The synthesis and characterisation of some aliphatic hyperbranched polyesters

Hamilton, Lesley M.

THE SYNTHESIS AND CHARACTERISATION OF SOME ALIPHATIC HYPERBRANCHED POLYESTERS

Lesley M. Hamilton.

A thesis submitted for the degree of Doctor of Philosophy at the University of Durham.

September 1996.

Abstract

The synthesis and characterisation of some aliphatic hyperbranched polyesters.

The attempted syntheses of potential AB_2 monomers for the production of hyperbranched polyesters has been described. The synthesis of poly(diethyl 3-hydroxyglutarate) has been reported and the characterisation of the products discussed fully. The use of soft ionisation mass spectrometry (MALDI-TOF MS) has been described and the results illustrate the number of different processes occurring during the polyesterification. ^{13}C nmr spectroscopy has been shown to be a viable technique in the determination of the degree of branching of these hyperbranched polymers.

The synthesis of core terminated hyperbranched polyesters has also been described. It was found that the coupling reactions of the core to the monomer/reactive focus was not efficient, hence only slightly improving the properties of the resulting hyperbranched polymers. The cross-linking of poly(diethyl 3-hydroxyglutarate) was attempted using two cross-linking agents, pentaerythritol tetra-acetate and 1,5-pentanediol, under a variety of conditions. Coupling of esters occurred, but the formation of an insoluble gel was not realised.

Contents

Appendix 3 **Analytical Data for Chapter 5**

FTIR spectra, GPC and DSC traces

Appendix 4 **Analytical Data for Chapter 6**

FTIR spectra, GPC and DSC traces

Colloquia, Lectures and Seminars Attended

Conferences and Courses Attended

Acknowledgements

I would like to acknowledge everyone who has helped me over the past three years throughout the course of my PhD studies. Firstly I must thank my supervisor, Professor Jim Feast who has constantly given me support and guidance. He has always ensured that I and the rest of the group have always had opportunities to travel and complete our work to the best of our abilities. Secondly I must thank my industrial supervisor, Dr. Steve Rannard. He is always a source of good ideas and his enthusiasm is totally inspiring.

I would also like to acknowledge all the support staff in Durham: Julia Say and Alan Kenwright for the excellent nmr service they provide, Gordon Forrest for the DSC and GPC service, Ray Hart and Gordon Haswell for their glass blowing skills and last but by no means least, Terry Harrison for his computer genius.

I must also thank the post-docs and students of the IRC in Durham, especially Helen who was always there for our early morning chats, Kate for living with me as well as working with me and Andy Grainger for helping me through my first two years. One other person who must be acknowledged is Lee; the love, support and understanding he has shown during the last stages of writing up has been incredible, he is one in a million.

Lastly, I must thank my parents, without them I would not be the person I am today. Words cannot express how much I appreciate all their love and support, not only throughout the past three years but throughout my life.

Memorandum

The work reported in this thesis has been carried out at the Durham site of the Interdisciplinary Research Centre in Polymer Science and Technology between October 1993 and September 1996. This work has not been submitted for any other degree either in Durham or elsewhere and is the original work of the author except where acknowledged by means of appropriate reference.

Financial Support

I gratefully acknowledge the provision of a CASE award from the Engineering and Physical Sciences Research Council and Courtaulds plc to support the work described herein.

Chapter 1.

A Review of Hyperbranched Polymers

1.1 INTRODUCTION

In recent years, the polymer community has sought novel synthetic routes for the production of polymers possessing unusual properties. The majority of the current commercially available polymers are synthesised via routes which were established many years ago. As the use of polymers has become more and more widespread over the past few decades, the demands on polymer properties and performance have become more rigorous. Properties depend on structure and organisation; structure, in its turn, depends on the details of the synthetic method used and so new structures generally require new synthetic strategies. The synthesis and study of polymers having novel topologies, for example polyrotaxanes[1] and catenanes,[2] has been an area of intensive research during recent years. It is hoped that the novel shapes and structures of these polymers will have profound effects on their properties which may prove technologically useful.

1.2 DENDRIMERS

The class of dendritic molecules encompasses both dendrimers[3] and hyperbranched[4] polymers. Both types of polymer have highly branched structures and, as a consequence, these polymers have numerous end groups. The first synthetic route to a dendritic wedge (dendron) was reported in 1978 by Vögtle.[5] As his "cascade" molecules were only of low molecular weight, polymer scientists showed little interest in this system. It wasn't until 1985, when both Tomalia[6] and Newkome[7] published papers on dendrimers within months of each other, that the polymer community began to take interest.

The synthesis of dendrimers requires a rigorous protection-deprotection, iterative, step-wise procedure.[8] At each stage of the reaction the product is purified as incomplete coupling reactions will result in defects within the structure. Dendrimers consist of concentric layers of repeat units around a central core. The core may be present from the beginning of the synthesis (divergent growth approach, Figure 1.1)[9]

or it may be introduced at a later stage and coupled to the dendrons (convergent approach, Figure 1.2).[10]

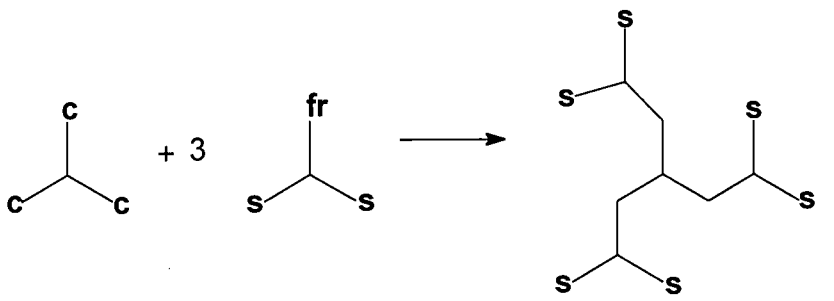

Figure 1.1 Divergent growth of a dendrimer.

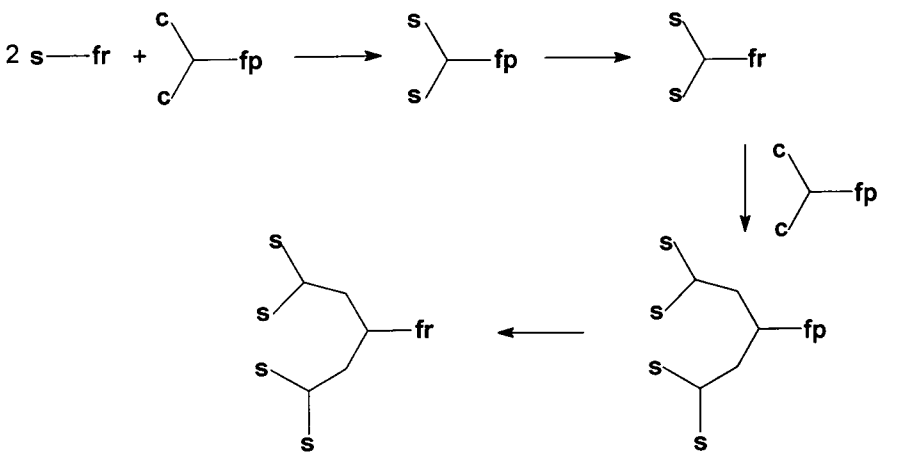

Figure 1.2 Convergent growth of a dendron.

Figures 1.1 and 1.2 exhibit the basic principles involved in the synthesis of monodisperse, highly branched macromolecules. In the diagrams, **c** refers to coupling sites which will only react with **fr**, the reactive functional groups. The surface moieties are labelled as **s**, whilst the protected functional groups are designated **fp**. In Figure 1.1, a threefold excess of the surface molecule is added to the core molecule to produce a zeroth generation dendrimer. The surface groups could be converted to coupling functionalities, and the process repeated to build a dendrimer. Figure 1.2 outlines a route to dendrimers via the convergent growth approach. In this method, the reactive functional groups are coupled to a molecule possessing only two coupling

sites. The product of this reaction may then be deprotected and reacted further to produce a dendritic wedge (dendron) which may ultimately be coupled to a core molecule to form a dendrimer.

Both synthetic methods have their advantages and disadvantages, however it would appear that the convergent approach is now favoured by most synthetic chemists. Due to the rigorous procedures required to construct these macromolecules, very few commercial dendrimers[11] are currently available. For highly branched molecules to find a niche in the market, they must either be easily prepared and inexpensive to produce or fulfil a demanding function. Initial investigations suggest that hyperbranched polymers fall into the categories of being easily made and inexpensive, hence generating industrial interest in these systems. It should be emphasised that ideal dendrimers are truly unique macromolecules, like many of the macromolecules of nature, whereas hyperbranched polymers resemble conventional synthetic polymers in as much as they consist of assemblies of molecules having a distribution of size and structure.

1.3 HYPERBRANCHED POLYMERS

Highly branched macromolecules were first discussed in detail by Flory in 1952.[12] His interest was purely theoretical and at that time few synthetic examples were available.[13,14] Flory predicted that hyperbranched molecules would be formed from AB_x monomers, where $x \geq 2$. The A and B functional groups must be able to react with each other, preferably on the addition of a catalyst or by the application of heat, to form highly branched, three dimensional structures free from cross-links. He assumed that, for polymers derived from an AB_2 monomer, the B groups would have the same reactivity independent of their location (Figure 1.3).

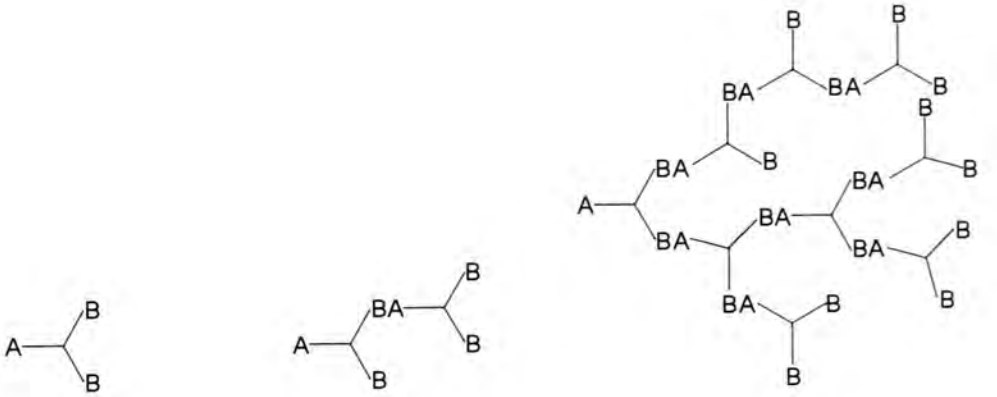

Figure 1.3 Schematic representation of an AB_2 monomer, dimer and oligomer.

As the molecule grows, it is clear that steric effects will become important. Perfect branching is impeded by these effects, giving rise to imperfections within the three dimensional structure. Hyperbranched molecules[i] can be considered to be imperfect dendrimers as there will be some unreacted B groups giving rise to linear segments within a highly branched environment. The schematic diagram below (Figure 1.4) colour codes the various structural features found in branched polymers and illustrates the differences between hyperbranched and dendritic macromolecules.

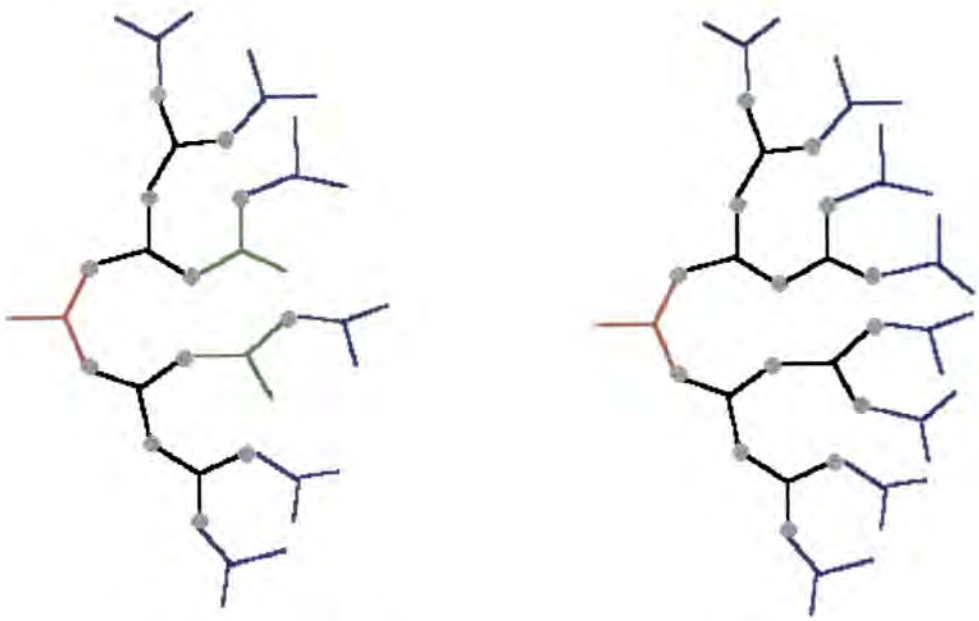

Hyperbranched wedge Dendron

Figure 1.4

Figure 1.4 illustrates the four types of sub-unit present within hyperbranched wedges. The red sub-unit represents the focus of the wedge which is the site of the only A group in the polymer. The black components denote the branched sub-units, whilst the blue groups represent the terminal sub-units. The linear sub-units are illustrated by the green sections of the polymer and it should be noted that these are only found within the hyperbranched structure.

1.4 THEORETICAL CONSIDERATIONS

The theoretical analysis of the polymerisation of AB_x monomers has been of interest for many years and was explored in detail by Flory[16] and Stockmayer.[17] The statistical arguments are based on the probabilities of reaction of A and B to provide a distribution of species of varied size and structure. An understanding of the approach is most easily obtained by first considering the much simpler case of the step-growth polymerisation of an AB monomer. To make the statistical analysis of the step-growth polymerisation of an AB monomer to form a linear polymer manageable, the following restrictions are applied:

i) the only reaction occurring in the system is the formation of a bond between the A and B functionalities,

ii) cyclisation reactions do not occur and

iii) the reactivity of A and B are assumed to be independent of the size of the molecule on which they reside.

An expression for the extent of reaction, p, can be written:-

$$p = \frac{N_0 - N}{N_0} \qquad \text{(Eq. 1.1)}$$

where N_0 is the number of monomer molecules at the beginning of the reaction and N is the number at a particular time. The term p could equally be called the probability of reaction of A or B; and, in this case, since we have stoichiometric balance of A and B, p_A and p_B are identical. The number average degree of polymerisation, $\overline{DP_n}$, ($\overline{\chi_n}$) is given by:-

$$\overline{\chi_n} = \frac{N_0}{N} \qquad \text{(Eq. 1.2)}$$

Elimination of N_0 and N from equations 1.1 and 1.2 gives the expression:-

$$\overline{\chi_n} = \frac{1}{1-p} \qquad \text{(Eq. 1.3)}$$

which is known as the Carother's equation. Equation 1.3 provides a measure of the number average size distribution in the product of an AB polymerisation. The ratio of the weight average distribution, $\overline{\chi_w}$, to the number average, $\overline{\chi_n}$ may also be obtained and is known as the polydispersity index (PDI).

The polymerisation equation:-

$$n\,(AB) \rightarrow A\text{-}(BA)_{n-1}\text{-}B$$

describes the formation of a species of degree of polymerisation n requiring (n-1) synthesis steps. The probability that A, or B, has reacted is p^{n-1}, the probability that A, or B, has not reacted is 1-p and so the probability of finding a molecule with a degree of polymerisation of n is the product of these two probabilities:-

$$(1-p)p^{n-1}$$

If we start with N_0 molecules of AB and have N molecules in the sample at a particular time, we can write an expression for the fraction of molecules, N_n, having a degree of polymerisation of n:-

$$N_n = N(1-p)p^{n-1} \qquad \text{(Eq. 1.4)}$$

substituting from equations 2 and 3, we obtain

$$N_n = N_o(1-p)^2 p^{n-1} \qquad \text{(Eq. 1.5)}$$

This expression, which gives the mole fraction of species N_n in the distribution, allows the number average distribution of species in a sample of an ideal AB step-growth polymer to be computed for any probability of reaction. One prediction of this expression is that however high the reaction conversion, small

oligomers (dimers and trimers) are always the numerically predominant species, as is illustrated in Figure 1.5.

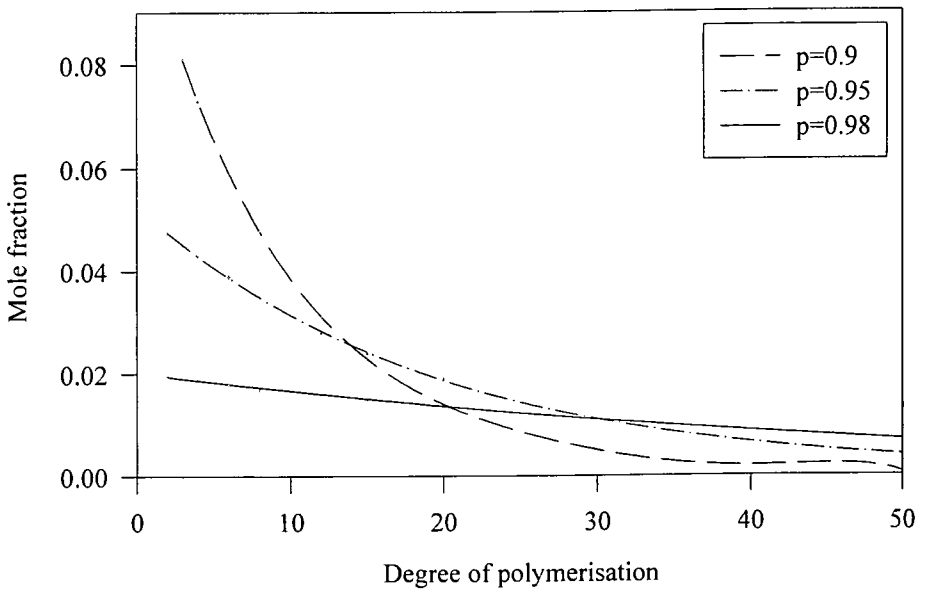

Figure 1.5 Graph showing the relationship between number average degree of polymerisation and mole fraction.

The weight average distribution can be obtained by multiplying the number average function by the weight fraction, w_n, as shown below:-

$$w_n = \frac{nN_n M_0}{N_0 M_0} \qquad \text{(Eq. 1.6)}$$

where M_0 is the repeat unit mass. Rearrangement and substitution of equation 1.5 into 1.6 gives:-

$$w_n = n(1-p)^2 p^{n-1} \qquad \text{(Eq. 1.7)}$$

When this expression, which gives the weight fraction of species of $\overline{DP} = n$ in the distribution, is plotted for various values of p, we are able to conclude that although low $\overline{DP}$ species may be the most numerous in a sample of material produced

by an AB step-growth polymerisation they constitute only a small part of the sample mass. Figures 1.5 and 1.6 demonstrate the differences.

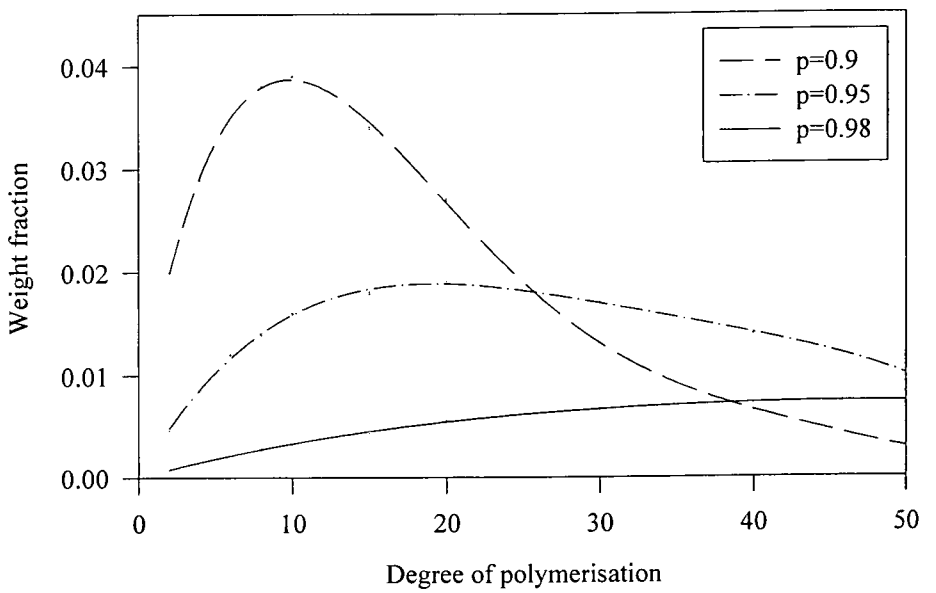

Figure 1.6 Graph showing the relationship between weight average degree of polymerisation and mole fraction.

We can use these results to establish an expression for the PDI. The number average molecular weight for this system is given by

$$\overline{M_n} = \frac{M_0}{1-p} \qquad \text{(Eq. 1.8)}$$

and the weight average molecular weight is defined as

$$\overline{M_w} = \sum_i w_i M_i \qquad \text{(Eq. 1.9)}$$

This expression for $\overline{M_w}$ can be rewritten for the species i having $\overline{DP} = n$

$$\overline{M_w} = \sum_n w_n n M_0 \qquad \text{(Eq. 1.10)}$$

Substituting for w_n we obtain

$$\overline{M_w} = \sum n(1-p)^2 p^{n-1} n M_0 \qquad \text{(Eq. 1.11)}$$

$$\overline{M_w} = M_0(1-p)^2 \sum n^2 p^{n-1} \qquad \text{(Eq. 1.12)}$$

The summation of this series, as n $\rightarrow \infty$, is known:

$$\sum n^2 p^{n-1} = \frac{1+p}{(1-p)^3} \qquad \text{(Eq. 1.13)}$$

Giving $$\overline{M_w} = \frac{1+p}{1-p} \qquad \text{(Eq. 1.14)}$$

and $$PDI = \frac{\overline{M_w}}{\overline{M_n}} = 1+p \qquad \text{(Eq. 1.15)}$$

Equation 15 leads to the prediction that as the reaction conversion tends to unity, the PDI tends to two.

Now let us consider the more complex case of the step-growth polymerisation of AB_x monomers. This is dealt with in detail in reference 16 pages 361-370 and here we will only outline the argument. The starting point is the same as for AB polymerisations, thus we assume:

i) the reactivity of a functional group is independent of the size of the molecule on which it resides or its position on that molecule

ii) intramolecular reactions do not occur and

iii) the reaction of A and B groups with each other is the only reaction which occurs.

Using these assumptions, consider x AB_{f-1} monomers reacting together (where f is the functionality, e.g. an AB_2 monomer is tri-functional), the resulting molecule will possess only one A group and (fx-2x+1) unreacted B groups. The branching probability, α, (defined as the probability that a functional group on a branch unit is connected to another branch unit) equals the fraction of B groups which have reacted, p_B. Hence:-

$$p_B = \frac{p_A}{f-1} = \alpha \qquad \text{(Eq. 1.16)}$$

The number average degree of polymerisation is defined by the consumption A groups and is the same as is given in equation 3:-

$$\overline{\chi}_n = \frac{1}{1-p_A} \qquad \text{(Eq. 1.3)}$$

Therefore:-

$$\overline{\chi}_n = \frac{1}{1-\alpha(f-1)} \qquad \text{(Eq. 1.17)}$$

To discuss molecular weight distributions in AB_{f-1} systems, Flory derived expressions for the number and weight average distributions and degrees of polymerisation. To achieve this he developed an argument based on counting the number of possible isomers at each stage of reaction. He made the assumption that the (f-1) B groups of a monomer, oligomer or polymer are readily distinguishable from each other even though they are identical in reactivity. This assumption was necessary to allow proper statistical counting of the numerous possibilities. Thus the dimers shown in Figure 1.7 are assumed to be different for this argument, although in practical terms B^1 and B^2 may be physically indistinguishable.

Figure 1.7 Statistically distinguishable isomers

The probability that a focal A group is attached to an x-mer is equivalent to the probability that a sequence of (x-1) B groups have reacted whilst (fx-2x+1) have not. The probability of this is defined as:-

$$\alpha^{x-1}(1-\alpha)^{(fx-2x+1)}$$

Therefore the probability that an A group is attached to an x-mer of any configuration is:-

$$N_x = \omega_x \alpha^{x-1}(1-\alpha)^{(fx-2x+1)} \qquad \text{(Eq. 1.18)}$$

where ω_x is the total number of configurations. As it is assumed that intramolecular condensation does not occur, each molecule must have one unreacted A group, hence N_x is also the mole fraction of the x-mer.

To evaluate the total number of configurations of an x-mer, Flory considered the hypothetical situation where monomer molecules are distinguishable from one another. To form an x-mer, (x-1) B groups are selected for reaction out of the total (f-1)x B's. The total number of sets which may be selected is given by:-

$$\frac{(fx-x)!}{(fx-2x+1)!(x-1)!}$$

The number of different ways in which (x-1) B's may react with (x-1) A's is (x-1)!. The total number of arrangements may be obtained by multiplying the expression above by (x-1)! to give:-

$$\frac{(fx-x)!}{(fx-2x+1)!}$$

As this assumption is physically unrealistic, dividing by x! (the number of monomer units for a given configuration) allows the determination of ω_x:-

$$\omega_x = \frac{(fx-x)!}{(fx-2x+1)!x!} \qquad \text{(Eq. 1.19)}$$

Equation 1.19 allows us to write an expression for the mole fraction distribution in an AB_{f-1} polymerisation:-

$$N_x = \frac{(fx-x)!}{(fx-2x+1)!x!}\alpha^{x-1}(1-\alpha)^{(fx-2x+1)} \qquad \text{(Eq. 1.20)}$$

The graph below shows the mole fraction distribution in an AB_2 polymerisation where α is replaced by equation 1.16 for simplicity.

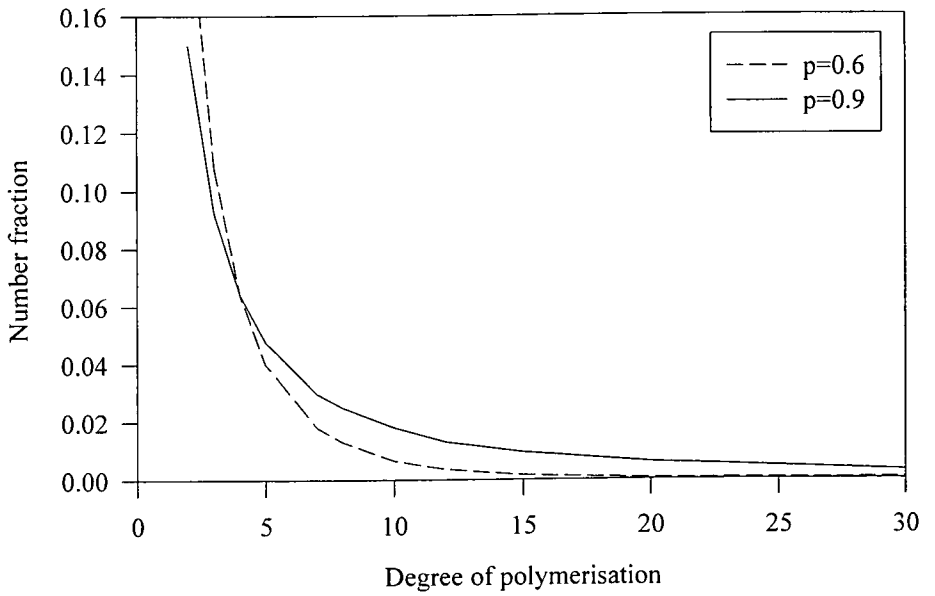

Figure 1.8 Graph showing the mole fraction distribution as fitted in accordance with equation 1.20.

Working through the mathematics Flory obtained, after some complicated series summations and differentiations, expressions for the weight fraction distribution, w_x, and weight average degree of polymerisation ($\overline{\chi_w}$). The weight fraction distribution is defined as:-

$$w_x = [1-\alpha(f-1)]x.\frac{(fx-x)!}{(fx-2x+1)!}\alpha^{x-1}(1-\alpha)^{(fx-2x+1)} \qquad \text{(Eq. 1.21)}$$

The graph overleaf shows the relationship between the weight fraction and the degree of polymerisation for an AB_2 system. Again, α is replaced by equation 1.16.

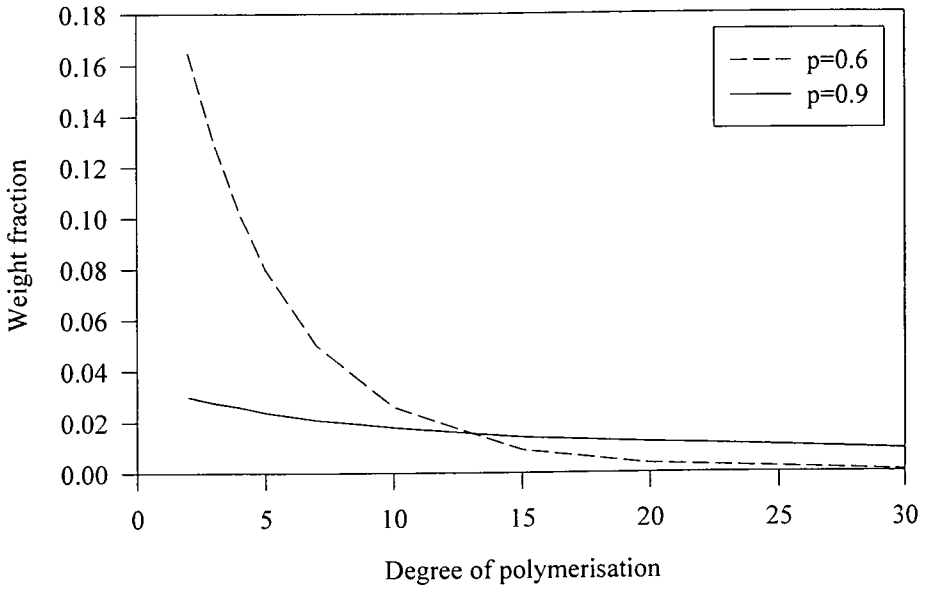

Figure 1.9 Graph showing the weight fraction distribution as fitted in accordance with equation 1.21

The weight average degree of polymerisation, $\overline{\chi_w}$, is given by:-

$$\overline{\chi_w} = \frac{1-\alpha^2(f-1)}{\left[1-\alpha(f-1)\right]^2} \qquad \text{(Eq 1.22)}$$

and he derived an expression for the polydispersity:-

$$\overline{\chi_w} \Big/ \overline{\chi_n} = \frac{1-\alpha^2(f-1)}{1-\alpha(f-1)} \qquad \text{(Eq 1.23)}$$

From equation 1.23, it can be seen that, for polymerisations based on AB_2 monomers, the equation simplifies to:-

$$\overline{\chi_w} \Big/ \overline{\chi_n} = \frac{1-2\alpha^2}{1-2\alpha} \qquad \text{(Eq. 1.24)}$$

This implies that as $\alpha \rightarrow \alpha_{max}$, i.e. 0.5, the polydispersity must be infinitely large. This is in marked contrast to the linear step-growth system where the PDI tends to 2 as conversion tends to 1. From this theoretical analysis it can be seen that large differences in the molecular weight distribution will be found for linear and hyperbranched polymers.

1.5 PROPERTIES OF DENDRITIC POLYMERS

When dendritic polymers were merely an academic curiosity, it was hoped that these highly branched macromolecules would possess different properties from analogous linear polymers due to their numerous end groups and branches. If one can assess the properties of the polymer and relate them to the structure and/or molecular weight it ought to be possible to tailor-make polymers for specific applications. The properties of hyperbranched polymers are not fully understood at the moment as they are a relatively new class of materials with few studied examples. It can be expected that they will require new theories to be developed to account for their properties.

The physical properties of dendrimers are perhaps easier to understand due to their regular structure. The viscosity, glass transition temperature and solubility of dendrimers may be empirically related to the number of end groups and branch points. As hyperbranched polymers possess several imperfections, reliable theories which describe the physical behaviour of these materials have not been fully developed, however, existing theories for dendrimers may be used in a slightly modified form.

The glass transition temperature of a linear polymer, which is defined as the onset of chain segmental motion, depends on several structural factors (chain stiffness, symmetry and polarity) and on molecular weight. A commonly used relationship is:-

$$T_g = T_{g_\infty} - \frac{K}{M} \qquad \text{(Eq. 1.25)}$$

which was introduced by Fox and Flory[18] and relates the observed T_g of the "infinite" molecular weight sample with the observed molecular weight. For dendrimers, a modified version of equation 1.25 has been introduced[19] by Fréchet:-

$$T_g = T_{g_\infty} - n_e \frac{K'}{M} \qquad \text{(Eq 1.26)}$$

The symbols T_g, $T_{g\infty}$ and M have the same meanings as in the Fox-Flory equation, K′ is a constant for a particular system and n_e represents the number of end groups. This expression provides a reasonable fit to Fréchet's data for dendrimers but there is some controversy about its applicability to hyperbranched systems. This will be discussed in greater detail in Chapter 4 where the experimental data accumulated in the course of this work is analysed.

Stutz[20] recently performed a detailed theoretical study of the glass transition of dendrimers. It was postulated that the large number of end groups decreases the glass transition temperature, whilst the large amount of branching increases it. Therefore these parameters tend to compensate each other and the difference in glass transition temperature between linear polymers and analogous dendrimers is smaller than first expected due to the cancellation of these opposing effects. It has been reported[21] that within one structural type of polymer, the T_g is independent of the architecture of the molecule. Thus, Wooley[21] found that, within experimental error, the glass transition temperature of linear, hyperbranched and dendritic meta-linked aromatic polyesters is constant at approximately 200°C for the phenolic terminated polymers.

The glass transition of highly branched systems cannot be defined as the onset of co-operative segmental motion as such systems do not possess the long unbranched segments usually associated with the back-bone of a linear polymer. Kim and Webster[22] modified the end groups of their hyperbranched polyphenylenes to show that the T_g is highly dependent on the structure and polarity of the end groups. As the internal structures and linkages remain the same in this series it was proposed that the glass transition of hyperbranched polymers is due to translational movements of the end groups.

The viscosity of dilute polymer solutions provides information on the hydrodynamic volume of the polymer. The intrinsic viscosity may also yield information on the amount of branching of the polymer by the Mark-Houwink-Sakurada relationship (equation 1.27):-

$$[\eta] = KM^a \qquad \text{(Eq 1.27)}$$

where K and a are constants for a particular polymer-solvent combination at a specified temperature. The values of a are especially informative as values lying between 0 and 0.5 indicate a highly branched, dense, globular structure. Turner *et al*[23] have found that hyperbranched aromatic polyesters, synthesised from 3,5-diacetoxybenzoic acid, give values of 0.3-0.4.

The viscosity of dendritic polymers has been investigated by several authors[23,24] and it has been shown that, generally, a non-linear behaviour is observed in Mark-Houwink plots. Figure 1.10 below illustrates the differing behaviours of linear, hyperbranched and dendritic polymers.[25]

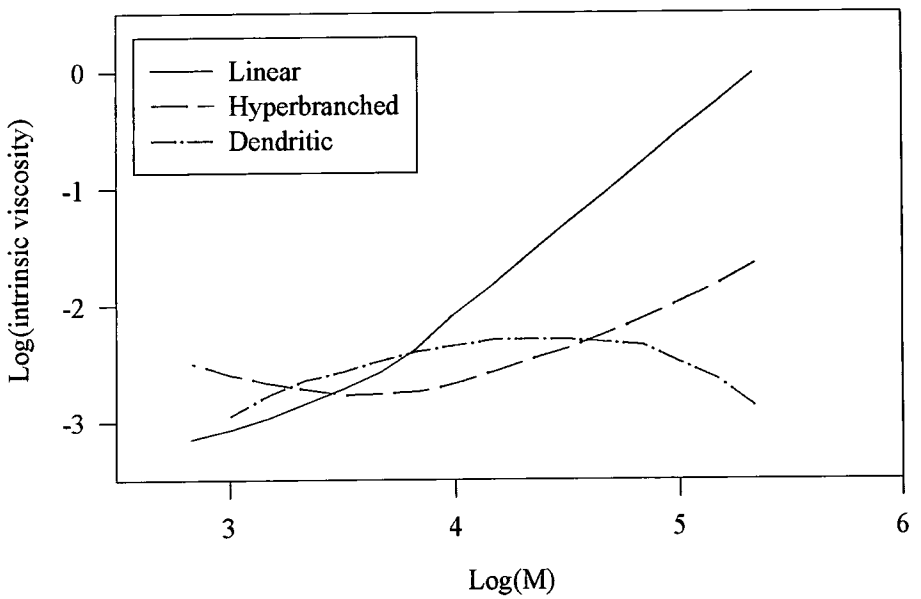

Figure 1.10 Graph showing the dependence of Log(η) on Log(M).

The plot above must be regarded as purely schematic as it represents results from different classes of polymer. As yet, no direct comparison of the viscosity behaviour of linear, hyperbranched and dendritic molecules having the same (or closely related) repeat motifs have been published.

It was proposed that[26] PAMAM (poly{amidoamine}) dendrimers [**1**] pass through a maximum in intrinsic viscosity due to a transition from an extended to globular shape as a function of molecular weight.

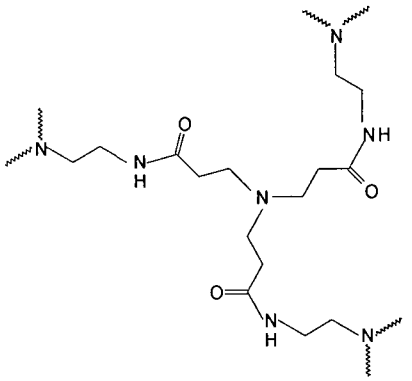

[**1**]

Dendrimers possessing unsymmetrical branch junctions,[26] e.g. polylysine dendrimers, show a linear dependence in Mark-Houwink plots. Much more work is required to elucidate the intrinsic viscosity-molecular weight relationships for hyperbranched systems.

1.6 CLASSES OF HYPERBRANCHED POLYMERS

1.6.1 Hyperbranched Aromatic Polyesters

When investigating the history of hyperbranched polyesters, it becomes clear that the majority of the work has centred around the polymerisation of aromatic AB_2 monomers. The first reported synthesis of an aromatic hyperbranched polyester[27] involved the polymerisation of 3,5-bis(trimethylsiloxy)benzoyl chloride [**2**].

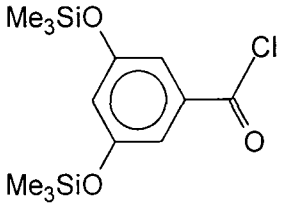

[**2**]

The use of [2] had previously been reported[28] as a branching agent in the synthesis of linear polymers. The reaction between [2] and 3-(trimethylsiloxy)benzoyl chloride gave copolymers displaying increasing solubility with increasing mole percent of the AB_2 monomer.

Verification of the microstructure of hyperbranched polymers is required to prove that highly branched structures have been formed. It was in the initial paper[27] by Hawker *et al* that the degree of branching (DB) was defined. The degree of branching provides information on the number of branches within a highly branched polymer. By definition, dendrimers have a degree of branching of 1 as every branch point reacts to give a perfectly branched structure, whilst infinitely long linear polymers have a DB of zero as they possess no branches. Hyperbranched macromolecules have DB's which lie between zero and one. To determine the DB, the following equation is used:

$$DB = \frac{N_t + N_b}{N_t + N_b + N_l} \qquad \text{(Eq. 1.28)}$$

where N_t is the number of terminal groups, N_b is the number of branched groups and N_l is the number of linear groups. It is therefore necessary to determine the number of terminal, linear and branched sub-units present in the polymer to calculate the DB. Hawker determined the number of constituent sub-units by synthesising model compounds which were direct analogues of the linear, terminal and branched sub-units within the polymer. The ^1H nmr spectra of these model compounds could then be used to assign the signals in the ^1H nmr of the hyperbranched polymer and the relative integrated intensities provided the number of discrete sub-units.

The use of [2] as an AB_2 monomer has been reported several times[29,30] since the initial paper in 1991. A systematic variance of amount and type of catalyst, duration of polymerisation and polymerisation temperature was described[31] in 1994. In this study, the highest molecular weight was achieved at 200°C in the presence of 10wt% of trimethylamine hydrochloride as catalyst, previously[27] polystyrene equivalent molecular weights of *ca* 180,000 were found in the absence of catalyst showing that [2] is highly active in AB_2 polymerisations. Kricheldorf[31] has also

reported the synthesis and subsequent polymerisation of silylated 5-acetoxyisophthalic acid [**3**] to give M_n's in the region of 10,000.

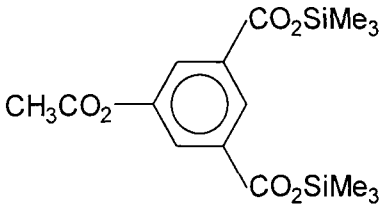

[**3**]

The polymerisation of aromatic acetate-acids has been investigated by two groups.[30,31,32,33] The polymerisation of 3,5-diacetoxybenzoic acid [**4**] reported by Voit and Turner[30] has largely been unexploited despite M_w's ranging from 60,000 to 100,000 Daltons (as determined by GPC using universal calibration).

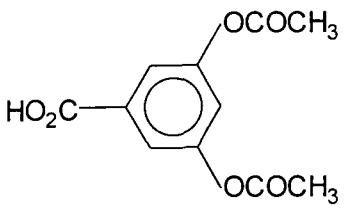

[**4**]

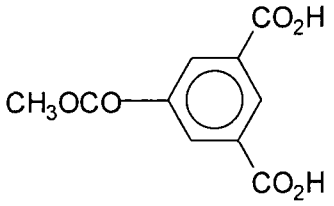

[**5**]

The direct A_2B analogue of [**4**], 5-acetoxyisophthalic acid, [**5**], has been the focus of two studies.[32,33] Turner *et al*[32] performed polymerisations of [**5**] in the absence of a catalyst to produce a hyperbranched polymer with a DB of 0.50, whilst Kricheldorf[33] polymerised [**5**] in the presence of AB monomers to produce aromatic copolyesters, although no indication of the DB was supplied by the authors.

Only one report of the polymerisation of aromatic diester-alcohols in the presence of a core molecule has been published thus far. Feast and Stainton[34] polymerised dimethyl 5-(2-hydroxyethoxy)isophthalate [**6**] in the presence of trimethyl 1,3,5-benzenetricarboxylate [**7**].

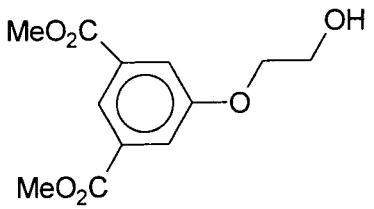

[6]

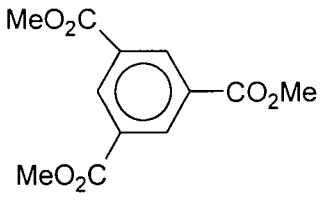

[7]

It was anticipated that the core molecule would regulate the molecular weight of the hyperbranched polymer by consuming the reactive focus and would give structures resembling dendrimers.

The polymerisation of [**6**] has successfully been performed by Turner *et al.*[32] The resulting hyperbranched polymer may be considered a hybrid aliphatic-aromatic polyester due to the ethoxy chain of the B group. This paper may have been the precursor to the studies performed by Hawker[35] and Kumar,[36] whose investigations involved the polymerisation of modified aromatic dihydroxy-esters [**8**] which contain short, oligomeric ethylene glycol units.

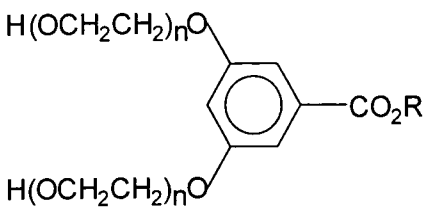

[**8**]

where R=Me or Et

n=1, 2, 3 or 6.

A comparison of a linear PEG sample with that of poly[**8**][35] reveals that the glass transition temperature of the hyperbranched analogues are slightly higher than that of the linear polymer, possibly due to the aromatic units within the hyperbranched samples. A melting transition is not observed for the hyperbranched species, proving that crystallisation is inhibited by the hyperbranched centres. The glass transition temperatures of the hyperbranched samples decreases as the length of the spacer unit increases as expected.

1.6.2 Aliphatic Hyperbranched Polyesters

Wholly aliphatic polyesters have, hitherto, only been reported by Hult and co-workers.[37] As previously described,[34] the polymerisation of hyperbranched molecules in the presence of a core molecule[38] effectively regulates the molecular weight of the polymer by "capping" the reactive focus. To obtain high degrees of branching,[38] Hult *et al* utilised a pseudo-one-step batch procedure.

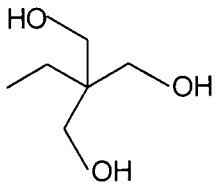

[9]

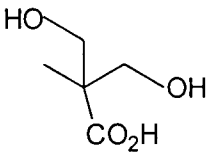

[10]

The core molecule, 2-ethyl-2-(hydroxymethyl)-1,3-propanediol [**9**] and 2,2-bis(hydroxymethyl) propionic acid [**10**] are polymerised in a 1:9 core:monomer ratio to give the equivalent of a second generation dendrimer. An additional 12 equivalents of monomer is added to produce a pseudo third generation macromolecule and the procedure is repeated in this manner. By the stepwise addition of monomer, a high degree of branching is obtained, which gives structures that may be considered almost dendritic. It has been postulated by the authors[38] that the high DB (0.8) is achieved due to the partial solubilisation of [**10**] into the melt. As the reaction proceeds, the monomer slowly dissolves allowing the hydroxyl groups on the hyperbranched skeleton to react with the carboxylic acid of [**10**]. This ensures that molecules possessing high DB's are formed rather than the statistical DB's of the hyperbranched systems formed in the absence of a core.

1.6.3 Polyethers

Uhrich *et al* reported[39] the synthesis of hyperbranched polyethers in 1991. The polymers were synthesised using 3,5-dihydroxybenzyl bromide [**11**] in the presence of potassium carbonate and 18-crown-6. Two syntheses were explored; a one

component system to provide an aromatic hydroxy terminated polyether and a two component system in which the monomer and an end-capping agent, [**12**], 3,5-dibenzyloxybenzyl bromide are polymerised under high dilution conditions to give benzylic groups at the periphery.

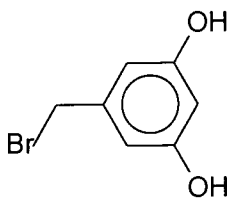

[**11**]

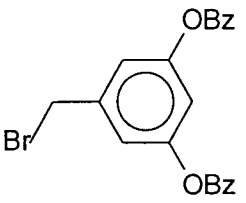

[**12**]

The molecular weight was found to be highly dependent on the solvent used in the polymerisations. Further work by Uhrich[40] showed that the timed addition of monomer to the reaction vessel throughout the polymerisation did not, to any great extent, effect the molecular weight of the resulting polymer.

1.6.4 Polyether ketones

As the linear analogues of polyether ketones are commonly used as engineering plastics, it was hoped that the hyperbranched polymers would possess improved properties. Two monomers were prepared by Chu and Hawker,[41] the first [**13**] was designed to give a fluoro-terminated hyperbranched polyether ketone, hence A=OH and B=F, whilst a hydroxy terminated polyether ketone was synthesised using A=F and B=OH, [**14**].

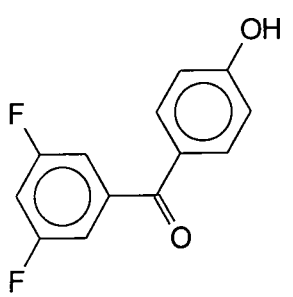

[**13**]

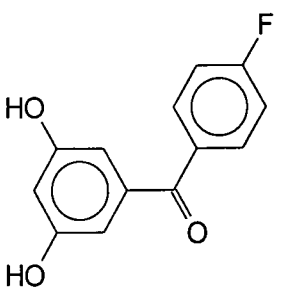

[**14**]

Several differences were noted in these isomeric polyether ketones, for example the hydroxy terminated polymer had a much higher molecular weight than the fluoro polymer, whilst the hydroxy polymer had a lower T_g than the fluoro terminated polymer. This was assumed to be due to the effect of the end groups on T_g.

Further work[42] into the properties of these polymers was performed. The DB's of these macromolecules ranged from 0.14 for the hydroxy terminated polymer to 0.49 for the fluoro terminated polymer. In an attempt to control the DB, AB_3 and AB_4 monomers were synthesised to produce fluoro terminated polyether ketones. It was found that the AB_3 polymer had a DB of 0.38 whilst the AB_4 polymer gave a DB of 0.71. No explanation was offered for the low DB of the hydroxy terminated polymer.

1.6.5 Polyamides

The first reported synthesis of "hyperbranched" polyamides was by Uhrich *et al.*[43] In this initial investigation "hyperbranched" polymers were grown onto a polymeric backbone by using the solid phase peptide synthesis pioneered by Merrifield.[44] It should be noted, that although these molecules are reported as hyperbranched, the synthetic route presented in the communication was developed to yield dendrimers. There was a lot of confusion in the early stages of dendritic syntheses as authors had not agreed on a universal nomenclature of highly branched polymers. The polyamides in this communication are in fact dendrimers, even though they are referred to as hyperbranched.

Kim[45] reported the synthesis of hyperbranched polyamides displaying liquid crystalline phases derived from aromatic acid chlorides [**15**].

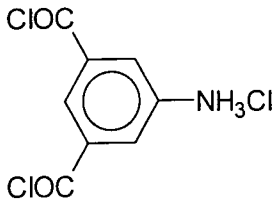

[15]

The polymer was precipitated into water to yield a carboxylic acid terminated hyperbranched polyamide. The polymer shows signs of forming aggregates[46] in dilute solutions in the absence of complexing ions and it is postulated that the liquid crystalline behaviour may be due to aggregation.

1.6.6 Polyamines

To date, only one example of a hyperbranched polyamine synthesis has been reported. Suzuki *et al*[47] polymerised 5,5-dimethyl-6-ethenylperhydro-1,3-oxazin-2-one [**16**] in the presence of a Pd(0) catalyst to produce a hyperbranched polyamine.

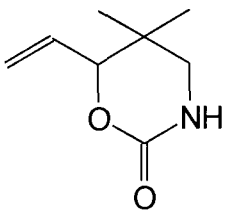

[**16**]

The authors refer to the formation of the hyperbranched polymer via ring-opening polymerisation as "multibranching polymerisation" (MBP). Molecular weights of 1860-5330 Daltons were achieved and DB's ranged from 0.44 to 0.52. It is clear that the process involves the loss of carbon dioxide, but the mechanism of the polymerisation is somewhat obscure.

1.6.7 Polyurethanes

Only two reports of hyperbranched polyurethanes have been published thus far. The synthesis of polyurethanes may be achieved via the reaction of an alcohol with an isocyanate. Spindler and Fréchet[48] reported some cross-linking at high concentrations of the protected isocyanate, 3,5-bis([benzoxycarbonyl]imino)benzyl alcohol [**17**] in THF.

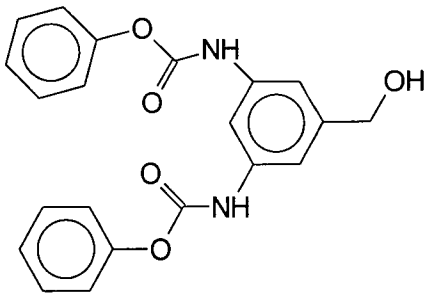

[17]

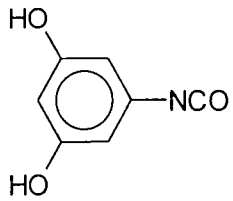

[18]

To prevent this occurring, either an equimolar amount of an alcohol was added at the start of the polymerisation to end cap the polymer or low monomer concentrations were used. The bis-isocyanate is formed when [**17**] is heated in the polymerisation vessel with the liberation of phenol.

Kumar[49] has reported the polymerisation of the *in situ* generated 3,5-dihydroxyphenyl isocyanate, [**18**], to give a hydroxy terminated polyurethane. The molecular weight of these polymers was disappointing (M_w=2500-9100) however cross-linking was not observed for this system. The DB of these polymers was found to be 0.59.

1.6.8 Polyphenylenes

The synthesis of hyperbranched polyphenylenes was first reported by Kim and Webster.[50] The polyphenylenes were synthesised via the polymerisation of 3,5-dihalophenyl Grignard reagents [**19**] in the presence of transition metal catalysts or from 3,5-dibromophenylboronic acid [**20**].

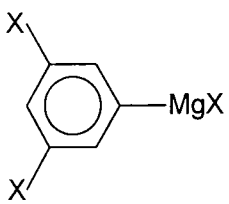

[19]

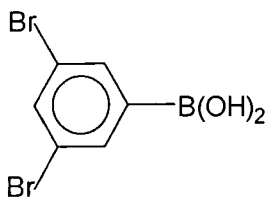

[20]

The polymers synthesised from [**18**] had, on average, molecular weights lower than those obtained from [**19**]. It was postulated that this may be due to decreased reactivity as a consequence of steric hindrance around the catalytic centre. The bromo-terminated polyphenylenes was blended with polystyrene (5:95 mix) in an attempt to assess the effect of this hyperbranched polymer on the properties of commodity polymers. It was found that the thermal stability of the blend was improved and the melt viscosity had decreased by 50% implying that hyperbranched polyphenylenes may have a profound impact as additives for commodity polymers.

1.6.9 Polysiloxysilanes

Mathias and Carothers[51] successfully polymerised AB_3 silicon containing monomers to produce polymers with silane and siloxane groups of an average molecular weight of 19,000 (as determined by GPC using polystyrene standards). The synthesis of [**21**] involved the addition of allyltrichlorosilane to three equivalents of dimethylchlorosilane to give [**21**] in good yield.

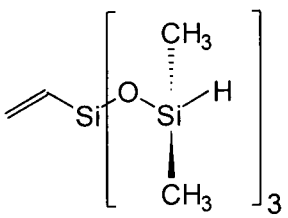

[**21**]

The polymerisation was performed in the presence of hydrogen hexachloroplatinate (IV) hydrate. The authors gave no information on the DB of the polymer.

1.6.10 Hyperbranched polymers prepared from vinyl monomers

Fréchet[52] introduced the concept of "self-condensing vinyl polymerisation" in 1995. This involves the hybrid polycondensation/vinyl polymerisation of an AB vinyl monomer to produce hyperbranched polymers, see Figure 1.11 below:

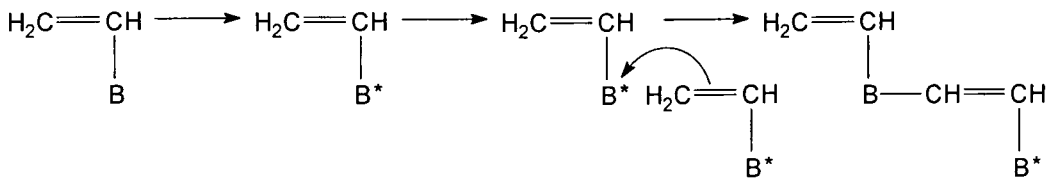

Figure 1.11 Self-condensing vinyl polymerisation

The AB monomer is activated by either a physical (application of heat or light) or chemical process to give an AB* activated monomer. This is then able to react with another AB* monomer to yield a dimer which possesses both an initiating (B*) centre and a propagating (CH*) centre to produce hyperbranched polymers. In this initial communication, 3-(1-chloroethyl)-ethenylbenzene [**22**] was chosen as the AB vinyl monomer.

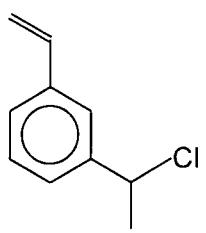

[**22**]

The polymerisation was performed in the presence of $SnCl_4$ as the activator to give number average molecular weights in the range of $5x10^3$-$68x10^3$ (as determined by GPC using universal calibration).

An analogous reaction was performed using [**23**][53] as the AB vinyl monomer to give hyperbranched polymers with weight average molecular weights of 6000 (determined by GPC using polystyrene standards).

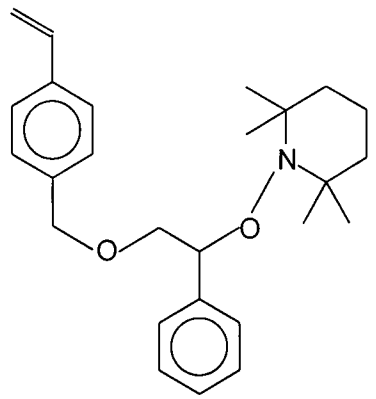

[**23**]

The polymerisation proceeds via a radical mechanism induced by the application of heat. As the carbon oxygen bond linking the nitroxide group is of low energy, thermal activation produces a propagating benzylic radical. This is then able to react with the vinyl group of another monomer to produce an AB_2 monomer with a polymerisable vinyl bond and two potential propagating sites. The reaction thus proceeds to form hyperbranched polymers.

Gaynor *et al*[54] polymerised *p*-(chloromethyl)styrene via an atom transfer radical process in the presence of Cu[1] and 2,2'-bipyridyl to give hyperbranched polymers with number average molecular weights of 1100-2800 (as determined by GPC using linear polystyrene standards).

1.7 CONCLUSIONS

The field of highly branched molecules has expanded rapidly, however few systems have been used for commercial applications. Tomalia's PAMAM™ starburst dendrimers are currently used in the pharmaceutical industry as carrier molecules in medical diagnostics and therapy. Dendritic structures have been suggested as components of adhesives or sealants, coatings or as rheology modifiers.

Hyperbranched molecules are already used in coatings[55] due to their low T_g's and ease of resin formation. High T_g polymers are used in blends[50] with polystyrene, the resulting copolymers have been used as reinforcing filler materials. It is clear that highly branched polymers are becoming an important part of technical materials advancement.

1.8 REFERENCES

1. H.W. Gibson, S. Liu, *Macromol. Symp.*, **102**, (1996), 55.
2. D.B. Amabiline, J.F. Stoddart, *Pure Appl. Chem.*, **65**, (1993), 2351.
3. J. Issberner, R. Moors, F. Vögtle, *Angew. Chem. Int. Ed. Engl.*, **33**, (1994), 2413.
4. B.I. Voit, *Acta. Polym.*, **46**, (1995), 87.
5. E. Buhleier, W. Wehner, F. Vögtle, *Synthesis*, (1978), 155.
6. D.A. Tomalia, H. Baker, J. Dewald, M. Hall. G. Kallos, S. Martin, J. Roeck, J. Ryder, P. Smith, *Polym. J.*, **17**, (1985), 2003.
7. G.R. Newkome, Z.Q. Yao, G.R. Baker, V.K. Gupta, *J. Org. Chem.*, **50**, (1985), 2003.
8. J.M.J. Fréchet, C.J. Hawker, K.L. Wooley, *J.M.S.-Pure Appl. Chem.*, **A31**, (1994), 1627.
9. D.A. Tomalia, H.D. Hurst, *Top. Curr. Chem.*, **165**, (1993), 193.
10. C.J. Hawker, J.M.J. Fréchet, *J. Am. Chem. Soc.*, **112**, (1990), 7638.
11. E.M.M. Brabender-van den Berg, E.W. Meijer, *Angew. Chem. Int. Ed. Engl.*, **32**, (1993), 1308.
12. P.J. Flory, *J. Am. Chem. Soc.*, **74**, (1952), 2718.
13. W.H. Hunter, G.H. Woolett, *J. Am. Chem. Soc.*, **43**, (1921), 135.
14. R.A. Jacobson, *J. Am. Chem. Soc.*, **54**, (1932), 1513.
15. Y.H. Kim, *Mcromol. Symp.*, **77**, (1994), 21.
16. P.J. Flory, "Principles of Polymer Chemistry", Cornell University Press, Ithaca, New York, (1953).
17. W.H. Stockmayer, *J. Chem. Phys.*, **11**, (1943), 45.
18. T.G. Fox, P.J. Flory, *J. Polym. Sci.*, **14**, (1954), 315.
19. K.L. Wooley, C.J. Hawker, J.M. Pochan, J.M.J. Fréchet, *Macromol.*, **26**, (1993), 1514.
20. H. Stutz, *J. Polym. Sci: Part B, Polym. Phys.*, **33**, (1995), 333.
21. K.L. Wooley, J.M.J. Fréchet, C.J. Hawker, *Polymer,* **35**, (1994), 4489.
22. Y.H. Kim, O.W. Webster, *Macromol.*, **25**, (1992), 5561.
23. S.R. Turner, B.I. Voit, T.H. Mourey, *Macromol.*, **26**, (1993), 4617.

24. T.H. Mourey, S.R. Turner, M. Rubinstein, J.M.J. Fréchet, C.J. Hawker, K.L. Wooley, *Macromol.*, **25**, (1992), 2401.
25. J.M.J. Fréchet, C.J. Hawker, *React. Funct. Polym.*, **26**, (1995), 127.
26. D.A. Tomalia, D.M. Hall, D. Hedstrand, *J. Am. Chem. Soc.*, **109**, (1987), 1601.
27. C.J. Hawker, R. Lee, J.M.J. Fréchet, *J. Am. Chem. Soc.*, **113**, (1991), 4583.
28. H.R. Kricheldorf, Q-Z Zang, G. Schwarz, *Polymer*, **23**, (1982), 1821.
29. K.L. Wooley, C.J. Hawker, R. Lee, J.M.J. Fréchet, *Polym. J.*, **26**, (1994), 187.
30. B.I. Voit, S.R. Turner, *Polym. Prepr.*, **33**, (1992), 184.
31. H.R. Kricheldorf, O. Stöber, *Macromol. Rapid Commun.*, **15**, (1994), 87.
32. S.R. Turner, F. Walter, B.I. Voit, T.H. Mourey, *Macromol.*, **27**, (1994), 1611.
33. H.R. Kricheldorf, O. Stöber, D. Lübbers, *Macromol. Chem. Phys.*, **196**, (1995), 3549.
34 W.J. Feast, N.M. Stainton, *J. Mater. Chem.*, **5**, (1995), 405.
35. C.J. Hawker, F. Chu, *Abs. Papers Am. Chem. Soc.*, **210**, (1995), 94.
36. A. Kumar, S. Ramakrishnan, *Macromol.*, **29**, (1996), 2524.
37. E. Malmström, M. Johansson, A. Hult, *Macromol.*, **28**, (1995), 1698.
38. E. Malmström, A. Hult, *Abs. Papers Am. Chem. Soc.*, **210**, (1995), 349.
39. K.E. Uhrich, C.J. Hawker, J.M.J. Fréchet, *Polym. Mater. Sci. Eng.*, **64**, (1991), 237.
40. K.E. Uhrich, C.J. Hawker, J.M.J. Fréchet, S.R. Turner, *Macromol.*, **25**, (1992), 4583.
41. F. Chu, C.J. Hawker, *Polym. Bull.*, **30**, (1993), 265.
42. C.J. Hawker, F. Chu, *Macromol.*, **29**, (1996), 4370.
43. K.E. Uhrich, S. Boegeman, J.M.J. Fréchet, S.R.Turner, *Polym. Bull.*, **25**, (1991), 551.
44. R.B. Merrifield, *J. Am. Chem. Soc.*, **85**, (1963), 2149.
45. Y.H. Kim, *J. Am. Chem. Soc.*, **114**, (1992), 4947.
46. Y.H. Kim, *Adv. Mater.*, **4**, (1992), 764.
47. M. Suzuki, A. Ii, T. Saegusa, *Macromol.*, **25**, (1992), 7071.
48. R. Spindler, J.M.J. Fréchet, *Macromol.*, **26**, (1993), 4809.
49. A. Kumar, S. Ramakrishnan, *J. Chem. Soc., Chem. Commun.*, (1993), 1453.

50. Y.H. Kim, O.W. Webster, *J. Am. Chem. Soc.*, **112**, (1990), 4590.

51. L.J. Mathias, T.W. Carothers, *J. Am. Chem. Soc.*, **113**, (1991), 4043.

52. J.M.J. Fréchet, M. Henmi, I. Gitsov, S. Aoshima, M.R. Leduc, R.B. Grubbs, *Science*, **269**, (1995), 1080.

53. C.J. Hawker, J.M.J. Fréchet, R.B. Grubbs, J. Dao, *J. Am. Chem. Soc.*, **117**, (1995), 10763.

54. S.G. Gaynor, S. Edelman, K. Matyjaszewski, *Macromol.*, **29**, (1996), 1079.

55. M. Johansson, E. Malmström, A. Hult, *J. Polym. Sci, Part A: Polym. Chem.*, **31**, (1993), 619.

Chapter 2.

Attempted Syntheses of AB_2 monomers for Polycondensation Reactions

2.1 INTRODUCTION

This chapter describes unsuccessful attempts to make suitable AB_2 monomers for the synthesis of hyperbranched aliphatic polyesters. The work is recorded here for the sake of completion.

An important criterion for suitable monomers is relatively low cost since, even in an academic laboratory, it is desirable to produce materials on a sufficiently large scale for assessment of properties. In an attempt to synthesise AB_2 monomers which may be used to produce aliphatic hyperbranched polyesters, it is necessary to contemplate which functional groups would fit the reaction criteria. The A and B functionalities must be capable of reacting with each other to eliminate a condensation product when either heat is applied or a catalyst is added to the monomer. As the purity of monomers for step-growth polymerisations is of paramount importance if high conversion is to be achieved, the scenario where A and B react spontaneously would make the verification of the purity of the compound very difficult, if not impossible. For example, small amounts of AB, A_2 or B_2 impurities would result in a polymer with extended linear segments, a cross-linked polymer or a core terminated polymer respectively. Therefore it is desirable to ensure that the monomer is pure before the reaction is performed.

Many industrial polyesterification processes are performed either by direct esterification or alcoholysis. Figure 2.1 below outlines the general reaction pathway used in the production of polyesters:

Figure 2.1

Direct esterification occurs when X=OH and Y=R'OH whereas alcoholysis, or transesterification, requires X=OR" and Y=R'OH. As these reactions are the most

commonly utilised in the synthesis of linear polyesters, it was decided to attempt to make analogous AB_2 monomers. Therefore diacid-alcohols or diol-acids must be synthesised for direct esterification whereas diester-alcohols or diol-esters may be synthesised to allow alcoholysis to be performed.

The range of reactions reported in this chapter show the variety of methods available for producing diester-alcohols. To date only one synthesis of a diol-ester has been attempted due to the lack of a facile route to the required type of product.

2.2 THE SYNTHESIS OF MONOMER PRECURSORS VIA MICHAEL ADDITION

In the author's initial foray into potential syntheses of suitable AB_2 monomers for polyesterification reactions, it was found that monomer precursors may be synthesised via Michael addition[1] reactions. The number of readily available precursors is limited by the constraints of the Michael addition, however two suitable precursors utilising malonate esters as the donor molecule were successfully synthesised.

The Michael addition is a base-catalysed addition reaction which forms carbon-carbon bonds. The outcome of the reaction is the addition of a donor molecule to the C-terminus of the conjugated system of an acceptor as shown below:

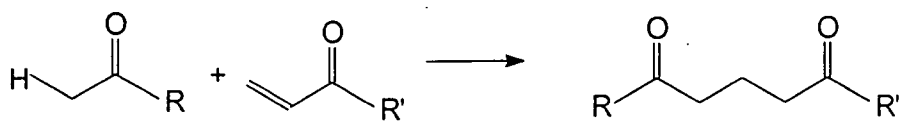

Figure 2.2

The donor molecule must have an α-hydrogen which can be extracted to form a carbanion. The base most commonly used in Michael additions is an alkoxide anion[2] which is formed by the reaction of a catalytic amount of an alkali metal with an alcohol, however recent work in this area suggests that water soluble inorganic

hydroxides used in conjunction with phase transfer catalysts[3,4] may be more effective than alkoxides. Figure 2.3 illustrates the abstraction of a proton by an alkoxide anion. The resulting carbanion is resonance stabilised, but reactive enough to attack the electropositive carbon atom of the Michael acceptor:

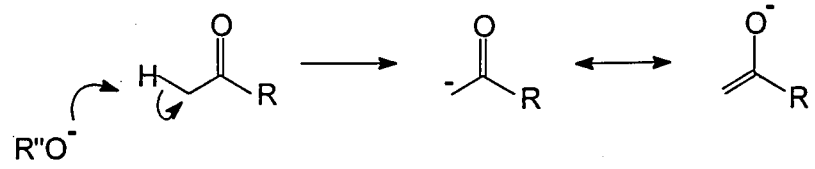

Figure 2.3

By definition, acceptor molecules must have a conjugated double bond system, Figure 2.2 shows an acceptor where R' is typically a hydrogen atom, alkyl or alkoxy group. However, in general terms, acceptors may be olefins which are activated by carbonyl, carboalkoxy, nitro[5] or nitrile functional groups. In the work presented in this chapter, the acceptor molecules are either acrolein (a vinyl aldehyde) or methyl vinyl ketone, whilst the donor molecule is dimethyl methylmalonate, hence the reaction may be represented as:

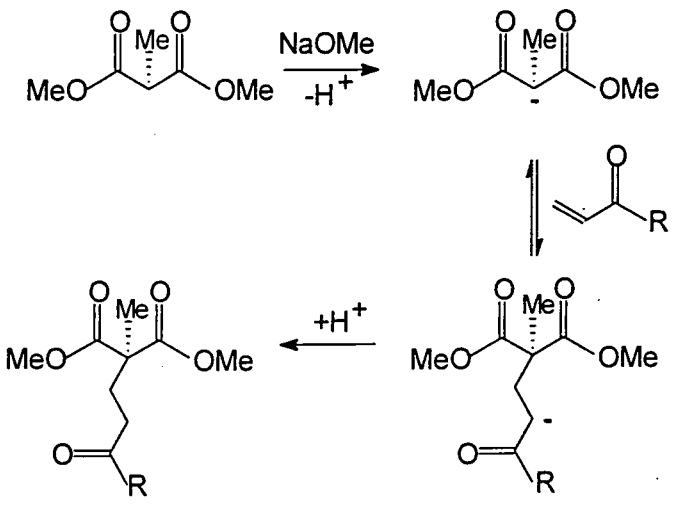

Figure 2.4

Michael additions involving acrolein must be carried out at low temperatures (0-5°C) as elevated temperatures promote retrogression[6] and acrolein polymerisation. As well as low temperatures being favoured, an excess of one of the reactants promotes Michael addition as the balance of equilibrium is shifted towards the products. One possible side reaction which may occur is that of the catalyst competing with the donor to form an adduct as shown below:

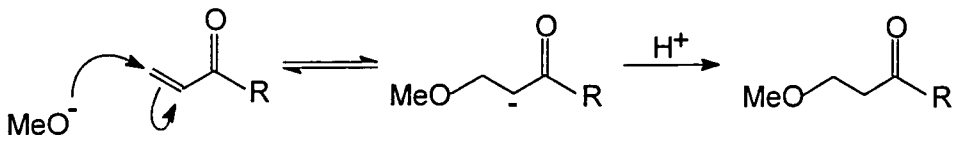

Figure 2.5

It is possible to perform Michael additions in the absence of a solvent,[7] which avoids this undesirable side reaction. The Michael additions presented in the following section proceed as expected without the 1,2 addition product, i.e. nucleophilic addition to the carbonyl, being formed or the alkoxide anions competing with the donor molecule.

2.2.1 Formation of dimethyl methyl-(3'-propionaldehydo)-malonate

Dimethyl methyl-(3'-propionaldehydo)-malonate, Figure 2.4 (R=H), was readily synthesised via the Michael Addition of dimethyl methylmalonate to acrolein.[8] The addition was performed below 5°C, under nitrogen, to prevent retrogression of the addition product to the starting materials. The resulting colourless liquid was acidified and distilled under reduced pressure to yield a slightly impure product. The identity of the impurity has not been established as it was present in low concentration which inhibited attempts to integrate the resolved peaks in the ^{1}H nmr spectrum accurately.

To isolate a pure sample of dimethyl methyl-(3'-propionaldehydo)-malonate, reduced pressure distillation was performed using a Fischer concentric tube fractional distillation apparatus. The impurity has a boiling point very close to that of the desired product, and consequently only 7.86g (15.7%) of pure material was recovered from fractionation of a 50g batch of crude product.

The ^{1}H nmr spectrum of dimethyl methyl-(3'-propionaldehydo)-malonate, Figure 2.6, is deceptively simple. On cursory inspection, the expected singlets due to the CH_3, OCH_3 and CHO protons are seen to be present, as are the triplets due to the methylene protons of the alkyl chain.

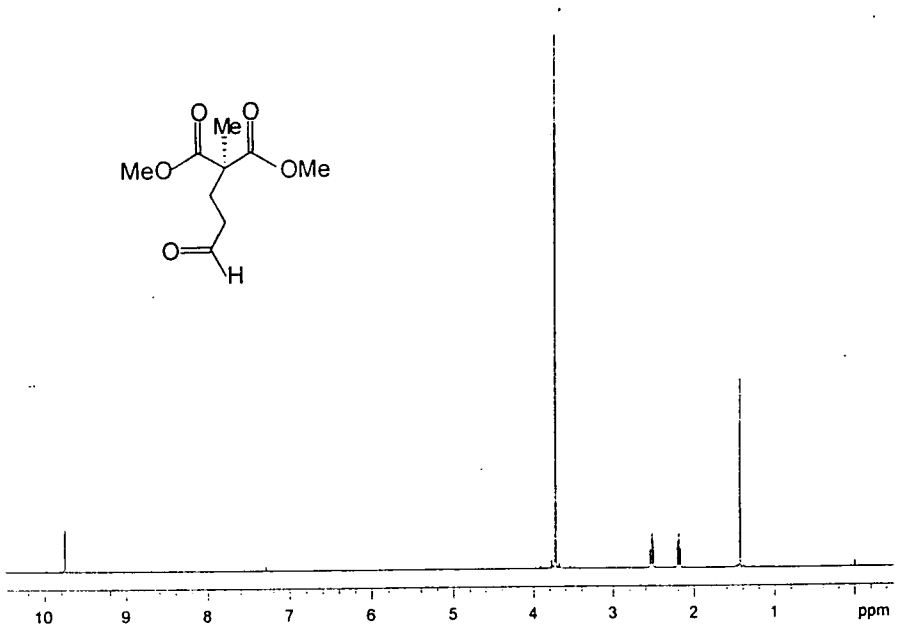

Figure 2.6 ^{1}H nmr spectrum of dimethyl methyl-(3'-propionaldehydo)-malonate

However, on expansion of the spectrum, Figure 2.7, much fine structure can be observed.

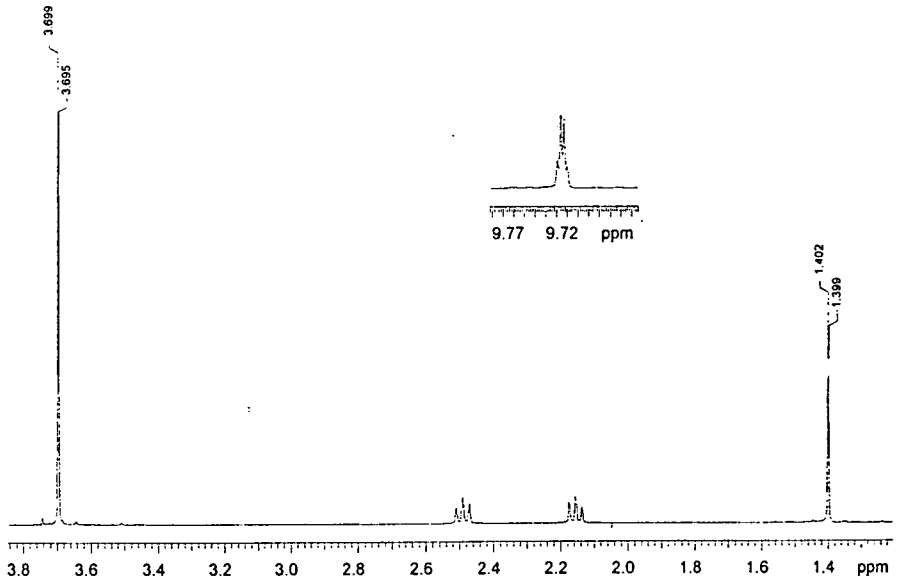

Figure 2.7 Expansion of the ^{1}H nmr spectrum of dimethyl methyl-(3'-propionaldehydo)-malonate

Thus, the aldehyde signal at 9.73ppm is observed to be a quartet, whilst the "singlets" at 1.40 and 3.70ppm (CH_3 and OCH_3) are partially resolved doublets with a coupling constant of 1.2Hz, the same as the coupling constant for the aldehyde proton quartet. This observation has eluded convincing explanation although the author is convinced that the structure assigned to the product is correct since the total spectroscopic characterisation (see 2.6.1) is unambiguous.

As the purification procedure was so time consuming and the impurity could not be identified, this monomer precursor was unsuitable for the large scale synthesis of AB_2 monomers, however reduction of the pure sample was attempted as reported in section 2.3.1.

2.2.2 Formation of dimethyl methyl-(3'-oxobutyl)-malonate

Dimethyl methyl-(3'-oxobutyl)-malonate was readily synthesised via the Michael addition of dimethyl methylmalonate to methyl vinyl ketone.[9] Both the ^{1}H and ^{13}C nmr spectra (Figures 2.8 and 2.9) are straightforward to assign. Three singlets

are observed in the ^{1}H nmr spectrum at 1.42ppm (CH_3), 2.15ppm ($CH_3C=O$) and 3.73ppm (OCH_3) as well as two triplets at 2.14 and 2.50ppm due to the methylene protons in the aliphatic chain. Two singlets at 1.43 and 3.75ppm are observed in low concentrations and it is postulated that these are due to unreacted dimethyl methylmalonate. Again, fine splitting is observed in the expanded spectra which remains unassigned.

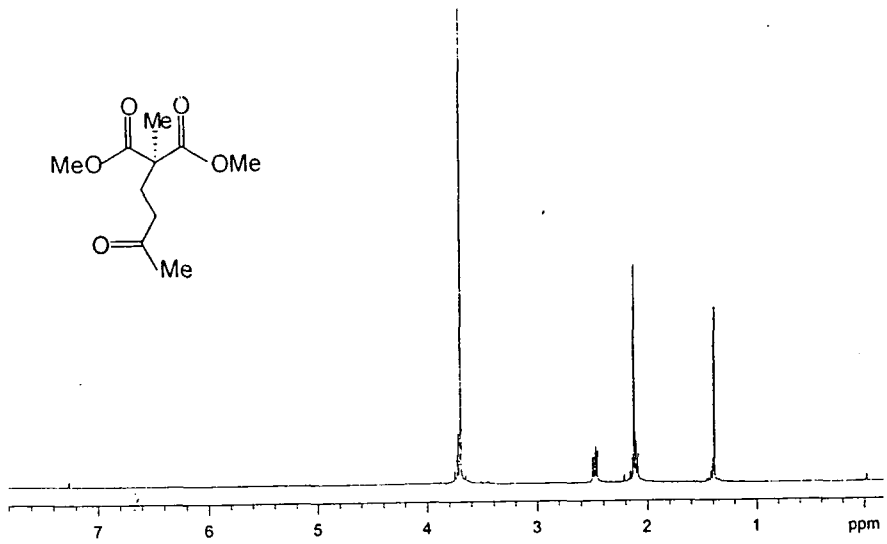

Figure 2.8 ^{1}H nmr spectrum of dimethyl methyl-(3'-oxobutyl)-malonate

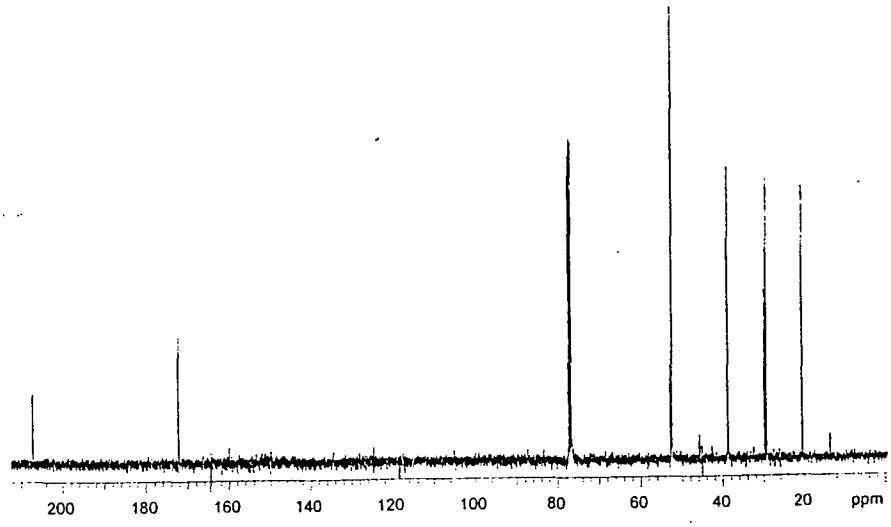

Figure 2.9 ^{13}C nmr spectrum of dimethyl methyl-(3'-oxobutyl)-malonate

Figure 2.9 displays the ^{13}C nmr spectrum of dimethyl methyl-(3'-oxobutyl)-malonate. The CH_3 signals of the product are found at 20.55 and 29.04ppm, whilst the methylene carbon signals of the alkyl chain are observed at 29.88 and 38.82ppm. The methoxy carbon and quaternary carbon signals are found at 52.53 and 52.77ppm respectively. The resonance of the methyl ester carbonyl is found at 172.34ppm, whilst that of the ketonic carbonyl occurs at 207.31ppm. The two resonances at 14ppm and 46ppm are assigned as the CH_3 and CH carbon signals of unreacted dimethyl methylmalonate. As this impurity could not be removed by careful reduced pressure distillation, it was hoped that it could be eliminated during the purification of the product from the next stage in the monomer preparation.

In conclusion, as expected, the Michael additions were successful; but, unfortunately, the products were difficult to purify on a reasonable scale in a reasonable time. It is therefore unlikely that these precursors will find a niche for AB_2 monomer preparations of the future.

2.3 SELECTIVE REDUCTION OF KETONES AND ALDEHYDES IN THE PRESENCE OF ESTERS

The selective reduction of aldehydes and ketones in the presence of other types of carbonyl functional groups has been an area of research interest for many decades. Early methods for the reduction of carbonyls[10] to alcohols were often harsh and gave low yields of the desired product. Chemoselective reductions require that the reaction is sufficiently mild to tolerate other functionalities in the molecule, whilst giving a high yield of the target molecule.

One class of reducing agents capable of chemoselective carbonyl reductions are boron hydrides. The selectivity of the hydride reagent is determined by a number of factors, for example judicious choice of solvent[11,12] in sodium borohydride reductions can either enhance or detract from its reducing capabilities, whereas introduction of substituents[13] to the parent hydride or variation of the cation[14] may be used to control the reducing power of the reagent. The following sections discuss the choice of reducing agents.

2.3.1 Attempted reduction of dimethyl methyl-(3'-propionaldehydo)-malonate

Due to the rigorous purification procedure required to isolate a pure sample of dimethyl methyl-(3'-propionaldehydo)-malonate a highly selective hydride reducing agent was desirable. A survey of the literature[15] revealed a modified borohydride reagent which is capable of reducing aldehydes in the presence of ketones, such selectivity suggested that the reagent, zinc borohydride,[16] would effectively reduce aldehydes without effecting esters. Therefore zinc borohydride was used in an attempt to make dimethyl methyl-(3'-hydroxypropyl)-malonate as outlined in Figure 2.10 below:

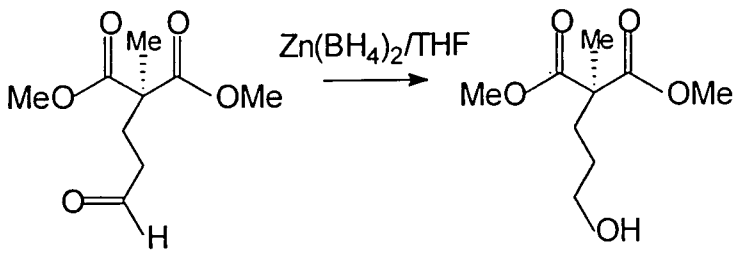

Figure 2.10

Zinc borohydride was generated in situ immediately prior to use by reacting stoichiometric amounts of zinc chloride with sodium borohydride in 1,2-dimethoxyethane at 2°C. The borohydride slurry was filtered under nitrogen into a solution of dimethyl methyl-(3'-propionaldehydo)-malonate in THF at -10°C and the reaction was quenched with water after 30 minutes. To isolate the product, the THF solution was extracted with ether (due to poor THF/water separation) and the organic fraction was collected and washed with brine. On drying and removal of the solvent it was found that only a small portion of the product had been isolated, therefore the aqueous fraction was extracted with dichloromethane. The organic fraction was dried and the solvent removed to give another portion of the organic product. Nmr analysis showed that both products were slightly impure, however as the impurity was not the starting material, it is postulated that side reactions must have occurred during reduction.

On close inspection of the product collected from the ether fraction it was clear that only a small amount of impurity was present. Gas chromatographic analysis (silicone elastomer SE30 capillary column, nitrogen carrier gas from 40 to 270°C at 10°Cmin^{-1}), Appendix 1.10, indicated that the product contained only one minor impurity, therefore reduced pressure distillation was performed in an attempt to purify the compound. Analysis of the distilled product's ^{1}H and ^{13}C nmr spectra (Figures 2.11 and 2.12) showed that the distillation had not only failed to isolate the desired product, but had increased the amount of impurity present in the sample.

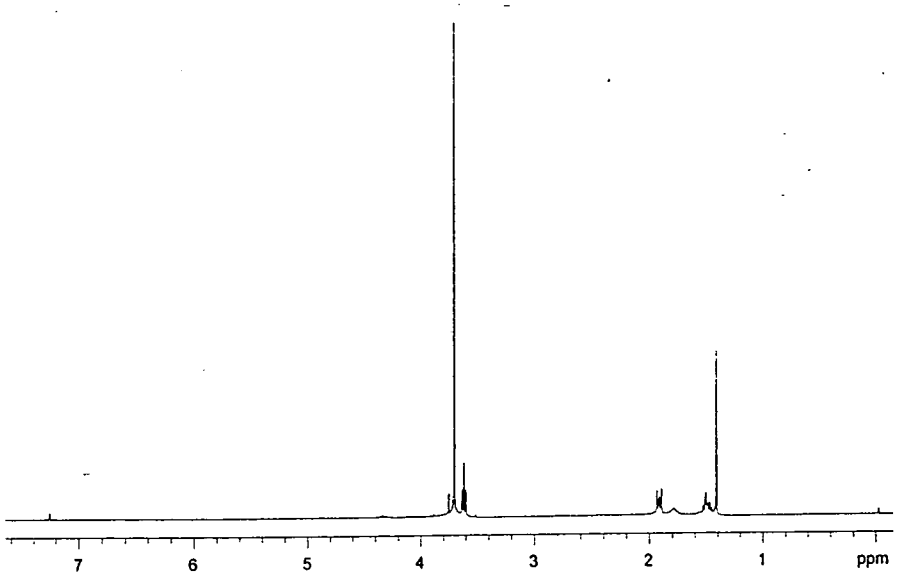

Figure 2.11 ^{1}H nmr spectrum of dimethyl methyl-(3'-hydroxypropyl)-malonate after distillation

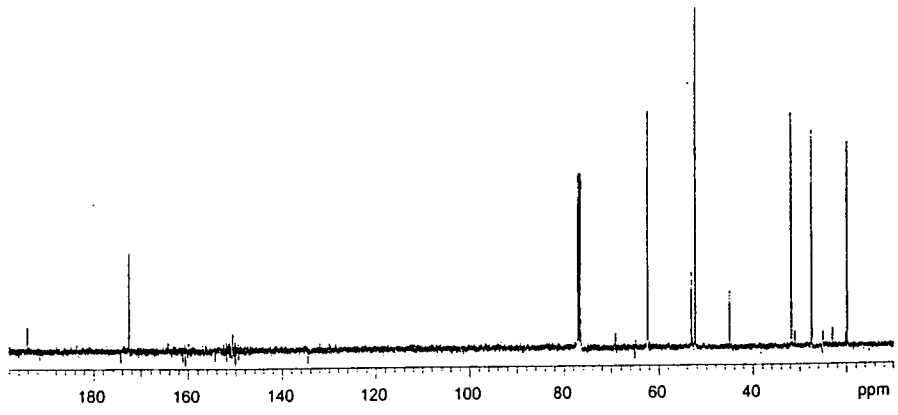

Figure 2.12 ^{13}C nmr spectrum of dimethyl methyl-(3'-hydroxypropyl)-malonate after distillation

Coupled gas chromatography mass spectral analysis was performed in an attempt to identify the impurity. The M+1 ion of the impurity was found at 173amu which corresponds to the cyclic product shown below:

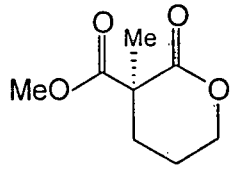

Figure 2.13

The presence of this impurity, in increasing amount following the application of heat during distillation, was verified by the signal at 194.3ppm in the ^{13}C nmr spectrum as lactone carbon carbonyl resonances occur at lower field than acyclic ester carbonyl carbons. The ^{1}H nmr spectrum also indicates the presence of a lactone, a minor multiplet at ~4.4ppm is assigned to the CH_2O in the lactone ring.

A small amount of impurity was also present in the product collected from the dichloromethane fraction. As it had been shown that the monomer cyclised on application of heat, there seemed little point in continuing with rigorous purification procedures as lactonisation would compete with the polymerisation.

In conclusion, purification of dimethyl methyl-(3'-hydroxypropyl)-malonate could not be achieved by simple means, therefore this avenue of investigation was closed.

2.3.2 Attempted reduction of dimethyl methyl-(3'-oxobutyl)-malonate

The reactions discussed in this section involve the selective reduction of a ketone in the presence of esters. Two modified sodium borohydride chemoselective reducing agents were used in an attempt to isolate a pure sample of a diester-alcohol which may be used as a monomer for AB_2 polycondensation reactions.

It has been reported[17] that sodium borohydride adsorbed on alumina ($NaBH_4$-Alox) is an effective reducing agent allowing aldehydes and ketones to be reduced in aprotic solvents, such as ether, to produce primary and secondary alcohols under very mild conditions. The synthesis of $NaBH_4$-Alox was performed by the addition of aqueous $NaBH_4$ to alumina with stirring. The resulting white solid was dried under vacuum and stored without any further precautions. The reduction procedure is very fast when a three-fold excess of $NaBH_4$ to carbonyl ratio is utilised, in practical terms this requires 1g $NaBH_4$-Alox:1mmol carbonyl compound.

The reduction of dimethyl methyl-(3'-oxobutyl)-malonate was attempted using $NaBH_4$-Alox, (see section 2.6.4). The GC trace, Appendix 1.11, of the distilled product, showed that there was at least one contaminant present. The difference in retention volumes between the two species was very small and an attempted separation via reduced pressure distillation was not successful. As the ^1H nmr spectrum of the distilled product was very complicated, an assignment of the impurity structure was not achieved. In light of this, an alternative reducing agent was sought in an attempt to avoid side reactions.

It was decided that the relative rate of the reduction of esters in the presence of aldehydes and ketones is sufficiently slow to attempt reduction using $NaBH_4$. A survey of the literature revealed a mixed solvent system of 1:1 v:v ether:ethanol[18] has been successful in the chemoselective reduction of ketones hence this method was attempted. The reduction of the ketone occurs very quickly, however complete conversion of dimethyl methyl-(3'-oxobutyl)-malonate to dimethyl methyl-(3'-hydroxybutyl)-malonate has proved difficult.

The ^1H nmr spectrum, Figure 2.14, of the product of the attempted reduction of dimethyl methyl-(3'-oxobutyl)-malonate was complicated and gas chromatographic analysis, Appendix 1.12, showed a mixture of components was present in the sample.

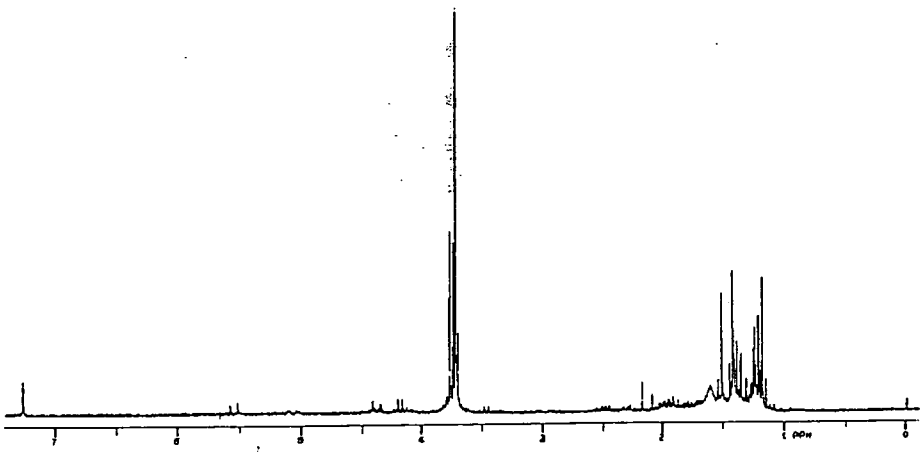

Figure 2.14 ^{1}H nmr spectrum of the attempted reduction dimethyl methyl-(3'-oxobutyl)-malonate

The quartet at 4.2ppm (assigned to C**H**(OH)) indicates that the ketone reduction has been achieved, but the relative integrated intensities of the C**H**(OH) signal to that of the O**CH**$_3$ signal at 3.72ppm shows that the reduction has not gone to completion. As this signal is a series of multiplets, it is clear that the sample consists of several components. Minor resonances at 5.1 and 5.5ppm, possibly indicative of hydrogens on non-conjugated carbon-carbon double bonds, are present which suggests that side reactions, or decomposition, has occurred giving rise to a mixture of products.

As the aldehyde derivative forms lactones on heating after reduction, it is possible that the reduced form of the ketone would also form rings with, in this case, several possibilities of isomeric structures. Therefore it was decided to leave this avenue of investigation.

2.3.3 Reduction of diethyl 3-oxopimelate

Diethyl 3-oxopimelate (Figure 2.15) is a readily available diester-ketone potential monomer precursor. The selective reduction of the ketone should be relatively facile under the correct conditions. It was hoped that the reduction could be performed quickly and easily to provide a simple route into AB_2 monomers. Sodium

borohydride was used in an attempt to achieve 100% chemoselective reduction of the ketone to a secondary alcohol.

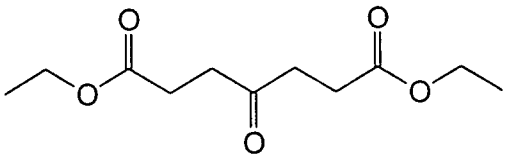

Figure 2.15

Both the ^{1}H and ^{13}C nmr spectra (Figures 2.16 and 2.17) are easy to assign due to the symmetry of the molecule. The ethyl ester signals (OCH_2, 4.12ppm and CH_3, 1.25ppm) in the ^{1}H nmr spectrum will remain unaffected by the reduction of the ketone functionality, it is therefore possible to monitor the success of the reduction by observing the two methylene triplets at 2.60 and 2.78ppm due to CH_2 and $CH_2C{=}O$ respectively. If complete reduction of the ketone takes place the triplet at 2.78ppm should be significantly shifted and changed in the product spectrum.

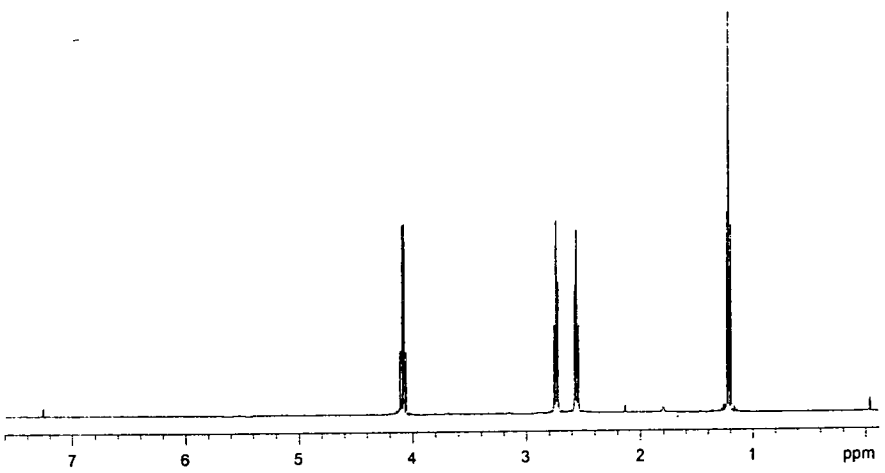

Figure 2.16 ^{1}H nmr spectrum of diethyl 3-oxopimelate

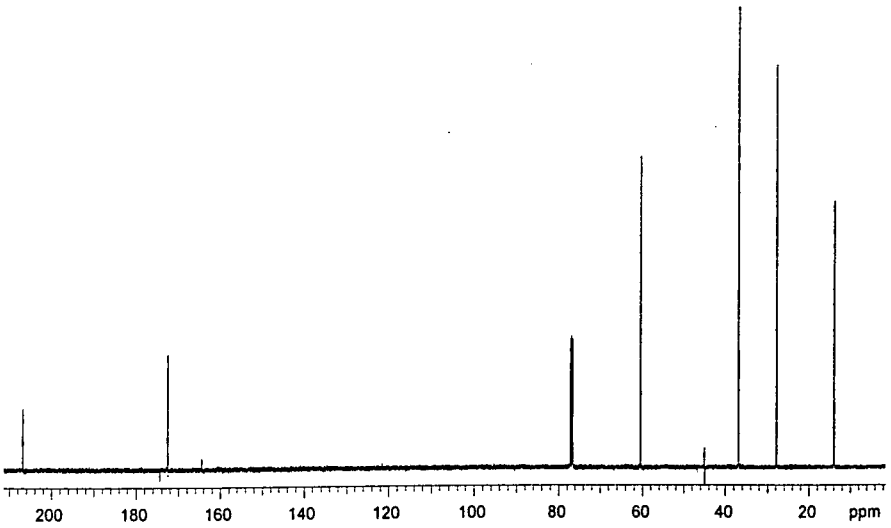

Figure 2.17 ^{13}C nmr spectrum of diethyl 3-oxopimelate

It was anticipated that the ^{13}C nmr spectrum would remain largely unchanged after reduction. The only carbons which would be in a different environment are those which are adjacent, or bound, to the ketone, i.e. those at 36.92ppm ($\mathbf{C}H_2C{=}O$) and 206.89ppm ($\mathbf{C}{=}O$) will be shifted in the product spectrum. The signals due to the ester groups, 14.00ppm ($\mathbf{C}H_3$), 60.47ppm ($O\mathbf{C}H_2$) and 172.52ppm ($\mathbf{C}{=}O$) and the methylene adjacent to the ester groups, 27.81ppm ($\mathbf{C}H_2$) should remain at approximately the same shifts.

To achieve the selective reduction of a ketone in the presence of esters, sodium borohydride in an ether-ethanol solution[18] was used. The reduction was totally successful as verified by only one peak in the gas chromatogram, Appendix 1.13 however the ^{1}H and ^{13}C nmr spectra, Figures 2.18 and 2.19, appear more complicated than expected.

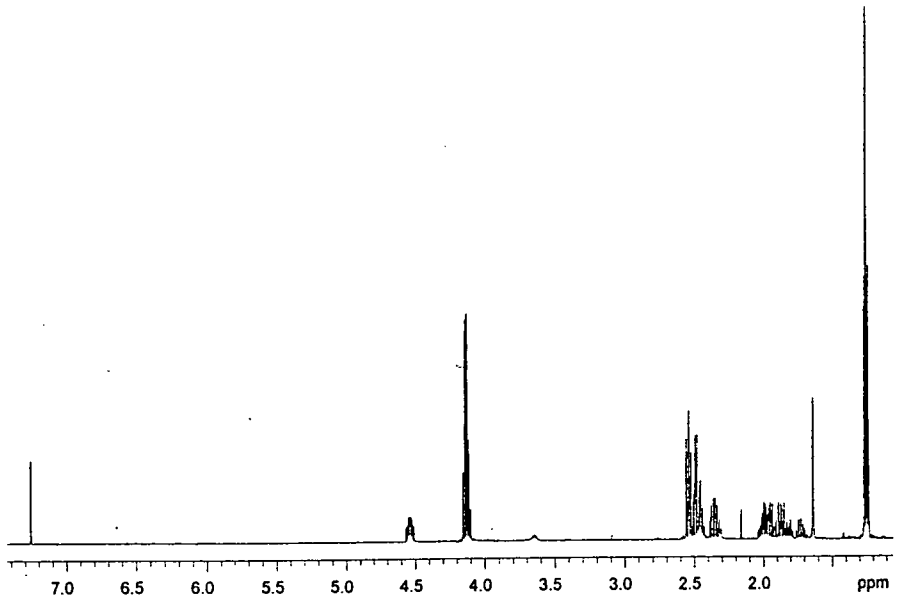

Figure 2.18 ^{1}H nmr spectrum of the product of the reduction of diethyl 3-oxopimelate

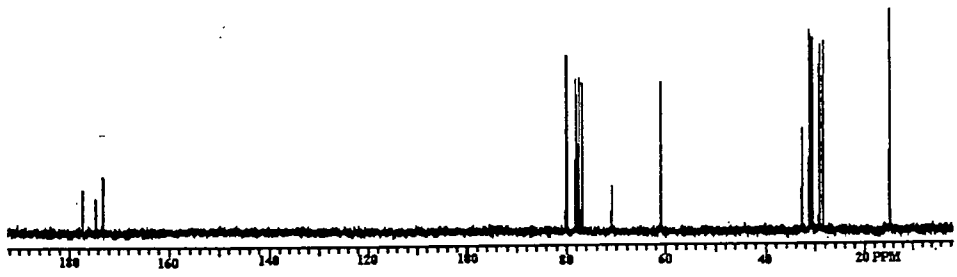

Figure 2.19 ^{13}C nmr spectrum of the product of the reduction of diethyl 3-oxopimelate

On close inspection, it would seem that there is more than one species present as the ethyl ester signals in the ^{1}H nmr spectrum appear as overlapping triplets (CH_3, 1.26ppm) and quartets (OCH_2, 4.13ppm). Two complicated multiplets are also observed at 3.65ppm and 4.55ppm. If the multiplet at low field is due to CH-OH, the relative integrated intensity of the ester OCH_2 signal at 4.13ppm should be four times that of the multiplet, clearly this is not the case. If the multiplet at high field is due to the CH-OH in the product, the relative integrated intensity of the ester OCH_2 signal is too great. Mass spectral analysis of the product was performed and showed a M+1 ion at m/e 187 amu which corresponds to the lactone shown overleaf:

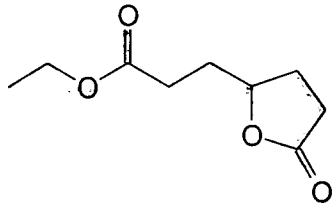

Figure 2.20

It would therefore appear that the lactone forms spontaneously on reduction, and is the only product at elevated temperatures which is why only one signal is observed when gas chromatographic analysis is performed. To verify that the lactone is the major product it is necessary to examine the ^{1}H nmr spectrum in some detail. If the multiplet at 4.55ppm is due to the C**H**-O- of the lactone ring and the multiplet at 3.65ppm is due to the C**H**-OH of the desired product, the integrated intensity of the ethyl ester O**C**$\mathbf{H}_2$ quartet should equal twice the intensity of the C**H**-O multiplet plus four times the intensity of the C**H**-OH multiplet, this is in fact true. The methylene region of the spectrum is very complicated but it is possible to determine the number of hydrogens due to the product and the lactone. The hydrogens due to the methylenes adjacent to C**H**OH in the desired product are observed at 1.64ppm (2H), and within the multiplet at 1.9ppm (2H), whilst the remaining four hydrogens are found in the multiplet at 2.5ppm. The methylene signals of the lactone are observed within the multiplet at 1.9ppm (3H), the sextet at 2.35ppm (1H) and within the multiplet at 2.5ppm (4H).

The ^{13}C nmr spectrum is difficult to assign unambiguously as many of the methylene carbons are in similar environments giving only slight changes in their chemical shifts. The methine carbons are readily distinguishable at 70.97ppm (**C**H-OH) and 80.16ppm (**C**H-O-), as are the carbonyl carbons at 173.14 and 174.56ppm (ethyl ester **C**=O) and 177.32ppm (lactone **C**=O). The FTIR spectrum (Appendix 1.7) confirms the presence of lactone due to the absorption observed at 1777.4cm^{-1} indicative of the carbonyl stretch of a five-membered lactone. It is therefore concluded that diethyl 3-hydroxypimelate is not a suitable monomer for AB_2 polycondensations due to the instantaneous formation of the lactone. It is well

documented[19] that 5-membered substituted lactones do not undergo ring-opening polymerisations, hence this avenue of investigation was not pursued further.

2.4 SELECTIVE REDUCTION OF ETHYL-4-ACETYL-5-OXOHEXANOATE

In an attempt to synthesise a diol-ester which would undergo alcoholysis, a diketo-ester was purchased from Aldrich. Selective reduction of the ketones in the presence of the ethyl ester would give the desired AB_2 monomer.

The ^{1}H and ^{13}C nmr spectra of ethyl-4-acetyl-5-oxohexanoate, Figures 2.21 and 2.22, are complicated due to the effects of keto-enol tautomerism.

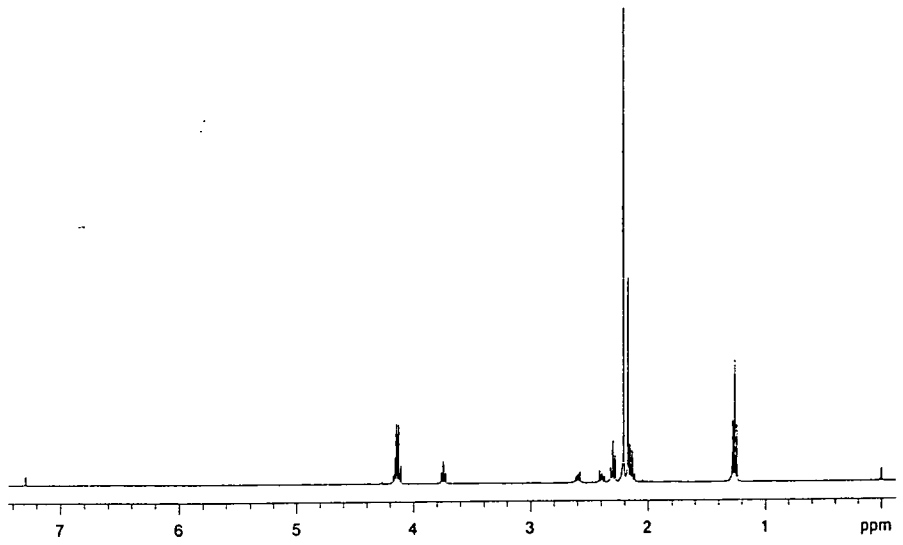

Figure 2.21 ^{1}H nmr spectrum of ethyl-4-acetyl-5-oxohexanoate

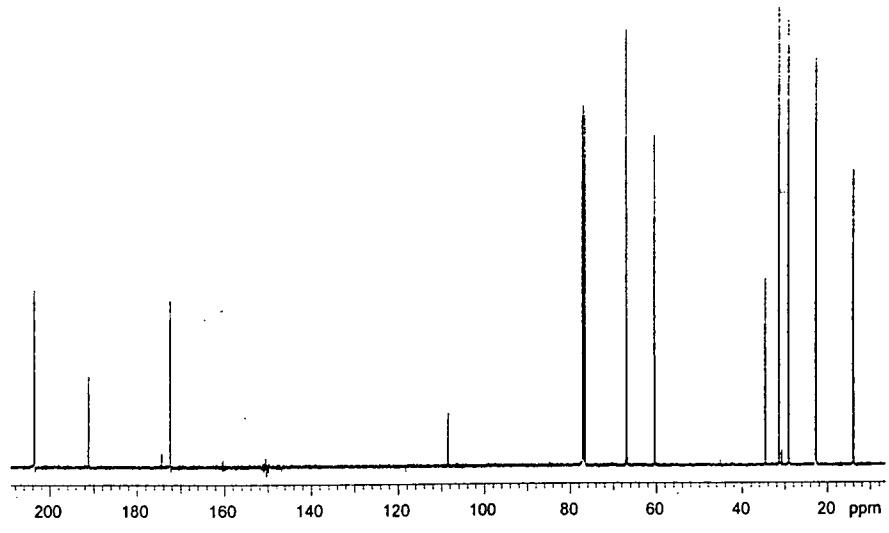

Figure 2.22 ^{13}C nmr spectrum of ethyl-4-acetyl-5-oxohexanoate

Analysis of the nmr spectra is possible by taking into account the tautomerism depicted in Figure 2.23:

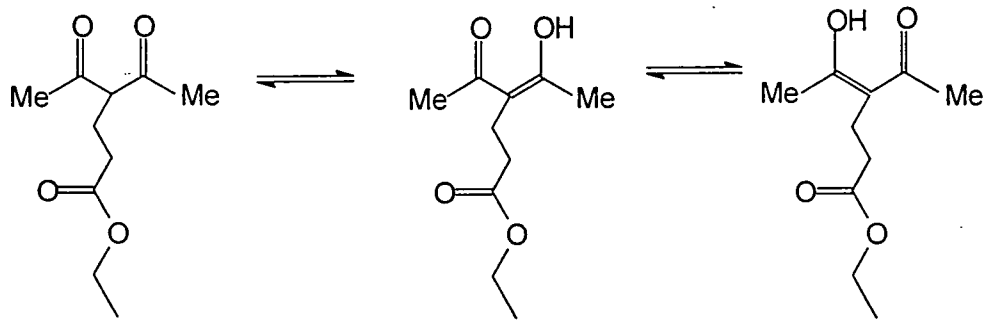

Figure 2.23 Tautomers of ethyl-4-acetyl-5-oxohexanoate

In the ^{1}H nmr spectrum, the ethyl ester signals (CH_3, 1.26 and 1.27ppm and OCH_2, 4.13 and 4.14ppm) are almost coincident. As the triplets of the methylenes in the alkyl chain are well resolved it is possible to determine the amount of enol tautomer present in the starting material. The minor signals at 2.42 and 2.58ppm are due to the methylenes of the enol tautomer, whilst the major triplets, those at 2.15 and 2.30ppm, are assigned to the methylenes of the keto tautomer and have twice the intensity of the methine hydrogen at 3.75ppm. Integration establishes a keto-enol ratio of 2:1.

The ^{13}C nmr spectrum could only be fully assigned after a DEPT (Distortionless Enhancement through Polarisation Transfer) nmr had been performed. The ethyl ester signals at 14.13ppm (CH_3) and 60.59ppm (OCH_2) are coincident for both tautomers whilst the other carbon signals are resolved. The methylene carbons of the keto isomer are observed at 22.81 and 31.54ppm, whilst the methyl signals of the ketone are found at 29.23ppm. The methine signal is observed at 67.06ppm and the carbonyl carbons of the ester and ketone are found at 172.49 and 203.23ppm respectively. The methylene carbons of the enol tautomer are observed at 22.97 and 34.80ppm assigned to the methylene adjacent to the carbon-carbon double bond and the CH_2 bonded to the ester carbonyl respectively. Only one additional methyl signal is observed at 22.86ppm implying that this is due to the methyl attached to the enolic COH carbon. The olefinic carbon of the tautomer is readily observed at 108.66ppm, whilst the conjugated carbonyl carbon is found at 191.26ppm. This phenomenon is also observed for acetylacetone.[20] The presence of tautomers in the starting material is acceptable with respect to the proposed synthesis as the enol form will revert back to the keto tautomer as the reduction is performed hence, in theory, it should be possible to recover 100% of the reduced version of this molecule.

2.4.1 Reduction of ethyl-4-acetyl-5-oxohexanoate using $NaBH_4$

The reduction of ethyl-4-acetyl-5-oxohexanoate can be monitored by measuring the disappearance of the methyl singlet at 2.21ppm in the ^1H nmr spectrum. As the ketone functionality is reduced, the integrated intensity of the methyl signal will diminish and be replaced by a more complicated multiplet at a different shift. In an attempt to promote the selective reduction of this diketo-ester, sodium borohydride in a mixed solvent system[18] was utilised.

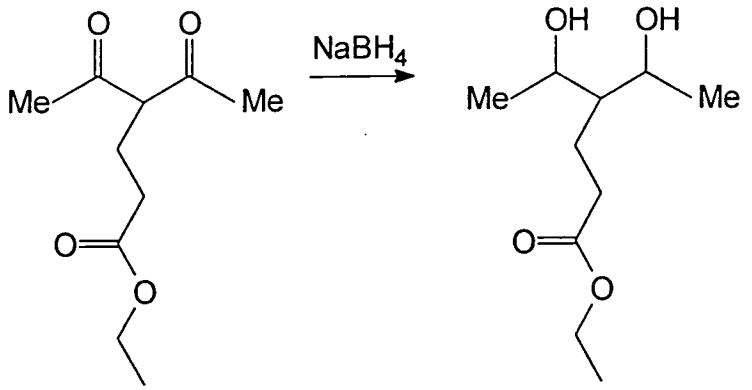

Figure 2.24 Representation of the reduction of ethyl-4-acetyl-5-oxohexanoate

The ^{1}H and ^{13}C nmr spectra, Figures 2.25 and 2.26, of the crude product are encouraging as the singlet at 2.21ppm in the ^{1}H nmr spectrum is present in a very small amount, hence by using prolonged reaction times this method should work.

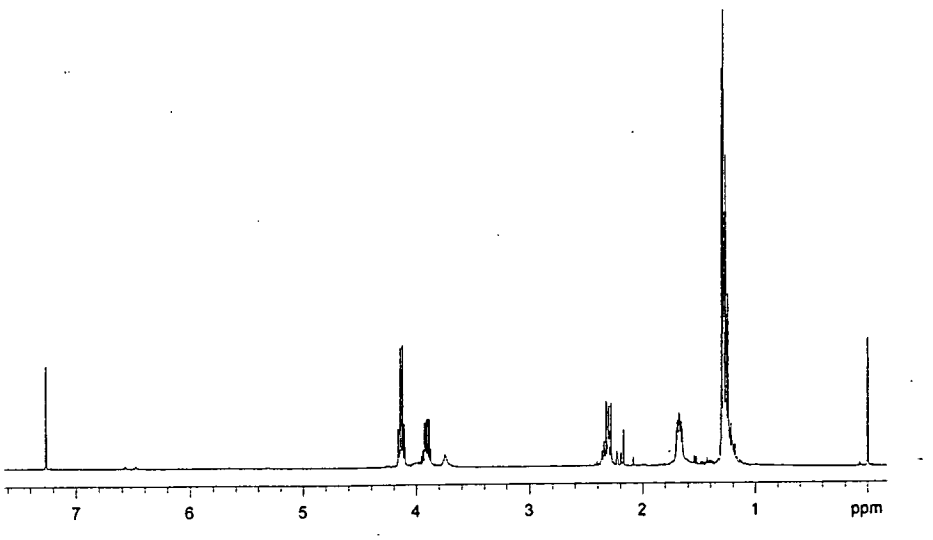

Figure 2.25 ^{1}H nmr of the attempted reduction of ethyl-4-acetyl-5-oxohexanoate

The spectrum above indicates that the reaction has been only partially successful. The integrated intensities and shifts of the main signals in the spectrum imply that the majority of the product is the diol-ester, however as there are several minor resonances which remain unexplained it proved impossible to fully assign the spectrum.

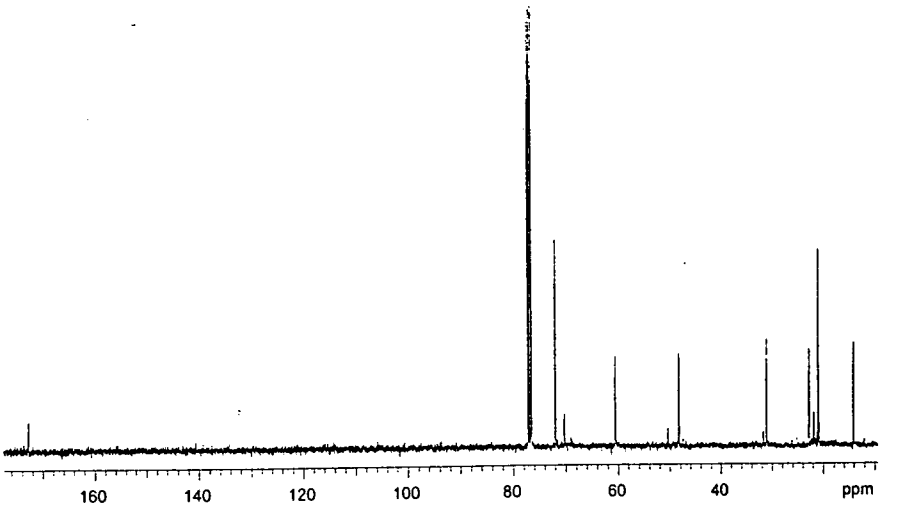

Figure 2.26 ^{13}C nmr of the attempted reduction of ethyl-4-acetyl-5-oxohexanoate

The ^{13}C nmr spectrum may be tentatively assigned using the signals of the starting material as a guide. The carbons of the ester (OCH_2, CH_3 and carbonyl) and the methylene adjacent to the ester carbonyl have the same chemical shift as in the starting material as expected. Several new resonances are found at 22.90ppm (assigned to the $CHCH_3$), 48.31ppm (assigned to the $CHCH_2$) and 72.06ppm assigned to the CHOH carbons of the product. The minor resonances are unassigned and are assumed to be due to a side product.

One disappointing aspect to this reaction is the low yield of the recovered crude product. Previously the yields for this reaction for other monomer precursors had been approximately 50%, however in this case the yield was only 12.2%. Due to the low yield, the route was not pursued any further.

2.5 CONCLUSIONS

In view of the rigorous purifications procedures necessary to provide pure samples for AB_2 polycondensation reactions, the techniques applied in the selective reduction of aldehydes and ketones in the presence of esters are not viable. A more useful approach would be to attempt to synthesise solid AB_2 monomers which may be purified by recrystallisation.

In the event these synthetic attempts ended in failure to obtain materials of satisfactory purity. Fortunately, as will be described subsequently a suitable monomer became commercially available (see chapter 4).

2.6 EXPERIMENTAL

All organic reagents were purchased from Aldrich Chemical Co. and used without further purification. FTIR spectra were recorded on a Perkin-Elmer 1600 series FTIR. ^{1}H and ^{13}C nmr spectra were recorded on a Varian 400MHz, 200MHz or a Bruker 500MHz spectrometer as indicated and were referenced to internal Me_4Si.

2.6.1 Preparation of dimethyl methyl-(3'-propionaldehydo)-malonate

Dimethyl methylmalonate (60g, 420 mmol) was added to a solution of sodium (0.04g, 1.74 mmol) in absolute methanol (240ml) in a two necked flask equipped with a dropping funnel with nitrogen inlet and a nitrogen outlet. The solution was cooled to 0°C using an ice bath and acrolein (24.16g, 420 mmol) was added dropwise. The reaction temperature was maintained at approximately 2°C. After the addition was complete, the reaction mixture was stirred for 4 hours and neutralised by careful addition of acetic acid. The solvent was removed using a rotary evaporator at water pump pressure and the resulting liquid was mixed with toluene (160ml) and extracted with 3 portions of water. The cloudy organic solution was dried over anhydrous magnesium sulphate and the solvent removed using a rotary evaporator at water pump pressure to give a colourless liquid. Reduced pressure distillation (10cm Vigreux column) gave four fractions: (i) solvent, identified by its boiling range (br 22-28°C, 4 mmHg), (ii) mixture of starting materials (br 58-100°C, 4 mmHg), (iii) impure product identified by its ^{1}H nmr spectrum (br 94-118°C, 5 mmHg) 15.40g, 18.16% and (iv) slightly impure product identified by its ^{1}H nmr spectrum (br 114-122°C, 4 mmHg) 34.71g, 40.9%.

Fractions (iii) and (iv) were combined and distilled under reduced pressure using a Fischer concentric tube fractional distillation column. In total 6 fractions were collected, only fraction 4, methyl-(3'-propionaldehydo)-malonate, proved to be pure by nmr analysis:^{1}H nmr ($CDCl_3$, 400 MHz) δ 1.44 (d, J=1.2Hz, 3H, CH_3), 2.19 (t, J=7.8Hz, 2H, CH_2C), 2.53 (t, J=7.8Hz, 2H, CH_2CHO), 3.73 (d, J=1.2Hz, 6H, CH_3O),

9.76 (q, *J*=1.2Hz, 1H, **CH**O). ^{13}C nmr ($CDCl_3$, 100 MHz) δ 20.43 (CH_3), 27.86 (CH_2), 39.32 (CH_2), 52.58 (CH_3O), 52.70 (CCH_2), 172.1 (**C**=O), 200.7 (CHO). FTIR, ν_{max}/cm^{-1}: 2995.7, 2954.9, 2843.5, 2729.6, 1733.6, 1435.1. MS M+1 ion = 203 determined by EI mass spectrometry.

2.6.2 Preparation of dimethyl methyl-(3'-oxobutyl)-malonate

Dimethyl methylmalonate (36.5g, 256 mmol) was added to a solution of sodium (0.862g, 38 mmol) in absolute methanol (38ml) in a two necked flask equipped with a dropping funnel with nitrogen inlet and a nitrogen outlet. The solution was cooled to -10°C using an acetone/solid CO_2 bath and a solution of dimethyl methylmalonate (34.05g, 239 mmol) and methyl vinyl ketone (21.8g, 311 mmol) in methanol (38ml) was added dropwise. The solution was stirred at room temperature for 7.5 hours and then neutralised with 6% aqueous acetic acid. The solution was extracted with ether and the organic fraction collected and the solvent removed on a rotary evaporator at water pump pressure. Reduced pressure distillation was performed twice to give three fractions: (i) dimethyl methylmalonate (bp 30°C, 1mmHg), (ii) a mixture of starting materials and product (br 54-84°C, 1mmHg) and (iii) slightly impure dimethyl methyl-(3'-oxobutyl)-malonate (46.17g, 68.7%) as a colourless liquid (br 85-98°C, 1mmHg). The product, dimethyl methyl-(3'-oxobutyl)-malonate, was characterised by ^1H nmr ($CDCl_3$, 400 MHz) δ 1.42 (s, 3H, C*H*$_3$), 2.13 (t, J=7.8Hz, 2H, C*H*$_2$), 2.15 (s, 3H, ketone C*H*$_3$), 2.50 (t, J=7.8Hz, 2H, **CH**$_2$), 3.73 (s, 6H, O**CH**$_3$), ^{13}C nmr ($CDCl_3$, 100 MHz) δ 20.55 (**CH**$_3$), 29.40 (ketone **CH**$_3$), 29.88 (**CH**$_2$), 38.82 (**CH**$_2$), 52.53 (O**CH**$_3$), 52.77 (quaternary **C**), 172.34 (O-**C**=O), 207.31 (Me-**C**=O).

FTIR, ν_{max}/cm^{-1}:2997.5, 2954.2, 2845.7, 1732.1.

(Found: C 54.9; H 7.14. $C_{10}H_{16}O_5$ requires C 55.6; H 7.40)

2.6.3 Preparation of dimethyl methyl-(3'-hydroxybutyl)-malonate.

Dimethyl methyl-(3'-propionaldehydo)-malonate (16.71g, 83 mmol) was stirred with zinc borohydride (7.89g, 83 mmol) in 40ml THF at -10°C for fifteen minutes. The reaction was quenched by careful dropwise addition of water (monitored by observing the liberation of hydrogen). The THF layer was separated and the aqueous layer extracted using ether. The combined THF and ether extract was washed with brine and dried ($MgSO_4$) and the solvent removed on a rotary evaporator at water pump pressure. The aqueous layer was washed with dichloromethane and the organic fraction collected, dried ($MgSO_4$) and the solvent removed on a rotary evaporator at water pump pressure. Both fractions were analysed to show slightly impure products, therefore reduced pressure distillation was performed to give one fraction (br 96-102°C, 1mmHg, 14.92g, 87.7%). The product was characterised by ^1H nmr ($CDCl_3$, 400 MHz) δ 1.44 (s, 3H, CH_3), 1.52 (m, 2H, CH_2) 1.94 (m, 2H, CH_2), 3.65 (t, J=6.4Hz, 2H, CH_2OH), 3.73 (s, 3H, CH_3O), 3.78 (d, J=0.8Hz, 0.15H, CH_3O) 4.35 (m, 0.1H, CH_2O). ^{13}C nmr ($CDCl_3$, 100 MHz) δ 20.03 (CH_3), 23.5 (lactone CH_3), 25.8 (lactone CH_2), 27.61 (CH_2), 30.9 (lactone CH_2), 31.97 (CH_2), 52.50 (CH_3O), 53.35 (CCH_2), 62.58 (CH_2OH), 69.5 (lactone CH_2O), 172.7 (C=O), 194.33 (lactone C=O). IR, ν_{max}/cm^{-1}: 3439.0, 2954.2, 2876.3, 1732.4.
(Found: C 53.14; H 8.18. $C_9H_{16}O_5$ requires C 52.9; H 7.80)

2.6.4 $NaBH_4$-Alox reduction of dimethyl methyl-(3'-oxobutyl)-malonate

A solution of dimethyl methyl-(3'-oxobutyl)-malonate (0.864g, 4 mmol) in ether (12ml) was added to a slurry of $NaBH_4$-Alox (4g) in ether (12ml) under an atmosphere of nitrogen. The mixture was stirred at room temperature for 20 minutes. The solid was removed by filtration and the residue washed copiously with ether to recover residual product. The filtrate was collected and the solvent removed on a rotary evaporator at water pump pressure. Any residual solvent was removed on the vacuum line. Reduced pressure distillation gave one fraction at 135°C, 0.3 torr which was found to be a mixture of three components by GC analysis. Separation of the

2.14 (s, 2.4H, CH_3), 2.50 (t, J=8.2Hz, 1.6H, CH_2), 3.71 (s, 5.9H, OCH_3), 3.77 (s, 0.4H).

2.6.5 Sodium borohydride reduction of dimethyl methyl-(3'-oxobutyl)-malonate

Sodium borohydride (0.3g, 8 mmol) in water (1.5ml) was added slowly to a cooled solution of dimethyl methyl-3-oxobutyl-malonate (3.46, 16 mmol) in 50ml 1:1 mixture of ether:ethanol. The solution was stirred for 1 hour at 5°C, on stirring a white precipitate formed. The reaction was quenched with aqueous acetic acid, diluted with water (15ml), extracted with ether, washed with aqueous sodium bicarbonate and then water. Reduced pressure distillation was performed to give one fraction at 140°C, 0.1 torr which was a mixture of starting material and product, separation could not be achieved. The mixture was characterised via ^1H nmr ($CDCl_3$, 200 MHz) δ 1.18 (m, 7.75H), 1.42 (m, 8.5H), 1.51 (s, 2.5H), 1.90 (m, 3.25H), 3.72 (s, 5.25H), 3.74 (s, 1.5H), 3.77 (s, 2.75H), 4.20 (q, 1H).

2.6.6 Reduction of diethyl 4-oxopimelate with sodium borohydride

Sodium borohydride (0.15g, 4 mmol) in water (0.75ml) was added slowly to a cooled solution of diethyl 4-oxopimelate (1.84g, 8 mmol) in 25ml 1:1 mixture of ether:ethanol. The solution was stirred for 30 minutes at 5°C, during which time a white precipitate formed from the yellow solution. The reaction was quenched with aqueous acetic acid (10 drops), diluted with water (7.5ml), extracted with ether, washed with aqueous sodium bicarbonate and then water. Reduced pressure distillation gave one fraction: 0.1 torr, 140°C, 0.72g which was found to be a mixture of the lactone and the desired product. Characterisation was performed by ^1H nmr $CDCl_3$, 500 MHz) δ 1.25 (t, J=7.5Hz, 6H, product CH_3), 1.26 (t, J=7.5Hz, 3H, lactone CH_3), 1.64 (p, J=7.5Hz, 2H, product CH_2), 1.9 (m, 3H, lactone CH_2 + 2H, product CH_2), 2.35 (s, J=7.5Hz, 2H, lactone CH_2), 2.50 (m, 4H, product CH_2 + 4H lactone CH_2), 3.65 (m, 1H, product CH), 4.12 (q, J=7.5Hz, 4H, product OCH_2), 4.13 (q, J=7.5Hz, 4H, product OCH_2), 4.55 (m, 1H, lactone CH). ^{13}C nmr ($CDCl_3$, 50 MHz) δ

CH_2), 2.35 (s, J=7.5Hz, 2H, lactone CH_2), 2.50 (m, 4H, product CH_2 + 4H lactone CH_2), 3.65 (m, 1H, product CH), 4.12 (q, J=7.5Hz, 4H, product OCH_2), 4.13 (q, J=7.5Hz, 4H, product OCH_2), 4.55 (m, 1H, lactone CH). ^{13}C nmr ($CDCl_3$, 50 MHz) δ 14.67 (CH_3), 28.36 (CH_2), 29.18 (CH_2), 30.65 (CH_2), 31.18 (CH_2), 31.23 (CH_2), 32.73 (CH_2), 60.98 (CH_2), 61.12 (CH_2), 70.97 (CH_2), 80.17 (CH_2), 173.14 (product C=O), 174.56 (lactone ester C=O), 177.32 (lactone C=O).

2.6.7 Reduction of ethyl 4-acetyl-5-oxohexanoate with $NaBH_4$

Sodium borohydride (0.3g, 7.93 mmol) in water (1.5ml) was added slowly to a cooled solution of ethyl 4-acetyl-5-oxohexanoate (1.6g, 8 mmol) in 25ml 1:1 mixture of ether:ethanol. The solution was stirred for 3 hours at 5°C, during which time the solution turned yellow. The reaction was quenched with aqueous acetic acid (10 drops), diluted with water (15ml), extracted with ether, washed with aqueous sodium bicarbonate and then water. The crude product was collected (0.2g, 12.3%). Reduced pressure distillation was not attempted due to the small amount of recovered material.

2.7 REFERENCES

1. J. Michael, *J. Prakt. Chem.*, [2], **35**, (1887), 349.
2. O.A. Moe and D.T.Warner, *J. Am. Chem. Soc.*, **70**, (1948), 2763.
3. M. Yamaguchi, N. Yokota and T. Minami, *J. Chem. Soc. Chem. Commun.*, (1991), 1088.
4. G.V. Kryshtal, V.V. Kulganek, V.F. Kucherov and L.A. Yanovskaya, *Synthesis*, (1979), 107.
5. A. Kamimura, H. Sasatani, T. Hashimoto, T. Kawai, K. Hori and N. Ono, *J. Org. Chem.*, **55**, (1990), 2437.
6. Dorrow and Boberg, *Ann.*, **578**, (1952), 101.
7. C.F. Koelsch, *J. Am. Chem. Soc.*, **65**, (1943), 437.
8. D.T. Warner and O.A. Moe, *J. Am. Chem. Soc.*, **70**, (1948), 3470.
9. T.A. Spencer, M.D. Newton and S.W. Baldwin, *J. Org. Chem.*, **29**, (1964), 787.
10. A.J. Hill, E.H Nason, *J. Am. Chem. Soc.*, **46**, (1924), 2236; F.C. Whitmore and T. Otterbacker, *Org. Synth. Coll. 2*, (1943), 317; W. Ponndorf, *Z. Angew. Chem.*, **39**, (1926), 138; S.O. Ford and C.S. Marvel, *Org. Synth. Coll. 2*, (1943), 372.
11. H.C. Brown, E.J. Mead and B.C. Subba Rao, *J. Am. Chem. Soc.*, **77**, (1955), 6204.
12. H.C. Brown and P.A. Tierney, *J. Am. Chem. Soc.*, **80**, (1958), 1552.
13. R.O. Hutchins, D. Kandasamy, C.A. Maryanoff, D. Masilamani and B.E. Maryanoff, *J. Org. Chem.*, **42**, (1977), 82.
14. R.F. Nystrom, S.W. Chaikin and W.G. Brown, *J. Am. Chem. Soc.*, **71**, (1949), 3245.
15. B.C. Ranu and R. Chakraborty, *Tet. Letters*, **31**, (1990), 7663.
16. P. Crabbe, G.A. Garcia and C.J. Rius, *J. Chem. Soc. Perkin Trans. 1*, (1973), 810.
17. E. Santaniello, F. Ponti and A. Manozocchi, *Syn.*, (1978), 891.
18. H. Nozaki, K. Kondo and O. Nakanisi, *Tet.*, **19**, (1963), 1617.

19. "Enclyclopedia of Polymer Science and Engineering", Eds. Mark, Bikales, Overberger, Menges, 2nd Edition, Volume 12, Pages 36-42.

20. "Carbon-13 nmr Spectroscopy", H-O Kalinowski, S. Berger and S. Braun, John Wiley and Sons Ltd., (1988).

Chapter 3.

Physical Techniques for the Characterisation of Hyperbranched Polymers

3.1 INTRODUCTION

The characterisation of polymers, both linear and highly branched, is of utmost importance to both academia and industry. If full characterisation, including determination of molecular weight, degree of branching, glass transition temperature and viscosity, could be achieved it might be possible to construct detailed structure/property correlations. Such an understanding could be the basis for "fine tuning" polymer syntheses to tailor make polymers for specific applications. Current characterisation techniques for linear polymers are well established and many methods are available for molecular weight determination, unfortunately this statement cannot be applied to hyperbranched polymers.

The characterisation of hyperbranched macromolecules may be regarded as being in its infancy. Several techniques have been attempted for molecular weight determination, however only two can be regarded as reasonably reliable as neither of these depend on linear polymers as calibration standards. Light scattering[1] has been shown to be a viable technique for molecular weight determination of dendrimers, and it seems reasonable to expect that it will also be applicable to hyperbranched polymers. Matrix assisted laser desorption-ionisation mass spectrometry (MALDI-MS)[2] may also be used as a method to determine the number average molecular weight of hyperbranched polymers.

Structural information may be determined via spectroscopy. Nuclear magnetic resonance spectroscopy (nmr) generally provides the most detailed structural information and, in favourable cases can give branching ratio data and other structural information. It is now routine to utilise both ^{1}H and ^{13}C nmr spectroscopy to characterise hyperbranched polymers. Of all the other spectroscopies, MALDI-MS, in favourable cases, provides sufficient information for unambiguous assignment of the structures present in the molecular weight distribution of the polymer sample. Even in this case, the data is usually least ambiguous for the low molecular weight oligomers of the distribution. The following sections discuss the variety of methods available for the structure and molecular weight determination of hyperbranched polymers and their individual merits.

3.2 MOLECULAR WEIGHT DETERMINATION

3.2.1 Gel Permeation Chromatography

As gel permeation chromatography (GPC) is a method which separates polymers according to their hydrodynamic volumes, it is necessary to understand the physical processes occurring during the acquisition of the molecular weight data. The columns employed in GPC consist of highly cross-linked gels which contain a distribution of pores of differing sizes, hence separation is determined by the size exclusion of the coils of the individual molecules. The polymer solution is injected onto the column and is transported by the solvent through the pores of the column. The higher the molecular weight of the polymer molecule, the larger its hydrodynamic volume. Therefore, high molecular weight species pass through the column faster than their smaller analogues as they will be able to permeate only into the largest pores which will be infrequent in the distribution. Large polymer molecules therefore have a much shorter and less tortuous pathway through the column than shorter polymer chains and hence emerge first. Polymer molecules which are too large to enter any of the pores are said to be above the exclusion limit of the column.

The molecular weight of the polymer may be determined using a calibration procedure. Calibration requires that a relationship between the retention volume and the molecular weight is established. Retention volume is related to hydrodynamic volume which is a measure of the size of the polymer coil in solution which, in turn, is dependant on both the solvent and temperature. A universal calibration curve is constructed, using linear standards of known narrow molecular weight distribution, which consists of a plot of $\log[\eta]M$ *vs* retention volume. To apply the calibration to a polymer of unknown molecular weight, a graph of weight fraction *vs* elution volume is created. It is therefore possible to extract a value of $[\eta]M$ using the universal calibration curve for a known retention volume. The intrinsic viscosity can be readily determined hence providing a molecular weight for the sample.

As the polymer molecules are separated on the basis of their hydrodynamic volume and it is probable that highly branched molecules will have a significantly different hydrodynamic volume than their linear analogues, it therefore seems unlikely

that an analysis calibrated on the basis of linear polymers will be reliable for hyperbranched polymers. Fréchet[3] has shown that, for hyperbranched aromatic polyethers, the determination of the weight average molecular weight (M_w) using low angle laser light scattering (LALLS) consistently yields values that are 3-5 times higher than those determined by GPC calibrated using linear polystyrene standards, supporting the hypothesis that the hydrodynamic volume is smaller for highly branched systems than for their linear analogues. Only one account describing the use of dendrimers as calibration standards for GPC has been reported[4] in the literature thus far. The dendrimers in question were designed for use in aqueous GPC (i.e. they are water soluble) and there have been no further reports of their success or failure as calibrants for other highly branched polymers.

It is reasonable to assume that the large number of end groups present in hyperbranched polymers play a major role in the properties of the polymer. Polar end groups may interact with the stationary phase of the GPC columns or the polar column surfaces giving erroneous results as is also seen with linear polymer samples, e.g. poly(acrylic acid).[5] If this is the case, the resulting weight average molecular weight computed for the hyperbranched polymers will be lower than expected since strong sample/column interactions will result in longer retention times.

It is clear that GPC may not be as reliable an indication of molecular weight for highly branched systems as for linear polymers when calibrated using linear standards. Calibration using dendrimers as the standards would, perhaps, give a more realistic view of the molecular weight distribution of hyperbranched polymers. However, as yet, this has not been proved so GPC molecular weight averages must always be quoted along with information on the calibration procedure and the results have to be treated with a measure of scepticism. Comparisons within a series of hyperbranched polymers having similar structural features certainly give reliable indications of the relative molecular weights but absolute values are uncertain. Since it seems likely that the hydrodynamic volume of a hyperbranched polymer will be a complex function of structure, degree of branching, solvent and temperature, it is clear that the results of using this technique will always be difficult to interpret in any absolute sense but may well be useful as qualitative "quality control" measures.

3.2.2 Matrix Assisted Laser Desorption-Ionisation Time of Flight Mass Spectrometry.

The underlying principles of matrix assisted laser desorption-ionisation time of flight mass spectrometry (MALDI-TOF MS) are, in essence, the same as for any other mass spectrometric technique. The sample to be analysed, the analyte, is placed in a low pressure environment where it is ionised into positive or negative ions. The ions are then accelerated towards a detector and the mass of the individual ions arriving at the detector is calculated. MALDI-TOF MS however, is a relatively new technique which utilises soft ionisation; this implies that fragmentation of the analyte does not occur, allowing intact desorbed species to be detected. In MALDI-TOF MS the analyte is uniformly mixed with a matrix which is UV active, i.e. has a large extinction coefficient at the irradiation wavelength. A pulse of laser light (3ns from a nitrogen laser of wavelength 337nm) is directed onto the sample area (typically 100μm in diameter) by condensing the laser light with an optical lens. This causes the matrix to be vapourised and the charged species in the gas phase are detected as either proton, cation or matrix ion adducts. The role of the matrix is to allow the desorption of analyte molecules without fragmentation. This occurs as the matrix absorbs more energy than the analyte encouraging ionisation of the UV active molecules. An excess of matrix is used to allow analyte particles to be surrounded by the matrix thus assisting facile analyte desorption.

The charged particles generated by MALDI-TOF MS are capable of free movement, hence they are drawn towards the detector by the potential difference, V_0, between the sample and the grid, see Figure 3.1. As the law of conservation of energy must be observed, the velocity of the ions may be determined by the following equations:-

$$zV_0 = \frac{mv^2}{2} \qquad \text{(Eq. 3.1)}$$

$$v = \sqrt{\frac{2zV_0}{m}} \qquad \text{(Eq. 3.2)}$$

where z is the charge on the ion, v is the velocity of the ion, m is the mass of the ion and V_0 is the potential difference between the sample and the grid.

The time the ions take to reach the detector may be determined by:-

$$t = \frac{L}{v} = L\sqrt{\frac{m}{2zV_0}} \qquad \text{(Eq. 3.3)}$$

where L is the distance between the grid and the detector. Rearranging equation 3.3 gives:-

$$\frac{m}{z} = \frac{2V_0 t^2}{L^2} \qquad \text{(Eq. 3.4)}$$

For one spectrometer, the potential difference and L will be constant, hence the shorter the flight time, the smaller the mass/charge ratio (as illustrated by equation 3.4). Therefore it can be seen that the circuitry required to measure the time differences between individual ions arriving at the detector must be very accurate. For example, for a device which has V_0=20kV and L=0.7m, a mass difference of 1amu would require a time resolution of ≤ 5.7ns.

There are currently two TOF modes available in MALDI-MS. Figure 3.1 below shows a schematic diagram of the instrument set-up available to the author.

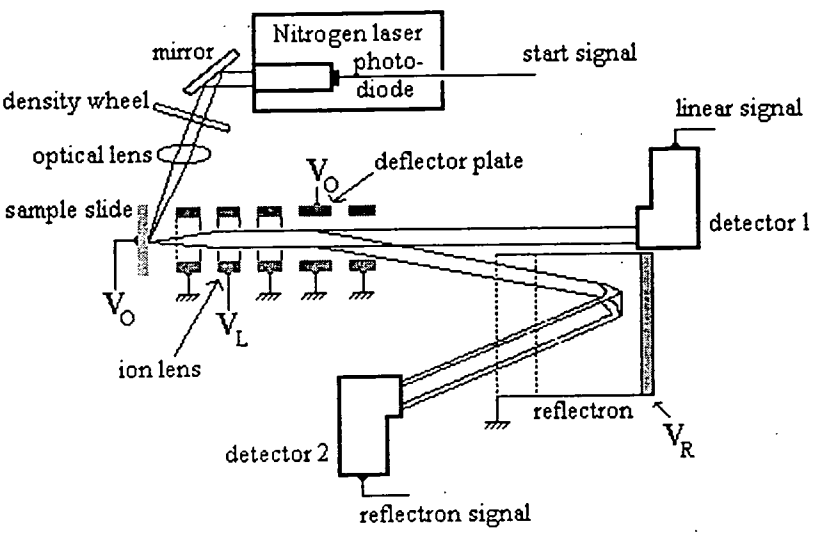

Figure 3.1 Schematic diagram of the instrument set-up in a Kratos Kompact MALDI IV time of flight mass spectrometer.

In linear TOF mass spectrometry, after the ions are created they drift towards the detector. Using this method, both neutral particles and metastable ions (those which decompose before reaching the detector) can be detected. Reflectron TOF mass spectrometry is used when high mass resolution is required. The ions are repelled by a deflector and, by applying a voltage to the reflectron, are made to turn back towards the ion source. Ions having a high energy penetrate deep into the reflectron, whilst ions of lower energy have a longer time of flight through the drift space, this causes the ions to be "time focused". This results in the distribution in the time of flight, caused by the initial energies when the ions are created, for ions of the same mass being eliminated. Using this technique, ions having equivalent mass/charge ratios are detected at essentially the same time regardless of their initial energy.

The detector, in both linear and reflectron TOF, operates by converting the kinetic energy of the incoming ions into an electric current. This is achieved by the ions striking a surface, the first dynode, which releases one or more electrons when the ion has an energy above a predetermined level. The released electron is accelerated towards the second dynode due to a potential difference between dynodes. Once again, electrons are released. By repeating this procedure, the number of electrons released increase in a geometric progression giving rise to a measurable current.

To summarise, the ions generated in the ion chamber, through laser irradiation, are separated on a time of flight basis depending on the magnitude of their mass and the charge carried. To measure the time of flight of ions, a very accurate timing circuit must be utilised. In Kompact MALDI, a photo-diode provides the start signal for the timing mechanism. The zero point is defined as the irradiation of the sample by the laser, i.e. the point at which ions are generated. As there are some errors introduced by signals travelling through wires and electronic circuitry it is necessary to make a time correction. Equation 3.5 shows the relationship used to convert the time of flight of the ions into mass information:-

$$time = A\sqrt{M} + C \qquad \text{(Eq. 3.5)}$$

where A is a proportionality coefficient and C is a constant correction term.

Although MALDI-MS was initially developed[6] to analyse proteins whose masses exceed 10,000 Daltons, it has now been extended to analyse synthetic polymers.[7] The ability of MALDI-TOF mass spectrometry to obtain very accurate masses is essential in determination of the composition of polymeric and oligomeric species present in a polymer sample.[8] A typical spectrum of a linear polymer[9] consists of a distribution of signals which correspond to the sodium, potassium or proton attached oligomers. As MALDI-TOF mass spectrometry does not induce fragmentation of the analyte, the mass spectrum of a polymer may be used to calculate the number average molecular weight. This is particularly useful for dendrimers and hyperbranched polymers whose molecular weights cannot be accurately determined by GPC.

The first report[10] of MALDI-TOF being used as an analytical tool for the mass determination of dendrimers merely showed that the coupling of core molecules to wedges was successful. As an extension to the study by Xu,[10] Kawaguchi *et al*[11] utilised MALDI-TOF MS to analyse phenylacetylene dendrimers. The synthesis of these dendrimers is *via* a double exponential growth scheme, Figure 3.2, where large structures can be obtained very quickly.

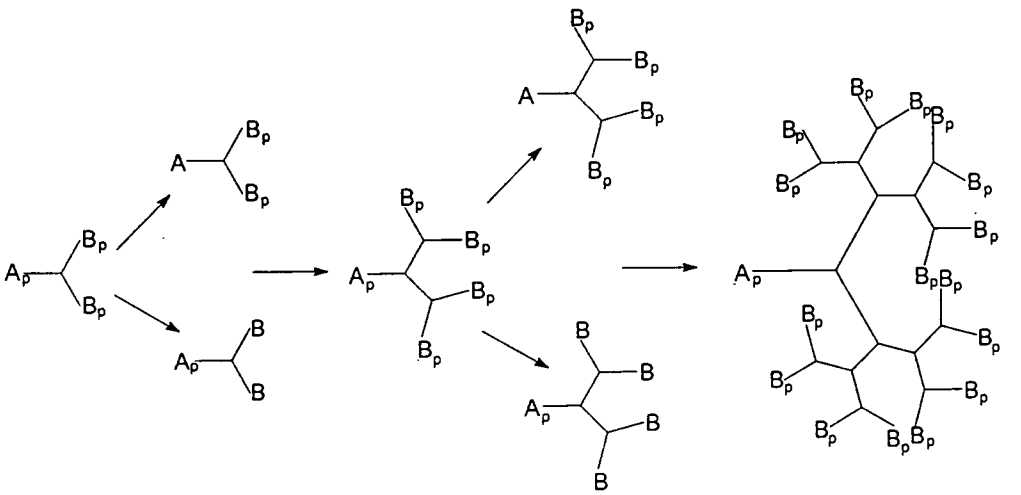

Figure 3.2 Double exponential dendrimer scheme

where A_p and B_p are protected functional groups.

As GPC and ^{1}H nmr spectroscopy were unable to resolve defects within the dendrons, MALDI-TOF MS was utilised. The mass spectrum proved that coupling of the A_pB_{16} molecule to 16 equivalents of AB_{16p} molecule had not gone to completion. A more detailed investigation into the applicability of MALDI for dendrimers was performed by Haddleton *et al.*[12] Two series of aromatic polyester dendrimers based on benzyl protected 3,5-dihydroxybenzoic acid were synthesised. One series had benzyloxy terminal groups, whilst the other series had hydroxy terminal groups. The mass spectra show only one peak proving that these dendrimers were truly monodisperse. In theory, this could also have been shown using GPC however hydroxy surface functionalities have a tendency to interact with GPC column packing hence giving errors in the molecular weight determination. It has been claimed[12] that MALDI is the only method available to test the success of synthesising a defect free dendrimer.

As low molecular weight hyperbranched polymers resemble linear polymers in as much as they display a molecular weight distribution tending to two, it was anticipated that such low molecular weight hyperbranched macromolecules might display a Gaussian polydispersity like linear polymers; this is indeed the case for hyperbranched poly(diethyl 3-hydroxyglutarate), Figure 3.3.

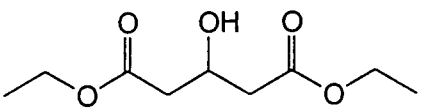

Figure 3.3 Diethyl 3-hydroxyglutarate

In most samples, not only are the sodium oligomer adduct peaks observed, but the potassium adduct is formed as a minor series. The inclusion of these cation adducts is most probably due to impurities in the matrix, 2,5-dihydroxybenzoic acid, DHB. In principle it is possible to remove the impurities by a series of recrystallisations from ethanol/water,[2] however as the cations are required for detection of the polymer molecules there seems little point in removing them only to have to dope the analyte with a salt.

To date, only two systematic investigations[13,14] into the influence of the laser power on the MALDI mass spectra of polymers have been published. Both groups essentially find that for linear polymers, the spectrum obtained from the laser at the threshold power (that power where a spectrum may be first obtained) is the most symmetrical and most representative of the polymer distribution. A slight increase in power gives a skewed distribution which is shifted to lower mass. It has been suggested[14] that this is due to degradation (scissions) of the polymer by the laser.

In an attempt to investigate the dependence of laser power on the quality of the observed MALDI-TOF mass spectra of hyperbranched poly(diethyl 3-hydroxyglutarate), a series of spectra were collected and scrutinised. The samples were prepared by laying down 0.5μL of a saturated solution of DHB in acetonitrile/water (60/40) followed by 0.5μL of the chloroform polymer solution (2-4mgml^{-1}) on a sample slide. The solutions were allowed to mix freely in the sample well and were dried at ambient temperature for 15 minutes before being introduced into the spectrometer. The power of the laser was varied from 36%-56% of the available power and the collected spectra were averaged over 100 shots, where one shot is defined as one pulse of laser irradiation. On inspection of the spectra, Figures 3.4, 3.5 and 3.6, it is clear that the recorded spectrum is a function of laser power and there is probably only a small "power window" where "representative spectra" of the analyte can be obtained. At very low power, i.e. the threshold power, the distribution observed is skewed towards low mass. Only when moving to higher power (44 and 47%) is a distribution found which resembles expectation; however, even in the small power range of 44 to 47% the observed distribution is very dependent on the incident laser power. If the power is too high, fragmentation of the analyte occurs.

These results are in direct opposition of the findings of Lehrle[14] and Belu *et al.*[13] Spectra observed for poly(diethyl 3-hydroxyglutarate) at the threshold laser power (Figure 3.4) have a skewed distribution, whilst at higher laser power (Figure 3.5) a symmetrical distribution is seen which becomes skewed in the opposite sense at even higher laser power. One other feature is that the larger oligomers are present at higher powers, as intuitively expected. The polystyrene samples of Belu *et al*[13] are of a similar molecular weight to the hyperbranched polymer displayed in Figures 3.4, 3.5 and 3.6 (a detailed discussion of the analysis of this polymer is given in Chapter 4),

hence the molecular weight of the polymer cannot be the reason for this discrepancy. An increase of only 3% (Figure 3.6) gives a slightly flatter distribution, however this small change in power does not affect the molecular weight distribution. Above this power level, symmetrical distributions are not observed and the molecular weight distribution is skewed towards low mass again, in agreement with other authors results. The factors determining the form of the distribution observed in MALDI-TOF MS of polymers are clearly much more complex than might be expected from the few papers published on the subject. There is clearly much to learn in the application of this comparatively new technique.

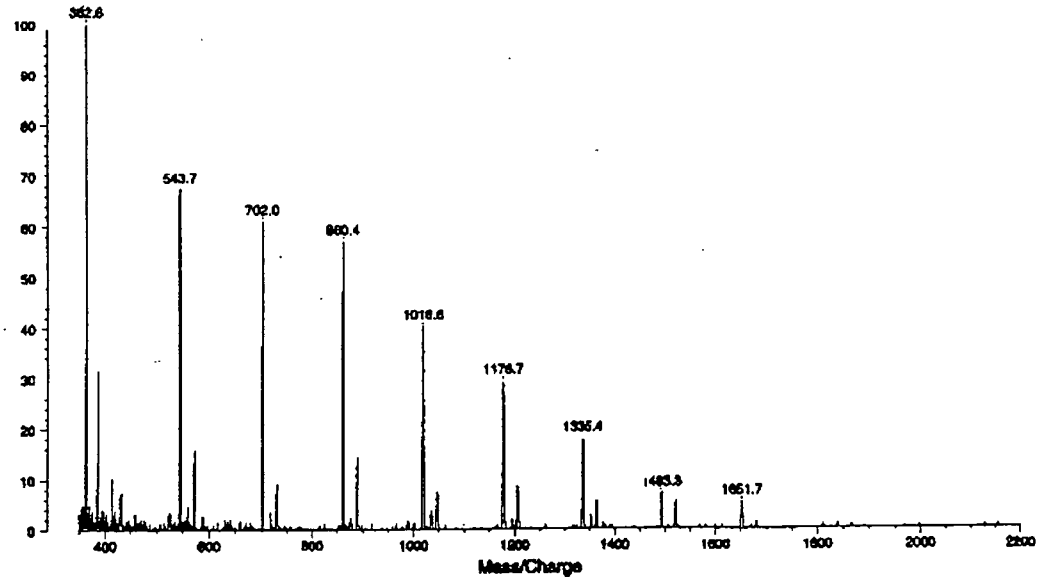

Figure 3.4 Spectrum obtained at threshold laser power (36%)

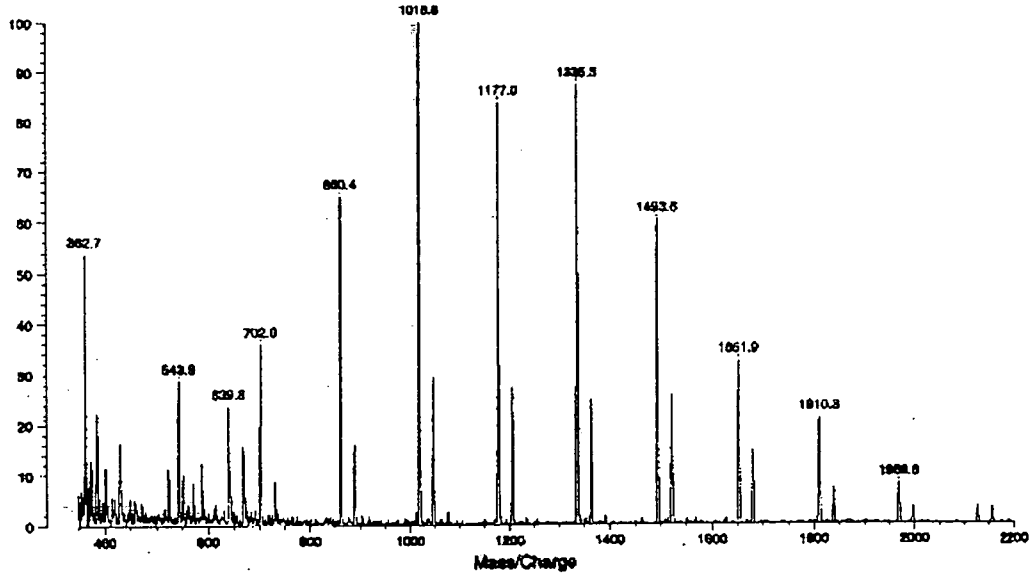

Figure 3.5 Spectrum obtained at optimum laser power (44%)

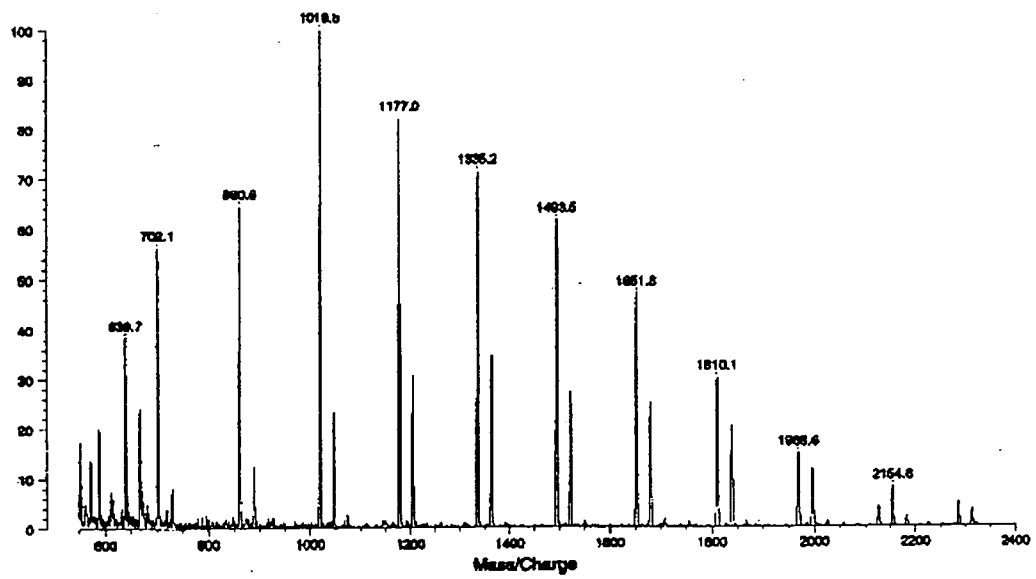

Figure 3.6 Spectrum obtained slightly above optimum laser power (47%)

In the above spectra, the major mass series is due to the hyperbranched oligomers of poly(diethyl 3-hydroxyglutarate), whilst the minor series is due to only one end group of the polymer being transesterified to butyl esters. A full analysis of the spectra obtained using MALDI-TOF MS is given in Chapter 4.

MALDI-TOF MS is still in the early stages of development for the molecular weight determination of polymers and as such several issues need to be addressed. For instance, what is the definition of optimum laser power, that which gives the strongest signals at the highest m/z ratio or that which gives a correct distribution? It is clear more work is required in this field, however MALDI-TOF MS has been found to be invaluable in oligomeric structure determination as will be shown in Chapter 4.

3.3 STRUCTURE DETERMINATION

3.3.1 ^{13}C nmr spectroscopy

Nuclear magnetic resonance (nmr) spectroscopy is an invaluable technique in the characterisation of polymers. It has been demonstrated that ^{13}C nmr spectroscopy may be used to determine the microstructure[15] of linear polymers and in highly branched polymers this technique is used to determine the extent of branching.[16]

A hyperbranched polymer may have several different architectures which correspond to any given molecular weight. It is essential, therefore to confirm the "degree of branching", DB, defined in chapter 1 as:

$$DB = \frac{N_t + N_b}{N_t + N_b + N_l}$$

where N_t is the number of terminal sub-units, N_b is the number of branched sub-units and N_l is the number of linear sub-units.

Figure 3.7 below highlights the four types of sub-unit present within a hyperbranched polymer.

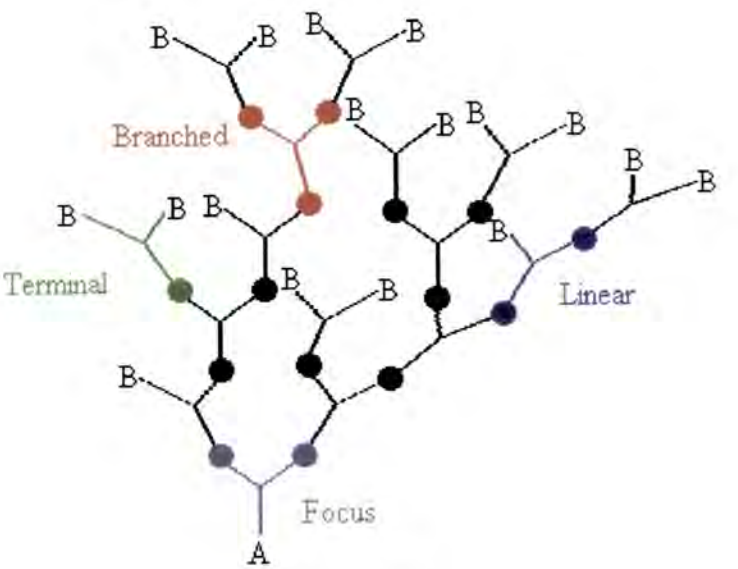

Figure 3.7

As described in Chapter 1, the focus of the hyperbranched wedge is the only sub-unit which has an unreacted A group associated with it. The branched sub-units may alternatively be named dendritic as both the B groups have reacted to incorporate two other monomer units into the hyperbranched structure. The linear groups possess only one unreacted B group and as such are considered as imperfections. The terminal groups possess two unreacted B groups and they may reside anywhere, i.e. internally or externally, on the polymer.

Ideal dendrimers have no linear sub-units as every monomer introduces a branch point into the growing polymer, therefore by definition, dendrimers have a DB of one, whilst linear polymers have a degree of branching (DB) equal to zero. Hyperbranched polymers, therefore have DB values that may lie between zero and one, although very low values would not be considered as truly hyperbranched. DB values between 0.5-0.7 are typical of the majority reported,[17,18] but statistically an AB_2 polymerisation would be expected to reach a value of 0.66 if no synthetic complications occurred. Exceptionally high branching factors of 0.8 have been reported by Hult *et al.*[19] One goal for AB_2 syntheses is to produce a DB approaching one as this would indicate a one-pot synthetic route to materials which would be expected to display some of the characteristics of dendrimers. Highly specific and efficient reactions would be required for this limit.

To determine the DB, it is necessary to assign signals in the spectrum to those arising from terminal, linear and branched sub-units. Typically within a monomer there will only be one, or possibly two, carbons which will be influenced sufficiently by their immediate environment to cause a slight shift, possibly giving rise to a multiplet. As the carbon in question will only be subtly influenced by the small environment change of the surrounding linear, branched and terminal sub-units, it may be necessary to perform a curve fitting procedure to separate the multiplet into its constituent signals. The expansion overleaf shows part of the ^{13}C nmr spectrum due to the methine carbon, marked with an asterisk, of poly(diethyl 3-hydroxyglutarate). As can be seen, the multiplet consists of four peaks which are assigned to the focus, linear, branched and terminal sub-units of the hyperbranched polymer. The resonance due to the focus is appreciably smaller than those of the other sub-units hence it may not always be readily detected.

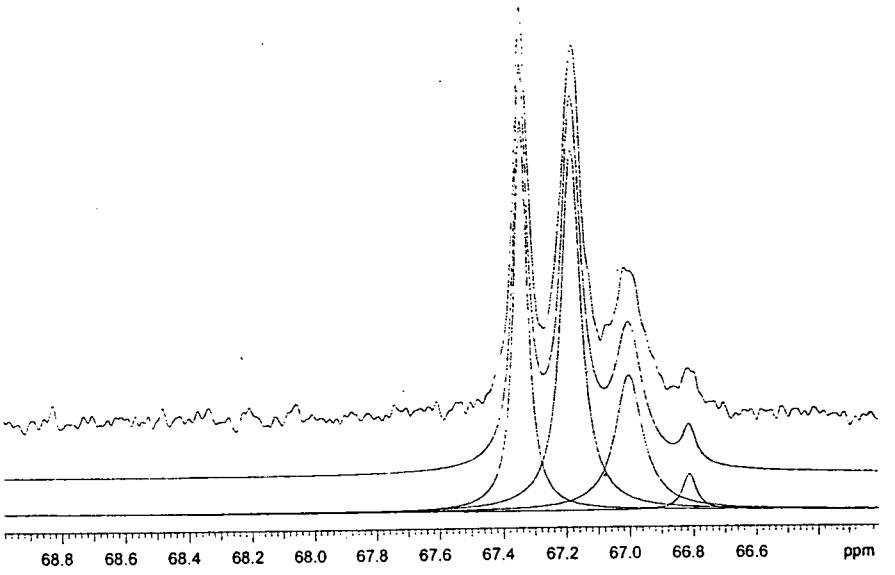

Figure 3.8 ^{13}C nmr expansion of the multiplet due to the methine carbon associated with terminal, linear, branched and focal sub-units present in poly(diethyl 3-hydroxyglutarate) and its Laurentzian deconvolution.

A Laurentzian deconvolution may be performed to allow integration of the areas beneath the three signals. The relative integrated areas give a direct method of calculating the amount of each species present in the polymer sample, when the peaks relating to terminal, linear and branched sub-units have been assigned. This analysis requires that the spectrum is recorded under quantitative conditions, that is that the differences in relaxation time have no effect on the relative integrated intensities.

If one considers the freedom of movement of the methine carbon of a terminal group, it becomes clear that it will have more freedom than the corresponding carbon of a branched sub-unit. In terms of ^{13}C nmr spectroscopy, the relaxation time of the carbon in a terminal environment will be shorter than that of a carbon in a branched environment, hence the line width of a terminal sub-unit will be narrower than a branched sub-unit. Using this assumption the signal at 67.04ppm must be due to a branched sub-unit (line width = 10.48Hz). whilst that at 67.34ppm is due to a terminal sub-unit (line width = 4.90Hz). Therefore, by analogy, the central signal must be due to a linear sub-unit (line width = 7.39Hz).

If the focal sub-unit is present in the ^{13}C nmr spectrum it would be possible, in theory, to calculate the molecular weight of the polymer. This may be achieved as the molecular mass of the individual sub-units is known and the number of species within a sub-unit is readily determined.

It has been reported[20] that selective chemical degradation may be used to determine the DB of hyperbranched polymers, however as this technique is time consuming and the degradation reactions must be highly selective to retain the distinct sub-units of the hyperbranched structure, this method has only been reported once to date.

3.4 CONCLUSIONS

The complete characterisation of hyperbranched polymers may only be achieved if both structural elucidation and molecular weight determination have been performed. It is clear, that neither of these objectives is undemanding hence the characterisation can be regarded as being as important, if not more so, than the synthesis of hyperbranched polymers.

The use of MALDI-TOF MS and ^{13}C nmr spectroscopy will be discussed in Chapter 4 in relation to the structural determination of poly(diethyl 3-hydroxyglutarate).

3.5 REFERENCES

1. P.M. Saville, J.W. White, C.J. Hawker, K.L. Wooley and J.M.J. Fréchet, *J. Phys. Chem.*, **97** (1993), 293.
2. B. Thomson, K. Suddaby, A. Rudin and G. Lajoie, *Eur. Polym. J.*, **32**, (1996), 239.
3. K.E. Uhrich, C.J. Hawker, J.M.J. Fréchet and S.R. Turner, *Macromol.*, **25**, (1992), 4583.
4. P.L. Dubin, S.L. Edwards, J.I. Kaplan, M.S. Mehta, D. Tomalia and J. Xia, *Anal. Chem.*, **64**, (1992), 2344.
5. "Comprehensive Polymer Science" Volume 1:Polymer Characterisation, Chapter 12, Eds. Booth, Price, (1989), Pergamon.
6. M. Karas and F. Hillenkamp, *Anal. Chem.*, **60**, (1988), 2299.
7. U. Bahr, A. Deppe, M. Karas and F. Hillenkamp, *Anal. Chem.*, **64**, (1992), 2866.
8. M. Dey, J.A. Castro and C.L. Wilkins, *Anal. Chem.*, **67**, (1995), 1575.
9. D. Braun, R. Ghahary and H. Pasch, *Polymer*, **37**, (1996), 777.
10. Z. Xu, M. Kahr, K.L.Walker, C.L. Wilkins and J.S. Moore, *J. Am. Chem. Soc.*, **116**, (1994), 4537.
11. T. Kawaguchi, K.L. Walker, C.L. Wilkins and J.S. Moore, *J. Am. Chem. Soc.*, **117**, (1995), 2159.
12. H.S. Sahota, P.M. Lloyd, S.G. Yeates, P.J. Derrick, P.C.Taylor and D.M. Haddleton, *J. Chem. Soc., Chem. Commun.*, (1994), 2445.
13. A.M. Belu, J.M. DeSimone, R.W. Linton, G.W. Lange and R.M. Friedman, *J. Am. Soc. Mass Spectrom.*, **7**, (1996), 11
14. R.S. Lehrle and D.S. Sarson, *Polym. Degrad. Stab.*, **51**, (1996), 197.
15. W.J. Feast and D.B. Harrison, *Polymer*, **32**, (1991), 558.
16. W.J. Feast and N.M. Stainton, *J. Mater. Chem.*, **5**, (1995), 405.
17. C.J. Hawker, R. Lee and J.M.J. Fréchet, *J. Am. Chem. Soc.*, **113**, (1991), 4583.
18. Y.H. Kim and O.W. Webster, *Macromol.*, **25**, (1992), 5561.
19. E. Malmström, M. Johansson and A. Hult, *Macromol.*, **28**, (1995), 1698.

20. P. Kambouris and C.J. Hawker, *J. Chem. Soc. Perkin Trans. 1*, (1993), 2717.

Chapter 4.

Synthesis, Characterisation and Physical Properties of Hyperbranched Poly(diethyl 3-hydroxyglutarate)

4.1 INTRODUCTION.

The production of linear polymers via polyesterification reactions has been known for the past 100 years and is well documented,[1-3] however the synthesis of polyesters using AB_2 monomers has been a somewhat neglected subject until recently. The initial interest in AB_2 systems was shown by Flory[4] in 1952. As discussed in Chapter 1, his work focused on the statistics of the processes leading to highly branched polymers.

This Chapter discusses the synthesis and characterisation of an aliphatic hyperbranched polyester based on the AB_2 monomer, diethyl 3-hydroxyglutarate. The principles of polyester formation and the expected properties of hyperbranched polymers are discussed in the following sections.

4.1.1 Synthetic methods utilised in the production of linear polymers.

In principle, there are a variety of reactions which may be used to produce polyesters however the majority of these are not industrially viable due to the limited availability of the monomers or the cost of the process. In general, direct esterification and alcoholysis[5] reactions are favoured by the chemical industry due to the high yields and low running costs. Direct esterification (Figure 4.1a) occurs between diacids and diols to produce linear polymers with water as the condensation product. However this synthetic route is not viable with tertiary diols due to their reduced reactivity in comparison with primary and secondary diols and their tendency to undergo dehydration reactions.

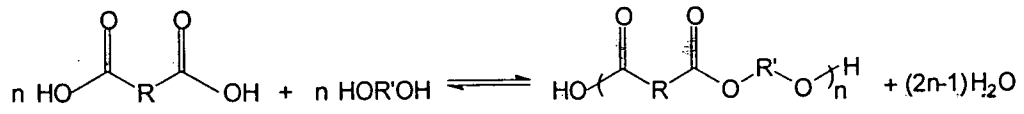

4.1a

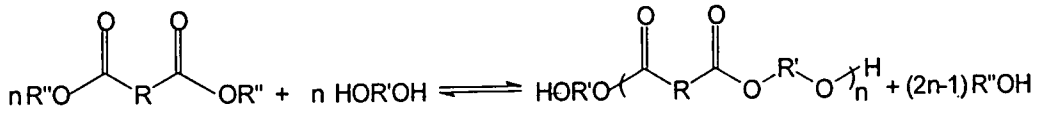

4.1b

Figure 4.1 (a) Direct esterification (b) Alcoholysis

Polyesterifications proceeding *via* an alcoholysis route (Figure 4.1b) may be described as a transesterification reaction[6] between an ester and an alcohol. In the case of linear polymers where the starting materials are diesters and diols, the resulting polymers are generally of a better quality than those made via a direct esterification route as the diesters can usually be obtained in higher purity than the corresponding diacids. One disadvantage of alcoholysis reactions is that they may not always be commercially viable due to the increased operating costs.

As the polyesterifications described above are step-growth condensation reactions,[7] it is necessary to efficiently remove the condensation product to achieve high conversions. This is normally done by a distillation process, often aided by passing a flow of inert gas, such as argon or nitrogen, through the reaction vessel. A vacuum may be applied during the final stages of the reaction to remove the last traces of the condensation product to give high molecular weight polymers.

4.1.2 Properties of linear aliphatic polyesters.

Linear aliphatic polyesters were, at first, rejected[3] as potentially useful materials because of their low melting and glass transition temperatures. Recently however, poly(β-hydroxyalkanoates) have fuelled interest as biodegradable polymers and may be regarded as the first commercial polymer produced using biotechnology.[8]

These polymers are produced in a stereoregular form and are higher melting semicrystalline thermoplastics. Typically the melting temperatures of most linear aliphatic polyesters occur between 40-90°C whilst the glass transition temperatures lie within the range of -70 to -30°C.[6] The melting temperatures are low compared to aromatic polyesters, e.g. polyethyleneterephthalate mp 245-265°C, so with the exception of poly(β-hydroxyalkanoates) aliphatic analogues have received little industrial interest.

Linear aliphatic polyesters are readily soluble in amides, ketones and phenols, but are insoluble in alcohols. Only moderate solubility is shown towards chlorohydrocarbons, tetrahydrofuran (THF) and aromatic hydrocarbons. It was anticipated that by introducing numerous branches, both the glass transition temperature and the solubility would be greatly effected with the former decreasing and the latter increasing.

4.1.3 Industrial applications of linear aliphatic polyesters.

The majority of polyesters which are of significant commercial importance are derived from aromatic compounds, however copolyesters of aliphatic and aromatic monomers have found use as films, fibres and moulding materials.[7] The only notable examples of linear aliphatic polyesters being utilised for commercial purposes are the poly(alkylene adipates), Figure 4.2, where x=2, 4 or 6.

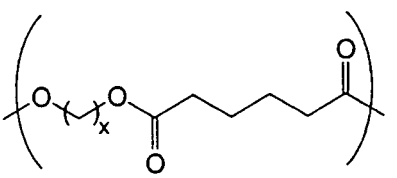

Figure 4.2

At low conversions (M_n<5000), and when both end groups are hydroxyls, this class of compound may be used as telechelic or macrodiols for the synthesis of polyurethanes.

Polyesters are used in a wide variety of forms, however they can easily be divided into two classes: coatings materials and fibres and plastics. High molecular weight linear polyesters are commonly used in the fibres and plastics industry. Polyesters required for coatings typically have a much lower mass and an ability to cross-link is desirable.

In summary, polyesters are a widely used class of polymeric materials, their properties are highly dependent on their structure and molecular weight and the introduction of branches may provide new materials for the coatings industry. The following chapter provides details of a study of the synthesis and characterisation of hyperbranched poly(diethyl 3-hydroxyglutarate) formed via a condensation alcoholysis reaction in the presence of titanium (IV) butoxide.

4.2 POLYMERISATION OF DIETHYL 3-HYDROXYGLUTARATE.

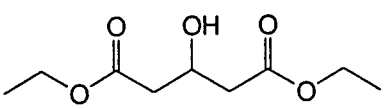

Figure 4.3 Diethyl 3-hydroxyglutarate

The polymerisation of diethyl 3-hydroxyglutarate was performed under a variety of conditions. Throughout the series of reactions, both the time of reaction and temperature of the reaction bath were controlled using a Eurotherm temperature controller. The catalyst, titanium (IV) butoxide, and monomer were added to the reaction vessel which was slowly lowered into a preheated oil bath at 80°C, the temperature was then increased to the desired polymerisation temperature (100-125°C) at a rate of 3°Cmin^{-1} and maintained at that temperature for 270-600 minutes. The diagram overleaf shows the apparatus used for the polymerisation reactions. Polycondensations of neat monomers involve systems in which the viscosity is expected to change dramatically during the course of the reaction which requires

efficient stirring. In the system used by the author, a Heidolph stirrer with a 6mm diameter stirrer rod, held in place by an Edwards vacuum seal, drives a propeller-like stirrer which forces the mass against the flat bottom of the cylindrical reaction vessel. The clearance between the stirrer blades and the vessel was ≤2mm. These mechanical manipulations of the reaction process have been found by experience to be essential for a successful outcome in such polycondensations.

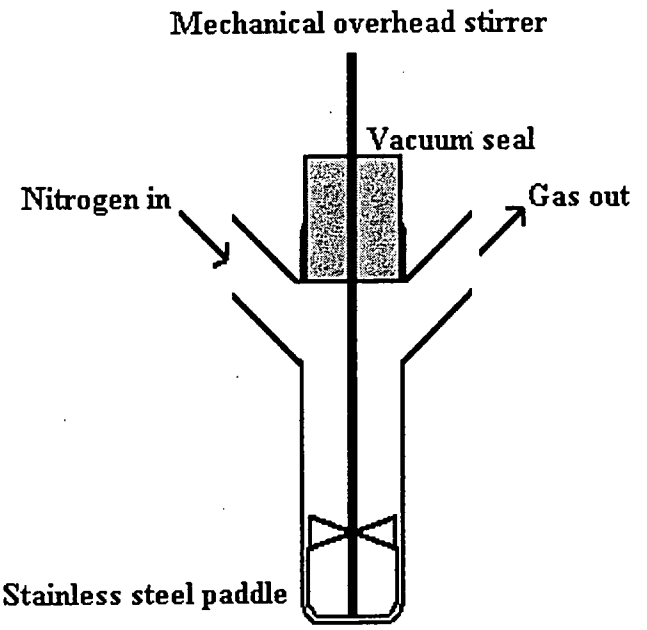

Figure 4.4 Schematic of polymerisation reaction vessel.

A systematic variation of reaction conditions was investigated in an attempt to find the optimum polymerisation conditions. For the initial reaction, an arbitrary time of 270 minutes and a temperature of 100°C was chosen for the polymerisation. A vacuum was applied (10mmHg) for the final 30 minutes of the reaction to aid removal of the condensate from the reaction vessel.

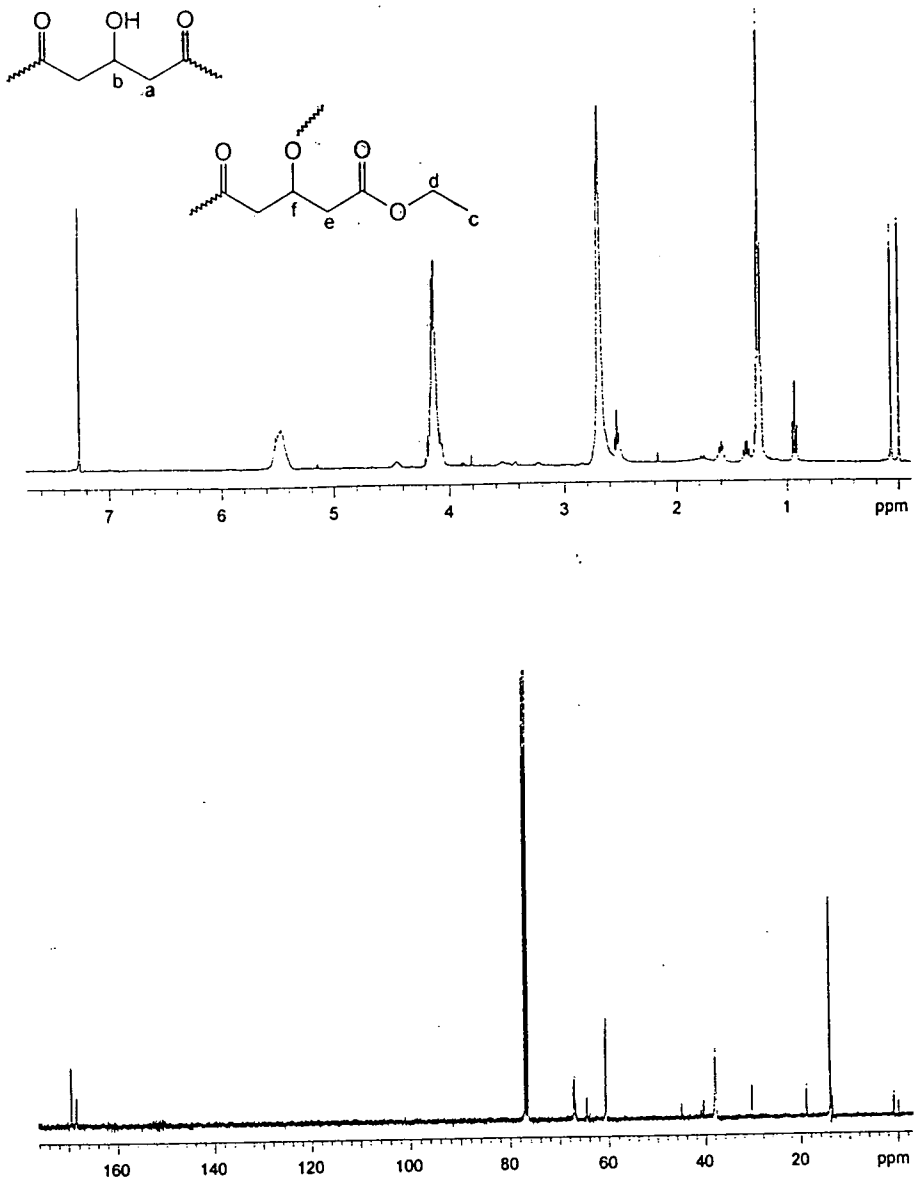

Figure 4.5 Representative ^{1}H and ^{13}C nmr spectra of poly(diethyl 3-hydroxyglutarate) of M_n=3190 (determined by GPC using $CHCl_3$ as eluent and linear polystyrene standards).

The ^{1}H and ^{13}C nmr spectra of poly(diethyl 3-hydroxyglutarate) are shown in Figure 4.5. The ^{1}H nmr spectrum shows a major triplet at 1.26ppm due to the CH_3 hydrogens (c) of the terminal ester units assigned by comparison with monomer signals, whilst the multiplet at 4.15ppm is due to the corresponding OCH_2 hydrogens (d). The minor multiplet at 2.54ppm coincides in chemical shift with the other CH_2 (a) of the monomer, hence it is assumed to correspond to the CH_2 hydrogens adjacent

to the polymer foci. The major signal at 2.69ppm is assigned to the CH_2 hydrogens (e) of the branched, linear or terminal sub-units of the polymer. The minor multiplet at 4.44ppm is due to the CH-OH hydrogen (b) of the focus, again assignment is based on coincidence of shift with the analogous monomer signal. If these assignments are correct relative integrated intensities of the CH-OH signal should be 0.25 of the intensity of the multiplet at 2.54ppm, experimentally it is 0.2 which lies within the error of the measurement of the integrals of these relatively weak signals. The signal at 5.51ppm is due to CH-O- (f) of a sub-unit, this integral gives a good indication of the success of the reaction when compared to the intensity of the signal at 4.44ppm (see section 4.2.3 for a full analysis). As hyperbranched polymers contain only one unreacted A group, in the absence of intramolecular reactions, the integrated intensities of the multiplets at 4.44 and 5.51ppm provide a method of determining the number of focal sub-units with respect to the number of terminal, linear and branched sub-units, therefore it should be possible to calculate the number average molecular weight of the sample from these data. The minor multiplets at 0.93, 1.36 and 1.60ppm are thought to be due to the methyl and two methylene units of a butoxy residue arising from exchange with the catalyst.

The ^{13}C nmr spectrum has been assigned by analogy with the monomer and from a DEPT analysis. The signal at 14.14ppm is due to the CH_3 (c) of the terminal esters, whilst the signal at 60.82ppm arises from the corresponding OCH_2 (d). The minor peak at 40.61ppm is due to the CH_2 (a) of the focal units whilst the multiplet at 38.23ppm is due to the CH_2 (e) of the remaining linear, terminal and branched sub-units. In theory, this signal could be deconvoluted to determine the degree of branching however the multiplet at 67.19ppm, due to the CH-O- (f), is well resolved making the assignment and relative intensity measurement of the constituent signals easier. This aspect of the analysis was discussed in Chapter 3 (page 79). The CH-OH (b) of the focus is readily observable at 64.73ppm. Only three signals are observed in the carbonyl region of the spectrum, however these have not been assigned unambiguously. The remaining minor signals at 13.68, 19.06 and 30.51ppm are assigned to transesterified butoxide groups. As all the catalyst is removed at the end of the reaction by washing a chloroform solution of the polymer with copious amounts of water, the residual butoxide signals are bound to the product and probably

due to a transesterification product as discussed later. Appendix 2, Tables 1-13 provide full ^{1}H nmr spectral data for the complete series of polymerisations of diethyl 3-hydroxyglutarate, whilst Tables 14-20 (Appendix 2) shows the complete ^{13}C nmr spectral data for the products of the polymerisation.

In principle, there are two classes of reaction which would explain butoxide incorporation into the polymer. The first involves the direct reaction of an alkoxide with an organic ester. The mechanism shown below has been suggested[9] as the most obvious mode of reaction:

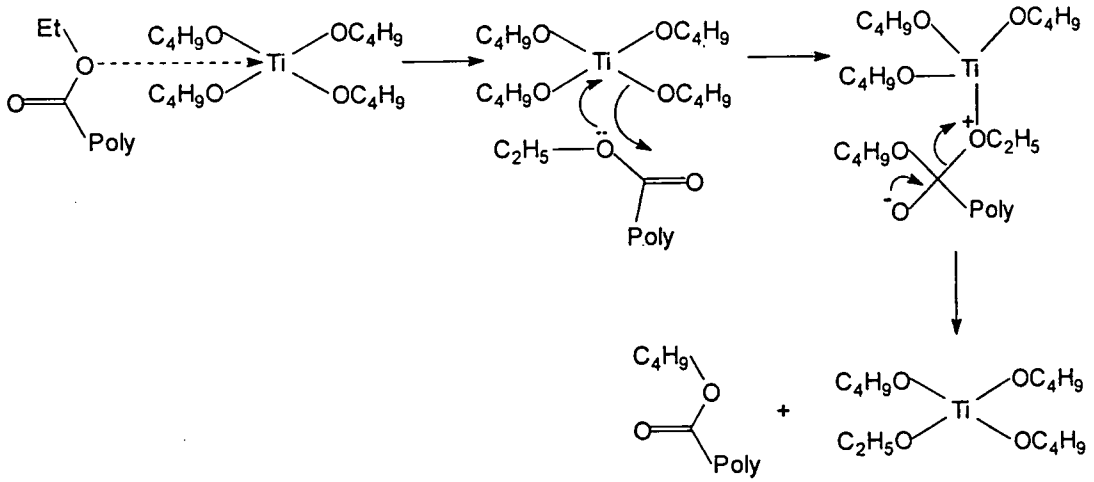

Figure 4.6

However, an alternative mechanism has been proposed which involves co-ordination through the carbonyl oxygen atom:

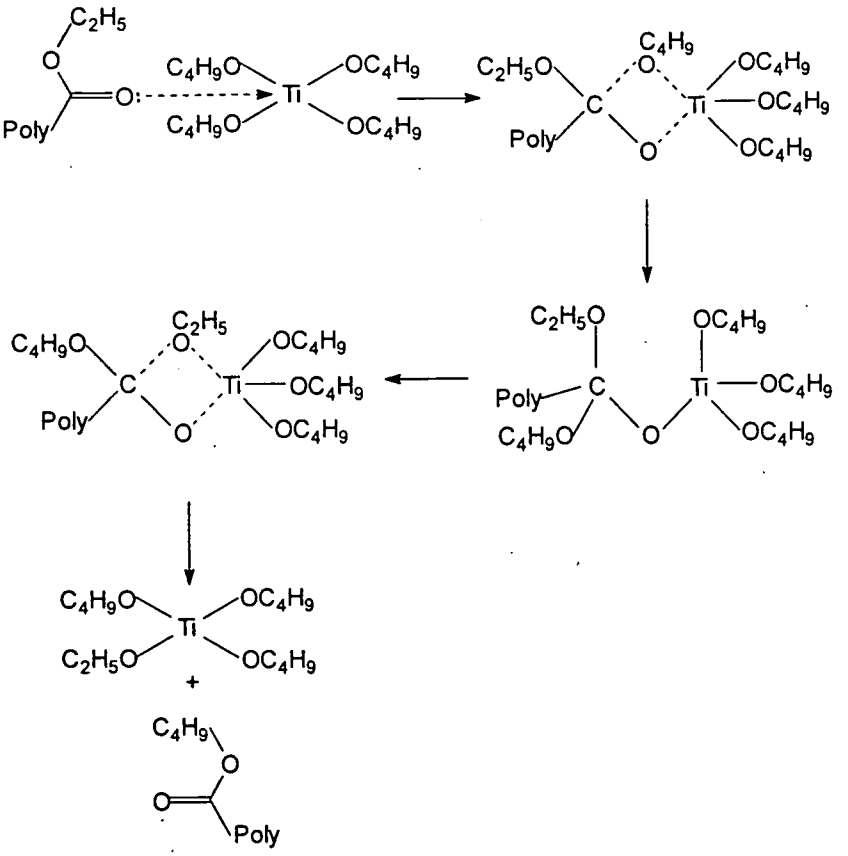

Figure 4.7

The actual mode of reaction is unclear, however Lappert[10] favours the mechanism outlined in Figure 4.7 based on an analogy with the results of his studies of the reactions of boron trichloride with organic esters.

Both the reaction schemes outlined in Figures 4.6 and 4.7 assume that it is the ester units of the monomer or polymer that react with the catalyst, however, an alternative may be transesterification with the eliminated alcohol. The polymerisation temperature of 100°C was chosen as it was assumed to be sufficiently higher than the boiling point of the condensation product, ethanol, to allow facile removal under a stream of nitrogen. As the reacting system becomes more viscous, it may be assumed that the efficiency of the removal of ethanol decreases. Hence, it is plausible that the ethanol exchanges with the catalyst to form butanol and a mixed alkoxide as shown in Figure 4.8.

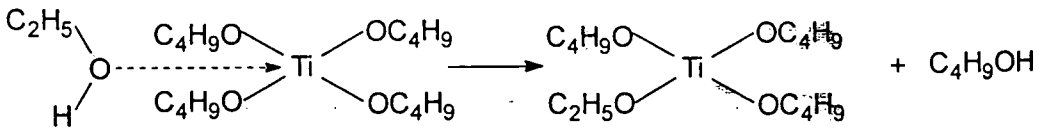

Figure 4.8

If the reaction represented above is occurring in the polymerisation vessel, butanol would be produced and as its boiling point is 117°C, a reaction temperature of 100°C would not be sufficient to remove it from the reaction vessel. Butanol may then transesterify with the growing polymer.

The extent of exchange of alkoxide groups will be discussed in greater detail in relation to the MALDI-TOF results in the following sections. This exchange side reaction provides a possible explanation for the observed decrease in catalytic activity during large scale reactions. If the catalyst is not added in aliquots throughout the reaction, it has been found that the polymerisation slows dramatically; it may be that mixed alkoxide catalysts, or in the limit titanium (IV) ethoxide, are less reactive than titanium (IV) butoxide. Alternatively, of course, there may simply be a degradation of catalyst in the reaction mixture with time.

It was unclear which reaction was responsible for the exchange of the butoxy groups, therefore model studies were performed. In an attempt to prove which reaction was the most plausible, both ethanol and ethyl caprate ($CH_3(CH_2)_8CO_2C_2H_5$) were heated in the presence of titanium (IV) butoxide. To monitor the success of the attempted ethanol exchange (see section 4.7.2 for experimental details), the volatile products were removed and the titanium compound dried under vacuum. The ^1H nmr spectrum (Figure 4.9) of the titanium compound shows two new resonances at 1.25 and 3.72ppm due to the CH_3 and OCH_2 protons of the incorporated ethoxide group, proving that ethanol is able to exchange with the catalyst to produce a mixed alkoxide species.

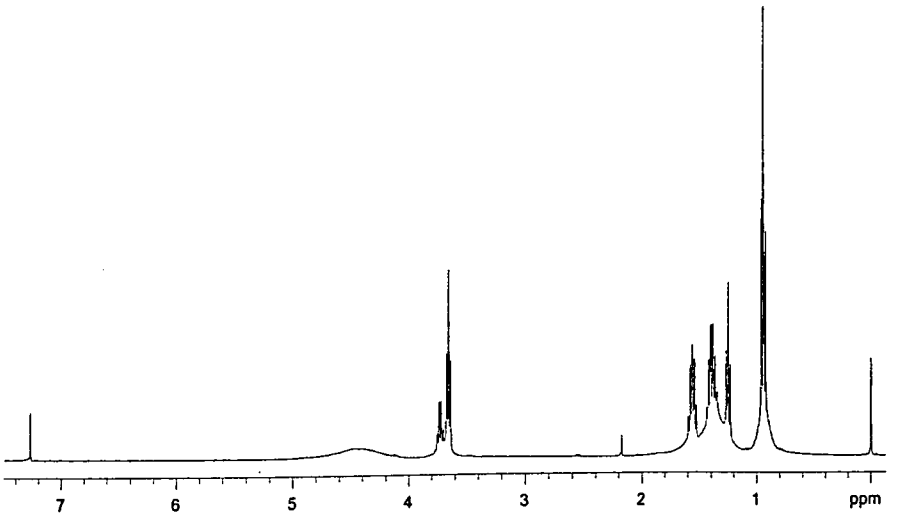

Figure 4.9 ^{1}H nmr of $Ti(OBu)_x(OEt)_y$ where x+y=4

To determine the outcome of the reaction of ethyl caprate with catalyst (section 4.7.3), the product was isolated by adding ethyl acetate and washing the solution with water to remove the catalyst. After distilling the isolated product under vacuum, ^{1}H nmr analysis was performed.

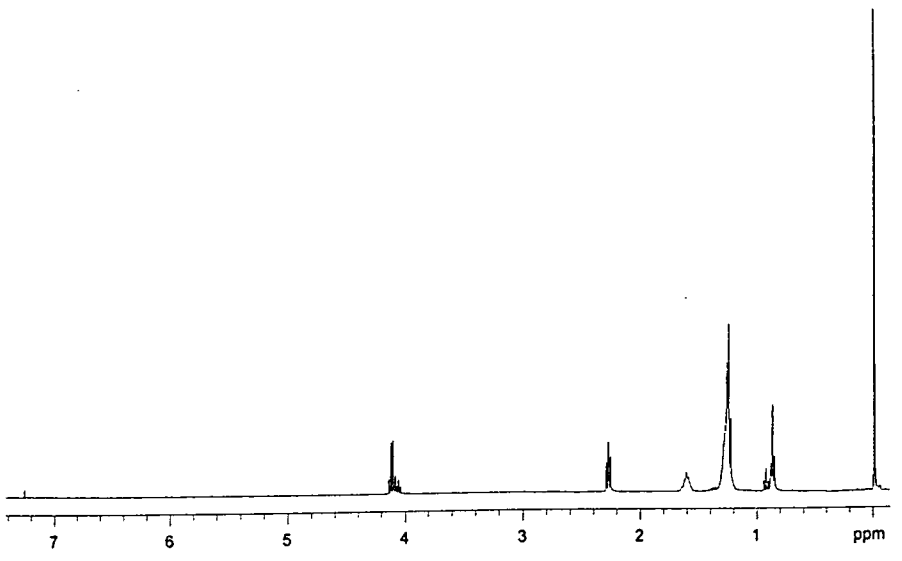

Figure 4.10 ^{1}H nmr spectrum of transesterified ethyl caprate

The ^1H nmr spectrum of the product (Figure 4.10) is essentially that of ethyl caprate but shows three additional multiplets, which can be assigned to the butyl ester product of the exchange reaction shown in Figure 4.11:

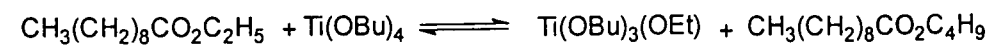

Figure 4.11 Reaction scheme showing the possible products formed in the initial step during the exchange between ethyl caprate and titanium (IV) butoxide.

The triplet at 0.94ppm in Figure 4.10 is assigned to the CH_3 of the butoxy of butyl caprate, whilst the triplet at 4.06ppm is due to the OCH_2 of the butoxy hydrogens. Only one other methylene signal for the butoxy residue is observed at 1.38ppm, the other multiplet is assumed to be coincident with the starting material signals at 1.6ppm. Integration of the appropriate resolved signals indicates exchange has occurred to the extent of 9%.

As both ester groups and ethanol have been shown to exchange with $Ti(OBu)_4$, it is impossible to conclude which reaction is responsible for the observed exchange in poly(diethyl 3-hydroxyglutarate), it is quite plausible that both reactions occur.

4.2.1 Variation of mass of catalyst.

In an attempt to determine the optimum catalyst level for polymerisation, the temperature and reaction time parameters were kept constant at 100°C and 270 minutes respectively, whilst the weight percent (relative to the monomer) of catalyst was increased from 2.5 - 25%. The graph overleaf shows the results.

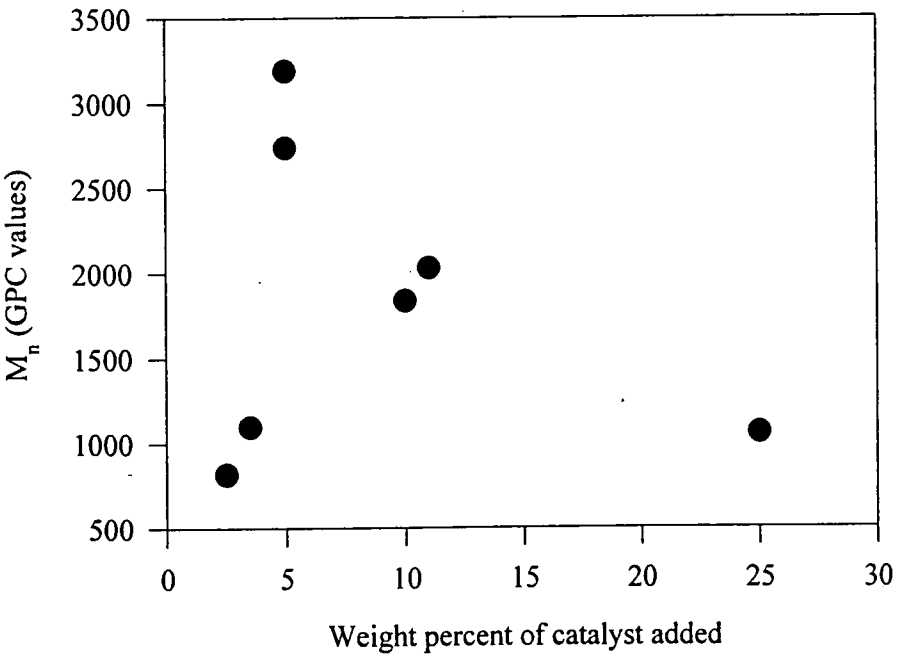

Figure 4.12 Graph showing the relationship between number average molecular weight (determined by GPC using $CHCl_3$ as eluent and linear polystyrene standards) and the amount of catalyst used.

From the graph, it would appear that the optimal amount of catalyst for polymerisation of diethyl 3-hydroxyglutarate at 100°C for 4.5 hours is in the region of 5 weight percent. This is, relatively speaking, a large amount of catalyst. Polyesterifications are usually performed in the presence of 0.05 - 0.5 weight percent titanium alkoxide catalysts,[11] however for this system the lower the amount of catalyst the lower the molecular weight. On inspection of the ^1H nmr spectra of the polymers produced with 2.5, 5, 10 and 25 weight percent catalyst, it is clear that the concentration of butoxy groups present in the polymer increases as the amount of catalyst increases. It is possible to determine the amount of exchanged butoxide present in the polymer from the relative integrated intensities of the ethyl triplet at 1.26ppm and the butoxide CH_3 triplet at 0.93ppm since these signals are reasonably well resolved.

Table 4.1 shows the initial amount of catalyst, the number average molecular weight of the polymer and the mole percent of butyl ester in the polymer.

M_n (GPC)[a]	Initial amount catalyst (wt%)	% BuO in polymer[b]	DB[c]
820	2.5	5.1	0.44
2740	5	6.8	0.54
1840	10	15.1	0.52
1060	25	51.9	0.53

a As determined using GPC with $CHCl_3$ as eluent and linear polystyrene standards
b Mole percent of butyl ester groups
c As determined *via* ^{13}C nmr spectroscopy

Table 4.1 Summary of results of the transesterification during polymerisation of diethyl 3-hydroxyglutarate with variation of amount of catalyst used.

As intuitively expected the relative amount of butyl ester present in the polymer increases as the initial amount of catalyst increases. However, it is also found that the molecular weight achieved decreases with increasing initial catalyst concentration above 5wt%. Transesterification reactions appear to consume a large amount of catalyst relative to that required for the condensation polymerisations and in this case it is not unreasonable to assume that transesterification is competing with polyesterification. Optimum polymerisation appears to occur at 5wt% catalyst under the experimental conditions. MALDI-TOF MS has been used to assess the amount of transesterified species relative to extent of formation of the desired hyperbranched polymer.

To illustrate the amount of butyl ester present within the desired hyperbranched polymer, the mass spectra of the products synthesised using 2.5 and 25wt% catalyst are shown overleaf:

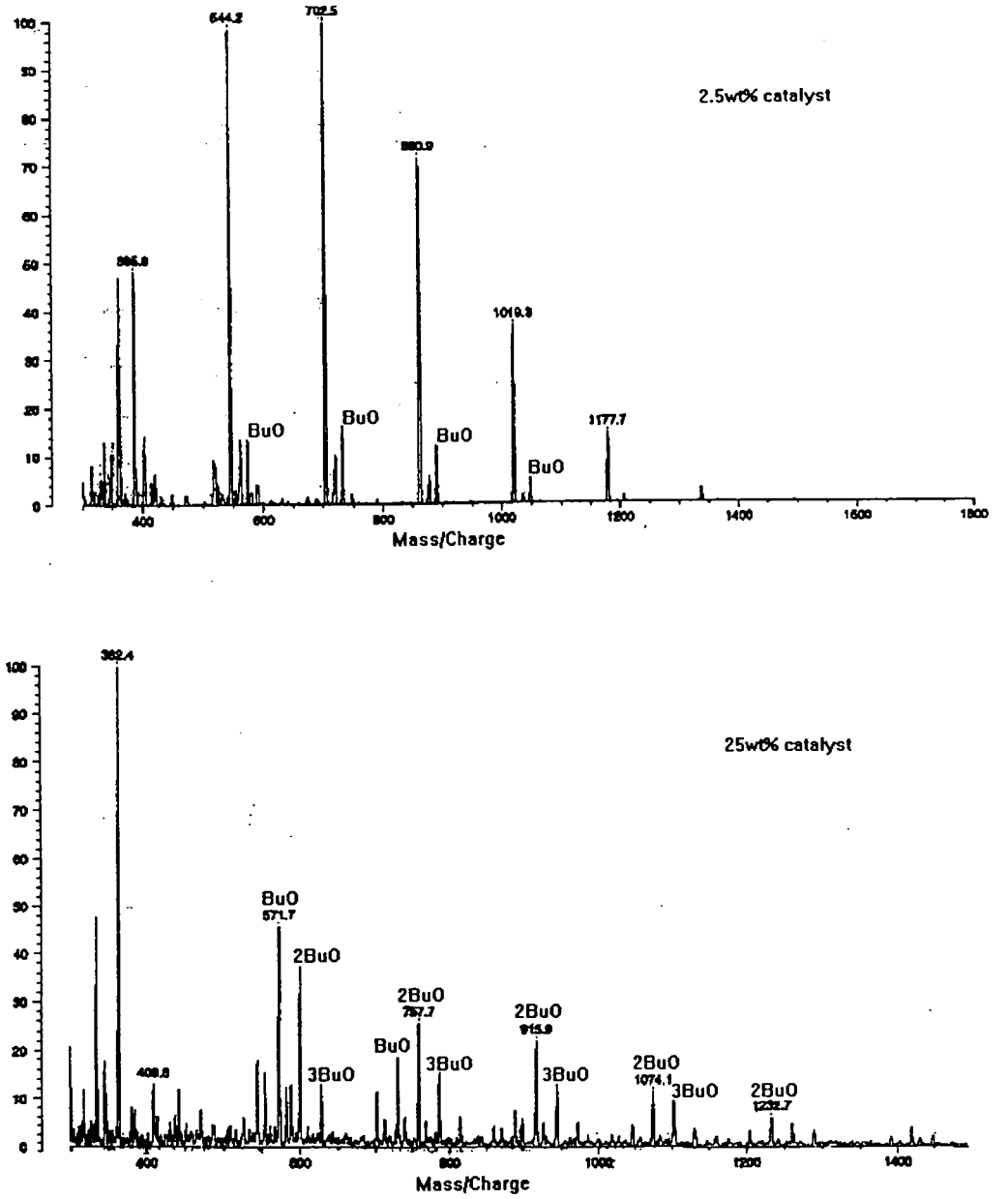

Figure 4.13 MALDI-TOF mass spectra of the products formed in the presence of 2.5 and 25wt% $Ti(OBu)_4$

The mass spectrum of the product formed in the presence of 2.5wt% $Ti(OBu)_4$ shows three series of m/e peaks, the major series is due to the desired hyperbranched poly(ethyl ester) oligomers displayed as MNa^+ ions. The next series of peaks (those at 402, 560, 718 and 876 amu) is due to the MK^+ hyperbranched poly(ethyl ester) oligomers (see Appendix 2, Table 21). The third series of peaks (marked with BuO) corresponds to the MNa^+ hyperbranched polymer containing one transesterified butyl

ester group per oligomer. Signals are observed for trimer, tetramer, pentamer and hexamer species. It is assumed that only one alkoxide is transesterified due to the small amount of catalyst present.

The mass spectrum of the product formed in the presence of 25wt% $Ti(OBu)_4$ appears totally different to the previous example. Only two peaks may be assigned to the MNa^+ hyperbranched poly(ethyl ester) oligomers, whilst only one can be attributed to the MK^+ polymer. The major peaks are due to either one, two or three transesterified butoxides within the polymer (see Appendix 2, Table 22). This result suggests that either the butyl ester polymer is more readily detected than the pure ethyl ester product in MALDI-TOF MS, or the relative amount of butyl ester present in the polymer, determined by ^1H nmr, is slightly low.

4.2.2 Variation of duration of reaction.

To determine the effect of the duration of reaction, four experiments were performed at 100°C using 5wt% $Ti(OBu)_4$ for 3.5, 4.5, 5.5 and 6.5 hours. The table and graph overleaf summarise the results.

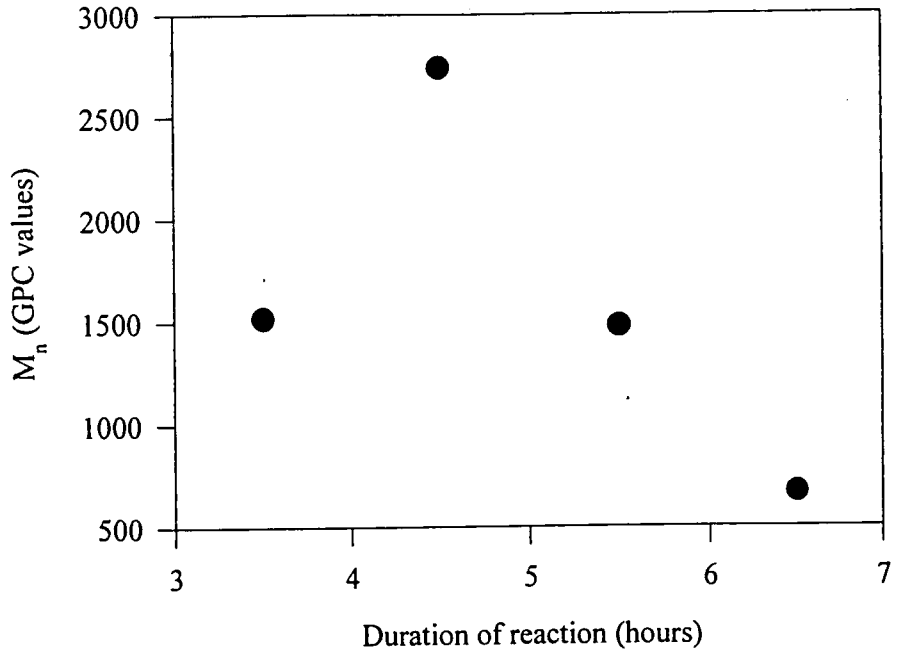

Figure 4.14 Graph showing the relationship between M_n (determined by GPC using $CHCl_3$ as eluent and linear polystyrene standards) and length of reaction.

Duration (Hours)	M_n[a]	%BuO[b]	DB[c]
3.5	1520	7.2	0.57
4.5	2740	6.8	0.54
5.5	1480	8.7	0.55
6.5	670	5.8	0.54

a As determined using GPC with $CHCl_3$ as eluent and linear polystyrene standards
b Mole percent of butyl ester groups
c As determined *via* ^{13}C nmr spectroscopy

Table 4.2 Summary of M_n results (determined via $CHCl_3$ GPC) as a function of the duration of reaction.

From these results it would appear that the percentage of transesterified butoxide and the degree of branching are largely unaffected by the duration of

reaction, however the molecular weight of the polymer is strongly influenced. For step-growth polymerisations, it is expected that high degrees of polymerisation will only occur at high reaction conversion and long reaction times favour this. However on prolonged heating, there is a risk of side-reactions and chain scission competing with the desired reaction. Clearly in this polymerisation, M_n passes through a maximum in the region of 4.5 hours reaction time.

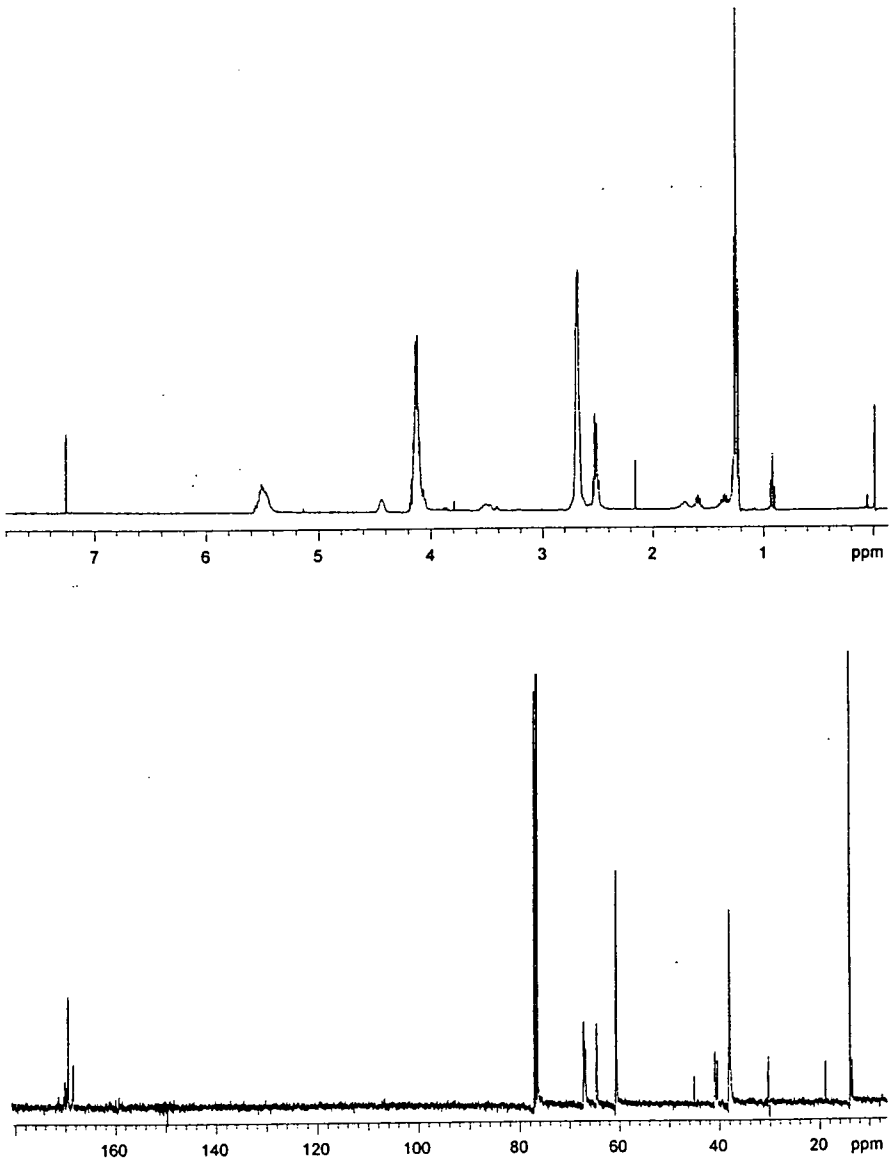

Figure 4.15 ^{1}H and ^{13}C nmr spectra of the product of the polymerisation of diethyl 3-hydroxyglutarate in the presence of 5wt% catalyst at 100°C for 3.5 hours.

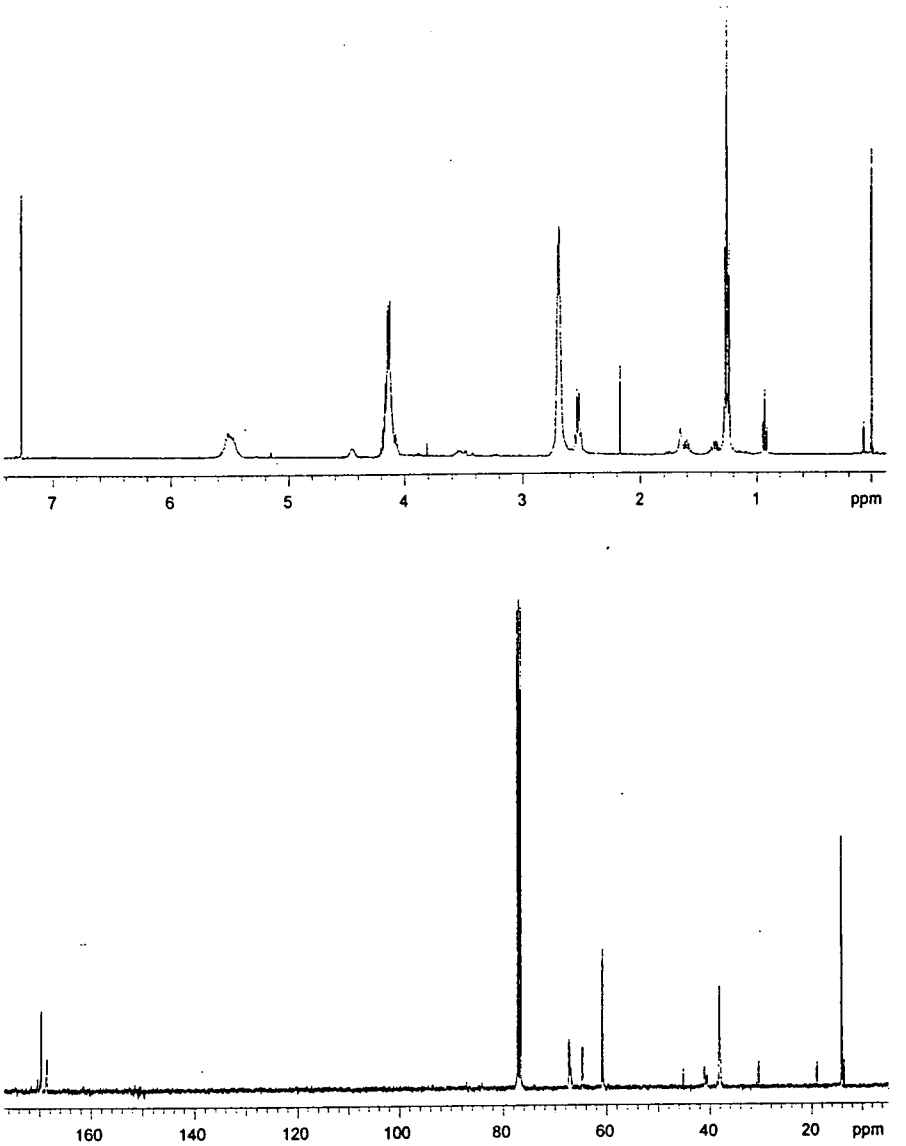

Figure 4.16 ^{1}H and ^{13}C nmr spectra of the product of the polymerisation of diethyl 3-hydroxyglutarate in the presence of 5wt% catalyst at 100°C for 5.5 hours.

On comparison of the ^{1}H and ^{13}C nmr spectra (Figures 4.15 and 4.16) of the 3.5 and 5.5 hour reactions there appear to be no anomalies indicative of side reactions having occurred. These observations are consistent with a competition between reactions leading to polymer growth (i.e. elimination of an alcohol unit) and degradation without introduction of a new structural feature; alcoholysis is an obvious candidate for the degradative step but the origin of the required alcohol is obscure. The immediate candidate for the source of the alcohol required for degradation is

hydrolysis of the titanium alkoxide by ingress of water, this seems unlikely since the reaction was continuously purged by dry nitrogen (activated molecular sieves).

In an attempt to investigate the polymerisation process in greater detail, MALDI-TOF MS analysis of the products was performed. Figure 4.17 shows the mass spectrum of the product of the 3.5 hour reaction.

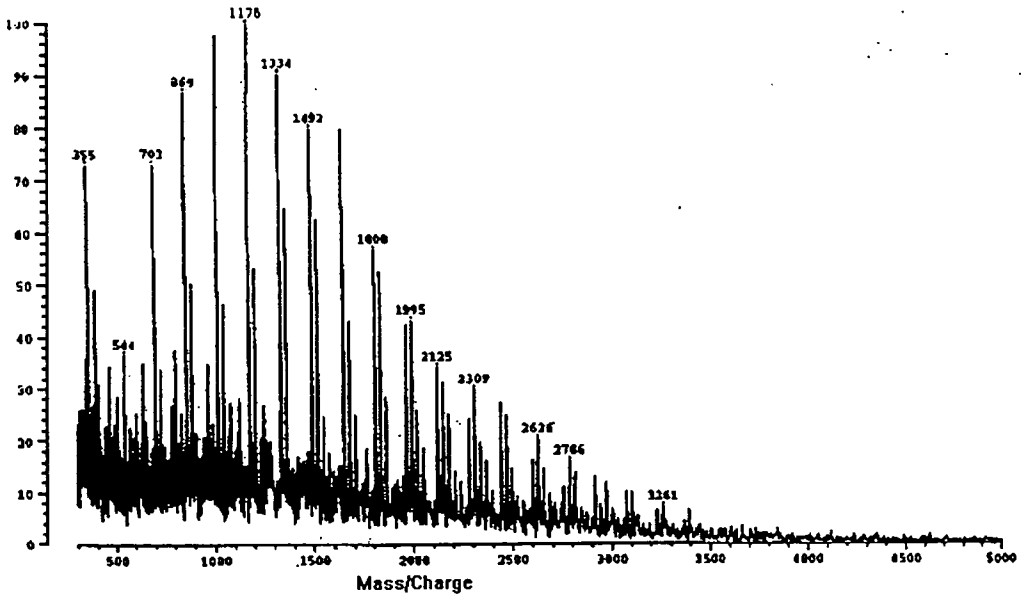

Figure 4.17 MALDI-TOF mass spectrum of poly(diethyl 3-hydroxyglutarate)

To assign all of the mass series present in the spectrum represented in Figure 4.17, it is necessary to determine all the possible side reactions which may have occurred during the polymerisation. During a typical step growth polymerisation process, one molecule of condensate will be eliminated during each monomer addition, hence for the first step in the polymerisation of diethyl 3-hydroxyglutarate, one molecule of ethanol will be produced as shown below:

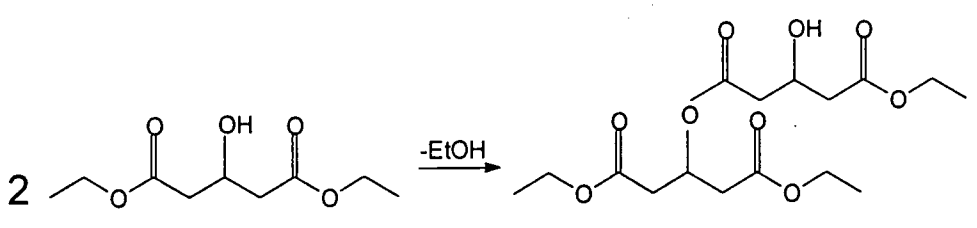

Figure 4.18

Hence the polymerisation process giving rise to a series of peaks in the mass spectrum may be represented as:

$$Y = n\text{M-}(n\text{-}1)\text{EtOH+x}$$

$$Y = n(\text{M-EtOH})+46+23$$

$$n = \frac{Y-69}{158} \qquad \text{(Eq. 4.1)}$$

Where Y is the observed peak mass from the spectrum, n is the number of monomer units, x is the molecular mass of the associated cation (in this case sodium=23), M is the monomer molecular mass (204) and the molecular mass of ethanol is 46. In this data analysis it is clear that n must be an integer, the signals in the recorded mass spectrum are only assigned to a specific process having occurred during polymerisation if the calculated n values lie within ± 0.06 of an integer. The value of 0.06 is arbitrarily chosen and examination of the accumulated data shows that the experimental fit is generally much better than ± 0.02.

As discussed in section 4.2 it would appear that as the polymerisation proceeds, the catalyst becomes less effective, possibly degraded, leading to a decrease in reaction rate, it is therefore postulated that transesterification side reactions may be responsible for the second and third mass series observed in the MALDI-TOF mass spectra. As the ^{1}H nmr spectrum exhibits signals corresponding to the hydrogens of butoxy groups, it was assumed that butoxide transesterification may be responsible for at least some of the additional mass series.

It has been calculated that the second series of peaks fits the following equation:

$$Y = n\text{M-}(n\text{-}1)\text{EtOH+x+}C_2H_4$$

$$n = \frac{Y-97}{158} \qquad \text{(Eq. 4.2)}$$

which corresponds to the transesterification process postulated above, in which only one butoxide has transesterified with an ethoxide.

A third mass series can be attributed to the exchange of two butoxides according to the following equation:

$$Y = n\text{M-}(n\text{-}1)\text{EtOH+x+2C}_2\text{H}_4$$

$$n = \frac{Y - 125}{158} \qquad \text{(Eq. 4.3)}$$

Other possible side reactions which may occur during the polyesterification of diethyl 3-hydroxyglutarate include cyclisation and dehydration, both of which would severely hinder the polymerisation by removing the reactive hydroxyl from the polymerising mixture. During the cyclisation process an additional molecule of ethanol will be eliminated as shown for the dimerisation below:

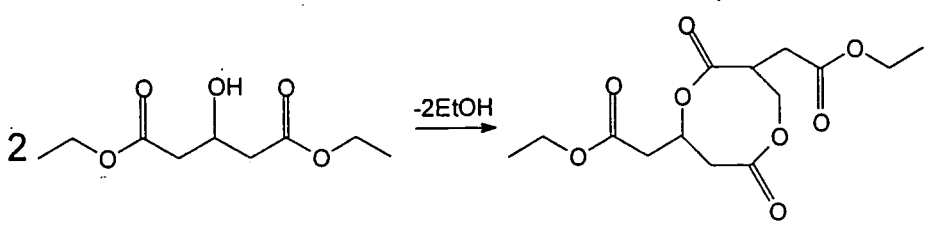

Figure 4.19

This process would give rise to a mass series calculated as follows:

$$Y = n\text{M-}n\text{EtOH+x}$$

$$n = \frac{Y - 23}{158} \qquad \text{(Eq. 4.4)}$$

A full listing of the analysis of MALDI-TOF MS results can be found in Appendix 2, Table 23, the major peaks in the spectrum (shown in italics) correspond to the full series of oligomers of a hyperbranched polymer from a trimer to twenty-one monomer units. These peaks are highlighted in bold type in the "Na+" column,

However, not all of the major peaks correspond with simple hyperbranched oligomers, the twelve, fourteen, sixteen, seventeen and twenty-mer most intense oligomer series correspond to the hyperbranched polymer containing one transesterified butoxide group. On inspection of the table it can be seen that masses corresponding to cyclisation occur for oligomers with n = 2, 3, 4, 5, 6 and 19 and that the major peak in the 19-mer set is due to a cyclic product. It seems reasonable to assume that cyclisation is the cause for the observed ceiling molecular weight of approximately 3000 Daltons. Interestingly, on inspection of Table 23 (Appendix 2) it can be seen that dehydration does not occur during the polymerisation as the signals required to prove this are not present in the MALDI mass spectrum.

Table 4.3 below is an extract from Table 23, Appendix 2. It is clear from this that additional signals are present in the mass spectrum.

	Na+	BuO	2 BuO	Cycl.
Peak mass	*n*	*n*	*n*	*n*
348	1.77	1.59	1.41	**2.06**
355	1.81	1.63	1.45	2.10
400	2.09	1.92	1.73	2.39
415	2.19	**2.01**	1.83	2.48
471	2.54	2.37	2.18	2.84
506	2.77	2.59	2.41	**3.06**
544	**3.01**	2.83	2.65	3.30
607	3.41	3.23	**3.04**	3.70
638	3.60	3.42	3.24	3.89
645	3.65	3.47	3.28	**3.94**
702	**4.01**	3.83	3.65	4.30
731	4.19	**4.01**	3.83	4.48
794	4.59	4.41	4.23	4.88
809	4.68	4.51	4.32	**4.97**
860	**5.01**	4.83	4.65	5.29
882	5.15	**4.97**	4.78	5.44

Table 4.3 Expansion of Table 23, Appendix 2.

On careful analysis of the data, it has been found that some of these signals correspond to three butoxide groups transesterifying with the ethoxide groups of the hyperbranched polymer. Incorporation of three butoxide groups into the polymer

have been found for four, five, twelve, thirteen and fourteen-mers. The signals at 355, 400 and 638 Daltons are the only mass peaks which have not been identified, it is possible that they correspond to the very small degree of fragmentation occurring in this form of mass spectrometry.

In an attempt to provide support for the concept of self-termination *via* cyclisation in the formation of poly(diethyl 3-hydroxyglutarate) several structures were examined using computer-assisted molecular modelling. This is becoming a widely used technique in the study of polymers.[12] Molecular modelling covers a wide variety of procedures including *ab initio* quantum mechanical calculations and forcefield approaches for predicting structures and properties of isolated molecules, and a number of Monte Carlo methods used in larger scale simulations of large molecules and assemblies. However in the following section, only molecular mechanics and molecular dynamics calculations will be discussed. Molecular mechanics explores the static characteristics of a configuration of atoms, i.e. the time evolution of the configuration is not considered. Transition states, equilibrium structures and harmonic vibrational frequencies may be determined using molecular mechanics. However, molecular dynamics solves the equations of motion for a given configuration, hence this process represents the time evolution of molecular motions. To appreciate the value of molecular dynamics one must first consider molecular mechanics.

The co-ordinates of the molecule on a potential energy surface and the forcefield data are combined to give an expression for the energy of the molecule. This expression (outlined below) is an equation which describes the potential energy surface as a function of its co-ordinates.

$$E_{total}=E_{bonded}+E_{angle}+E_{tortional}+E_{nonbonded}$$

The forcefields used in molecular mechanics utilise interatomic distances to describe the electrostatic and van der Waals (i.e. non-bonded) interactions between atoms and the internal co-ordinates (bond distances, torsional and bond angles) to describe the bonded section of the potential energy surface. A forcefield is considered successful if it is applicable to the description of several classes of molecules with

reasonable accuracy. That is to say its predictions are tested against molecules with known structures.

The potential energy surface is then utilised to find the minimised structure for a given configuration of atoms. The minimised structure represents the conformation about which fluctuations occur during molecular dynamics. To determine the minimised conformation, an algorithm must be applied. The first step is to define an equation which describes the energy of the conformation as a function of its co-ordinates, this equation is then evaluated and the conformation is subsequently adjusted to lower the value of the energy expression of the molecule. The minimisation process is iterative and the number of iterations required to find a minimum is dependent on the nature of the algorithm, the size of the molecule and the form of the energy expression.

The algorithm used in the minimisation of the hyperbranched macromolecules is the Steepest Descent algorithm of the BioSym molecular mechanics package. This method is extremely robust and may be used in highly strained systems, however one disadvantage is that convergence to a minimum may be slow. Energy minimisation however, has a major disadvantage; the structure it obtains as a minimum may not be the global minimum structure. The algorithms locate a minimum which is related to the starting conformation; they do not explore higher energy conformations, hence the 'minimised' structure may only be a local minimum.

Molecular dynamics may be used to ensure that the global minimum is achieved. The technique solves the equations of motion for the configuration of atoms, this represents the time evolution (trajectory) of the molecular motions of the configuration. Hence molecular dynamics allows molecules to cross energy barriers (maxima) and explore other stable conformations, one of which may be the global minimum.

A disadvantage of molecular dynamics with current hardware is the time scale of the trajectories. At the moment, simulations are limited to only a few nanoseconds, or often much less, whereas actual transitions of interest may occur on the scale of milliseconds or even minutes in the case of polymers. However, molecular dynamics has proved a useful tool in the simulations of polymers when used in conjunction with

appropriate building techniques. Both amorphous[13] and crystalline[14,15] phases of linear polymers have been modelled and a variety of properties calculated.

Polymer analysis by MALDI-TOF MS had indicated that, although low mass oligomers (n = 2, 3, 4, 5, 6) gave peaks associated with cyclisation, intermediate sized molecules showed no tendency to cyclise except for the 19-mer. Therefore it seemed appropriate to investigate this molecule. As a first approximation, five structures were constructed from 19 monomer units in a systematic procedure to give an oligomer with a degree of branching of 0.58. It can be envisaged that there are a myriad of possibilities for the number of different configurations which would possess a DB of 0.58, but limitations of computing time restrict the extent of the investigation. In total five molecules were constructed and minimised, however only one, chosen at random, was submitted to a molecular dynamics simulation. Figure 4.20 below shows the two dimensional representation of the 19-mer before the simulation. For the purposes of this discussion we define 10 exterior terminal functional groups (highlighted in blue) and 10 interior terminal functional groups (highlighted in green).

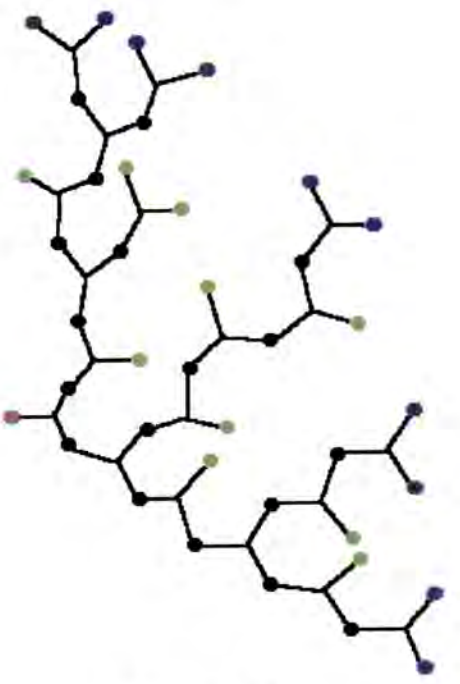

Figure 4.20

As the reaction temperature is 100°C, the simulation was performed at 373K for 100,000 steps. It was clear, from the simulation, that only the inner groups came within bonding distance of the focus. Figure 4.21 shows frame 38 of the dynamics simulation. This conformation highlights the possibility of cyclisation occurring between an ethyl ester and the hydroxyl focus of the hyperbranched wedge. The distance between the carbonyl carbon and the hydroxyl oxygen is only 3.34Å which implies that the atoms are close enough for bonding to occur.

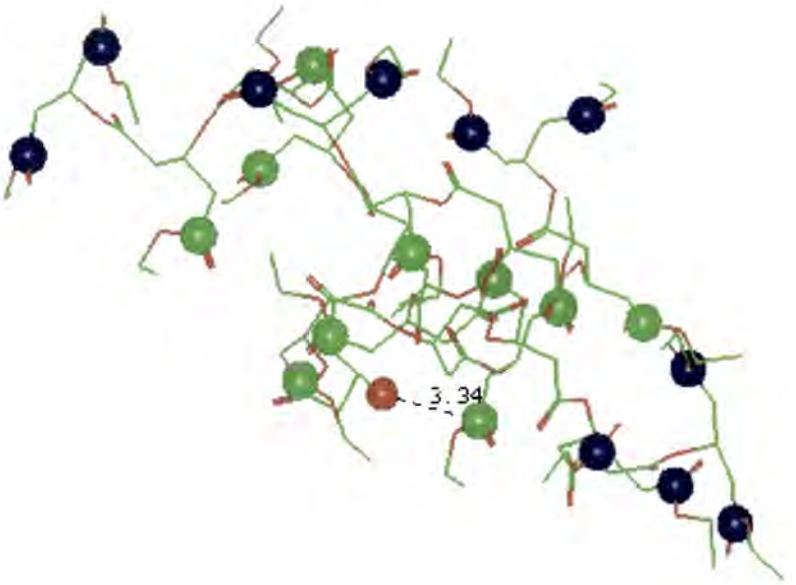

Figure 4.21

This modelling procedure merely shows that cyclisation may be possible. It is impossible to unequivocally prove that cyclisation of a 19-mer will occur as the extact structure of the oligomer undergoing cyclisation can never be absolutely confirmed. This molecular modelling approach demonstrates that it is not unreasonable to expect cyclisation in aliphatic hyperbranched structures based on diethyl 3-hydroxyglutarate. The question remains, why does cyclisation not occur for every oligomer? Modelling studies were performed on cyclic molecules of diethyl 3-hydroxyglutarate of various sizes. Ring formation was shown to be possible for many structures. It may be postulated that, above a certain size, the bulk of the polymer encourages cyclisation through constraint of the inner terminal groups in the vicinity of the focus, therefore

inducing cyclisation. However, cyclisation was also observed for low molecular weight oligomers. The formation of hyperbranched polymers provides a mixture of numerous molecules with the same DP, but with differing isomeric structures, hence it may be deduced that some structures will favour cyclisation whilst others will not and it is not at all clear why the cyclisation route appears to be favoured for a specific set of oligomers.

In summary, this molecular modelling exercise supports the hypothesis that cyclisation is a reasonable process but did not really provide any insight into the apparent size selectivity of the process.

4.2.3 Variation of reaction temperature.

To determine the effect of reaction temperature on the molecular weight of the hyperbranched polymer, three experiments were performed keeping the catalyst at 5wt% (of the mass of the monomer) and duration of reaction at 4.5 hours. The chosen temperatures were 100, 115 and 125°C. It was decided that 100°C would be the lower limit as it was anticipated that working below this temperature would merely make the removal of the eliminated ethanol more difficult, hence possibly increasing the number of butoxide groups per molecule. The table and graph overleaf summarise the results.

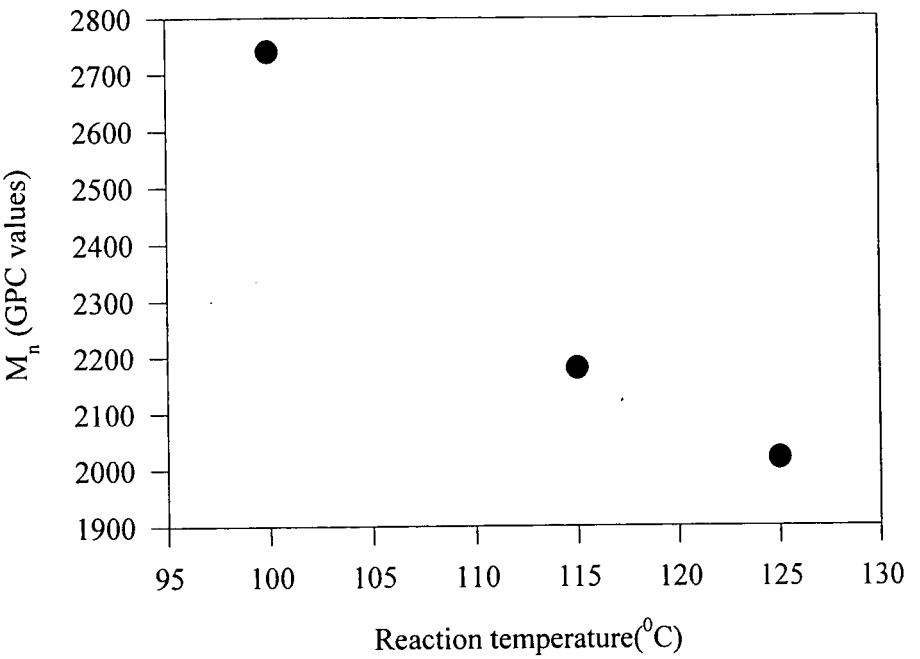

Figure 4.22 Graph showing the relationship between M_n (determined by GPC using $CHCl_3$ as eluent and linear polystyrene standards) and reaction temperature.

Temperature (°C)	M_n[a]	%BuO[b]	DB[c]
100	2740	6.8	0.54
115	2180	7.3	0.57
125	2020	7.9	0.57

a As determined using GPC with $CHCl_3$ as eluent and linear polystyrene standards
b Mole percent of butyl ester groups
c As determined *via* ^{13}C nmr spectroscopy

Table 4.4 Summary of the variance of M_n with temperature for the products of the polymerisation of diethyl 3-hydroxyglutarate

From the results listed in Table 4.4, it would appear that an increase in temperature induces a very slight increase in the degree of branching, an increase in

the extent of alkoxy exchange and a significant molecular weight decrease. We observed earlier that there is a decrease in molecular weight with increased reaction time (section 4.2.2) and with this result we see that there must be an optimum time and temperature range for maximising the molecular weight of the polymer. It seems, therefore, that there must be a competition between polymerisation and degradation which is complicated by the effects of alkoxy exchange and catalyst degradation.

If the exchange reaction depended upon the presence of butanol produced by hydrolysis of the catalyst in the reaction vessel, an increase in temperature would allow facile removal inducing a decrease in the amount of butanol available for transesterification. As the percentage of incorporated butoxide actually increases with an increase in temperature, it may be deduced that the mechanism for the transesterification of butoxide does not involve free alcohol but most probably occurs *via* direct interaction with the catalyst.

4.2.4 Comparison of the molecular weights as determined via nmr, MALDI-TOF MS and GPC.

In an attempt to estimate the validity of the determination of the molecular weight of these hyperbranched polymers using GPC (with $CHCl_3$ as eluent and linear polystyrene standards), a graph of M_n versus the relative integrals of the CH_2 signals of the terminal, linear and branched sub-unit hydrogens at 2.69ppm to the CH_2 signals of the focal sub-unit protons (2.54ppm) was plotted. The data points lie on an approximate straight line, correlation coefficient 0.84, indicating a reasonably good correlation between the two methods of determining M_n. The nmr method is expected to be reliable only at relatively low M_n.

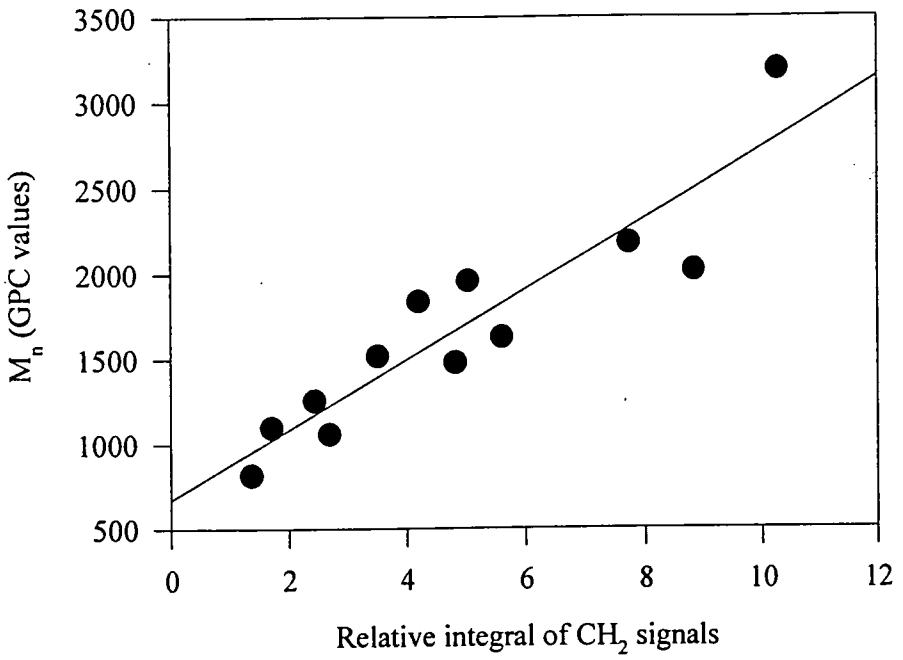

Figure 4.23 Graph showing the correlation of M_n determined *via* GPC using $CHCl_3$ as eluent and linear polystyrene standards.

In theory, the number average degree of polymerisation of these hyperbranched polyesters may be determined from the ^1H nmr data in two ways. As the spectra are fully assigned, it should be possible to calculate the number average molecular weight using the relative integrated intensities of both the CH_2 signals and the CH-O- signals. The number of CH_2 hydrogens due to the focal sub-unit can be normalised to one, as for every wedge there will only be one focal unit if cyclisation does not occur. Using this assumption the molecular weight can be determined by comparing the integrated intensities of the coincident multiplet of the terminal, linear and branched CH_2 sub-units with that of the focal sub-unit. An analogous process can be applied to the CHO- resonances. For every n monomers which react together, n-1 molecules of ethanol are eliminated, hence a general equation relating degree of polymerisation and molecular weight may be formulated as shown overleaf:

$$mw=204n-46(n-1) \qquad \text{(Eq. 4.5)}$$

where 204 is the monomer mass and 46 is the mass of ethanol.

Table 4.5 below lists the average molecular weights as determined by GPC (both $CHCl_3$ and THF as eluents calibrated using linear polystyrene standards), MALDI-TOF MS and ^1H nmr. The values in column A are calculated from the relative integrated intensities of the C**H**$_2$ signals of the focus with those of the terminal, linear and branched sub-units, whilst those in column B are calculated from the relative integrated intensities of the C**H**-O- signals of the focus with those of the remaining sub-units.

GPC data			^1H nmr data	
$M_n(CHCl_3)$	M_n(THF)	M_n(MALDI)	A (CH_2)	B (CHO-)
3190	2240	-	1990	2070
2740	3150	1870	2390	2570
2180	1780	1200	1480	1780
2030	1510	1110	1240	1570
2020	1300	1150	1670	2120
1960	1410	1190	1000	1070
1840	950	1100	870	990
1630	1800	1180	1090	1250
1520	960	1230	760	850
1480	1350	1090	970	1220
1260	730	920	590	600
1100	720	980	470	470
1060	650	800	630	680
820	390	720	420	440

Table 4.5 Summary of molecular weight results obtained for a series of poly(diethyl 3-hydroxyglutarate) using different procedures.

In general, although the scatter is quite large, the MALDI-TOF results compare most favourably with the ^1H nmr results, it is clear that the discrepancies between the GPC results, when using either $CHCl_3$ or THF as eluent, and those obtained from MALDI-TOF MS are generally larger. A discrepancy between the GPC results is not unexpected as this technique is highly size and shape dependent. It may be deduced that THF encourages hyperbranched poly(diethyl 3-hydroxyglutarate) to contract into a smaller, more globular shape than $CHCl_3$, this would give a smaller hydrodynamic volume and longer retention time with consequent assignment of a lower molecular weight. Thus, $CHCl_3$ is a better solvent for these polymers than THF which is qualitatively borne out by the ease of dissolving them.

It was anticipated that the results determined *via* GPC would be smaller than those determined via other methods. As the hydrodynamic volumes of hyperbranched polymers are expected to be smaller than their linear analogues, it was assumed that GPC would underestimate the M_n of hyperbranched macromolecules. However, from the results listed in Table 4.5, the molecular weights found using GPC are generally larger than those determined via MALDI-TOF MS and nmr. This result is puzzling, however may be explained as MALDI-TOF MS has been found[16] to give M_n values skewed to low molecular weight. This is thought to be due to the MALDI process preferentially volatising the lower molecular weight species. If this is true, the MALDI results may be expected to be lower than the true molecular weight, i.e. pessimistic. On the other hand we know there is some cyclisation removing focal groups so the nmr analysis ought to be optimistic. It can be seen that there are slight variations in the molecular weights calculated via nmr analysis, but they are generally lower than GPC but higher than MALDI values. Hence it would appear that all the values listed in Table 4.5 are subject to errors and as such should not be considered as absolute values but rough indications of molecular size.

4.3 ENZYMATIC POLYMERISATION OF DIETHYL 3-HYDROXYGLUTARATE.

As discussed in the beginning of this chapter, linear polymers are expected to possess different properties than their hyperbranched analogues. In an attempt to investigate this, a procedure was sought which would allow the synthesis of linear poly(diethyl 3-hydroxyglutarate). A review of the literature suggested that a possible method would involve the use of enzymes.

Enzymes are currently used to synthesise linear aliphatic polyesters from hydroxy acids[17] and hydroxy esters,[18] however this area has not been extensively developed yet. It has been reported[19] that dimethyl 3-hydroxyglutarate can be polymerised in the presence of several enzymes. The reaction is very slow, requiring ten days to produce a trimer, however as enzymes are able to positively discriminate between enantiomeric groups of a prochiral AB_2 molecule, a linear enantiomeric polyester may ultimately be formed. Since these results were so close to the linear polymer synthesis desired it was decided to make an attempt to use enzymes for the synthesis of a linear polyester, the general method outlined by Gutman[19] was followed. As it has been reported[18] that an increase in temperature increases the DP of polyesters, the reaction temperature was increased to 55°C from 40°C. The reaction was performed using a suspension of "porcine liver acetone powder" (which is a complex extract containing, *inter alia*, porcine lipase) in hexane and diethyl 3-hydroxyglutarate in a thermostatted chamber for 10 days. The author is indebted to Dr. D. O'Hagan for supervision of this aspect of the work. To recover the material, the suspension containing the enzyme and product was filtered, giving a brown filtrate. The residue was washed with cold chloroform to remove any unreacted monomer, the solvents were then removed from the combined organic extracts to give a mobile brown liquid for analysis. On nmr analysis, the filtrate was found to be unreacted monomer (40% recovery) indicating that the reaction is not very efficient.

In an attempt to recover higher oligomers from the solid residue, it was added to chloroform and the mixture refluxed for an hour, after filtration and solvent evaporation the slightly viscous brown fluid was analysed by MALDI-TOF (Appendix 2, Table 24) to show a mixture of, trimers and tetramers, as well as two

cyclic species (dimer and tetramer) and dehydrated species (dimer, trimer and tetramer). Separation of the linear products was attempted using the chromatographic method given by Gutman[19] for the dimethyl analogue. It was found that a 95:5 ether:hexane solution did not give separation using preparative t.l.c., therefore a range of solvents and solvent mixtures were tried. All either produced a "streak" or failed to move the components. As separation could not be achieved, ^{13}C nmr analysis was performed to assess the success of producing linear oligomers. The multiplet at 67ppm, usually due to hyperbranched formation, was replaced by a singlet with a slight shoulder to high field. The shift of this signal corresponds to linear sub-units. Surprisingly there were no observable signals for the terminal sub-units, however this may be due to a poor S/N ratio. The ^{1}H nmr spectrum shows the expected multiplets for oligomer formation at 5.57ppm (CH-O-) and 2.70ppm (CH_2CH-O-). As separation of the constituent species cannot be achieved it was decided to leave this line of investigation. It would appear that linear oligomers of the condensation product of diethyl 3-hydroxyglutarate have formed to a very small extent, therefore this reaction is not suitable for the production of linear analogues of hyperbranched poly(diethyl 3-hydroxyglutarate), hence a direct comparison of the properties of linear and hyperbranched polymers was thwarted.

4.4 GLASS TRANSITION TEMPERATURES OF HYPERBRANCHED WEDGES.

The glass transition theory for linear polymers is well known and understood, however dendrimers and hyperbranched molecules provide a new challenge to existing theories. The glass transition of linear polymers increases as molecular mass increases until it reaches a maximum value, $T_{g\infty}$. The equation below shows the relationship between T_g and $T_{g\infty}$.

$$T_g = T_{g\infty} - K/M_n \qquad \text{(Eq. 4.6)}$$

where K is a constant.

A plot of T_g *vs.* $1/M_n$, based on the previous equation, allows us to calculate $T_{g\infty}$ and K from the intercept and slope of the graph respectively. Highly branched polymers are assumed not to follow the previous relationship due to the large number of end groups present in the polymer. Fréchet[20] has proposed equation 4.7 to account for the observed T_g's of dendrimers and to take into account the considerable number of end groups:

$$T_g = T_{g\infty} - K'(n_e/M_n) \qquad \text{(Eq. 4.7)}$$

$$\text{where } K' = \rho N\theta/\alpha$$

(where ρ is the chain end density, N is Avagadro's number, θ is the chain end free volume, α is the free volume expansion coefficient and n_e is the number of chain ends.)

As can be seen in Figure 4.24, a linear dependence of T_g on $1/M_n$ is shown for the diethyl 3-hydroxyglutarate hyperbranched polyester (correlation coefficient R=0.76), although it should be noted that the molecular weight range examined for this polymer is relatively small. Thus, it appears at first sight that this narrow molecular weight range hyperbranched system resembles linear polymers rather than dendritic polymers since no account of the number of chain ends, chain end free volume or density effects have been included. Alternatively, it may be concluded that these effects cancel out in this particular system.

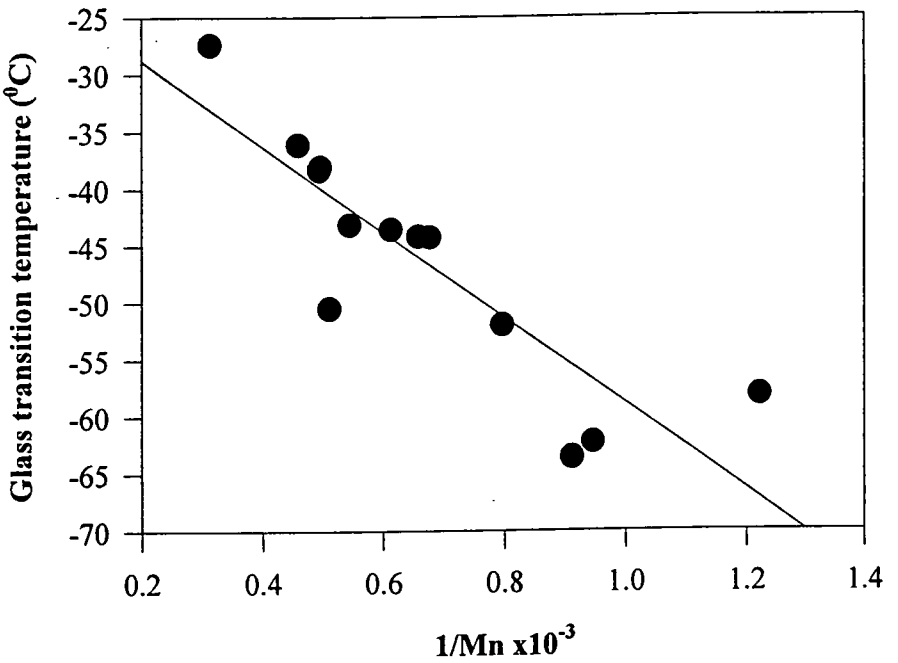

Figure 4.24 Graph showing the relationship between T_g and reciprocal molecular weight (as determined by GPC)of hyperbranched wedges.

Terminal groups on the periphery of the molecule must have a larger free volume than those within the bulk polymer. As a consequence of the extensive branching of hyperbranched polymers, the free volume of chain ends must decrease with increasing molecular mass due to the increasing amount of chain ends being trapped inside the wedge. Hence the decrease in chain end free volume with increasing M_n is quite plausible for hyperbranched systems. The variation of chain end density is much more difficult to predict because of the variety of isomeric hyperbranched structures possible.

Several authors[21,22] have reported very little variance in T_g with number average molecular weight. Perhaps the most notable invariance was found in hyperbranched polyphenylenes[21] where the T_g remained at approximately 240°C in the M_n range of 2000-35000. It is clear, from Figure 4.24, that the glass transition temperature is dependant on M_n, as intuitively expected. Similar findings have been

reported[20] for dendrimers, where T_g increases with generation number and hence molar mass.

4.5 INTRINSIC VISCOSITY OF POLY(DIETHYL 3-HYDROXYGLUTARATE).

The viscosity of dilute polymer solutions depends on several variables: the concentration of the polymer, the nature of the polymer and the solvent, M_n and temperature. In very dilute polymer solutions the limiting viscosity number, [η], also known as the intrinsic viscosity, is defined as:

$$[\eta] = \lim_{c \to 0} \frac{\eta_{sp}}{c} \qquad \text{(Eq. 4.8)}$$

where c is the polymer concentration and η_{sp} is the specific viscosity, i.e. $(t-t_0)/ct_0$ where t_0 is the time taken for the pure solvent to run through the viscometer and t is the time taken for the polymer solution to run through the viscometer.

The evaluation of [η] greatly simplifies the interpretation of experimental results as it effectively eliminates intermolecular polymer-polymer interactions and several factors such as the presence of branching in linear polymers, molecular dimensions and molecular weight have been related to [η]. An empirical relationship between molecular weight of the polymer and the intrinsic viscosity was derived by Mark and Houwink[21] in 1940:

$$[\eta] = KM^a \qquad \text{(Eq. 4.9)}$$

where K and a are constants for a particular polymer-solvent pair at a designated temperature.

Generally, a graph of log[η] *vs.* log(M) is plotted which shows a linear dependence, hence K and *a* can be easily extracted. These plots are essentially linear over large ranges of M_n however it has been found[24,25,26] that deviations from linearity occur at low masses.

Branched polymers usually exhibit lower viscosities than linear molecules of the same molecular weight, due to their smaller hydrodynamic volume. Branching may be determined from the *a* values obtained from a Mark-Houwink plot. Linear polymers generally have values of *a* exceeding 0.5, whilst lower values are obtained for branched systems. Hence for hyperbranched molecules it is anticipated that the *a* values will lie between 0 and 0.5.

4.5.1 Determination of intrinsic viscosity

Initially 15ml of a polymer stock solution ($0.1 gdL^{-1}$ in dichloromethane) was transferred to an Ubbelohde viscometer, thermostated at 25°C and several time of flow readings recorded. When the standard deviation was deemed small enough the stock solution was diluted using dichloromethane (10ml) and the procedure repeated. In total four dilutions were made. Graphs of *b* (see below) *vs.* concentration are plotted to give straight lines which allow the intrinsic viscosities to be determined from the intercepts.

$$a = \frac{t - t_0}{t_0} \qquad \text{(Eq. 4.10)}$$

$$b = \frac{a}{conc.} \qquad \text{(Eq. 4.11)}$$

The graph overleaf shows the results obtained from the intrinsic viscosities of the hyperbranched wedges. The values of [η] obtained were all very small, in the range 0.01 to 0.05, as is expected for relatively low molecular weight hyperbranched structures.

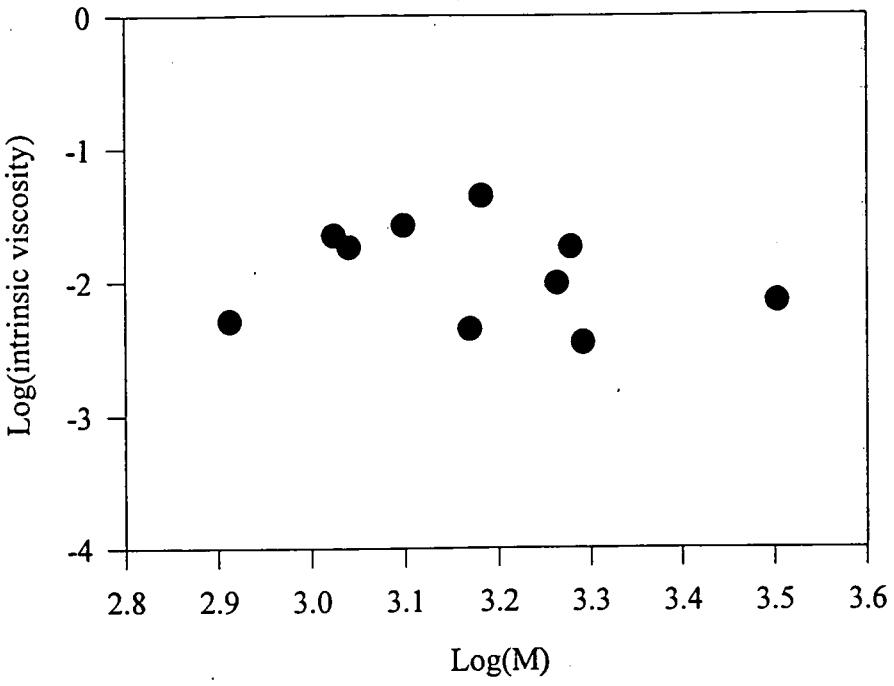

Figure 4.25 Graph showing the relationship between log[η] and log(M) where M is determined by GPC using $CHCl_3$ as eluent and linear polystyrene standards

A linear dependence has been shown for aromatic hyperbranched polyesters,[27] where the extracted *a* constants lie between 0.3 and 0.4 for these systems indicating a highly branched structure. However, it can be seen that a linear dependence is not shown by the aliphatic hyperbranched polyesters represented above, indeed a least squares fit to these data give a correlation coefficient of 0.6 and a negative value for the slope, i.e. *a* in the Mark-Houwink equation. Such results are virtually meaningless although a very low value for *a* is consistent with a hyperbranched structure. The scatter and low molecular weight values mean that no firm conclusions can be based on these data.

4.6 CONCLUSIONS

The formation of hyperbranched aliphatic polyesters via a condensation step-growth mechanism, has been shown to be moderately successful. The molecular weights found for poly(diethyl 3-hydroxyglutarate) have been disappointing, however it has been shown that the polymerisation is "self-terminating". MALDI-TOF MS has proved to be an invaluable tool in the determination of the structures of oligomers for this system, whilst ^{13}C nmr spectroscopy provided a method for the determination of the DB. The degrees of branching of these polymers have been found to lie between 0.48 and 0.57 indicating hyperbranched formation.

Some controversy over the determination of M_n has been discussed and it has been concluded that all methods examined for the molecular weight determination are subject to errors and uncertainties of interpretation, hence it is impossible to report an absolute value of M_n for this system. The glass transition temperatures have been found to be dependent on the reciprocal molecular weight, whilst the viscosity results appear to be anomalous due to the low molecular weight of these compounds.

Therefore there seems little doubt that hyperbranched polymers have actually been formed, however their full analysis has been hampered by the low molecular weights attained.

4.7 EXPERIMENTAL

All organic reagents were purchased from Aldrich Chemical Co. and used without further purification. IR spectra were recorded on a Perkin-Elmer 1600 series FTIR. ^{1}H and ^{13}C nmr spectra were recorded on a Varian 400MHz spectrometer and were referenced to internal Me_4Si. DSC measurement were recorded using a Perkin Elmer DSC7, at a scanning rate of $10°Cmin^{-1}$. GPC was performed using a Viscotek differential refractometer as detector with two mixed PL-gel columns (10μm) and THF as eluent or using a Waters differential diffractometer three PL-gel columns (exclusion limits 100,10^3 and 10^5Å) as detector and $CHCl_3$ as solvent. Columns were calibrated using polystyrene standards (Polymer Labs). Viscometry measurements were taken using a Schott-Geräte Ubbelohde viscometer (bore size 0.46mm) immersed in a constant temperature water bath at 25°C.

4.7.1 General polymerisation procedure.

Diethyl 3-hydroxyglutarate (2g, 9.8mmol) was mixed with titanium (IV) butoxide in the glass reaction vessel. The vessel was lowered into a pre-heated oil bath and the temperature ramped up to the desired polymerisation temperature. The reaction remained at that temperature for a pre-determined length of time and a vacuum was applied (10mmHg) for the final 30 minutes of the reaction. After reaction, the yellow, viscous liquid was dissolved in chloroform and the solution washed with water to remove the catalyst. The organic layer was collected and the solvent removed under reduced pressure. The final traces of solvent were removed by placing the product in a vacuum oven for 4 hours at 35°C.

4.7.2 Transesterification of ethanol in the presence of $Ti(OBu)_4$.

Ethanol (45ml) was added to titanium (IV) butoxide (2.5g, 7.4mmol) and the reaction refluxed overnight. The solvent was removed under reduced pressure and the yellow liquid (2.37g) analysed.

^1H nmr ($CDCl_3$, 400MHz) δ 0.94ppm (t, J=7.2Hz, 3H, butyl CH_3), 1.25ppm (t, J=6.8Hz, 1.2H, ethyl CH_3), 1.38ppm (s, 8.0Hz, 3.1H, butyl CH_2), 1.56ppm (p, J=8.0Hz, 1.7H, butyl CH_2), 3.66ppm (t, J=6.8Hz, 1.1H, butyl OCH_2), 3.72ppm (q, J=7.2Hz, 0.5H, ethyl OCH_2). ^{13}C nmr ($CDCl_3$, 100MHz) δ 13.84ppm (butyl CH_3), 18.41ppm (ethyl CH_3), 18.88ppm (CH_2), 38.86ppm (CH_2), 58.48ppm (ethyl OCH_2), 62.76ppm (butyl OCH_2).

4.7.3 Transesterification of ethyl caprate in the presence of $Ti(OBu)_4$.

Ethyl caprate (1.963g, 9.8mmol) and titanium (IV) butoxide (0.1g, 0.3mmol) were heated at 100°C, under a stream of nitrogen, for 4.5 hours. When the reaction had cooled to room temperature, ethyl acetate was added and the solution poured into water. The two phase system was stirred vigorously for 30 minutes, the white solid was removed by filtration and the organic fraction collected. The solvent was removed under reduced pressure to yield a colourless product. This was distilled under reduced pressure to give one fraction: a mixture of starting material and product, bp 150°C, 0.6torr, 1.745g.

^1H nmr ($CDCl_3$, 400MHz) δ 0.88ppm (t, J=7.2Hz, 2.7H, ethyl CH_3), 0.94ppm (t, J=7.2Hz, 0.6H, butyl CH_3), 1.25ppm (t, J=6.8Hz, 14.7H, CH_2), 1.39ppm (t, J=7.2Hz, 0.5H, butyl CH_2), 1.62ppm (m, 2.5H, CH_2), 2.29ppm (t, 7.6Hz, 2H, $CH_2C=O$), 4.05ppm (t, J=7.2Hz, 0.4H, Butyl OCH_2), 4.12ppm (q, J=7.2Hz, 1.45H, ethyl OCH_2). ^{13}C nmr ($CDCl_3$, 100MHz) δ 13.73ppm (butyl CH_3), 14.12ppm (ethyl CH_3), 14.27ppm (ethyl CH_3), 19.17ppm (butyl CH_2), 22.69ppm (CH_2), 25.01ppm (CH_2), 25.05ppm (butyl CH_2), 29.17ppm (CH_2), 29.28ppm (CH_2), 29.44ppm (CH_2), 30.73ppm (butyl CH_2), 31.88ppm (CH_2), 34.42ppm (CH_2), 60.16ppm (ethyl OCH_2), 64.11ppm (butyl OCH_2), 173.94ppm ($C=O$).

4.7.4 Polymerisation of diethyl 3-hydroxyglutarate catalysed by enzymes.

Diethyl 3-hydroxyglutarate (1g, 4.9mmol) was added to a suspension of porcine liver acetone powder (1g) in dry hexane (25ml). The conical flask was sealed (to prevent solvent loss) and shaken at 200rpm for 10 days at 55°C. The monomer was recovered from the enzyme by filtration (0.4g, 40%), the oligomers were recovered by refluxing the enzyme in chloroform for one hour. The solid was removed by filtration and the filtrate was collected. The solvent was removed to give a mixture of oligomers (0.2g, 20%).

^{1}H nmr ($CDCl_3$, 400MHz) δ 1.27 (overlapping t, 30.3H, CH_3), 2.54 (m, 18.7H, CH_2CH-OH), 2.69 (m, 4.3H, CH_2CH-O), 4.16 (m, 18.3H, OCH_2), 4.46 (p, J=6.0Hz, 4.3H, CH-OH), 5.59 (m, 1H, CH-O).). ^{13}C nmr ($CDCl_3$, 100MHz) δ 14.02 (CH_3), 38.27 (CH_2CH-O), 40.50 (CH_2CH-OH), 41.06 (CH_2CH-O cyclic), 60.70 (OCH_2), 61.39 (OCH_2), 64.49 (CH-OH), 64.63 (CH-OH), 67.04 (CH-O), 171.70 (C=O).

4.8 REFERENCES

1. J. Berzelius, *Rapp. Ann.*, (1847), 26.
2. A.V. Laurenco, *Ann. Chim. Phys.*, **67**, (1863), 293.
3. W.H. Carothers et al, *J. Am. Chem. Soc.*, **51**, (1929), 2560; **52**, (1930), 711; **54**, (1932), 761, 1557, 1559.
4. P.J. Flory, *J. Am. Chem. Soc.*, **74**, (1952), 2718.
5. N. Ogata and S. Okamoto, *J. Polym. Sci., Polym. Chem. Ed.*, **11**, (1973), 1095.
6. Encyclopedia of Polymer Science and Engineering, 2nd Ed., (1989), Vol. 12, H.F. Mark, N.M. Bikales, C.G. Overberger and G. Menges, Wiley-Interscience.
7. Encyclopedia of Polymer Science and Engineering, 2nd Ed., (1989), Vol. 6, H.F. Mark, N.M. Bikales, C.G. Overberger and G. Menges, Wiley-Interscience.
8. E.R. Howells, *Chem. Ind.* (London), (1982), 508.
9. Metal Alkoxides, D.C. Bradley, R.C. Mehrotra and D.P. Gaur, Academic Press, 1978.
10. M.F. Lappert, *J. Chem. Soc.*, (1962), 542.
11. Comprehensive Polymer Science, Vol. 5:Step Polymerization, Chapter 17, (1989), G.C. Eastmond, A. Ledwith, S. Russo and P. Sigwalt, Pergamon Press.
12. Computer Simulation of Polymers, Ed. E.A. Colbourn, Longman Scientific and Technical, (1994).
13. U. Trommsdorff and I. Tomka, *Macromol.*, **28**, (1995), 6128.
14. D.N. Theodora and U.W. Suter, *Macromol.*, **18**, (1985), 1467.
15. M. Hutnik, F.T. Gentile, P.J. Ludovice, U.W. Suter and A.S. Argon, *Macromol.*, **24**, (1991), 5962.
16. R.S. Lehrle and D.S Sarson, *Polym. Degrad. Stab.*, **51**, (1996), 197.
17. D. O'Hagan and N.A. Zaidi, *Polymer*, **35**, (1994), 3576.
18. D. Knani, A.L. Gutman and D.H. Kohn, *J. Polym. Sci, Part A, Polym. Chem.*, **31**, (1993), 1221.
19. A.L. Gutman and D.H. Kohn, *J. Org. Chem.*, **54**, (1989), 5645.

20. K.L. Wooley, C.J. Hawker, J.M. Pochan and J.M.J. Fréchet, *Macromol.*, **26**, (1993). 1514.

21. Y.H. Kim and O.W. Webster, *Macromol.*, **25**, (1992), 5561.

22. E. Malmström, M. Johansson and A. Hult, *Macromol.*, **28**, (1995). 1698.

23. R. Houwink, *J. Prakt. Chem.*, **157**, (1940), 15.

24. G. Meyerhoff and B. Appelt, *Macromol.*, **12**, (1979), 968.

25. E.Cohn-Ginsberg, T.G. Fox and H.F. Mason, *Polymer*, **3**, (1962), 97.

26. U. Bianchi and A. Peterlin, *J. Polym. Sci., Polym. Phys. Ed.*, **6**, (1968), 1759.

27. S.R. Turner, B.I. Voit and T.H. Mourey, *Macromol.*, **26**, (1993), 4617.

Chapter 5.

The synthesis and characterisation of core-terminated aliphatic hyperbranched polyesters

5.1 INTRODUCTION

The synthesis of core-terminated hyperbranched polymers has received little attention thus far. The role of a core molecule is to react with the focus of the hyperbranched wedges to form a macromolecule resembling a dendrimer. The synthesis of core terminated polymers may take one of two routes. If the hyperbranched wedge is pre-formed, the synthesis of a core-terminated polymer will be analogous to the convergent[1] dendrimer methodology; whilst if the polymerisation is performed in the presence of a core molecule, the synthesis would be similar to the divergent[2] growth approach. In reality, if the core is present from the beginning of the polymerisation, it is anticipated that a hybrid divergent/convergent polymerisation will ensue. The core molecule may react with the monomer, but as the monomer is in large excess over the core-terminator, hyperbranched wedges will also form. These wedges may then couple to the core or may remain as wedges, the determining factors for these reactions will be the relative reactivity of the core molecule and the focus of the wedge and steric restrictions. If the convergent approach is utilised, the coupling reaction between the core and the focus of the wedge must be high yielding to encourage full core incorporation.

The formation of core-terminated hyperbranched polymers has, thus far, only been reported by two groups. Feast and Stainton[3] synthesised core-terminated aromatic polyesters whilst Malmström *et al*[4] produced aliphatic polyesters. The work reported by Stainton centred around the incorporation of a 1,3,5-trisubstituted aromatic ester with an AB_2 aromatic diester-alcohol. This paper refers to the core molecule as a "trifunctional terminator unit" implying that the hyperbranched growth will be impeded by the presence of core molecules. The copolymerisations were performed in ratios of 9:1, 21:1, 45:1 and 93:1 of the monomer to the core molecule to mimic the relative ratios of core molecule required to form consecutive generations of dendrimers prepared via a stepwise methodology. It was found that the masses of the resulting polymers are dependent on the amount of core present in the reaction vessel in the anticipated sense, i.e. the higher the core monomer concentration the lower the molecular weight.

(hydroxymethyl)-1,3-propanediol (255°C as opposed to 60°C) and the monomer has a melting point intermediate between the two (180-190°C). When 2-ethyl-2-(hydroxymethyl)-1,3-propanediol is used as the core, the solid monomer reacts with the molten core whereas when pentaerythritol is used as a core, the solid core slowly dissolves in the molten monomer. It is postulated that it is this dissolution behaviour which gives an increase in reaction rate in the case of pentaerythritol.

In this work, an attempt to produce core-terminated highly branched polymers, the core molecules were polymerised with the AB_2 monomer, diethyl 3-hydroxyglutarate, to produce "copolyesters". The ratio of core:monomer was varied to assess the effect of a core molecule on the properties and molecular weight of the hyperbranched polymer. It was hoped that the presence of a core would provide a method of circumventing the problem of the ceiling molecular weight by capping the reactive focus of the growing polymer. It was anticipated that the consumption of the focus by a core terminator would effectively prevent cyclisation which would encourage hyperbranched growth. By varying the molar ratio of core:monomer it was hoped that high molecular weight samples might be obtained. Additional investigations concerning the comparison of B_2 and B_3 aromatic cores were performed. The results discussed in the following sections are concerned with the full characterisation of core terminated aliphatic hyperbranched polyesters and the effects of the core molecule on the physical properties of the products.

5.2 INCORPORATION OF TRIMETHYL 1,3,5-BENZENETRICARBOXYLATE

The synthesis of core-terminated polyesters requires a B_x core molecule which should be highly reactive towards the AB_2 monomer to encourage core incorporation. It was anticipated that the use of aromatic cores would be advantageous in the determination of the percentage of core incorporation into the hyperbranched polymer. As poly(diethyl 3-hydroxyglutarate) is an aliphatic polyester, the resonances due to the core molecule, both in the ^1H and ^{13}C nmr spectra, will not coincide with the signals due to the wedges allowing degree of incorporation measurements to be performed. Trimethyl 1,3,5-benzenetricarboxylate [**1**] was anticipated to be reactive enough to allow preferential reaction with the monomer.

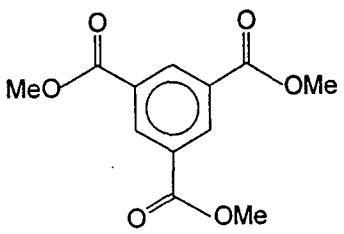

[**1**]

The synthesis of [**1**] was achieved by stirring benzene 1,3,5-tricarbonyl trichloride in dry methanol to give the product in good yield. The ^1H nmr spectrum exhibited only 2 signals; a singlet at 3.96ppm (OCH_3) and a singlet at 8.83ppm due to the aromatic hydrogens. It was anticipated that the percentage of the core incorporation could easily be determined by measuring the disappearance of the singlet at 3.96ppm relative to the resonances of the aromatic hydrogens. As it was expected that the hyperbranched polymer will induce a shift in the aryl signals, the sum of the intensities of the signals in the aromatic region of the ^1H nmr spectra should allow facile determination of the degree of core incorporation.

In total, four different ratios were used to assess the effect of an aromatic core molecule on the physical properties of the polymer. To ensure the results are reproducible, two experiments were repeated. The table overleaf summarises the M_n's

(as determined by GPC using linear polystyrene standards and $CHCl_3$ as eluent), glass transition temperatures and the DB's of the products. A full listing of all ^1H and ^{13}C nmr spectral data may be found in Appendix 3, Tables 1-6 and 20-22.

Ratio[a]	M_n[b]	T_g(°C)[c]	DB[d]
1:25	920	-45.6	0.58
1:50	710	-58.9	0.52
1:50	900	-51.7	0.60
1:75	870	-52.2	0.60
1:90	1150	-51.4	0.56
1:90	920	-53.3	0.61

a Molar ratio of core:monomer present at the start of the reaction
b M_n determined by GPC using linear polystyrene standards and $CHCl_3$ as eluent
c As determined *via* DSC
d As determined *via* ^{13}C nmr spectroscopy

Table 5.1 Summary of glass transition temperatures and degrees of branching of core-terminated aliphatic hyperbranched polyesters.

It is clear that the ratio of core:monomer does not effect the molecular weight to any appreciable extent. This is in direct contrast to those results obtained by Hult[4] and Feast.[3] In those studies, as the degree of incorporation decreased, an increase in the molecular weight was observed. The results reported by the author in this section may be complicated by possible transesterification of the core with the condensate, ethanol. As the experiments were all performed under the optimum conditions for the formation of a hyperbranched wedge (5wt% $Ti(OBu)_4$, 100°C for 270 minutes), it can be deduced that the presence of a core molecule has the effect of significantly lowering the molecular weight. On comparison of the glass transition temperatures with those found for hyperbranched wedges of poly(diethyl 3-hydroxyglutarate), those of the core terminated samples are slightly higher than those for the wedges of similar molecular weight as is illustrated in the graph overleaf:

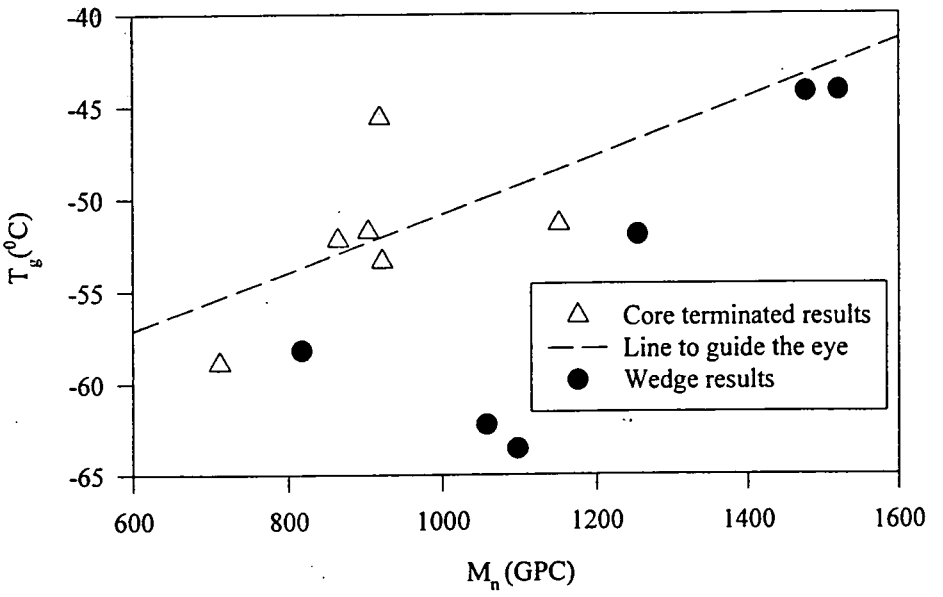

Figure 5.2 Graph comparing the T_g's of the core-terminated samples and those of analogous hyperbranched wedges.

The apparent increase in T_g for the core-terminated species may indicate the incorporation of the core molecule as it was anticipated that the aromatic core would increase the glass transition temperature of the system due to the induced conformational rigidity.

To ensure that the above assumption is correct, it is necessary to calculate the success of the coupling reaction. Careful scrutiny of the ^1H nmr spectra provide several interesting findings. Figure 5.3 overleaf shows the ^1H nmr spectrum of the product obtained using a core:monomer ratio of 1:90.

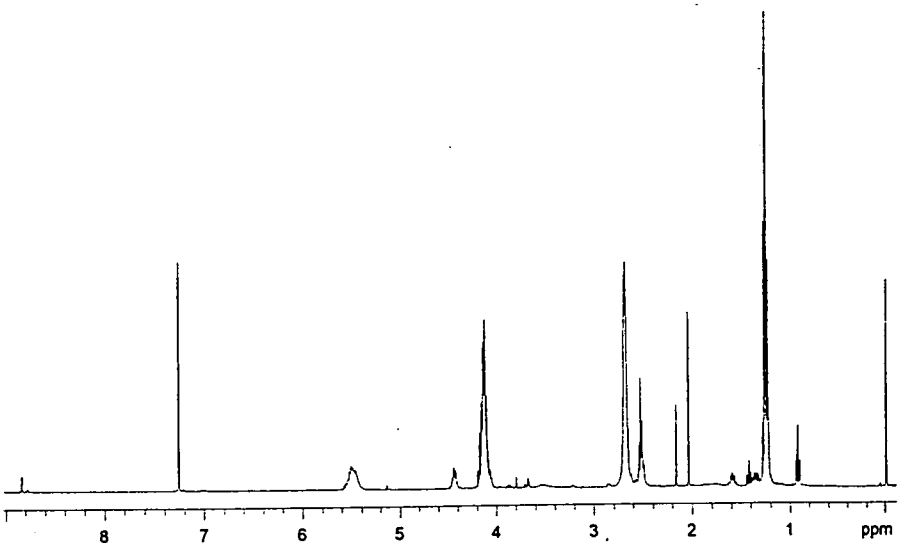

Figure 5.3 ^{1}H nmr spectrum of a core-terminated hyperbranched polyester.

On inspection of Figure 5.3, it is clear, by comparison with earlier work (Chapter 4), that the expected hyperbranched signals are observed. The ethyl ester signals are clearly visible at 1.26 and 4.14ppm (CH_3 and OCH_2 respectively), whilst the signals assigned to the methylene groups at the focus and those of the terminal, linear and branched sub-units are observed at 2.54 and 2.69ppm respectively. The multiplet at 5.54ppm denotes hyperbranched formation and is assigned to the CH of the terminal, linear and branched sub-units. The minor resonances observed at 0.93, 1.33 and 1.60ppm are due to the hydrogens of the transesterified butyl ester groups. On close inspection of the aromatic region, Figure 5.4, a multiplet is observed at 8.78ppm and is assigned to the hydrogens of the aromatic core which is bound to one or more wedges, whilst two singlets are observed at 8.846 and 8.836ppm. These singlets are tentatively assigned to ethyl esters formed by exchange between the condensate and the core molecule. The line widths of these of these latter signals are qualitatively narrower than the other aromatic hydrogen signals consistent with their association with an unbound aromatic residue. If this analysis is correct, it implies that exchange between the condensate and the 1,3,5-trimethyl ester is facile and effectively ties up the catalyst in a non-productive side reaction.

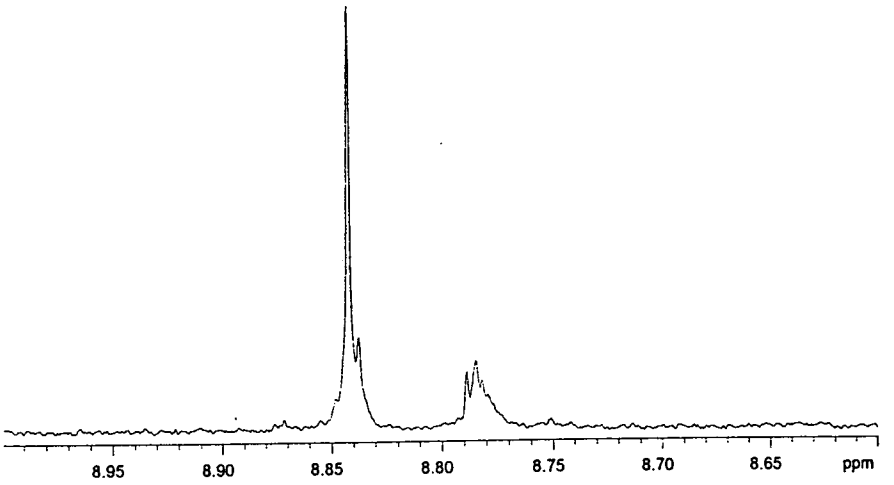

Figure 5.4 Expansion of the aromatic region of the ^{1}H nmr spectrum of a core-terminated hyperbranched polyester.

Additional support for this hypothesis is provided by new resonances observed at 1.44ppm (triplet) and a quartet overlapping with the CHOH focal signals at 4.44ppm. These signals have been found to correspond to the CH_3 and OCH_2 ester signals of triethyl 1,3,5-benzenetricarboxylate (see section 5.3).

The information in Table 5.2 summarises the ^{1}H nmr analysis of the percentage of core incorporation. The results were determined by dividing the integrated intensity of the multiplet, assumed to be due to the hydrogens of the incorporated cores, by the sum of the integrated intensities of the aromatic signals (both the multiplet and the singlets). Thus, the value indicates the mole percent of the aromatic residues in the product which are bound into the core-terminated hyperbranched structure, the rest are due to the triethyl ester of benzene 1,3,5-tricarboxylic acid; the fact that more than one signal is observed in this region may indicate the presence of mixed methyl/ethyl triesters or partial reaction with a wedge.

Ratio[a]	% Core incorporated[b]	M_n[c]
1:25	24.3	920
1:50	12.7	710
1:50	22.8	900
1:75	16.5	870
1:90	31.0	1150
1:90	21.5	920

a Molar ratio of core:monomer at the start of the reaction
b Percentage of core incorporated determined *via* ^{1}H nmr spectroscopy
c M_n determined by GPC using linear polystyrene standards and $CHCl_3$ as eluent

Table 5.2 Summary of the percentage of core incorporation for the reactions of diethyl 3-hydroxyglutarate and trimethyl 1,3,5-benzenetricarboxylate.

It is clear from the table above, that a trend between the ratio of core:monomer and the amount of core incorporated does not exist. However, a trend is observed between the molecular weight (as determined by GPC) and the amount of core incorporated into the polymer. The graph overleaf (Figure 5.5) shows an approximately linear relationship between the observed M_n and the percentage of core attached to the polymer (correlation coefficient, R=0.90).

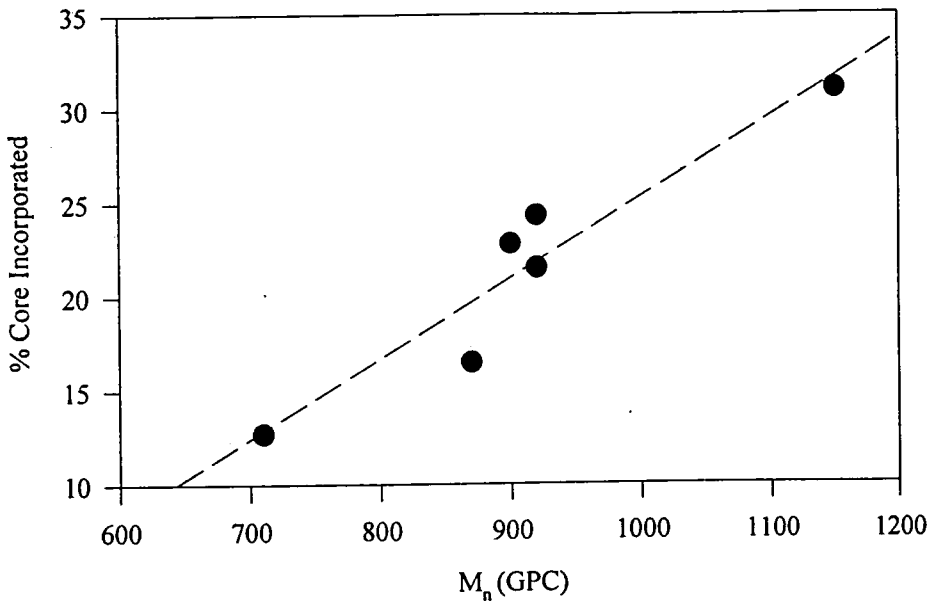

Figure 5.5 Graph showing the relationship between the amount of core incorporation and the M_n

The graph shows that as the amount of core incorporation increases the molecular weight increases. It seems that the relative amount of core present in the reaction vessel is immaterial, which is surprising. It is perhaps worth noting that this set of results was obtained using the same batch of monomer and core and the same reaction conditions.

When considering the ^{13}C nmr spectra, it is only possible to say if the reaction has been successful by observing both the decrease of the ethyl ester carbon signals and the appearance of the aromatic carbon signals. Figure 5.6 shows the ^{13}C nmr spectrum of the product of the reaction performed in the presence of 1:90 molar ratio of core:monomer.

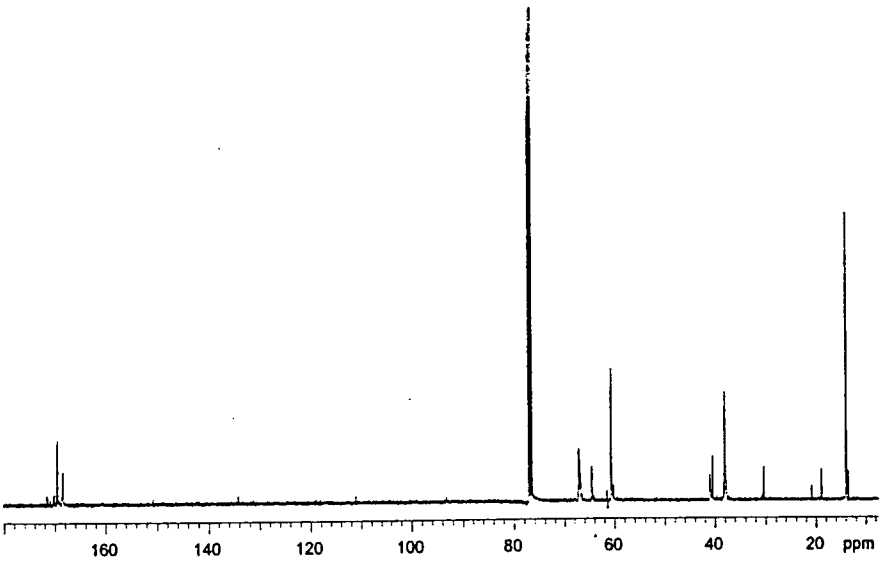

Figure 5.6 ^{13}C nmr spectrum of a core-terminated hyperbranched polyester

Again, the expected signals of the hyperbranched oligomers are found at 14.12 (CH_3), 38.35 (multiplet assigned to the CH_2 of the terminal, linear and branched sub-units), 40.62 (CH_2 of the focal sub-units), 60.83 (OCH_2), 64.72 (focal CH), 67.20 (CH assigned to terminal, linear and branched sub-units) and the signals of the ester carbonyls at 168.59 and 169.68ppm. As the signals due to the focal sub-units are readily observed, it is clear that incorporation of the core has not occurred fully. As there is a small amount of core present, the aromatic signals are difficult to observe in the ^{13}C nmr spectrum. However, as ^{13}C nmr allows us to determine the DB of the polymer, this may provide important clues to the success of the reaction.

Before performing a Laurentzian deconvolution curve fitting procedure, all samples are referenced using the $CDCl_3$ signal. It is therefore possible to accurately measure the shifts of the carbon signals and compare the values found in the hyperbranched wedges to those of the core terminated samples. It was anticipated that the peak positions of the multiplet centred around 67ppm (due to the CH-O of the hyperbranched polymer) would shift slightly due to the focus being attached to an aromatic molecule as shown in Figure 5.7 overleaf:

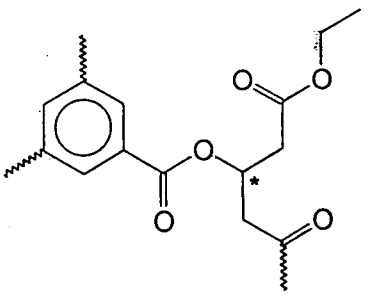

Figure 5.7 Possible structure of the core molecule attached to a hyperbranched fragment.

On analysis of the peak positions of the terminal, linear, branched and focal sub-units of the core terminated polyester, it is clear that the signals due to the focus, branched and linear sub-units have shifted to low field with respect to those of the wedge, by 0.046, 0.065 and 0.115ppm respectively. This shift is assumed to be due to incorporation of the core terminator to the hyperbranched molecule. In these low molecular weight samples the line widths do not provide useful information as was the case with higher molecular weight samples (see section 3.3.1 page 79).

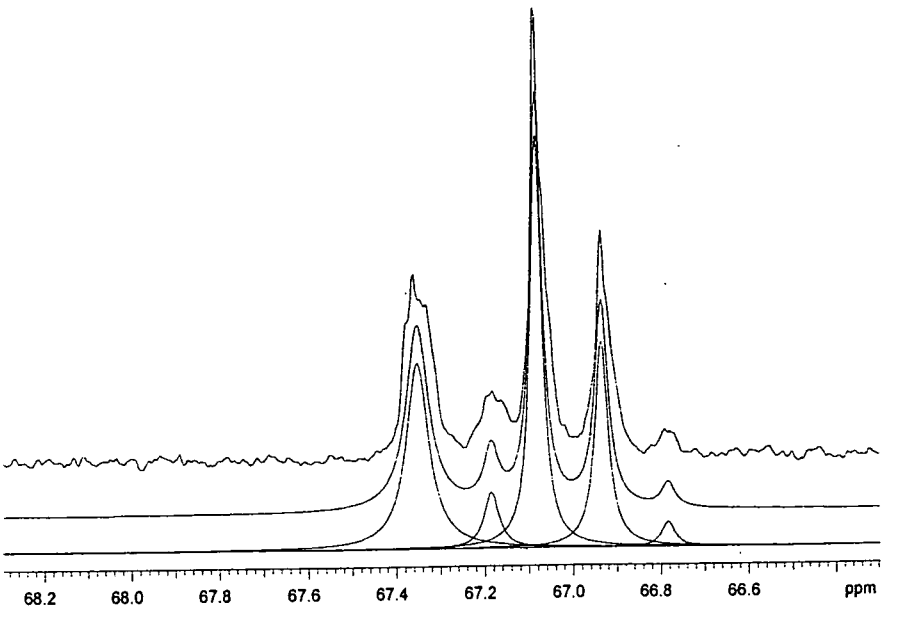

Figure 5.8 Laurentzian deconvolution of a hyperbranched wedge

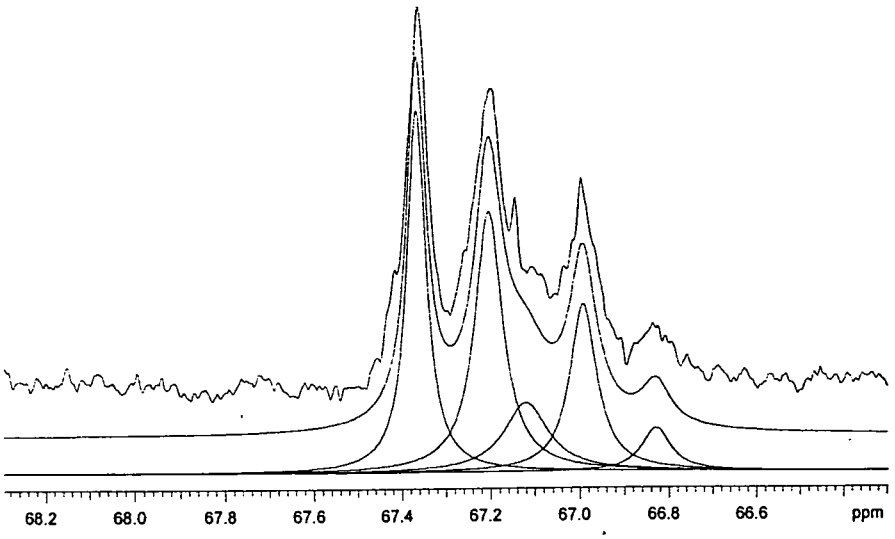

Figure 5.9 Laurentzian deconvolution of a core-terminated hyperbranched polyester

As can be seen in Figure 5.8, some of the low molecular weight hyperbranched wedge samples possess two lines due to the linear sub-units (as determined from their shifts and earlier assignment, see page 79). It is postulated that two environments of the linear sub-units may be observed due to the low degrees of polymerisation. If the linear sub-unit is directly bonded to a partially reacted focal group (see Figure 5.10) the methine carbon (marked with an asterisk) may be able to detect the difference in environment between this situation and the case where the focal unit is fully branched.

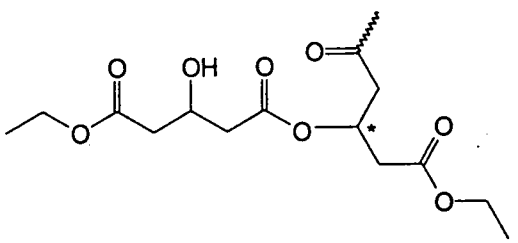

Figure 5.10 Representation of a linear sub-unit bonded to a focal group.

In an attempt to estimate the number of "arms" of the B_3 core which have reacted with the hyperbranched wedge, MALDI-TOF mass spectral analysis was performed. As the core is a methyl ester, methanol would be eliminated on reaction of the core with the monomer. It was hoped that by formulating equations relating to the

number of monomers transesterifying with the core, the number of arms of the core which had reacted may be determined. However, as the core molecule appears to preferentially transesterify with the condensate to form an ethyl ester, the analysis of the MALDI-TOF spectra was very complicated. The formulation of equations taking into account the core molecule transesterifying with both ethanol and butyl groups, of either butanol or the catalyst, was practically impossible due to the large number of permutations available to the molecule. The structures below show a small sample of the variety of possible products of the transesterification of 1,3,5-benzenetricarboxylate.

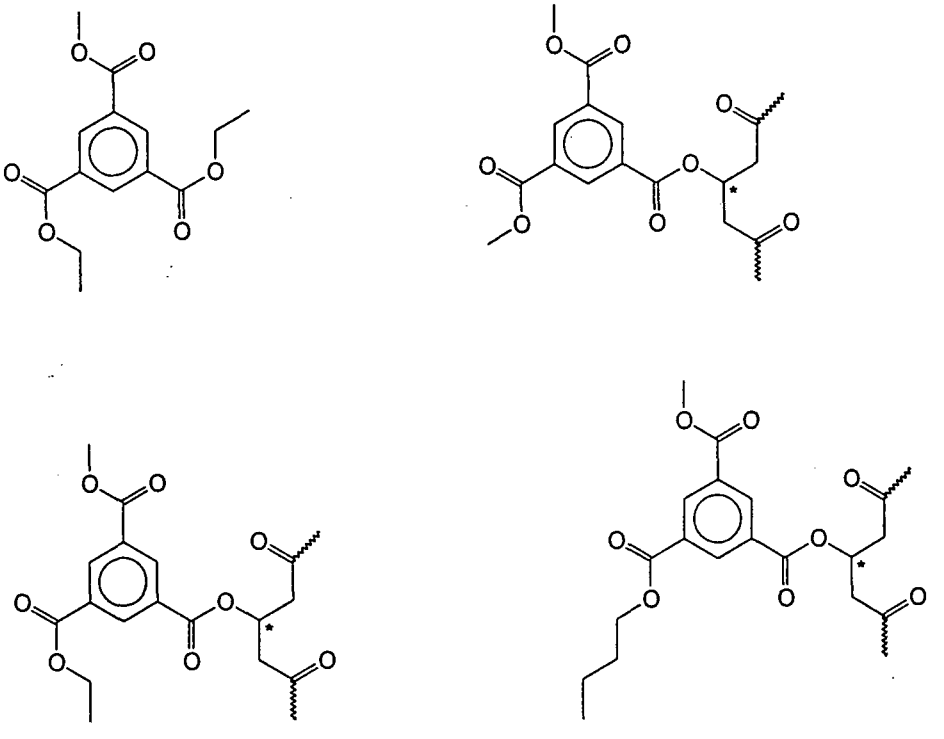

Figure 5.11 Possible structures arising from the transesterification of diethyl 3-hydroxyglutarate in the presence of trimethyl 1,3,5-benzenetricarboxylate.

It is clear that the methyl ester may react to form up to three new classes of compound. For example, it may become a mono-, di- or tri-substituted ethyl or butyl ester or it may react with the monomer to produce the desired core terminated species. The resulting compound may then produce species with butyl ester end groups and so on. In view of this, the MALDI-TOF spectra were not analysed in great detail. Figure

5.12 below shows a representative MALDI-TOF mass spectrum of the product of a ratio of core:monomer of 1:25.

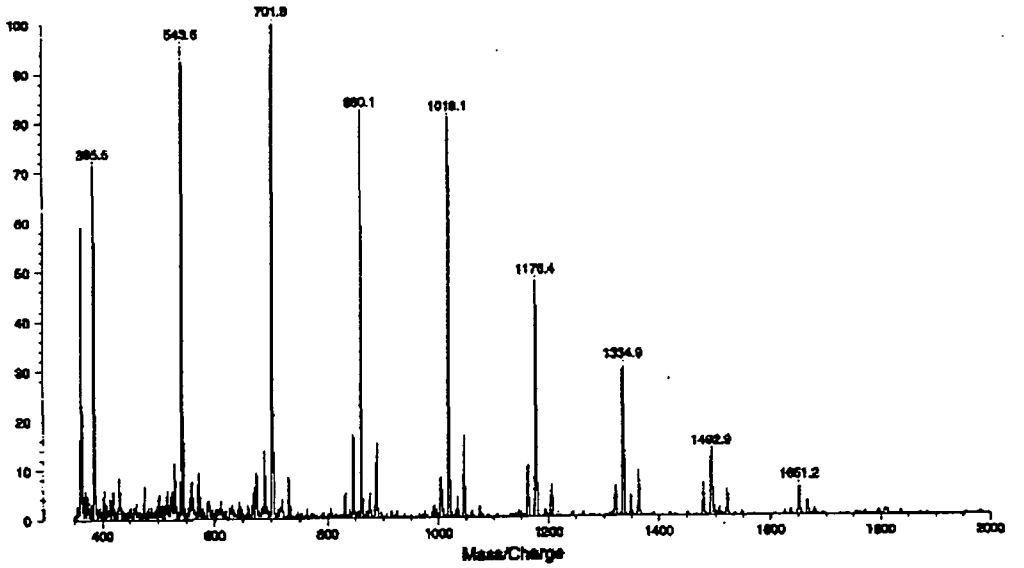

Figure 5.12 MALDI-TOF spectrum of the product of the copolymerisation of diethyl 3-hydroxyglutarate in the presence of trimethyl 1,3,5-benzenetricarboxylate.

The following equations are derived in Chapter 4, section 4.2.1 and may be used to determine if cyclisation, dehydration, hyperbranched formation or hyperbranched formation coupled with butoxide transesterification has occurred:-

Hyperbranched formation $$n = \frac{Y - 69}{158}$$ (Eq. 5.1)

Transesterified hyperbranched $$n = \frac{Y - x}{158}$$ (Eq. 5.2)

where x is either 97 or 125 corresponding to one or two butoxides transesterifying with the ethyl end groups

Cyclisation $$n = \frac{Y - 23}{158}$$ (Eq. 5.3)

Dehydration $$n = \frac{Y - 51}{158}$$ (Eq. 5.4)

where n is the number of monomer residues present in the oligomer and Y is the observed peak mass.

Applying the above equations to the observed peak masses, the major signals are due to the hyperbranched oligomers, whilst the minor peaks to slightly higher mass are due to hyperbranched oligomers with one and two transesterifed butoxide groups. The minor peaks to low mass are assigned to dehydrated hyperbranched species, see Appendix 3, Table 30. As all the signals above an intensity of 10% have been assigned to hyperbranched formation, it would appear that the detection of core terminated species is difficult.

In conclusion, the incorporation of trimethyl 1,3,5-benzenetricarboxylate has occurred to some extent, however preferential reaction with ethanol appears to be detrimental to formation of core-terminated hyperbranched polymers. Therefore it was decided to utilise an ethyl ester core in an attempt to simplify the interpretation of analytical data and possibly encourage core incorporation.

5.3 INCORPORATION OF TRIETHYL 1,3,5-BENZENETRICARBOXYLATE

The synthesis of triethyl 1,3,5-benzenetricarboxylate [2] is detailed in section 5.5.2. The complete characterisation of [2] is necessary as, in theory, it will be possible to determine the degree of incorporation of the core molecule by monitoring the disappearance of the ethyl ester signals in the ^{1}H nmr spectra.

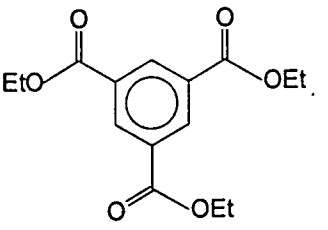

[2]

Due to the symmetry of the molecule, the nmr analysis is easy. The ^{1}H nmr spectrum, Figure 5.13, exhibits a triplet at 1.44ppm (CH_3), a quartet at 4.46ppm (OCH_2) and a singlet at 8.85pm (aromatic CH), whilst the ^{13}C nmr spectrum, Figure 5.14, is comprised of five distinct carbon resonances. The ester signals of interest are found at 14.32ppm (CH_3) and 61.70ppm (OCH_2).

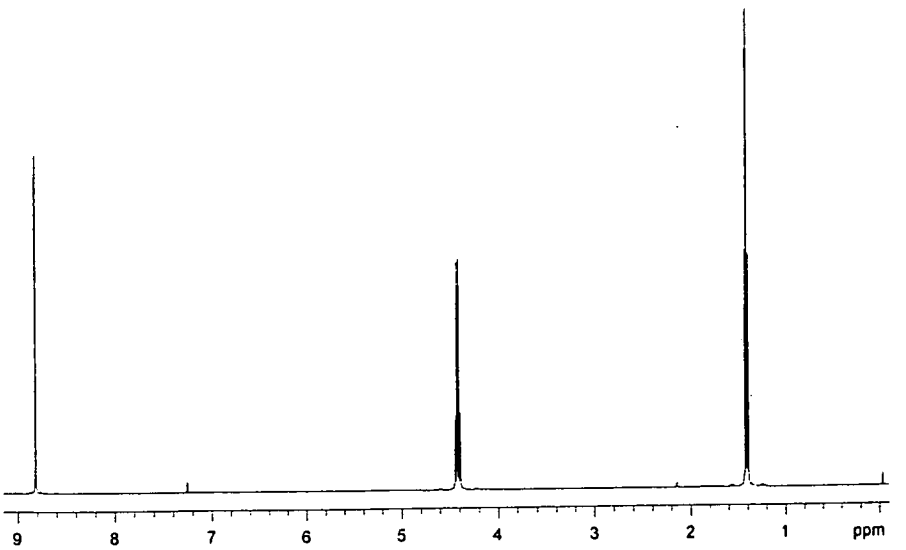

Figure 5.13 ^{1}H nmr spectrum of triethyl 1,3,5-benzenetricarboxylate

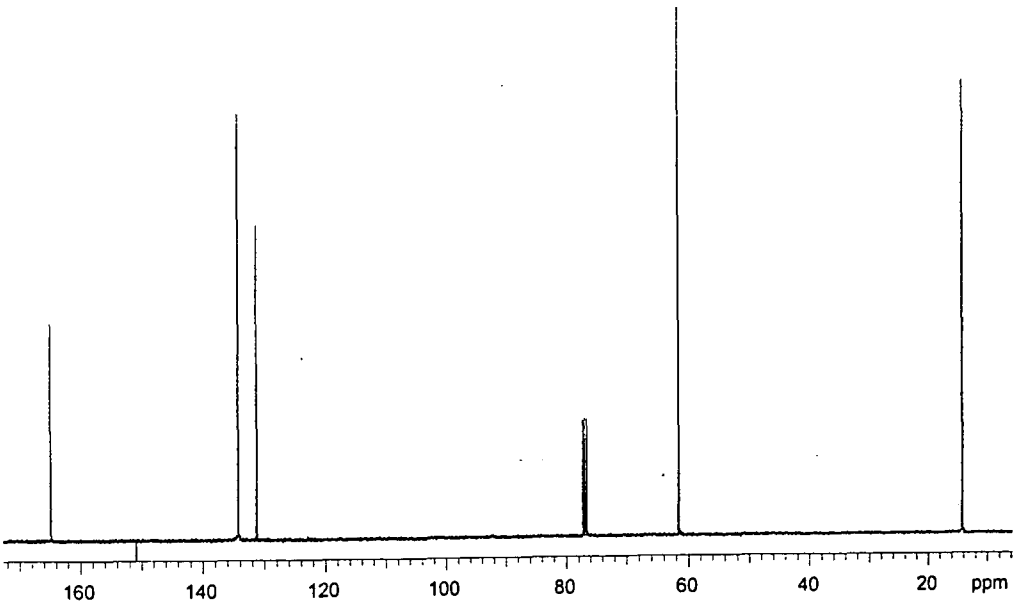

Figure 5.14 ^{13}C nmr spectrum of triethyl 1,3,5-benzenetricarboxylate

It was anticipated that the ^{1}H nmr spectrum would provide the most accurate and easiest way of monitoring the success of the reaction by measuring the relative integrated intensities of the CH_3 signal and the aromatic hydrogen signal. The results of six polymerisation attempts are summarised overleaf. A full listing of the ^{1}H and ^{13}C nmr spectral data may be found in Appendix 3, Tables 7-12 and 23-25.

Ratio[a]	M_n[b]	T_g(°C)[c]	DB[d]
1:25	1280	-45.3	0.59
1:50	1490	-39.3	0.56
1:50	880	-58.0	0.59
1:75	1380	-49.5	0.57
1:90	1370	-47.4	0.57
1:90	1360	-46.7	0.59

a Molar ratio of core:monomer at the start of the reaction
b M_n determined by GPC using linear polystyrene standards and $CHCl_3$ as eluent
c As determined *via* DSC
d As determined *via* ^{13}C nmr spectroscopy

Table 5.3 Summary of glass transition temperatures and degrees of branching of core-terminated aliphatic hyperbranched polyesters.

On cursory inspection, it appears that the molecular weight of the resulting polymer is independent of the amount of core present. This was unexpected as it was anticipated that the molecular weight would increase with a decreasing amount of core. If a graph of T_g versus M_n (as determined by GPC) is plotted, the glass transition temperatures increase linearly with M_n. On comparison of these values with those of the hyperbranched wedges, Figure 5.15, it can be seen that they lie roughly about the same line.

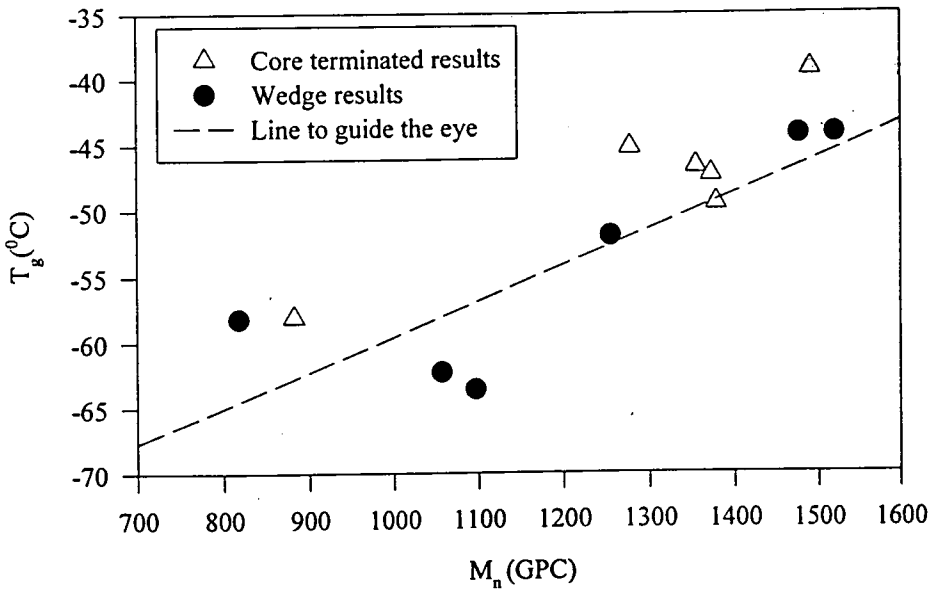

Figure 5.15 Graph comparing the T_g's of hyperbranched wedges and core-terminated samples.

The plot above suggests that the core may either have a negligible effect on the T_g of the polymer, or it may not be incorporated to any great extent.

In an attempt to determine how much of the core has reacted to form a core-terminated hyperbranched polyester, the ^{1}H nmr spectra were scrutinised. It was hoped that the triplet at 1.44ppm and the singlet at 8.85ppm would be instructive in the determination of the success of the coupling reaction. Figure 5.16 shows a representative ^{1}H nmr spectrum of the product of the polymerisation performed using a ratio of 1:50 triethyl 1,3,5-benzenetricarboxylate:diethyl 3-hydroxyglutarate.

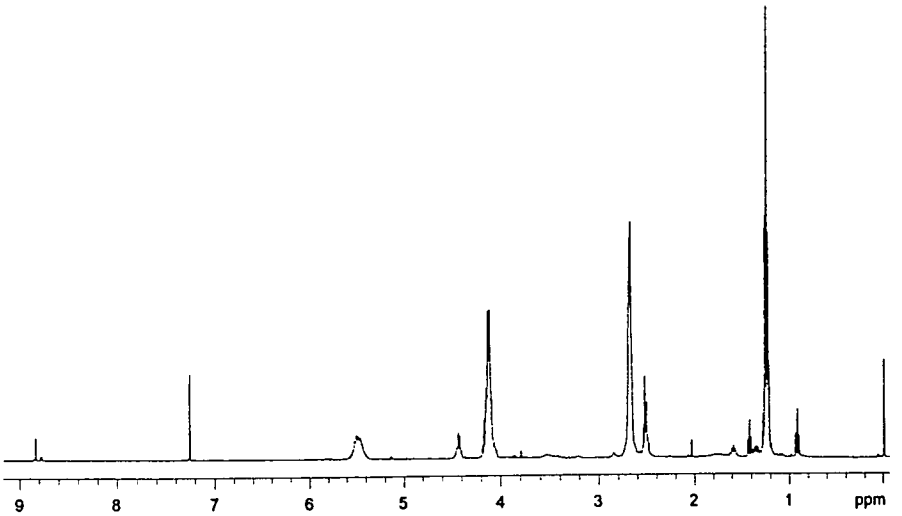

Figure 5.16 ^{1}H nmr spectrum of a core-terminated hyperbranched polyester.

On close inspection of the product spectrum, it was found that the CH_3 core triplet at 1.44ppm slightly overlaps with a methylene multiplet of the transesterified butoxide signals, therefore the integral of this signal is not as accurate as required for this analysis. An alternative method to determine the success of the reaction is to consider the relative integrated intensities of the C**H** signals in the aromatic region of the ^{1}H nmr spectrum, Figure 5.17.

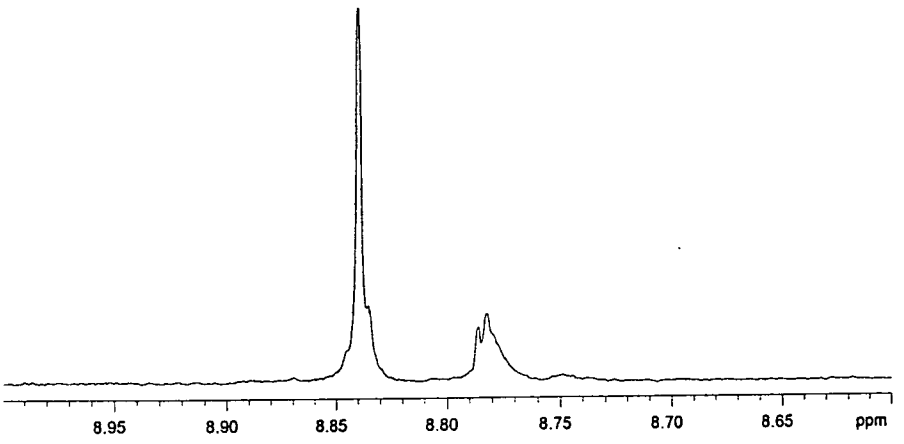

Figure 5.17 Expansion of ^{1}H nmr spectrum of a core-terminated hyperbranched polyester

Prior to reaction, only one singlet was observed at 8.85ppm, however in the product spectra, two signals are found. The major signal at 8.84ppm, is assigned to

the hydrogens of the unreacted core molecule, whilst a minor broad multiplet at 8.78ppm is assigned to the aromatic protons of the core molecule attached to a hyperbranched wedge as in the case of the methyl ester core molecule. The sum of the integrals of these two signals should be equivalent to the three hydrogens of [2], page 147, therefore the relative amount of the new signal to the sum of the aromatic hydrogen signals should allow the determination of the amount of core incorporated into the polymer. The table below shows the percentage of core attached to the hyperbranched polymer:

Ratio[a]	% Core incorporated[b]	M_n[c]
1:25	25.0	1280
1:50	31.9	1490
1:50	9.09	880
1:75	28.1	1380
1:90	30.4	1370
1:90	28.9	1360

a Molar ratio of core:monomer at the start of the reaction
b Percentage of core incorporated determined *via* ^{1}H nmr spectroscopy
c M_n determined by GPC using linear polystyrene standards and $CHCl_3$ as eluent

Table 5.4 Summary of the percentage of core incorporation for the reactions of diethyl 3-hydroxyglutarate and triethyl 1,3,5-benzenetricarboxylate.

It would appear that the percentage of available core molecules incorporated into the polymer never exceeds approximately 30% and of those incorporated, the multiplicity of the signal at 8.78ppm suggest that a mixture of singly, doubly and triply derivatised species are formed. Only one result in Table 5.4 shows a deviation from the almost constant amount of core incorporation and on analysis of the product, it would appear that the monomer had absorbed moisture from the atmosphere resulting in a low molecular weight sample due to the reduction in catalytic activity of $Ti(OBu)_4$ due to the ingressed water.

In an attempt to further investigate the incorporation of [2], the ^{13}C nmr spectrum, Figure 5.18, was analysed.

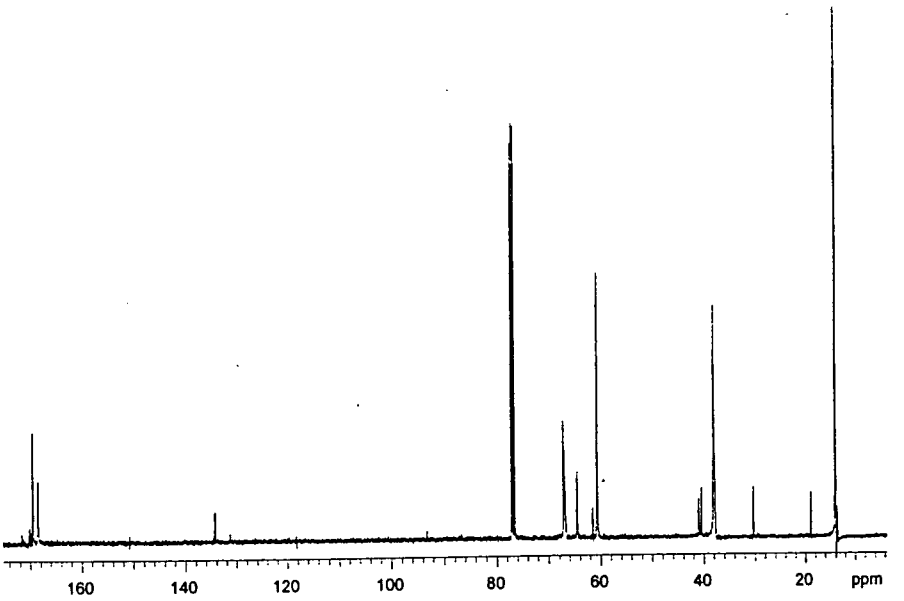

Figure 5.18 ^{13}C nmr spectrum of a core-terminated hyperbranched polyester

As expected, the signals due to hyperbranched structures are present, as is the core ethyl ester CH_3 signal at 14.33ppm, confirming that total incorporation has not been achieved. Expansion of the multiplet centred on 67.2ppm, Figure 5.19, shows that the peak positions of the terminal, linear and branched methine signals of the hyperbranched wedges have not shifted in the core terminated polymer. This can be interpreted on the basis that the core molecule does not induce a significant change in environment of the focal sub-unit or that the signals due to the methine carbons of the wedge focus bound to the core are coincident with other sub-unit resonances.

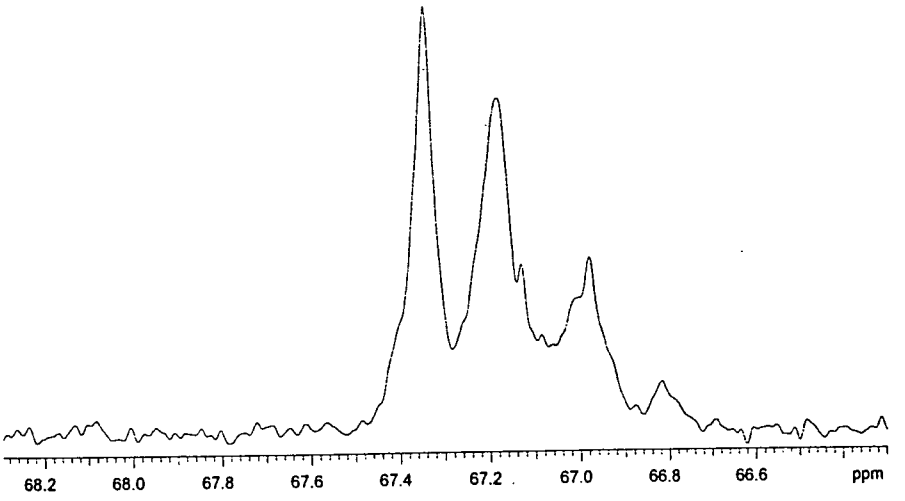

Figure 5.19 Expansion of the methine multiplet of a core-terminated hyperbranched polyester

To confirm the limited amount of core present in the hyperbranched samples, MALDI-TOF mass analysis was performed. As the nmr results suggest that only 30% of the core has reacted to give core-terminated species, it was anticipated that the signals due to the core terminated hyperbranched polymer would be small compared to the hyperbranched wedges, hence they may be difficult, if not impossible to detect.

The MALDI-TOF spectra of the products look very similar to the hyperbranched wedges confirming that the incorporation of core had only occurred to a small extent. The samples exhibited the expected signals for the hyperbranched polymers and the hyperbranched polymer containing one transesterified butoxide group, see Appendix 3, Table 31. In all cases, there was no evidence for cyclisation implying that the core molecule did indeed help to prevent this phenomenon. All of the samples contained signals due to the core terminated hyperbranched species with three transesterified butoxide groups. As an illustration of the spectra of the core-terminated samples, Figure 5.20 overleaf shows the mass spectrum of the product made with a core:monomer ratio of 1:90.

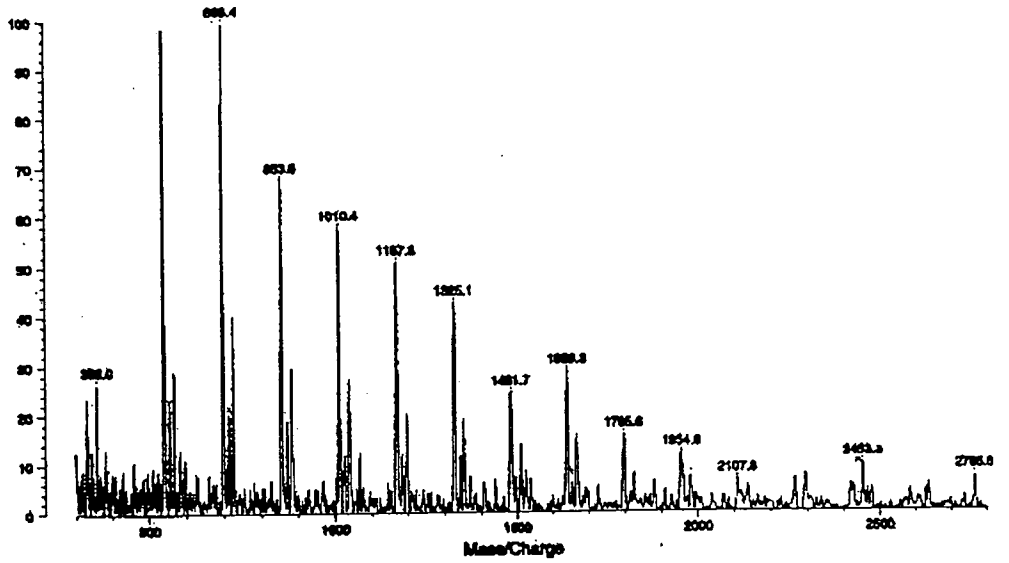

Figure 5.20 MALDI-TOF mass spectrum of the product of the polymerisation of diethyl 3-hydroxyglutarate in the presence of triethyl 1,3,5-benzenetricarboxylate (Ratio = 1:90)

As for the trimethyl ester core, to fully assign the MALDI-TOF spectrum it is necessary to consider all possible reactions which may occur during the polymerisation. If no core incorporation occurs it can be assumed that the major reaction will be the formation of hyperbranched polymers as discussed in section 5.2.

If the core molecule reacts with a monomer, one molecule of ethanol will be eliminated, therefore it is possible to derive a general equation to determine if core incorporation has occurred. Consider Figure 5.21 below:

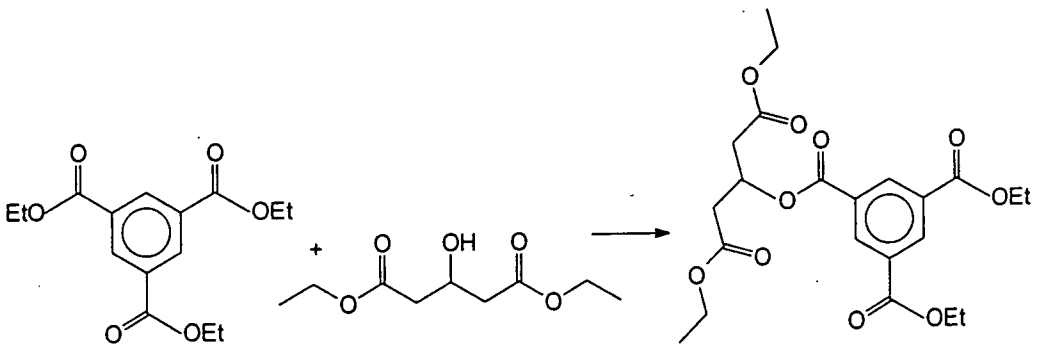

Figure 5.21 Incorporation of diethyl 3-hydroxyglutarate

An expression may derived to predict the masses of ions produced by this and related reactions:-

$$Y = n\mathrm{M} + \mathrm{c} + \mathrm{Na} - n\mathrm{EtOH}$$

$$Y = 158n - 317$$

$$n = \frac{Y - 317}{158} \qquad \text{(Eq. 5.5)}$$

where Y is the observed peak mass, c is the molar mass of the core molecule (294), Na is the attached ion mass (23) and the mass of ethanol is 46.

MALDI-TOF MS is unable to determine how many of the arms have reacted due to the condensation product, ethanol, being the same as when hyperbranched molecules are formed. An additional reaction results in the ethyl esters transesterifying with butoxide. The following equations represent one, two and three butoxide groups transesterifying with a core terminated sample:-

$$n = \frac{Y - 345}{158} \qquad \text{(Eq. 5.6)}$$

$$n = \frac{Y - 373}{158} \qquad \text{(Eq. 5.7)}$$

$$n = \frac{Y - 401}{158} \qquad \text{(Eq. 5.8)}$$

To detect the small amounts of core terminated species present in the polymer sample, it was necessary to acquire the spectrum using linear mode, unfortunately this gives relatively poor mass resolution resulting in questionable data. The spreadsheet of the results from the spectrum in Figure 5.20 (see Appendix 3, Table 31) illustrates the difficulties in assigning the peaks to oligomer structures. For example, the peak at 1167amu may be assigned to either a 7-mer which has undergone dehydration or a core terminated 5-mer which has two transesterified butoxide groups attached.

It is clear that there is a limitation in the analysis of the MALDI-TOF mass spectra; the equations derived to predict the masses of species arising from the processes occurring during the polymerisation should be distinct enough to give unambiguous conclusions and this only occurs in favourable cases. When it works, see Chapter 4, MALDI-TOF MS analysis provides convincing proof of structure but it is of little use in identifying all the species present in the products of the reactions described in this section.

5.4 INCORPORATION OF DIETHYL ISOPHTHALATE

In an attempt to overcome the problem of limited core incorporation, a B_2 core was synthesised to investigate the possible steric inhibition to hyperbranched growth around the core. Diethyl isophthalate [3] was synthesised from isophthalic acid *via* a standard esterification procedure in the presence of concentrated sulphuric acid (see section 5.5.3). The colourless liquid was distilled to give the desired product in good yield.

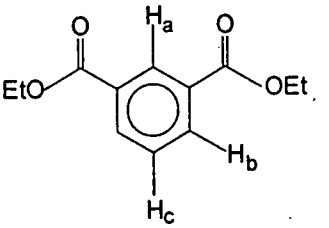

[3]

As the ethyl ester CH_3 signal at 1.43ppm overlaps with the CH_2 multiplet of the butyl ester in the hyperbranched ^1H nmr spectra, only the integrals of the aromatic CH signals will provide a method for the determination of the percentage of core incorporated. Figure 5.22 below shows the ^1H nmr spectrum of [3].

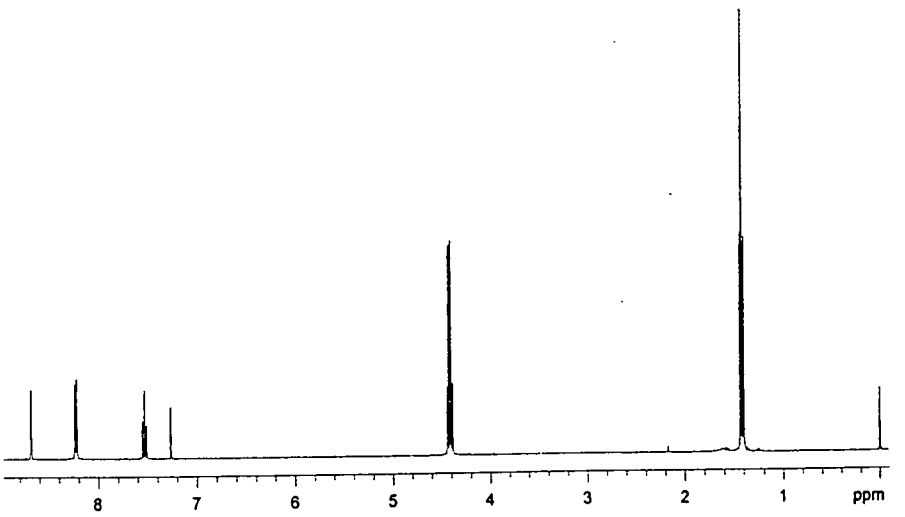

Figure 5.22 ^1H nmr spectrum of diethyl isophthalate.

The aromatic region of the above spectrum is expected to be the most informative when determining the amount of core present in the hyperbranched sample. The three types of aromatic hydrogen in Figure 5.22 will have different chemical shifts due to their differing environments, hence their assignment is facile. The triplet at 7.53ppm is assigned to H_c, the doublet of doublets at 8.23ppm is assigned to H_b whilst the singlet at 8.69ppm is assigned to H_a. When **[3]** is incorporated into the polymer there should be three new signals corresponding to the new aromatic **CH** resonances, therefore it will be possible to calculate the percentage of incorporation by measuring the relative integrated intensity of the new signals and comparing them to the sum of the original and new aromatic hydrogen resonances. Figure 5.23 shows the ^{13}C nmr spectrum of diethyl isophthalate.

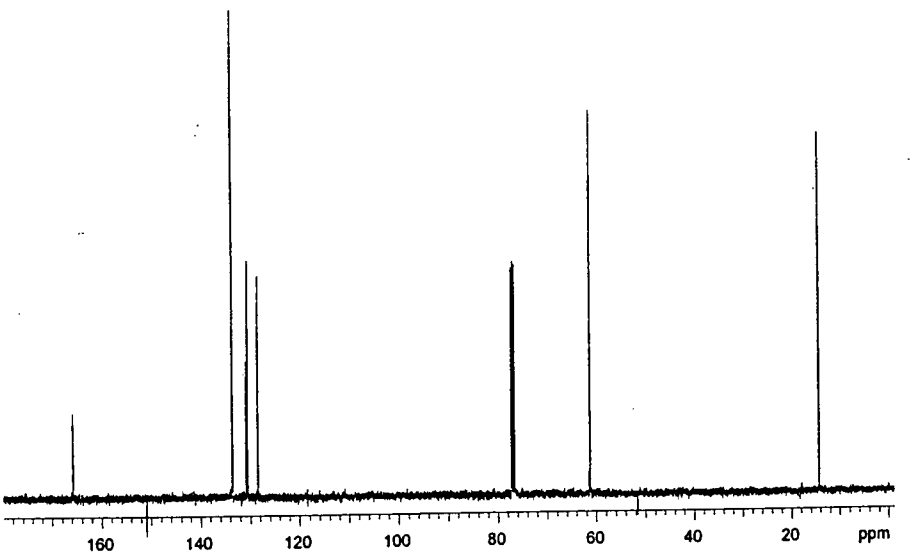

Figure 5.23 ^{13}C nmr spectrum of diethyl isophthalate.

The assignment of the above ^{13}C nmr spectrum is straightforward, the ethyl ester signals are observed at 14.31 ($\mathbf{C}H_3$), 61.32 ($O\mathbf{C}H_2$) and 165.82ppm ($\mathbf{C}$=O). The aromatic carbons are found at 128.49, 130.58 and 130.86ppm assigned to the carbons bearing H_c, H_b, H_a respectively, whilst the signal at 133.66ppm is assigned to the carbon bonded to the carbonyl.

Once again, a variety of molar ratios of core:monomer were used to assess the effect of a B_2 core on the polymer properties. A full listing of the ^1H and ^{13}C nmr

spectral data of the products of reaction can be found in Appendix 3, Tables 13-19 and 26-29. The table below summarises the results:

Ratio[a]	M_n[b]	T_g(°C)[c]	DB[d]
1:25	1080	-49.6	0.59
1:50	1100	-50.2	0.60
1:50	800	-65.2	0.50
1:75	1470	-40.8	0.54
1:75	1110	-52.6	0.60
1:90	1140	-48.0	0.60
1:150	1190	-47.1	0.59

a Molar ratio of core:monomer at the start of the reaction
b M_n determined by GPC using linear polystyrene standards and $CHCl_3$ as eluent
c As determined *via* DSC
d Determined *via* ^{13}C nmr spectroscopy

Table 5.5 Summary of glass transition temperatures and degrees of branching of core-terminated aliphatic hyperbranched polyesters.

The ratio of core:monomer does not appear to influence the molecular weight which implies that the incorporation of the core is small. To compare these results with those found for triethyl 1,3,5-benzenetricarboxylate, a graph of the glass transition temperatures of both ethyl ester core-terminated systems and hyperbranched wedges of similar molecular weight *versus* molecular weight was plotted. Figure 5.24 overleaf shows the results:

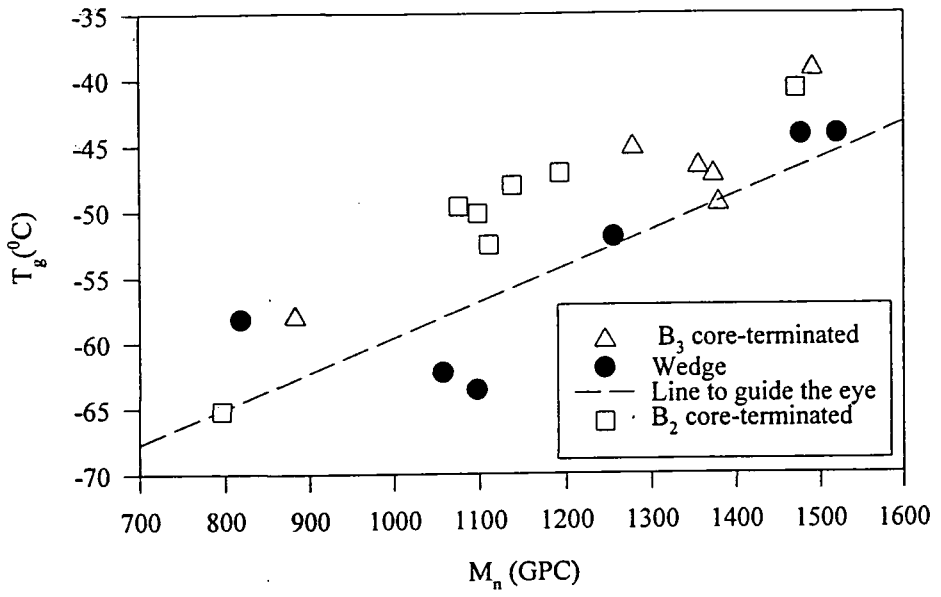

Figure 5.24 Graph comparing the T_g's of wedges and core terminated polyesters.

It can be seen that generally the core-terminated samples possess slightly higher T_g's than the wedges of similar molecular weight. This is assumed to be a consequence of the incorporated aromatic group introducing rigidity into the system.

The degrees of branching for the diethyl isophthalate polymers are marginally higher than those of the hyperbranched wedges yet comparable to the triethyl 1,3,5-benzenetricarboxylate results. The similarities in these core terminated samples suggest that the functionality of the core is not an important factor in the synthesis of core-terminated hyperbranched poly(diethyl 3-hydroxyglutarate). In an attempt to assess the degree of incorporation, the ^{1}H nmr spectra were analysed.

Figure 5.25 overleaf shows the ^{1}H nmr spectrum of the product of a 1:50 core terminated polymerisation.

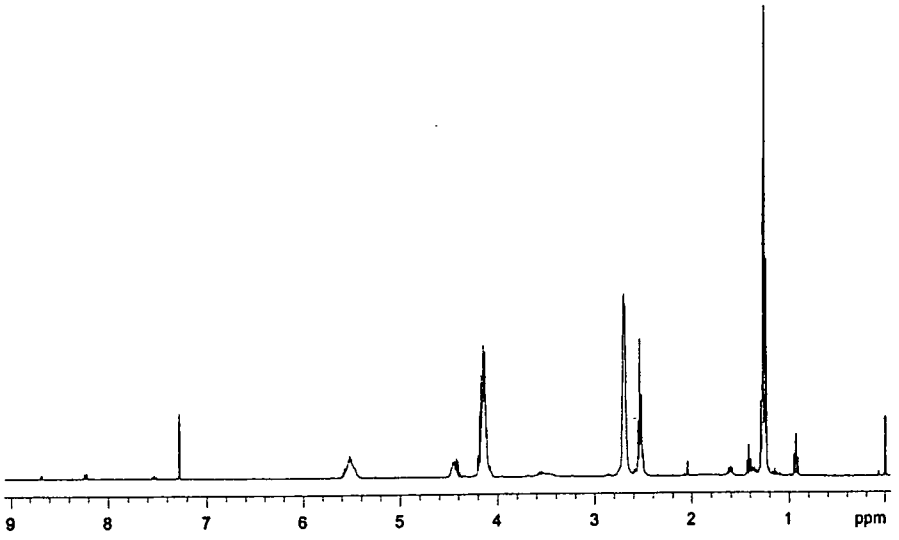

Figure 5.25 ^{1}H nmr spectrum of a core terminated hyperbranched polyester synthesised using a 1:50 ratio of core:monomer

The signals due to formation of hyperbranched structures are as expected, however it is clear that the core ethyl ester signals overlap with some of the hyperbranched signals. Thus, the CH_3 triplet slightly overlaps with a methylene multiplet of the transesterified butoxide at 1.43ppm, whilst the OCH_2 quartet is coincident with the focal methine signal at 4.44ppm. It is therefore clear, as in the case of the triethyl derivative, that only the aromatic hydrogen signals may be used to determine the percentage of incorporation. Expansion of the aromatic region of the ^{1}H nmr spectrum, Figure 5.26, shows several new resonances indicative of the presence of core terminated species.

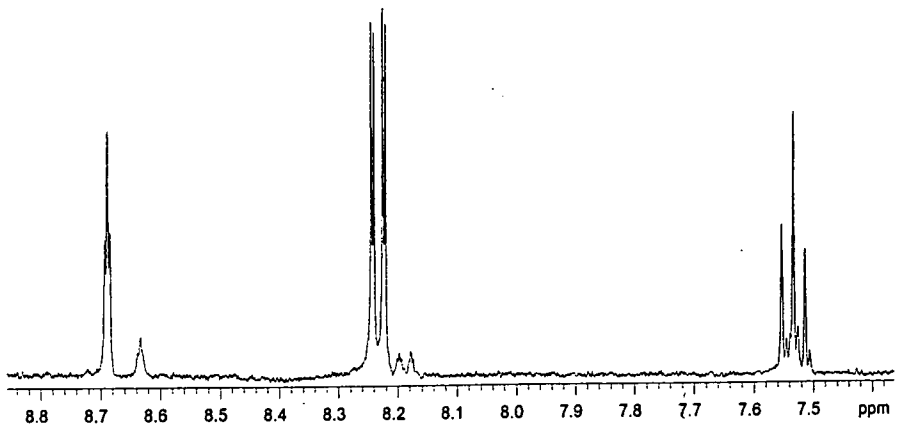

Figure 5.26 Expansion of ^{1}H nmr of core terminated polyester.

It was anticipated that the resonances to high field of the unreacted triethyl 1,3,5-benzenetricarboxylate are due to the aromatic hydrogens of the core terminated hyperbranched polyester. If this is true, it will be possible to determine the degree of incorporation by dividing the relative integrated intensities of the new signals by the sum of the integrated intensities of the unreacted core and core terminated signals. To perform this analysis, the signals between 8.1 and 8.3ppm, namely the starting material doublet of doublets at 8.23ppm and its corresponding signals to high field were chosen as these were the most intense, well resolved signals. Table 5.6 below summarises the results of this analysis:

Ratio[a]	% Core incorporated[b]	M_n[c]
1:25	10.26	1080
1:50	8.69	1100
1:50	9.04	800
1:75	-	1470
1:75	11.35	1110
1:90	9.46	1140
1:150	14.02	1190

a Molar ratio of core:monomer at the start of the reaction
b Percentage of core determined *via* ^{1}H nmr spectroscopy
c M_n determined by GPC using linear polystyrene standards using $CHCl_3$ as eluent

Table 5.6 Summary of the percentage of core incorporation for the diethyl isophthalate core terminated polyesters

It can be seen from the above table that the percentage of incorporation remains practically constant and low. This implies that the core molecule does not play an active role in the polymerisation of diethyl 3-hydroxyglutarate. To confirm the small amount of reaction of [**3**], the ^{13}C nmr product spectra were analysed. Figure 5.27 shows the ^{13}C nmr spectrum of the product of the reaction performed in the presence of a ratio of 1:50 core:monomer.

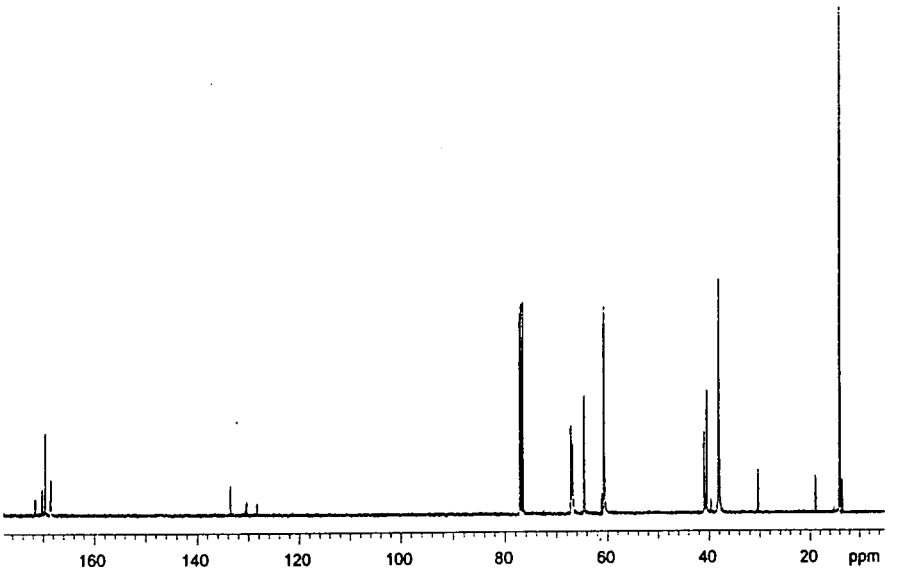

Figure 5.27 ^{13}C nmr spectrum of a core-terminated hyperbranched polyester synthesised using a ratio of 1:50 core:monomer

As expected, the signals due to the unreacted diethyl isophthalate are observable in the product spectrum at 14.4ppm (CH_3) and 61.32ppm (OCH_2). The aromatic carbons are readily observed between 128 and 134ppm, whilst the expected carbonyl signal is not visible above the S/N level. As the aromatic region is devoid of new resonances it must be concluded that the core terminated species are present in very low concentrations.

In an attempt to characterise the products of the reactions between diethyl isophthalate and diethyl 3-hydroxyglutarate, MALDI-TOF mass spectral analyses were performed. As in the previous two systems, the equations representing the usual hyperbranched formation may be applied to the hyperbranched polymers. To allow full analysis to be performed, consider the Figure overleaf:

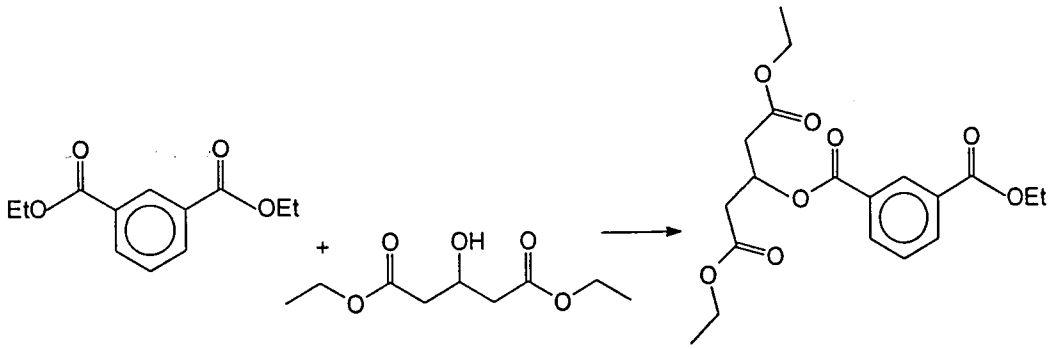

Figure 5.28 Reaction scheme showing the condensation of diethyl 3-hydroxyglutarate with diethyl isophthalate.

It is clear that as one molecule of monomer reacts with the wedge, one molecule of ethanol will be eliminated, therefore an expression may derived for the above reaction:-

$$Y = n\mathrm{M} + \mathrm{c} + \mathrm{Na} - n\mathrm{EtOH}$$

$$Y = 158n - 245$$

$$n = \frac{Y - 245}{158} \qquad \text{(Eq. 5.9)}$$

There is also the possibility of the ethyl end groups transesterifying to butyl esters hence additional equations must be derived to account for this. Equations 5.10, 5.11 and 5.12 correspond to one, two and three ethyl groups transesterifying to butyl ester end groups.

$$n = \frac{Y - 273}{158} \qquad \text{(Eq. 5.10)}$$

$$n = \frac{Y - 301}{158} \qquad \text{(Eq. 5.11)}$$

$$n = \frac{Y - 329}{158} \qquad \text{(Eq. 5.12)}$$

On application of the above equations to the spectrum shown in Figure 5.29, (see Appendix 3, Table 32) it is found that the major series of peaks is due to hyperbranched formation.

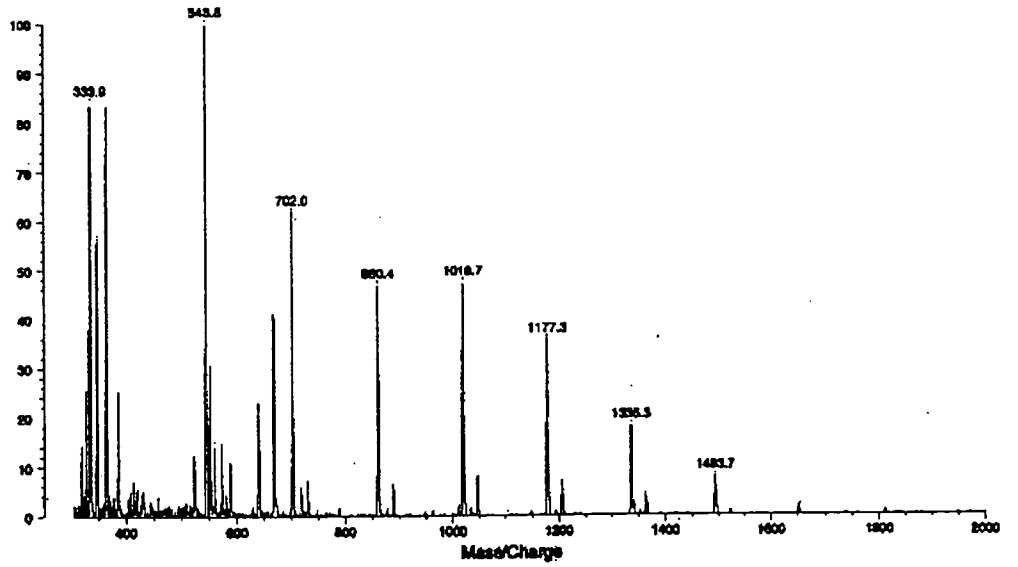

Figure 5.29 MALDI-TOF mass spectrum of the product of the copolymerisation of diethyl 3-hydroxyglutarate in the presence of diethyl isophthalate in a ratio of 1:25 core:monomer.

The signal at 299 amu is found to be due to the dibutyl isophthalate, i.e. both ethyl esters have transesterified during the reaction. Only two signals in the spectrum can be assigned to core terminated polyester. The minor peaks at 587 and 639 amu correspond to a core terminated hyperbranched dimer with one and three butyl ester groups. The lack of other core terminated signals in the spectrum prove that the extent of core incorporation is very small.

In conclusion, it would appear that the formation of core-terminated hyperbranched polyesters via this method is not viable. As the molecular weights of the polymers, in all cases, have been lower than the hyperbranched wedges formed under the same conditions, it would seem that the reactions only yield low molecular weight oligomers.

5.5 EXPERIMENTAL

All organic reagents were purchased from Aldrich Chemical Co. and used without further purification. IR spectra were recorded on a Perkin-Elmer 1600 series FTIR. ^{1}H and ^{13}C nmr spectra were recorded on a Varian 400MHz spectrometer and were referenced to internal Me_4Si. DSC measurement were recorded using a Perkin Elmer DSC7, at a scanning rate of $10°Cmin^{-1}$. GPC was performed with a guard column and three PL-gel columns (exclusion limits 100,10^3 and 10^5Å) using a Waters differential diffractometer and $CHCl_3$ as eluent. Columns were calibrated using polystyrene standards (Polymer Labs).

5.5.1 Synthesis of trimethyl-1,3,5-benzenetricarboxylate

1,3,5-Benzene tricarbonyl trichloride (5.00g, 18.8mmol) was added to pre-dried methanol (50ml) and the mixture stirred at room temperature for 30 minutes to form a white suspension. The precipitate was collected by filtration and washed with cold methanol to yield trimethyl-1,3,5-benzenetricarboxylate as a white solid (2.897g, 18.8mmol, 61%, m.p. 144.3-146.4°C, lit[6] 144°C) which was characterised by ^{1}H nmr ($CDCl_3$, 400MHz) δ3.96 (s, 9H, C**H**$_3$) 8.83 (s, 3H, Ar**H**), ^{13}C nmr ($CDCl_3$, 100MHz) δ 52.60 (**C**H_3), 131.12 (aromatic **C**-H), 134.53 (aromatic **C**-R), 165.34 (**C**=0), FTIR (KBr disc) ν_{max}/cm^{-1} 3086.1, 3014.3, 2957.2, 2847.5, 1731.4, 1611.6.
Found C 57.17, H 4.73 $C_{12}H_{12}O_6$ requires C 57.14, H 4.76.

5.5.2 Synthesis of triethyl-1,3,5-benzenetricarboxylate

1,3,5-Benzene tricarbonyl trichloride (5.00g, 18.8mmol) was added to pre-dried ethanol (50ml) and the mixture stirred at room temperature for 45 minutes to form a white suspension. The precipitate was collected by filtration and washed with cold ethanol to yield triethyl-1,3,5-benzenetricarboxylate as a white solid (3.482g, 11.84mmol, 63%, m.p. 133-135°C, lit[7] 134°C) which was characterised by ^{1}H nmr

($CDCl_3$, 400MHz) δ 1.44 (t, J=7.2Hz, 9H, C**H**$_3$), 4.44 (q, J=7.2Hz, 6H, OC**H**$_2$), 8.85 (s, 3H, Ar**H**), ^{13}C nmr ($CDCl_3$, 100MHz) δ 14.26 (**C**H_3), 61.65 (O**C**H_2), 131.37 (aromatic **C**-H), 134.36 (aromatic **C**-R), 164.99 (**C**=0), FTIR (KBr disc) ν_{max}/cm^{-1} 3814.2, 2997.5, 1718.6.

Found C 61.16, H 6.16 $C_{15}H_{18}O_6$ requires C 61.22, H 6.12.

5.5.3 Synthesis of diethyl isophthalate

Isophthalic acid (2.3g, 0.014 moles) was refluxed in methanol (40ml) in the presence of concentrated sulphuric acid (1.5ml) for 15 hours. The solution was concentrated, chloroform added and poured into water. The organic fraction was collected and dried on the vacuum line. The product was distilled to yield one fraction (bp 125°C, 0.1 torr, lit.[7] 302°C) 2.54g, 11.44mmol, 81.7% which was characterised by ^{1}H nmr ($CDCl_3$, 400MHz) δ 1.43 (t, J=7.4Hz, 6H, C**H**$_3$), 4.41 (q, J=7.4Hz, 4H, OC**H**$_2$), 7.53 (t, J=7.4Hz, 1H, Ar**H**), 8.23 (AB, J=1.6Hz, 2H, Ar**H**), 8.69 (t, J=1.6Hz, 1H, Ar**H**), ^{13}C nmr ($CDCl_3$, 100MHz) δ 14.31 (**C**H_3), 61.32 (O**C**H_2), 128.49 (aromatic **C**-H), 130.58 (aromatic **C**-H), 130.86 (aromatic **C**-H), 133.67 (aromatic **C**-R), 164.99 (**C**=0), FTIR NaCl plates ν_{max}/cm^{-1} 3427.8, 2982.0, 1726.1.

Found C 64.85, H 6.35 $C_{12}H_{14}O_4$ requires C 64.86, H 6.31.

5.5.4 General core terminated polymerisation procedure.

Diethyl 3-hydroxyglutarate (2g, 9.8mmol) was mixed with titanium (IV) butoxide (0.1g, 0.29mmol) and core terminator in the glass reaction vessel. The vessel was lowered into a pre-heated oil bath and the temperature ramped up to 100°C. The reaction remained at that temperature for a 270 minutes and a vacuum was applied (10mmHg) for the final 30 minutes of the reaction. After reaction, the yellow, viscous liquid was dissolved in dichloromethane and the solution washed with water to remove the catalyst. The organic layer was collected and the solvent removed under

reduced pressure. The final traces of solvent were removed by placing the product in a vacuum oven for 4 hours at 35°C.

5.5.5. Large scale polymerisation of diethyl 3-hydroxyglutarate

Diethyl 3-hydroxyglutarate (40g, 0.196mol) was mixed with titanium (IV) butoxide (0.1g, 2.94mmol) in the glass reaction vessel. The vessel was lowered into a pre-heated oil bath and the temperature ramped up to 100°C. Throughout the reaction additional portions of titanium (IV) butoxide (0.1g per portion) was added to the reaction vessel. The reaction remained at 100°C for 510 minutes and a vacuum was applied (10mmHg) for the final 30 minutes of the reaction. After reaction, the yellow, viscous liquid was dissolved in dichloromethane and the solution washed with water to remove the catalyst. The organic layer was collected and the solvent removed under reduced pressure. The final traces of solvent were removed by placing the product in a vacuum oven for 4 hours at 35°C. The product was characterised by ^{1}H nmr ($CDCl_3$, 400MHz) δ 0.93 (t, J=7.6Hz, 1.8H, butyl CH_3), 1.26 (t, J=7.2Hz, 54.9H, ethyl CH_3), 1.36 (m, 1.6H, butyl CH_2), 1.62 (p, 1.1H, butyl CH_2), 2.54 (m, 5.4H, focal CH_2), 2.69 (m, 70.4H, linear, branched and terminal CH_2), 4.14 (m, 44.0H, OCH_2), 4.44 (m, 1H, focal CH), 5.47 (m, 19.1H, linear, branched and terminal CH), ^{13}C nmr ($CDCl_3$, 200MHz) δ 13.9 (butyl CH_3), 14.09 (ethyl CH_3), 19.01 (butyl CH_2), 30.46 (butyl CH_2), 38.19 (terminal, linear and branched CH_2), 40.59 (butyl CH_2), 41.20 (focal CH_2), 60.77 (ethyl OCH_2), 64.69 (focal CH), 67.15 (terminal, linear and branched CH), 168.55 (C=O), 168.64 (C=O), 169.63 (C=O), FTIR NaCl plates ν_{max}/cm^{-1} 3620.5, 3536.1, 3461.7, 2982.5, 2988.4, 1730.8.

5.6 REFERENCES

1. C.J. Hawker and J.M.J. Fréchet, *J. Am., Chem. Soc.*, **112**, (1990), 7638.
2. D.A. Tomalia and H.D. Hurst, *Top. Curr. Chem.*, **165**, (1993), 193.
3. E. Malmström, M. Johansson and A. Hult, *Macromol.*, **28**, (1995), 1698.
4. W.J. Feast and N.M. Stainton, *J. Mater. Chem.*, **5**, (1995), 405.
5. E. Malmström and A. Hult, *Macromol.*, **29**, (1996), 1222.
6. "Dictionary of Organic Compounds" (5th edn.), J. Buckingham and S.M. Donaghy (Eds.), Chapman and Hall (1982).
7. "Handbook of Chemistry and Physics" (68th edn.), R.C. Weast, CRC Press, Inc. (1987).

Chapter 6.

Cross-linking studies of hyperbranched aliphatic polyesters

6.1 INTRODUCTION

As described in previous chapters, the synthesis of hyperbranched polymers occurs without cross-linking, however for certain systems cross-linking may be desirable. For example, polymers designed to be incorporated into coatings[1,2] are often required to undergo some cross-linking.

To date, there is only one report of a dendrimer being modified to produce a cross-linked system. Moszner[3] adapted the poly(propyleneimine) dendrimers, introduced by DSM,[4] by converting the amine groups to methacrylic end groups, allowing the modified dendrimer to be cross-linked in the presence of 2,2'-azoisobutryonitrile (AIBN) to form an insoluble gel. Figure 6.1 below shows a schematic representation of a fragment of a second generation poly(propyleneimine) dendrimer. The authors reacted the terminal primary amine functions with a mixed acrylate/methacrylate ester of ethylene glycol. The acrylate undergoes selective Michael Addition at both N-H bonds to give a methacrylate terminated dendrimer in which all the nitrogen atoms occur as simple tertiary amines.

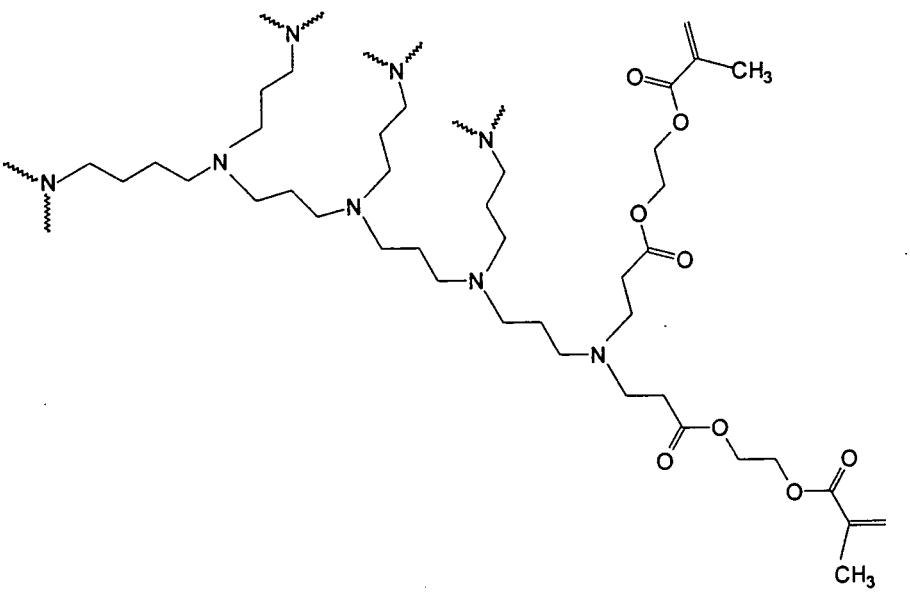

Figure 6.1 Modified poly(propyleneimine) dendrimer

The authors report an increase in glass transition temperature of the cross-linked products of, on average, 90°C when compared to the modified uncross-linked starting materials. This increase is assumed to be due to the cross-links introducing rigidity into the system.

The most notable work performed in the area of cross-linked hyperbranched systems has been that of aliphatic polyesters.[5] Several hyperbranched polyesters have been synthesised and the hydroxyl end groups converted to acrylates[6] which may undergo cross-linking when irradiated with UV. It was found that 100% conversion of the hydroxyls was not achieved and the remaining terminal hydroxyl groups could be converted to benzoates or propionates, providing a family of UV curable cross-linking polymers. Hult[7] has also prepared and photo-cured allyl ether-maleate resins based on the same set of hyperbranched polyesters.

A review of the literature reveals that several hyperbranched systems undergo unintentional cross-linking as a consequence of the reaction conditions. For example, the synthesis of hyperbranched polyurethanes[8] is hampered by the formation of a cross-linked network due to the numerous side-reactions of the terminal isocyanate groups. Reversible cross-linking has been discovered during the synthesis of hyperbranched aromatic polyesters.[9] It has been reported that, in this case, cross-linking occurs via intermolecular anhydride formation at high temperatures; these cross-links however may be cleaved by the addition of boiling THF and water. Partial cross-linking has also been observed for polyesters synthesised from 3,5-diacetoxybenzoic acid[10] at 280°C, however no explanation of the cross-linking mechanism was reported.

The cross-linking of hyperbranched systems reported thus far has relied on the chemical modification of end groups to introduce cross-linkable termini. As yet there have been no reports relating cross-linking to cross-linking agents added to hyperbranched polymers. This chapter describes an investigation of potential protocols for the cross-linking of hyperbranched aliphatic polyesters produced in the study with added polyol or polyacetate cross-linking agents.

6.2 POLYMERISATION OF DIETHYL 3-HYDROXYGLUTARATE IN THE PRESENCE OF CROSS-LINKING AGENTS

In an attempt to produce cross-linked hyperbranched polymers, the copolymerisation of a potential cross-linking molecule and diethyl 3-hydroxyglutarate was investigated. It was hoped that an insoluble gel would form in the reaction vessel which would prove that the reaction had been successful. The reaction was performed as described in section 6.6.2. The cross-linking agents were added at different times during the polymerisation to investigate the affect on the molecular weight of the resulting hyperbranched polymer. To provide a direct comparison with the hyperbranched wedges discussed in Chapter 4, the polymerisations were performed at 100°C in the presence of 5wt% $Ti(OBu)_4$ for 270 minutes. Only two cross-linking agents were used in an attempt to produce an insoluble gel.

Initially, pentaerythritol tetra-acetate (PTA) was used as it was anticipated that a multifunctional cross-linking agent would have the greatest chance of success due to the large number of reactive sites on both the A'_4 cross-linking molecule and the AB_x wedge. To contrast the A'_4 molecule, an A_2 diol was used. 1,5-Pentanediol was considered a suitable cross-linking agent for several reasons: it should possess a large degree of conformational flexibility hence making it easy to approach the terminal groups of the AB_x wedge; it has a high boiling point (242°C) and therefore will not be removed by a flow of nitrogen through the reaction vessel and it is a primary diol hence it should be relatively reactive. One potential problem with the diol may be the formation of loops with the same wedge, see Figure 6.2.

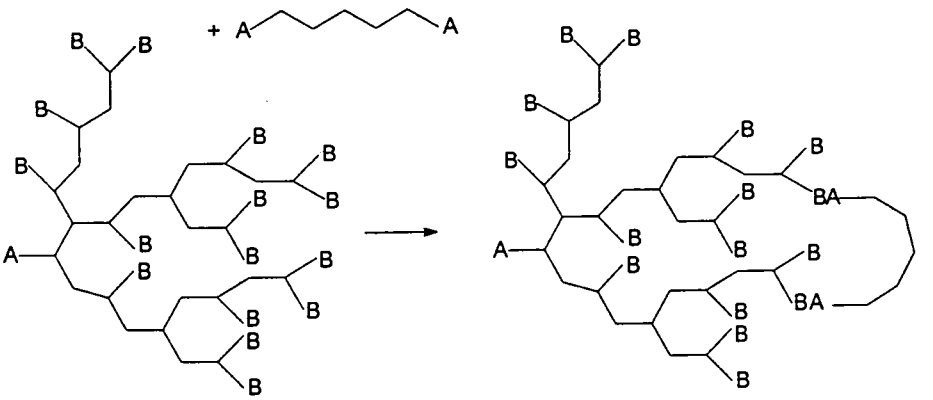

Figure 6.2 Possible reaction between a hyperbranched wedge and 1,5-pentanediol

The following sections discuss the results of the attempted cross-linking reactions of both PTA and 1,5-pentanediol.

6.2.1 Cross-linking in the presence of PTA.

The ^{1}H nmr spectrum of PTA, Figure 6.3, was straightforward to assign. The singlet at 2.07ppm was assigned to the CH_3 hydrogens whilst the singlet at 4.13ppm was assigned to the methylene signals.

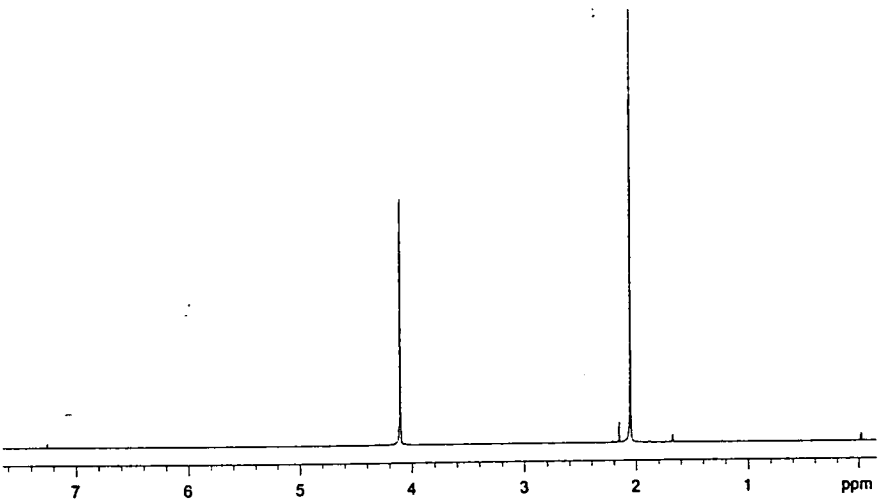

Figure 6.3 ^{1}H nmr spectrum of PTA.

In the initial investigation the monomer and the PTA were present in the reaction vessel in a 3:1 molar ratio from the beginning of the experiment. A full listing of the ^{1}H and ^{13}C nmr results of the reactions reported in this section may be found in Appendix 4, Tables 1-3 and 16-18. The resulting yellow product did not appear as viscous as the hyperbranched wedge synthesised under the same conditions, suggesting that the compound was of lower molecular weight. Gel permeation chromatography (using linear polysytrene standards as calibrants) was performed and showed an M_n of 610, which would correspond to a tetramer, with a polydispersity of only 1.1.

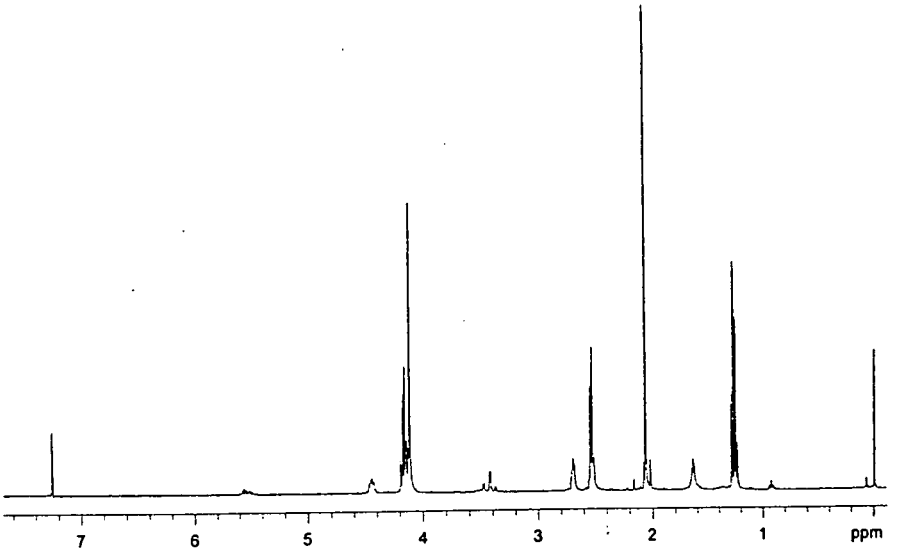

Figure 6.4 ^{1}H nmr spectrum of the product of the copolymerisation of PTA and diethyl 3-hydroxyglutarate.

On analysis of the ^{1}H nmr product spectrum, Figure 6.4, it is clear that there is a small amount of monomer still present due to the observed hydroxyl doublet at 3.44ppm. This signal is assigned to the hydrogen of the hydroxyl coupling with the methine C**H** in the structure shown below, Figure 6.5. This signal is only detected for the monomer species, the hydroxyl of the focus of the hyperbranched wedges is not observed in their ^{1}H nmr spectra.

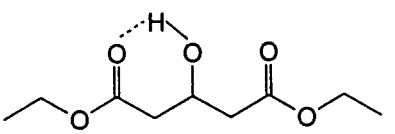

Figure 6.5 Diethyl 3-hydroxyglutarate

As the products of the homopolymerisations of diethyl 3-hydroxyglutarate do not exhibit this signal, it seems plausible to propose that PTA preferentially reacts with the monomer to form a 4:1 condensation product, Figure 6.6, and this is sterically inhibited from further reaction. The product of a 4:1 simple ester exchange has a molar mass of 720 which is reasonably consistent with the GPC measurement.

The ^{1}H nmr spectrum, Figure 6.4, is consistent with the presence of the proposed 4:1 condensation product, residual PTA and wedge formation.

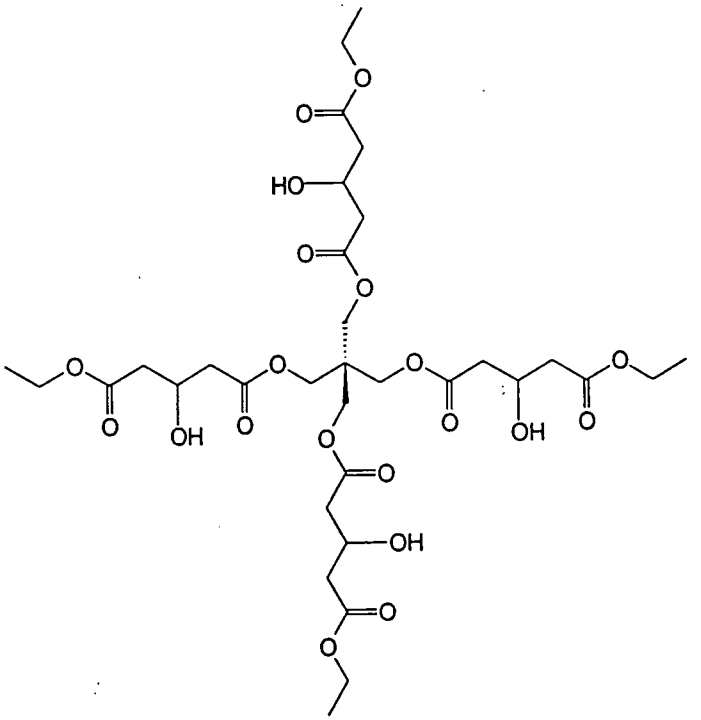

Figure 6.6

The ^{13}C nmr spectrum (Figure 6.7) is also consistent with this proposal and shows very little evidence of hyperbranched formation.

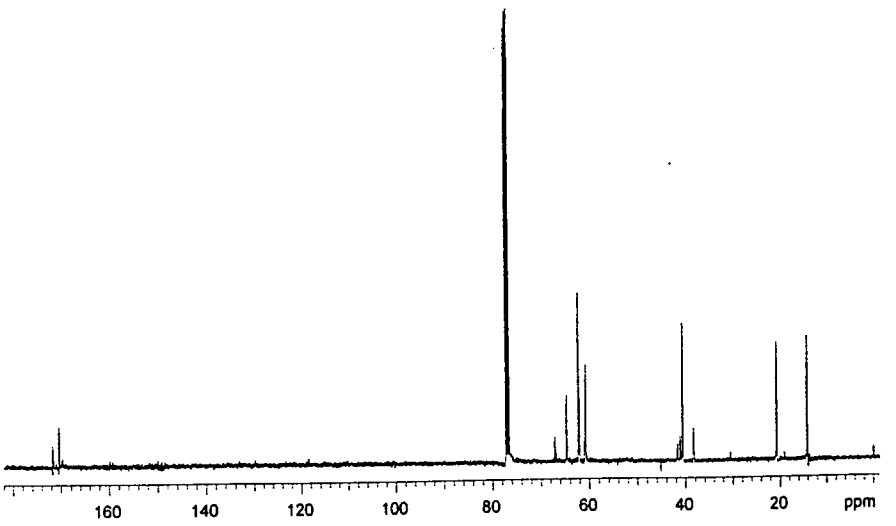

Figure 6.7 ^{13}C nmr spectrum of the product of the copolymerisation of PTA and diethyl 3-hydroxyglutarate.

The expected multiplet at 67ppm, due to the CH-O of the terminal, linear and branched sub-units in a hyperbranched segment is not observed and is replaced by three distinct weak signals at 66.87, 67.15 and 67.43ppm. The strongest signal of this set (67.15ppm) corresponds to the linear sub-unit in a hyperbranched wedge (see Chapter 4) which is consistent with the picture deduced from the ^{1}H nmr spectrum. Thus, the majority of the linear signal is assigned to the CH-O of the structure shown in Figure 6.6 and the other minor methine peaks are indicative of wedge formation. These results indicate that PTA preferentially reacts with the monomer to consume the ester groups in competition with the polymerisation process, under the appropriate conditions it ought therefore to be an effective cross-linking agent.

In an attempt to encourage true cross-linking, PTA was added to the reaction vessel 2 hours after the polymerisation had commenced. It was anticipated that this method would allow hyperbranched formation before the cross-linking molecule was added, providing a technique for the successful coupling of hyperbranched wedges. When the reaction reached completion, the viscous yellow liquid was analysed using a variety of techniques to assess the success of the cross-linking reaction.

The molecular weight, determined by GPC, was 820 with a PDI of 1.3. Both the ^{1}H and ^{13}C nmr spectra, Figures 6.8 and 6.9, exhibit, in addition to the signals from the unreacted PTA, the anticipated hyperbranched signals proving that this protocol overcomes the problem of the monomer transesterifying preferentially with the cross-linking agent.

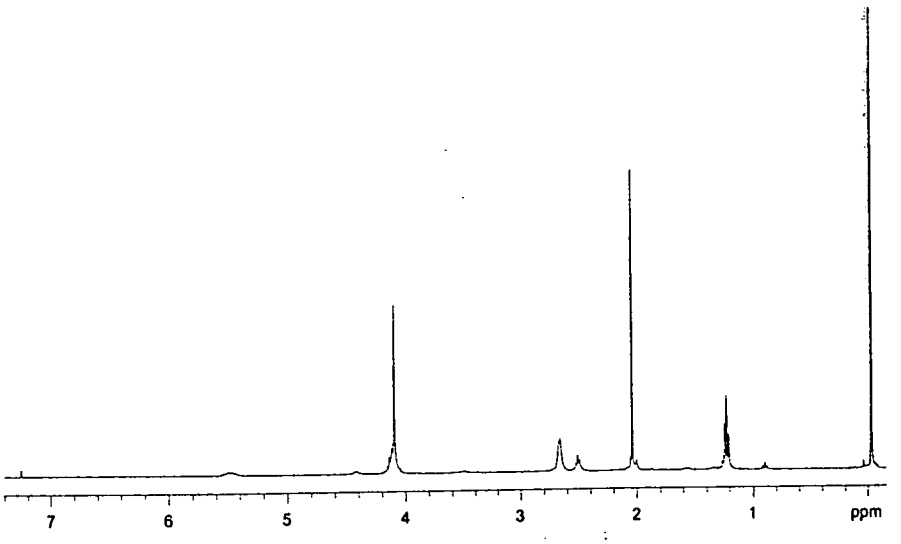

Figure 6.8 ^{1}H nmr of diethyl 3-hydroxyglutarate polymerised for two hours before the addition of PTA.

The multiplets observed at 2.51 and 2.66ppm (assigned to the hydrogens of the methylene groups of the focal and polymeric sub-units respectively) and those at 4.44 and 5.51ppm (assigned to the methine hydrogen of the focal and polymeric sub-units) imply that hyperbranched formation had occurred. It is impossible to determine the extent of incorporation of PTA *via* ^{1}H nmr spectroscopy due to the singlet of the CH_2O of the cross-linking agent being coincident on the OCH_2 of the hyperbranched ethyl ester multiplet. However, if coupling has occurred, the glass transition temperature of the system should have increased due to the inclusion of quaternary centres. These centres will possess restricted mobility, hence comparison of a hyperbranched wedge of similar molecular weight with the coupled sample will provide a method of determining if coupling has occurred. As the T_g of the cross-linked sample is -48.1°C and a hyperbranched wedge of similar molecular weight has a T_g of approximately -57°C it is postulated that coupling has occurred to a small extent.

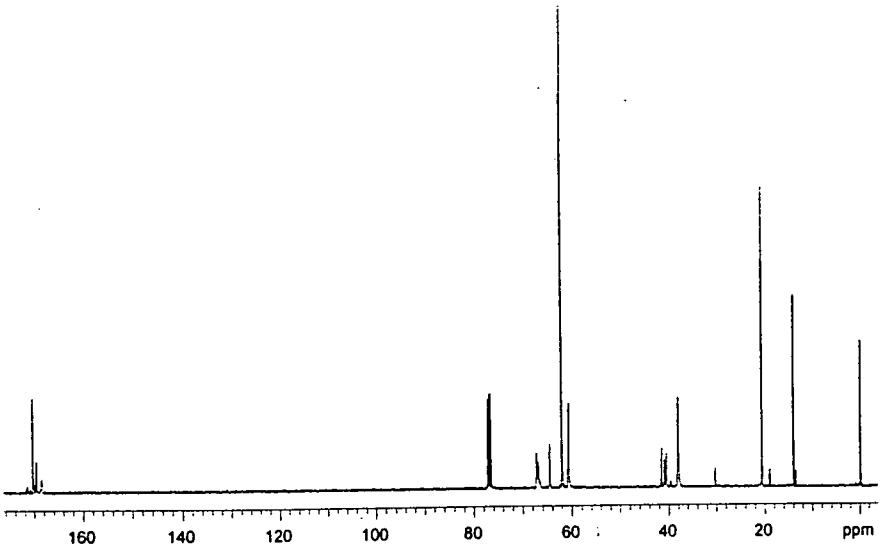

Figure 6.9 ^{13}C nmr of diethyl 3-hydroxyglutarate polymerised for two hours before the addition of PTA.

The ^{13}C nmr spectrum displays all the expected signals due to hyperbranched formation along with the signals of PTA at 20.69ppm (CH_3), 41.57ppm (CCH_2), 62.22ppm (OCH_2) and 170.47ppm (C=O). It was hoped that the degree of branching (DB) would be highly dependent on the amount of coupling in the system. When cross-linking occurs, the linear or terminal sub-units will be consumed providing more branched and linear sub-units respectively. If these new sub-units possess a slightly different shift to those of the hyperbranched polymer, it may be possible to determine the extent of cross-linking.

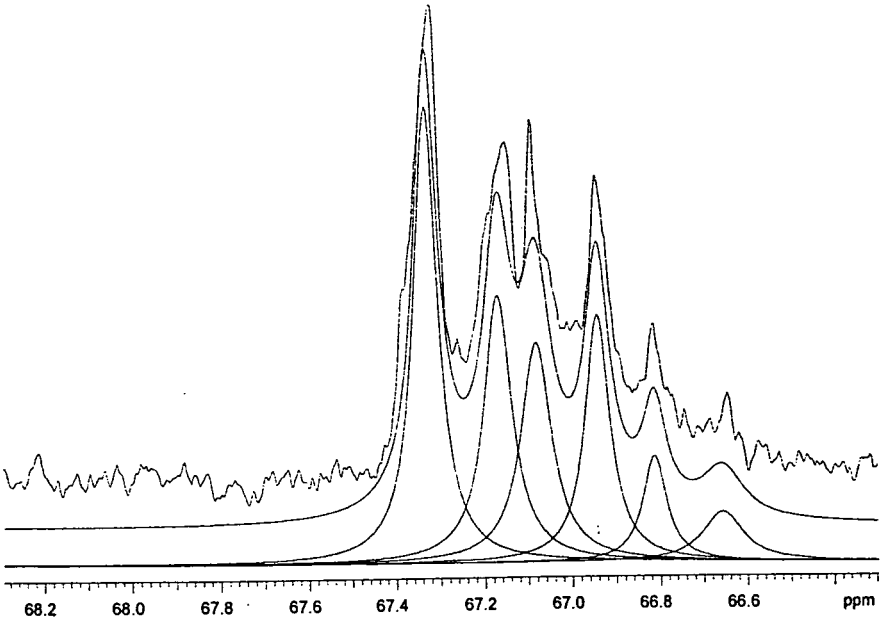

Figure 6.10 Expansion of ^{13}C nmr spectrum and its Laurentzian deconvolution of a cross-linked sample of poly(diethyl 3-hydroxyglutarate).

On inspection of an expansion of the ^{13}C nmr spectrum (Figure 6.10) of the polymer sample, it is clear that the multiplet centred at 67ppm is more complicated than was the case for the hyperbranched wedge samples. An additional signal is found at 66.66ppm, it is postulated that this is due to the cross-link between the wedge and PTA, see Figure 6.11. The presence of this signal suggests that cross-linking has occurred, albeit to a small extent. In an attempt to quantify the amount of cross-linking, the percentage of this postulated cross-link methine sub-unit was calculated from the deconvoluted methine peak areas. It was found to be 5% of the total number of sub-units present within the molecule.

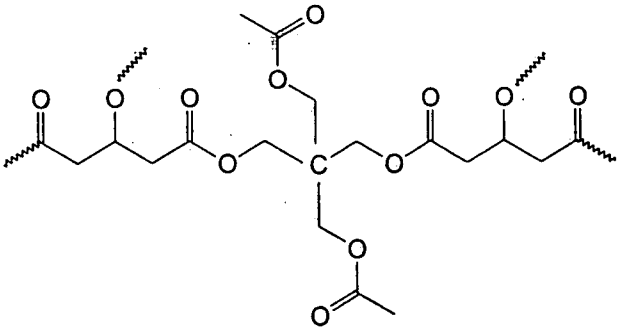

Figure 6.11 Example of a cross-linked section of poly(diethyl 3-hydroxyglutarate).

A third cross-linking reaction was attempted, where the monomer was polymerised for three hours before the addition of PTA. The GPC trace (Appendix 4.18) shows a slightly bimodal distribution with an M_n of 1140. Both the ^1H and ^{13}C nmr spectra, Figures 6.12 and 6.13, show the presence of hyperbranched polymer as well as unreacted PTA.

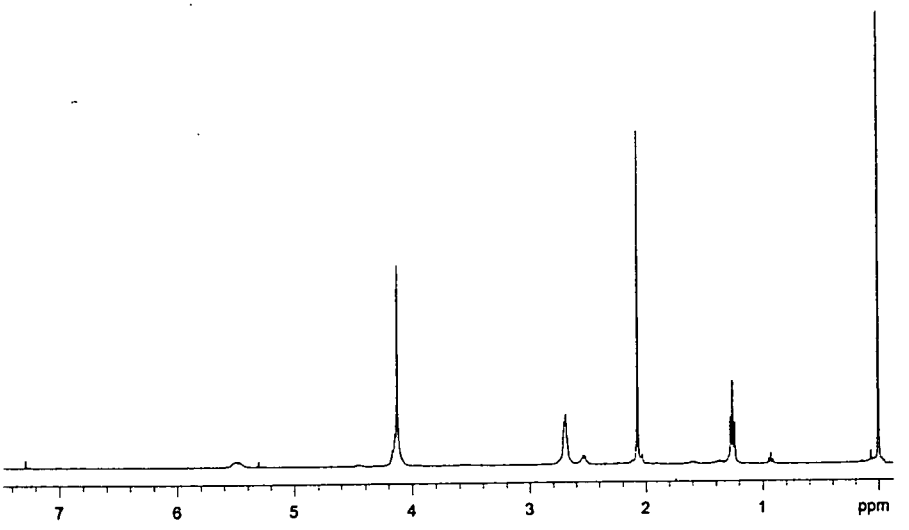

Figure 6.12 ^1H nmr of diethyl 3-hydroxyglutarate polymerised for three hours before the addition of PTA.

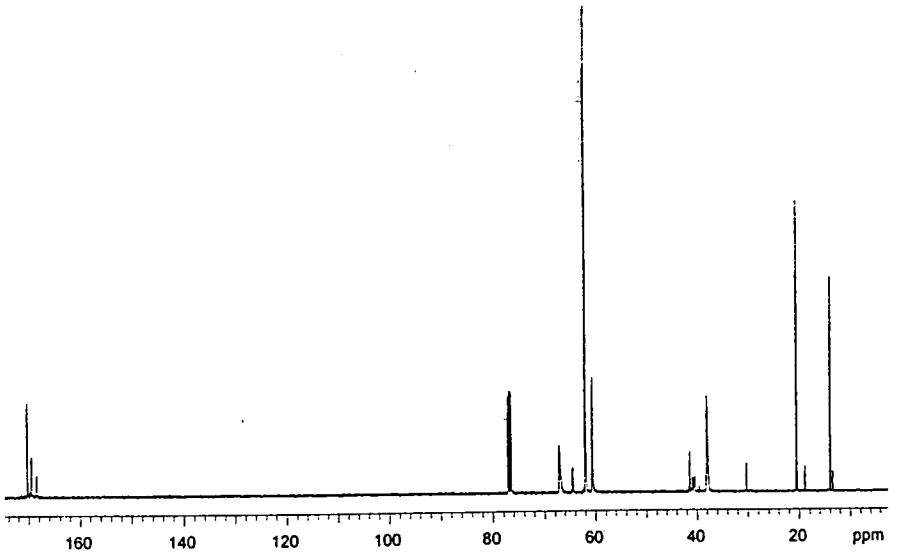

Figure 6.13 ^{13}C nmr of diethyl 3-hydroxyglutarate polymerised for three hours before the addition of PTA.

The DB of this sample was determined to be 0.62 which is higher than that of the previous sample. This may be due to the extended polymerisation time of reaction before the coupling agent was added. Again, an additional peak was found at 66.65ppm, assigned to the methine in a PTA based cross-link. The percentage of this sub-unit was found to be 5%.

The glass transition temperature of this polymer was found to be -47.4°C which is very similar to hyperbranched wedges of similar molecular weight. From this, it may be deduced that very few cross-links have been formed in this sample. This may also be a consequence of the shorter reaction time provided for cross-linking.

From the characterisation data of these reactions, it would seem that the optimum condition for cross-linking is to allow the formation of hyperbranched polymer before the addition of PTA. However, if the cross-linking agent is added towards the end of the polymerisation reaction, it has difficulty in successfully reacting with the ester groups to form a cross-linked sample which might be due to a mixing or incompatibility problem. All reactions discussed in this section are disappointing in that an insoluble gel did not form. The following section discusses

the use of 1,5-pentanediol as a cross-linking agent in the polymerisation of diethyl 3-hydroxyglutarate.

6.2.2 Cross-linking in the presence of 1,5-pentanediol

Only two reactions were performed using 1,5-pentanediol and the full listing of the ^{1}H and ^{13}C nmr results of the products of the reactions reported in this section can be found in Appendix 4, Tables 4-5 and 19-20. The first attempted cross-linking reaction involved the addition of 1,5-pentanediol to the reaction vessel after the monomer had been allowed to react for two hours to provide a direct comparison with the PTA experiment. A 3:2 molar ratio of monomer to diol was used so that the ratio of ester units to potential cross-linking hydroxyl units was the same as in the PTA case. The results of this reaction looked promising; an M_n of 2250 was found (GPC) and the trace indicated a bimodal distribution (Appendix 4.19). The sample appeared to exhibit two glass transition temperatures, DSC, Figure 6.14. The minor transition at -38.3°C is postulated to be a consequence of uncross-linked material as this value correlates well with results obtained from hyperbranched wedges of similar molecular weight, whilst the major transition at -29.6°C is attributed to material which has been coupled through the diol.

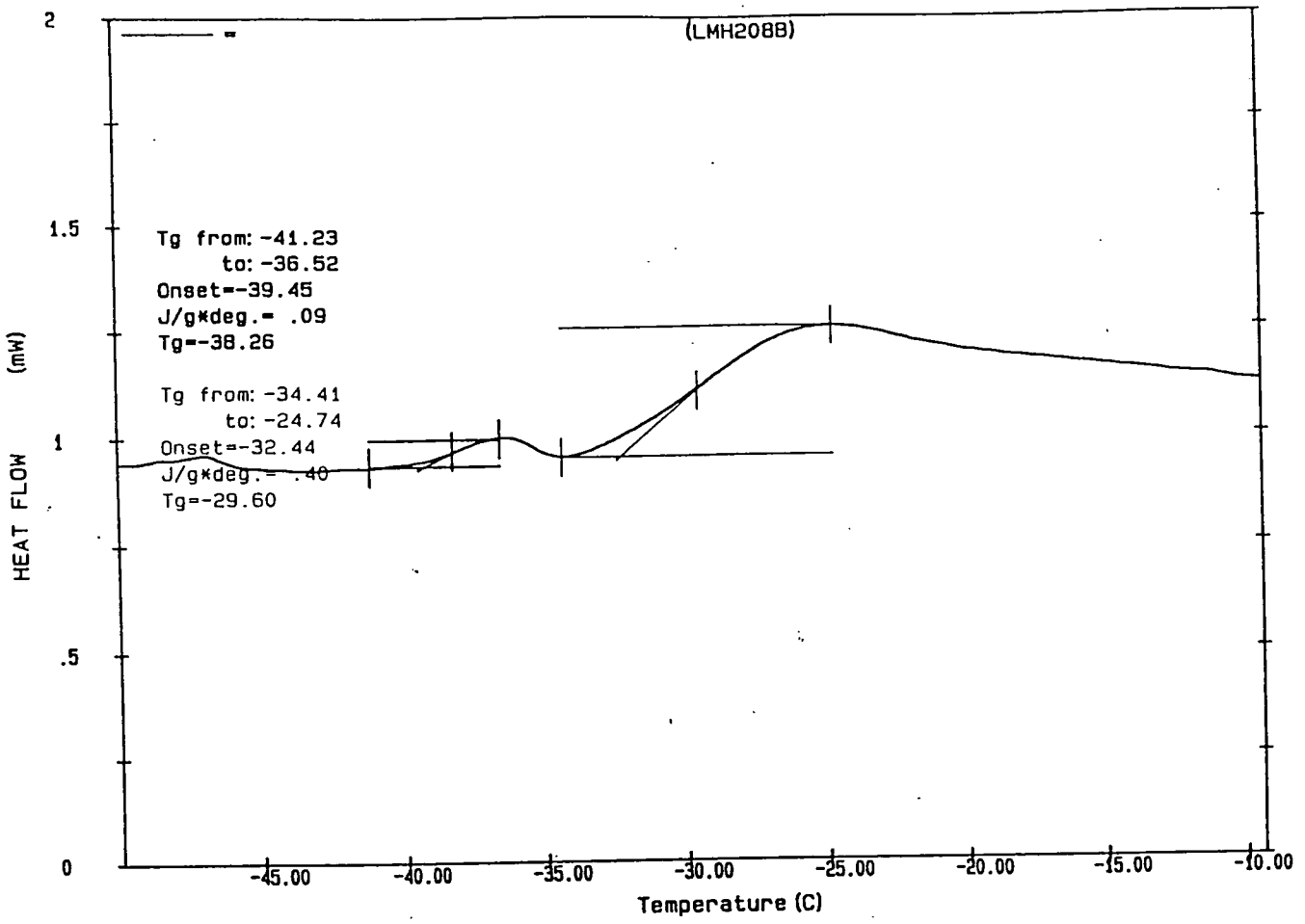

Figure 6.14 DSC trace of coupled hyperbranched polymer.

Analysis of the ^{1}H and ^{13}C nmr spectra, Figures 6.15 and 6.16, show that it is not possible to determine the number of cross-links incorporated into the polymer due to the lack of diagnostic 1,5-pentanediol signals. On close inspection of the ^{1}H nmr spectrum, broad multiplets are found at 1.61ppm (CH_2) and 3.55ppm (OCH_2) of the cross-linking molecule, the other methylene multiplet is not observed in the spectrum, possibly due to some overlap between this methylene and that of the butyl esters. As the signals due to the OCH_2 are expected to be shifted when bonded to a carbonyl group, it is possible that the new resonances are overlapping with the ethyl ester OCH_2 signals at 4.13ppm. It was hoped that the CH_2O signals (readily observed as a triplet at 3.66ppm in the ^{1}H nmr spectrum) would be distinguishable in the product spectrum, however a sharp resonance in this region is not found.

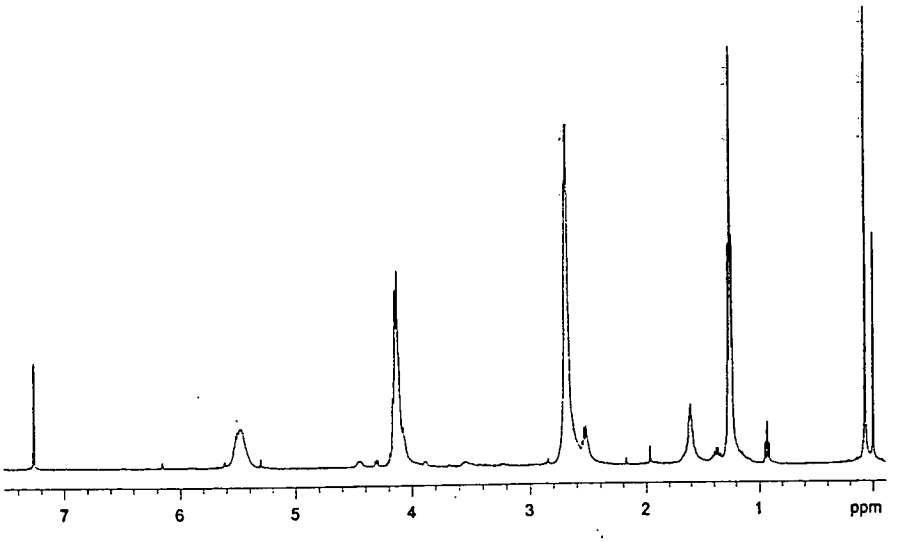

Figure 6.15 ^{1}H nmr of diethyl 3-hydroxyglutarate polymerised for two hours before the addition of 1,5-pentanediol.

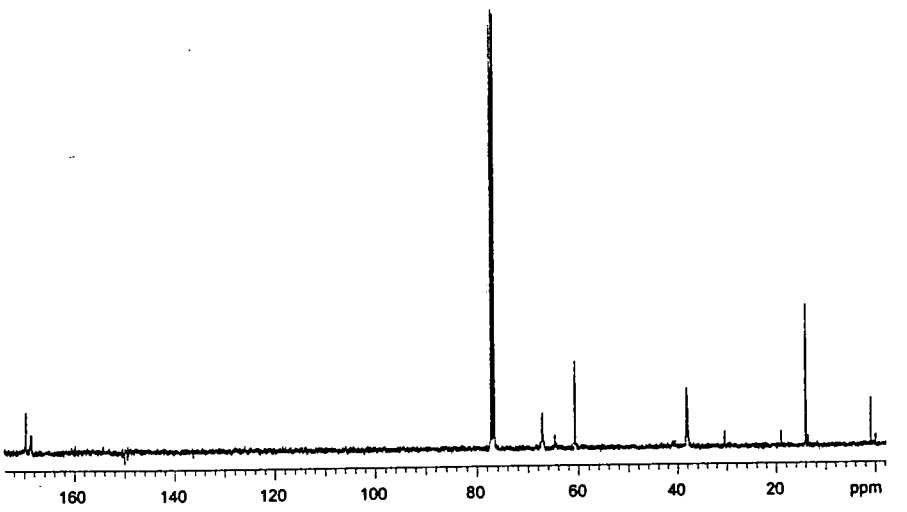

Figure 6.16 ^{13}C nmr of diethyl 3-hydroxyglutarate polymerised for two hours before the addition of 1,5-pentanediol.

The ^{13}C nmr spectrum is uninformative with respect to the amount of coupling reagent incorporated into the hyperbranched polymer. The expected signals due to 1,5-pentanediol 21.91ppm ($\mathbf{C}H_2$), 32.20ppm ($\mathbf{C}H_2$) and 62.59ppm ($O\mathbf{C}H_2$) are not observed, which is assumed to be a consequence of the S/N ratio being rather poor. The multiplet centred at 67ppm in the ^{13}C nmr spectrum, Figure 6.17, provides

information on the DB of the polymer. Unlike the PTA samples, a distinct resonance for the cross-linked sub-units was not detected. This may be due to several factors: the S/N ratio may not have been good enough or the cross-linked sections may not have been significantly different to the other linkages in the molecule.

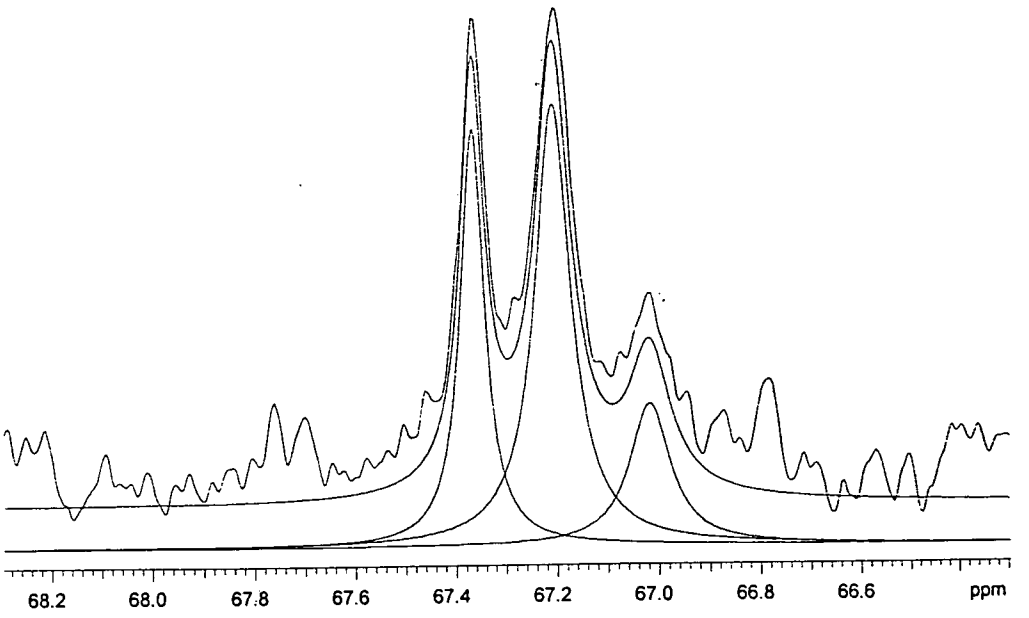

Figure 6.17 Expanded ^{13}C nmr spectrum and its Laurentzian deconvolution

If cross-linking occurs, sub-units of the type shown in Figure 6.18a will be present. It is possible that ^{13}C nmr spectroscopy may not be sensitive enough to distinguish between a sub-unit containing a 1,5-pentanediol and a terminal sub-unit, Figure 6.18b.

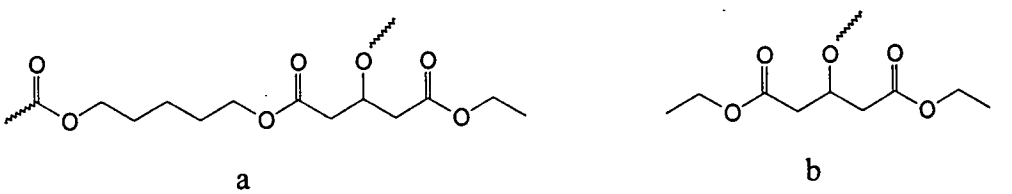

a b

Figure 6.18

a)Example of a cross-linked section of poly(diethyl 3-hydroxyglutarate).

b) Example of a terminal group of poly(diethyl 3-hydroxyglutarate).

The methine carbon of the monomer residue is the carbon which is used to distinguish between the differing types of sub-units present in the hyperbranched molecule. It can be seen that the difference in structure between Figure 6.18a and b is slight due to the presence of four identical bonds between the methine carbon and the CH_2 of the terminal ester group, it is only the fifth bond which would provide a change in environment. It is therefore postulated that ^{13}C nmr spectroscopy would not be able, under the conditions used in this analysis, to distinguish between an ethyl ester terminal group and a cross-linked moiety. The DB of this polymer was determined to be 0.50 suggesting that there are numerous linear sub-units present within the polymeric sample. The relatively low DB value may be due to the presence of cross-links.

In an attempt to further understand the reaction, 1,5-pentanediol was added to the reaction vessel after three hours of polymerisation. From both the DSC and GPC analysis, only one type of species was present in the sample. The M_n was found to be 2100 (GPC), whilst the T_g was -41.3°C. These results suggest that if cross-linking has occurred it is only to a very small extent as the M_n and T_g values correlate well with hyperbranched wedges of similar molecular weight. Again, the ^1H and ^{13}C nmr spectra, Figures 6.19 and 6.20, are relatively uninformative due to the lack of distinct cross-linking signals.

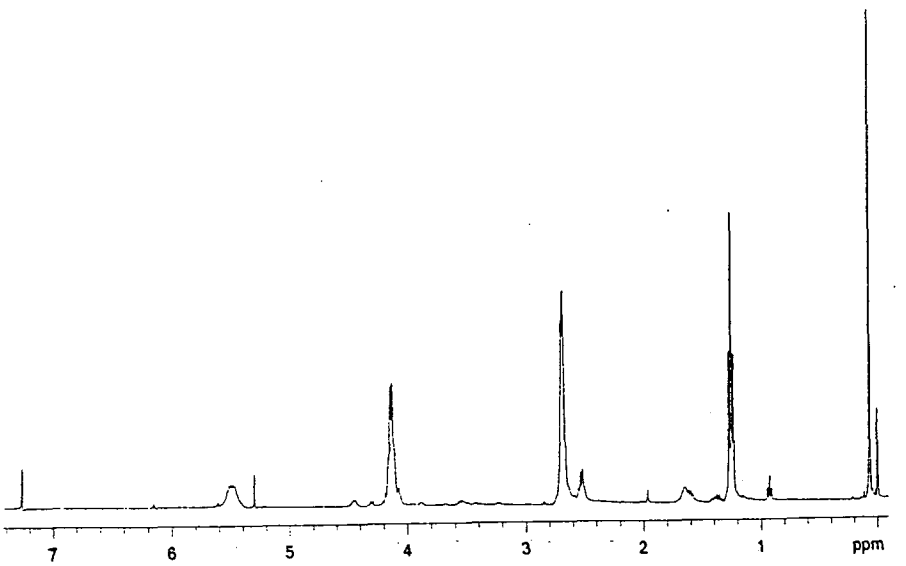

Figure 6.19 ^1H nmr of diethyl 3-hydroxyglutarate polymerised for three hours before the addition of 1,5-pentanediol.

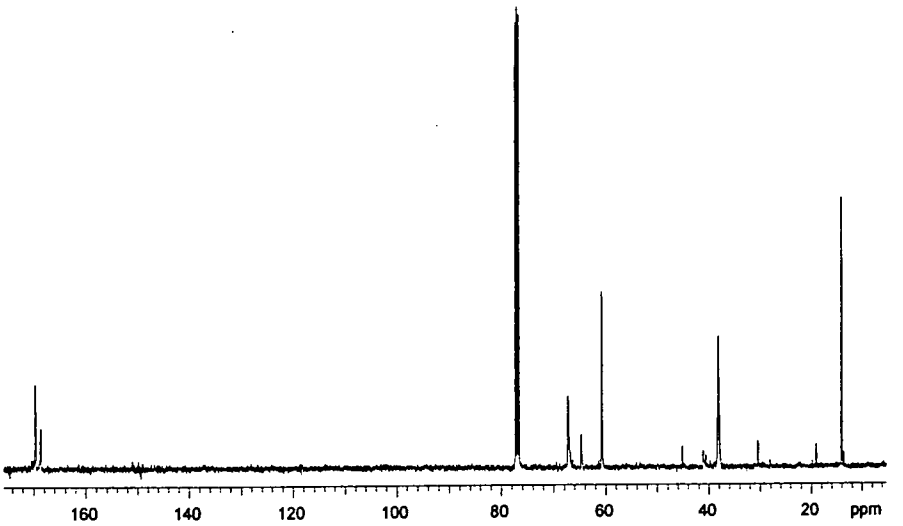

Figure 6.20 ^{13}C nmr of diethyl 3-hydroxyglutarate polymerised for three hours before the addition of 1,5-pentanediol.

The DB, Figure 6.21, of this hyperbranched polymer was calculated to be 0.58, again no signals due to the cross-linked sub-units were resolved.

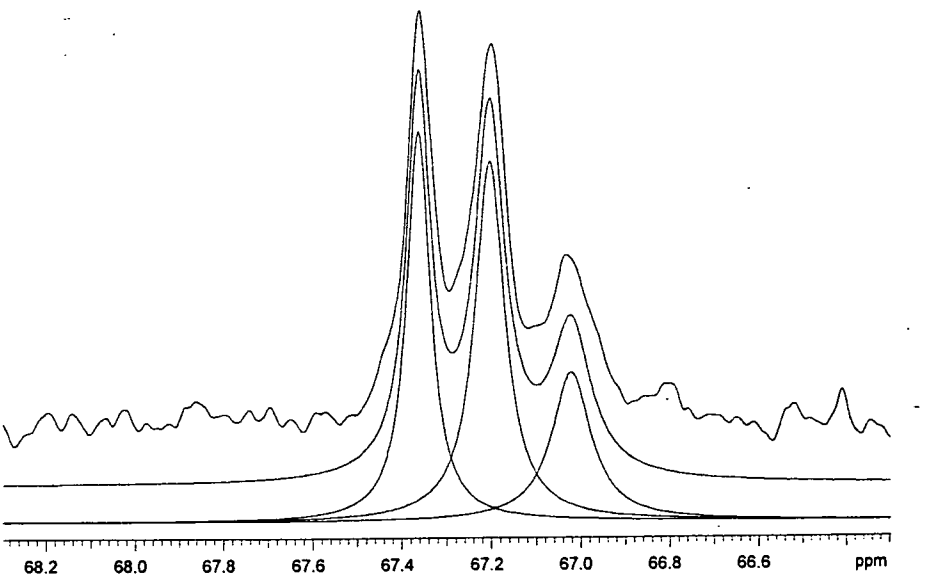

Figure 6.21 Expansion of the ^{13}C nmr spectrum and its Laurentzian deconvolution

In conclusion, as the DB correlates well with hyperbranched wedges of similar molecular weight, it would seem that cross-linking has been unsuccessful in this particular case.

6.2.3 Conclusions

It would appear that neither cross-linking molecule provides a method for producing a totally insoluble network. This was both surprising and disappointing as it was anticipated that the numerous B groups would easily react with the cross-linking reagents. It is unclear why only a small extent of cross-linking occurred, the proposed chemistry has been demonstrated to work for the PTA case so the most likely explanation of the relatively poor level of coupling must involve poor mixing. A survey of the literature reveals that ester groups are not generally used in commercial cross-linking reactions.

Table 6.1 summarises the results discussed above.

PTA				1,5-Pentanediol			
Time(mins)[a]	M_n[b]	T_g(°C)[c]	DB[d]	Time(mins)[a]	M_n[b]	T_g(°C)[c]	DB[d]
0	610	-66.9	-	-	-	-	-
120	820	-48.1	0.54	120	2250	-29.6	0.50
180	1140	-47.4	0.62	180	2100	-41.3	0.58

a Time after which the cross-linking molecule is added
b Determined by GPC with linear polystyrene standards and $CHCl_3$ as eluent
c Determined using DSC
d Calculated from ^{13}C nmr spectroscopy

Table 6.1 Summary of polymerisations in the presence of cross-linking reagents.

From Table 6.1, it would appear that the optimum conditions for coupling occurs when the hyperbranched wedge has been allowed to form for 120 minutes before the addition of the coupling agent, this provides a further 150 minutes for the coupling reaction to proceed. Both the PTA and 1,5-pentanediol copolymer samples have glass transition temperatures higher than those of the corresponding wedges indicating the presence of links between hyperbranched sub-units. Both samples also exhibit lower DBs than are observed for simple AB_2 analogues which may indicate a coupled structure.

The large discrepancies in molecular weight between the two systems is puzzling. On cursory inspection, it may be concluded that the polymerisations in the presence of PTA are unsuccessful, however it has been shown in section 6.2.1 that reaction does occur for the latter 2 cases. It may be envisaged that although the PTA does react with the growing wedges, it does not effectively couple the wedges together. The product of this reaction would be hyperbranched wedges with numerous pendant A'_3 groups. If this is true, the increase in T_g for the low molecular weight samples may be due to the A' end groups. As 1,5-pentanediol is a more reactive and conformationally flexible molecule, it may be postulated that the increase in M_n is due to the diol forming cross-links and coupling the wedges together. Hence, if these theories are correct, 1,5-pentanediol is a more effective cross-linking agent than PTA in this system.

6.3 LARGE SCALE SYNTHESIS OF HYPERBRANCHED POLY(DIETHYL 3-HYDROXYGLUTARATE).

To ensure the same batch of poly(diethyl 3-hydroxyglutarate) was used throughout the series of proposed wedge cross-linking reactions, a large scale reaction, using 40g of monomer, was performed in the presence of 0.5g titanium (IV) butoxide. As described earlier (Chapter 4, section 4.2), the catalyst appears to become 'poisoned' as the reaction proceeds. To circumvent this, the catalyst was added in 0.1g units at the start of reaction and after 1, 2, 3 and 5 hours in a reaction of 8.5 hours duration.

The number average molecular weight, as determined by GPC was 2800amu. This compares well with the ^{1}H nmr average molecular weight of 2260, determined from the relative integrals of the CH_2 of the focus and the CH_2 of the terminal, linear and branched sub-units as described in chapter 4, section 4.2.4. The DSC analysis shows a T_g of -38.8°C which correlates well with the values obtained in the small scale reactions reported in Chapter 4. The degree of branching for this wedge is calculated, from a ^{13}C nmr deconvolution procedure, to be 0.52. Figures 6.22 and 6.23 show the ^{1}H and ^{13}C nmr spectra of poly(diethyl 3-hydroxyglutarate).

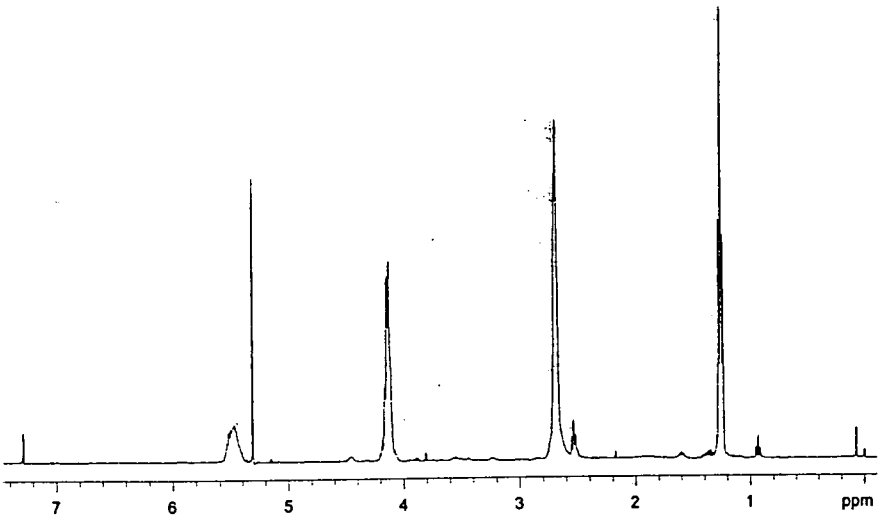

Figure 6.22 ^{1}H nmr spectrum of poly(diethyl 3-hydroxyglutarate)

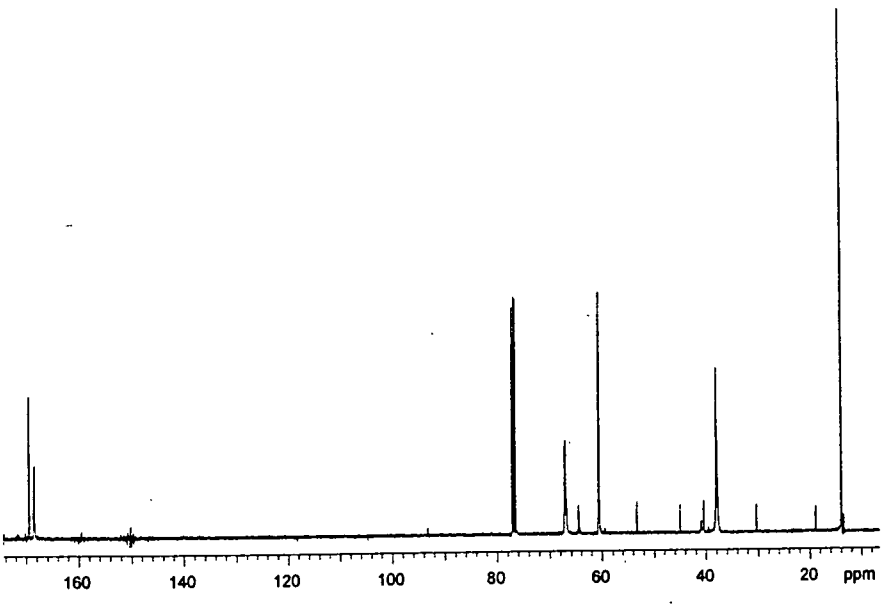

Figure 6.23 ^{13}C nmr spectrum of poly(diethyl 3-hydroxyglutarate)

As discussed in Chapter 5, the sample exhibits all the expected hyperbranched signals in both the ^{1}H and ^{13}C nmr spectra. The singlet found at 5.31ppm is assigned to residual dichloromethane from the work-up.

6.4 CROSS-LINKING OF PRE-FORMED POLYMER SAMPLES

The following sections discuss the attempted cross-linking reactions between hyperbranched wedges and A_x cross-linking molecules. As the polymer had a molecular weight of 2800amu it was anticipated that these reactions ought to occur more easily than in the experiments designed to probe the feasibility of the process (section 6.2). Thus, large hyperbranched units will have many potential coupling or cross-linking sites and the result of coupling on molecular weight and properties should be easily detected.

6.4.1 Attempted cross-linking of poly(diethyl 3-hydroxyglutarate) with PTA

Pentaerythritol tetra-acetate (PTA) was used as a cross-linking reagent due to its solubility in a number of solvents, unlike its parent compound pentaerythritol. Figure 6.24 below shows the apparatus used to perform the reaction.

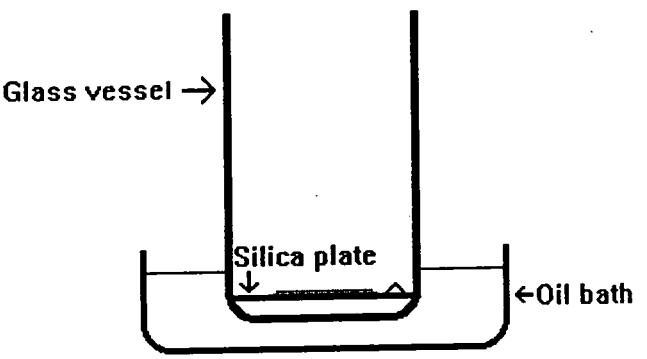

Figure 6.24

Poly(diethyl hydroxyglutarate) (M_n=2800) was mixed with PTA on a silica plate in a 5:2 wt for wt basis, as described in section 6.6.4, and placed in the glass reaction vessel which was lowered into a pre-heated oil bath. Several reactions were performed under varying conditions. A small amount of white solid sublimed around the lip of the reaction vessel when the temperature of the oil bath was 110°C, this was

analysed and found to be unreacted PTA. A lower temperature was used (90°C) and the amount of sublimation decreased. A full listing of ^{1}H and ^{13}C nmr results of the products of the reactions reported in this section may be found in Appendix 4, Tables 6-12 and 21-27.

It was initially anticipated that the percentage of cross-linking might be calculated from the relative intensities of the singlets of the OCH_2 and CH_3 of PTA normalised to a signal in the starting polymer. However, on analysis of a cross-linked sample it is clear that the degree of cross-linking cannot be determined using this method due to the overlap of the relevant cross-link and polymer signals. Figure 6.25 below shows the ^{1}H nmr spectrum of the product of the attempted cross-linking of poly(diethyl 3-hydroxyglutarate) and PTA at 110°C for 17 hours. The OCH_2 signals of both the polymer and the cross-linking agent are coincident at 4.13ppm, hence it is impossible to determine the success of the reaction *via* this method.

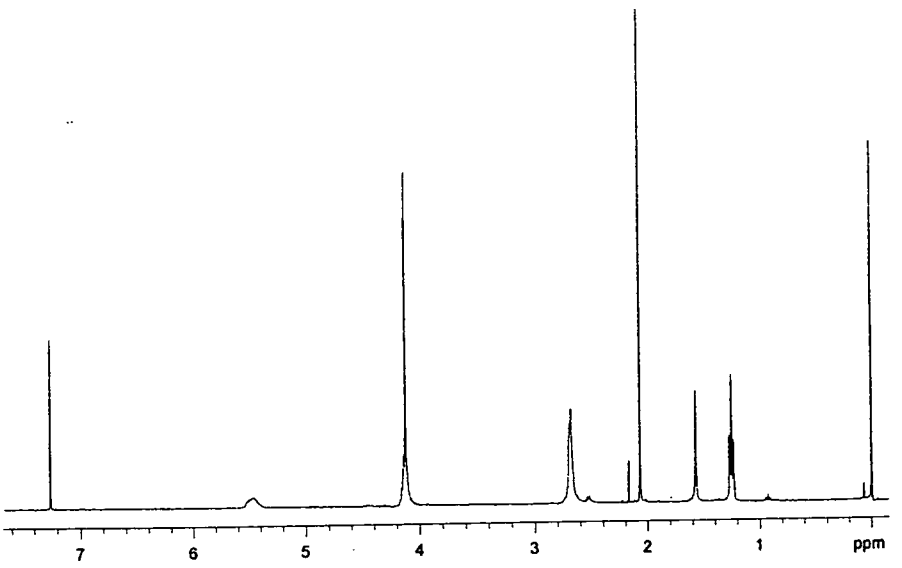

Figure 6.25 ^{1}H nmr spectrum of post cross-linked poly(diethyl 3-hydroxyglutarate).

An alternative method to evaluate the success of the cross-linking process was utilised. This involved comparison of the relative integrated intensities of the CH_3 of the PTA at 2.07ppm with that of the CH_2 of the polymeric wedge at 2.69ppm. The table overleaf summarises the results:

Temp(°C)/ Time(hours)[a]	1.26ppm signals[b]	2.07ppm signals[b]	2.69ppm signals[b]	DB[c]
90/2.5	0.84	0.13	1	0.52
90/5	0.76	0.59	1	-
90/17	0.71	0.29	1	-
110/2.5	0.81	0.03	1	0.47
110/5	0.80	0.05	1	0.48
110/17	0.68	0.46	1	0.51
185/0.25	0.80	0.67	1	-

a Reaction conditions
b Refers to the relative intensity of those signals compared to that of the 2.69ppm multiplet
c As determined *via* ^{13}C nmr spectroscopy

Table 6.2 Summary of ^{1}H and ^{13}C nmr results of the cross-linking of pre-formed poly(diethyl 3-hydroxyglutarate).

If cross-linking is successful, the relative integrated intensity of the peak at 2.07ppm (due to the CH_3 group of PTA) should decrease, as should the triplet at 1.26ppm due to the ethyl ester CH_3 hydrogens of the polymer. To monitor the success of the reaction, it is necessary to quantify these integrals by comparing them to a polymer signal which will not be consumed during the cross-linking process. The signal at 2.69ppm (due to the CH_2 hydrogens of the polymeric wedge) will not increase or decrease during the reaction, hence, when the CH_3 signals of the wedge and cross-linker are normalised with respect to this, it should be possible to estimate the degree of reaction of both esters.

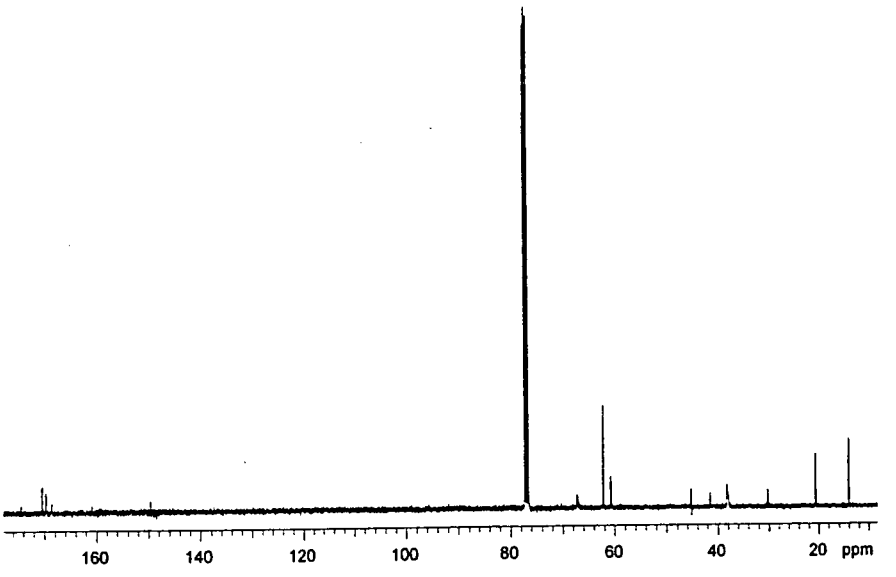

Figure 6.26 ^{13}C nmr spectrum of post cross-linked poly(diethyl 3-hydroxyglutarate).

Considering those reactions performed at the same temperature but differing reaction times, it would appear, from Table 6.2, that the amount of cross-linking is dependent on the duration of the reaction. For example, for both families of reactions performed at 90 and 110°C, the relative amount of $\mathbf{CH_3}$ ester protons steadily decreases as the reaction time increases implying that cross-linking is time dependent. However, it should be noted that the amount of $\mathbf{CH_3}$ of the cross-linking agent still present in the sample may not be reliable due to sublimation. Hence only the $\mathbf{CH_2}$ and $\mathbf{CH_3}$ polymer signals may be used to assess the success of the reaction from ^{1}H nmr spectroscopy.

When the degree of branching (DB) values are examined, it would appear that within the limits of measurement, they remain constant. It should be noted however, that the samples possessing the lowest DB also possess the highest T_g values (shown in Table 6.3). This may be interpreted as evidence in favour of coupling having occurred. Consider Figure 6.27 overleaf:

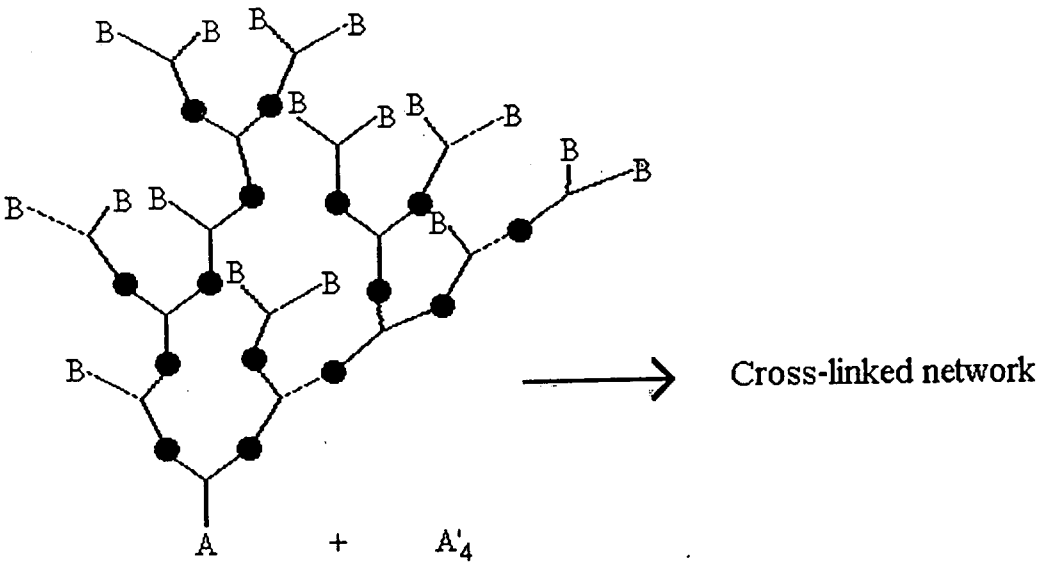

Figure 6.27

If coupling occurs, it can be seen that the ester end groups must be consumed, increasing the number of linear and branched sub-units within the molecule. As coupling must be regarded as a purely statistical process, it is impossible to predict how the DB will change. It may be possible that the reaction will occur in such a way that the DB remains constant, therefore it is not feasible to predict the amount of cross-linking using the DB values.

Table 6.3 overleaf shows the number average molecular weights (as determined GPC) and the glass transition temperatures of the attempted wedge cross-linking reactions:

Temp(°C)/Time(hours)[a]	M_n[b]	T_g(°C)[c]	DB[d]
90/2.5	2210	-27.7	0.52
90/5	1970	-32.9	-
90/17	2050	-27.9	-
110/2.5	2570	-23.4	0.47
110/5	2060	-21.5	0.48
110/17	1690	-24.3	0.51
185/0.25	1550	-28.9	-

a Temperature and duration of the reaction
b Determined by GPC using linear polystyrene standards and $CHCl_3$ as eluent
c Determined by DSC
d As determined *via* ^{13}C nmr spectroscopy

Table 6.3 Summary of the M_n values (as determined GPC) and the glass transition temperatures.

It is both interesting and surprising to note that the observed M_n values are consistently lower than that determined for the hyperbranched wedge (M_n = 2800). If cross-linking had been highly successful, the decrease in M_n may have been explained by the removal of the gel particles via filtration. This would only leave the lower molecular weight species in solution, however as the solubility of the polymer has not decreased to any appreciable extent, this explanation is unlikely. An alternative explanation may be a change in the hydrodynamic volume of the coupled hyperbranched polymers. If the samples go through a "shape" change during the reaction, the products may be able to contract into a smaller hydrodynamic volume. One other possible explanation of this observation is that the proposed cross-linking reaction results predominantly in intramolecular coupling of esters rather than intermolecular coupling. This would explain the observed lowering of the M_n value determined by GPC.

The glass transition temperatures of the products of the coupling reaction have all increased, by on average 10°C, implying that reaction has occurred, but only to a limited extent. The introduction of cross-links introduces limited mobility in the polymer, this enforced rigidity increases the T_g. The result observed is consistent with the intramolecular coupling hypothesis introduced to account for the GPC results.

In conclusion, it is impossible to quantify the degree of coupling, however it would appear that relatively few cross-links are introduced into the hyperbranched polymer. The lack of reaction is disappointing.

6.4.2 Attempted cross-linking of poly(diethyl 3-hydroxyglutarate) with 1,5-pentanediol

In an attempt to provide a comparable analogue of the product using PTA, an identical molar amount of 1,5-pentanediol was used. A full listing of ^{1}H and ^{13}C nmr results of the products of the reactions performed in this section may be found in Appendix 4, Tables 13-15 and 28-30. The initial reaction was performed at 90°C for 5 hours. The results were somewhat disappointing as there was no appreciable change in the glass transition temperature or the number average molecular weight. The T_g had increased slightly from -38.8°C to -35.0°C, whilst the M_n had, in effect remained constant at 2790. These results imply that this coupling reaction had not been successful under the conditions of reaction. It was therefore decided to increase the molar amount of 1,5-pentanediol by a factor of three to increase the number of available cross-linking groups.

As in section 6.2.2, the ^{1}H and ^{13}C nmr spectra, Figures 6.29 and 6.30, were not as informative as hoped for the determination of cross-links.

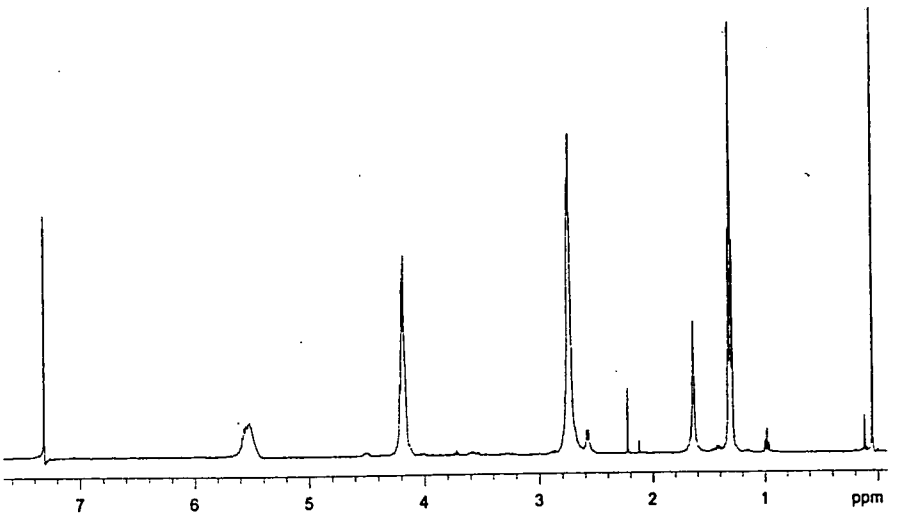

Figure 6.29 ^{1}H nmr spectrum of the product of the attempted cross-linking of a pre-formed hyperbranched wedge with 1,5-pentanediol.

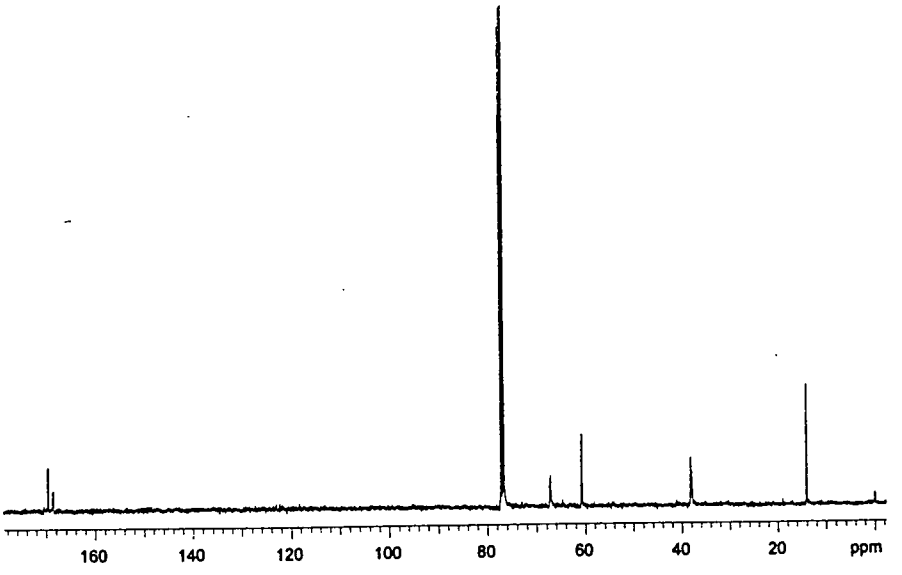

Figure 6.30 ^{13}C nmr spectrum of the product of the attempted cross-linking of a pre-formed hyperbranched wedge with 1,5-pentanediol.

The expected signals due to 1,5-pentanediol were not present in the ^{1}H and ^{13}C nmr spectra. This is thought to be due to the signals being coincident on the polymer signals. As nmr spectroscopy cannot be used to determine the success of the cross-linking reaction, it was hoped that the DSC results may be more informative.

To complete the study, two reaction temperatures were investigated and the results can be seen in Table 6.4 overleaf:

Temp(°C)/Time(hours)[a]	Intensity of 1.26ppm signal[b]	Intensity of 2.69ppm signal[b]	DB[c]
90/5	0.73	1	0.50
90/17	0.74	1	0.46
110/17	0.81	1	0.48

a Reaction conditions
b Refers to the relative intensity of those signals compared to that of the 2.69ppm multiplet
c As determined *via* ^{13}C nmr spectroscopy

Table 6.4 Summary of ^{1}H and ^{13}C nmr results.

From the results listed in Table 6.4, it is impossible to comment on the degree of cross-linking. The relative amount of ethyl ester CH_3 hydrogens remains close to the values obtained for the wedge, whilst the degree of branching has decreased slightly. A small amount of cross-linking is therefore assumed to have occurred as the DB has decreased implying an increase in the number of linear sub-units coupled with a decrease in terminal sub-units.

Temp(°C)/Time(hours)[a]	M_n[b]	T_g(°C)[c]
90/5	2770	-23.0
90/17	2360	-23.6
110/17	2920	-39.2

a Temperature and duration of the reaction
b Determined by GPC using linear polystyrene standards and $CHCl_3$ as eluent
c Determined by DSC

Table 6.5 Summary of GPC results and glass transition temperature results.

The results tabulated above indicate that cross-linking has occurred at 90°C, but not at 110°C. It is impossible to quantify the degree of incorporation of cross-links into the hyperbranched wedge using the techniques available, hence it may be concluded that coupling does occur but the extent cannot be readily determined.

6.5 CONCLUSIONS

The results presented in this chapter indicate that the cross-linking of hyperbranched polymers with terminal ester groups is not an efficient method to produce insoluble gels. It would seem that 1,5-pentanediol is a more reactive coupling agent when polymerisations in the presence of the coupling agent are performed, however when the coupling of wedges is attempted both PTA and 1,5-pentanediol are equally poor. In view of this, further work in this area was curtailed as it was apparent that the systems investigated in this thesis would not form cross-linked networks.

Any future work in this area should examine possible the end-group modification of hyperbranched polyesters in an attempt to produce a system which will undergo efficient cross-linking.

6.6 EXPERIMENTAL

All organic reagents were purchased from Aldrich Chemical Co. and used without further purification. IR spectra were recorded on a Perkin-Elmer 1600 series FTIR. ^{1}H and ^{13}C nmr spectra were recorded on a Varian 400MHz spectrometer and were referenced to internal Me_4Si. DSC measurement were recorded using a Perkin Elmer DSC7, at a scanning rate of $10°Cmin^{-1}$. GPC was performed with a guard column and three PL-gel columns (exclusion limits 100,10^3 and 10^5Å) using a Waters differential diffractometer and $CHCl_3$ as eluent. Columns were calibrated using polystyrene standards (Polymer Labs).

6.6.1 Synthesis of pentaerythritol tetra-acetate (PTA)

An excess of acetyl chloride (25g, 0.318 moles) was added slowly, with stirring, to pentaerythritol (10g, 0.074 moles) under an atmosphere of nitrogen. The

mixture was stirred at room temperature overnight to give a solid white mass. This was broken up and dissolved in hot water. The solution was added dropwise to iced water to form a white precipitate which was collected by filtration and washed with cold water to remove any unreacted acetyl chloride. The white solid (PTA) was dried at 25°C under vacuum overnight (8.39g, 27.6mmol, 37%, m.p. 77-78°C, lit.[11] 78-79°C) and characterised by ^{1}H nmr ($CDCl_3$, 400MHz) δ 2.07 (s, 12H, CH_3), 4.13 (s, 8H, OCH_2), ^{13}C nmr ($CDCl_3$, 100MHz) δ 20.72 (CH_3), 41.61 (quaternary **C**), 62.26 (OCH_2), 170.51 (**C**=O).
CHN Found C 51.27%, H 6.55%, calculated C 51.32%, H 6.58%.

6.6.2 General method for the polymerisation of diethyl 3-hydroxyglutarate in the presence of PTA

Diethyl hydroxyglutarate (2g, 9.8mmol) and titanium (IV) butoxide (0.1g, 2.94 x 10^{-4} moles) were heated at 100°C under a stream of nitrogen for a pre-determined time. PTA (1g, 3.289mmol) was added to the forming polymer and heating continued. A vacuum was applied for the final half hour of the reaction. The reaction vessel was allowed to cool and dichloromethane (40ml) was added to dissolve the yellow viscous polymer. The solution was washed several times with water to remove the residual catalyst. The solvent was removed on a rotary evaporator at water pump pressure to give a yellow viscous oil which was placed in a vacuum oven at 40°C overnight to remove any traces of solvent.

6.6.3 General method for the polymerisation of diethyl 3-hydroxyglutarate in the presence of 1,5-pentanediol

Diethyl hydroxyglutarate (2g, 9.8mmol) and titanium (IV) butoxide (0.1g, 2.94 x 10^{-4} moles) were heated at 100°C under a stream of nitrogen for a pre-determined time. 1,5-Pentanediol (0.65g, 6.25mmol) was added to the forming polymer and heating continued. A vacuum was applied for the final half hour of the

reaction. The reaction vessel was allowed to cool and dichloromethane (40ml) was added to dissolve the yellow viscous polymer. The solution was washed several times with water to remove the residual catalyst. The solvent was removed on a rotary evaporator at water pump pressure to give a yellow viscous oil which was placed in a vacuum oven at 40°C overnight to remove any traces of solvent.

6.6.4 Large scale polymerisation of diethyl 3-hydroxyglutarate

Diethyl 3-hydroxyglutarate (40g, 0.196mol) was mixed with titanium (IV) butoxide (0.1g, 2.94mmol) in the glass reaction vessel. The vessel was lowered into a pre-heated oil bath and the temperature ramped up to 100°C. Throughout the reaction additional portions of titanium (IV) butoxide (0.1g per portion) was added to the reaction vessel. The reaction remained at 100°C for 510 minutes and a vacuum was applied (10mmHg) for the final 30 minutes of the reaction. After reaction, the yellow, viscous liquid was dissolved in dichloromethane and the solution washed with water to remove the catalyst. The organic layer was collected and the solvent removed under reduced pressure. The final traces of solvent were removed by placing the product in a vacuum oven for 4 hours at 35°C. The product was characterised by ^{1}H nmr ($CDCl_3$, 400MHz) δ 0.93 (t, J=7.6Hz, 1.8H, butyl CH_3), 1.26 (t, 7.2Hz, 54.9H, ethyl CH_3), 1.36 (m, 1.6H, butyl CH_2), 1.62 (p, 1.1H, butyl CH_2), 2.54 (m, 5.4H, focal CH_2), 2.69 (m, 70.4H, linear, branched and terminal CH_2), 4.14 (m, 44.0H, OCH_2), 4.44 (m, 1H, focal CH), 5.47 (m, 19.1H, linear, branched and terminal CH), ^{13}C nmr ($CDCl_3$, 200MHz) δ 13.9 (butyl CH_3), 14.09 (ethyl CH_3), 19.01 (butyl CH_2), 30.46 (butyl CH_2), 38.19 (terminal, linear and branched CH_2), 40.59 (butyl CH_2), 41.20 (focal CH_2), 60.77 (ethyl OCH_2), 64.69 (focal CH), 67.15 (terminal, linear and branched CH), 168.55 (C=O), 168.64 (C=O), 169.63 (C=O), FTIR NaCl plates ν_{max}/cm^{-1} 3620.5, 3536.1, 3461.7, 2982.5, 2988.4, 1730.8.

6.6.5 General method for the cross-linking of a preformed hyperbranched wedge with PTA

Poly(diethyl hydroxyglutarate) (0.102g) was mixed with PTA (0.041g, 0.135mmol) on a silica plate. The plate was placed in a glass reaction vessel which was lowered into a pre-heated oil bath. The vessel was heated at a constant temperature for a pre-determined length of time and a vacuum was applied towards the end of the reaction. The silica plate was removed and washed with dichloromethane (60ml), the solvent was removed on a rotary evaporator at water pump pressure to give a clear polymer.

6.6.6 General method for the cross-linking of a preformed hyperbranched wedge with 1,5-pentanediol

Poly(diethyl hydroxyglutarate) (0.102g) was mixed with 1,5-pentanediol (0.040g, 0.389mmol) on a silica plate. The plate was placed in a glass reaction vessel which was lowered into a pre-heated oil bath. The vessel was heated at a constant temperature for a pre-determined length of time and a vacuum was applied towards the end of the reaction. The silica plate was removed and washed with dichloromethane (60ml), the solvent was removed on a rotary evaporator at water pump pressure to give a clear polymer.

6.7 REFERENCES

1. A.S. Baker, D.J. Walbridge, US Patent 3,669,939, (1972).
2. G.D. Figuly, US Patent 5,136,014, (1992)
3. N. Moszner, T. Völkel, V. Rheinberger, *Macromol. Chem. Phys.*, **197**, (1996), 621.
4. E.M.M. de Brabander-van den Berg, A. Nijenhuis, M. Mure, J. Keulen, R. Reintjens, F. Vandenbooren, B. Bosman, R. de Raat, T., Frijns, S. v.d. Wal, M. Castelijns, J. Put, E.W. Meijer, *Macromol. Symp.* **77**, (1994), 51.
5. M. Johansson, A. Hult, PMSE, (1995),178.
6. M. Johansson, A. Hult, *J. Coatings Tech.*, **67**, (1995), 35.
7. M. Johansson, E. Malmstöm, A. Hult, *J. Polym. Sci.:Part A, Polym. Chem.*, **31**, (1993), 619.
8. R. Spindler, J.M.J. Fréchet, *Macromol.*, **26**, (1993), 4809.
9. F. Walter, S.R. Turner, B.I. Voit, *Polym. Prepr. (Am. Chem. Soc., Div. Polym. Chem.)*, **34**, (1993), 79.
10. H.R. Kricheldorf, O. Stöber, D. Lübbers, *Macromol.*, **28**, (1995), 2118.
11. "Purification of Laboratory Chemicals" (3rd edn), Perrin D.D. and Armarego W.L.F., Butterworth-Heinemann Ltd. (1988).

Chapter 7.

Conclusions and Proposals for Future Work

7.1 CONCLUSIONS

The work performed during the course of this study into aliphatic hyperbranched polyesters has highlighted several interesting features. The routes into the required monomers for hyperbranched growth are not as facile as first imagined. The purification of these AB_2 monomers indicated the potential problems of competing lactonisation reactions which would severely hinder the desired polymerisation process. It would therefore be necessary to synthesise monomers which would be too sterically strained to undergo ring closure.

The synthesis of poly(diethyl 3-hydroxyglutarate) was achieved, however the molecular weights achieved were somewhat disappointing. It has been postulated that these low molecular weight oligomers are a consequence of the cyclisation process which has been shown to occur. The attempts to prevent cyclisation by the introduction of a core molecule, proved to be relatively unsuccessful. The cyclisation reactions could not be detected when the co-polyesters were analysed using MALDI-TOF MS, hence in that sense the reactions served their purpose, however the molecular weights of the products were lower than those of the hyperbranched wedges synthesised under the same conditions. This observation indicates that the core molecule acts as a core "terminator" by consuming the reactive focus of the hyperbranched wedge. It was therefore concluded that although the core did prevent cyclisation the decrease in molecular weight was unacceptable.

In an attempt to produce insoluble gels, cross-linking of the pre-formed polymeric wedges and cross-linking during the polymerisation process was attempted. The results were singularly disappointing. As the glass transition temperatures had increased it was concluded that coupling had occurred to a small extent, however the solubility of the products did not appear to be appreciably diminished. These observations lead the author to conclude that, although a small amount of coupling had occurred it was probably predominantly due to intramolecular reaction, hence these systems will never be utilised in the manufacture of coatings with the cross-linking agents reported in this thesis.

In conclusion, the synthesis of aliphatic hyperbranched polyesters has been achieved, however the overall results have been a little disappointing.

7.2 FUTURE WORK

As it has been shown that aliphatic AB_2 polyesters may have the tendency to lactonise, the synthesis of monomers which will be suitable for polymerisation must involve molecules which would form 3, 4, 7 or higher membered rings. One synthesis which would achieve this is the addition of formaldehyde to dimethyl methylmalonate:

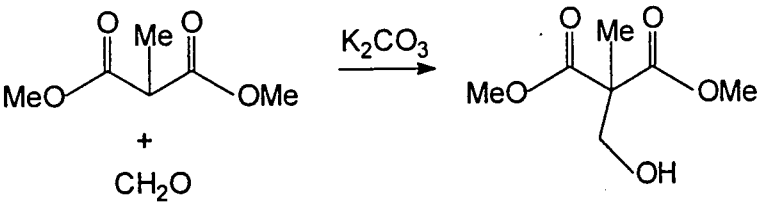

Figure 7.1

This reaction may be performed at 0°C under nitrogen in the presence of K_2CO_3.[1] The product may then be purified to give the desired AB_2 monomer which should be suitable for hyperbranched growth, one potential problem however, may be steric hindrance. As the A and B groups are in close proximity to each other the hyperbranched growth may be impeded by steric effects. Of course, the only method of testing this hypothesis is to perform the reaction.

An alternative route to a suitable monomer may the modification of diethyl 3-hydroxyglutarate. If the secondary alcohol could be modified to a primary, the monomer should be more reactive and it may be envisaged that polymerisation may be more facile. The modification may be performed by chain extending the hydroxyl group through reaction with an halo-alcohol to produce an ether linkage as well as a primary hydroxyl group as shown in Figure 7.2 overleaf:

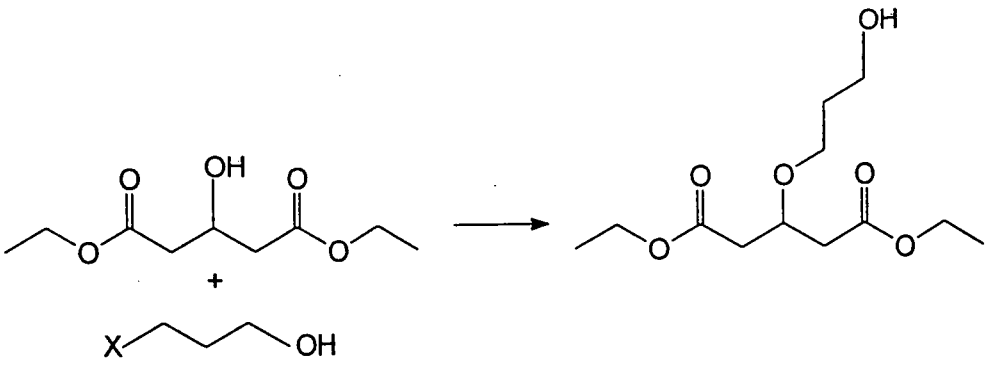

Figure 7.2

Potential problems with this approach may be the possibility of cyclisation of the product, or ester exchange between the reagents. If the alkyl chain of the halo-alcohol has one or two methylenes, five and six membered rings may form in preference to hyperbranched polymer. Therefore, it would advantageous to use halo-alcohols possessing three or more methylene units to prevent this.

As the incorporation of core has not been successful, an alternative approach may be to react benzene 1,3,5-tricarbonyl trichloride with the monomer in an attempt to produce a B_6 core. This may then encourage reaction between the monomer and the core. A direct analogue of this would be to react the triacid chloride with a pre-formed hyperbranched wedge in an attempt to increase the molecular weight of the system.

In conclusion, the synthesis of high molecular weight hyperbranched aliphatic polyesters may be achieved if suitable monomers can be synthesised, whether by the production of new monomers or by the modification of the existing monomer.

7.3 REFERENCES

1. H. Gault and A. Roesch, *Compt. Rend.*, **199**, (1934), 613.

Appendix 1

Analytical data for Chapter 2

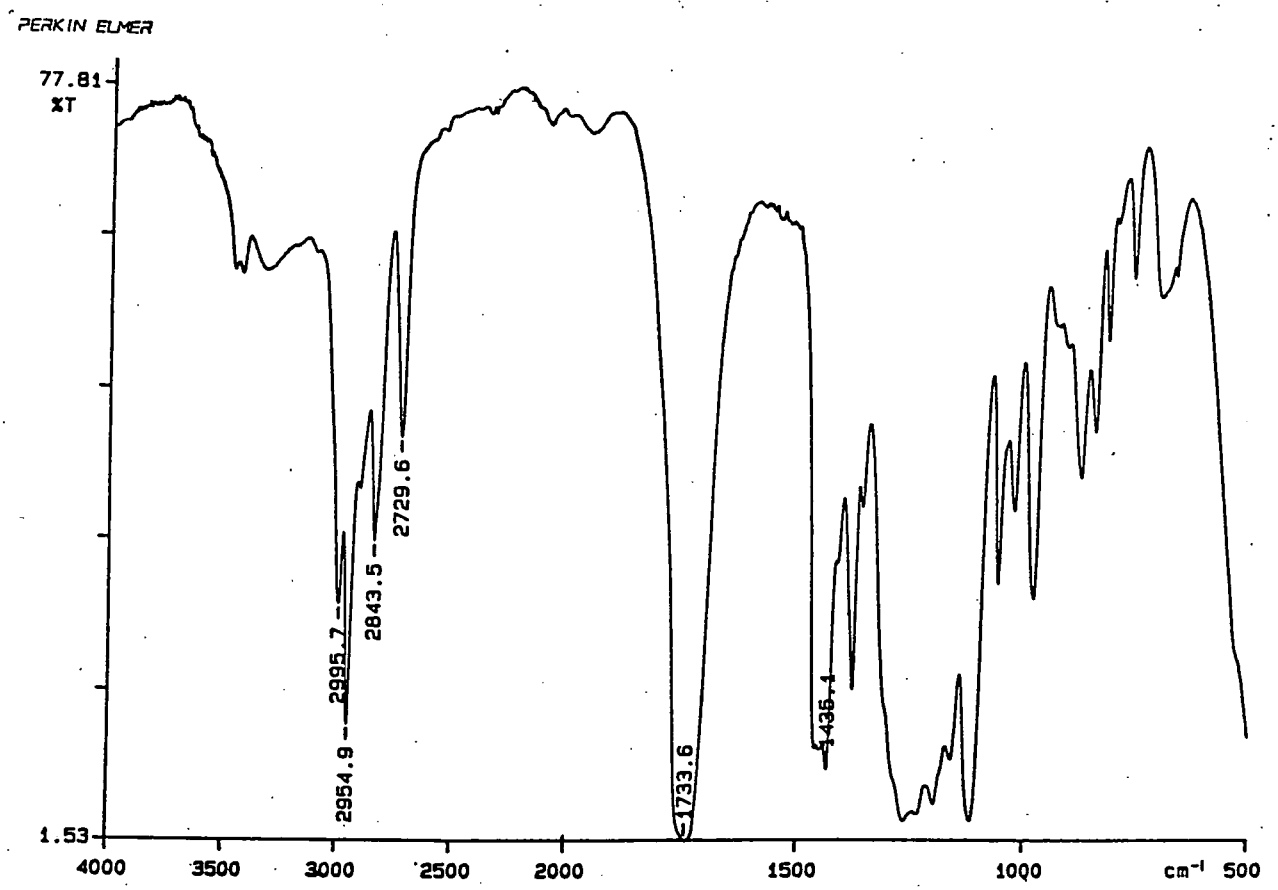

Appendix 1.1 FTIR spectrum of dimethyl methyl-(3'-propionaldehydo)-malonate

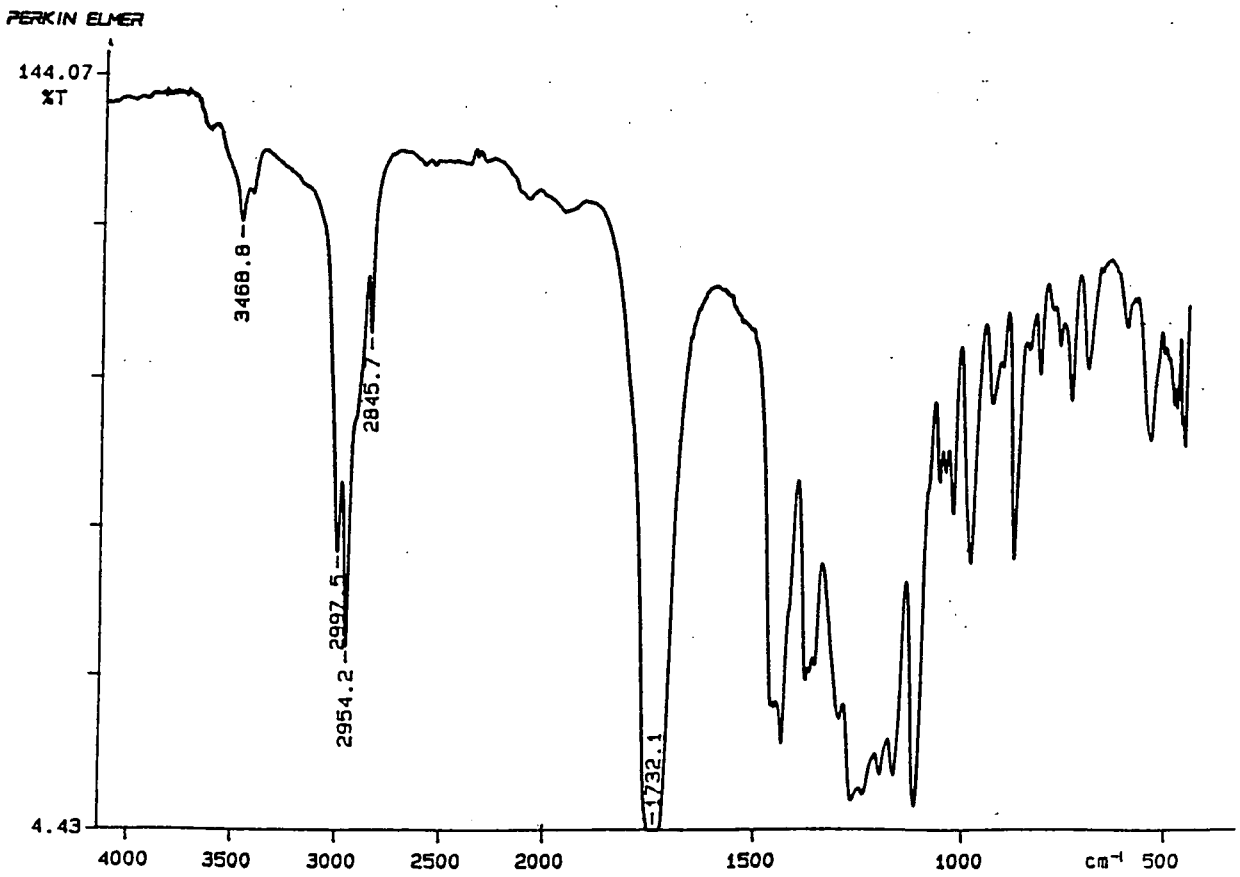

Appendix 1.2 FTIR spectrum of dimethyl methyl-(3'-oxobutyl)-malonate

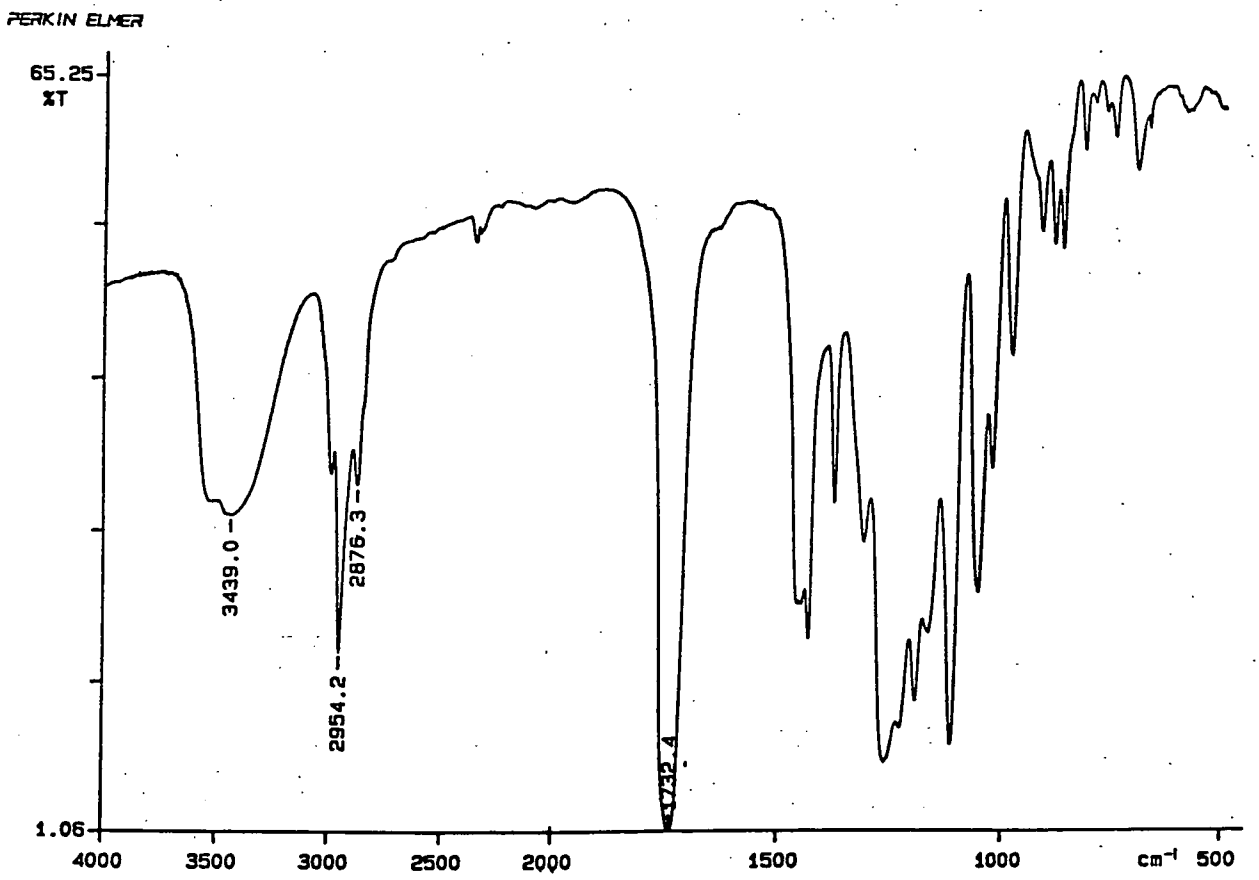

Appendix 1.3 FTIR spectrum of the product of the attempted reduction of dimethyl methyl-(3'-propionaldehydo)-malonate

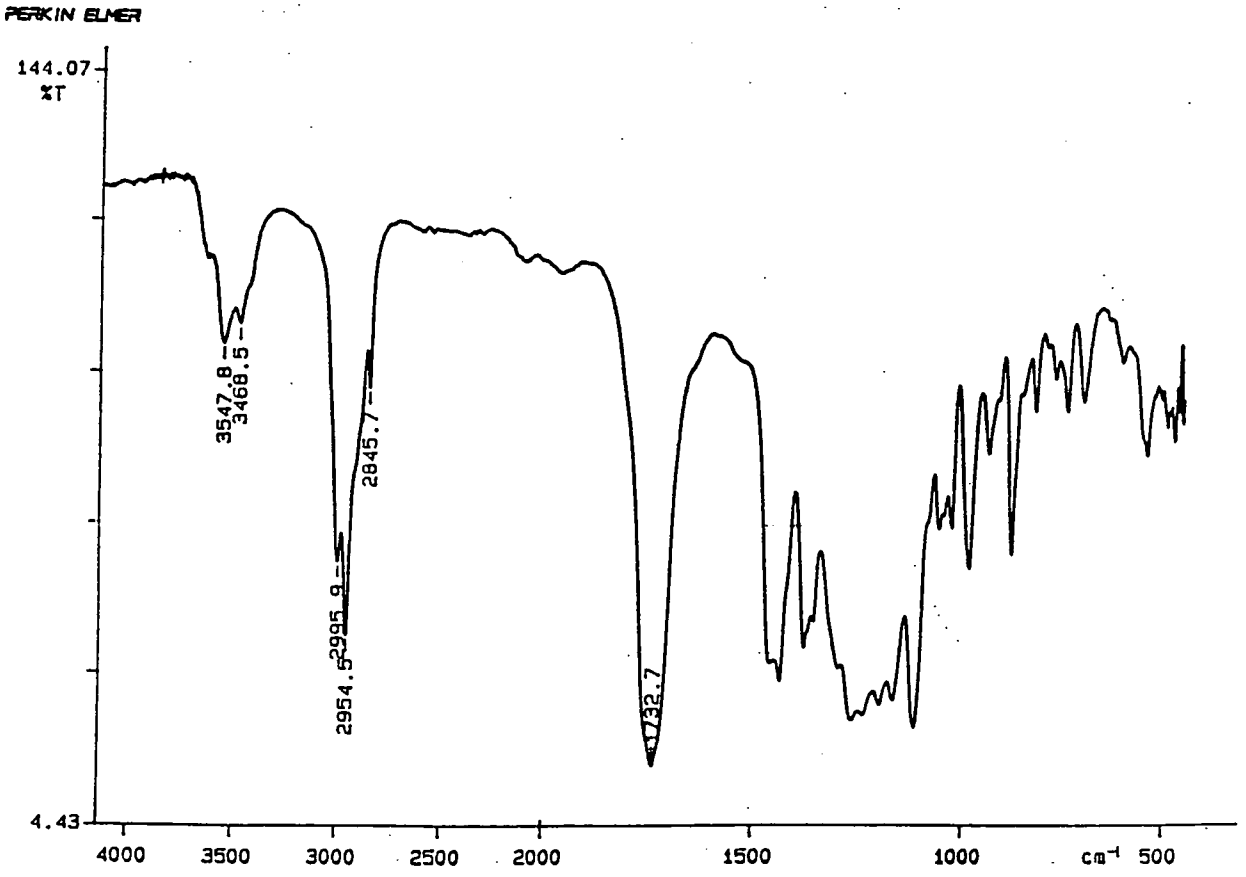

Appendix 1.4 FTIR spectrum of the product of the attempted reduction (using $NaBH_4$-Alox) of dimethyl methyl-(3'-oxobutyl)-malonate

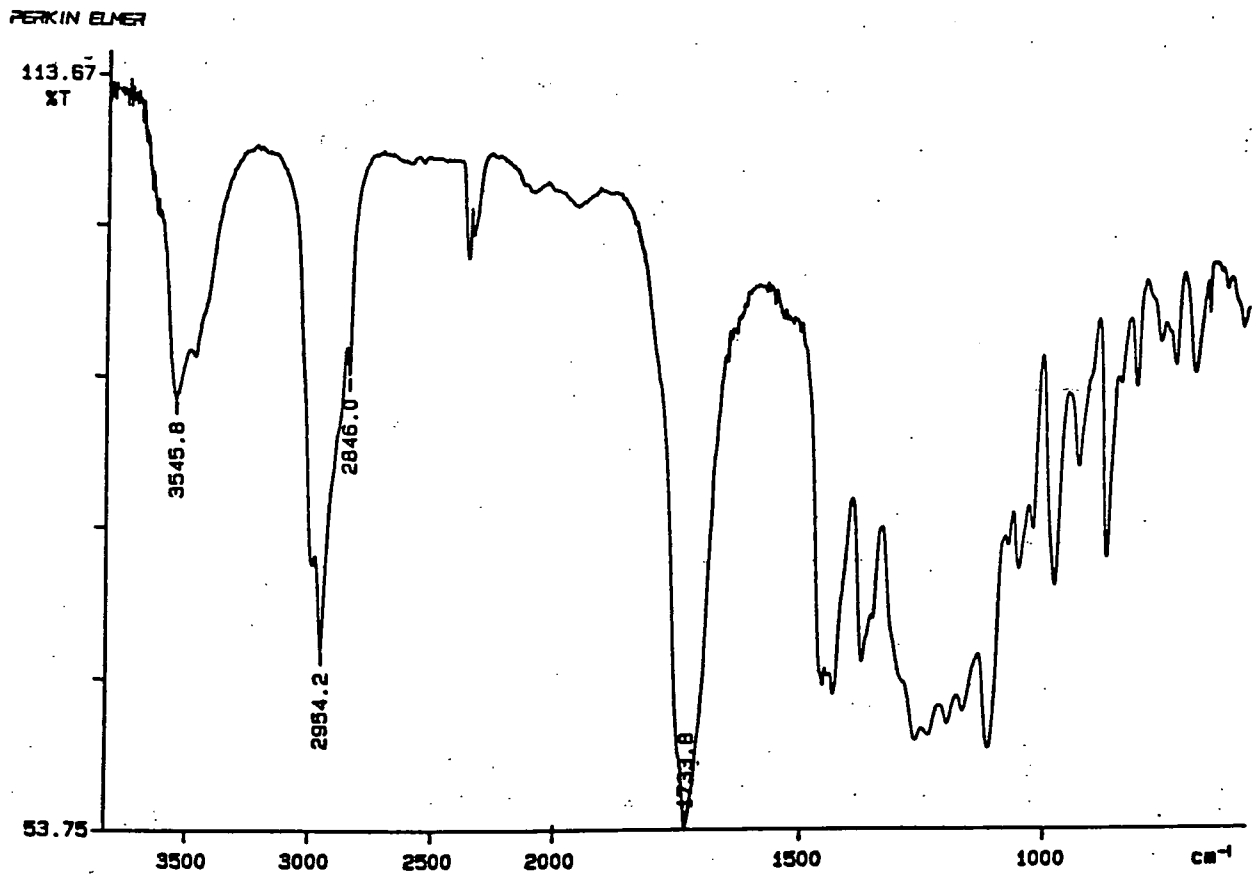

Appendix 1.5 FTIR spectrum of the product of the attempted reduction (using $NaBH_4$) of dimethyl methyl-(3'-oxobutyl)-malonate

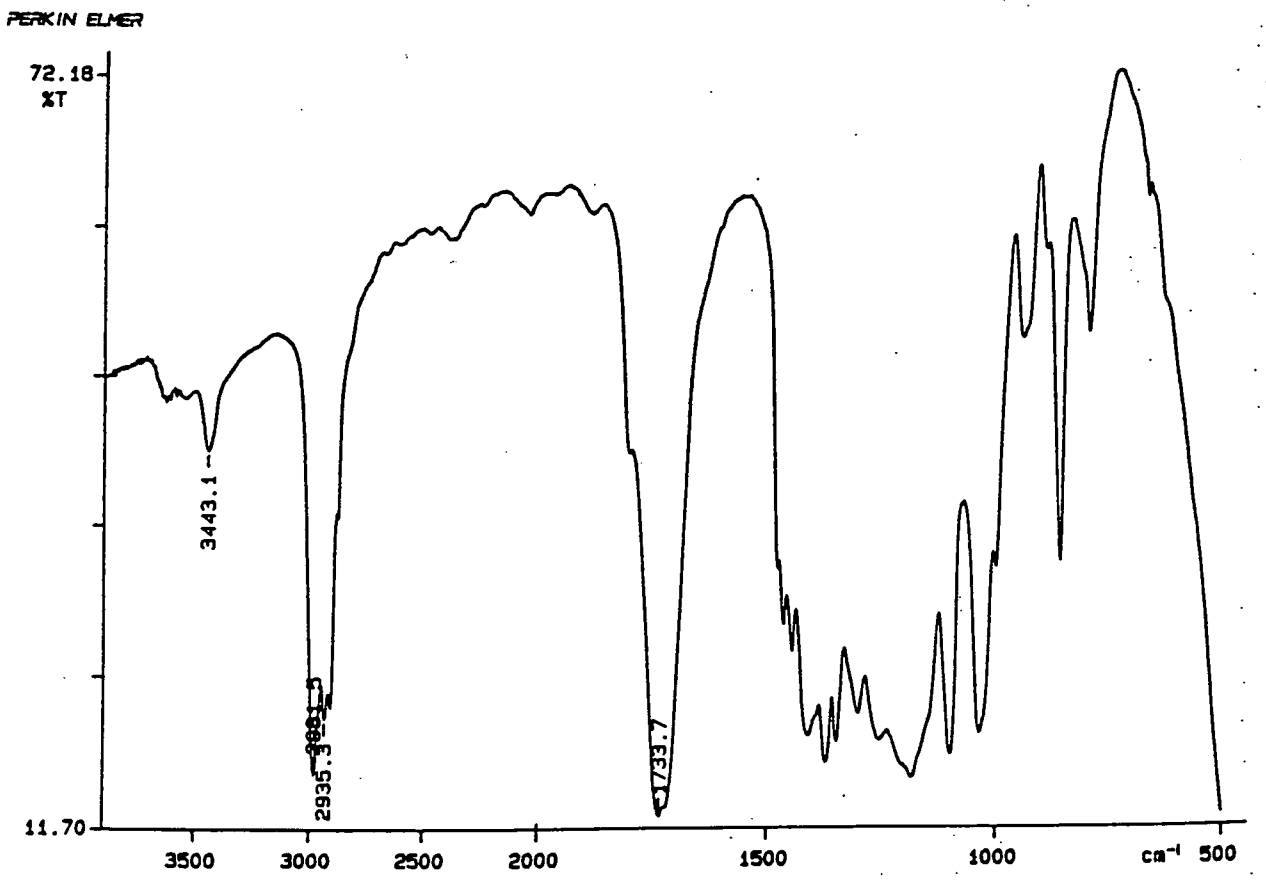

Appendix 1.6 FTIR spectrum of diethyl 3-oxopimelate

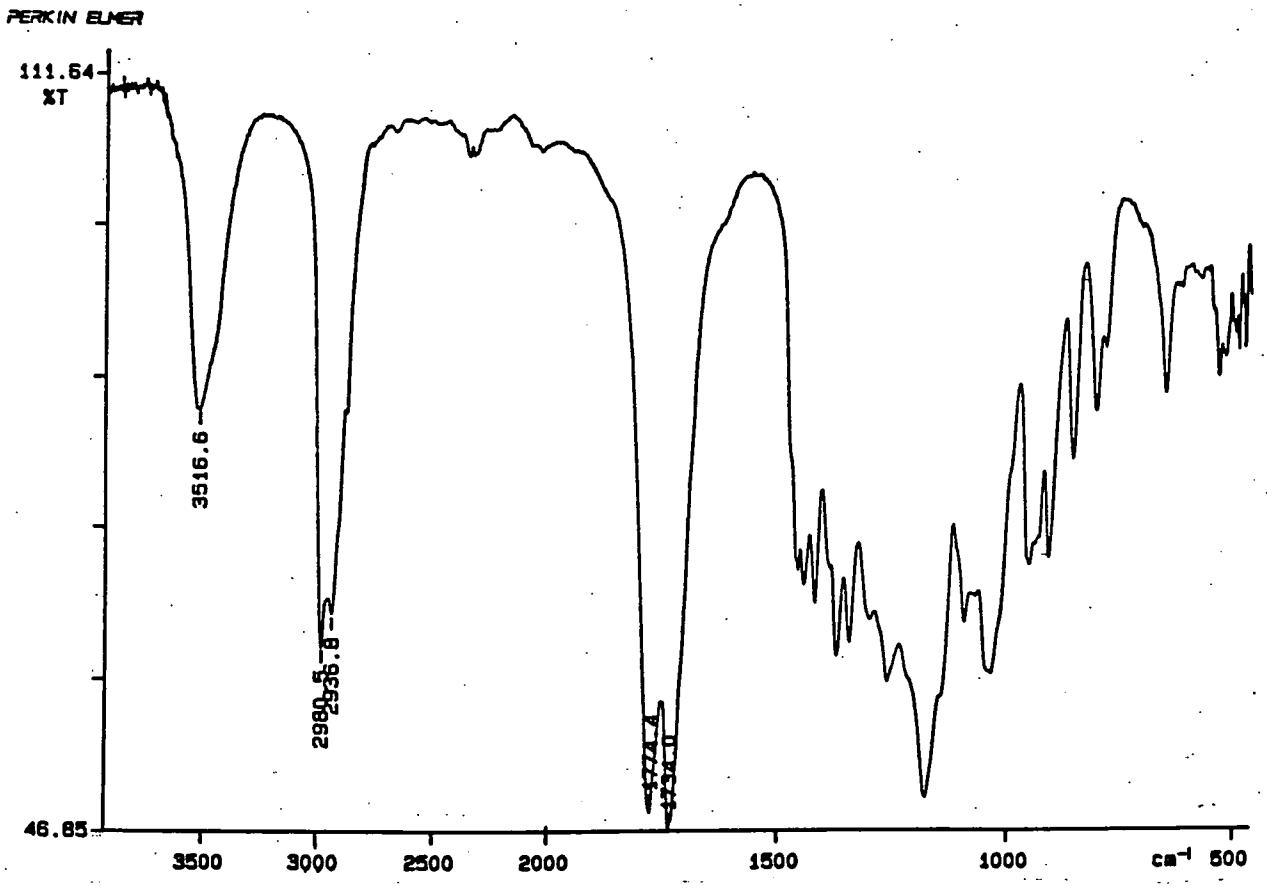

Appendix 1.7 FTIR spectrum of the product of the attempted reduction (using $NaBH_4$) of diethyl 3-oxopimelate

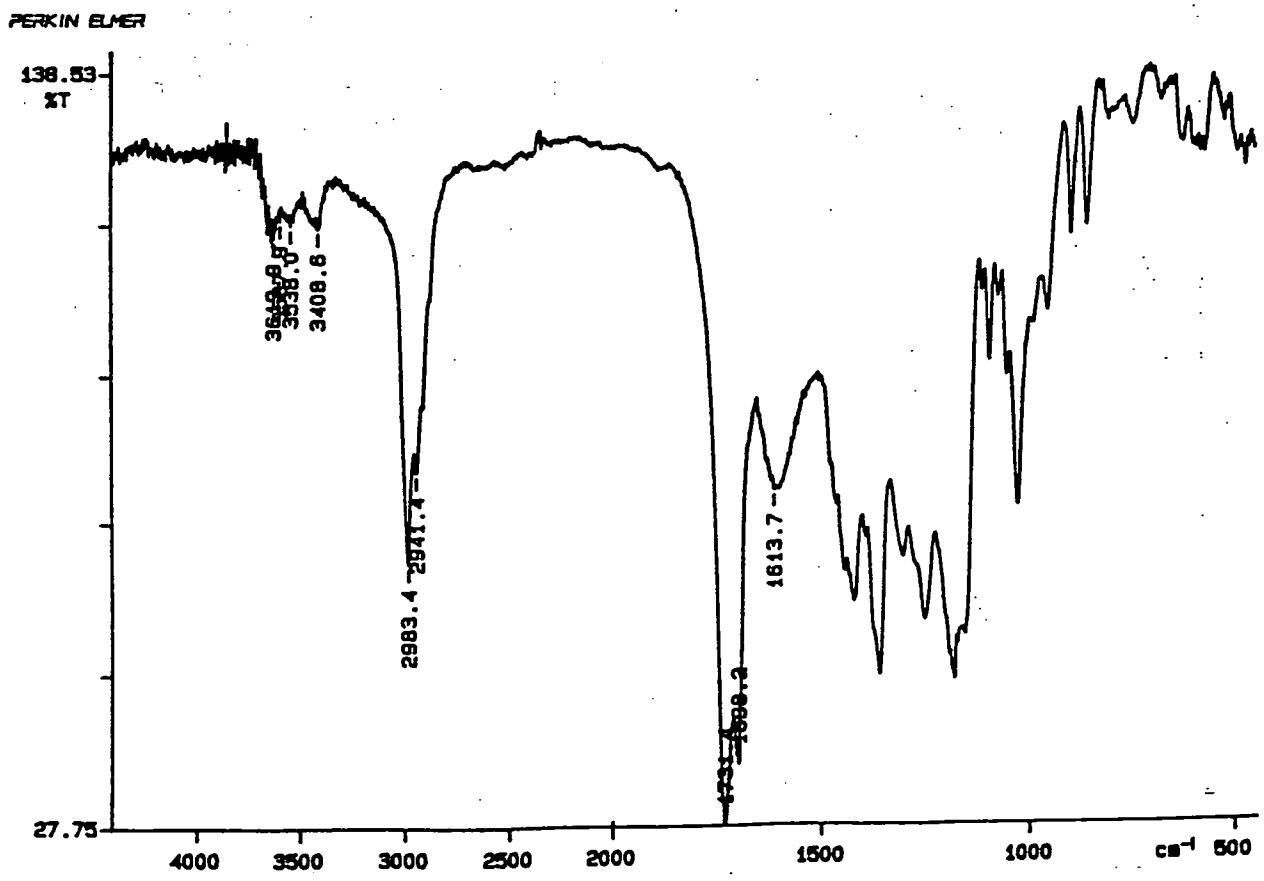

Appendix 1.8 FTIR spectrum of ethyl-4-acetyl-5-oxohexanoate

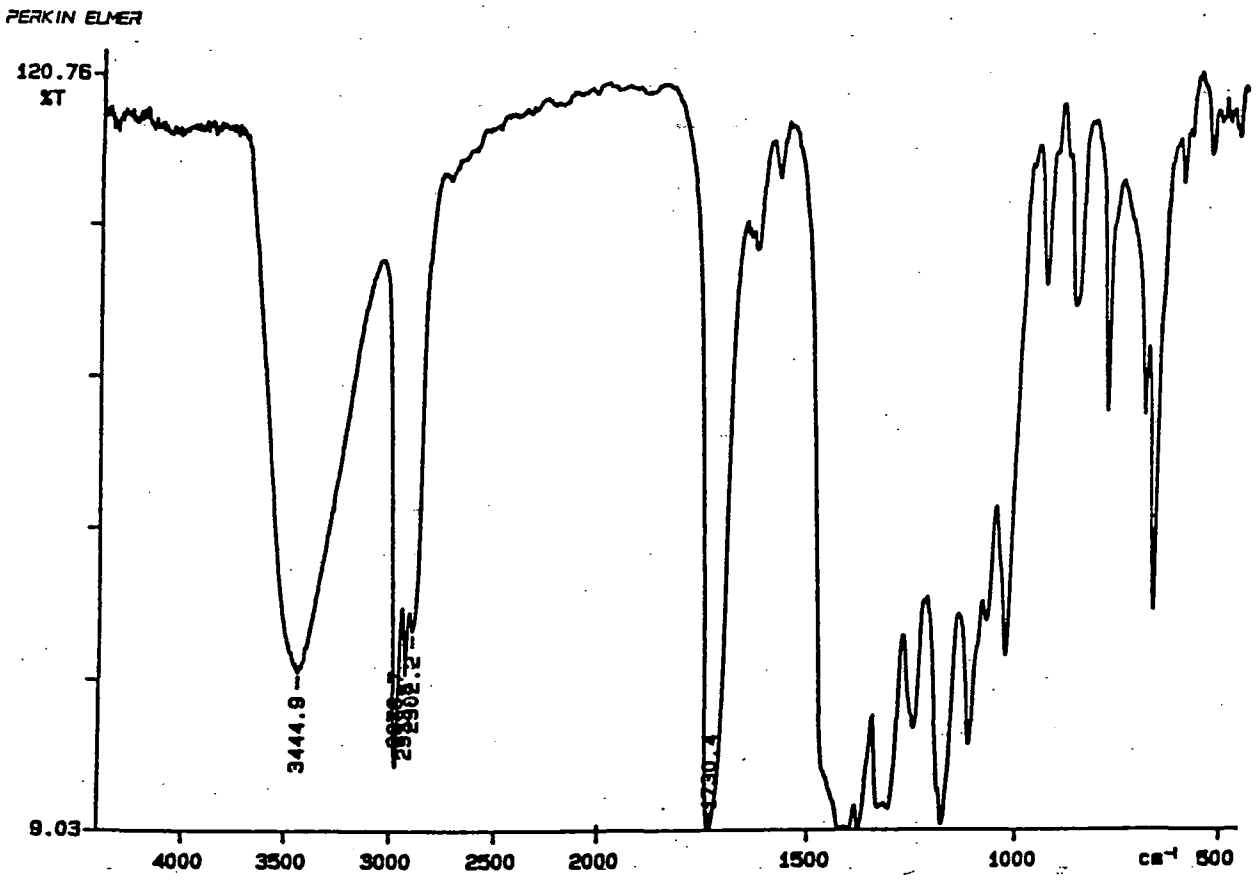

Appendix 1.9 FTIR spectrum of the product of the attempted reduction (using $NaBH_4$) of ethyl-4-acetyl-5-oxohexanoate

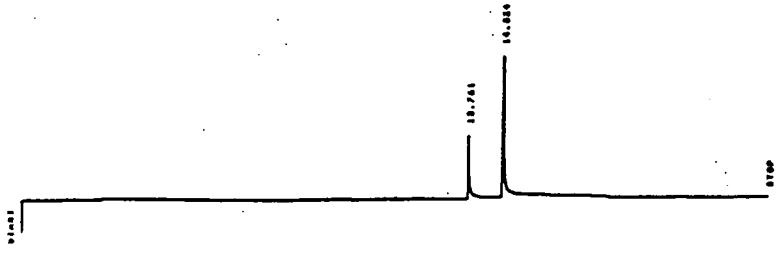

Appendix 1.10 GC trace of the product of the attempted reduction of dimethyl methyl-(3'-propionaldehydo)-malonate

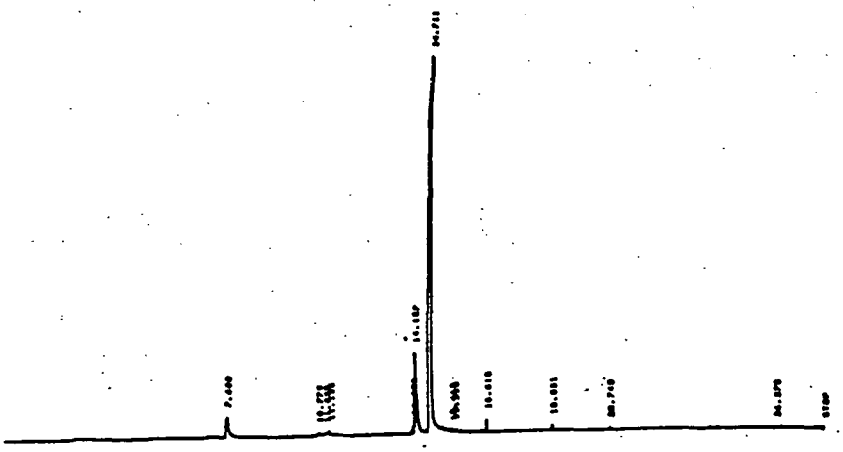

Appendix 1.11 GC trace of the product of the attempted reduction (using $NaBH_4$-Alox) of dimethyl methyl-(3'-oxobutyl)-malonate

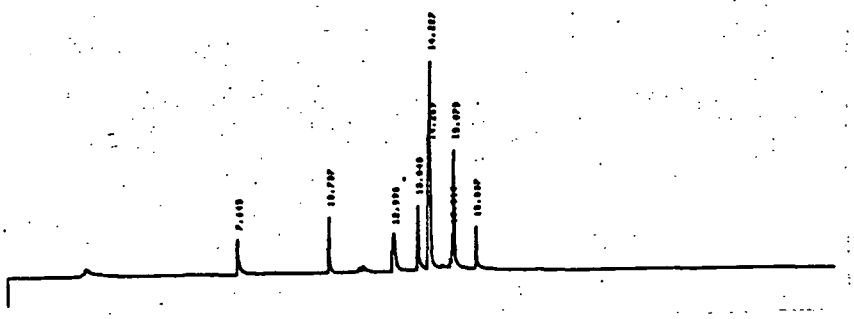

Appendix 1.12 GC trace of the product of the attempted reduction (using $NaBH_4$) of dimethyl methyl-(3'-oxobutyl)-malonate

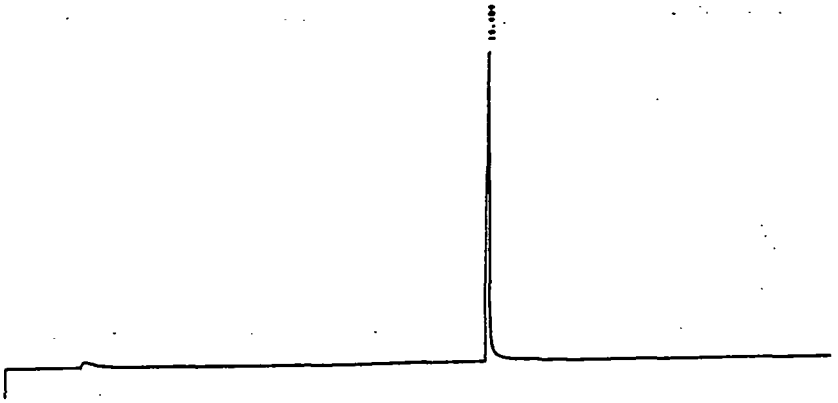

Appendix 1.13 GC trace of the product of the attempted reduction (using $NaBH_4$) of diethyl 3-oxopimelate

Appendix 2

Analytical data for Chapter 4

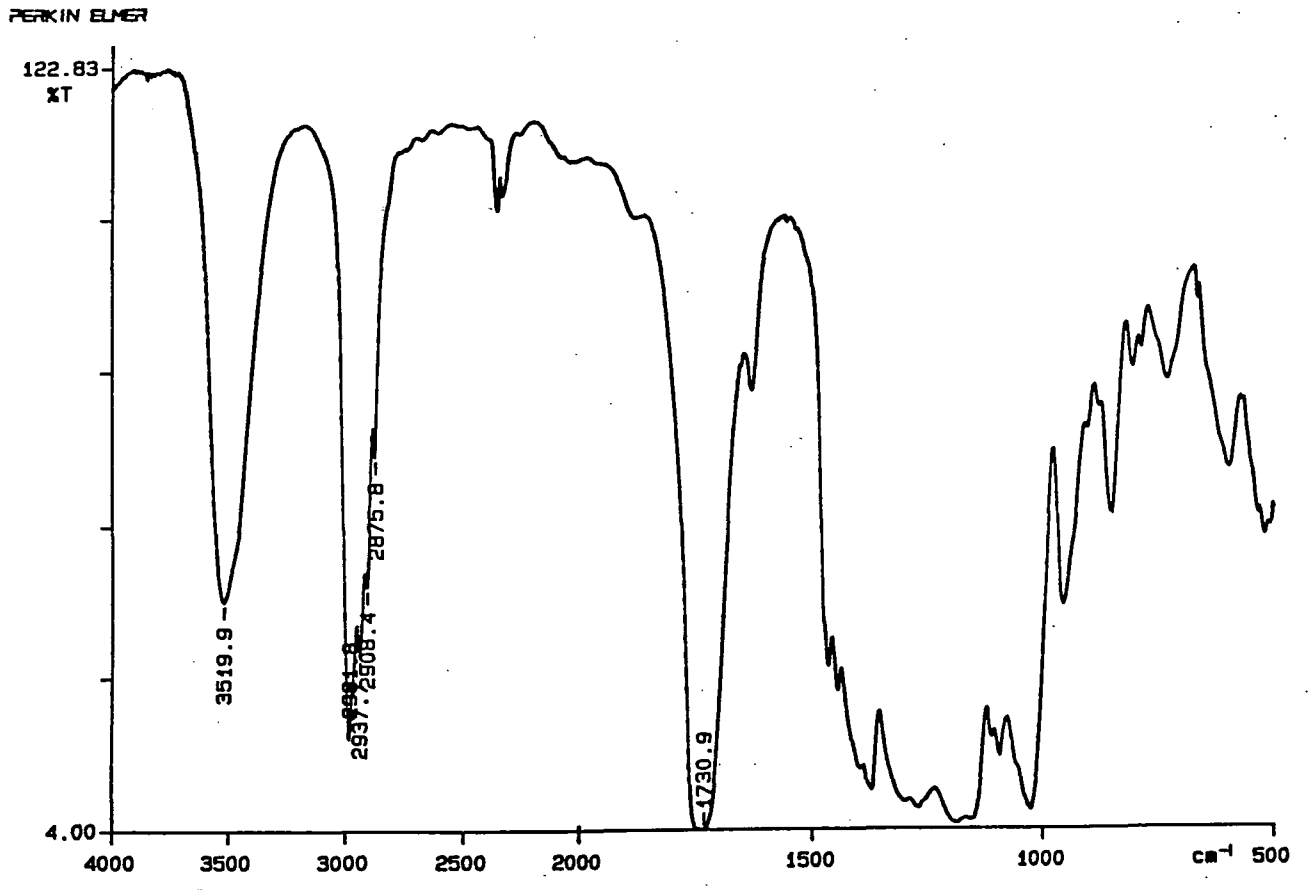

Appendix 2.1 FTIR spectrum of poly(diethyl 3-hydroxyglutarate) performed in the presence of 2.5wt% $Ti(OBu)_4$ at 100°C for 270 minutes

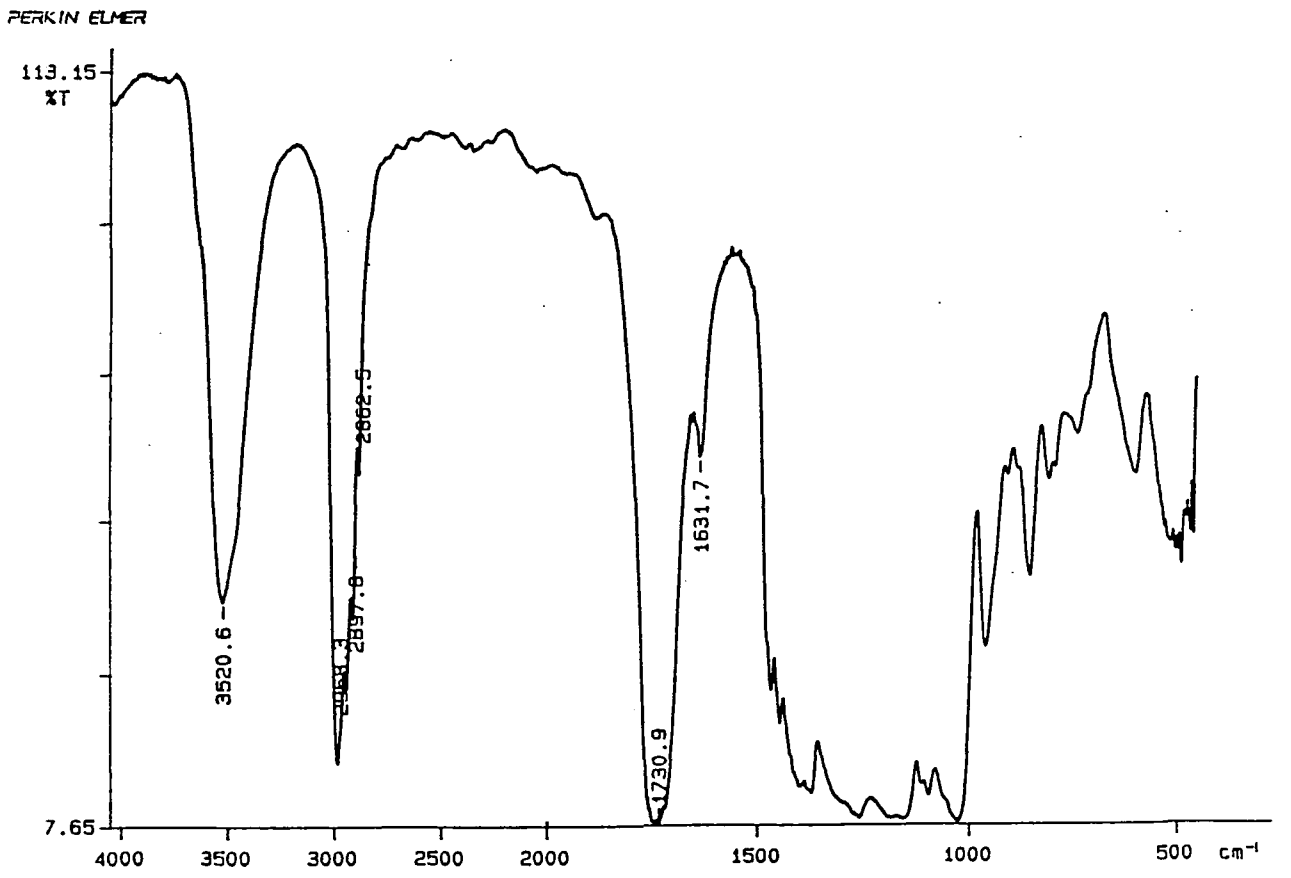

Appendix 2.2 FTIR spectrum of poly(diethyl 3-hydroxyglutarate) performed in the presence of 3.5wt% $Ti(OBu)_4$ at 100°C for 270 minutes

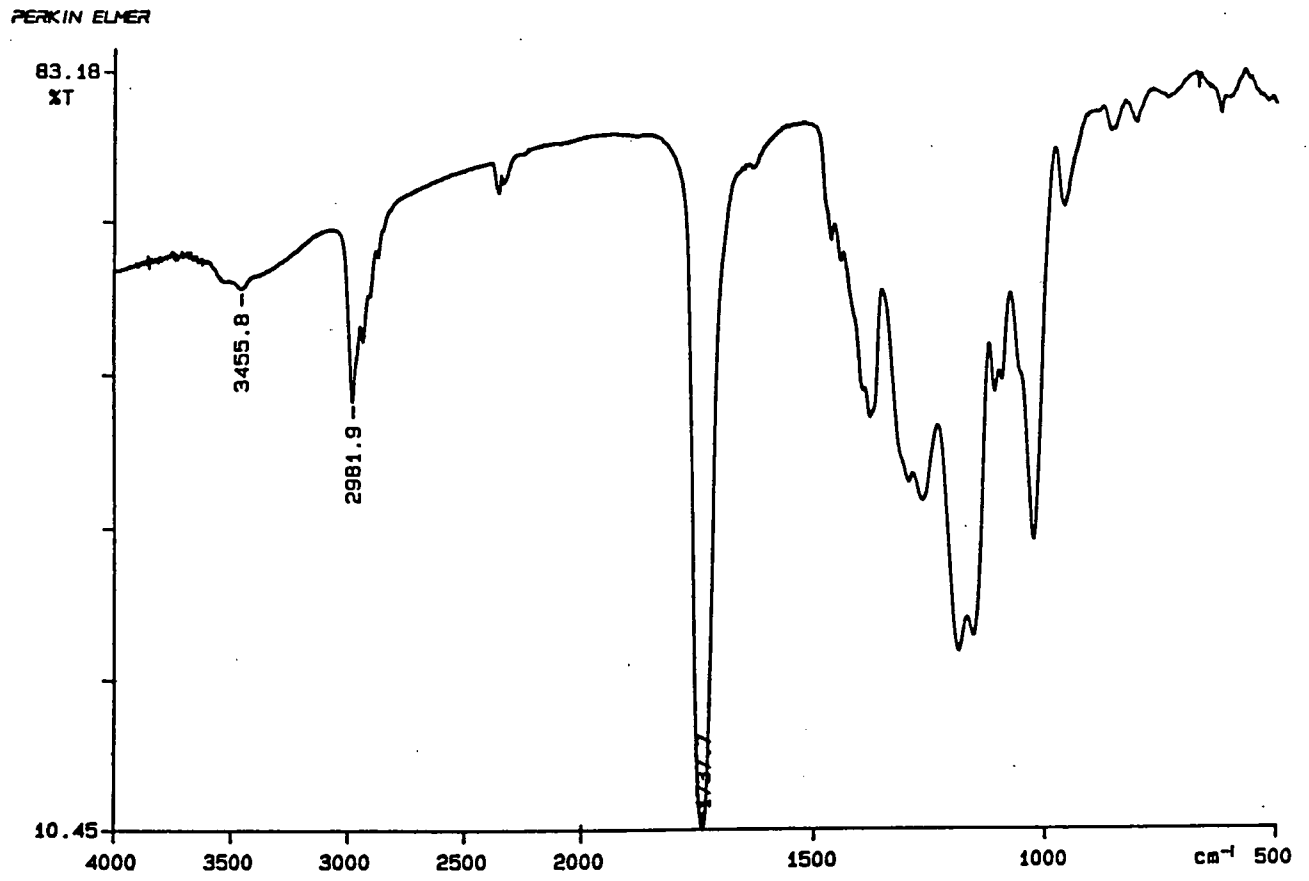

Appendix 2.3 FTIR spectrum of poly(diethyl 3-hydroxyglutarate) performed in the presence of 5wt% $Ti(OBu)_4$ at 100°C for 270 minutes

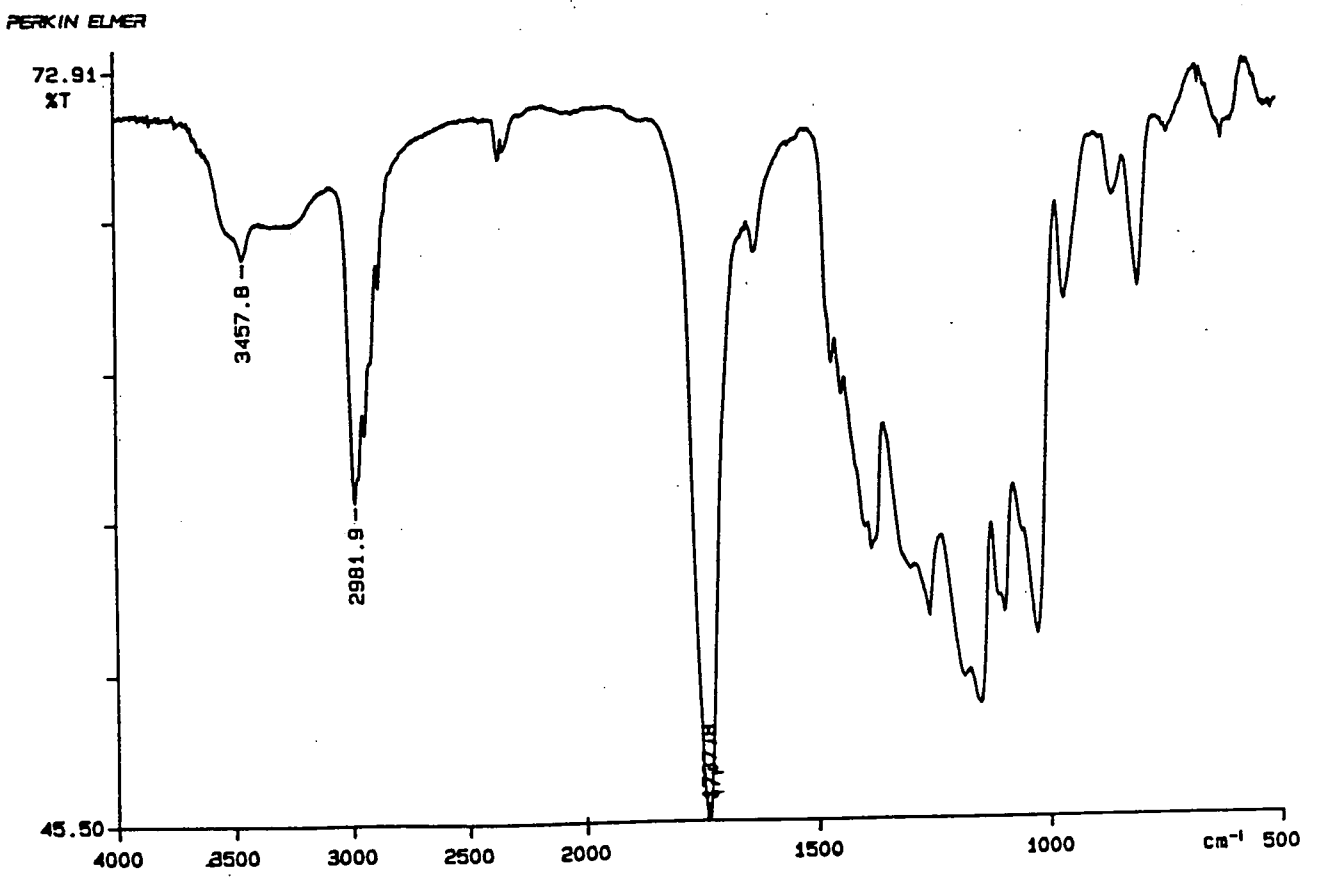

Appendix 2.4 FTIR spectrum of poly(diethyl 3-hydroxyglutarate) performed in the presence of 5wt% $Ti(OBu)_4$ at 100°C for 270 minutes

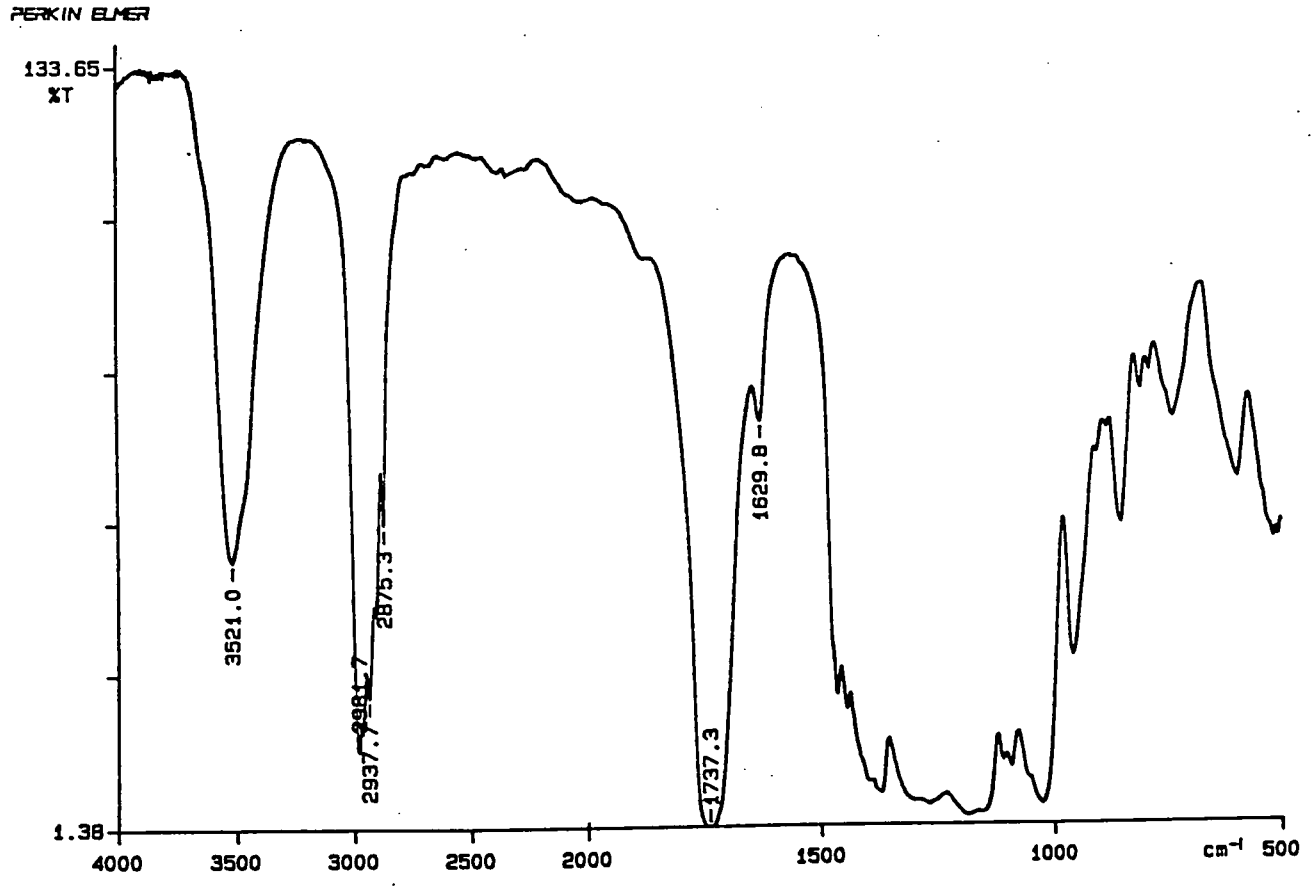

Appendix 2.5 FTIR spectrum of poly(diethyl 3-hydroxyglutarate) performed in the presence of 7wt% $Ti(OBu)_4$ at 100°C for 270 minutes

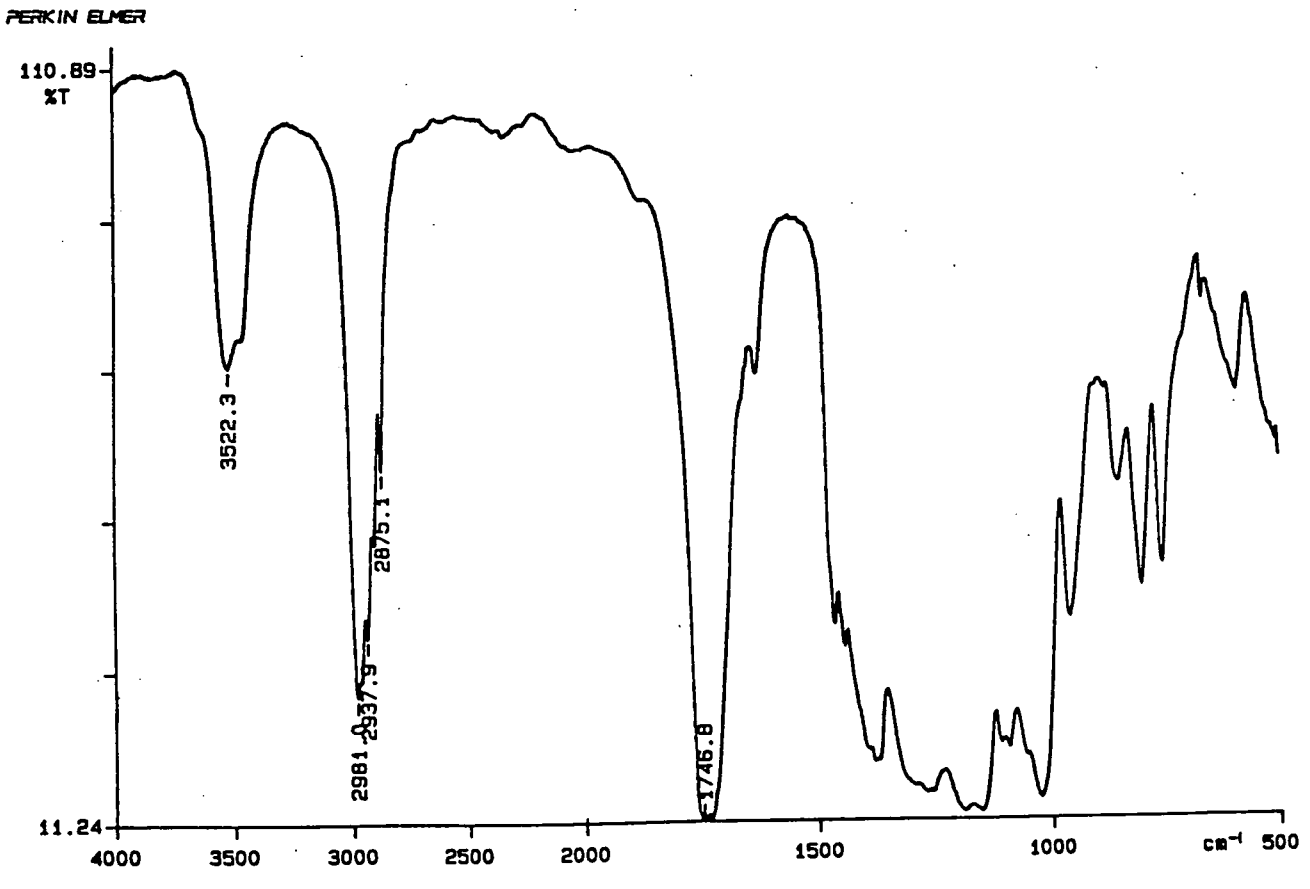

Appendix 2.6 FTIR spectrum of poly(diethyl 3-hydroxyglutarate) performed in the presence of 10wt% $Ti(OBu)_4$ at 100°C for 270 minutes

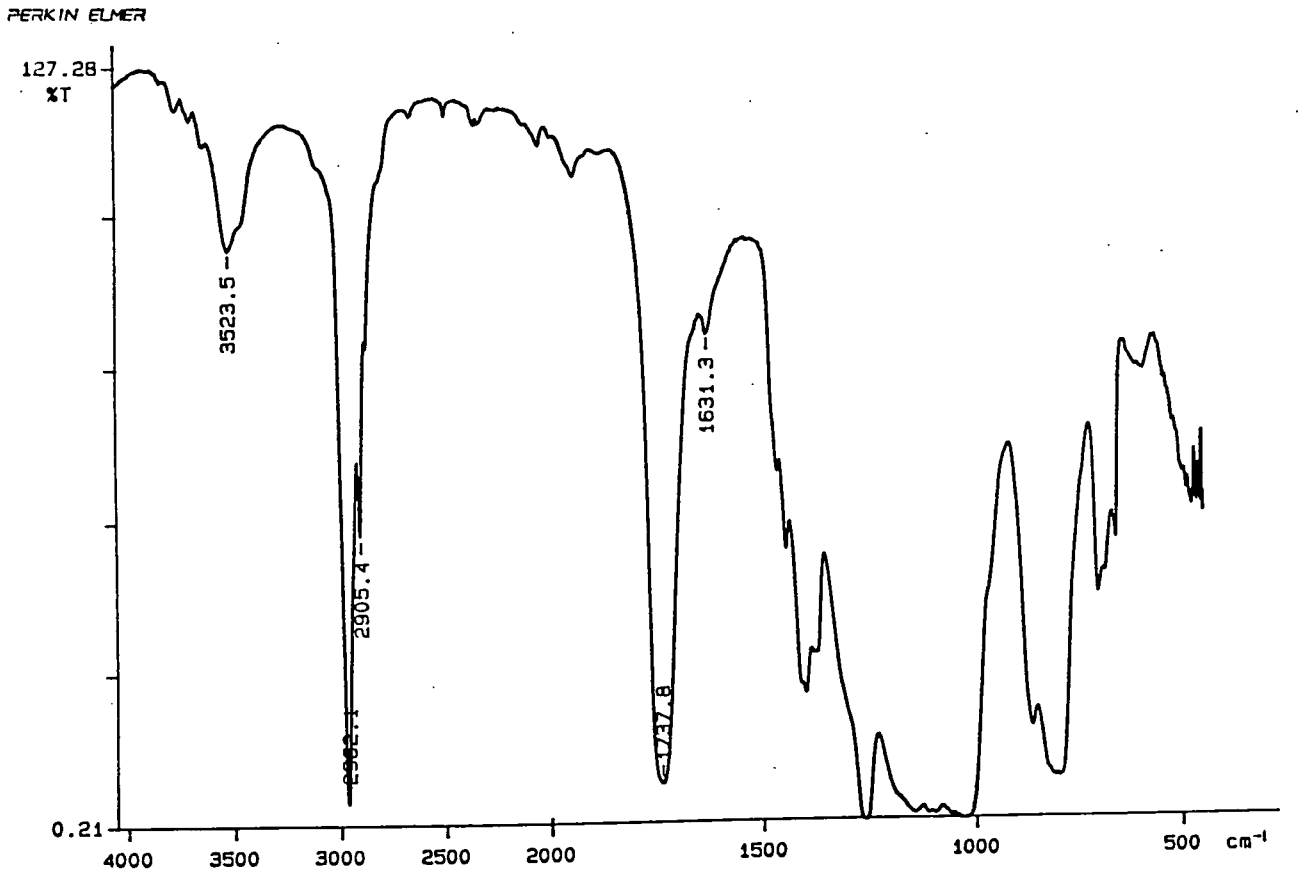

Appendix 2.7 FTIR spectrum of poly(diethyl 3-hydroxyglutarate) performed in the presence of 10wt% $Ti(OBu)_4$ at 100°C for 270 minutes

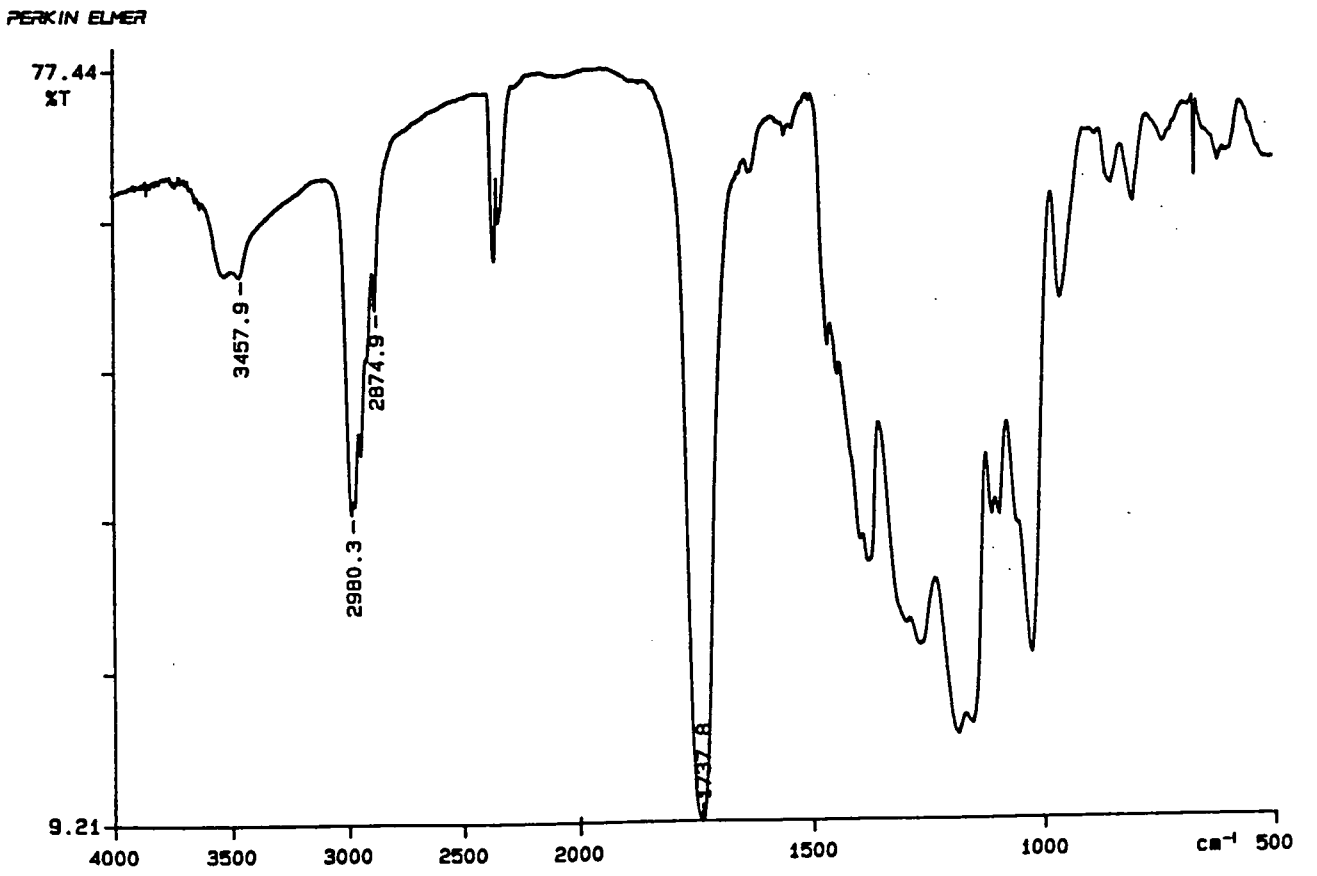

Appendix 2.8 FTIR spectrum of poly(diethyl 3-hydroxyglutarate) performed in the presence of 11wt% $Ti(OBu)_4$ at 100°C for 270 minutes

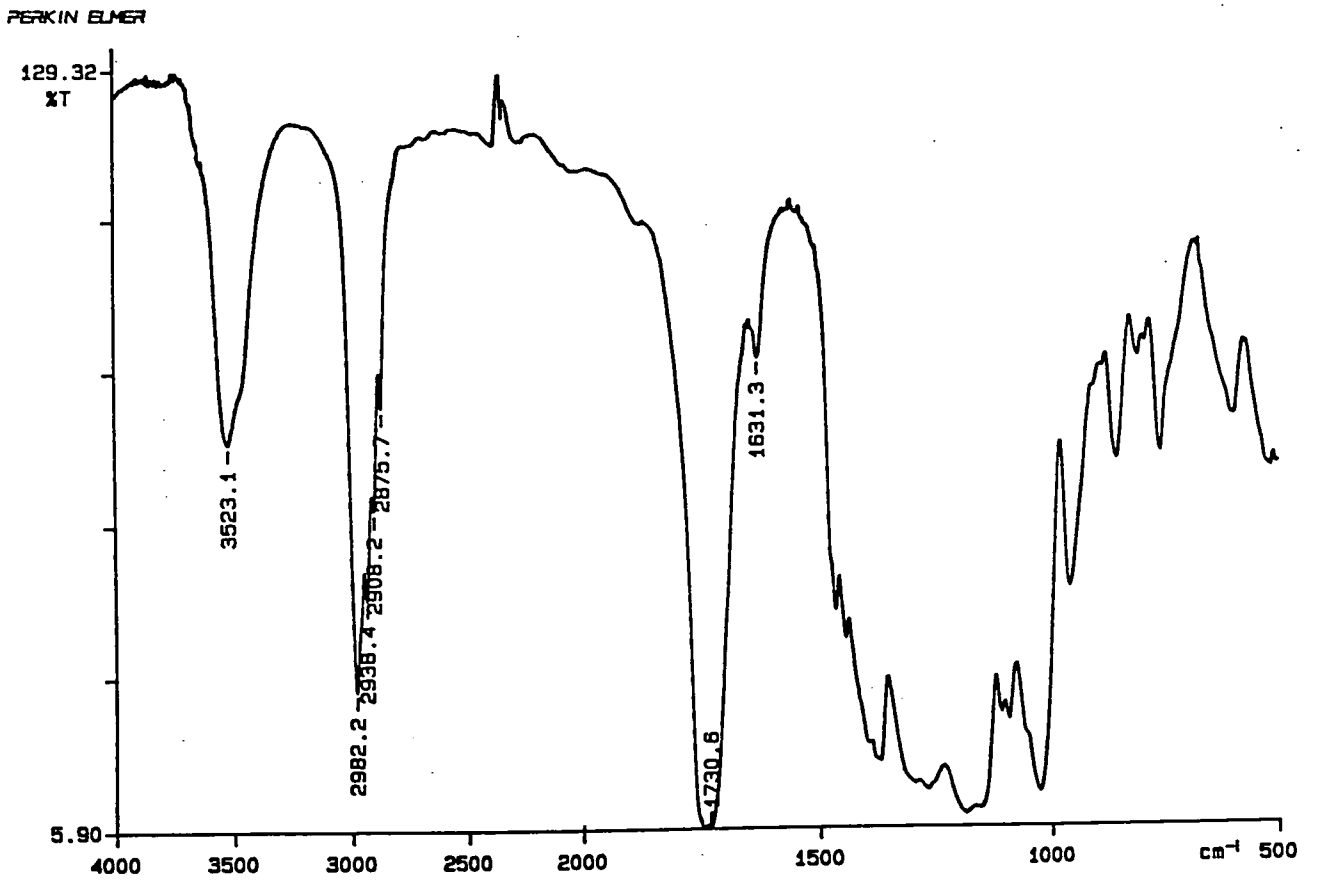

Appendix 2.9 FTIR spectrum of poly(diethyl 3-hydroxyglutarate) performed in the presence of 25wt% $Ti(OBu)_4$ at 100°C for 270 minutes

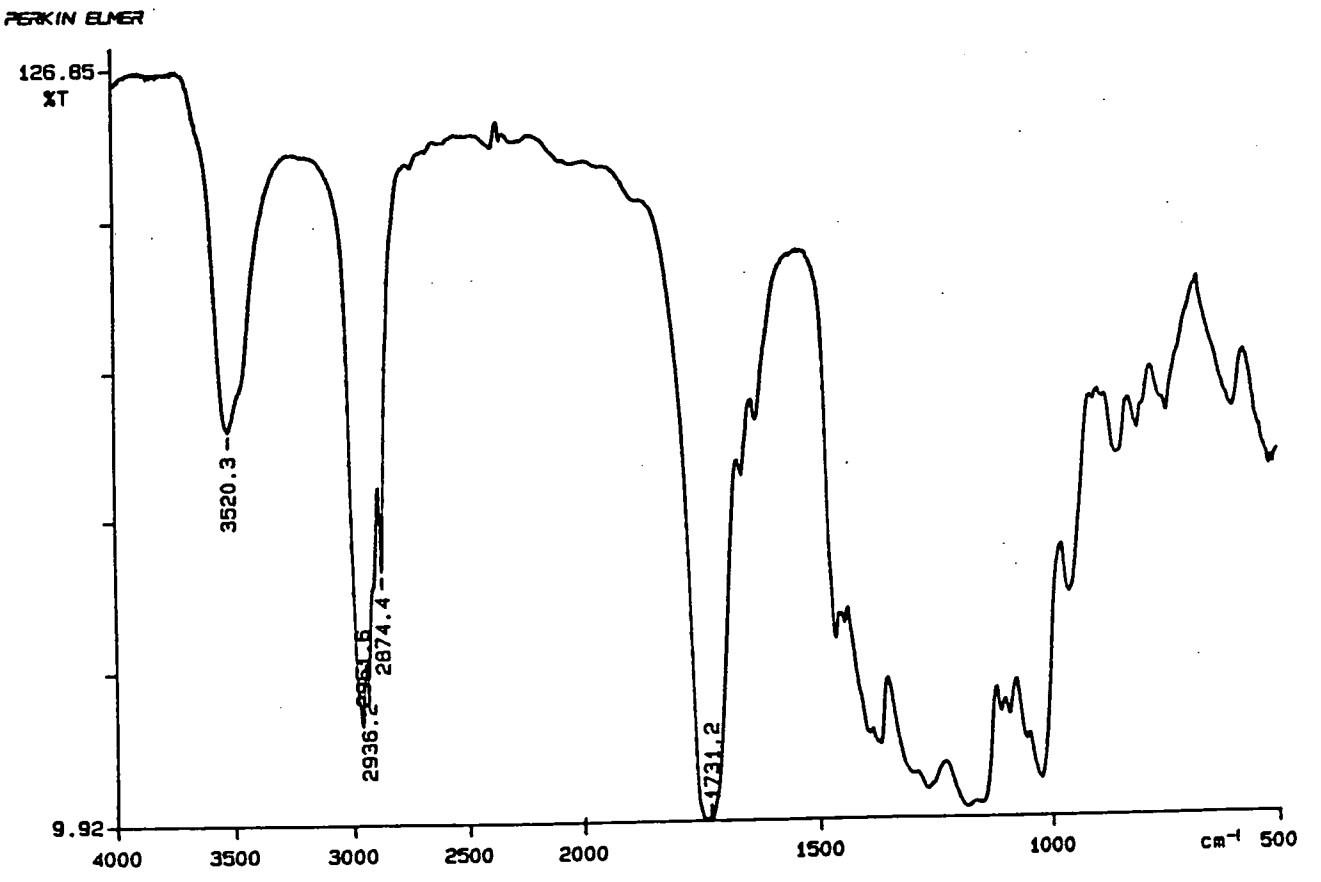

Appendix 2.10 FTIR spectrum of poly(diethyl 3-hydroxyglutarate) performed in the presence of 5wt% $Ti(OBu)_4$ at 100°C for 210 minutes

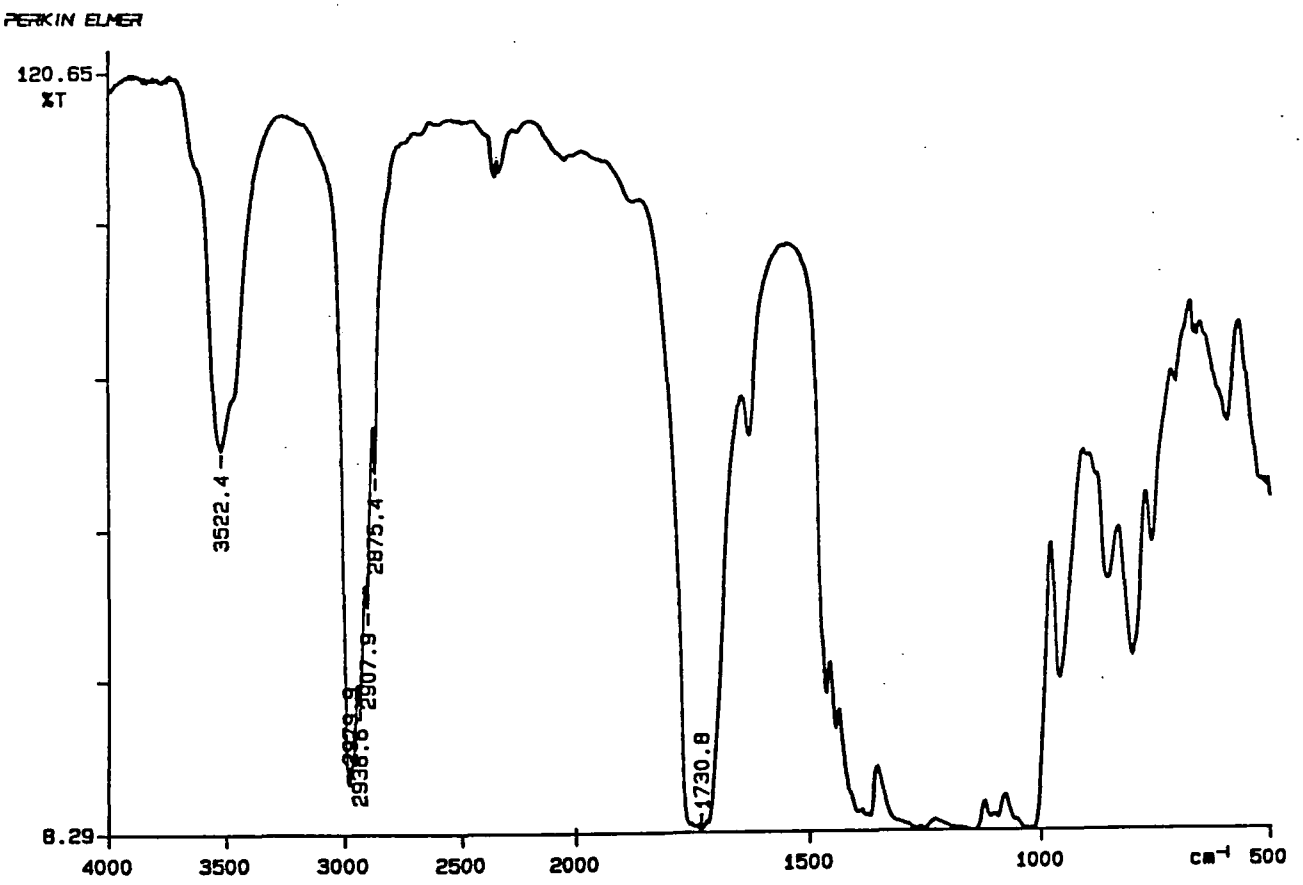

Appendix 2.11 FTIR spectrum of poly(diethyl 3-hydroxyglutarate) performed in the presence of 5wt% $Ti(OBu)_4$ at 100°C for 330 minutes

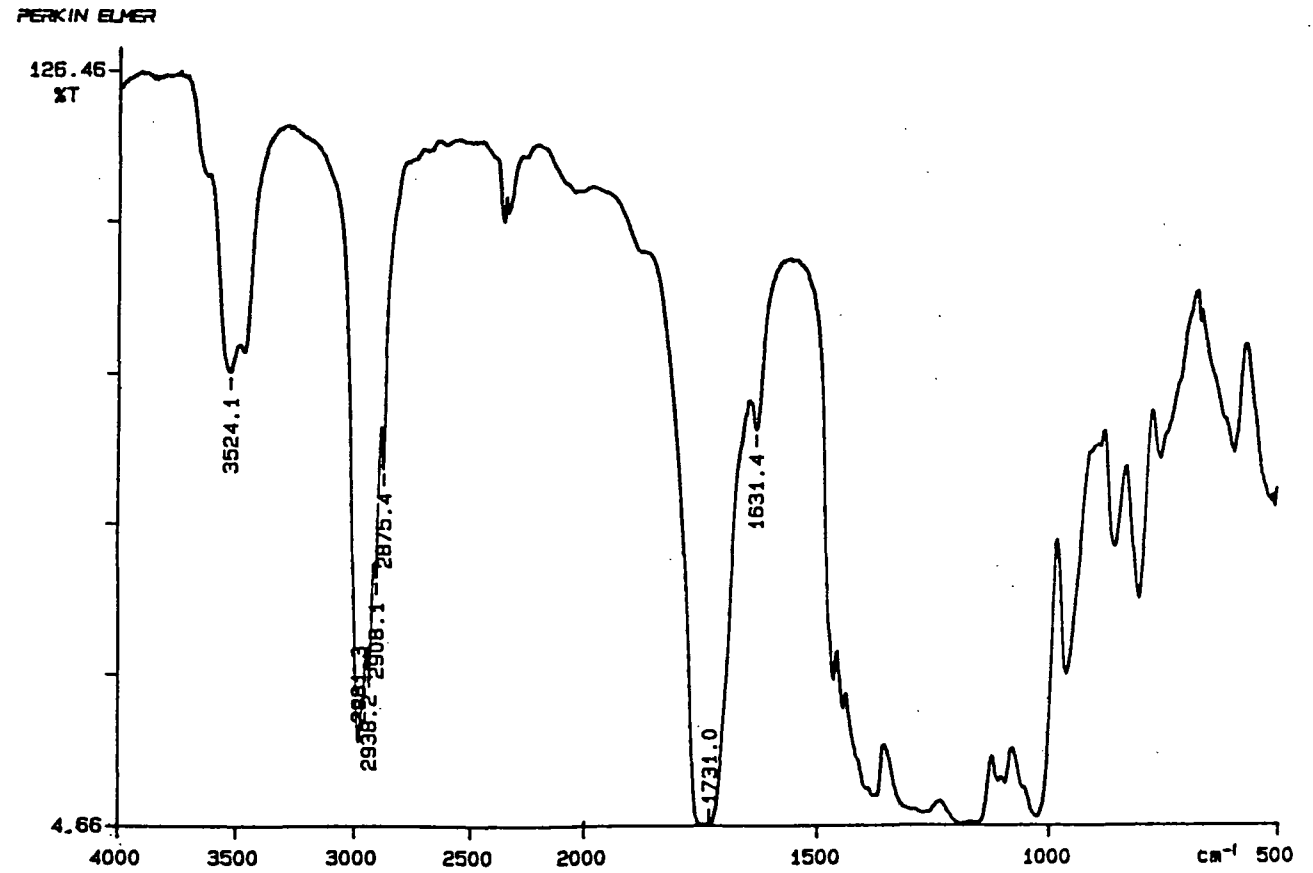

Appendix 2.12 FTIR spectrum of poly(diethyl 3-hydroxyglutarate) performed in the presence of 5wt% $Ti(OBu)_4$ at 115°C for 270 minutes

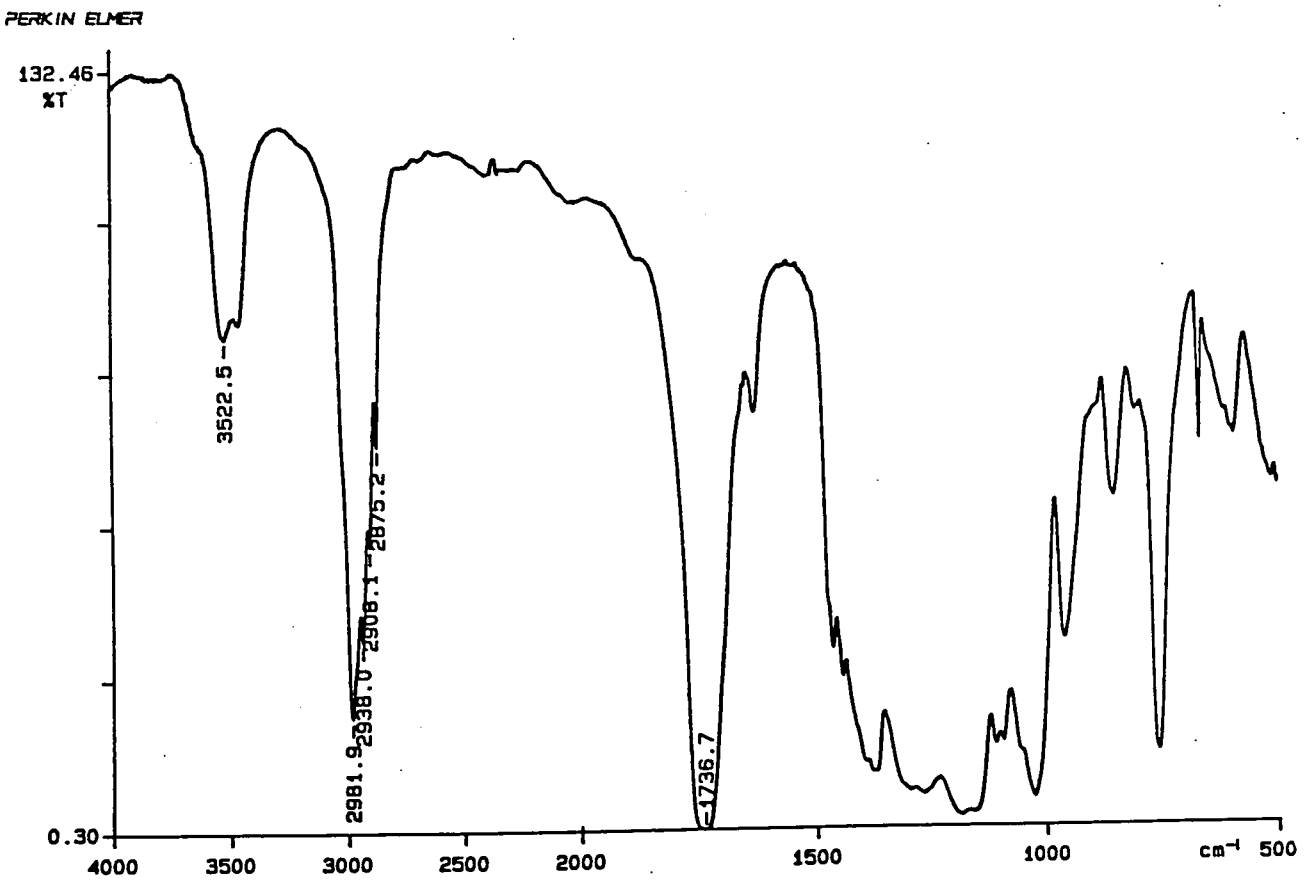

Appendix 2.13 FTIR spectrum of poly(diethyl 3-hydroxyglutarate) performed in the presence of 5wt% $Ti(OBu)_4$ at 125°C for 270 minutes

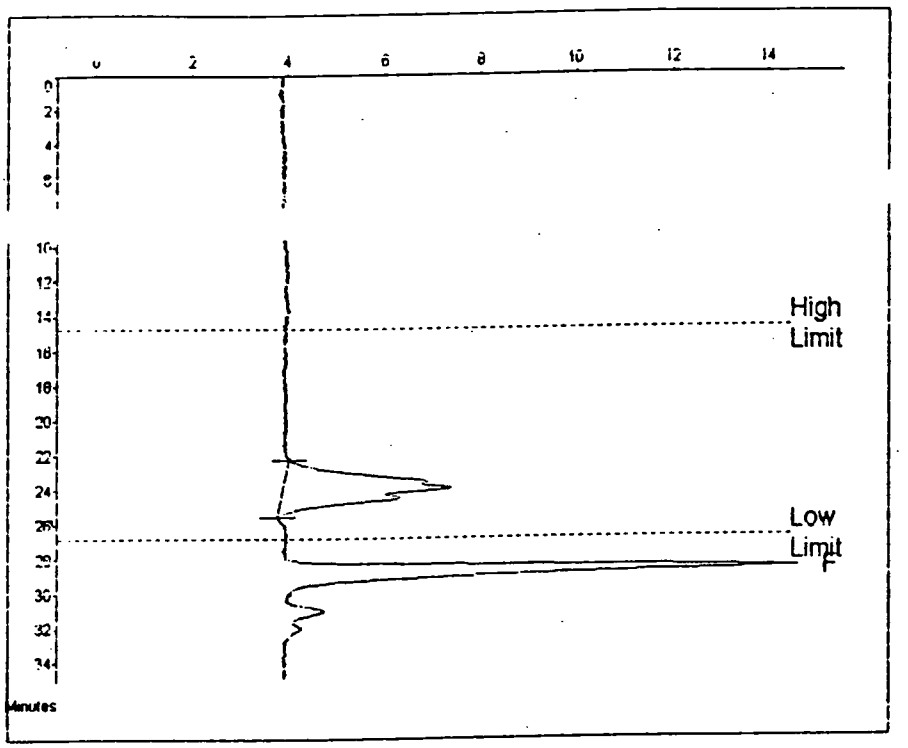

Molecular Weight Averages

Mp =	644	Mz =	1045
Mn =	819	Mz+1 =	1171
Mw =	928	Mv =	909
Polydispersity =	1.131	Peak Area =	62592

Appendix 2.14 $CHCl_3$ GPC trace of the poly(diethyl 3-hydroxyglutarate) performed in the presence of 2.5wt% $Ti(OBu)_4$ at 100°C for 270 minutes

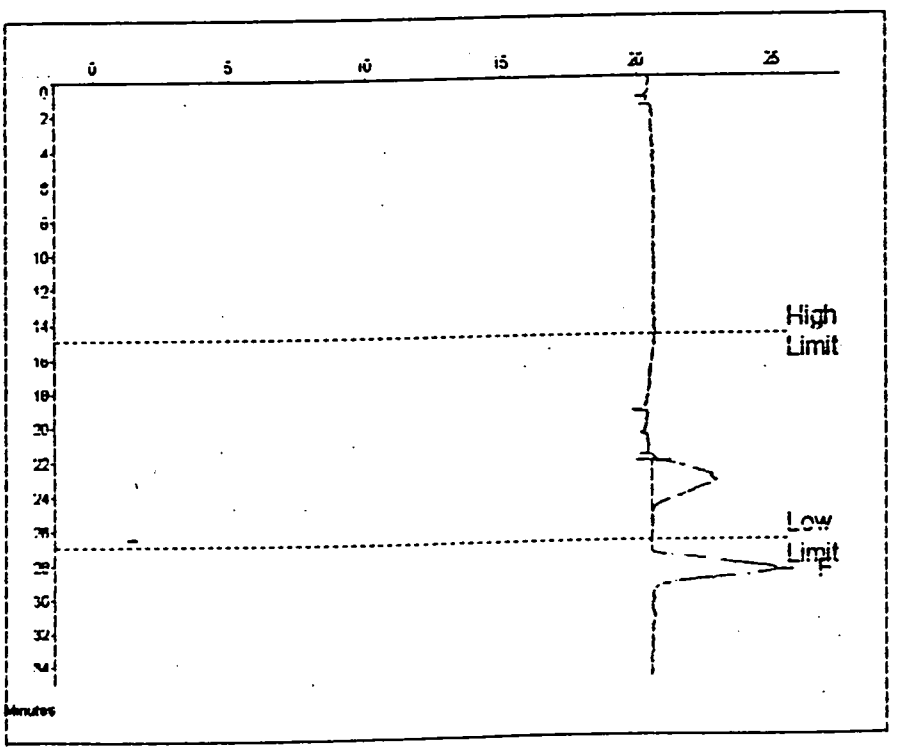

Molecular Weight Averages

Mp =	1152	Mz =	1378
Mn =	1097	Mz+1 =	1507
Mw =	1236	Mv =	1215
Polydispersity =	1.127	Peak Area =	46102

Appendix 2.15 $CHCl_3$ GPC trace of the poly(diethyl 3-hydroxyglutarate) performed in the presence of 3.5wt% $Ti(OBu)_4$ at 100°C for 270 minutes

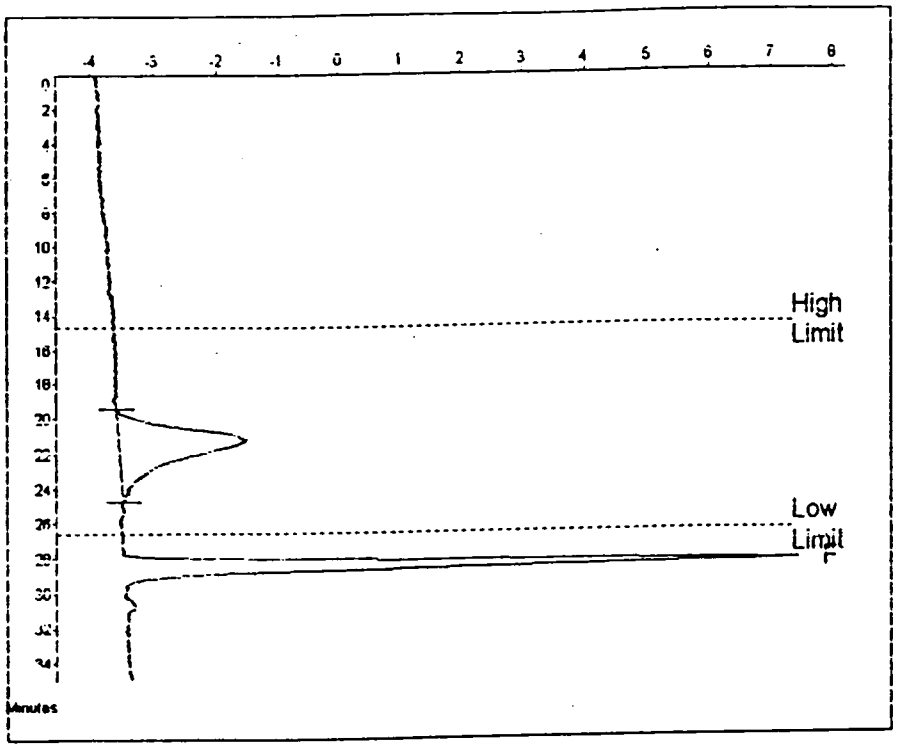

Molecular Weight Averages

Mw =	3783	Mv =	3633
Polydispersity =	1.379	Peak Area =	47982

Appendix 2.16 $CHCl_3$ GPC trace of the poly(diethyl 3-hydroxyglutarate) performed in the presence of 5wt% $Ti(OBu)_4$ at 100°C for 270 minutes

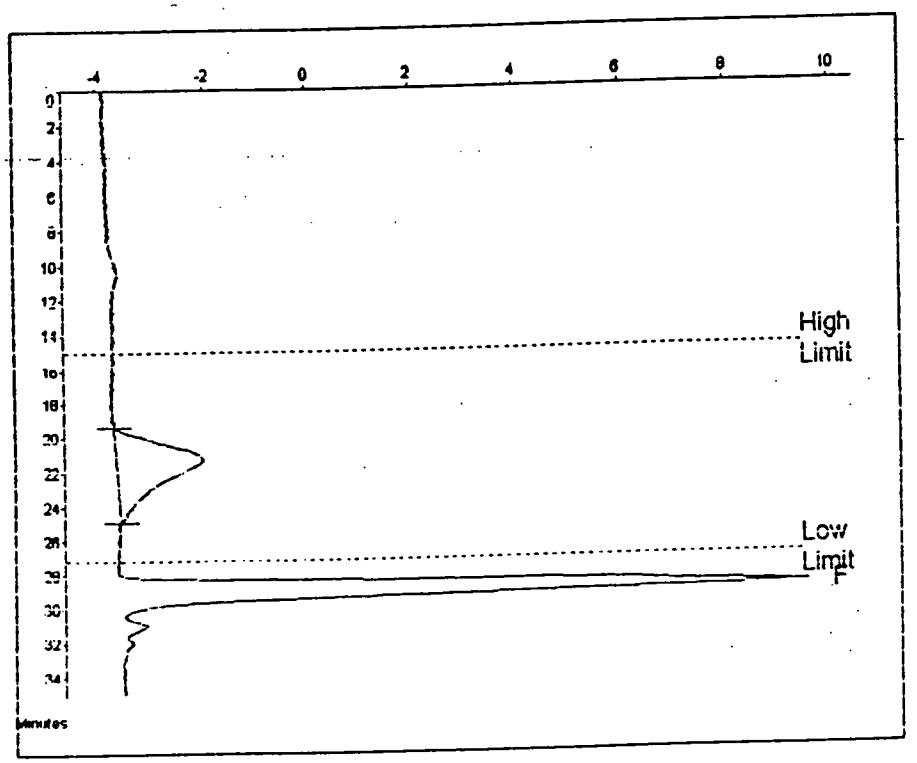

Molecular Weight Averages

Mw =	5034	Mv =	4741
Polydispersity =	1.580	Peak Area =	50348

Appendix 2.17 $CHCl_3$ GPC trace of poly(diethyl 3-hydroxyglutarate) performed in the presence of 5wt% $Ti(OBu)_4$ at 100°C for 270 minutes

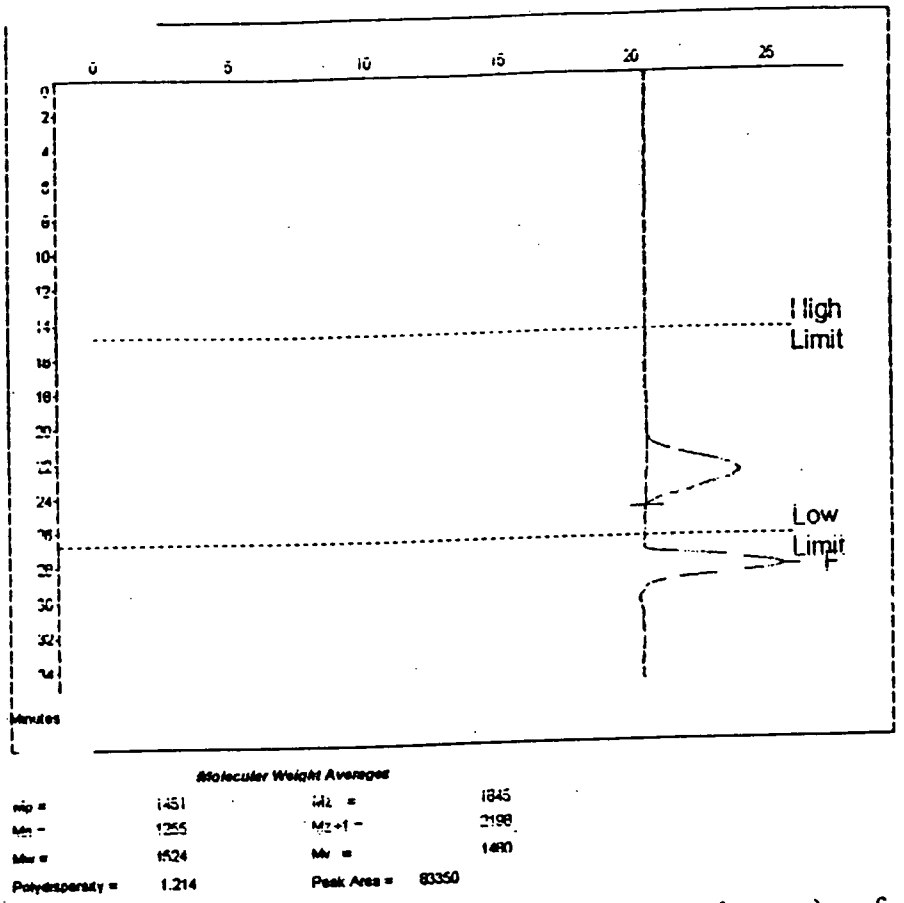

Molecular Weight Averages

Mp =	1451	Mz =	1845
Mn =	1255	Mz+1 =	2198
Mw =	1524	Mv =	1490
Polydispersity =	1.214	Peak Area =	83350

Appendix 2.18 $CHCl_3$ GPC trace of poly(diethyl 3-hydroxyglutarate) performed in the presence of 7wt% $Ti(OBu)_4$ at 100°C for 270 minutes

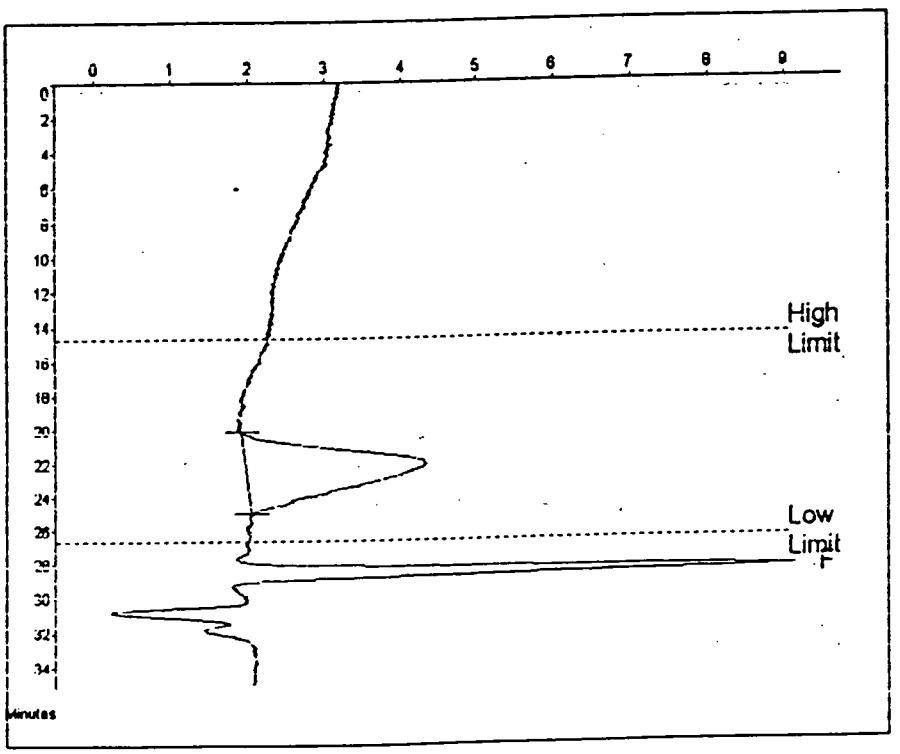

Molecular Weight Averages

Mp =	2308	Mz =	3006
Mn =	1631	Mz+1 =	3737
Mw =	2269	Mv =	2166
Polydispersity =	1.391	Peak Area =	71601

Appendix 2.19 $CHCl_3$ GPC trace of poly(diethyl 3-hydroxyglutarate) performed in the presence of 10wt% $Ti(OBu)_4$ at 100°C for 270 minutes

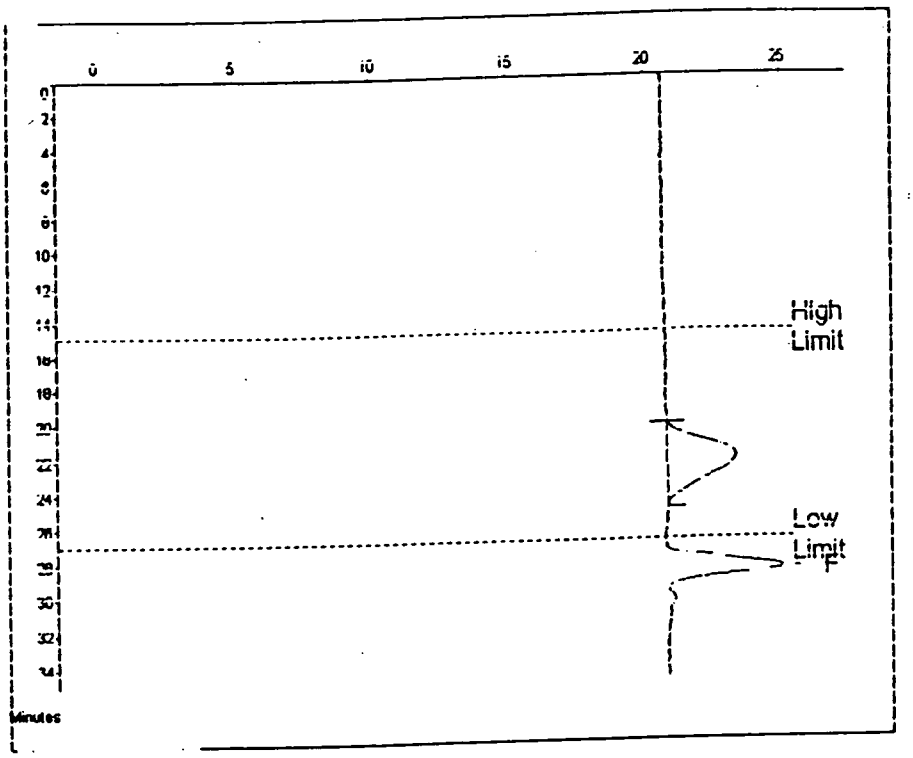

Molecular Weight Averages

Mp =	2499	Mz =	3154
Mn =	1835	Mz+1 =	3075
Mw =	2446	Mv =	2347
Polydispersity =	1.332	Peak Area =	74244

Appendix 2.20 $CHCl_3$ GPC trace of poly(diethyl 3-hydroxyglutarate) performed in the presence of 10wt% $Ti(OBu)_4$ at 100°C for 270 minutes

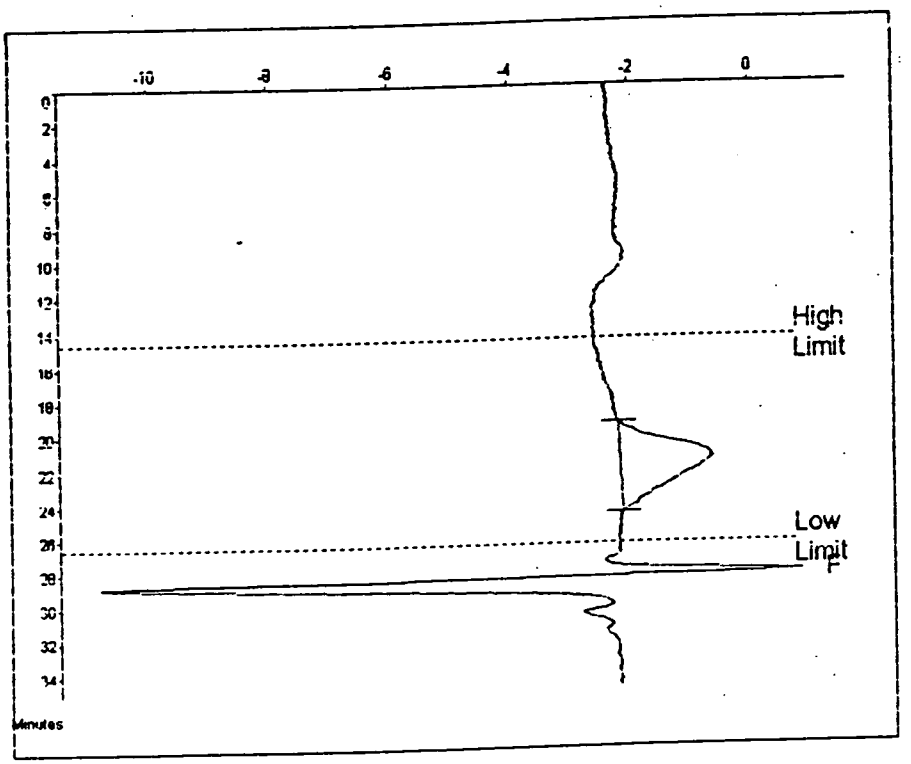

Molecular Weight Averages

Mp =	3050	Mz =	4316
Mn =	2012	Mz+1 =	5581
Mw =	3056	Mv =	2883
Polydispersity =	1.519	Peak Area =	49816

Appendix 2.21 $CHCl_3$ GPC trace of poly(diethyl 3-hydroxyglutarate) performed in the presence of 11wt% $Ti(OBu)_4$ at 100°C for 270 minutes

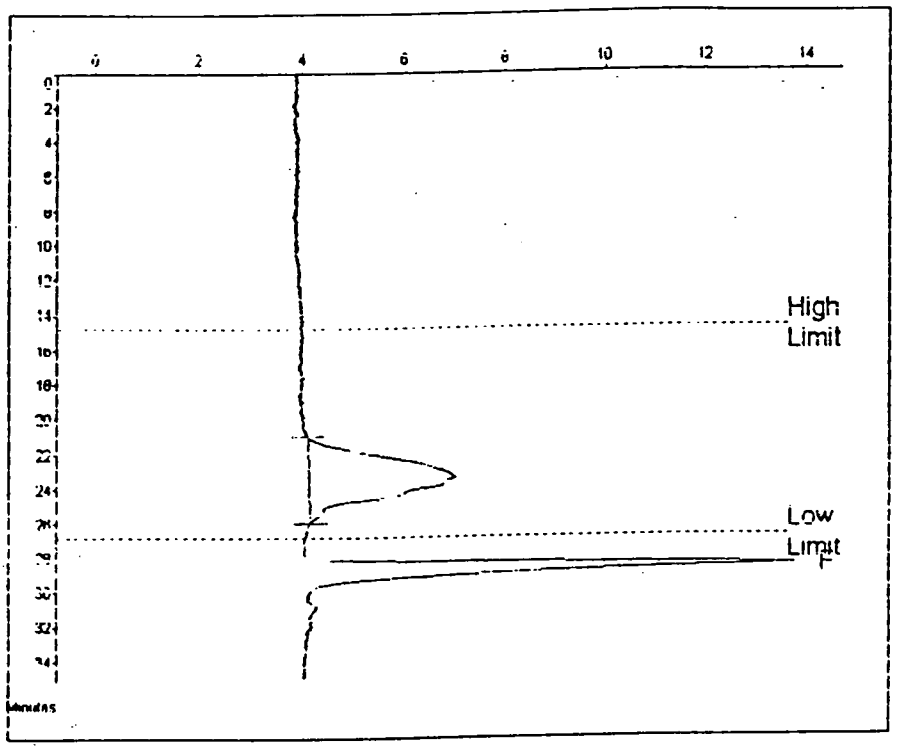

Molecular Weight Averages

Mp =	1157	Mz =	1793
Mn =	1057	Mz+1 =	2226
Mw =	1397	Mv =	1332
Polydispersity =	1.312	Peak Area =	81410

Appendix 2.22 $CHCl_3$ GPC trace of poly(diethyl 3-hydroxyglutarate) performed in the presence of 25wt% $Ti(OBu)_4$ at 100°C for 270 minutes

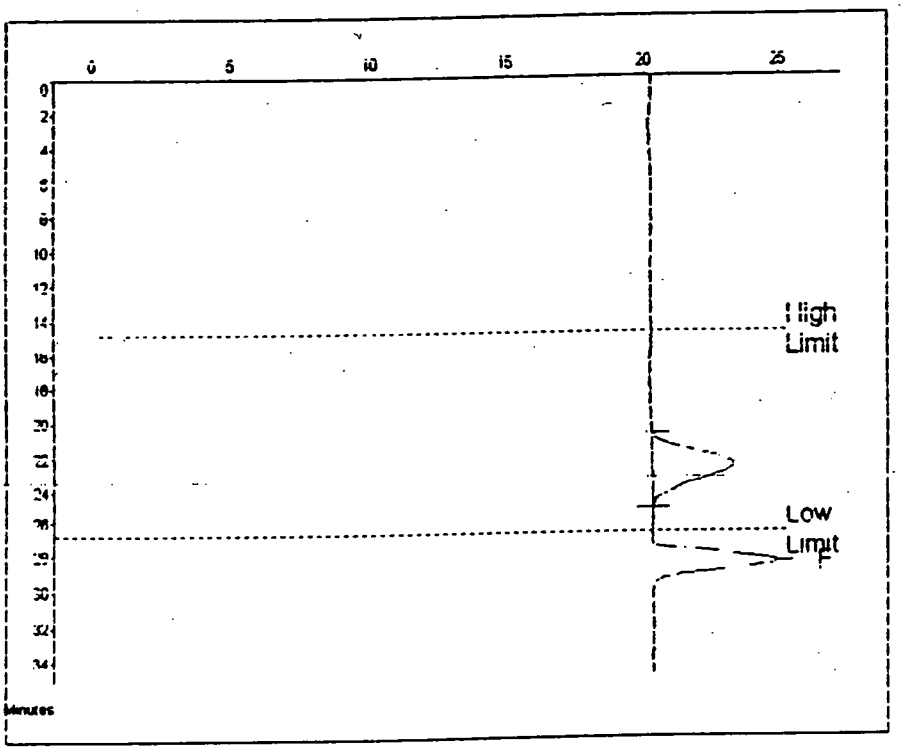

Molecular Weight Averages

Mp =	1777	Mz =	2285
Mn =	1530	Mz+1 =	2696
Mw =	1884	Mv =	1677
Polydispersity =	1.230	Peak Area =	73856

Appendix 2.23 $CHCl_3$ GPC trace of poly(diethyl 3-hydroxyglutarate) performed in the presence of 5wt% $Ti(OBu)_4$ at 100°C for 210 minutes

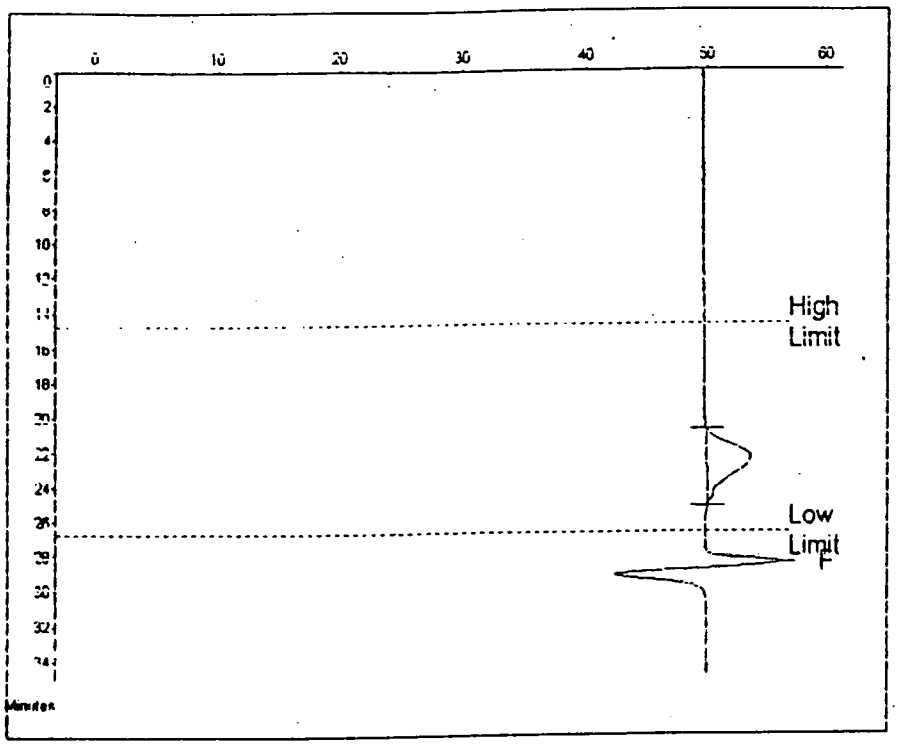

Molecular Weight Averages

Mw =	1954	Mz =	2356
Mn =	1477	Mz+1 =	2709
Mv =	1883	Mv =	1922
Polydispersity =	1.275	Peak Area =	93066

Appendix 2.24 $CHCl_3$ GPC trace of poly(diethyl 3-hydroxyglutarate) performed in the presence of 5wt% $Ti(OBu)_4$ at 100°C for 330 minutes

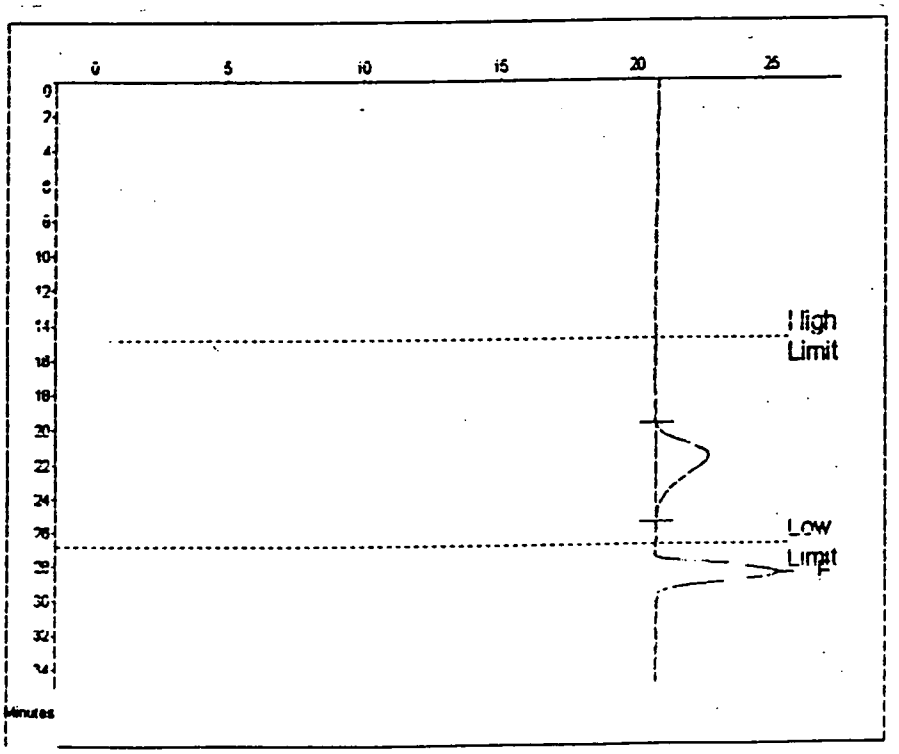

Molecular Weight Averages

Mw =	3464	Mz =	4176
Mn =	2161	Mz+1 =	5172
Mv =	3151	Mv =	3004
Polydispersity =	1.445	Peak Area =	58688

Appendix 2.25 $CHCl_3$ GPC trace of poly(diethyl 3-hydroxyglutarate) performed in the presence of 5wt% $Ti(OBu)_4$ at 115°C for 270 minutes

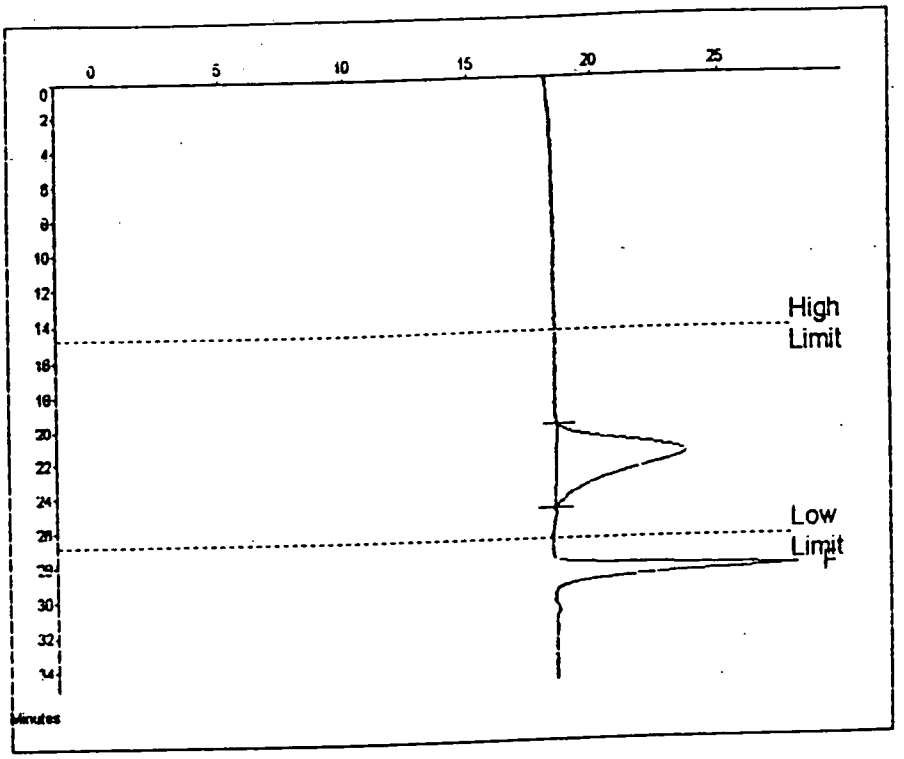

Molecular Weight Averages

Mp =	2922	Mz =	3452
Mn =	2016	Mz+1 =	4160
Mw =	2717	Mv =	2611
Polydispersity =	1.346	Peak Area =	133801

Appendix 2.26 $CHCl_3$ GPC trace of poly(diethyl 3-hydroxyglutarate) performed in the presence of 5wt% $Ti(OBu)_4$ at 125°C for 270 minutes

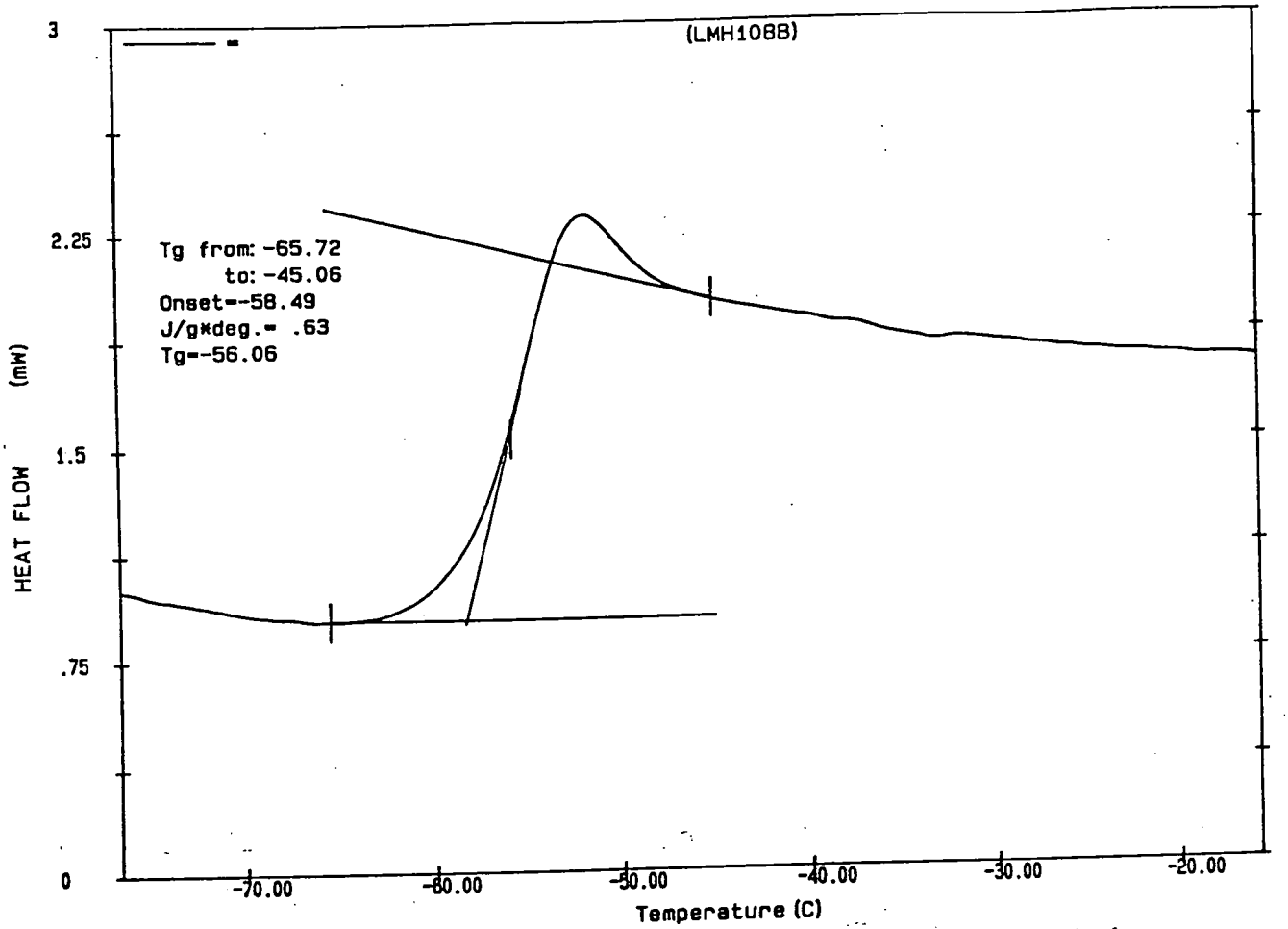

Appendix 2.27 DSC trace of poly(diethyl 3-hydroxyglutarate) performed in the presence of 2.5wt% $Ti(OBu)_4$ at 100°C for 270 minutes

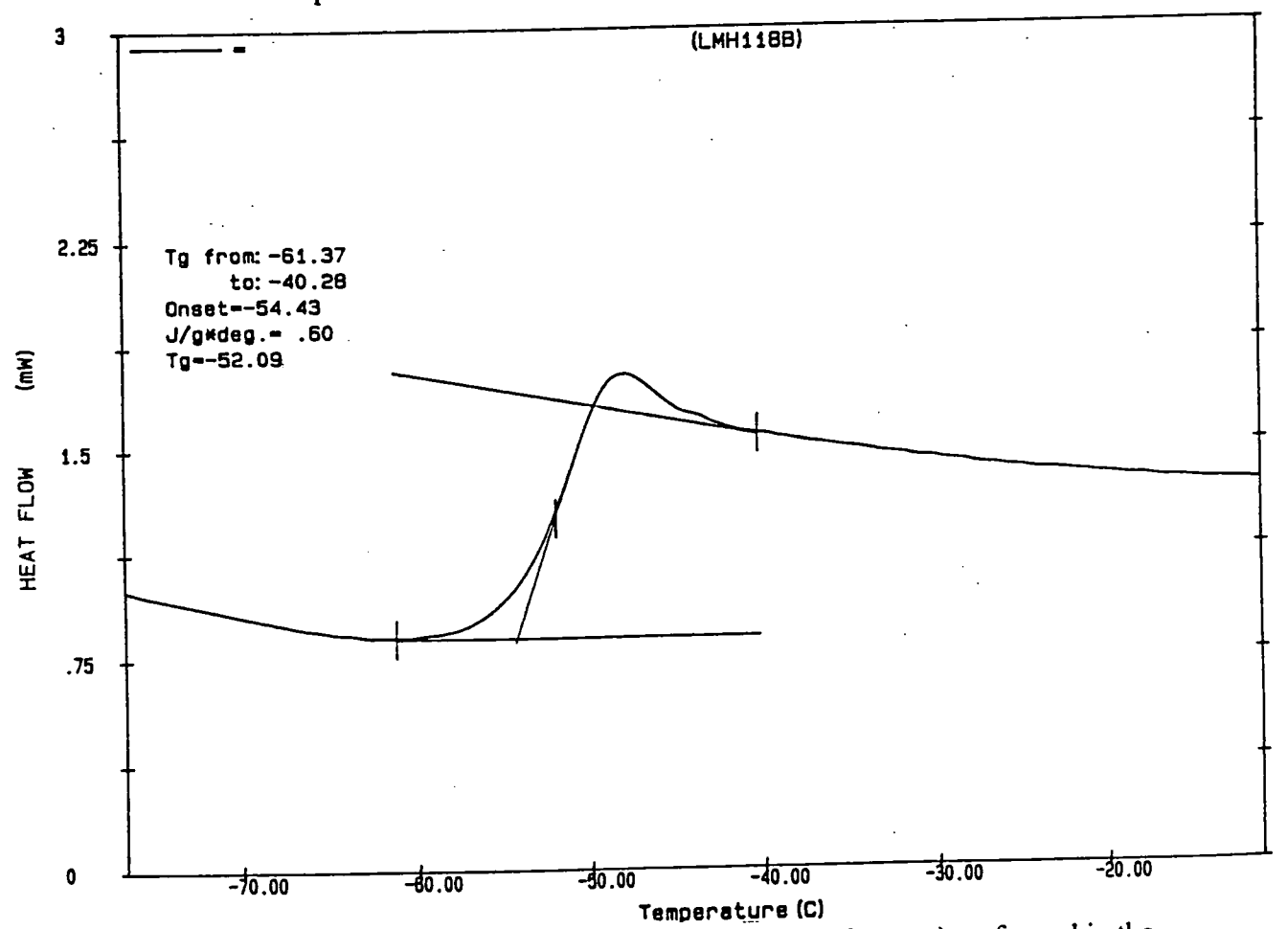

Appendix 2.28 DSC trace of poly(diethyl 3-hydroxyglutarate) performed in the presence of 3.5wt% $Ti(OBu)_4$ at 100°C for 270 minutes

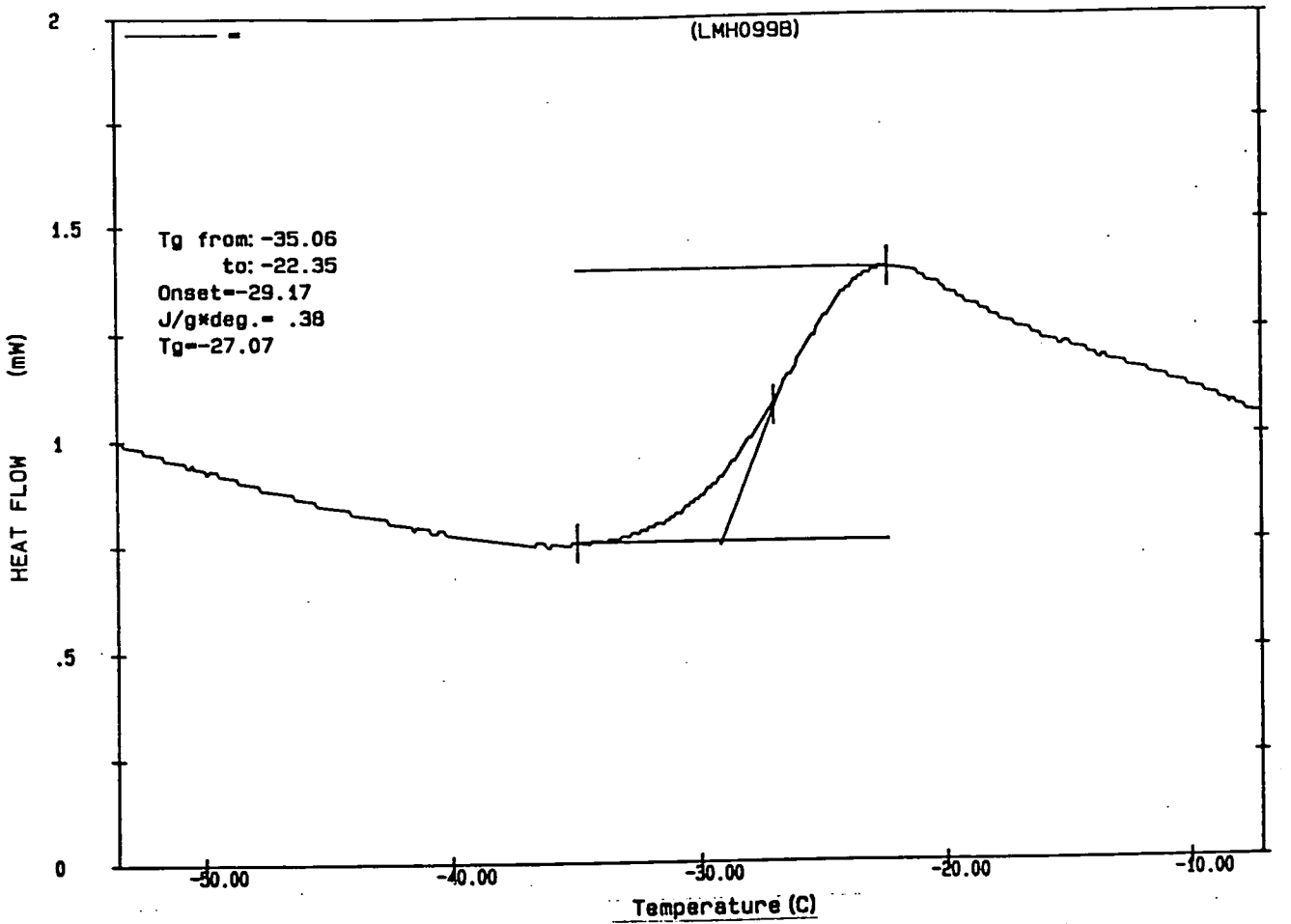

Appendix 2.29 DSC trace of poly(diethyl 3-hydroxyglutarate) performed in the presence of 5wt% $Ti(OBu)_4$ at 100°C for 270 minutes

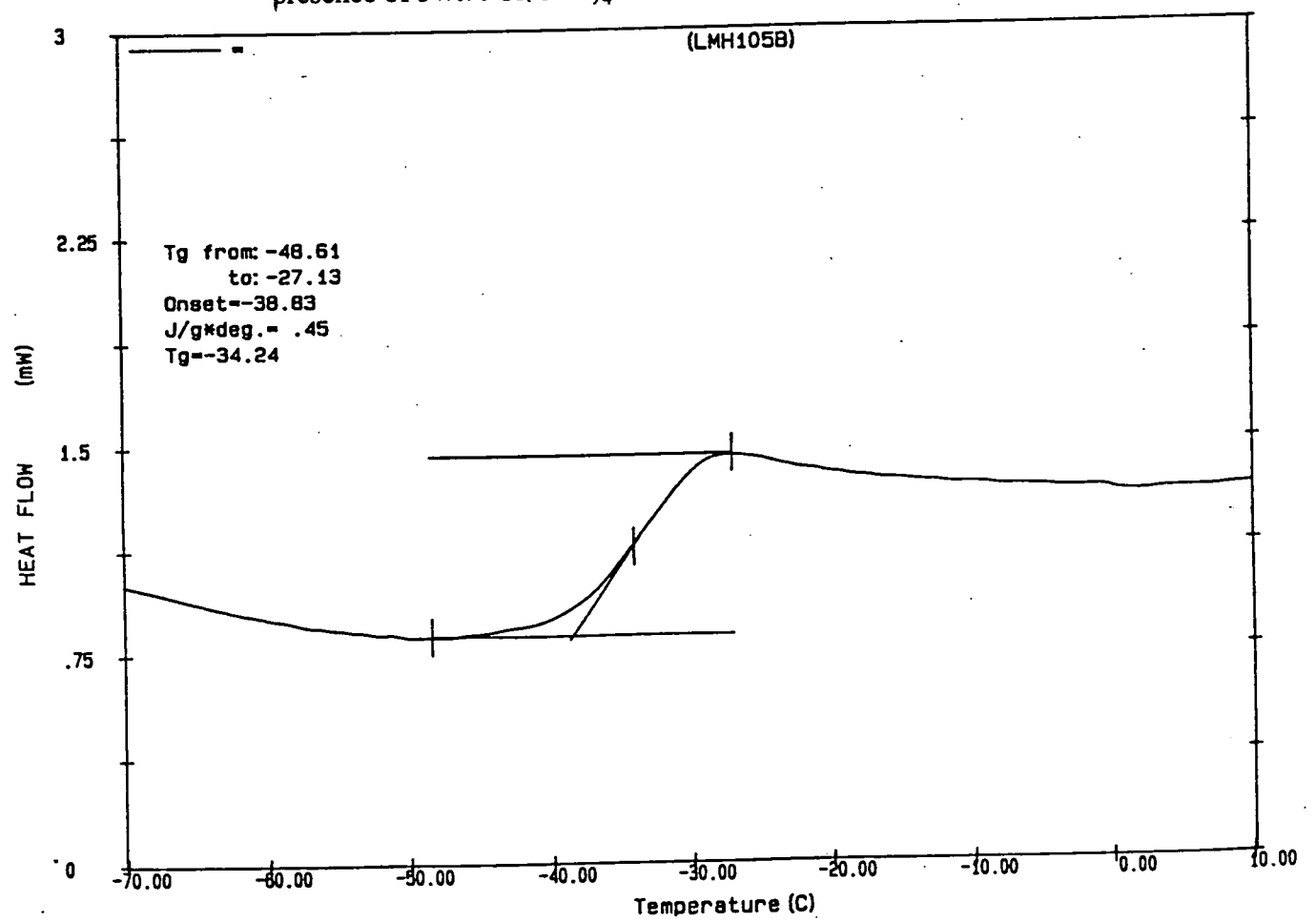

Appendix 2.30 DSC trace of poly(diethyl 3-hydroxyglutarate) performed in the presence of 5wt% $Ti(OBu)_4$ at 100°C for 270 minutes

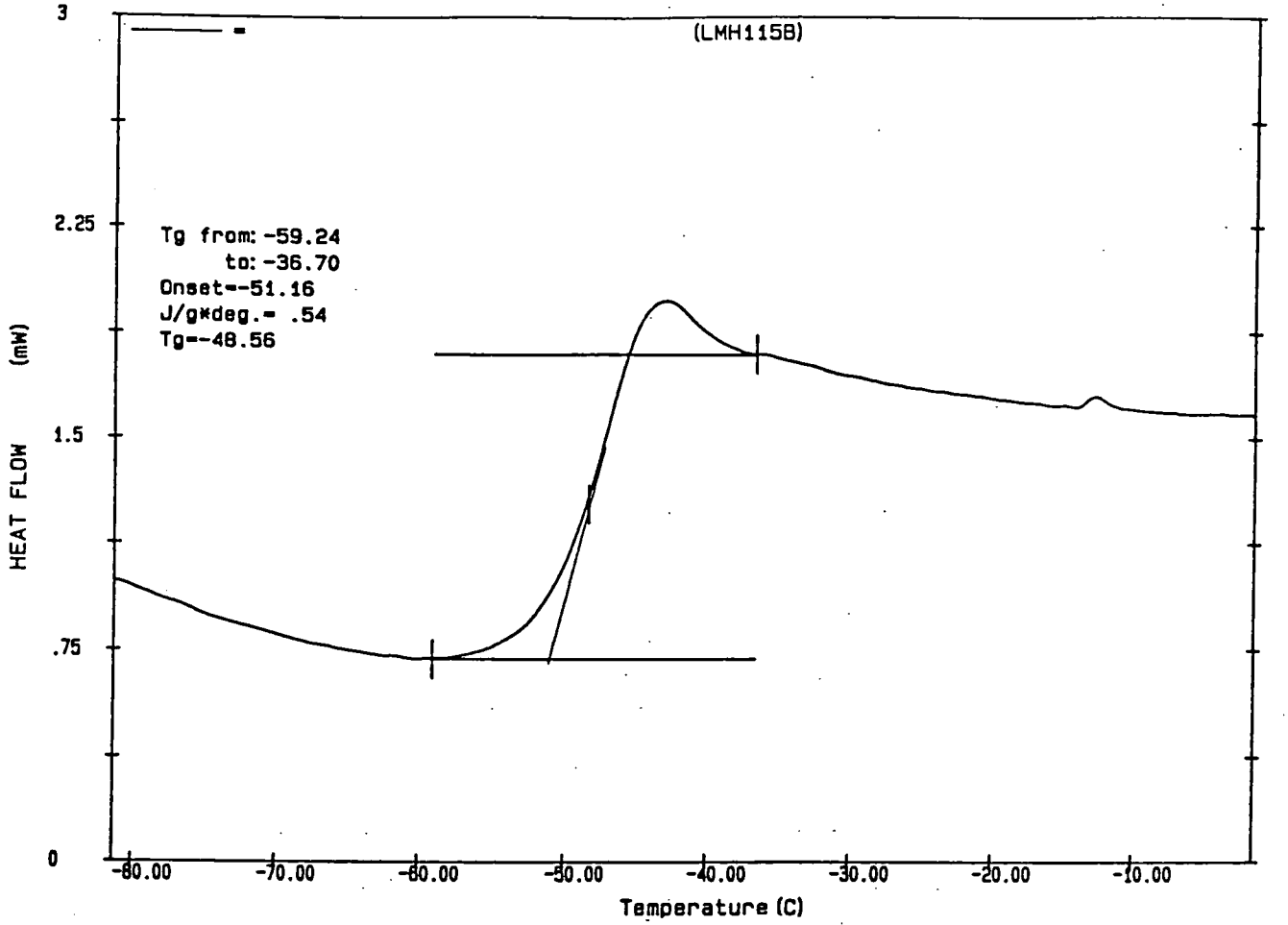

Appendix 2.31 DSC trace of poly(diethyl 3-hydroxyglutarate) performed in the presence of 7wt% $Ti(OBu)_4$ at 100°C for 270 minutes

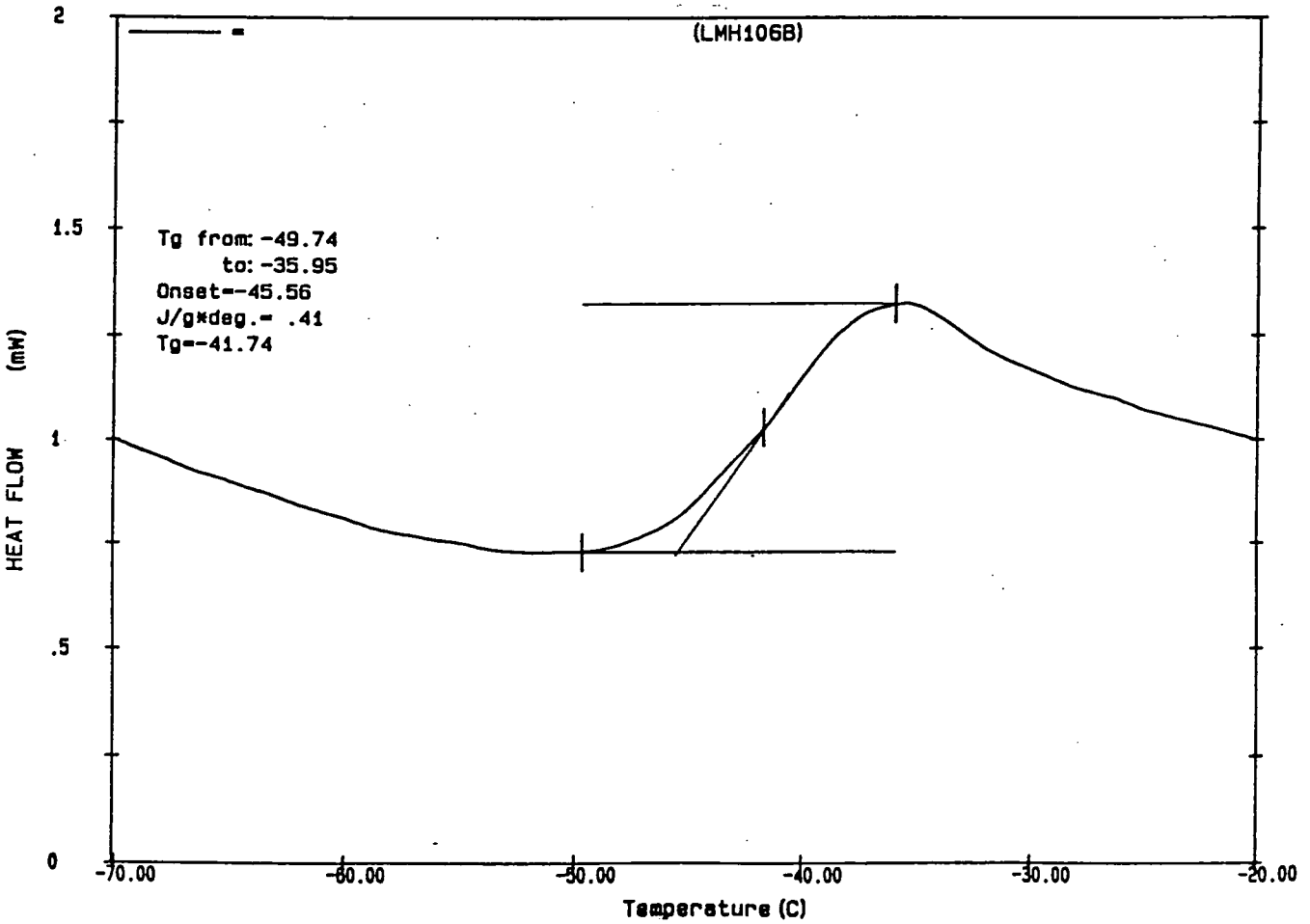

Appendix 2.32 DSC trace of poly(diethyl 3-hydroxyglutarate) performed in the presence of 10wt% $Ti(OBu)_4$ at 100°C for 270 minutes

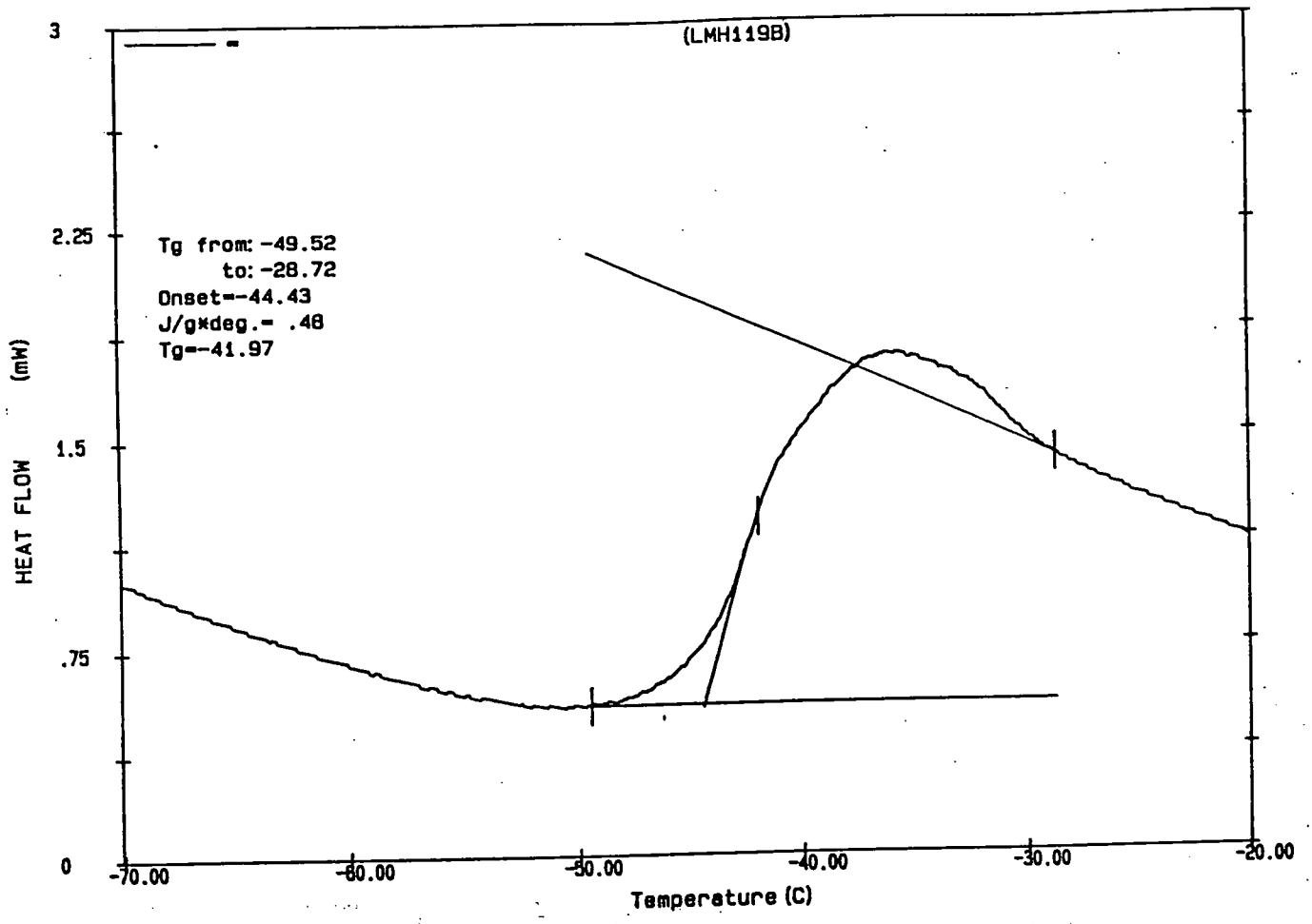

Appendix 2.33 DSC trace of poly(diethyl 3-hydroxyglutarate) performed in the presence of 10wt% $Ti(OBu)_4$ at 100°C for 270 minutes

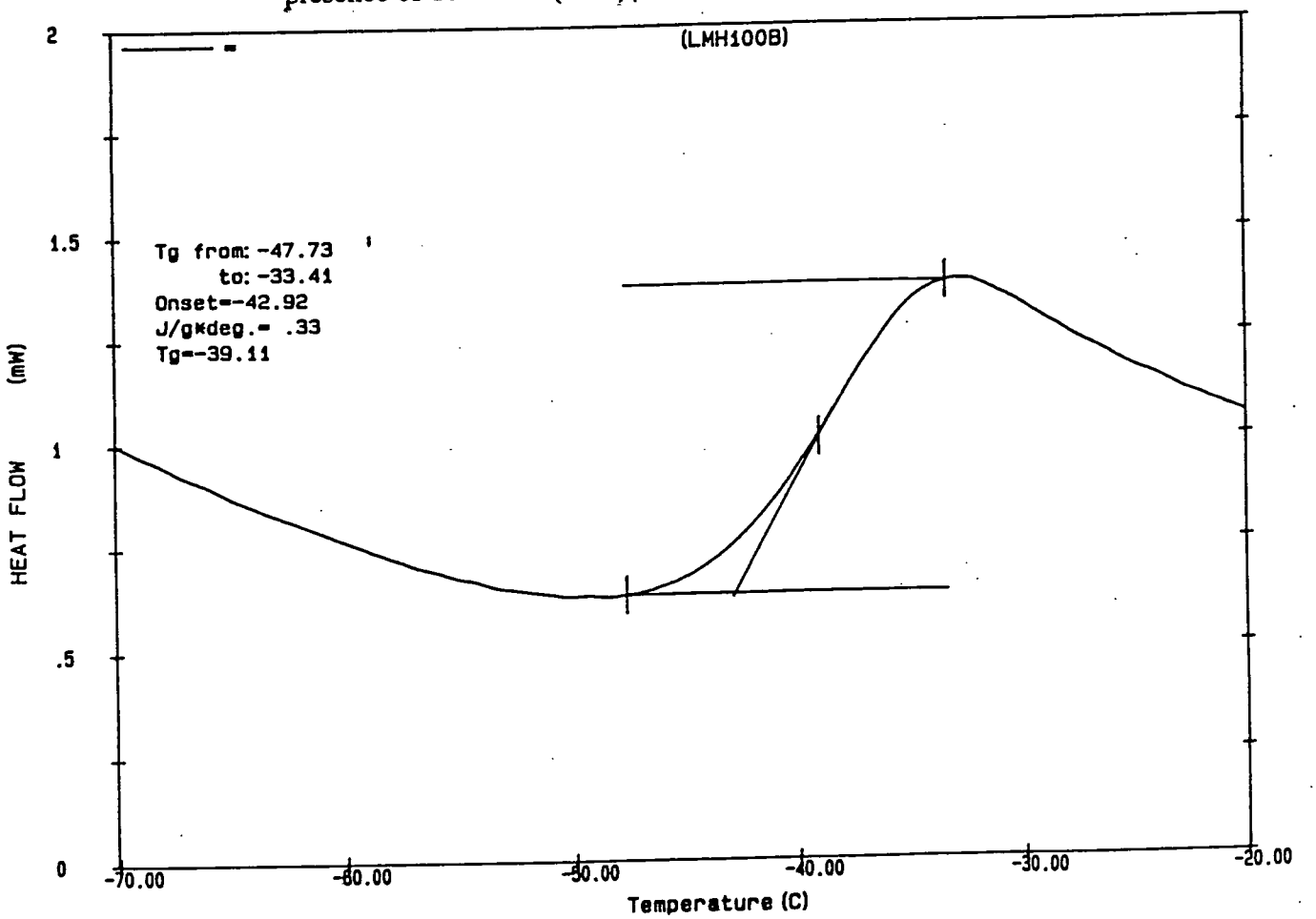

Appendix 2.34 DSC trace of poly(diethyl 3-hydroxyglutarate) performed in the presence of 11wt% $Ti(OBu)_4$ at 100°C for 270 minutes

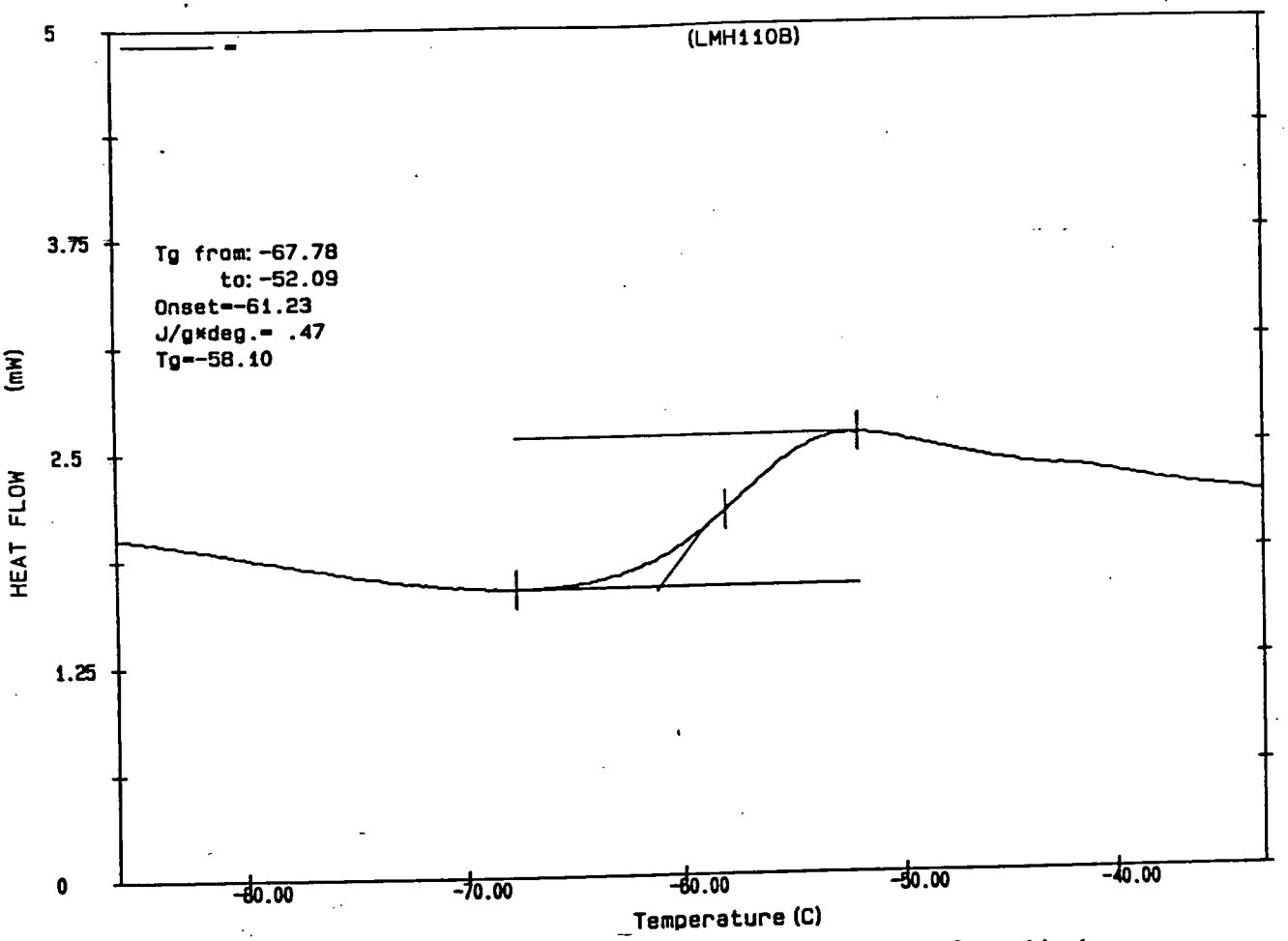

Appendix 2.35 DSC trace of poly(diethyl 3-hydroxyglutarate) performed in the presence of 25wt% $Ti(OBu)_4$ at 100°C for 270 minutes

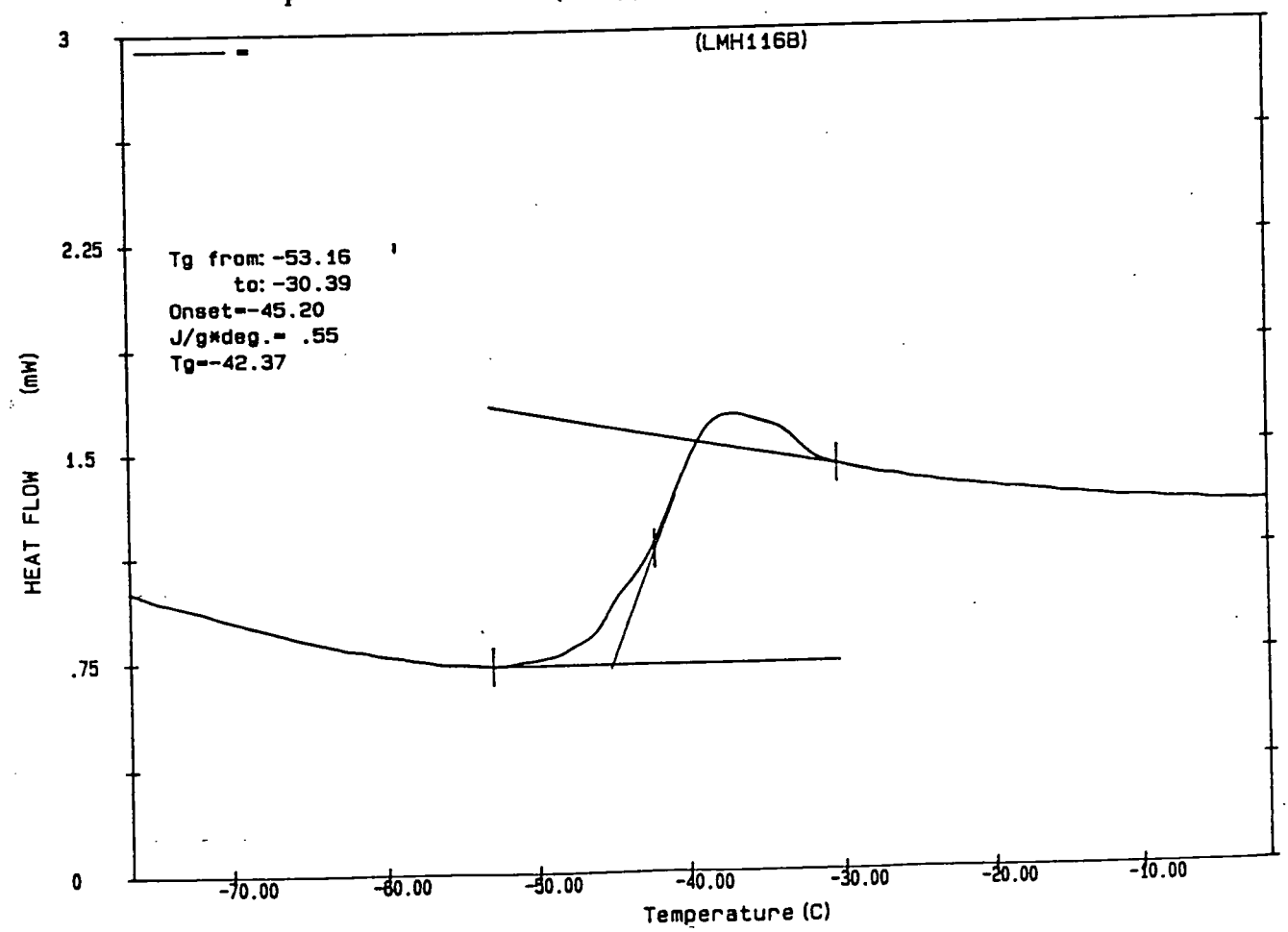

Appendix 2.36 DSC trace of poly(diethyl 3-hydroxyglutarate) performed in the presence of 5wt% $Ti(OBu)_4$ at 100°C for 210 minutes

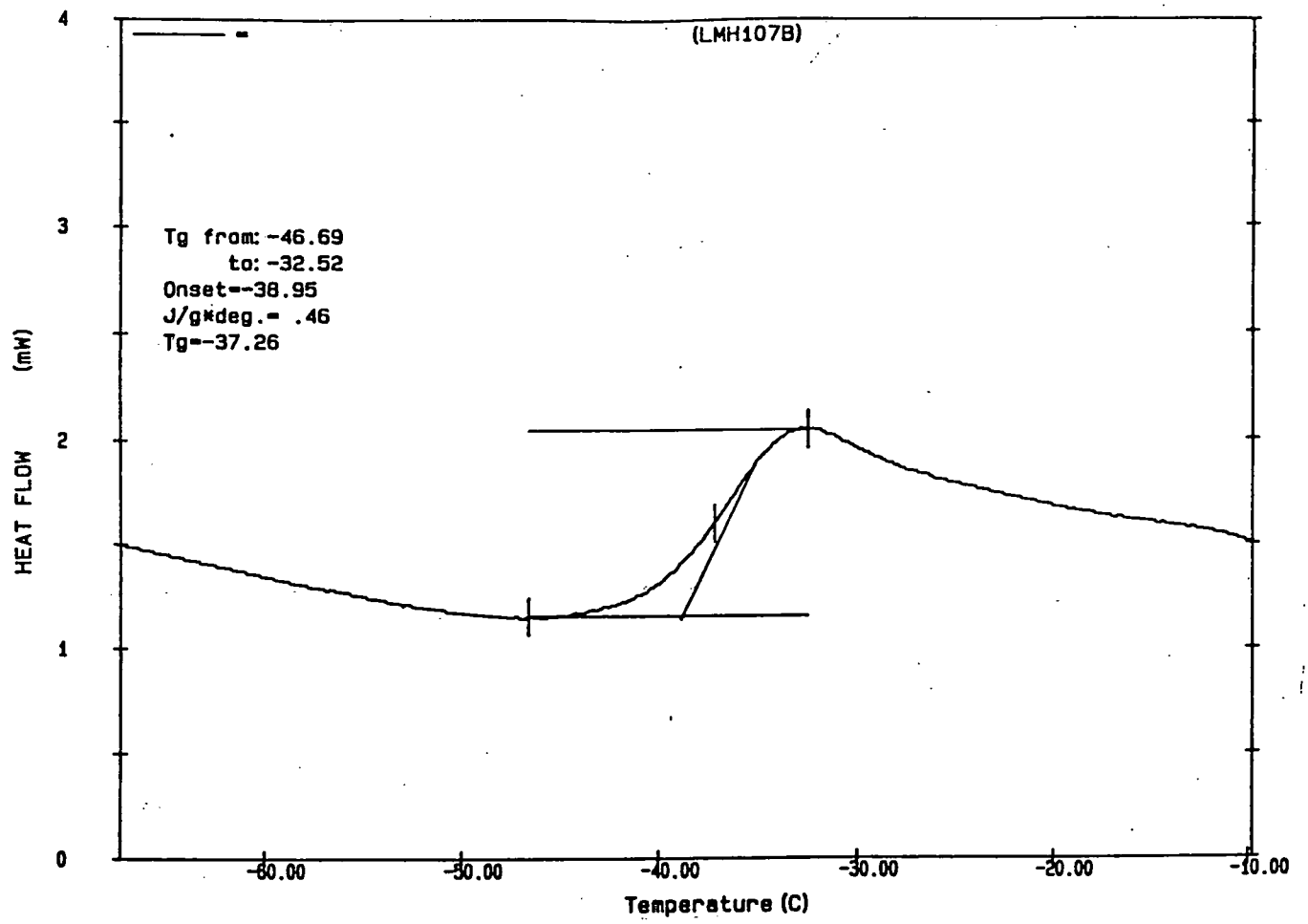

Appendix 2.37 DSC trace of poly(diethyl 3-hydroxyglutarate) performed in the presence of 5wt% $Ti(OBu)_4$ at 100°C for 330 minutes

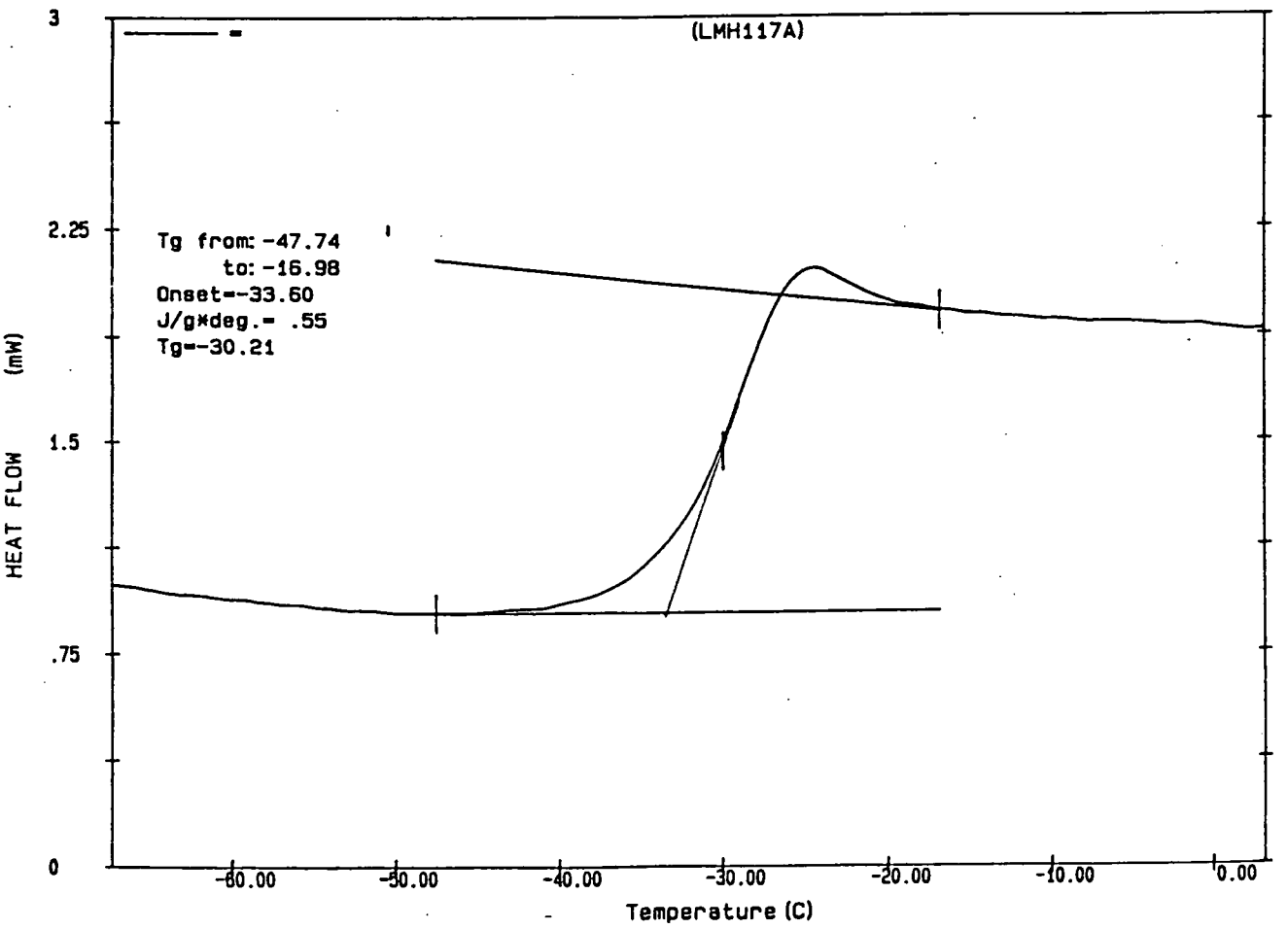

Appendix 2.38 DSC trace of poly(diethyl 3-hydroxyglutarate) performed in the presence of 5wt% $Ti(OBu)_4$ at 115°C for 270 minutes

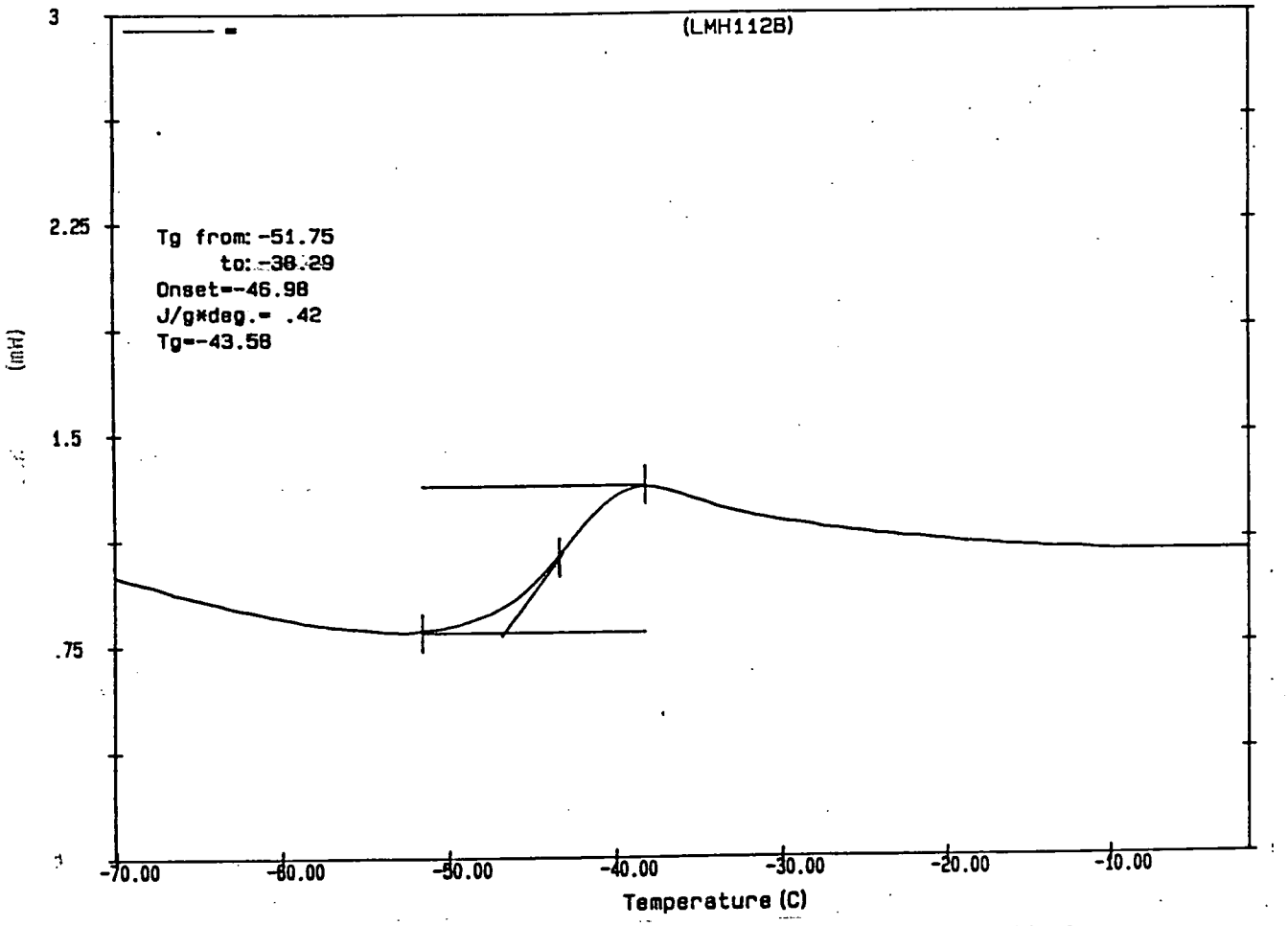

Appendix 2.39 DSC trace of poly(diethyl 3-hydroxyglutarate) performed in the presence of 5wt% $Ti(OBu)_4$ at 125°C for 270 minutes

APPENDIX 2

^{1}H and ^{13}C nmr data for hyperbranched poly(diethyl 3-hydroxyglutarate) whose synthesis is discussed in Chapter 4.

Peak/ppm	Integral	Multiplicity	Assignment
0.93	0.45	t	Butyl CH_3
1.26	8.76	t	Ethyl CH_3
1.33	0.32	m	Butyl CH_2
1.6	0.34	m	Butyl CH_2
2.54	4.24	m	Focal CH_2
2.69	5.79	m	Polymeric CH_2
3.50	1	m	Monomer
4.16	7.88	m	Ethyl OCH_2
4.56	1	m	Focal CH
5.56	1.52	m	Polymeric CH

Table 1. ^{1}H nmr data for the product of reaction at 100°C in the presence of 2.5wt%$Ti(OBu)_4$ for 270 minutes.

Peak/ppm	Integral	Multiplicity	Assignment
0.93	0.25	t	Butyl CH_3
1.26	5.63	t	Ethyl CH_3
1.33	0.18	m	Butyl CH_2
1.6	0.14	m	Butyl CH_2
2.54	2.38	m	Focal CH_2
2.69	4.06	m	Polymeric CH_2
4.16	4.44	m	Ethyl OCH_2
4.44	0.59	m	Focal CH
5.56	1	m	Polymeric CH

Table 2. ^{1}H nmr data for the product of reaction at 100°C in the presence of 3.5wt%$Ti(OBu)_4$ for 270 minutes.

Peak/ppm	Integral	Multiplicity	Assignment
0.93	4.5	t	Butyl CH_3
1.26	66.5	t	Ethyl CH_3
1.33	4.5	m	Butyl CH_2
1.6	3.5	m	Butyl CH_2
2.54	6.6	m	Focal CH_2
2.69	91.25	m	Polymeric CH_2
4.16	54	m	Ethyl OCH_2
4.44	1	m	Focal CH
5.56	22.5	m	Polymeric CH

Table 3. ^{1}H nmr data for the product of reaction at 100°C in the presence of 5wt%$Ti(OBu)_4$ for 270 minutes.

Peak/ppm	Integral	Multiplicity	Assignment
0.93	4	t	Butyl CH_3
1.26	41.25	t	Ethyl CH_3
1.33	2.8	m	Butyl CH_2
1.6	2.9	m	Butyl CH_2
2.54	5.5	m	Focal CH_2
2.69	56.5	m	Polymeric CH_2
4.16	37	m	Ethyl OCH_2
4.44	1	m	Focal CH
5.56	14.75	m	Polymeric CH

Table 4. ^{1}H nmr data for the product of reaction at 100°C in the presence of 5wt%$Ti(OBu)_4$ for 270 minutes.

Peak/ppm	Integral	Multiplicity	Assignment
0.93	0.54	t	Butyl CH_3
1.26	4.37	t	Ethyl CH_3
1.33	0.32	m	Butyl CH_2
1.6	0.33	m	Butyl CH_2
2.54	1.64	m	Focal CH_2
2.69	4	m	Polymeric CH_2
4.16	3.89	m	Ethyl OCH_2
4.44	0.4	m	Focal CH
5.56	1	m	Polymeric CH

Table 5. ^{1}H nmr data for the product of reaction at 100°C in the presence of 7wt%$Ti(OBu)_4$ for 270 minutes.

Peak/ppm	Integral	Multiplicity	Assignment
0.93	3.29	t	Butyl CH_3
1.26	20.64	t	Ethyl CH_3
1.33	2.0	m	Butyl CH_2
1.6	2.1	m	Butyl CH_2
2.54	4.5	m	Focal CH_2
2.69	25.21	m	Polymeric CH_2
4.16	18.43	m	Ethyl OCH_2
4.56	1	m	Focal CH
5.56	6.64	m	Polymeric CH

Table 6. ^{1}H nmr data for the product of reaction at 100°C in the presence of 10wt%$Ti(OBu)_4$ for 270 minutes.

Peak/ppm	Integral	Multiplicity	Assignment
0.93	0.54	t	Butyl CH_3
1.26	3.59	t	Ethyl CH_3
1.33	0.34	m	Butyl CH_2
1.6	0.36	m	Butyl CH_2
2.54	1	m	Focal CH_2
2.69	4.20	m	Polymeric CH_2
4.16	3.45	m	Ethyl OCH_2
4.56	0.23	m	Focal CH
5.56	1.14	m	Polymeric CH

Table 7. ^{1}H nmr data for the product of reaction at 100°C in the presence of 10wt%$Ti(OBu)_4$ for 270 minutes.

Peak/ppm	Integral	Multiplicity	Assignment
0.93	5.5	t	Butyl CH_3
1.26	25.6	t	Ethyl CH_3
1.33	3.4	m	Butyl CH_2
1.6	3.6	m	Butyl CH_2
2.54	5.25	m	Focal CH_2
2.69	32.75	m	Polymeric CH_2
4.16	24	m	Ethyl OCH_2
4.56	1	m	Focal CH
5.56	8.63	m	Polymeric CH

Table 8. ^1H nmr data for the product of reaction at 100°C in the presence of 11wt%$Ti(OBu)_4$ for 270 minutes.

Peak/ppm	Integral	Multiplicity	Assignment
0.93	16.5	t	Butyl CH_3
1.26	31.8	t	Ethyl CH_3
1.33	10	m	Butyl CH_2
1.6	10.5	m	Butyl CH_2
2.54	13	m	Focal CH_2
2.69	35	m	Polymeric CH_2
4.16	37.25	m	Ethyl OCH_2
4.44	3	m	Focal CH
5.56	9.13	m	Polymeric CH

Table 9. ^1H nmr data for the product of reaction at 100°C in the presence of 25wt%$Ti(OBu)_4$ for 270 minutes.

Peak/ppm	Integral	Multiplicity	Assignment
0.93	0.27	t	Butyl CH_3
1.26	3.73	t	Ethyl CH_3
1.33	0.16	m	Butyl CH_2
1.6	0.20	m	Butyl CH_2
2.54	1.09	m	Focal CH_2
2.69	3.83	m	Polymeric CH_2
4.16	3.20	m	Ethyl OCH_2
4.56	0.24	m	Focal CH
5.56	1	m	Polymeric CH

Table 10. ^{1}H nmr data for the product of reaction at 100°C in the presence of 5wt%$Ti(OBu)_4$ for 210 minutes.

Peak/ppm	Integral	Multiplicity	Assignment
0.93	1.79	t	Butyl CH_3
1.26	20.64	t	Ethyl CH_3
1.33	1.10	m	Butyl CH_2
1.6	1.12	m	Butyl CH_2
2.54	4.86	m	Focal CH_2
2.69	23.43	m	Polymeric CH_2
4.16	17.79	m	Ethyl OCH_2
4.44	1	m	Focal CH
5.56	6.43	m	Polymeric CH

Table 11. ^{1}H nmr data for the product of reaction at 100°C in the presence of 5wt%$Ti(OBu)_4$ for 330 minutes.

Peak/ppm	Integral	Multiplicity	Assignment
0.93	0.45	t	Butyl CH_3
1.26	6.18	t	Ethyl CH_3
1.33	0.25	m	Butyl CH_2
1.6	0.30	m	Butyl CH_2
2.54	1	m	Focal CH_2
2.69	7.73	m	Polymeric CH_2
4.16	5.23	m	Ethyl OCH_2
4.44	0.18	m	Focal CH
5.56	2.05	m	Polymeric CH

Table 12. ^{1}H nmr data for the product of reaction at 115°C in the presence of 5wt%$Ti(OBu)_4$ for 270 minutes.

Peak/ppm	Integral	Multiplicity	Assignment
0.93	0.55	t	Butyl CH_3
1.26	6.95	t	Ethyl CH_3
1.33	0.32	m	Butyl CH_2
1.6	0.35	m	Butyl CH_2
2.54	1	m	Focal CH_2
2.69	8.83	m	Polymeric CH_2
4.16	6.0	m	Ethyl OCH_2
4.44	0.21	m	Focal CH
5.56	2.31	m	Polymeric CH

Table 13. ^{1}H nmr data for the product of reaction at 125°C in the presence of 5wt%$Ti(OBu)_4$ for 270 minutes.

a) 2.5wt% $Ti(OBu)_4$		b) 3.5wt% $Ti(OBu)_4$	
Peak/ppm	Assignment	Peak/ppm	Assignment
13.59	Butyl CH_3	13.67	Butyl CH_3
14.06	Ethyl CH_3	14.13	Ethyl CH_3
18.98	Butyl CH_2	19.06	Butyl CH_2
30.44	Butyl CH_2	30.51	Butyl CH_2
38.18	Polymeric CH_2	38.36	Polymeric CH_2
38.29	Polymeric CH_2	40.68	Focal CH_2
40.61	Focal CH_2	41.13	Butyl CH_2
40.72	Focal CH_2	60.88	Ethyl OCH_2
41.07	Butyl CH_2	64.75	Focal CH
41.14	Butyl CH_2	67.15 (multiplet)	Polymeric CH
60.70	Ethyl OCH_2	168.64	C=O
60.86	Ethyl OCH_2	169.69	C=O
64.68	Focal CH	169.77	C=O
64.70	Focal CH	169.93	C=O
67 (multiplet)	Polymeric CH	170.32	C=O
168.73	C=O	170.44	C=O
169.70	C=O	-	-
169.90	C=O	-	-
170.35	C=O	-	-
170.35	C=O	-	-
171.70	C=O	-	-

Table 14. ^{13}C nmr data for the product of reaction at 100°C for 270 minutes

a) in the presence of 2.5wt% $Ti(OBu)_4$

b) in the presence of 3.5wt% $Ti(OBu)_4$

a) 5wt% $Ti(OBu)_4$		b) 5wt% $Ti(OBu)_4$	
Peak/ppm	Assignment	Peak/ppm	Assignment
13.55	Butyl CH_3	13.68	Butyl CH_3
14.01	Ethyl CH_3	14.14	Ethyl CH_3
18.93	Butyl CH_2	19.06	Butyl CH_2
30.39	Butyl CH_2	30.51	Butyl CH_2
38.11	Polymeric CH_2	38.23	Polymeric CH_2
60.70	Ethyl OCH_2	40.61	Focal CH_2
64.68	Focal CH	41.13	Butyl CH_2
64.70	Focal CH	60.82	Ethyl OCH_2
67.07 (multiplet)	Polymeric CH	64.73	Focal CH
168.46	C=O	67.19 (multiplet)	Polymeric CH
169.54	C=O	168.59	C=O
-	-	169.68	C=O
-	-	169.67	C=O

Table 15. ^{13}C nmr data for the product of reaction at 100°C for 270 minutes

a) in the presence of 5wt% $Ti(OBu)_4$

b) in the presence of 5wt% $Ti(OBu)_4$

a) 7wt% $Ti(OBu)_4$		b) 10wt% $Ti(OBu)_4$	
Peak/ppm	Assignment	Peak/ppm	Assignment
13.66	Butyl CH_3	13.66	Butyl CH_3
14.12	Ethyl CH_3	14.12	Ethyl CH_3
19.05	Butyl CH_2	19.05	Butyl CH_2
30.51	Butyl CH_2	30.51	Butyl CH_2
38.24	Polymeric CH_2	38.23	Polymeric CH_2
40.63	Focal CH_2	40.61	Focal CH_2
64.74	Focal CH	41.11	Butyl CH_2
67.15 (multiplet)	Polymeric CH	60.82	Ethyl OCH_2
168.66	C=O	64.73	Focal CH
169.66	C=O	67.19 (multiplet)	Polymeric CH
-	-	168.58	C=O
-	-	169.66	C=O

Table 16. ^{13}C nmr data for the product of reaction at 100°C for 270 minutes

a) in the presence of 7wt% $Ti(OBu)_4$

b) in the presence of 10wt% $Ti(OBu)_4$

a) 10wt% $Ti(OBu)_4$		b) 11wt% $Ti(OBu)_4$	
Peak/ppm	Assignment	Peak/ppm	Assignment
13.67	Butyl CH_3	13.68	Butyl CH_3
14.13	Ethyl CH_3	14.13	Ethyl CH_3
19.06	Butyl CH_2	19.06	Butyl CH_2
30.51	Butyl CH_2	30.51	Butyl CH_2
38.24	Polymeric CH_2	38.23	Polymeric CH_2
40.62	Focal CH_2	40.61	Focal CH_2
41.12	Butyl CH_2	60.81	Ethyl OCH_2
41.19	Butyl CH_2	64.72	Focal CH
60.83	Ethyl OCH_2	67.19 (multiplet)	Polymeric CH
64.74	Focal CH	168.60	C=O
67.20 (multiplet)	Polymeric CH	169.68	C=O
168.59	C=O	-	-
169.68	C=O	-	-

Table 17. ^{13}C nmr data for the product of reaction at 100°C for 270 minutes

a) in the presence of 10wt%

b) in the presence of 11wt%

25wt% $Ti(OBu)_4$	
Peak/ppm	Assignment
13.66	Butyl CH_3
14.12	Ethyl CH_3
19.05	Butyl CH_2
30.51	Butyl CH_2
38.24	Polymeric CH_2
40.63	Focal CH_2
41.18	Butyl CH_2
60.78	Ethyl OCH_2
64.69	Focal CH
67.17 (multiplet)	Polymeric CH
168.59	C=O
169.67	C=O
171.78	C=O

Table 18. ^{13}C nmr data for the product of reaction at 100°C for 270 minutes in the presence of 25wt% $Ti(OBu)_4$.

a) 210 minutes		b) 330 minutes	
Peak/ppm	Assignment	Peak/ppm	Assignment
13.54	Butyl CH_3	13.69	Butyl CH_3
14.00	Ethyl CH_3	14.15	Ethyl CH_3
18.93	Butyl CH_2	19.07	Butyl CH_2
30.38	Butyl CH_2	30.53	Butyl CH_2
38.12	Polymeric CH_2	38.26	Polymeric CH_2
40.56	Focal CH_2	40.64	Focal CH_2
41.00	Butyl CH_2	41.20	Butyl CH_2
60.70	Ethyl OCH_2	60.86	Ethyl OCH_2
64.62	Focal CH	64.76	Focal CH
67.09 (multiplet)	Polymeric CH	67.23 (multiplet)	Polymeric CH
168.46	C=O	168.61	C=O
169.55	C=O	169.70	C=O
169.63	C=O	170.45	C=O
167.30	C=O	-	-

Table 19. ^{13}C nmr data for the product of reaction at 100°C in the presence of 5wt% $Ti(OBu)_4$

a) for 210 minutes

b) for 330 minutes

a) 115°C		b) 125°C	
Peak/ppm	Assignment	Peak/ppm	Assignment
13.55	Butyl CH_3	13.66	Butyl CH_3
14.01	Ethyl CH_3	14.13	Ethyl CH_3
18.93	Butyl CH_2	19.05	Butyl CH_2
30.43	Butyl CH_2	30.92	Butyl CH_2
38.12	Polymeric CH_2	38.24	Polymeric CH_2
60.70	Ethyl OCH_2	40.64	Focal CH_2
64.61	Focal CH	41.20	Butyl CH_2
67.08 (multiplet)	Polymeric CH	60.82	Ethyl OCH_2
168.47	C=O	64.74	Focal CH
169.55	C=O	67.20 (multiplet)	Polymeric CH
174.35	C=O	168.59	C=O
-	-	169.66	C=O

Table 20. ^{13}C nmr data for the product of reaction at 100°C in the presence of 5wt% $Ti(OBu)_4$

a) at 115°C

b) at 125°C

lmh108	Na+	BuO	2xBuO	Cyclisation	Dehyd
Peak mass					
387.24	**2.014**	1.837	1.660	2.305	2.128
402.32	2.110	1.932	1.755	2.401	2.224
420.14	2.222	**2.045**	1.868	2.514	2.336
544.89	**3.012**	2.835	2.658	3.303	3.126
561.35	3.116	2.939	2.762	3.407	3.230
572.31	3.186	**3.008**	2.831	3.477	3.299
702.55	**4.010**	3.833	3.655	4.301	4.124
719	4.114	3.937	3.759	4.405	4.228
731.34	4.192	**4.015**	3.838	4.483	4.306
861.58	**5.016**	4.839	4.662	5.307	5.130
878.03	5.120	4.943	4.766	5.412	5.234
890.37	5.199	**5.021**	4.844	5.490	5.312
1019.23	**6.014**	5.837	5.660	6.305	6.128
1048.02	6.196	**6.019**	5.842	6.487	6.310
1178.26	**7.021**	6.843	6.666	7.312	7.135
1337.28	**8.027**	7.850	7.673	8.318	8.141

Table 21. MALDI-TOF MS results for the product of the polymerisation of diethyl 3-hydroxyglutarate at 100°C for 270 minutes in the presence of 2.5wt% $Ti(OBu)_4$ for explanation see text page 98.

lmh110	Na+	BuO	2xBuO	3xBuO	Cycl	Dehyd
Peak mass						
758.31	4.363	4.186	**4.008**	3.831	4.654	4.477
786.34	4.540	4.363	4.186	**4.008**	4.831	4.654
859.77	**5.005**	4.828	4.650	4.473	5.296	5.119
870.45	5.072	4.895	4.718	4.541	5.364	5.186
889.15	5.191	**5.014**	4.836	4.659	5.482	5.305
898.49	5.250	5.073	4.896	4.718	5.541	5.364
915.85	5.360	5.183	**5.005**	4.828	5.651	5.474
943.88	5.537	5.360	5.183	**5.006**	5.828	5.651
971.92	5.715	5.527	5.360	5.183	**6.006**	5.829
1018.65	**6.010**	5.833	5.656	5.479	6.302	6.124
1045.35	6.179	**6.002**	5.825	5.648	6.471	6.293
1074.72	6.365	6.188	**6.011**	5.834	6.656	6.479
1102.76	6.543	6.366	6.188	**6.011**	6.834	6.657
1130.8	6.720	6.543	6.366	6.189	**7.011**	6.834
1204.23	7.185	**7.008**	6.831	6.653	7.476	7.299
1232.26	7.362	7.185	**7.008**	6.831	7.654	7.476
1260.3	7.540	7.363	7.185	**7.008**	7.831	7.654
1288.34	7.717	7.540	7.363	7.186	**8.008**	7.831
1361.77	8.182	**8.005**	7.828	7.650	8.473	8.296
1391.14	8.368	8.191	**8.014**	7.836	8.659	8.482
1417.84	8.537	8.360	8.183	**8.005**	8.828	8.651
1447.21	8.723	8.546	8.368	8.191	**9.014**	8.837
1576.72	9.543	9.365	9.188	**9.011**	9.834	9.656
1735.59	10.548	10.371	10.194	**10.016**	10.839	10.662

Table 22. MALDI-TOF MS results for the product of the polymerisation of diethyl 3-hydroxyglutarate at 100°C for 270 minutes in the presence of 25wt% $Ti(OBu)_4$ for explanation see text page 99.

	Na+	BuO	2xBuO	Cycl.	Dehyd.
Peak mass	n	n	n	n	n
348	1.77	1.59	1.41	**2.06**	1.88
355	1.81	1.63	1.45	2.10	1.92
400	2.09	1.92	1.73	2.39	2.21
415	2.19	**2.01**	1.83	2.48	2.30
471	2.54	2.37	2.18	2.84	2.66
506	2.77	2.59	2.41	**3.06**	2.88
544	**3.01**	2.83	2.65	3.30	3.12
607	3.41	3.23	**3.04**	3.70	3.52
638	3.60	3.42	3.24	3.89	3.72
645	3.65	3.47	3.28	**3.94**	3.76
702	**4.01**	3.83	3.65	4.30	4.12
731	4.19	**4.01**	3.83	4.48	4.30
794	4.59	4.41	4.23	4.88	4.70
809	4.68	4.51	4.32	**4.97**	4.80
860	**5.01**	4.83	4.65	5.29	5.12
882	5.15	**4.97**	4.78	5.44	5.26
942	5.53	5.35	5.16	5.82	5.64
964	5.66	5.49	5.30	**5.96**	5.78
986	5.80	5.63	5.44	6.09	5.92
1015	**5.99**	5.81	5.63	6.28	6.10
1038	6.13	**5.96**	5.77	6.42	6.25
1071	6.34	6.16	**5.98**	6.63	6.46
1115	6.62	6.44	6.26	6.91	6.73
1176	**7.01**	6.83	6.65	7.30	7.12
1202	7.17	**6.99**	6.61	7.46	7.28
1334	**8.01**	7.83	7.65	8.30	8.12
1359	8.16	**7.99**	7.80	8.46	8.28
1493	**9.01**	8.84	8.65	9.30	9.13
1522	9.20	**9.02**	8.84	9.49	9.31
1545	9.34	9.16	**8.98**	9.63	9.46
1653	**10.03**	9.85	9.66	10.32	10.14
1675	10.16	**9.99**	9.80	10.46	10.28
1697	10.30	10.13	**9.94**	10.59	10.42
1808	**11.06**	10.83	10.65	11.30	11.12
1833	11.16	**10.99**	10.80	11.46	11.28
1855	11.30	11.13	**10.94**	11.59	11.42
1969	**12.03**	11.85	11.66	12.32	12.14
1995	12.19	**12.01**	11.83	12.48	12.30
2017	12.33	12.15	**11.97**	12.62	12.44
2046	12.51	12.34	12.15	12.80	12.63
2125	**13.01**	12.84	12.65	13.30	13.13
2148	13.16	**12.98**	12.80	13.45	13.27
2171	13.30	13.13	**12.94**	13.59	13.42
2200	13.49	13.31	13.13	13.78	13.60
2286	**14.03**	13.85	13.67	14.32	14.15
2309	14.18	**14.00**	13.82	14.47	14.29
2334	14.36	14.16	**13.97**	14.63	14.45
2357	14.48	14.30	14.12	14.77	14.59
2442	**15.02**	14.84	14.66	15.44	15.13
2465	15.16	**14.99**	14.80	15.46	15.28
2487	15.30	15.13	**14.94**	15.59	15.42

2603	**16.04**	15.86	15.68	16.33	16.15
2626	16.18	**16.00**	15.82	16.47	16.30
2649	16.33	16.15	**15.97**	16.62	16.44
2758	**17.02**	16.84	16.66	17.31	17.13
2786	17.20	**17.02**	16.84	17.49	17.31
2809	17.34	17.16	**16.98**	17.63	17.46
2915	**18.01**	17.84	17.65	18.30	18.13
2937	18.15	**17.97**	17.79	18.44	18.27
2962	18.31	18.13	**17.95**	18.60	18.56
3028	18.73	18.55	18.37	**19.02**	18.84
3079	**19.05**	18.87	18.69	19.34	19.16
3238	**20.06**	19.88	19.70	20.35	20.17
3261	20.20	**20.03**	19.84	20.49	20.32
3391	**21.03**	20.85	20.66	21.32	21.14

All the values in bold print are within +/- 0.06 of the nearest integer.

Table 23. MALDI-TOF MS results for the product of the polymerisation of diethyl 3-hydroxyglutarate at 100°C for 210 minutes in the presence of 5wt% $Ti(OBu)_4$ for explanation see text page 104.

lmh311#2	Na+	Cycl.	Dehyd.
Peak mass			
344.05	1.741	**2.032**	1.855
353.9	1.803	2.094	1.917
359.44	1.838	2.129	**1.952**
381.61	**1.979**	2.270	2.092
496.76	2.707	**2.998**	2.821
519.55	2.852	3.143	**2.966**
538.63	**2.972**	3.263	3.086
616.84	3.467	3.758	3.581
632.23	3.565	3.856	3.679
644.55	3.643	3.934	3.757
659.33	3.736	**4.027**	3.850
672.88	3.822	4.113	3.936
685.19	3.900	4.191	**4.014**
698.12	**3.982**	4.273	4.096
728.3	4.173	4.464	4.287
754.16	4.336	4.628	4.450
768.94	4.430	4.721	4.544
781.25	4.508	4.799	4.622
804.04	4.652	4.943	4.766

Table 24. MALDI-TOF MS results for the product of the enzymatic polymerisation of diethyl 3-hydroxyglutarate

Appendix 3

Analytical data for Chapter 5

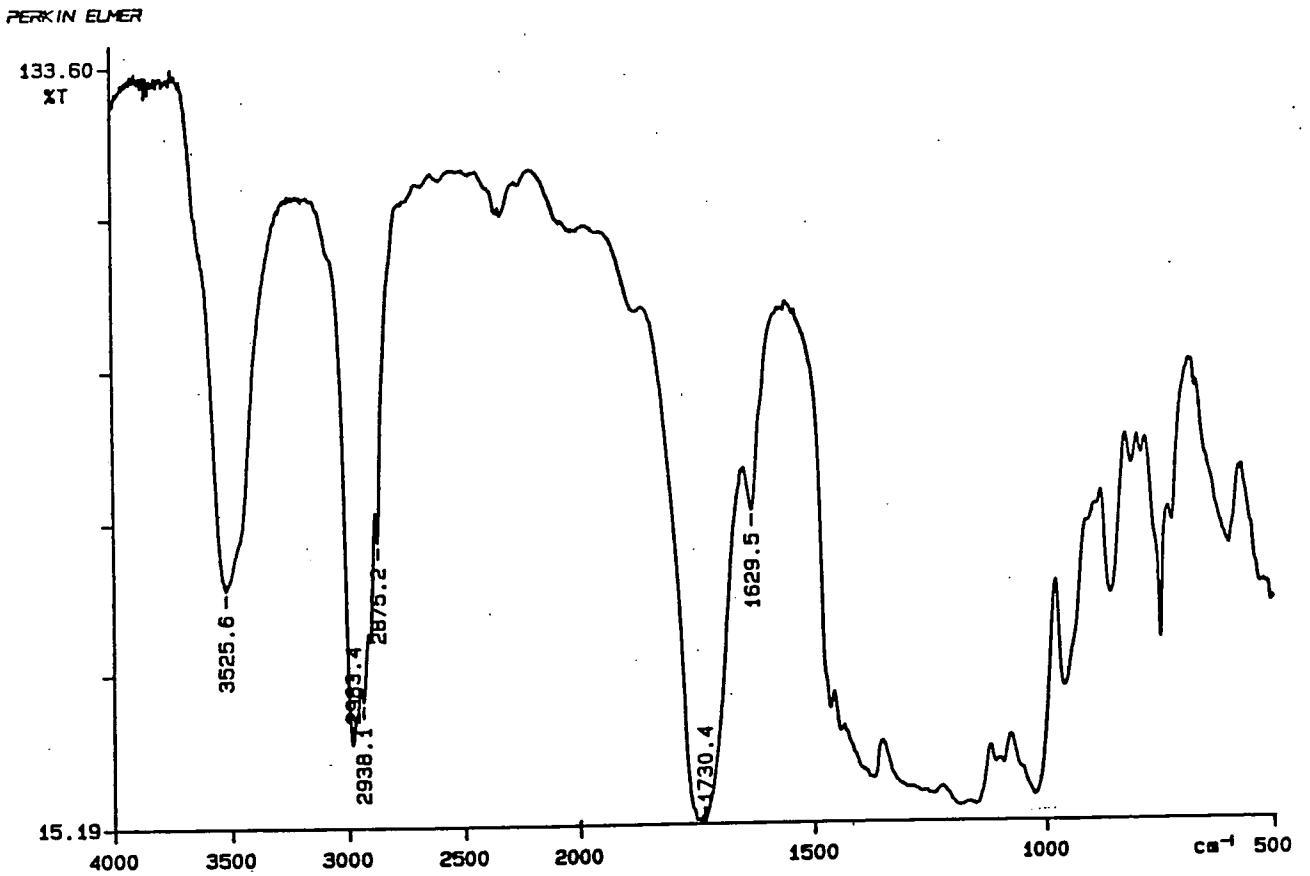

Appendix 3.1 FTIR spectrum of trimethyl 1,3,5-benzenetricarboxylate core terminated poly(diethyl 3-hydroxyglutarate), ratio core:monomer = 1:25

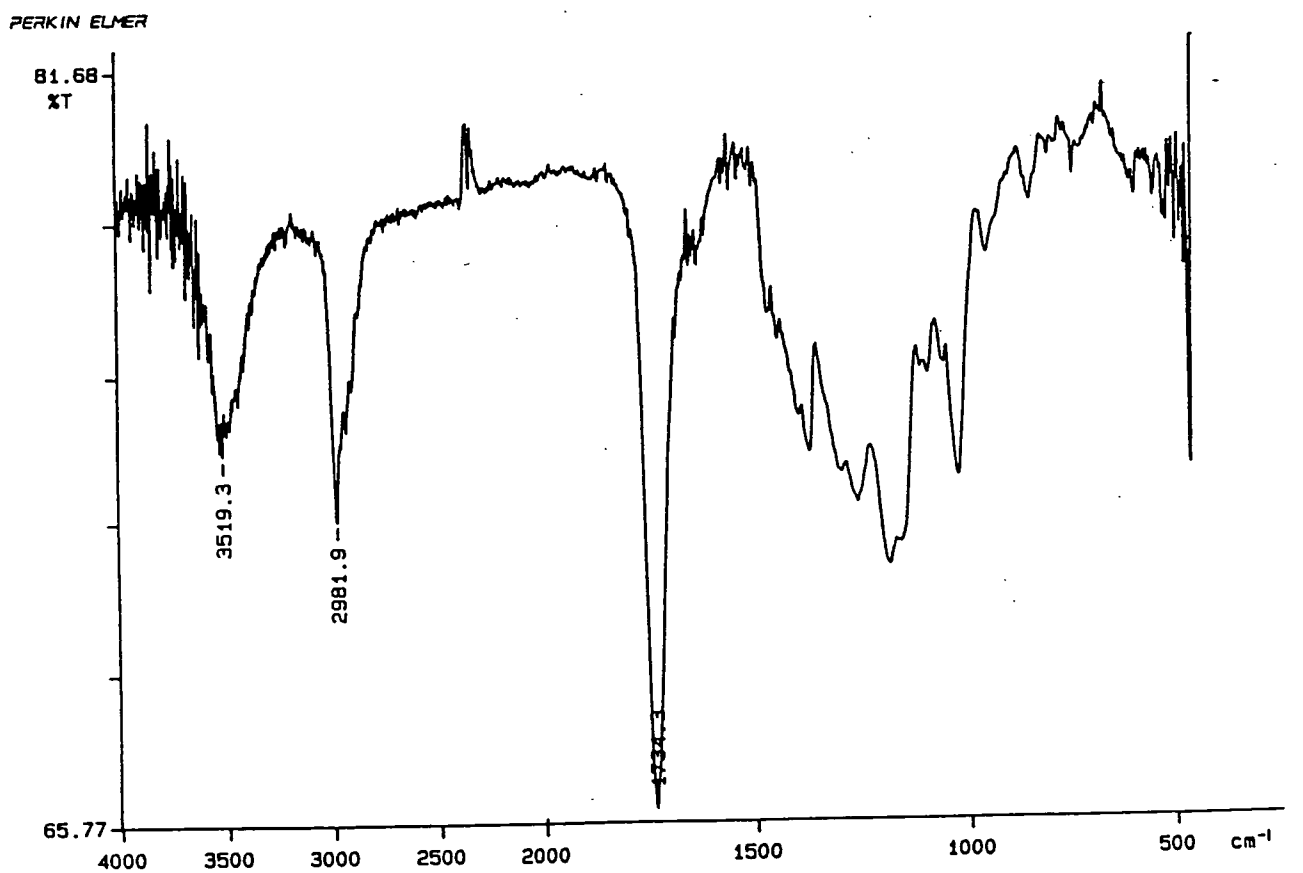

Appendix 3.2 FTIR spectrum of trimethyl 1,3,5-benzenetricarboxylate core terminated poly(diethyl 3-hydroxyglutarate), ratio core:monomer = 1:50

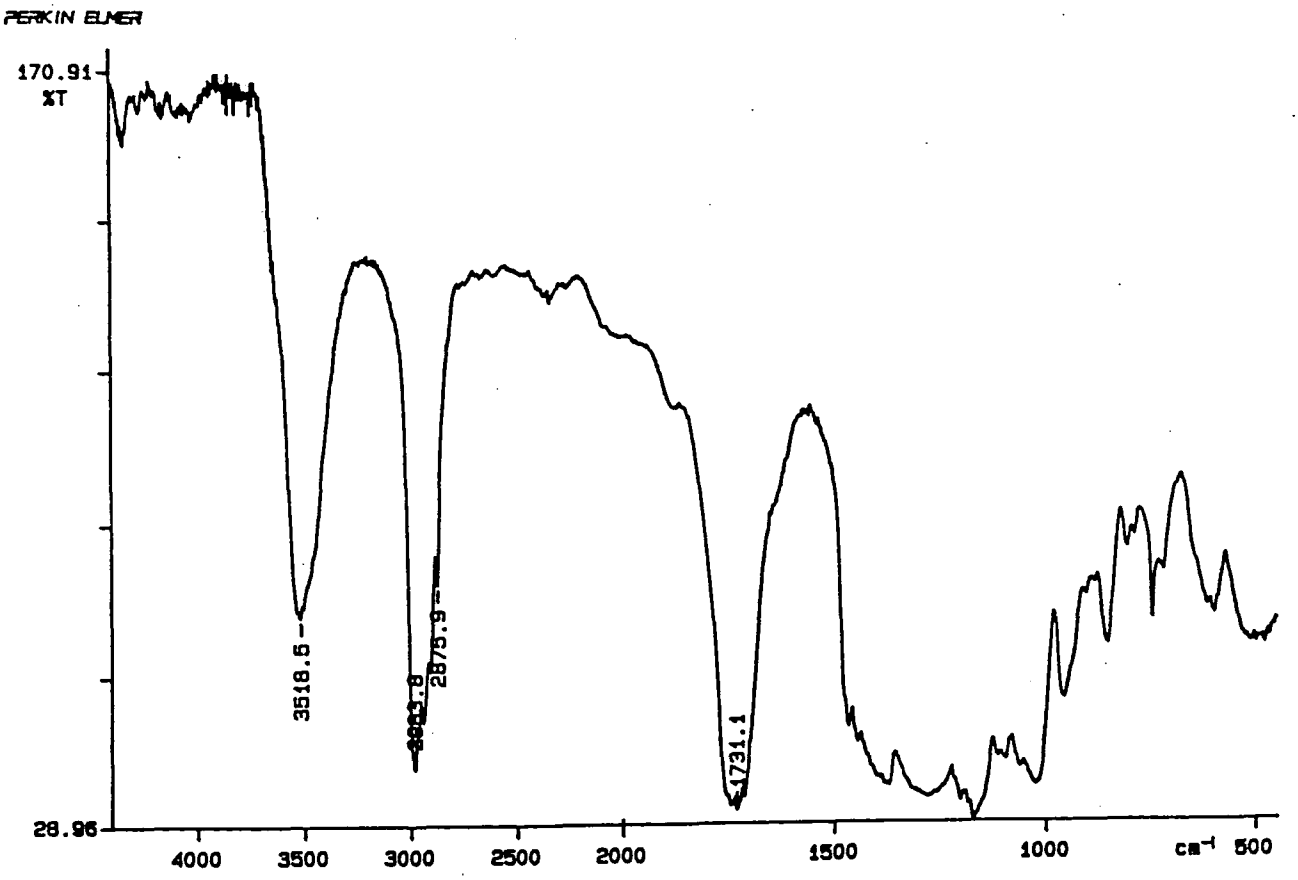

Appendix 3.3 FTIR spectrum of trimethyl 1,3,5-benzenetricarboxylate core terminated poly(diethyl 3-hydroxyglutarate), ratio core:monomer = 1:50

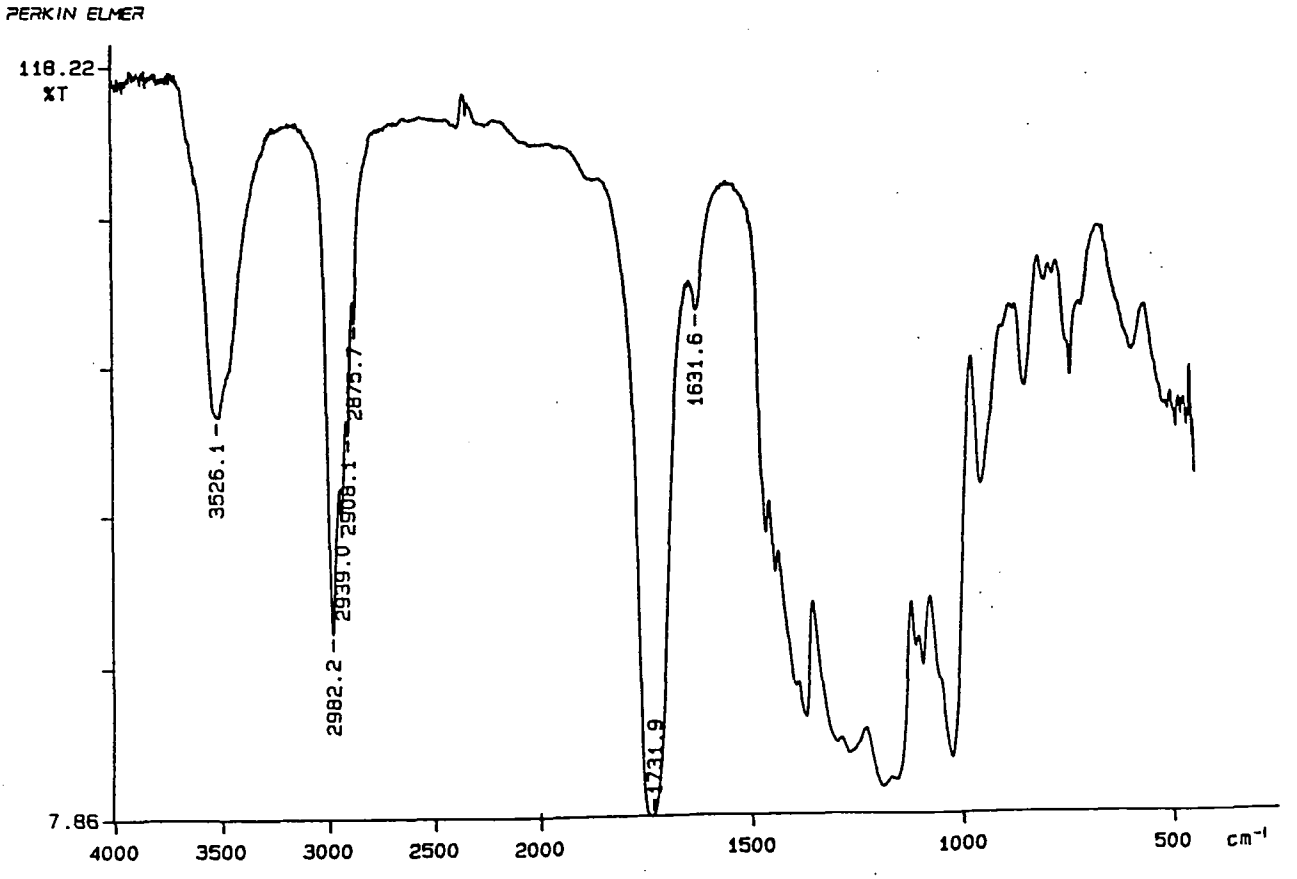

Appendix 3.4 FTIR spectrum of trimethyl 1,3,5-benzenetricarboxylate core terminated poly(diethyl 3-hydroxyglutarate), ratio core:monomer = 1:75

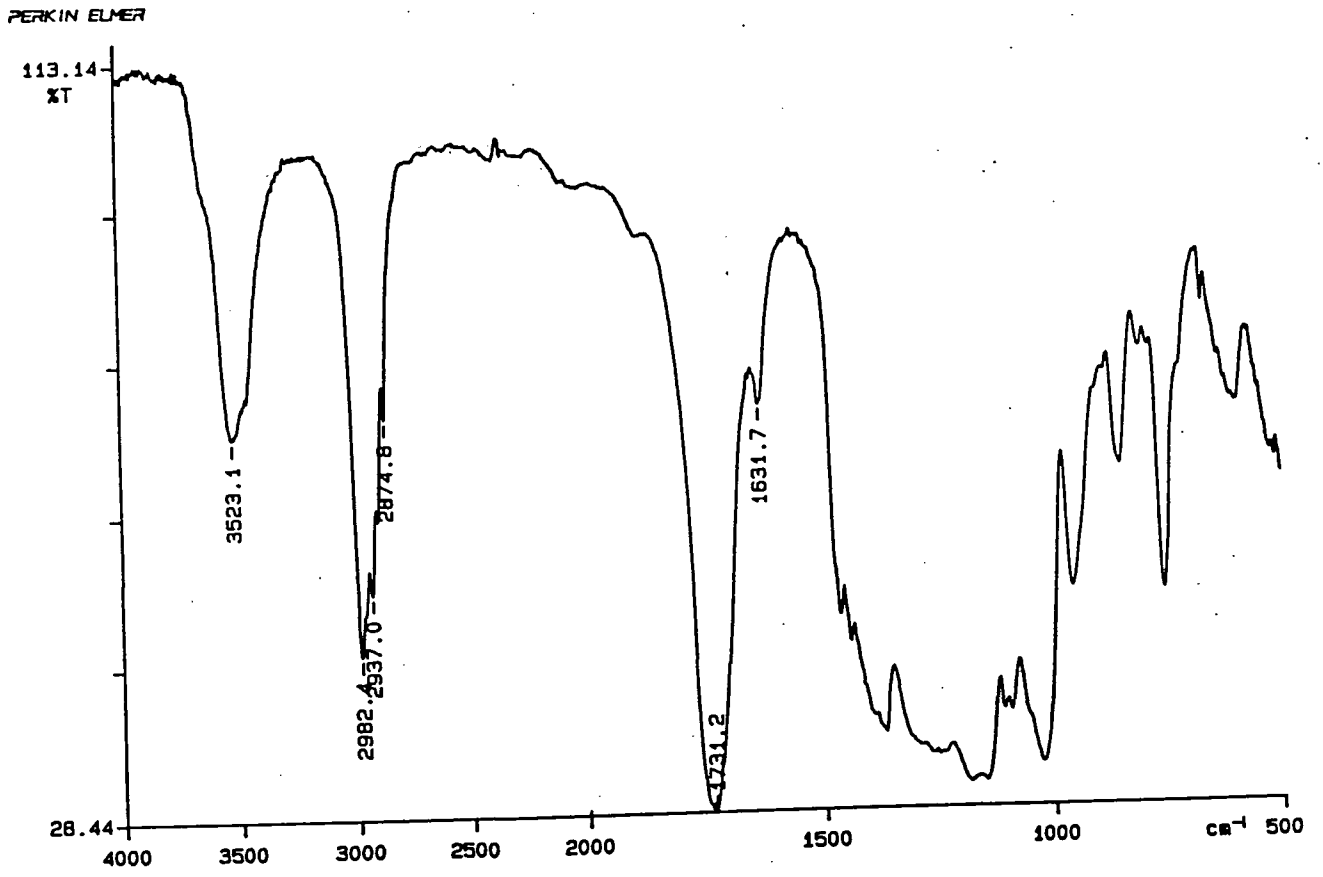

Appendix 3.5 FTIR spectrum of trimethyl 1,3,5-benzenetricarboxylate core terminated poly(diethyl 3-hydroxyglutarate), ratio core:monomer = 1:90

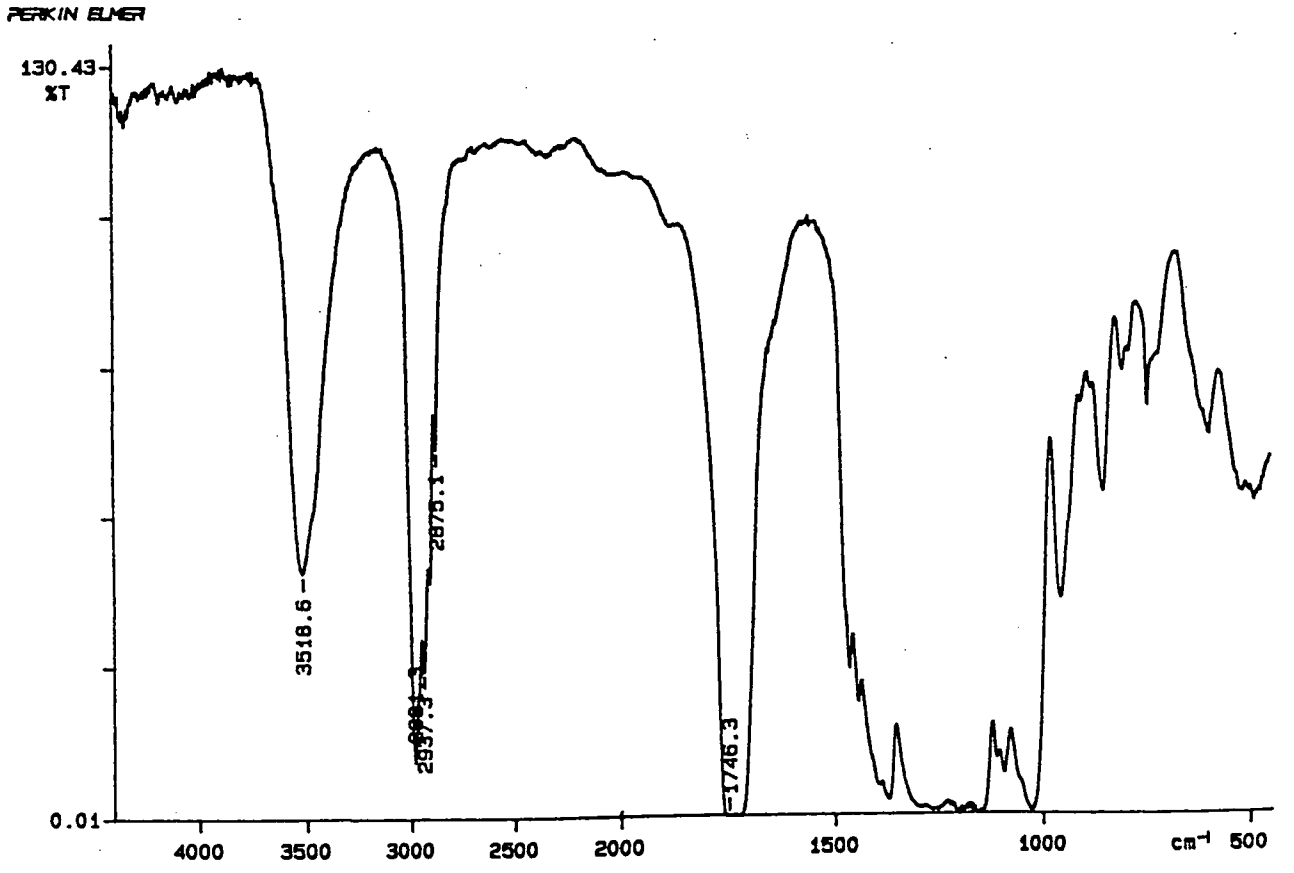

Appendix 3.6 FTIR spectrum of trimethyl 1,3,5-benzenetricarboxylate core terminated poly(diethyl 3-hydroxyglutarate), ratio core:monomer = 1:90

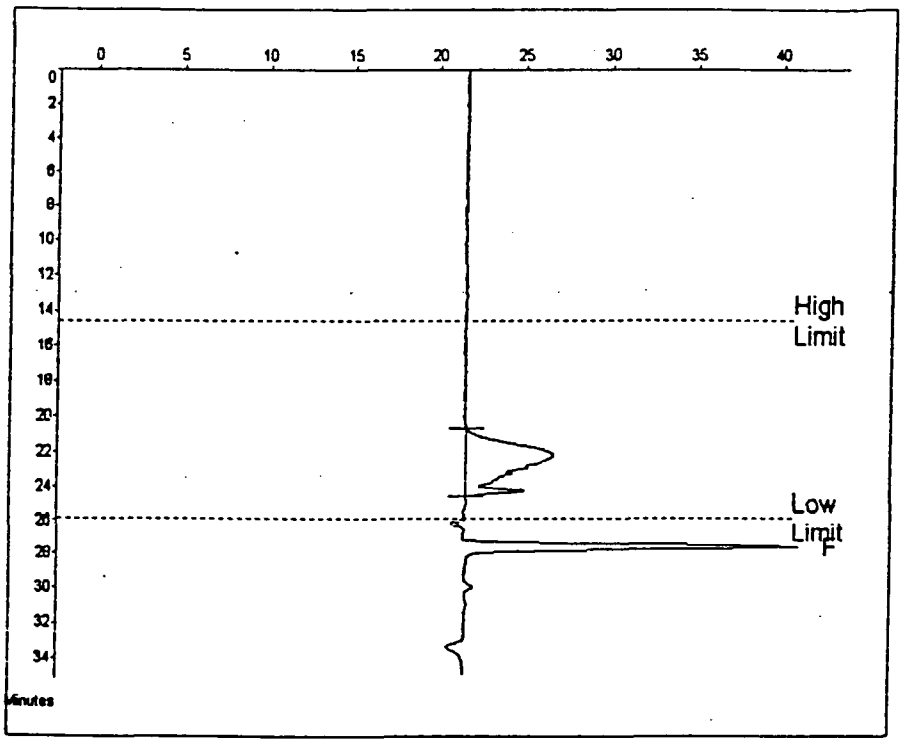

Molecular Weight Averages

Mp =	1465	Mz =	1597
Mn =	919	Mz+1 =	1911
Mw =	1250	Mv =	1199
Polydispersity =	1.360	Peak Area =	122882

Appendix 3.7 $CHCl_3$ GPC trace of trimethyl 1,3,5-benzenetricarboxylate core terminated poly(diethyl 3-hydroxyglutarate), ratio core:monomer = 1:25

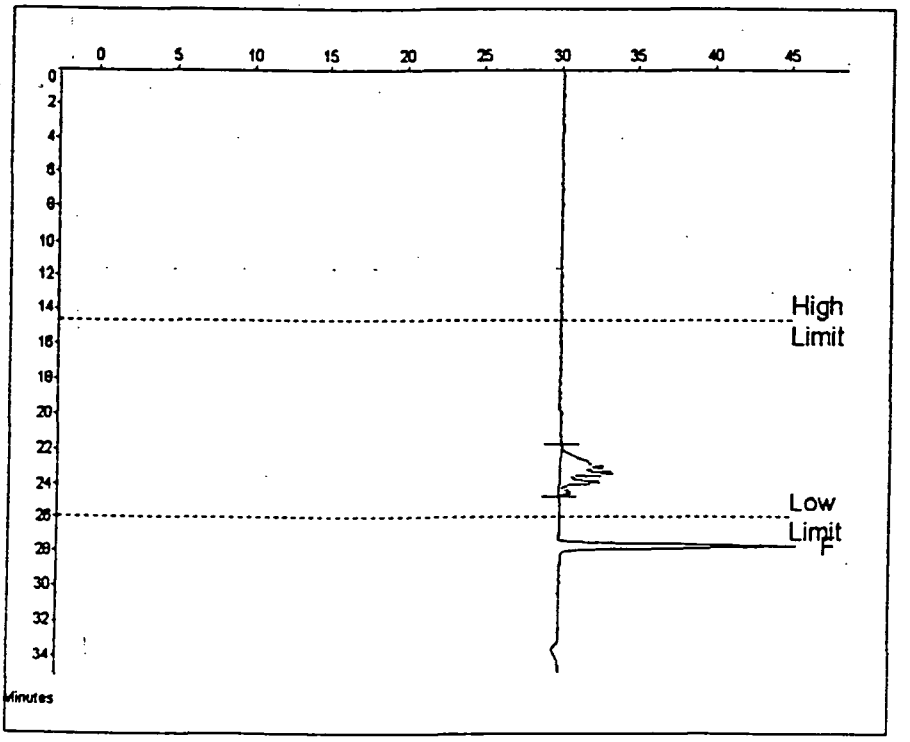

Molecular Weight Averages

Mp =	733	Mz =	910
Mn =	712	Mz+1 =	1014
Mw =	808	Mv =	793
Polydispersity =	1.134	Peak Area =	43734

Appendix 3.8 $CHCl_3$ GPC trace of trimethyl 1,3,5-benzenetricarboxylate core terminated poly(diethyl 3-hydroxyglutarate), ratio core:monomer = 1:50

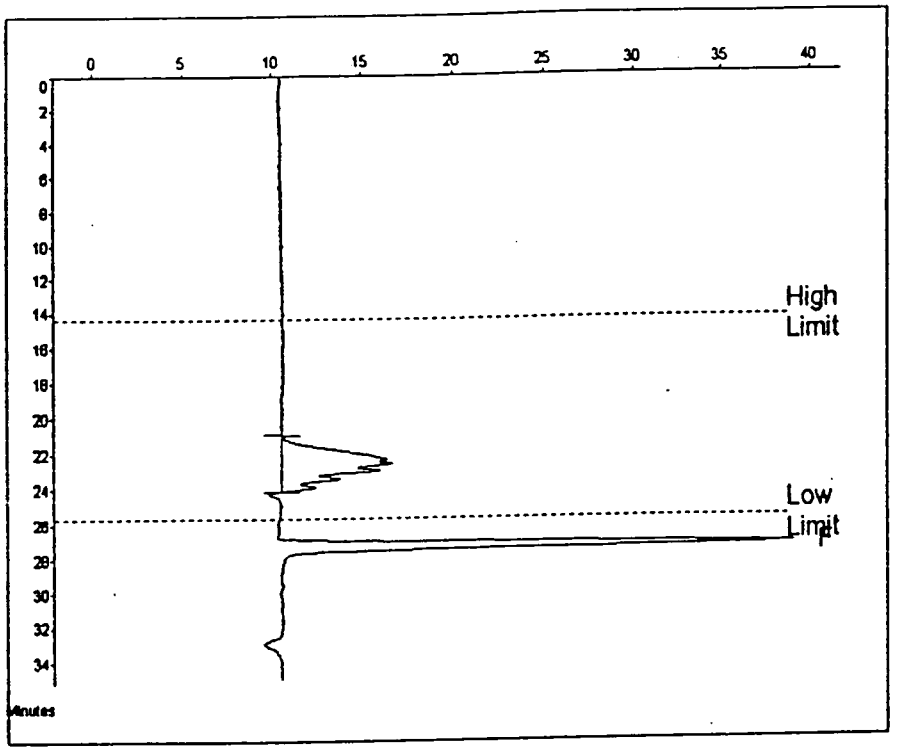

Molecular Weight Averages

Mp =	1008	Mz =	1255
Mn =	904	Mz+1 =	1440
Mw =	1072	Mv =	1046
Polydispersity =	1.187	Peak Area =	114059

Appendix 3.9 $CHCl_3$ GPC trace of trimethyl 1,3,5-benzenetricarboxylate core terminated poly(diethyl 3-hydroxyglutarate), ratio core:monomer = 1:50

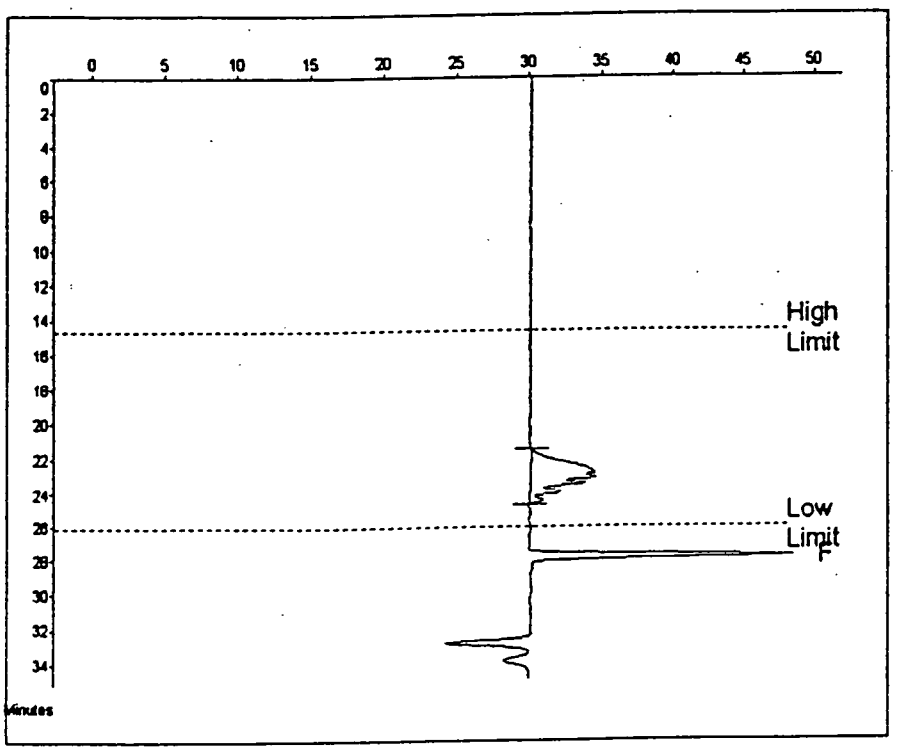

Molecular Weight Averages

Mp =	902	Mz =	1159
Mn =	865	Mz+1 =	1318
Mw =	1016	Mv =	993
Polydispersity =	1.174	Peak Area =	80869

Appendix 3.10 $CHCl_3$ GPC trace of trimethyl 1,3,5-benzenetricarboxylate core terminated poly(diethyl 3-hydroxyglutarate), ratio core:monomer = 1:75

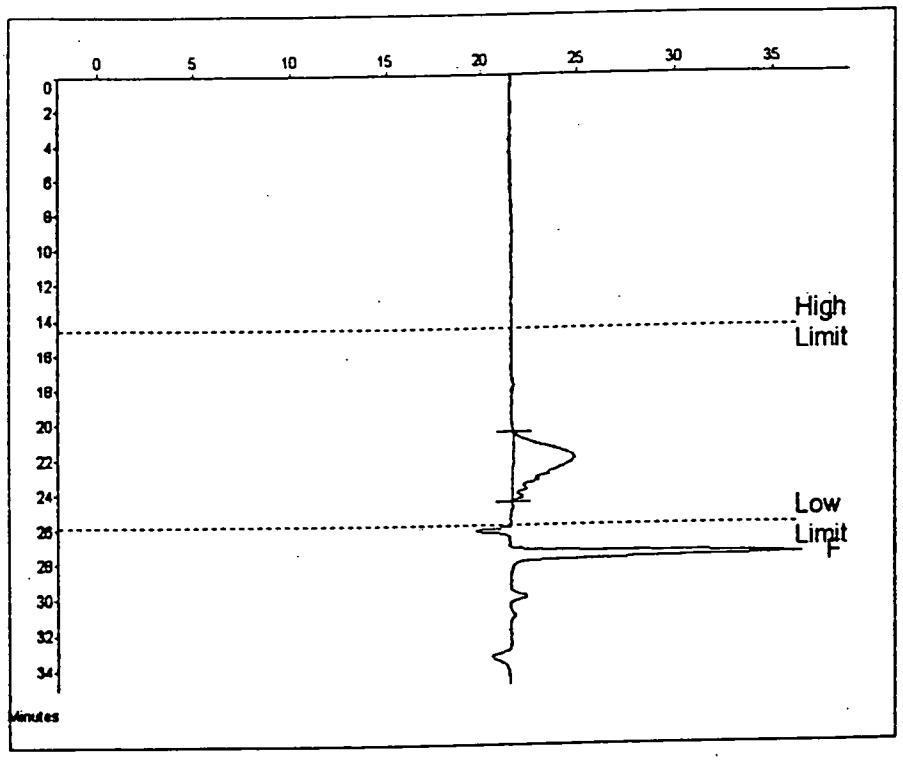

Molecular Weight Averages

Mp =	1623	Mz =	1870
Mn =	1151	Mz+1 =	2215
Mw =	1505	Mv =	1451
Polydispersity =	1.307	Peak Area =	71518

Appendix 3.11 $CHCl_3$ GPC trace of trimethyl 1,3,5-benzenetricarboxylate core terminated poly(diethyl 3-hydroxyglutarate), ratio core:monomer = 1:90

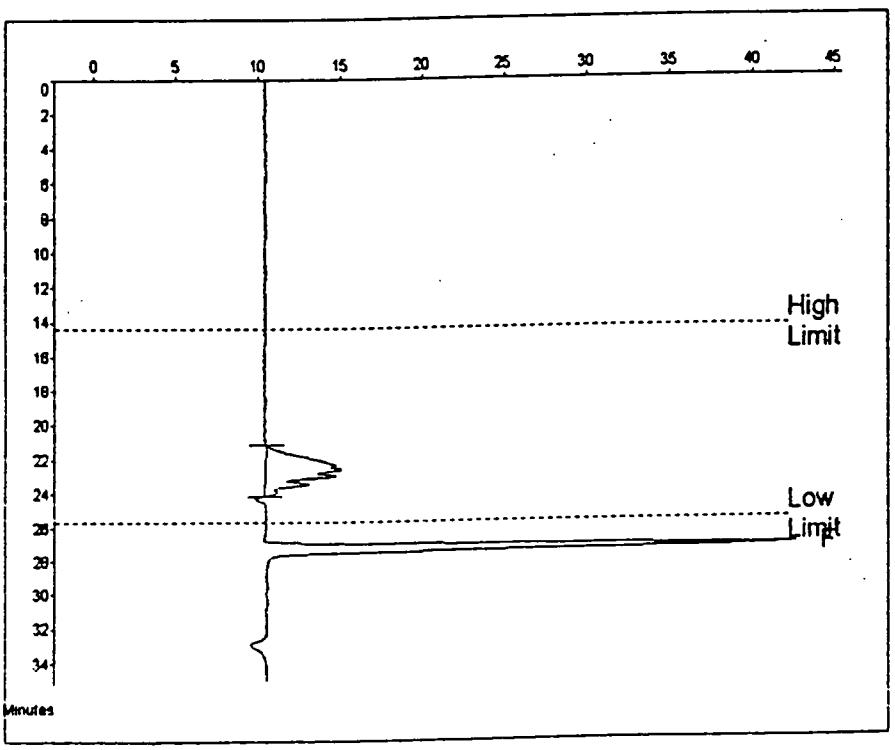

Molecular Weight Averages

Mp =	1006	Mz =	1235
Mn =	922	Mz+1 =	1388
Mw =	1072	Mv =	1049
Polydispersity =	1.163	Peak Area =	81993

Appendix 3.12 $CHCl_3$ GPC trace of trimethyl 1,3,5-benzenetricarboxylate core terminated poly(diethyl 3-hydroxyglutarate), ratio core:monomer = 1:90

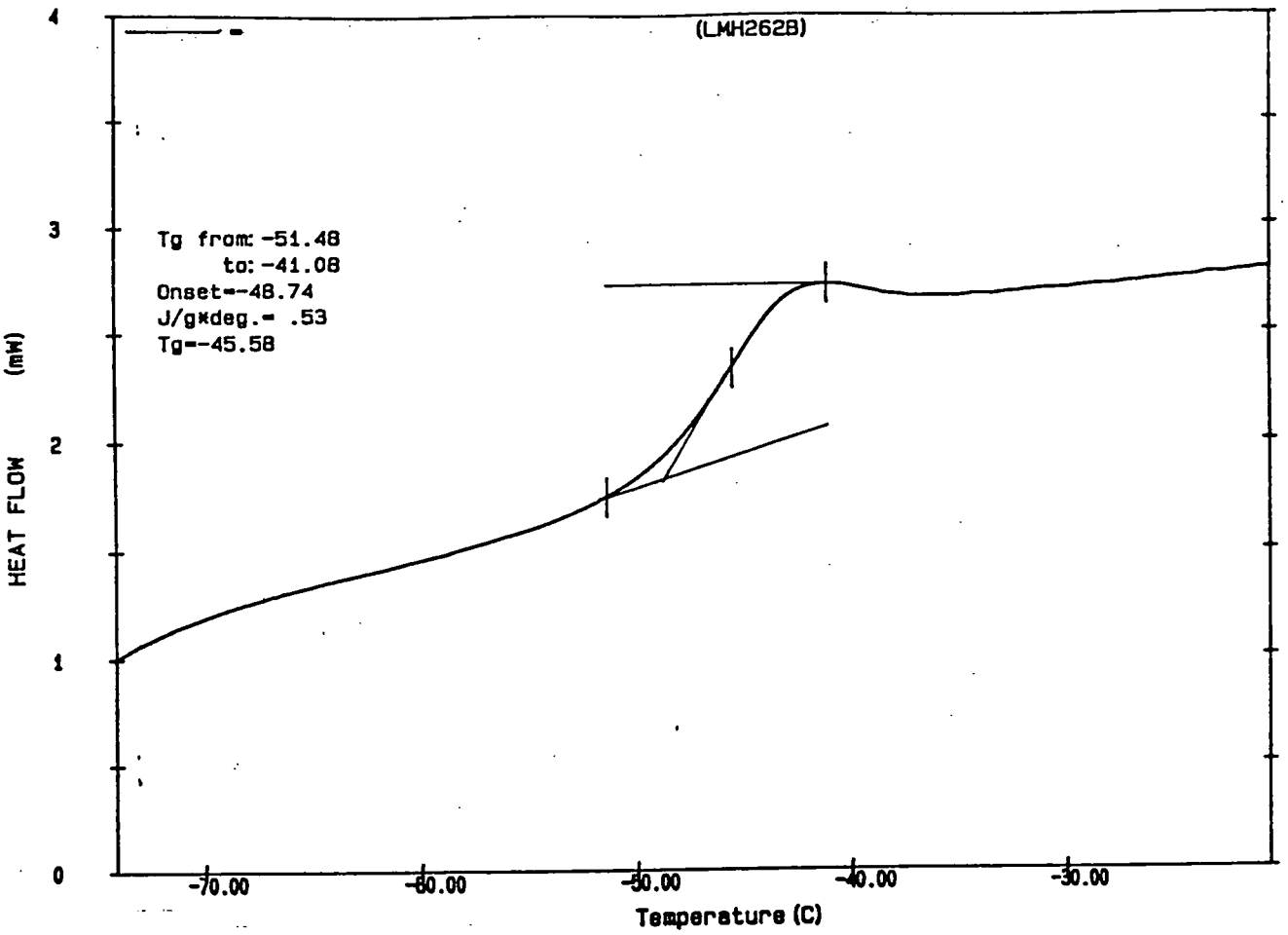

Appendix 3.13 DSC trace of trimethyl 1,3,5-benzenetricarboxylate core terminated poly(diethyl 3-hydroxyglutarate), ratio core:monomer = 1:25

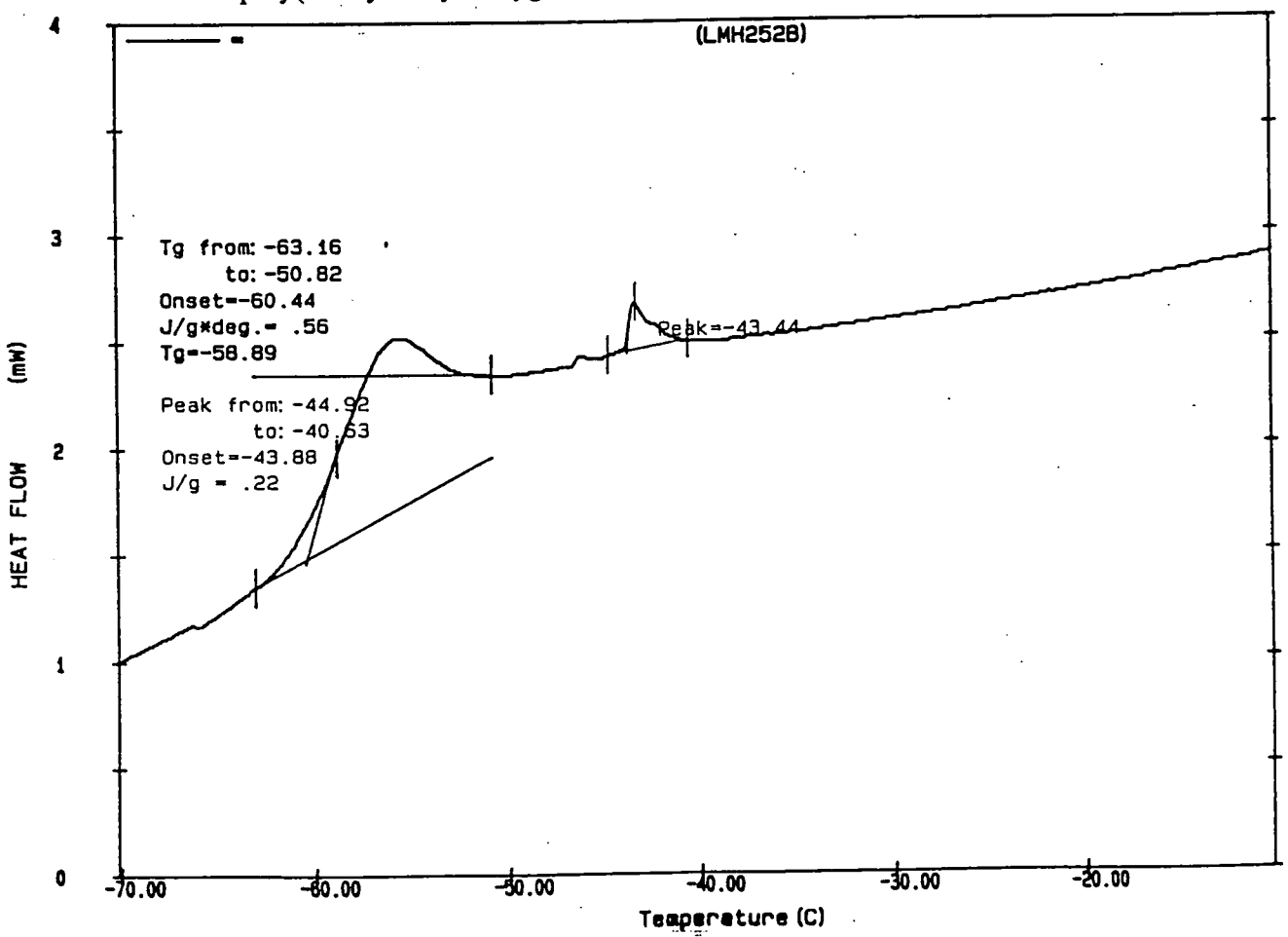

Appendix 3.14 DSC trace of trimethyl 1,3,5-benzenetricarboxylate core terminated poly(diethyl 3-hydroxyglutarate), ratio core:monomer = 1:50

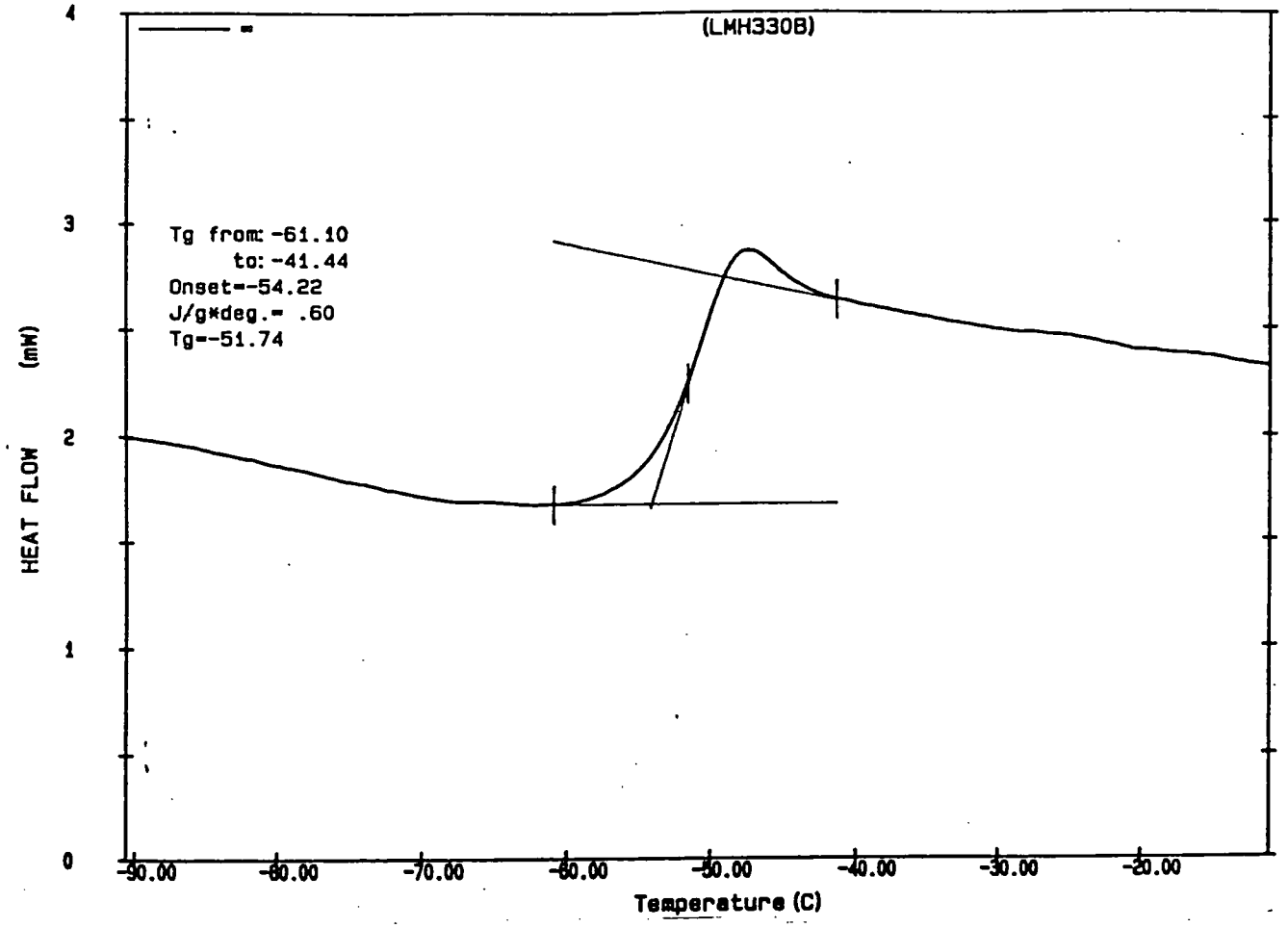

Appendix 3.15 DSC trace of trimethyl 1,3,5-benzenetricarboxylate core terminated poly(diethyl 3-hydroxyglutarate), ratio core:monomer = 1:50

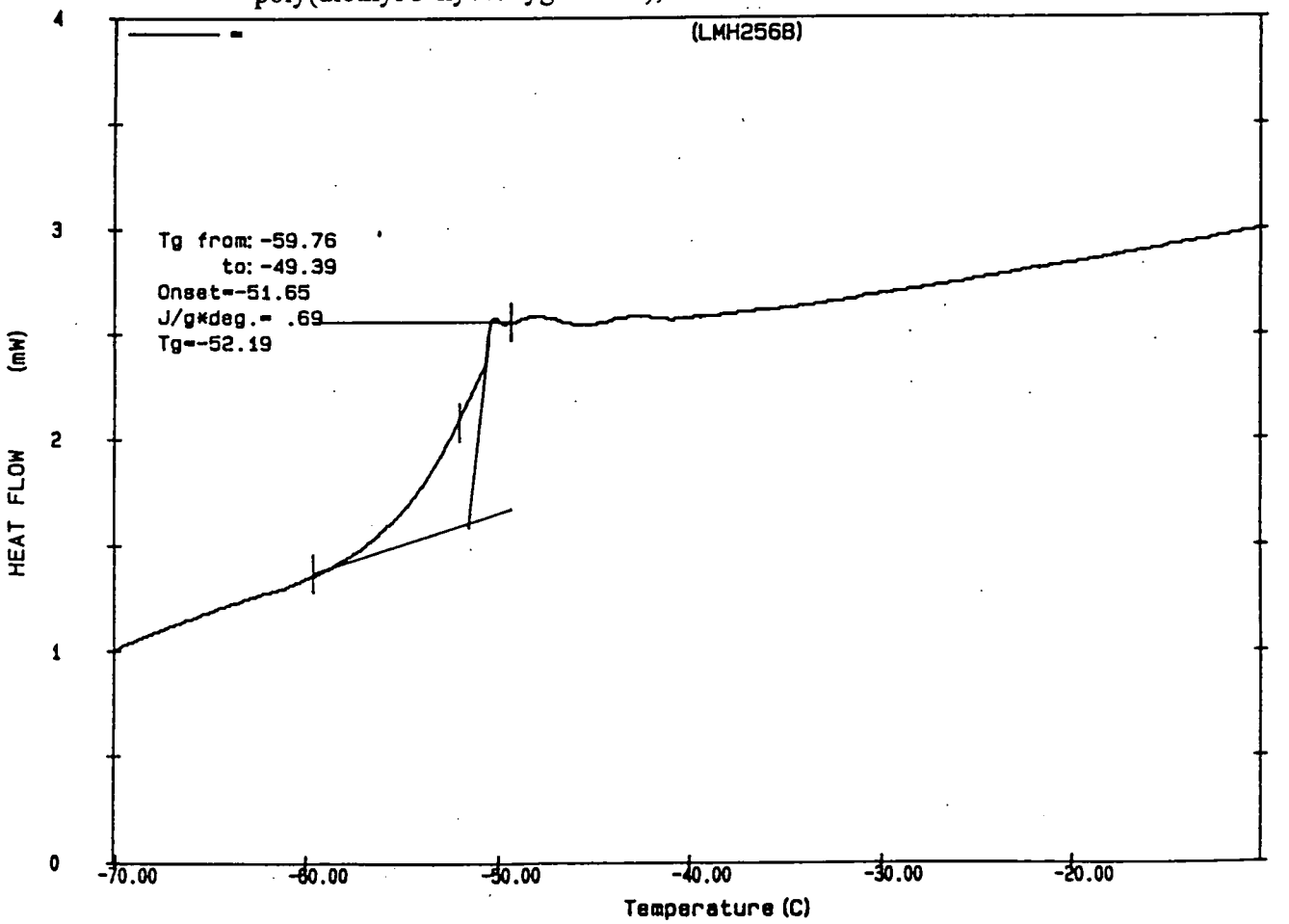

Appendix 3.16 DSC trace of trimethyl 1,3,5-benzenetricarboxylate core terminated poly(diethyl 3-hydroxyglutarate), ratio core:monomer = 1:75

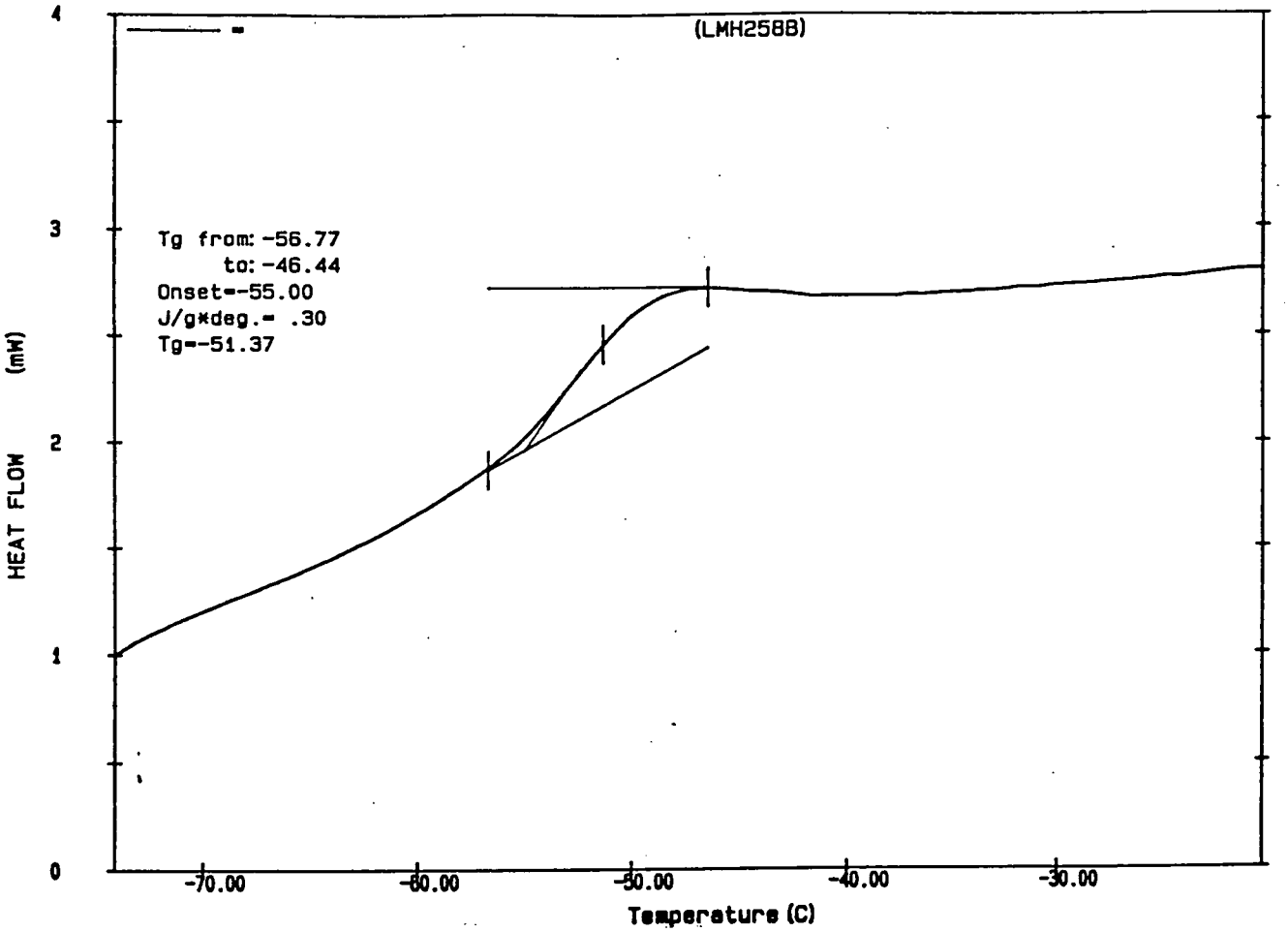

Appendix 3.17 DSC trace of trimethyl 1,3,5-benzenetricarboxylate core terminated poly(diethyl 3-hydroxyglutarate), ratio core:monomer = 1:90

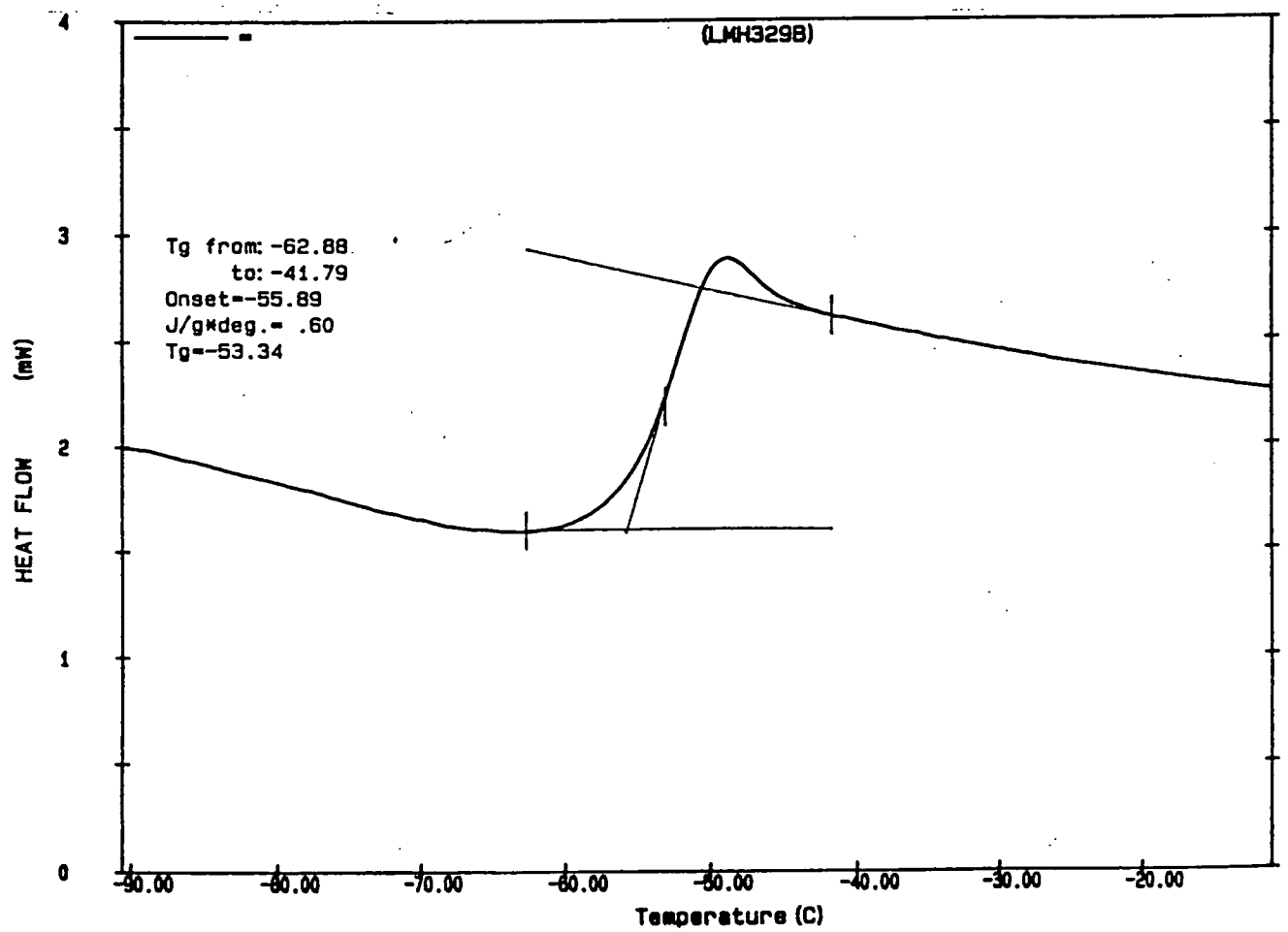

Appendix 3.18 DSC trace of trimethyl 1,3,5-benzenetricarboxylate core terminated poly(diethyl 3-hydroxyglutarate), ratio core:monomer = 1:90

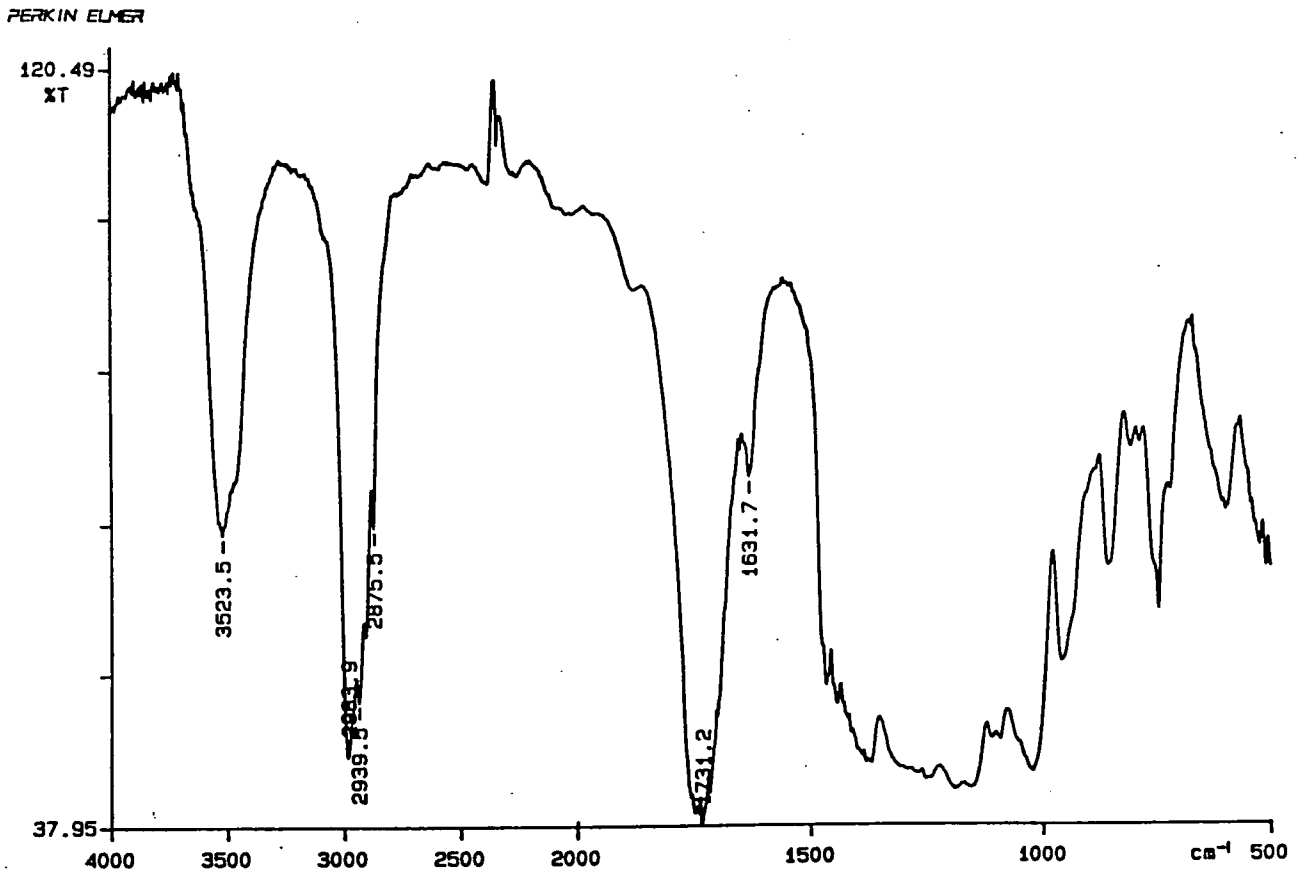

Appendix 3.19 FTIR spectrum of triethyl 1,3,5-benzenetricarboxylate core terminated poly(diethyl 3-hydroxyglutarate), ratio core:monomer = 1:25

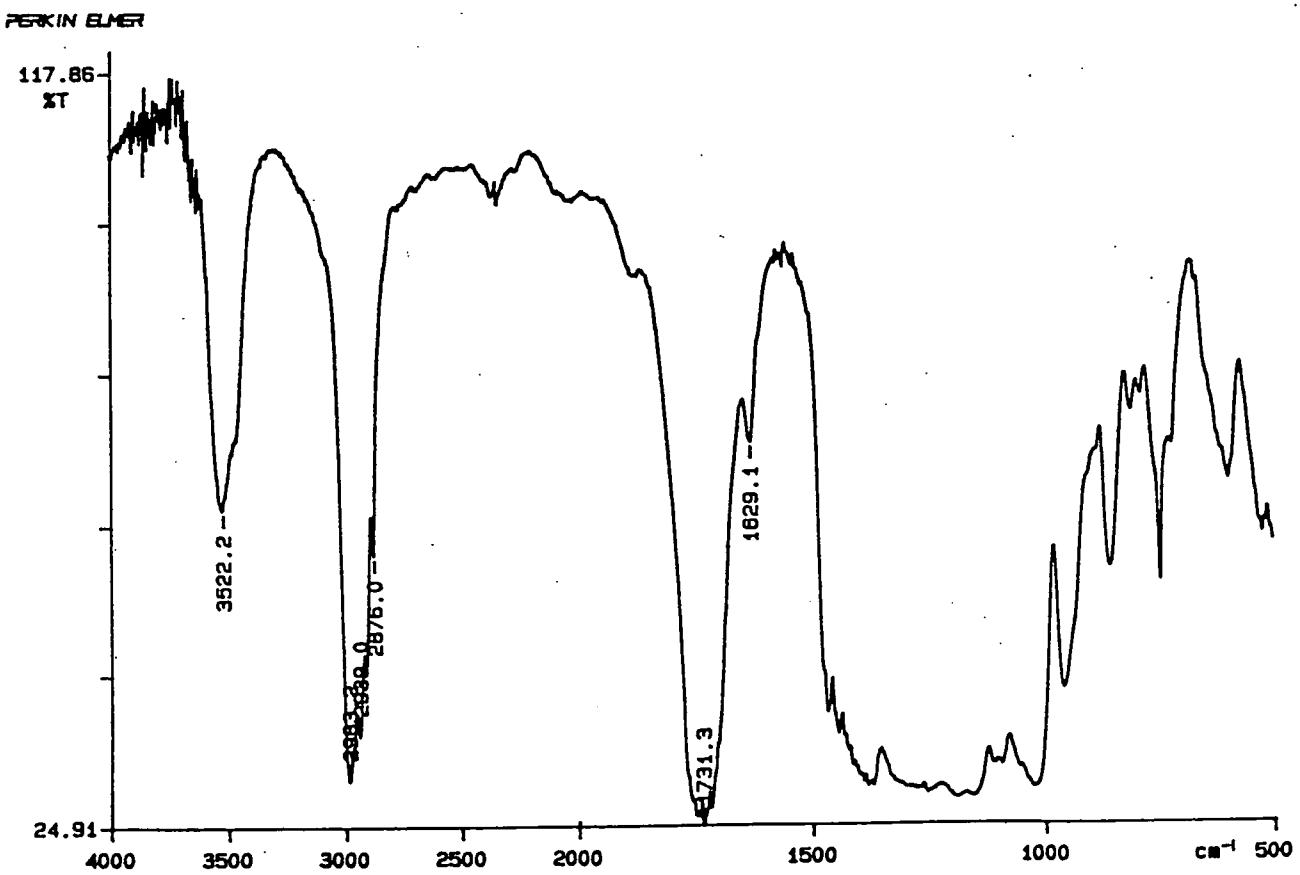

Appendix 3.20 FTIR spectrum of triethyl 1,3,5-benzenetricarboxylate core terminated poly(diethyl 3-hydroxyglutarate), ratio core:monomer = 1:50

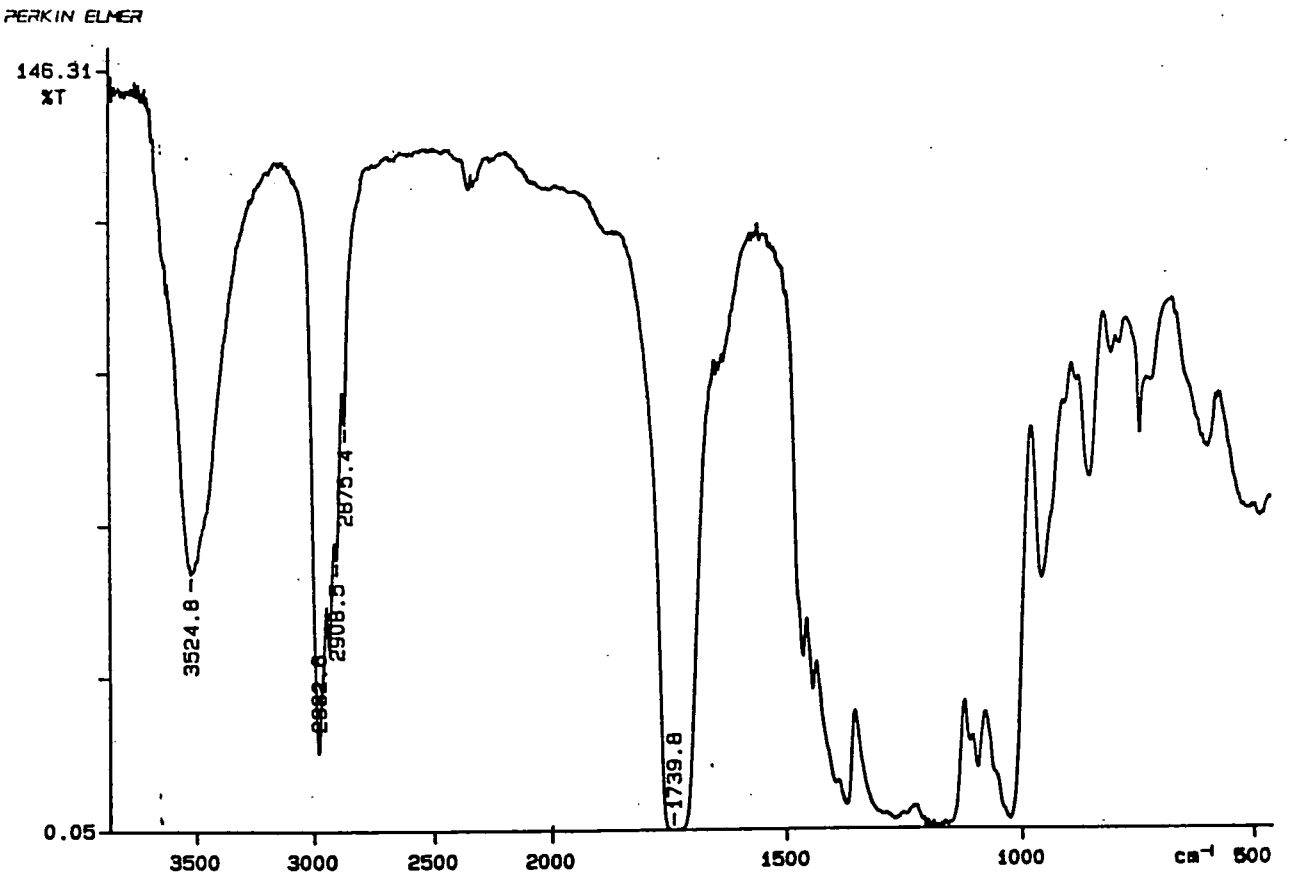

Appendix 3.21 FTIR spectrum of triethyl 1,3,5-benzenetricarboxylate core terminated poly(diethyl 3-hydroxyglutarate), ratio core:monomer = 1:50

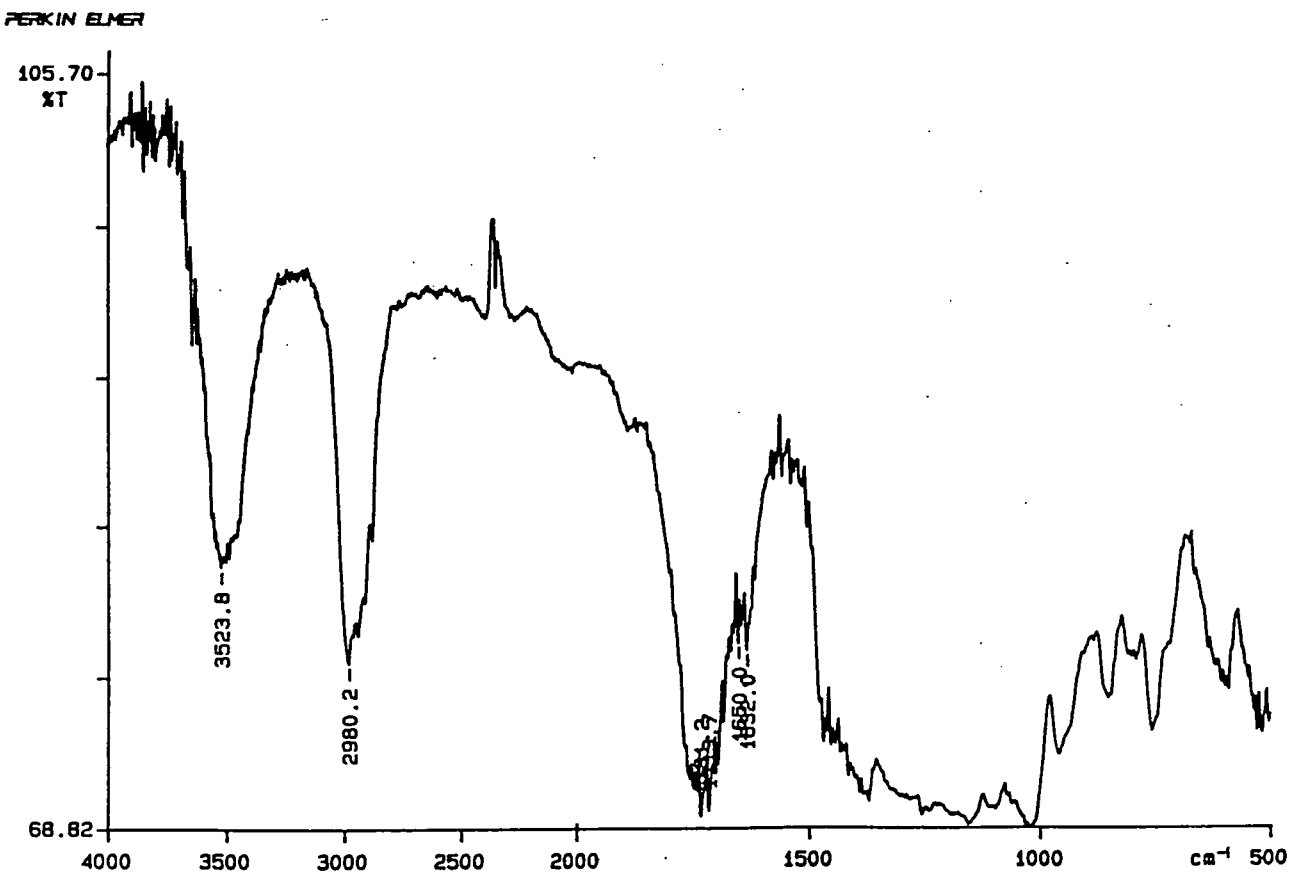

Appendix 3.22 FTIR spectrum of triethyl 1,3,5-benzenetricarboxylate core terminated poly(diethyl 3-hydroxyglutarate), ratio core:monomer = 1:75

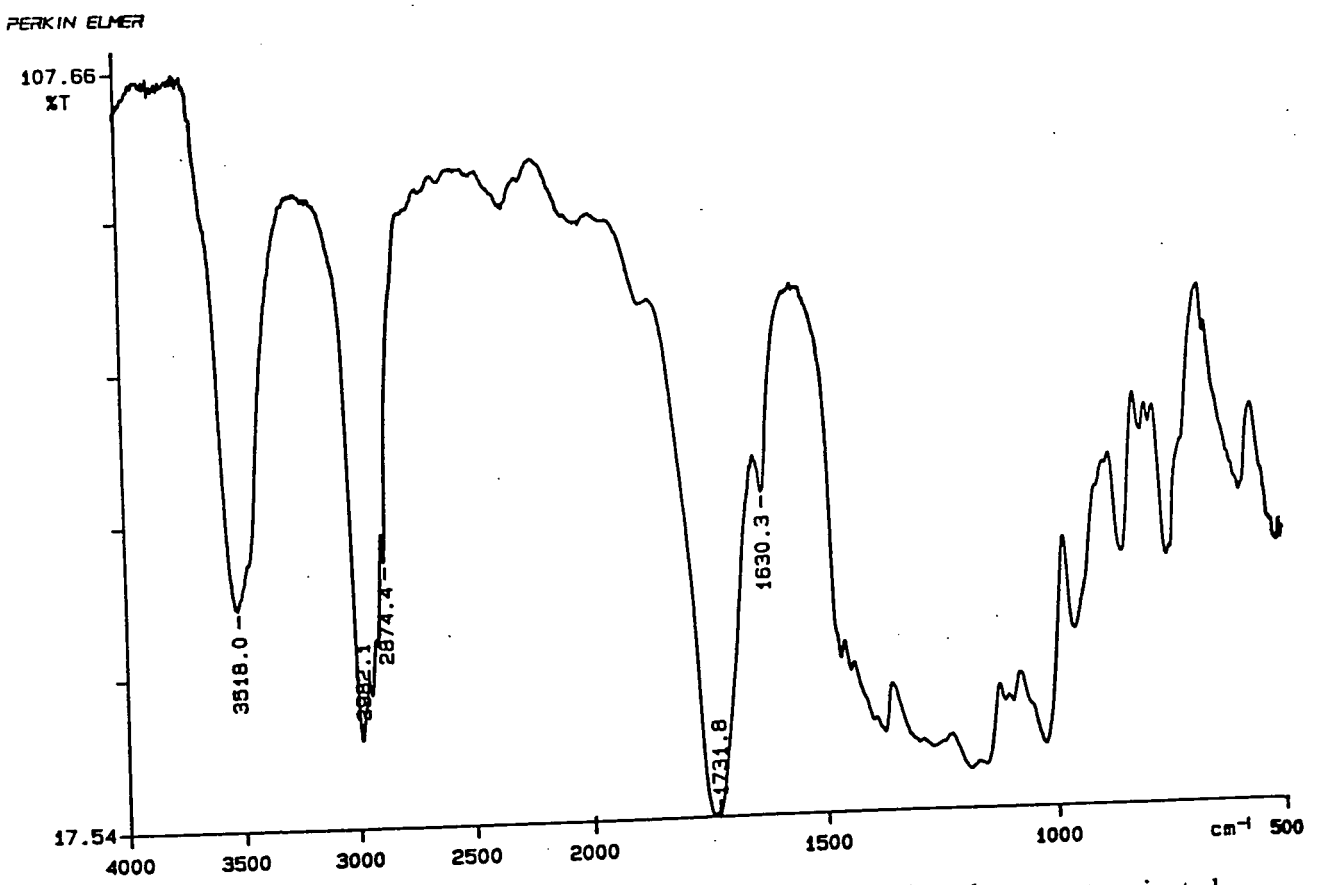

Appendix 3.23 FTIR spectrum of triethyl 1,3,5-benzenetricarboxylate core terminated poly(diethyl 3-hydroxyglutarate), ratio core:monomer = 1:90

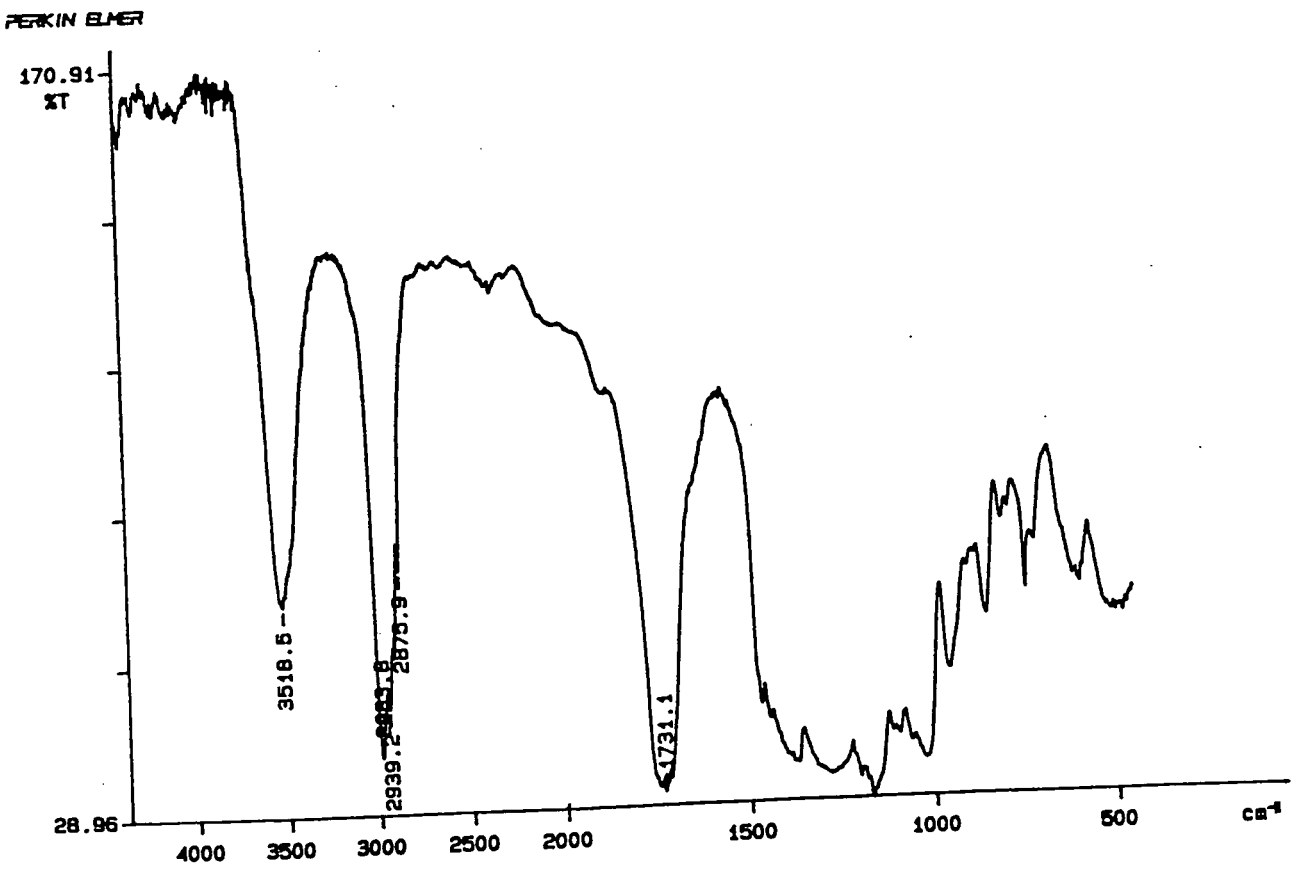

Appendix 3.24 FTIR spectrum of triethyl 1,3,5-benzenetricarboxylate core terminated poly(diethyl 3-hydroxyglutarate), ratio core:monomer = 1:90

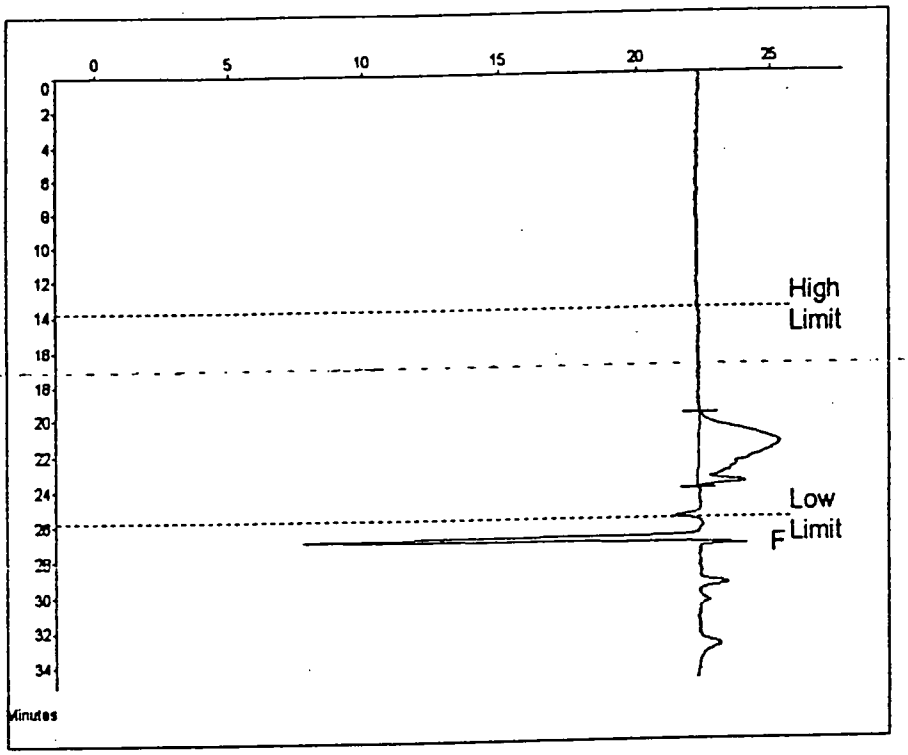

Molecular Weight Averages

Mp =	2073	Mz =	2435
Mn =	1279	Mz+1 =	3009
Mw =	1830	Mv =	1744
Polydispersity =	1.431	Peak Area =	76721

Appendix 3.25 $CHCl_3$ GPC trace of triethyl 1,3,5-benzenetricarboxylate core terminated poly(diethyl 3-hydroxyglutarate), ratio core:monomer = 1:25

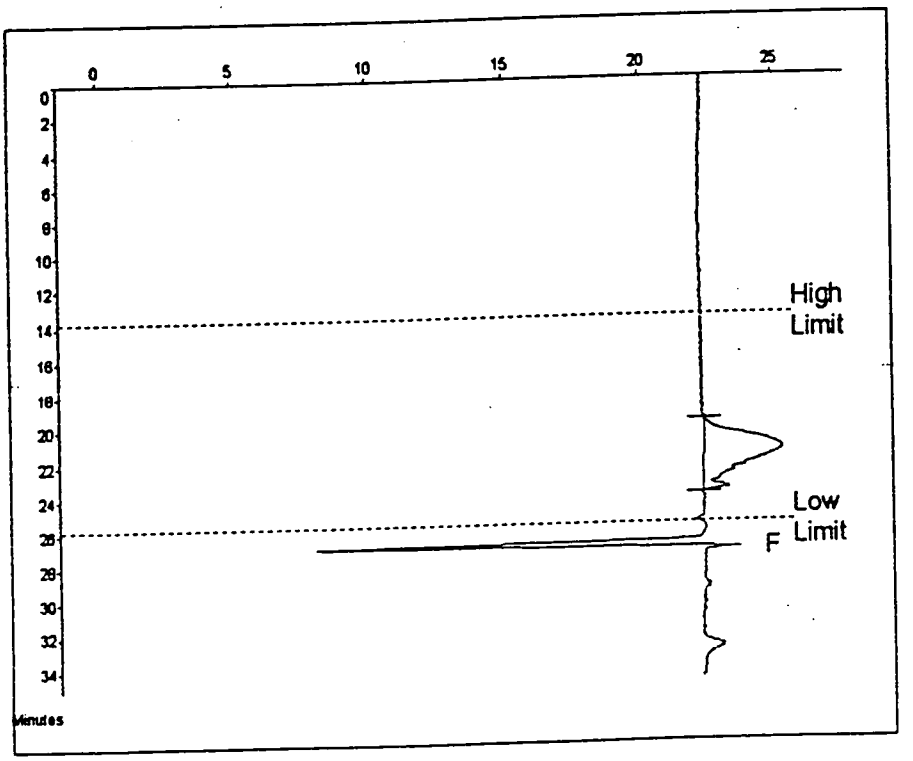

Molecular Weight Averages

Mp =	2214	Mz =	2729
Mn =	1491	Mz+1 =	3338
Mw =	2092	Mv =	2001
Polydispersity =	1.403	Peak Area =	71022

Appendix 3.26 $CHCl_3$ GPC trace of triethyl 1,3,5-benzenetricarboxylate core terminated poly(diethyl 3-hydroxyglutarate), ratio core:monomer = 1:50

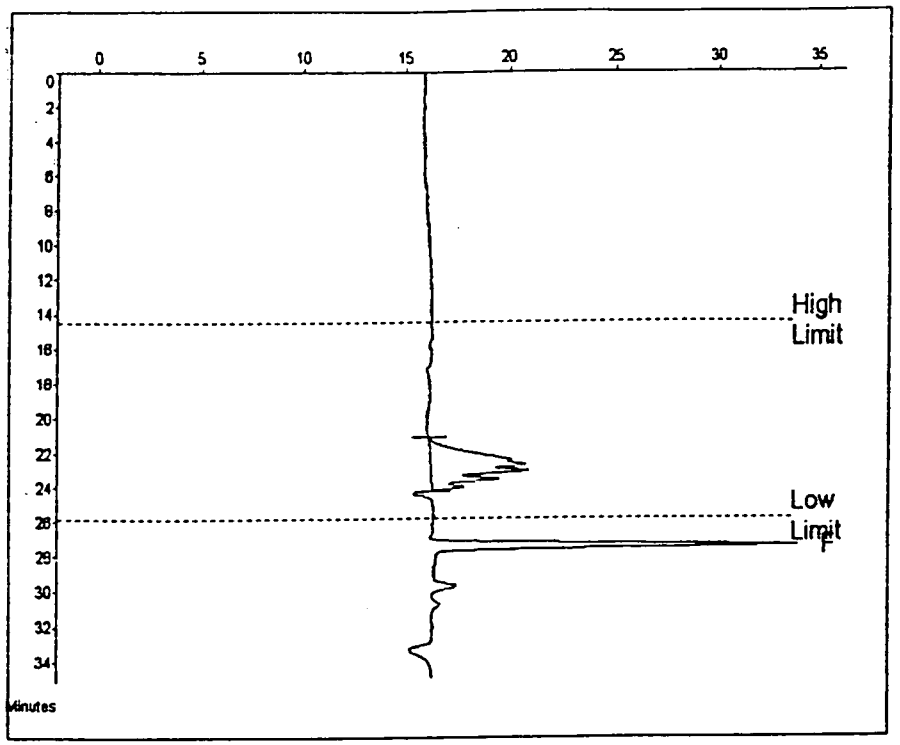

Molecular Weight Averages

Mp =	820	Mz =	1209
Mn =	882	Mz+1 =	1392
Mw =	1035	Mv =	1010
Polydispersity =	1.173	Peak Area =	81103

Appendix 3.27 $CHCl_3$ GPC trace of triethyl 1,3,5-benzenetricarboxylate core terminated poly(diethyl 3-hydroxyglutarate), ratio core:monomer = 1:50

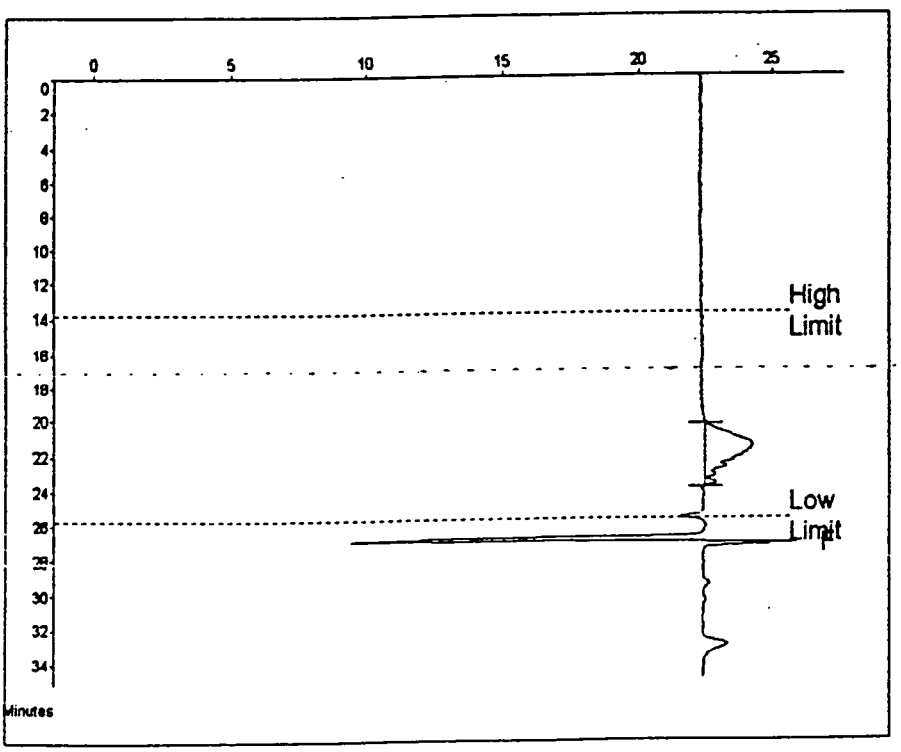

Molecular Weight Averages

Mp =	1878	Mz =	2122
Mn =	1379	Mz+1 =	2455
Mw =	1754	Mv =	1699
Polydispersity =	1.272	Peak Area =	36064

Appendix 3.28 $CHCl_3$ GPC trace of triethyl 1,3,5-benzenetricarboxylate core terminated poly(diethyl 3-hydroxyglutarate), ratio core:monomer = 1:75

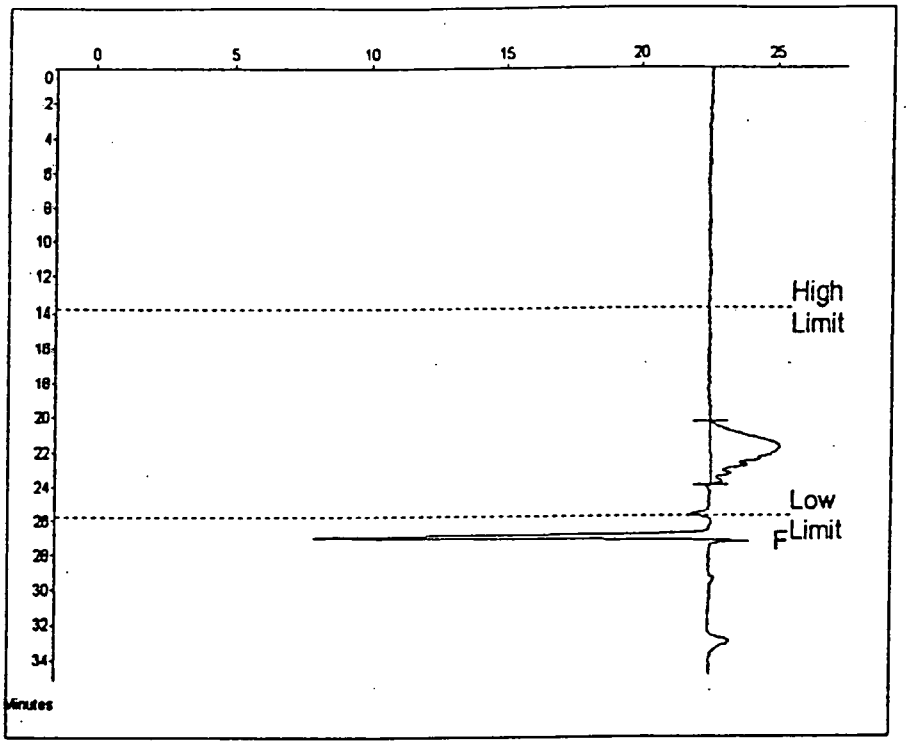

Molecular Weight Averages

Mp =	1665	Mz =	2116
Mn =	1373	Mz+1 =	2497
Mw =	1732	Mv =	1678
Polydispersity =	1.261	Peak Area =	53502

Appendix 3.29 $CHCl_3$ GPC trace of triethyl 1,3,5-benzenetricarboxylate core terminated poly(diethyl 3-hydroxyglutarate), ratio core:monomer = 1:90

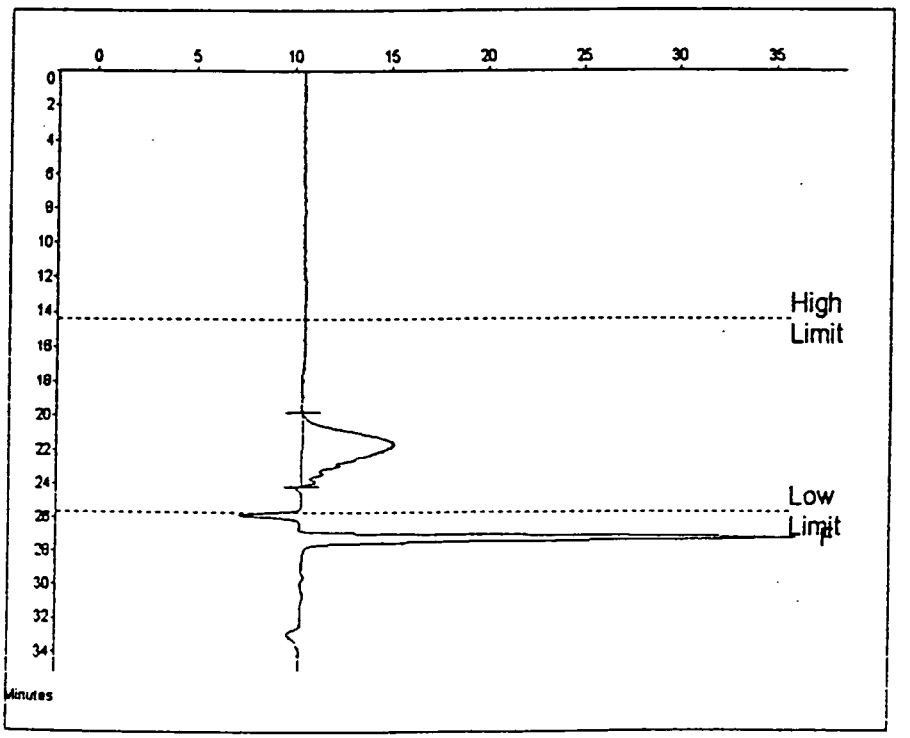

Molecular Weight Averages

Mp =	1804	Mz =	2346
Mn =	1355	Mz+1 =	2981
Mw =	1824	Mv =	1751
Polydispersity =	1.346	Peak Area =	112179

Appendix 3.30 $CHCl_3$ GPC trace of triethyl 1,3,5-benzenetricarboxylate core terminated poly(diethyl 3-hydroxyglutarate), ratio core:monomer = 1:90

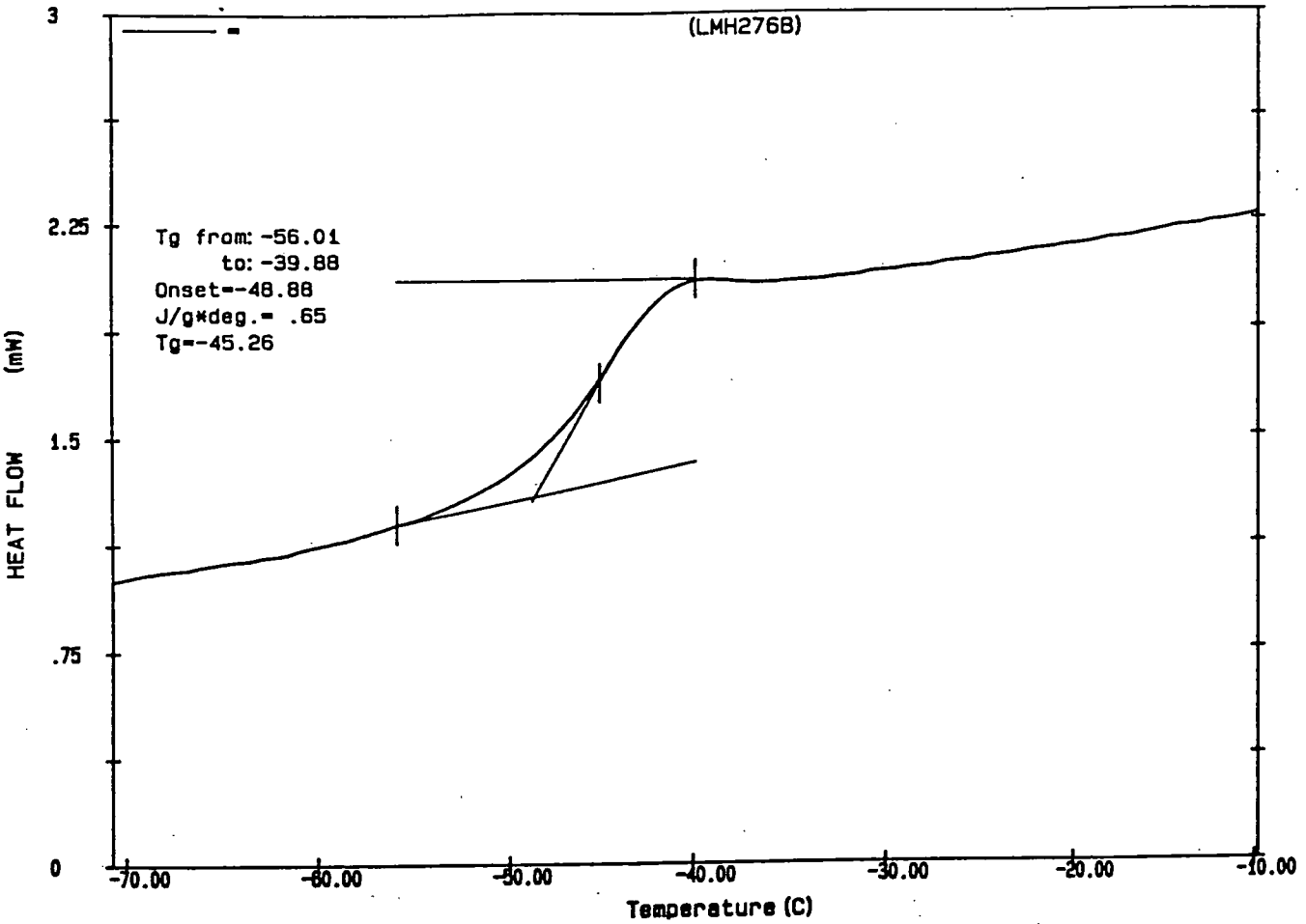

Appendix 3.31 DSC trace of triethyl 1,3,5-benzenetricarboxylate core terminated poly(diethyl 3-hydroxyglutarate), ratio core:monomer = 1:25

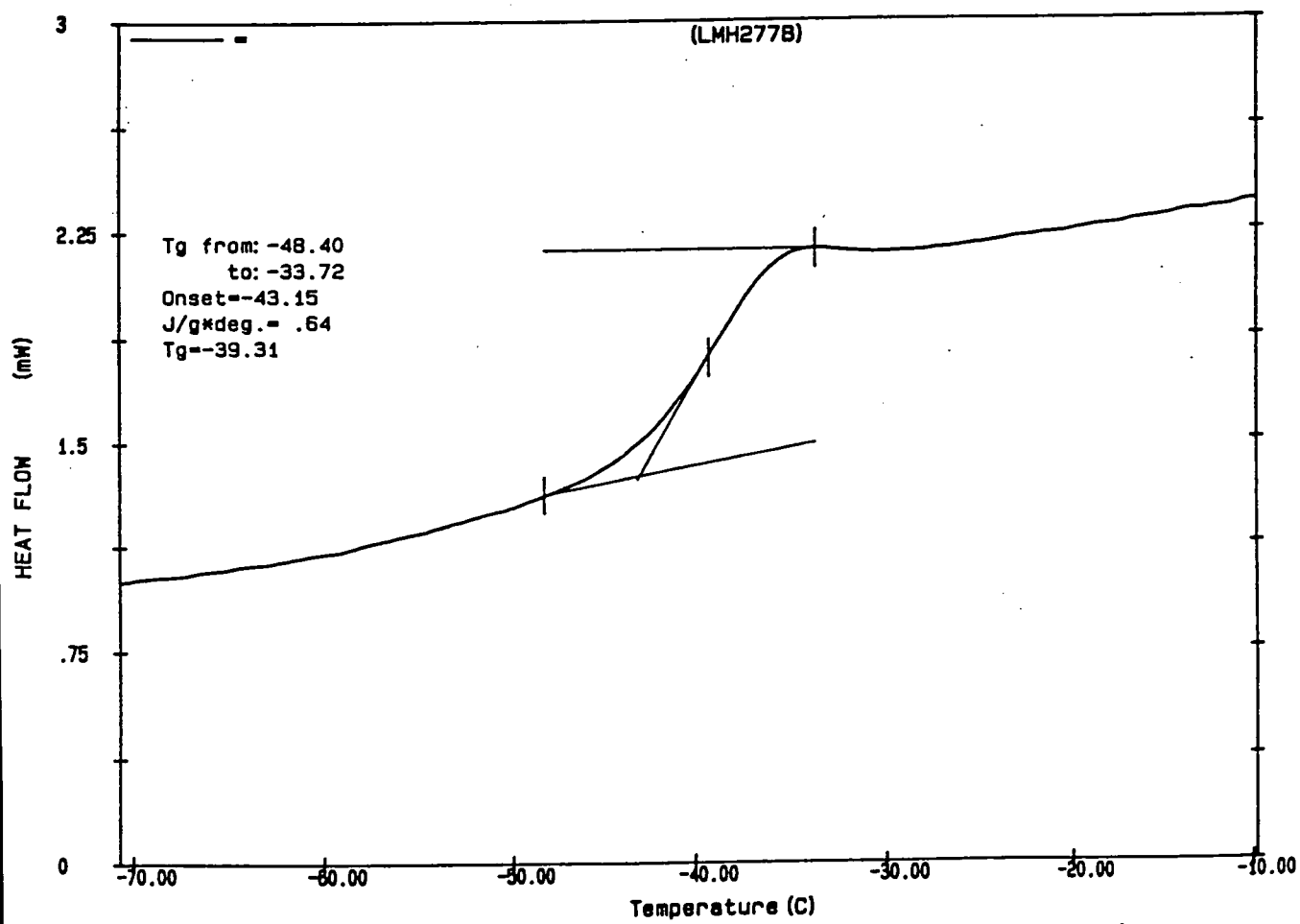

Appendix 3.32 DSC trace of triethyl 1,3,5-benzenetricarboxylate core terminated poly(diethyl 3-hydroxyglutarate), ratio core:monomer = 1:50

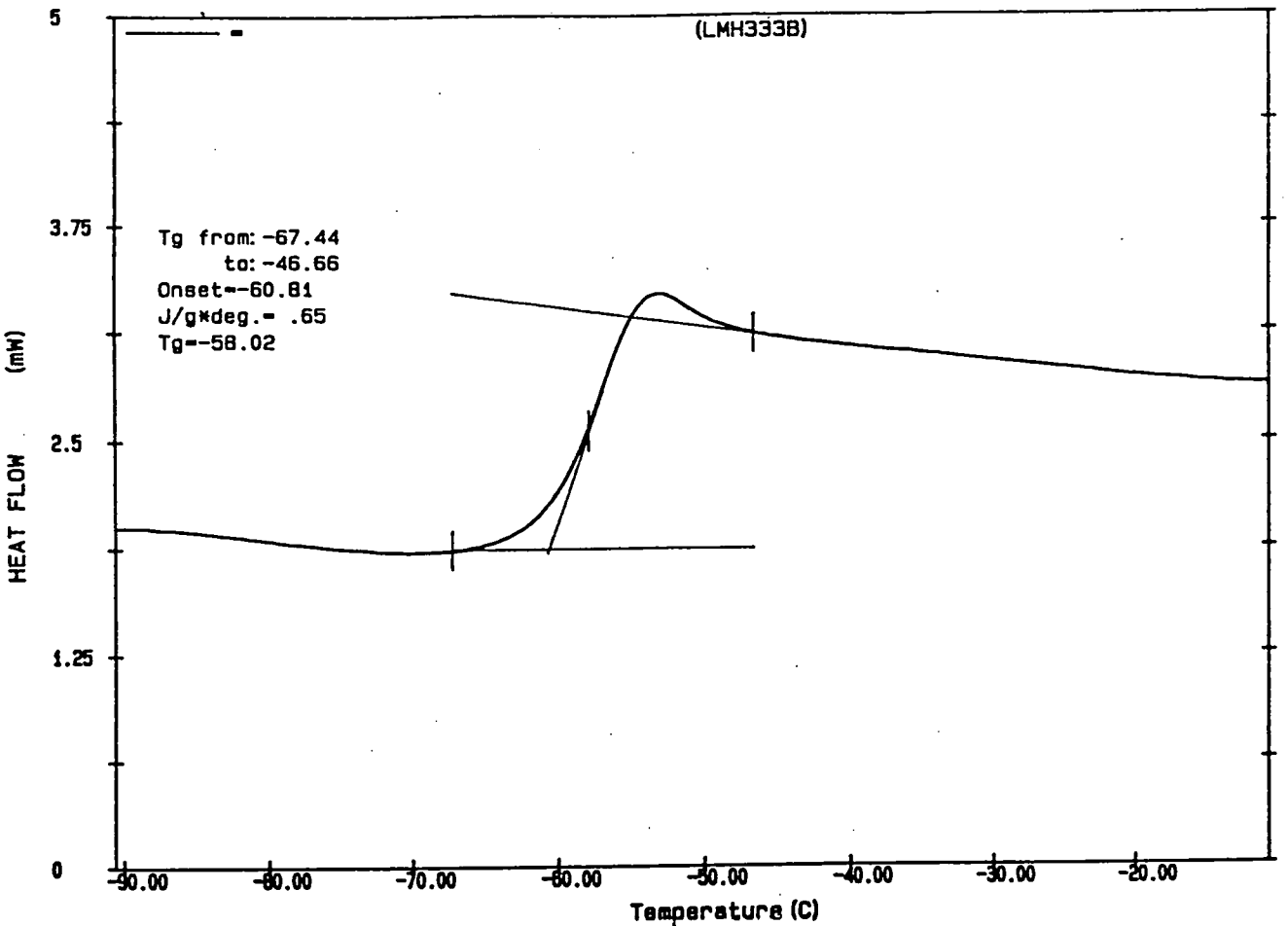

Appendix 3.33 DSC trace of triethyl 1,3,5-benzenetricarboxylate core terminated poly(diethyl 3-hydroxyglutarate), ratio core:monomer = 1:50

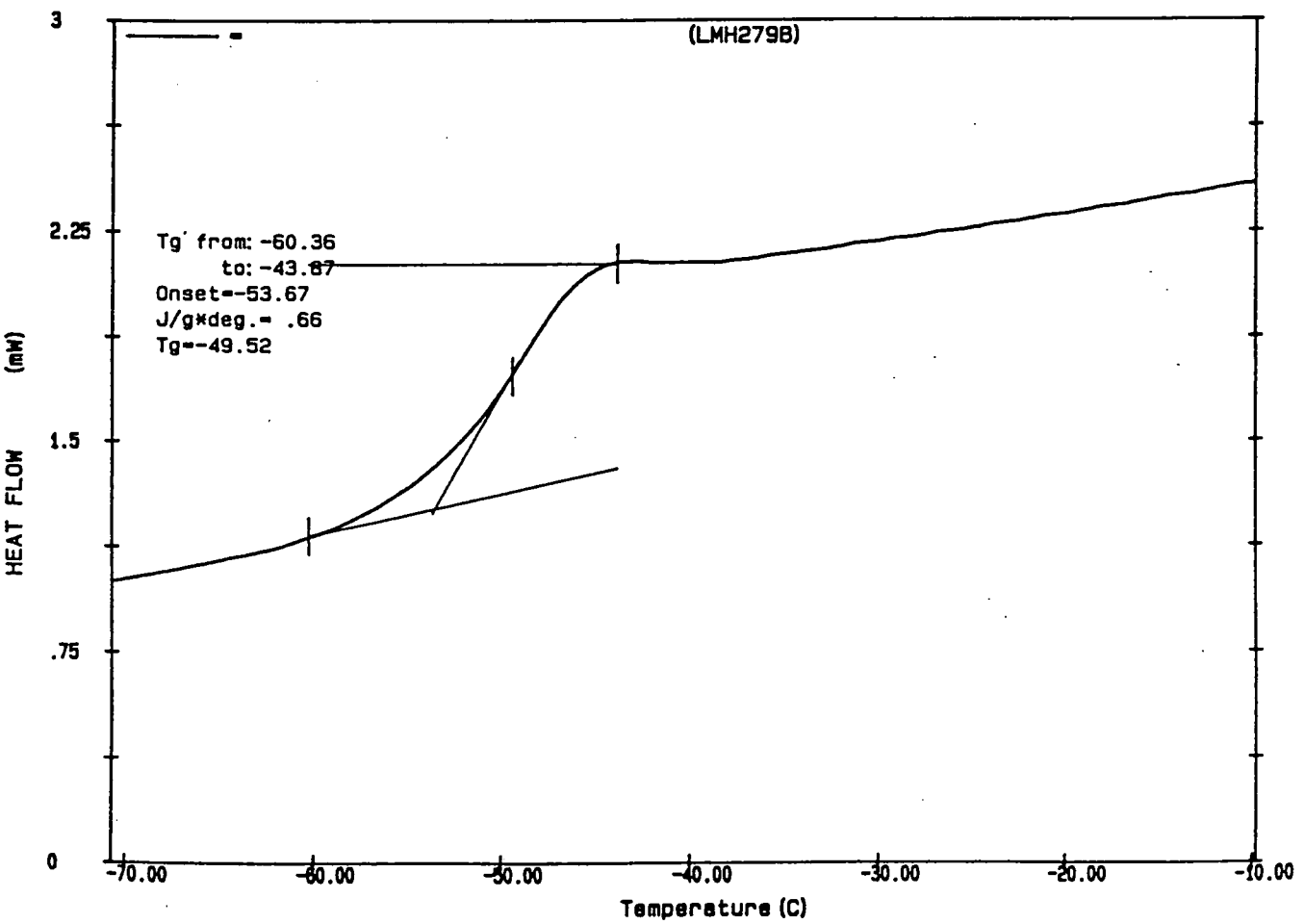

Appendix 3.34 DSC trace of triethyl 1,3,5-benzenetricarboxylate core terminated poly(diethyl 3-hydroxyglutarate), ratio core:monomer = 1:75

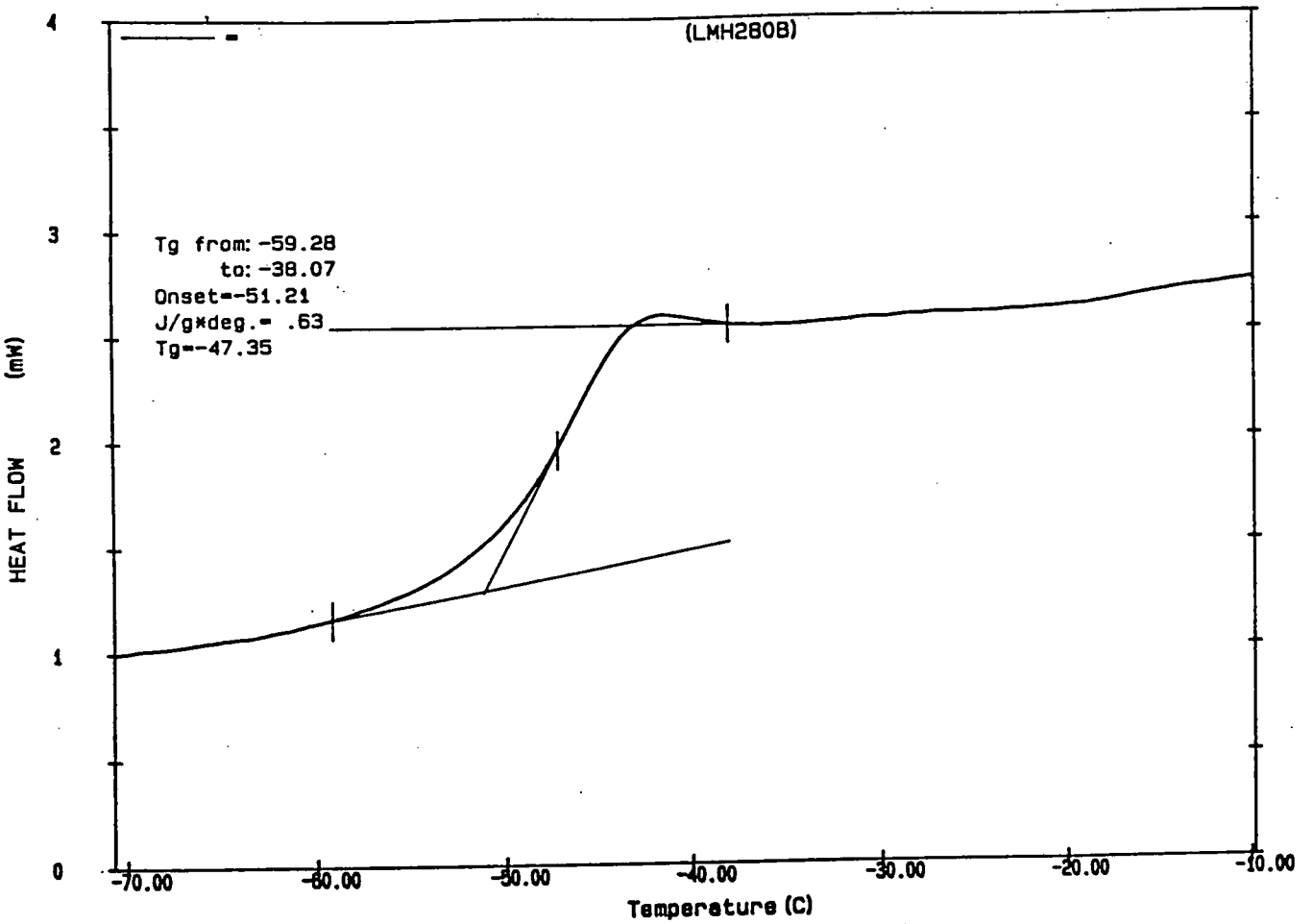

Appendix 3.35 DSC trace of triethyl 1,3,5-benzenetricarboxylate core terminated poly(diethyl 3-hydroxyglutarate), ratio core:monomer = 1:90

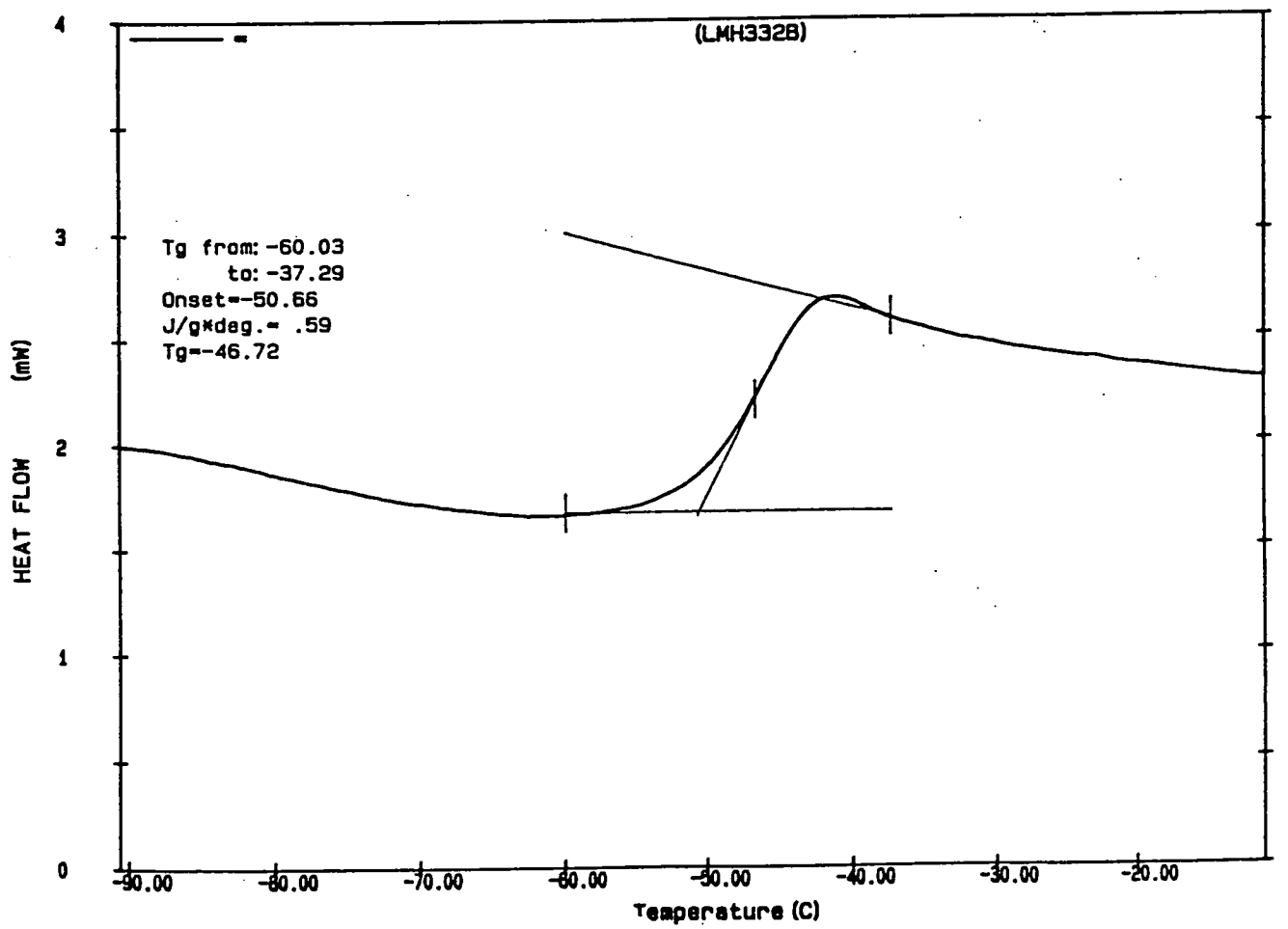

Appendix 3.36 DSC trace of triethyl 1,3,5-benzenetricarboxylate core terminated poly(diethyl 3-hydroxyglutarate), ratio core:monomer = 1:90

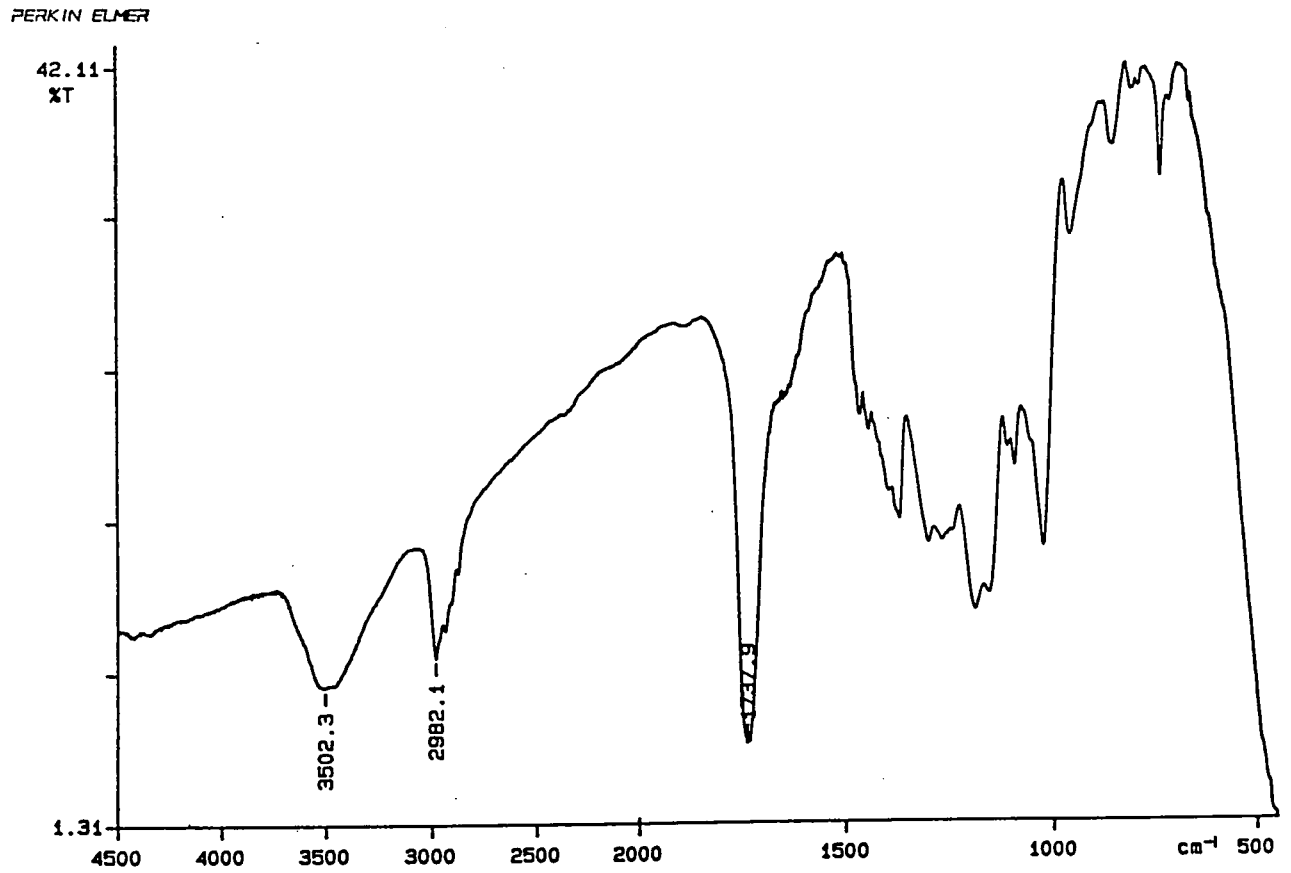

Appendix 3.37 FTIR spectrum of diethyl isophthalate core terminated poly(diethyl 3-hydroxyglutarate), ratio core:monomer = 1:25

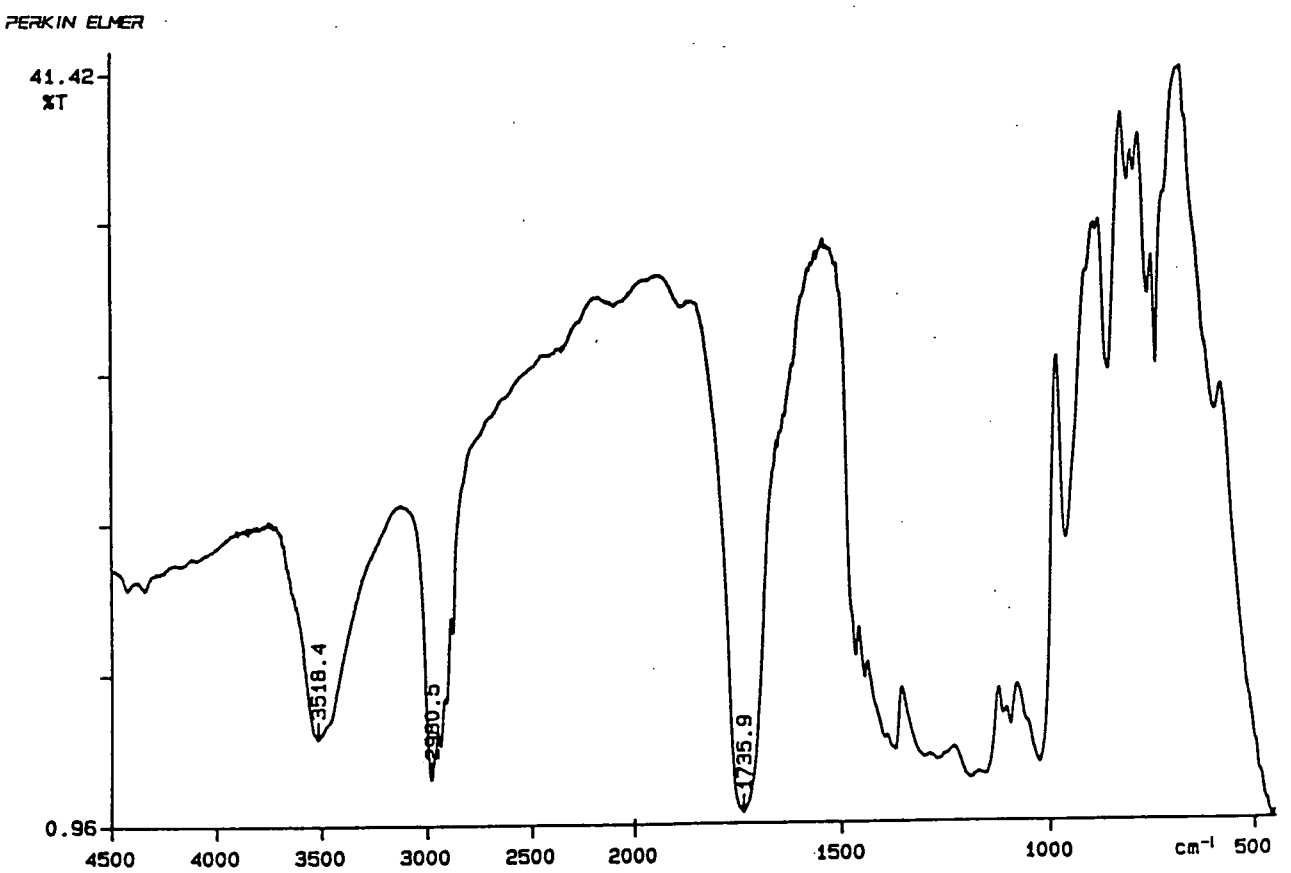

Appendix 3.38 FTIR spectrum of diethyl isophthalate core terminated poly(diethyl 3-hydroxyglutarate), ratio core:monomer = 1:50

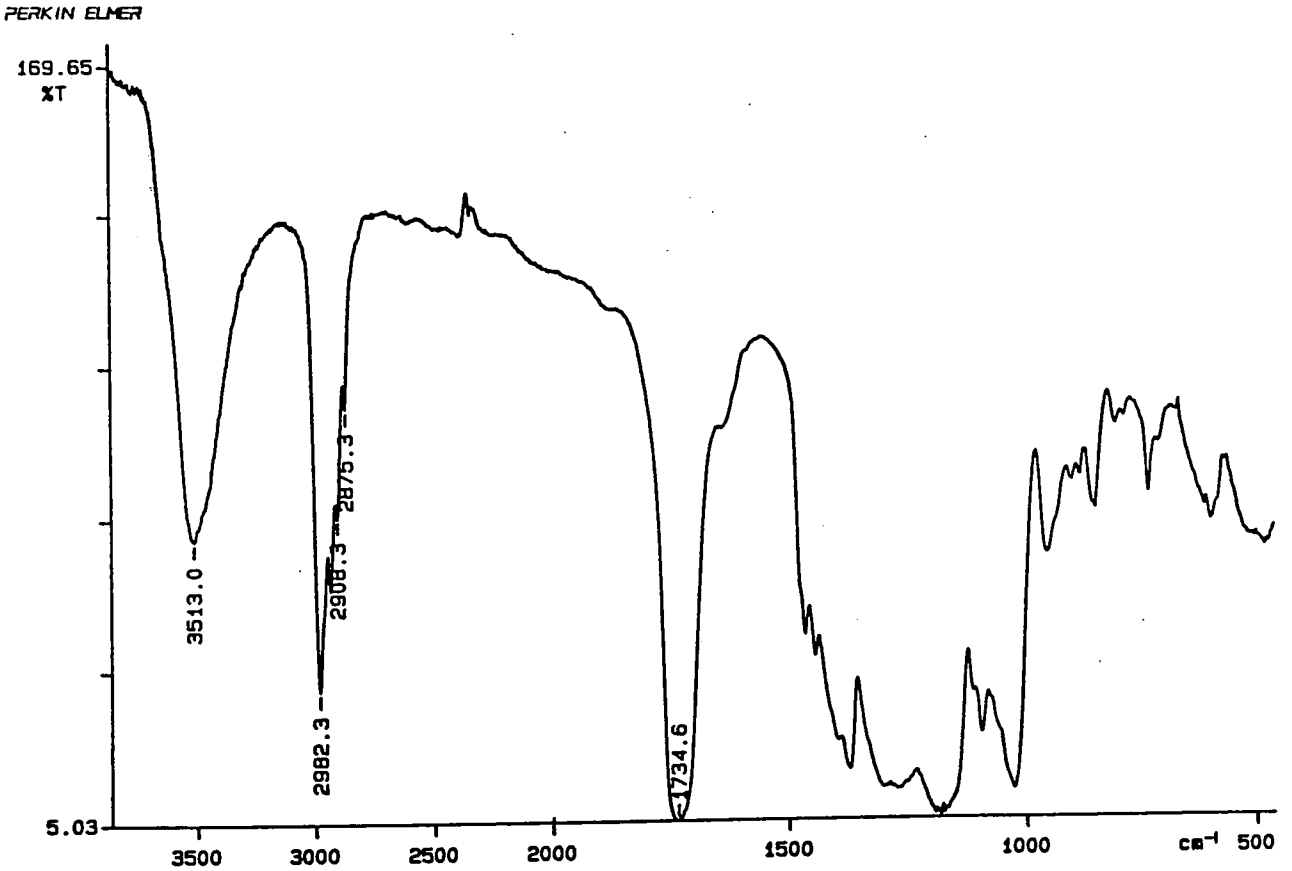

Appendix 3.39 FTIR spectrum of diethyl isophthalate core terminated poly(diethyl 3-hydroxyglutarate), ratio core:monomer = 1:50

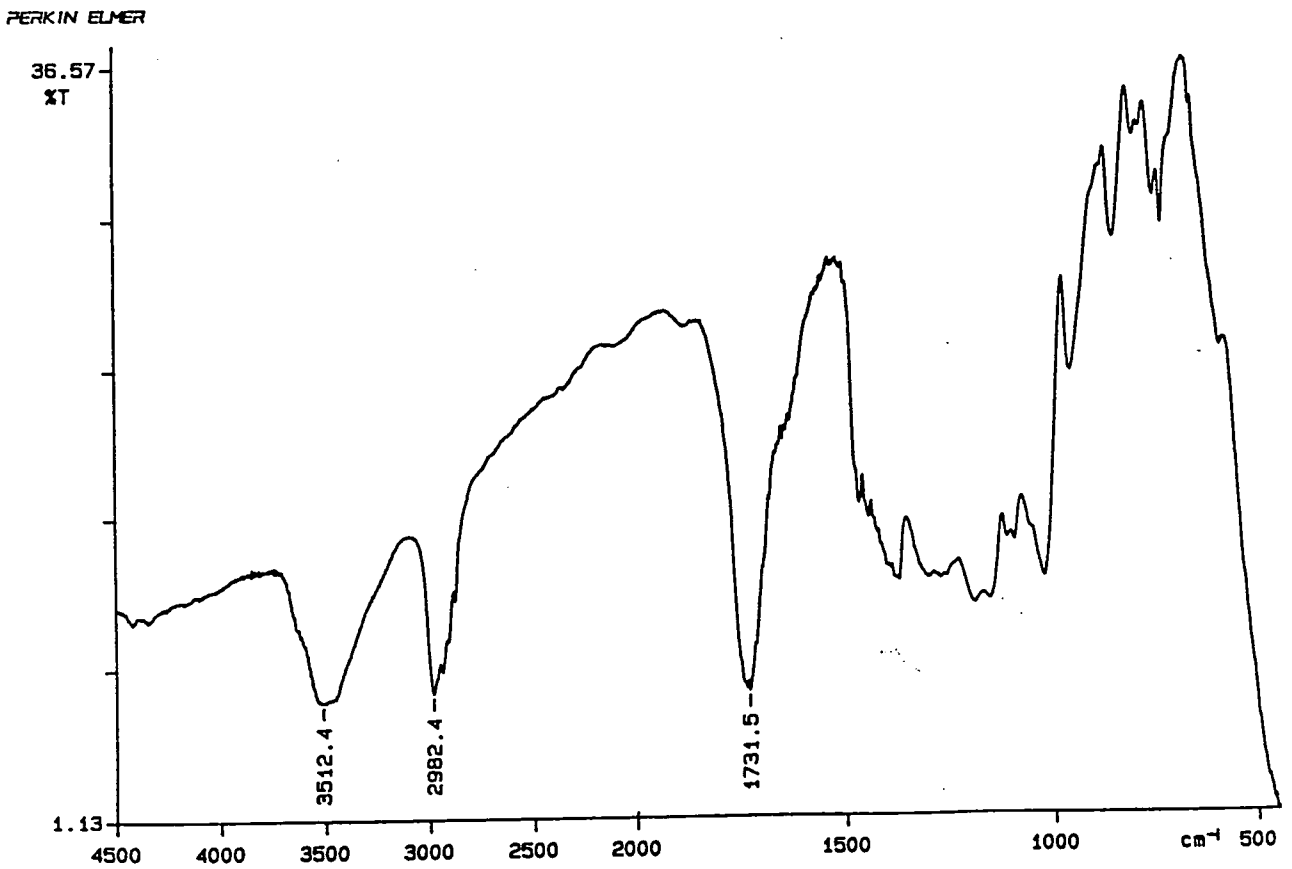

Appendix 3.40 FTIR spectrum of diethyl isophthalate core terminated poly(diethyl 3-hydroxyglutarate), ratio core:monomer = 1:75

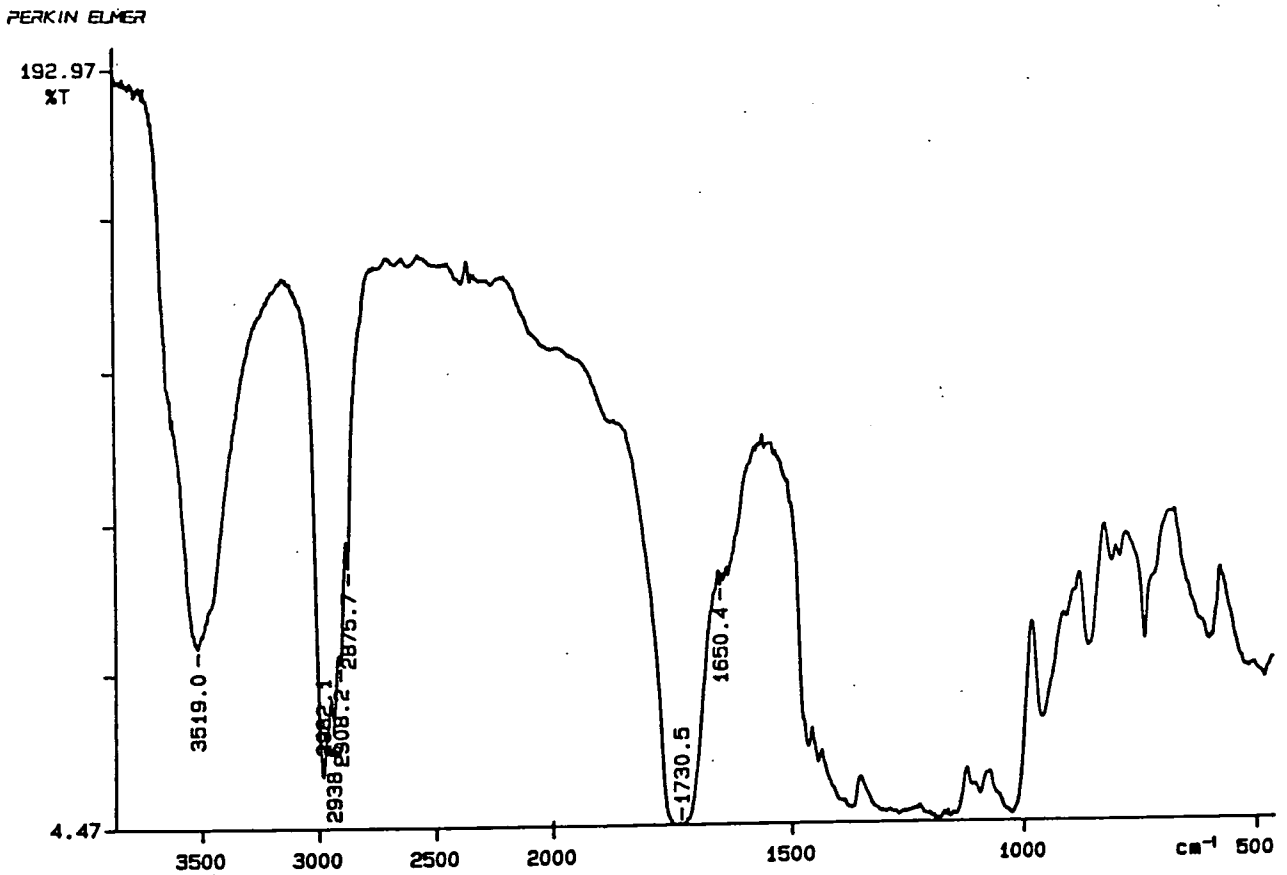

Appendix 3.41 FTIR spectrum of diethyl isophthalate core terminated poly(diethyl 3-hydroxyglutarate), ratio core:monomer = 1:75

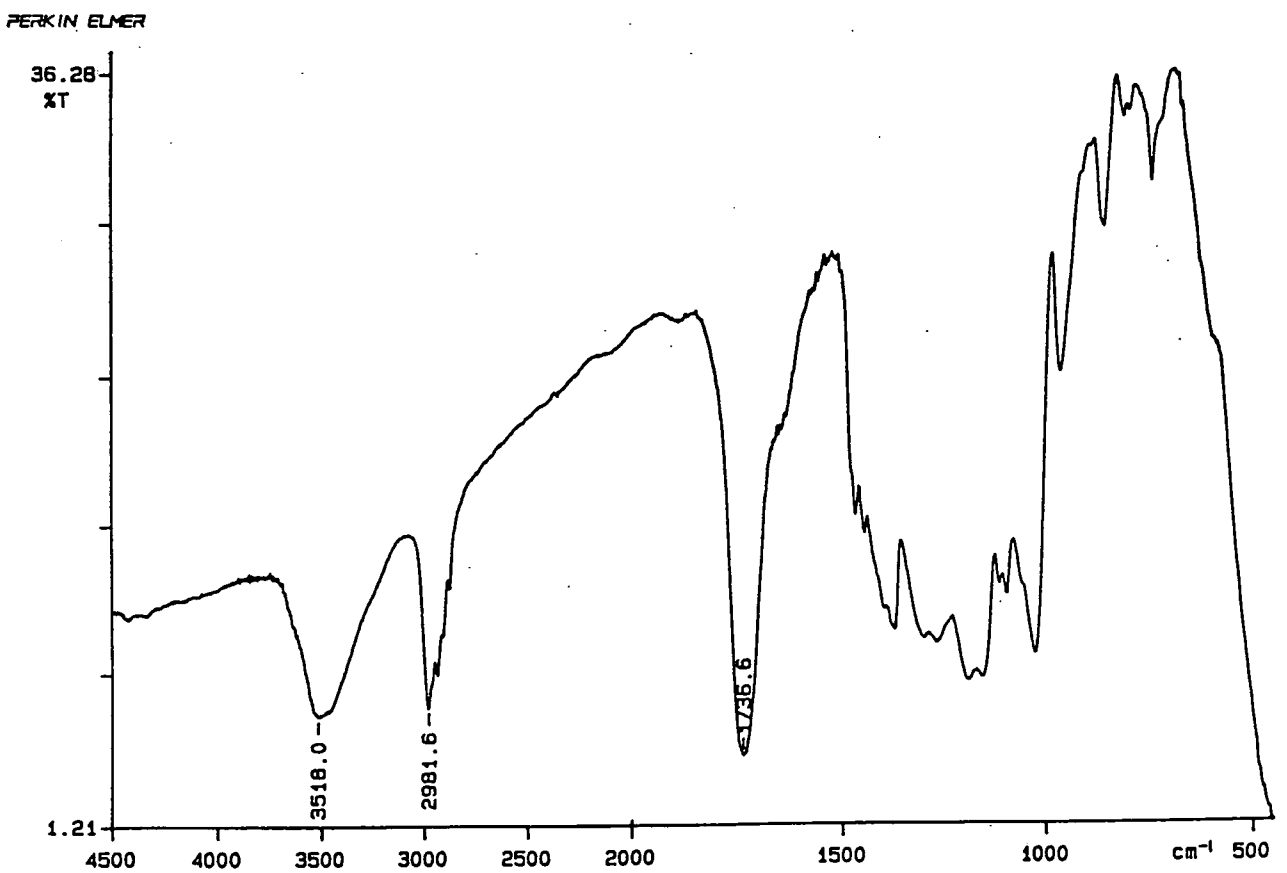

Appendix 3.42 FTIR spectrum of diethyl isophthalate core terminated poly(diethyl 3-hydroxyglutarate), ratio core:monomer = 1:90

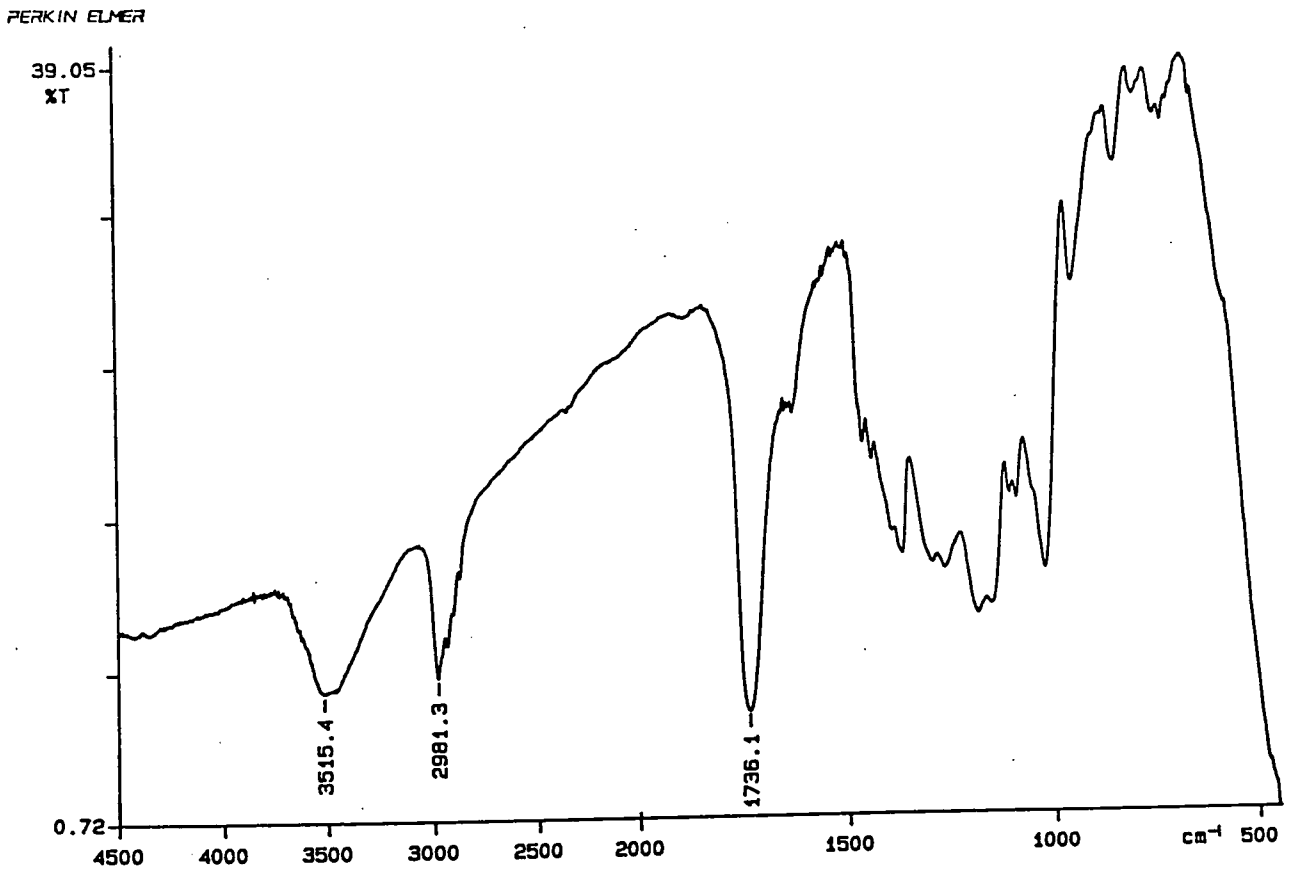

Appendix 3.43 FTIR spectrum of diethyl isophthalate core terminated poly(diethyl 3-hydroxyglutarate), ratio core:monomer = 1:150

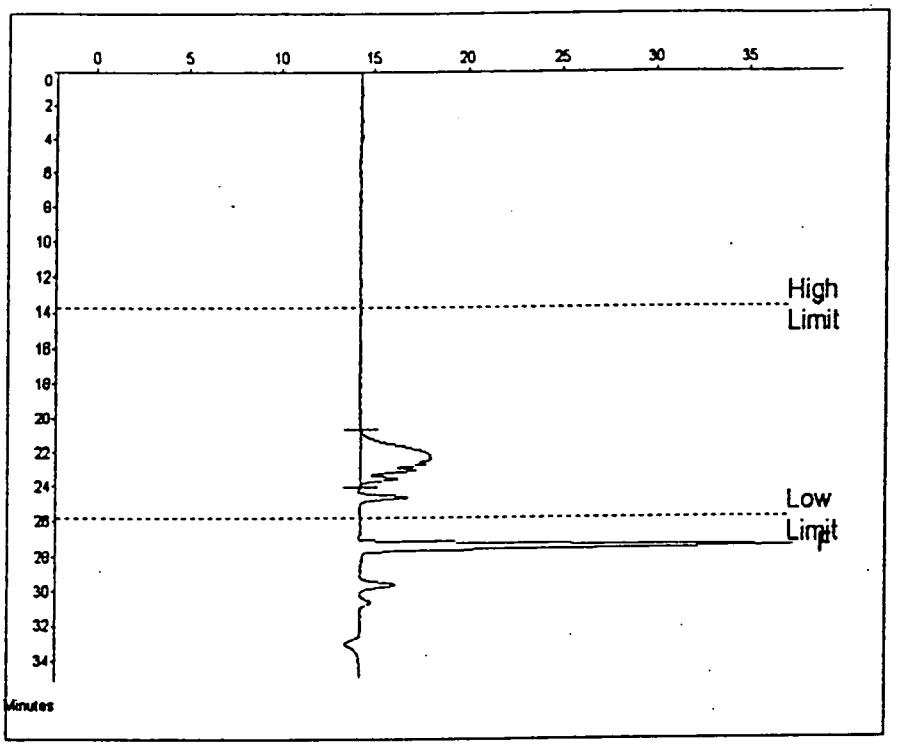

Molecular Weight Averages			
Mp =	1183	Mz =	1503
Mn =	1076	Mz+1 =	1739
Mw =	1277	Mv =	1245
Polydispersity =	1.187	Peak Area =	75697

Appendix 3.44 $CHCl_3$ GPC trace of diethyl isophthalate core terminated poly(diethyl 3-hydroxyglutarate), ratio core:monomer = 1:25

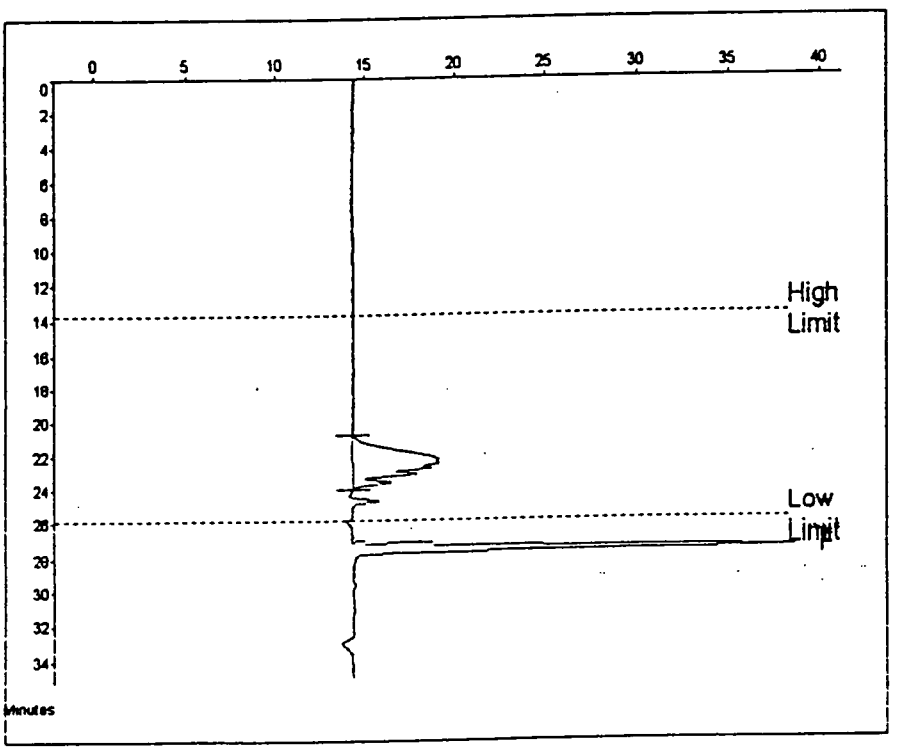

Molecular Weight Averages			
Mp =	1181	Mz =	1517
Mn =	1088	Mz+1 =	1751
Mw =	1295	Mv =	1263
Polydispersity =	1.179	Peak Area =	92764

Appendix 3.45 $CHCl_3$ GPC trace of diethyl isophthalate core terminated poly(diethyl 3-hydroxyglutarate), ratio core:monomer = 1:50

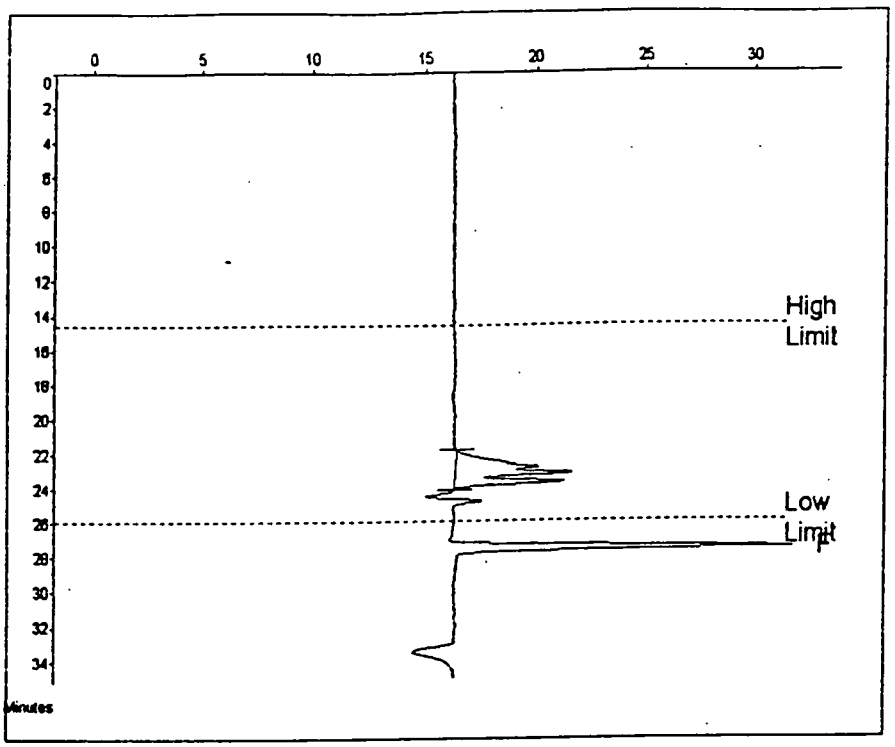

Molecular Weight Averages

Mp =	805	Mz =	955
Mn =	798	Mz+1 =	1046
Mw =	870	Mv =	858
Polydispersity =	1.093	Peak Area =	60904

Appendix 3.46 $CHCl_3$ GPC trace of diethyl isophthalate core terminated poly(diethyl 3-hydroxyglutarate), ratio core:monomer = 1:50

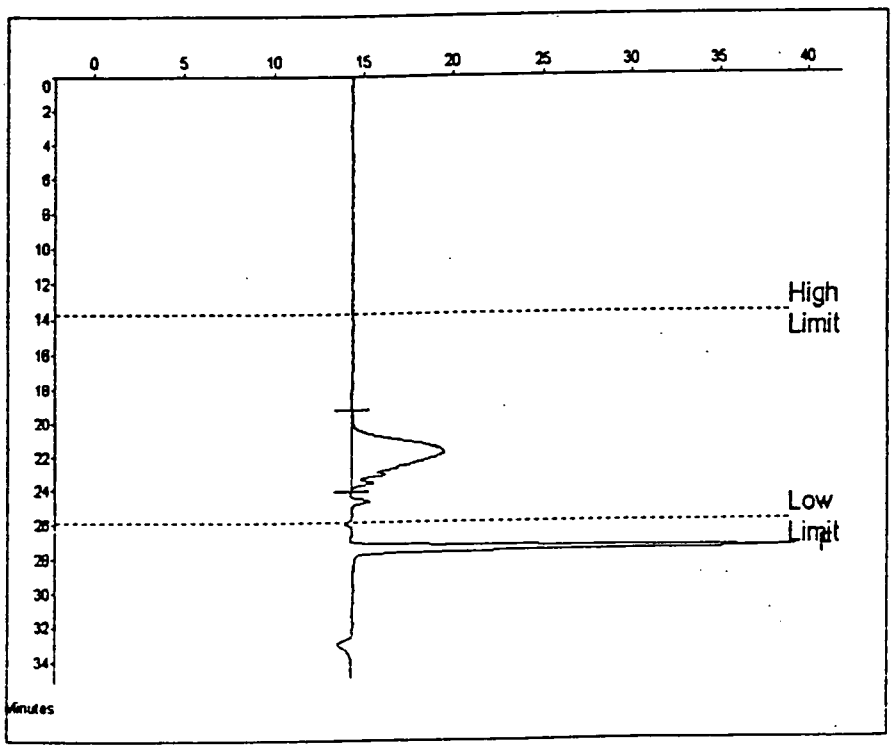

Molecular Weight Averages

Mp =	1904	Mz =	2470
Mn =	1471	Mz+1 =	3297
Mw =	1907	Mv =	1835
Polydispersity =	1.296	Peak Area =	114573

Appendix 3.47 $CHCl_3$ GPC trace of diethyl isophthalate core terminated poly(diethyl 3-hydroxyglutarate), ratio core:monomer = 1:75

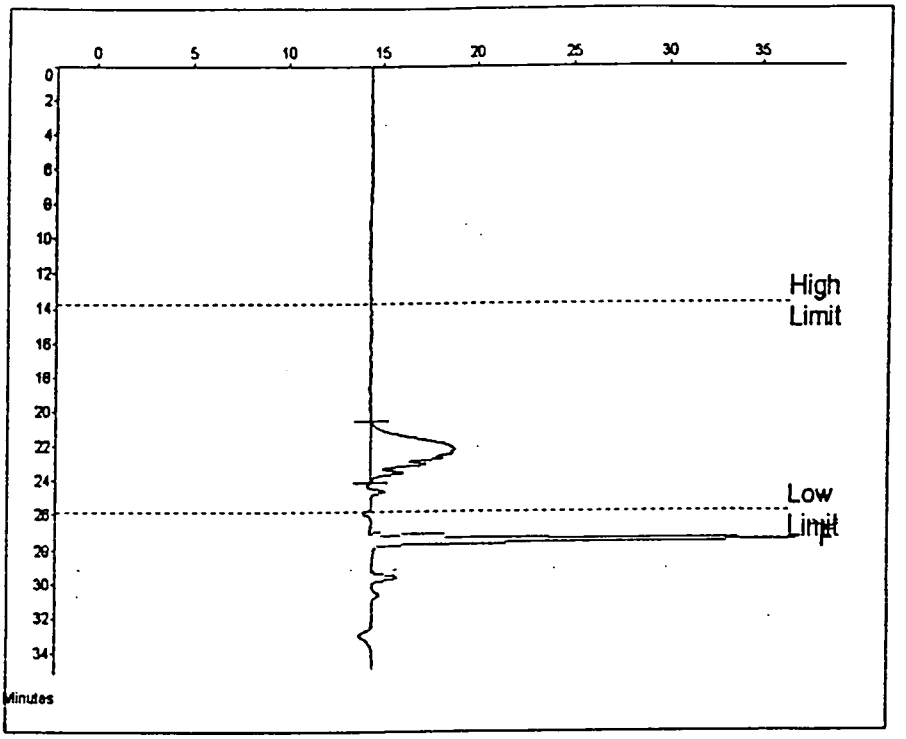

Molecular Weight Averages

Mp =	1381	Mz =	1609
Mn =	1138	Mz+1 =	1871
Mw =	1359	Mv =	1324
Polydispersity =	1.194	Peak Area =	87382

Appendix 3.48 $CHCl_3$ GPC trace of diethyl isophthalate core terminated poly(diethyl 3-hydroxyglutarate), ratio core:monomer = 1:75

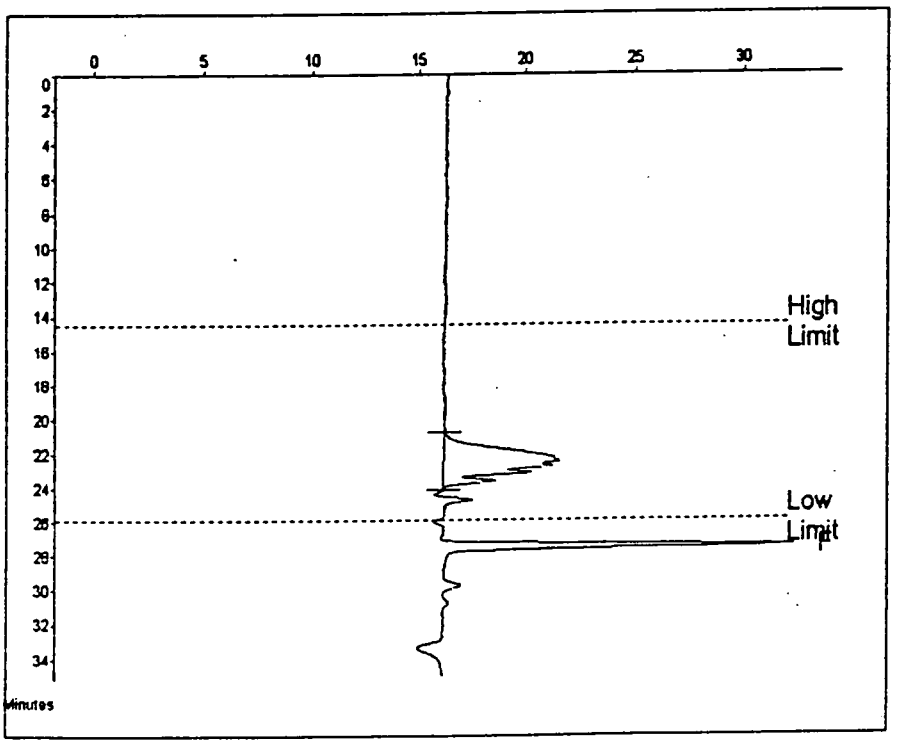

Molecular Weight Averages

Mp =	1242	Mz =	1520
Mn =	1111	Mz+1 =	1755
Mw =	1302	Mv =	1272
Polydispersity =	1.172	Peak Area =	99743

Appendix 3.49 $CHCl_3$ GPC trace of diethyl isophthalate core terminated poly(diethyl 3-hydroxyglutarate), ratio core:monomer = 1:90

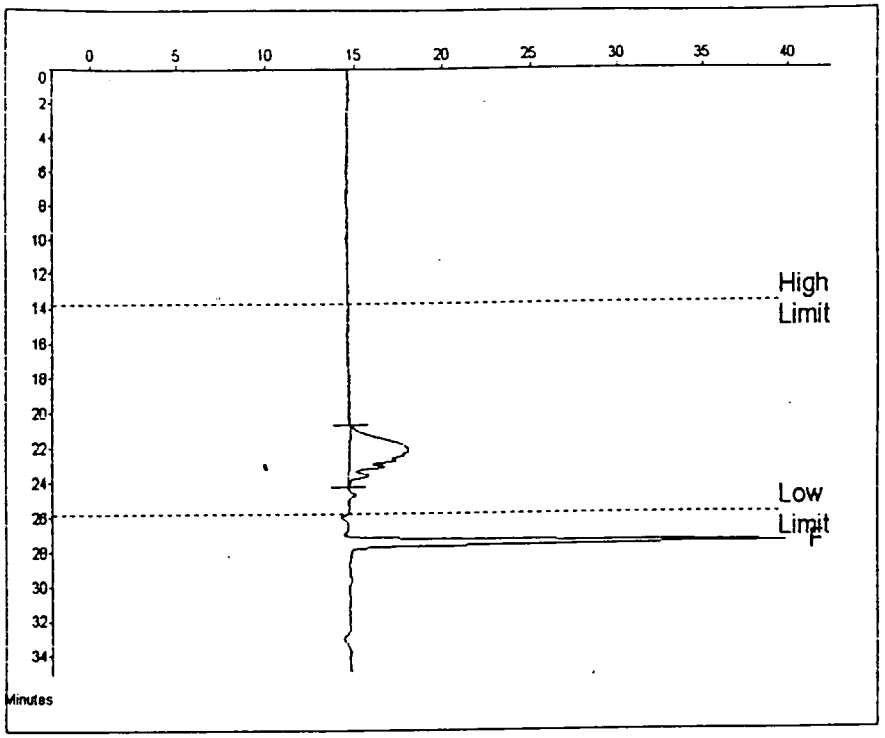

Molecular Weight Averages

Mp =	1429	Mz =	1703
Mn =	1187	Mz+1 =	1874
Mw =	1435	Mv =	1396
Polydispersity =	1.208	Peak Area =	67029

Appendix 3.50 $CHCl_3$ GPC trace of diethyl isophthalate core terminated poly(diethyl 3-hydroxyglutarate), ratio core:monomer = 1:150

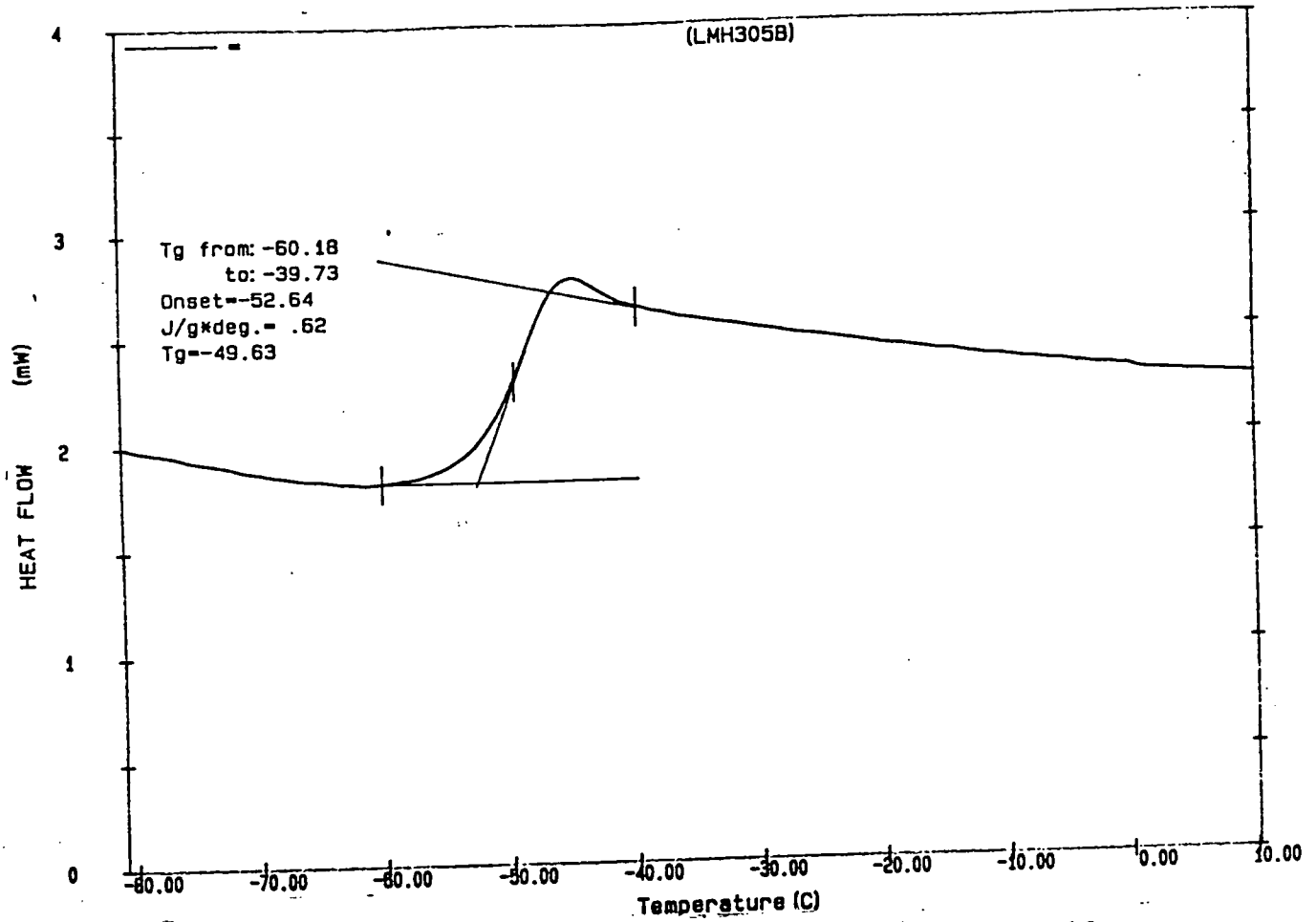

Appendix 3.51 DSC trace of diethyl isophthalate core terminated poly(diethyl 3-hydroxyglutarate), ratio core:monomer = 1:25

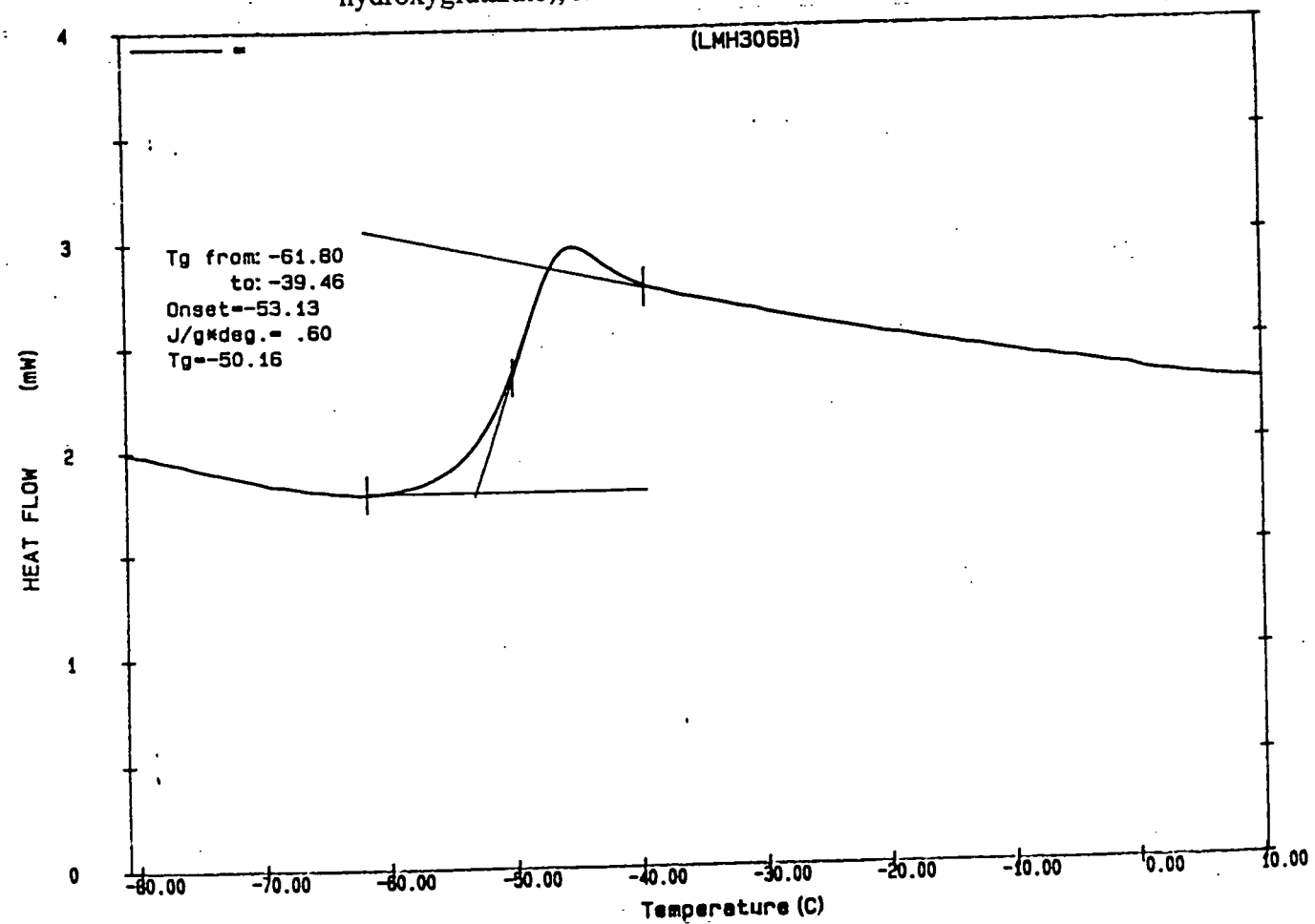

Appendix 3.52 DSC trace of diethyl isophthalate core terminated poly(diethyl 3-hydroxyglutarate), ratio core:monomer = 1:50

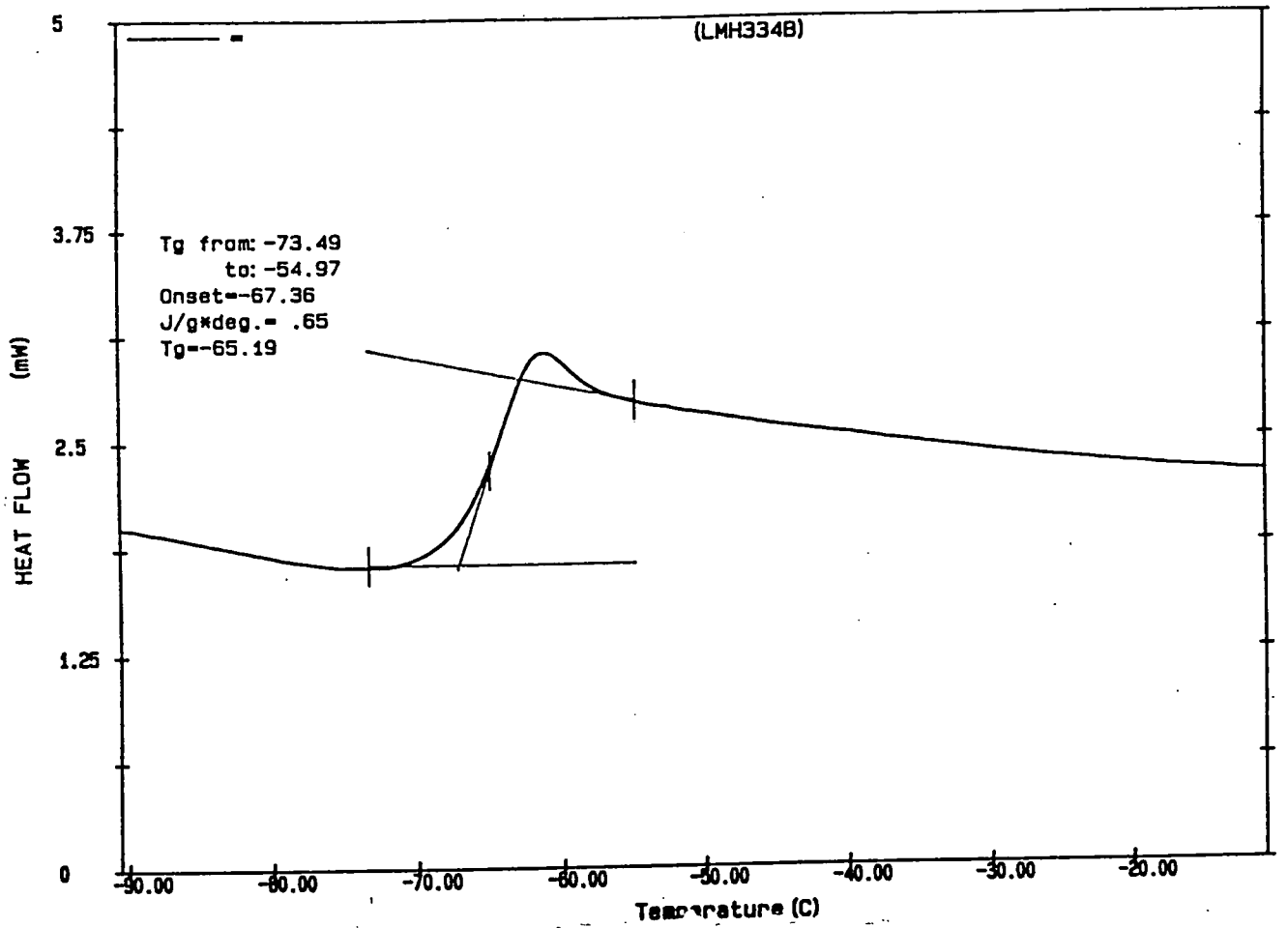

Appendix 3.53 DSC trace of diethyl isophthalate core terminated poly(diethyl 3-hydroxyglutarate), ratio core:monomer = 1:50

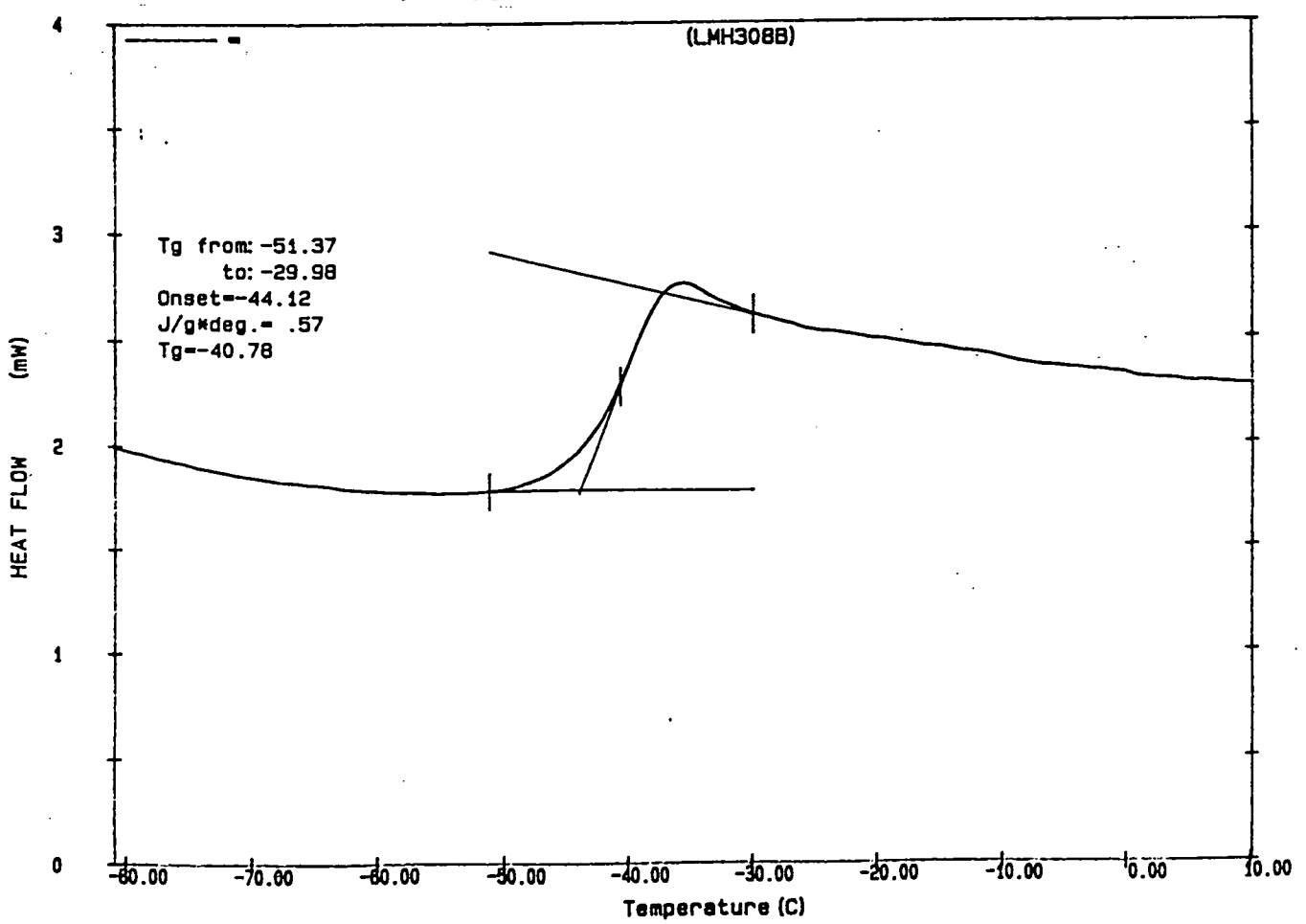

Appendix 3.54 DSC trace of diethyl isophthalate core terminated poly(diethyl 3-hydroxyglutarate), ratio core:monomer = 1:75

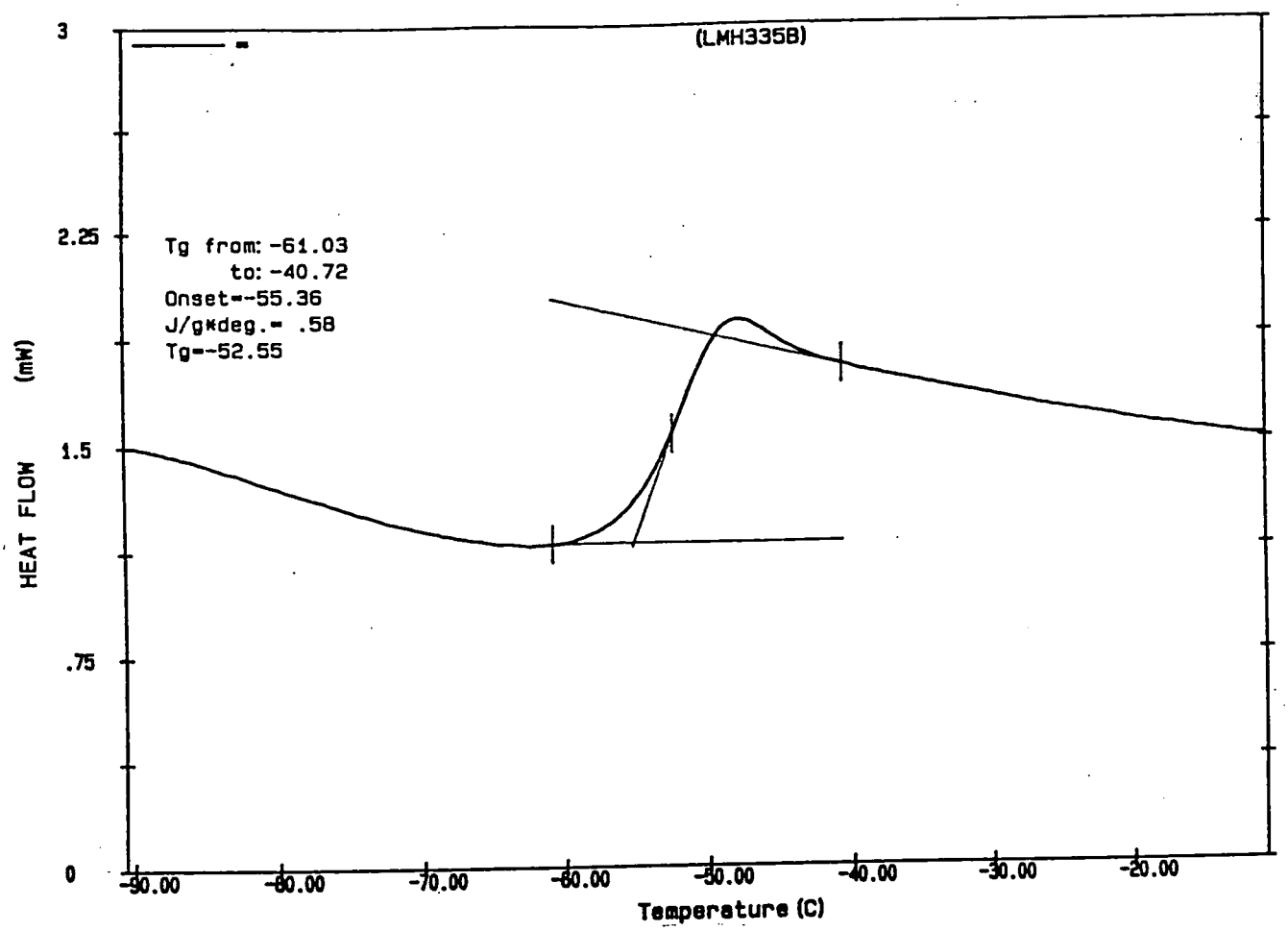

Appendix 3.55 DSC trace of diethyl isophthalate core terminated poly(diethyl 3-hydroxyglutarate), ratio core:monomer = 1:75

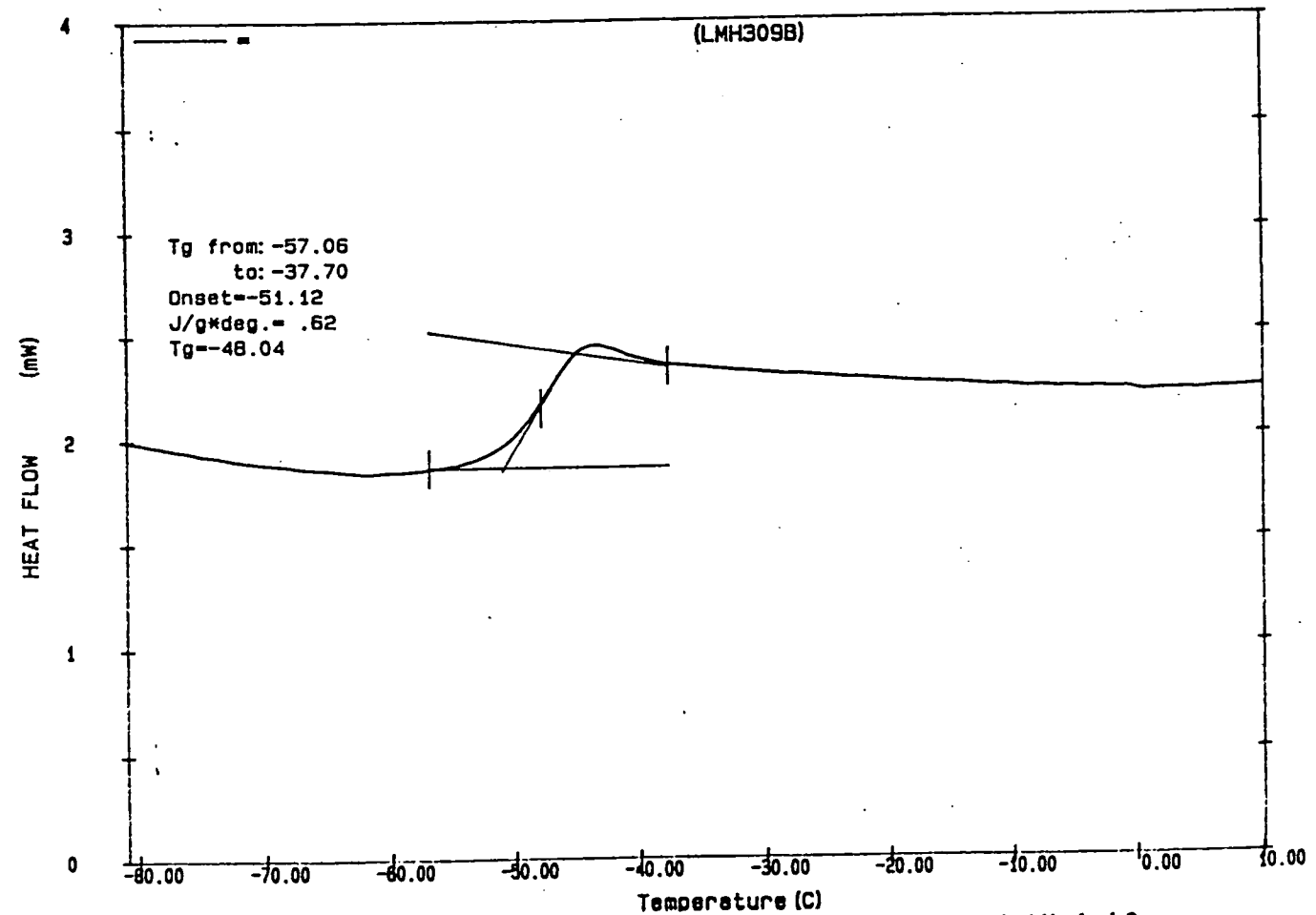

Appendix 3.56 DSC trace of diethyl isophthalate core terminated poly(diethyl 3-hydroxyglutarate), ratio core:monomer = 1:90

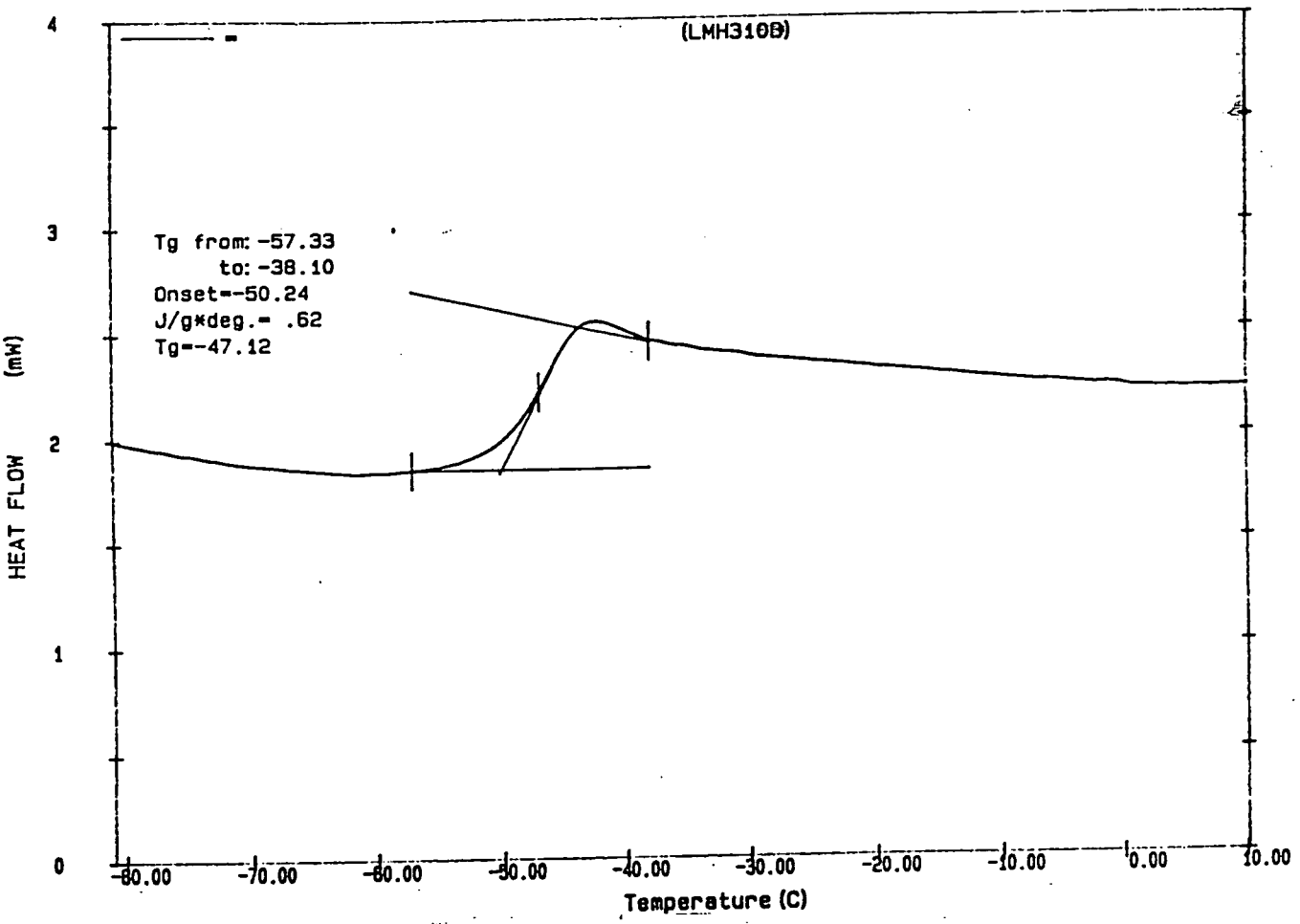

Appendix 3.57 DSC trace of diethyl isophthalate core terminated poly(diethyl 3-hydroxyglutarate), ratio core:monomer = 1:150

APPENDIX 3

^{1}H and ^{13}C nmr data for the core terminated hyperbranched polymers discussed in Chapter 5.

* Indicates an aromatic ester signal of the unreacted core molecule

Peak/ppm	Integral	Multiplicity	Assignment
0.93	1	t	Butyl CH_3
1.26	15.4	t	Ethyl CH_3
1.33	1.1	m	Butyl CH_2
1.44	1.2	t	Ethyl CH_3*
1.64	2	m	Butyl CH_2
2.54	4.1	m	Focal CH_2
2.69	12.6	m	Polymeric CH_2
3.69	0.2	s	Methyl CH_3*
4.14	10.5	m	Ethyl OCH_2
4.44	1.7	m	Focal CH
5.56	3.1	m	Polymeric CH
8.80	0.12	s	Core CH
8.86	0.41	s	Ethyl CH*

Table 1 ^{1}H nmr summary of the product of the co-polymerisation of diethyl 3-hydroxyglutarate and trimethyl 1,3,5-benzenetricarboxylate in a ratio of 25:1

Peak/ppm	Integral	Multiplicity	Assignment
0.93	3	t	Butyl CH_3
1.26	78.8	t	Ethyl CH_3
1.33	3.2	m	Butyl CH_2
1.44	1	t	Ethyl CH_3*
1.64	2	m	Butyl CH_2
2.54	32.8	m	Focal CH_2
2.69	41.2	m	Polymeric CH_2
3.69	1.6	s	Methyl CH_3*
4.14	55.2	m	Ethyl OCH_2
4.44	8.2	m	Focal CH
5.56	10	m	Polymeric CH
8.80	0.1	s	Core CH
8.86	0.7	s	Ethyl CH*

Table 2 ^{1}H nmr summary of the product of the co-polymerisation of diethyl 3-hydroxyglutarate and trimethyl 1,3,5-benzenetricarboxylate in a ratio of 50:1

Peak/ppm	Integral	Multiplicity	Assignment
0.93	1.5	t	Butyl CH_3
1.26	23	t	Ethyl CH_3
1.33	1.25	m	Butyl CH_2
1.44	1	t	Ethyl CH_3*
1.64	1	m	Butyl CH_2
2.54	8.63	m	Focal CH_2
2.69	16.63	m	Polymeric CH_2
4.14	16.38	m	Ethyl OCH_2
4.44	2.5	m	Focal CH
5.56	3.88	m	Polymeric CH
8.80	0.15	s	Core CH
8.86	0.55	s	Ethyl CH*

Table 3 ^{1}H nmr summary of the product of the co-polymerisation of diethyl 3-hydroxyglutarate and trimethyl 1,3,5-benzenetricarboxylate in a ratio of 50:1

Peak/ppm	Integral	Multiplicity	Assignment
0.93	2.25	t	Butyl CH_3
1.26	48.75	t	Ethyl CH_3
1.33	2	m	Butyl CH_2
1.44	1	t	Ethyl CH_3*
1.64	1.5	m	Butyl CH_2
2.54	16	m	Focal CH_2
2.69	36	m	Polymeric CH_2
3.69	0.25	s	Methyl CH_3*
4.14	33.75	m	Ethyl OCH_2
4.44	4.25	m	Focal CH
5.56	8.75	m	Polymeric CH
8.80	0.1	s	Core CH
8.86	0.5	s	Ethyl CH*

Table 4 ^{1}H nmr summary of the product of the co-polymerisation of diethyl 3-hydroxyglutarate and trimethyl 1,3,5-benzenetricarboxylate in a ratio of 75:1

Peak/ppm	Integral	Multiplicity	Assignment
0.93	3.5	t	Butyl CH_3
1.26	47.5	t	Ethyl CH_3
1.33	1.75	m	Butyl CH_2
1.44	1	t	Ethyl CH_3*
1.64	1.75	m	Butyl CH_2
2.54	10.75	m	Focal CH_2
2.69	41.25	m	Polymeric CH_2
4.14	34	m	Ethyl OCH_2
4.44	3.38	m	Focal CH
5.56	10	m	Polymeric CH
8.80	0.1	s	Core CH
8.86	0.2	s	Ethyl CH*

Table 5 ^{1}H nmr summary of the product of the co-polymerisation of diethyl 3-hydroxyglutarate and trimethyl 1,3,5-benzenetricarboxylate in a ratio of 90:1

Peak/ppm	Integral	Multiplicity	Assignment
0.93	2.4	t	Butyl CH_3
1.26	38	t	Ethyl CH_3
1.33	1.6	m	Butyl CH_2
1.44	1	t	Ethyl CH_3*
1.64	2	m	Butyl CH_2
2.54	14.8	m	Focal CH_2
2.69	27.6	m	Polymeric CH_2
4.14	28.4	m	Ethyl OCH_2
4.44	4	m	Focal CH
5.56	6.4	m	Polymeric CH
8.80	0.1	s	Core CH
8.86	0.37	s	Ethyl CH*

Table 6 ^{1}H nmr summary of the product of the co-polymerisation of diethyl 3-hydroxyglutarate and trimethyl 1,3,5-benzenetricarboxylate in a ratio of 90:1

Peak/ppm	Integral	Multiplicity	Assignment
0.93	1.29	t	Butyl CH_3
1.26	24.14	t	Ethyl CH_3
1.33	1.43	m	Butyl CH_2
1.44	2	t	Ethyl CH_3*
1.64	1	m	Butyl CH_2
2.54	5	m	Focal CH_2
2.69	21	m	Polymeric CH_2
4.14	16.86	m	Ethyl OCH_2
4.44	2.43	m	Focal CH
5.56	5.14	m	Polymeric CH
8.80	0.2	s	Core CH
8.85	0.8	s	Ethyl CH*

Table 7 ^{1}H nmr summary of the product of the co-polymerisation of diethyl 3-hydroxyglutarate and triethyl 1,3,5-benzenetricarboxylate in a ratio of 25:1

Peak/ppm	Integral	Multiplicity	Assignment
0.93	1.15	t	Butyl CH_3
1.26	19.47	t	Ethyl CH_3
1.33	1.02	m	Butyl CH_2
1.44	1	t	Ethyl CH_3*
1.64	1.1	m	Butyl CH_2
2.54	4.20	m	Focal CH_2
2.69	18.70	m	Polymeric CH_2
4.14	14.50	m	Ethyl OCH_2
4.44	1.53	m	Focal CH
5.56	4.77	m	Polymeric CH
8.80	0.2	s	Core CH
8.85	0.44	s	Ethyl CH*

Table 8 ^{1}H nmr summary of the product of the co-polymerisation of diethyl 3-hydroxyglutarate and triethyl 1,3,5-benzenetricarboxylate in a ratio of 50:1

Peak/ppm	Integral	Multiplicity	Assignment
0.93	1.57	t	Butyl CH_3
1.26	27.57	t	Ethyl CH_3
1.33	1.14	m	Butyl CH_2
1.44	1	t	Ethyl CH_3*
1.64	1.14	m	Butyl CH_2
2.54	11.43	m	Focal CH_2
2.69	17.43	m	Polymeric CH_2
4.14	19.86	m	Ethyl OCH_2
4.44	3.29	m	Focal CH
5.56	4	m	Polymeric CH
8.80	0.2	s	Core CH
8.85	2	s	Ethyl CH*

Table 9 ^{1}H nmr summary of the product of the co-polymerisation of diethyl 3-hydroxyglutarate and triethyl 1,3,5-benzenetricarboxylate in a ratio of 50:1

Peak/ppm	Integral	Multiplicity	Assignment
0.93	1.41	t	Butyl CH_3
1.26	27.53	t	Ethyl CH_3
1.33	1.18	m	Butyl CH_2
1.44	1	t	Ethyl CH_3*
1.64	1.18	m	Butyl CH_2
2.54	6.35	m	Focal CH_2
2.69	23.53	m	Polymeric CH_2
4.14	19.29	m	Ethyl OCH_2
4.44	1.88	m	Focal CH
5.56	5.88	m	Polymeric CH
8.80	0.1	s	Core CH
8.85	0.26	s	Ethyl CH*

Table 10 ^{1}H nmr summary of the product of the co-polymerisation of diethyl 3-hydroxyglutarate and triethyl 1,3,5-benzenetricarboxylate in a ratio of 75:1

Peak/ppm	Integral	Multiplicity	Assignment
0.93	2.18	t	Butyl CH_3
1.26	36.36	t	Ethyl CH_3
1.33	1.45	m	Butyl CH_2
1.44	1	t	Ethyl CH_3*
1.64	1.82	m	Butyl CH_2
2.54	8.73	m	Focal CH_2
2.69	28.73	m	Polymeric CH_2
4.14	24.73	m	Ethyl OCH_2
4.44	2.54	m	Focal CH
5.56	7.27	m	Polymeric CH
8.80	0.09	s	Core CH
8.85	0.21	s	Ethyl CH*

Table 11 ^{1}H nmr summary of the product of the co-polymerisation of diethyl 3-hydroxyglutarate and triethyl 1,3,5-benzenetricarboxylate in a ratio of 90:1

Peak/ppm	Integral	Multiplicity	Assignment
0.93	2.4	t	Butyl CH_3
1.26	40.4	t	Ethyl CH_3
1.33	1.6	m	Butyl CH_2
1.44	1	t	Ethyl CH_3*
1.64	1.4	m	Butyl CH_2
2.54	5.6	m	Focal CH_2
2.69	36	m	Polymeric CH_2
4.14	28.4	m	Ethyl OCH_2
4.44	2.6	m	Focal CH
5.56	8.6	m	Polymeric CH
8.80	0.08	s	Core CH
8.85	0.2	s	Ethyl CH*

Table 12 ^{1}H nmr summary of the product of the co-polymerisation of diethyl 3-hydroxyglutarate and triethyl 1,3,5-benzenetricarboxylate in a ratio of 90:1

Peak/ppm	Integral	Multiplicity	Assignment
0.93	1	t	Butyl CH_3
1.26	16.25	t	Ethyl CH_3
1.33	0.67	m	Butyl CH_2
1.44	1	t	Ethyl CH_3*
1.64	0.67	m	Butyl CH_2
2.54	4.83	m	Focal CH_2
2.69	12.5	m	Polymeric CH_2
4.14	11.58	m	Ethyl OCH_2
4.44	1.83	m	Focal CH
5.56	2.92	m	Polymeric CH
7.53	0.43	t^+	Core CH
8.18	0.11	m	Core CH
8.23	0.98	dd	Ethyl CH*
8.63	0.06	t	Core CH
8.69	0.49	t	Ethyl CH*

Table 13 ^{1}H nmr summary of the product of the co-polymerisation of diethyl 3-hydroxyglutarate and diethyl isophthalate in a ratio of 25:1

t^+ indicates an overlapping triplet

Peak/ppm	Integral	Multiplicity	Assignment
0.93	1.83	t	Butyl CH_3
1.26	31	t	Ethyl CH_3
1.33	0.83	m	Butyl CH_2
1.44	1	t	Ethyl CH_3*
1.64	1	m	Butyl CH_2
2.54	9.67	m	Focal CH_2
2.69	24.17	m	Polymeric CH_2
4.14	22	m	Ethyl OCH_2
4.44	2.83	m	Focal CH
5.56	5.83	m	Polymeric CH
7.53	0.17	t^+	Core CH
8.18	0.03	m	Core CH
8.23	0.31	dd	Ethyl CH*
8.63	0.03	t	Core CH
8.69	0.15	t	Ethyl CH*

Table 14 ^{1}H nmr summary of the product of the co-polymerisation of diethyl 3-hydroxyglutarate and diethyl isophthalate in a ratio of 50:1

Peak/ppm	Integral	Multiplicity	Assignment
0.93	1.5	t	Butyl CH_3
1.26	25	t	Ethyl CH_3
1.33	0.75	m	Butyl CH_2
1.44	1	t	Ethyl CH_3*
1.64	1.75	m	Butyl CH_2
2.54	11.75	m	Focal CH_2
2.69	11.63	m	Polymeric CH_2
4.14	17.75	m	Ethyl OCH_2
4.44	3.13	m	Focal CH
5.56	2.63	m	Polymeric CH
7.53	0.12	t^+	Core CH
8.18	0.02	m	Core CH
8.23	0.20	dd	Ethyl CH*
8.63	0.02	t	Core CH
8.69	0.10	t	Ethyl CH*

Table 15 ^{1}H nmr summary of the product of the co-polymerisation of diethyl 3-hydroxyglutarate and diethyl isophthalate in a ratio of 50:1

Peak/ppm	Integral	Multiplicity	Assignment
0.93	1.83	t	Butyl CH_3
1.26	29.5	t	Ethyl CH_3
1.33	1.17	m	Butyl CH_2
1.44	1	t	Ethyl CH_3*
1.64	1.33	m	Butyl CH_2
2.54	6.33	m	Focal CH_2
2.69	28.67	m	Polymeric CH_2
4.14	21	m	Ethyl OCH_2
4.44	1.83	m	Focal CH
5.56	6.83	m	Polymeric CH
7.53	-	t^+	Core CH
8.18	-	dd	Core CH
8.23	-	dd	Ethyl CH*
8.63	-	t	Core CH
8.69	-	t	Ethyl CH*

Table 16 ^{1}H nmr summary of the product of the co-polymerisation of diethyl 3-hydroxyglutarate and diethyl isophthalate in a ratio of 75:1

Peak/ppm	Integral	Multiplicity	Assignment
0.93	1.43	t	Butyl CH_3
1.26	27.57	t	Ethyl CH_3
1.33	1.14	m	Butyl CH_2
1.44	1	t	Ethyl CH_3*
1.64	1.14	m	Butyl CH_2
2.54	9	m	Focal CH_2
2.69	21.14	m	Polymeric CH_2
4.14	19.71	m	Ethyl OCH_2
4.44	2.43	m	Focal CH
5.56	4.86	m	Polymeric CH
7.53	0.11	t+	Core CH
8.18	0.03	m	Core CH
8.23	0.24	dd	Ethyl CH*
8.63	0.01	t	Core CH
8.69	0.10	t	Ethyl CH*

Table 17 ^{1}H nmr summary of the product of the co-polymerisation of diethyl 3-hydroxyglutarate and diethyl isophthalate in a ratio of 75:1

Peak/ppm	Integral	Multiplicity	Assignment
0.93	1.4	t	Butyl CH_3
1.26	38.6	t	Ethyl CH_3
1.33	1.2	m	Butyl CH_2
1.44	1	t	Ethyl CH_3*
1.64	1.2	m	Butyl CH_2
2.54	11.6	m	Focal CH_2
2.69	30.6	m	Polymeric CH_2
4.14	27.4	m	Ethyl OCH_2
4.44	3	m	Focal CH
5.56	7.6	m	Polymeric CH
7.53	0.14	t^+	Core CH
8.18	0.019	m	Core CH
8.23	0.20	dd	Ethyl CH*
8.63	0.018	t	Core CH
8.69	0.12	t	Ethyl CH*

Table 18 ^{1}H nmr summary of the product of the co-polymerisation of diethyl 3-hydroxyglutarate and diethyl isophthalate in a ratio of 90:1

Peak/ppm	Integral	Multiplicity	Assignment
0.93	3	t	Butyl CH_3
1.26	54	t	Ethyl CH_3
1.33	2	m	Butyl CH_2
1.44	1	t	Ethyl CH_3*
1.64	2	m	Butyl CH_2
2.54	14.33	m	Focal CH_2
2.69	45.33	m	Polymeric CH_2
4.14	38	m	Ethyl OCH_2
4.44	3.67	m	Focal CH
5.56	11	m	Polymeric CH
7.53	0.09	t+	Core CH
8.18	0.03	m	Core CH
8.23	0.20	dd	Ethyl CH*
8.63	0.015	t	Core CH
8.69	0.09	t	Ethyl CH*

Table 19 ^{1}H nmr summary of the product of the co-polymerisation of diethyl 3-hydroxyglutarate and diethyl isophthalate in a ratio of 150:1

Ratio 25:1		Ratio 50:1	
Peak/ppm	Assignment	Peak/ppm	Assignment
13.85	Butyl CH_3	13.65	Butyl CH_3
14.12	Ethyl CH_3	14.10	Ethyl CH_3
14.30	Ethyl CH_3*	14.23	Ethyl CH_3*
19.06	Butyl CH_2	19.04	Butyl CH_2
30.51	Butyl CH_2	30.48	Butyl CH_2
38.24	Polymeric CH_2	38.25	Polymeric CH_2
40.62	Focal CH_2	40.66	Focal CH_2
41.12	Butyl CH_2	41.10	Butyl CH_2
60.84	Ethyl OCH_2	52.61	Methyl CH_3*
61.51	Ethyl OCH_2*	60.86	Ethyl OCH_2
61.70	Ethyl OCH_2*	61.50	Ethyl OCH_2*
64.74	Focal CH	64.71	Focal CH
67.20	Polymeric CH	67.13	Polymeric CH
131.50	Aromatic CH	131.48	Aromatic CH
134.42	Aromatic C	134.45	Aromatic C
168.60	C=O	169.67	C=O
169.68	C=O	169.75	C=O
-	-	169.95	C=O
-	-	170.42	C=O
-	-	171.62	C=O

Table 20 ^{13}C nmr summary of the products of the co-polymerisation of diethyl 3-hydroxyglutarate and trimethyl 1,3,5-benzenetricarboxylate

Ratio 50:1		Ratio 75:1	
Peak/ppm	Assignment	Peak/ppm	Assignment
13.63	Butyl CH_3	13.66	Butyl CH_3
14.08	Ethyl CH_3	14.12	Ethyl CH_3
14.26	Ethyl CH_3*	14.21	Ethyl CH_3*
19.02	Butyl CH_2	19.05	Butyl CH_2
30.47	Butyl CH_2	30.49	Butyl CH_2
38.31	Polymeric CH_2	38.24	Polymeric CH_2
40.65	Focal CH_2	40.66	Focal CH_2
41.16	Butyl CH_2	41.17	Butyl CH_2
60.81	Ethyl OCH_2	60.85	Ethyl OCH_2
61.66	Ethyl OCH_2*	61.51	Ethyl OCH_2*
64.71	Focal CH	64.71	Focal CH
67.18	Polymeric CH	67.21	Polymeric CH
131.38	Aromatic CH	131.48	Aromatic CH
134.37	Aromatic C	134.42	Aromatic C
168.56	C=O	168.64	C=O
169.65	C=O	169.68	C=O
169.73	C=O	169.76	C=O
169.89	C=O	170.32	C=O
170.27	C=O	171.79	C=O
171.59	C=O	-	-

Table 21 ^{13}C nmr summary of the products of the co-polymerisation of diethyl 3-hydroxyglutarate and trimethyl 1,3,5-benzenetricarboxylate

Ratio 90:1		Ratio 90:1	
Peak/ppm	Assignment	Peak/ppm	Assignment
13.66	Butyl CH_3	13.63	Butyl CH_3
14.12	Ethyl CH_3	14.08	Ethyl CH_3
14.24	Ethyl CH_3*	14.26	Ethyl CH_3*
19.05	Butyl CH_2	19.02	Butyl CH_2
30.50	Butyl CH_2	30.47	Butyl CH_2
38.24	Polymeric CH_2	38.21	Polymeric CH_2
40.61	Focal CH_2	40.65	Focal CH_2
41.11	Butyl CH_2	41.16	Butyl CH_2
60.83	Ethyl OCH_2	60.81	Ethyl OCH_2
61.64	Ethyl OCH_2*	61.53	Ethyl OCH_2*
64.72	Focal CH	64.70	Focal CH
67.20	Polymeric CH	67.19	Polymeric CH
131.35	Aromatic CH	131.44	Aromatic CH
134.40	Aromatic C	134.38	Aromatic C
168.59	C=O	168.60	C=O
169.68	C=O	169.73	C=O
-	-	170.39	C=O
-	-	171.59	C=O
-	-	171.75	C=O

Table 22 ^{13}C nmr summary of the products of the co-polymerisation of diethyl 3-hydroxyglutarate and trimethyl 1,3,5-benzenetricarboxylate

Ratio 25:1		Ratio 50:1	
Peak/ppm	Assignment	Peak/ppm	Assignment
13.65	Butyl CH_3	13.65	Butyl CH_3
14.10	Ethyl CH_3	14.11	Ethyl CH_3
14.28	Ethyl CH_3*	14.23	Ethyl CH_3*
19.03	Butyl CH_2	19.04	Butyl CH_2
30.48	Butyl CH_2	30.49	Butyl CH_2
38.21	Polymeric CH_2	38.33	Polymeric CH_2
40.60	Focal CH_2	40.60	Focal CH_2
41.16	Butyl CH_2	41.17	Butyl CH_2
60.81	Ethyl OCH_2	60.82	Ethyl OCH_2
61.67	Ethyl OCH_2*	61.58	Ethyl OCH_2*
64.71	Focal CH	64.72	Focal CH
67.18	Polymeric CH	67.18	Polymeric CH
131.39	Aromatic CH	131.40	Aromatic CH
134.39	Aromatic C	134.41	Aromatic C
168.58	C=O	168.58	C=O
169.66	C=O	169.66	C=O
		169.75	C=O
-	-	170.30	C=O

Table 23 ^{13}C nmr summary of the products of the co-polymerisation of diethyl 3-hydroxyglutarate and triethyl 1,3,5-benzenetricarboxylate

Ratio 50:1		Ratio 75:1	
Peak/ppm	Assignment	Peak/ppm	Assignment
13.61	Butyl CH_3	13.64	Butyl CH_3
14.06	Ethyl CH_3	14.11	Ethyl CH_3
14.25	Ethyl CH_3*	14.23	Ethyl CH_3*
19.00	Butyl CH_2	19.04	Butyl CH_2
30.44	Butyl CH_2	30.48	Butyl CH_2
38.22	Polymeric CH_2	38.33	Polymeric CH_2
40.60	Focal CH_2	40.60	Focal CH_2
41.14	Butyl CH_2	41.17	Butyl CH_2
60.73	Ethyl OCH_2	60.82	Ethyl OCH_2
61.64	Ethyl OCH_2*	61.57	Ethyl OCH_2*
64.69	Focal CH	64.72	Focal CH
67.17	Polymeric CH	67.18	Polymeric CH
131.36	Aromatic CH	131.39	Aromatic CH
134.40	Aromatic C	134.41	Aromatic C
168.55	C=O	168.58	C=O
169.60	C=O	169.67	C=O
169.64	C=O	169.75	C=O
169.73	C=O	169.95	C=O
169.91	C=O	170.30	C=O
170.26	C=O	170.50	C=O
170.37	C=O	171.78	C=O
171.57	C=O	-	-
171.73	C=O	-	-

Table 24 ^{13}C nmr summary of the products of the co-polymerisation of diethyl 3-hydroxyglutarate and triethyl 1,3,5-benzenetricarboxylate

Ratio 90:1		Ratio 90:1	
Peak/ppm	Assignment	Peak/ppm	Assignment
13.63	Butyl CH_3	13.62	Butyl CH_3
14.08	Ethyl CH_3	14.08	Ethyl CH_3
14.24	Ethyl CH_3*	14.23	Ethyl CH_3*
19.01	Butyl CH_2	19.01	Butyl CH_2
30.46	Butyl CH_2	30.46	Butyl CH_2
38.19	Polymeric CH_2	38.20	Polymeric CH_2
40.59	Focal CH_2	40.59	Focal CH_2
41.14	Butyl CH_2	41.15	Butyl CH_2
60.79	Ethyl OCH_2	60.78	Ethyl OCH_2
61.62	Ethyl OCH_2*	61.59	Ethyl OCH_2*
64.70	Focal CH	64.70	Focal CH
67.17	Polymeric CH	67.16	Polymeric CH
131.36	Aromatic CH	131.37	Aromatic CH
134.40	Aromatic C	134.39	Aromatic C
168.56	C=O	168.55	C=O
168.64	C=O	169.63	C=O
169.65	C=O	169.72	C=O
169.73	C=O	170.26	C=O
169.89	C=O	170.38	C=O
170.28	C=O	-	-
170.39	C=O	-	-
171.59	C=O	-	-
171.75	C=O	-	-

Table 25 ^{13}C nmr summary of the products of the co-polymerisation of diethyl 3-hydroxyglutarate and triethyl 1,3,5-benzenetricarboxylate

Ratio 25:1		Ratio 50:1	
Peak/ppm	Assignment	Peak/ppm	Assignment
13.62	Butyl CH_3	13.64	Butyl CH_3
14.08	Ethyl CH_3	14.09	Ethyl CH_3
14.26	Ethyl CH_3*	14.23	Ethyl CH_3*
19.00	Butyl CH_2	19.02	Butyl CH_2
30.46	Butyl CH_2	30.47	Butyl CH_2
38.19	Polymeric CH_2	38.32	Polymeric CH_2
40.60	Focal CH_2	40.65	Focal CH_2
41.15	Butyl CH_2	41.10	Butyl CH_2
60.79	Ethyl OCH_2	60.81	Ethyl OCH_2
61.28	Ethyl OCH_2*	61.48	Ethyl OCH_2*
64.70	Focal CH	64.71	Focal CH
67.17	Polymeric CH	67.18	Polymeric CH
128.45	Aromatic CH	128.46	Aromatic CH
130.53	Aromatic CH	130.55	Aromatic CH
130.81	Aromatic CH	130.80	Aromatic CH
133.61	Aromatic C	133.63	Aromatic C
165.77	C=O*	168.61	C=O
168.60	C=O	169.74	C=O
169.73	C=O	169.90	C=O
169.92	C=O	170.28	C=O
170.26	C=O	170.46	C=O
170.38	C=O	171.60	C=O
171.58	C=O	171.76	C=O
171.74	C=O	-	-

Table 26 ^{13}C nmr summary of the products of the co-polymerisation of diethyl 3-hydroxyglutarate and diethyl isophthalate

Ratio 50:1		Ratio 75:1	
Peak/ppm	Assignment	Peak/ppm	Assignment
13.60	Butyl CH_3	13.65	Butyl CH_3
14.04	Ethyl CH_3	14.11	Ethyl CH_3
14.24	Ethyl CH_3*	14.22	Ethyl CH_3*
19.01	Butyl CH_2	19.04	Butyl CH_2
30.43	Butyl CH_2	30.49	Butyl CH_2
38.29	Polymeric CH_2	38.22	Polymeric CH_2
40.61	Focal CH_2	40.61	Focal CH_2
41.14	Butyl CH_2	41.10	Butyl CH_2
60.71	Ethyl OCH_2	60.81	Ethyl OCH_2
61.24	Ethyl OCH_2*	64.72	Focal CH
64.67	Focal CH	67.18	Polymeric CH
67.08	Polymeric CH	128.46	Aromatic CH
128.44	Aromatic CH	130.54	Aromatic CH
130.51	Aromatic CH	130.82	Aromatic CH
133.60	Aromatic C	133.62	Aromatic C
168.60	C=O	168.58	C=O
169.64	C=O	169.66	C=O
169.73	C=O	170.30	C=O
169.91	C=O	-	-
170.25	C=O	-	-
170.36	C=O	-	-
171.57	C=O	-	-
171.72	C=O	-	-

Table 27 ^{13}C nmr summary of the products of the co-polymerisation of diethyl 3-hydroxyglutarate and diethyl isophthalate

Ratio 75:1		Ratio 90:1	
Peak/ppm	Assignment	Peak/ppm	Assignment
13.62	Butyl CH_3	13.64	Butyl CH_3
14.07	Ethyl CH_3	14.11	Ethyl CH_3
14.21	Ethyl CH_3*	14.22	Ethyl CH_3*
19.01	Butyl CH_2	19.04	Butyl CH_2
30.45	Butyl CH_2	30.48	Butyl CH_2
38.31	Polymeric CH_2	38.22	Polymeric CH_2
40.65	Focal CH_2	40.61	Focal CH_2
41.15	Butyl CH_2	41.12	Butyl CH_2
60.80	Ethyl OCH_2	60.82	Ethyl OCH_2
61.24	Ethyl OCH_2*	64.72	Focal CH
64.69	Focal CH	67.30	Polymeric CH
67.17	Polymeric CH	128.46	Aromatic CH
128.45	Aromatic CH	130.54	Aromatic CH
130.53	Aromatic CH	133.64	Aromatic C
133.61	Aromatic C	168.58	C=O
168.56	C=O	169.63	C=O
168.61	C=O	169.67	C=O
169.65	C=O	169.91	C=O
169.73	C=O	170.30	C=O
169.89	C=O	170.41	C=O
170.27	C=O	171.54	C=O
170.38	C=O	171.70	C=O
171.58	C=O	-	-
171.74	C=O	-	-

Table 28 ^{13}C nmr summary of the products of the co-polymerisation of diethyl 3-hydroxyglutarate and diethyl isophthalate

Ratio 150:1	
Peak/ppm	Assignment
13.63	Butyl CH_3
14.09	Ethyl CH_3
14.20	Ethyl CH_3*
19.03	Butyl CH_2
30.45	Butyl CH_2
38.20	Polymeric CH_2
40.60	Focal CH_2
41.16	Butyl CH_2
60.81	Ethyl OCH_2
64.71	Focal CH
67.18	Polymeric CH
128.44	Aromatic CH
130.54	Aromatic CH
133.61	Aromatic C
168.56	C=O
168.61	C=O
169.65	C=O
169.74	C=O
170.28	C=O
170.37	C=O
171.56	C=O
171.74	C=O

Table 29 ^{13}C nmr summary of the products of the co-polymerisation of diethyl 3-hydroxyglutarate and diethyl isophthalate

262#2	Na+	BuO	2xBuO	Cyc.	Dehyd	1 arm	2 arms	3 arms
Peak mass								
384.54	**1.997**	1.896	1.820	2.288	2.111	0.605	0.516	0.427
543.16	**3.001**	2.900	2.824	3.292	3.115	1.609	1.520	**1.431**
570.19	**3.172**	3.071	2.995	3.463	3.286	1.780	1.691	1.602
672.93	3.822	3.721	3.645	4.113	3.936	2.430	2.341	2.253
687.35	3.914	3.812	3.736	4.205	**4.028**	2.521	2.433	2.344
701.77	**4.005**	3.904	3.828	4.296	4.119	2.612	2.524	2.435
728.81	4.176	4.075	3.999	4.467	4.290	2.784	2.695	2.606
844.17	4.906	4.805	4.729	5.197	**5.020**	3.514	3.425	3.337
858.59	4.997	4.896	4.820	5.289	5.111	3.605	3.516	3.428
874.81	5.100	**4.999**	4.923	5.391	5.214	3.708	3.619	3.530
887.43	5.180	5.079	**5.003**	5.471	5.294	3.788	3.699	3.610
1002.79	5.910	5.809	5.733	6.201	**6.024**	4.518	4.429	4.340
1017.21	**6.001**	5.900	5.824	6.292	6.115	4.609	4.520	4.432
1033.43	6.104	**6.003**	5.927	6.395	6.218	4.712	4.623	4.534
1046.05	6.184	6.083	**6.007**	6.475	6.298	4.791	4.703	4.614
1161.41	6.914	6.813	6.737	7.205	**7.028**	5.522	5.433	5.344
1175.83	**7.005**	6.904	6.828	7.296	7.119	5.613	5.524	5.436
1204.67	7.188	7.087	**7.011**	7.479	7.302	5.795	5.707	5.618
1320.03	7.918	7.817	7.741	8.209	8.032	6.526	6.437	6.348
1334.45	**8.009**	7.908	7.832	8.300	8.123	6.617	6.528	6.440
1361.48	8.180	8.079	**8.003**	8.471	8.294	6.788	6.699	6.611
1478.64	8.922	8.821	8.745	9.213	9.036	7.529	7.441	7.352
1491.26	**9.002**	8.900	8.824	9.293	9.116	7.609	7.521	7.432
1520.1	9.184	9.083	**9.007**	9.475	9.298	7.792	7.703	7.615
1649.88	**10.006**	9.904	9.828	10.297	10.119	8.613	8.525	8.436

Table 30 MALDI-TOF MS data of the product of the copolymerisation of diethyl 3-hydroxyglutarate and trimethyl 1,3,5-benzenetricarboxylate (Ratio 25:1)

280#2	Na+	BuO	Cyc.	Dehyd.	Core	Core BuO	Core 2BuO	Core 3BuO
Peak mass								
297.28	1.445	1.268	1.736	1.559	-0.125	-0.302	-0.479	-0.656
329.89	1.651	1.474	1.942	1.765	0.082	-0.096	-0.273	-0.450
356.57	1.820	1.643	2.111	1.934	0.250	0.073	-0.104	-0.281
380.28	**1.970**	1.793	2.261	2.084	0.401	0.223	**0.046**	-0.131
538.39	**2.971**	2.794	3.262	3.085	1.401	1.224	**1.047**	0.870
554.04	3.070	2.893	3.361	3.184	1.500	1.323	1.146	**0.969**
565.21	3.141	**2.963**	3.432	3.254	1.571	1.394	1.217	1.039
583.09	3.254	3.077	3.545	3.368	1.684	1.507	1.330	1.152
594.26	3.324	3.147	3.616	3.438	1.755	1.578	1.400	1.223
694.47	**3.959**	3.781	4.250	4.073	2.389	2.212	**2.035**	1.857
710.47	4.060	3.883	4.351	4.174	2.490	2.313	2.136	1.959
721.14	4.127	3.950	4.419	4.241	2.558	2.381	2.203	**2.026**

739.52	4.244	**4.067**	4.535	4.358	2.674	2.497	2.320	2.143
853.49	**4.965**	4.788	5.256	5.079	3.396	3.218	**3.041**	2.864
869.13	5.064	4.887	5.355	5.178	3.494	3.317	3.140	2.963
880.31	5.135	**4.958**	5.426	5.249	3.565	3.388	3.211	**3.034**
1009.92	5.955	5.778	6.246	6.069	4.386	4.208	**4.031**	3.854
1023.48	**6.041**	5.864	6.332	6.155	4.471	4.294	4.117	3.940
1036.74	6.125	**5.948**	6.416	6.239	4.555	4.378	4.201	**4.024**
1065.79	6.309	6.132	6.600	6.423	4.739	4.562	4.385	4.208
1166.36	6.945	6.768	7.236	**7.059**	5.376	5.198	**5.021**	4.844
1182	**7.044**	6.867	7.335	7.158	5.475	5.297	5.120	4.943
1195.39	7.129	**6.952**	7.420	7.243	5.559	5.382	5.205	5.028
1325.02	7.949	7.772	8.241	8.063	6.380	6.203	**6.025**	5.848
1340.63	**8.048**	7.871	8.339	8.162	6.479	6.301	6.124	5.947
1351.84	8.119	**7.942**	8.410	8.233	6.550	6.372	6.195	**6.018**
1405.47	8.459	8.281	8.750	8.573	6.889	6.712	6.535	6.357
1481.46	8.940	8.762	9.231	**9.054**	7.370	7.193	**7.016**	6.838
1494.76	**9.024**	8.847	9.315	9.138	7.454	7.277	7.100	6.923
1510.51	9.123	**8.946**	9.415	9.237	7.554	7.377	7.199	**7.022**
1523.92	9.208	**9.031**	9.499	9.322	7.639	7.462	7.284	7.107
1637.89	9.930	9.752	10.221	**10.044**	8.360	8.183	**8.006**	7.828
1664.7	10.099	9.922	10.391	10.213	8.530	8.353	8.175	**7.998**
1689.29	10.255	10.078	10.546	10.369	8.685	8.508	8.331	8.154
1794.13	10.919	10.741	11.210	**11.032**	9.349	9.172	**8.994**	8.817
1823.77	11.106	10.929	11.397	11.220	9.537	9.359	9.182	**9.005**
1879.24	11.457	11.280	11.748	11.571	9.888	9.710	9.533	9.356
1952.99	11.924	11.747	12.215	**12.038**	10.354	10.177	**10.000**	9.823
1979.8	12.094	11.916	12.385	12.208	10.524	10.347	10.170	**9.992**
2107.18	12.900	12.723	13.191	**13.014**	11.330	11.153	**10.976**	10.799
2132.03	**13.057**	12.880	13.348	13.171	11.488	11.310	11.133	**10.956**
2265.42	13.901	13.724	14.193	**14.015**	12.332	12.155	**11.977**	11.800
2292.09	14.070	13.893	14.361	14.184	12.501	12.323	12.146	**11.969**
2422.51	14.896	14.718	15.187	**15.010**	13.326	13.149	**12.972**	12.794
2452.15	15.083	14.906	15.374	15.197	13.514	13.336	13.159	**12.982**

Table 31 MALDI-TOF MS data of the product of the copolymerisation of diethyl 3-hydroxyglutarate and triethyl 1,3,5-benzenetricarboxylate (Ratio 90:1)

lmh305#1	Na+	BuO	Cyc.	Dehyd.	Core	Core BuO	Core 2BuO	Core 3BuO
Peak mass								
299.38	1.458	1.281	1.749	1.572	0.344	0.167	**-0.010**	-0.187
332.52	1.668	1.491	1.959	1.782	0.554	0.377	0.199	**0.022**
345.77	1.752	1.574	**2.043**	1.866	0.638	0.461	0.283	0.106
362.34	1.857	1.679	2.148	**1.971**	0.743	0.565	0.388	0.211
385.54	**2.003**	1.826	2.295	2.117	0.889	0.712	0.535	0.358
542.94	**3.000**	2.822	3.291	3.114	1.886	1.708	1.531	1.354
551.23	3.052	2.875	3.343	3.166	1.938	1.761	1.584	1.407
559.51	3.104	2.927	3.396	3.218	**1.991**	1.813	1.636	1.459
571.11	3.178	**3.001**	3.469	3.292	2.064	1.887	1.710	1.532
587.68	3.283	3.106	3.574	3.397	2.169	**1.992**	1.814	1.637
639.04	3.608	3.431	3.899	3.722	2.494	2.317	2.139	**1.962**
667.21	3.786	3.609	4.077	3.900	2.672	2.495	2.318	2.141
702	**4.006**	3.829	4.297	4.120	2.892	2.715	2.538	2.361
859.4	**5.003**	4.825	5.294	5.116	3.889	3.711	3.534	3.357
887.57	5.181	**5.004**	5.472	5.295	4.067	3.890	3.712	3.535
1018.46	**6.009**	5.832	6.300	6.123	4.895	4.718	4.541	4.364
1044.97	6.177	**6.000**	6.468	6.291	5.063	4.886	4.709	4.531
1175.86	**7.005**	6.828	7.297	7.119	5.892	5.714	5.537	5.360
1204.03	7.184	**7.007**	7.475	7.298	6.070	5.893	5.715	5.538
1334.92	**8.012**	7.835	8.303	8.126	6.898	6.721	6.544	6.367
1363.09	8.190	**8.013**	8.482	8.304	7.077	6.899	6.722	6.545
1492.32	**9.008**	8.831	9.299	9.122	7.894	7.717	7.540	7.363

Table 32. MALDI-TOF MS data of the product of the copolymerisation of diethyl 3-hydroxyglutarate and diethyl isophthalate (Ratio 25:1)

Appendix 4

Analytical data for Chapter 6

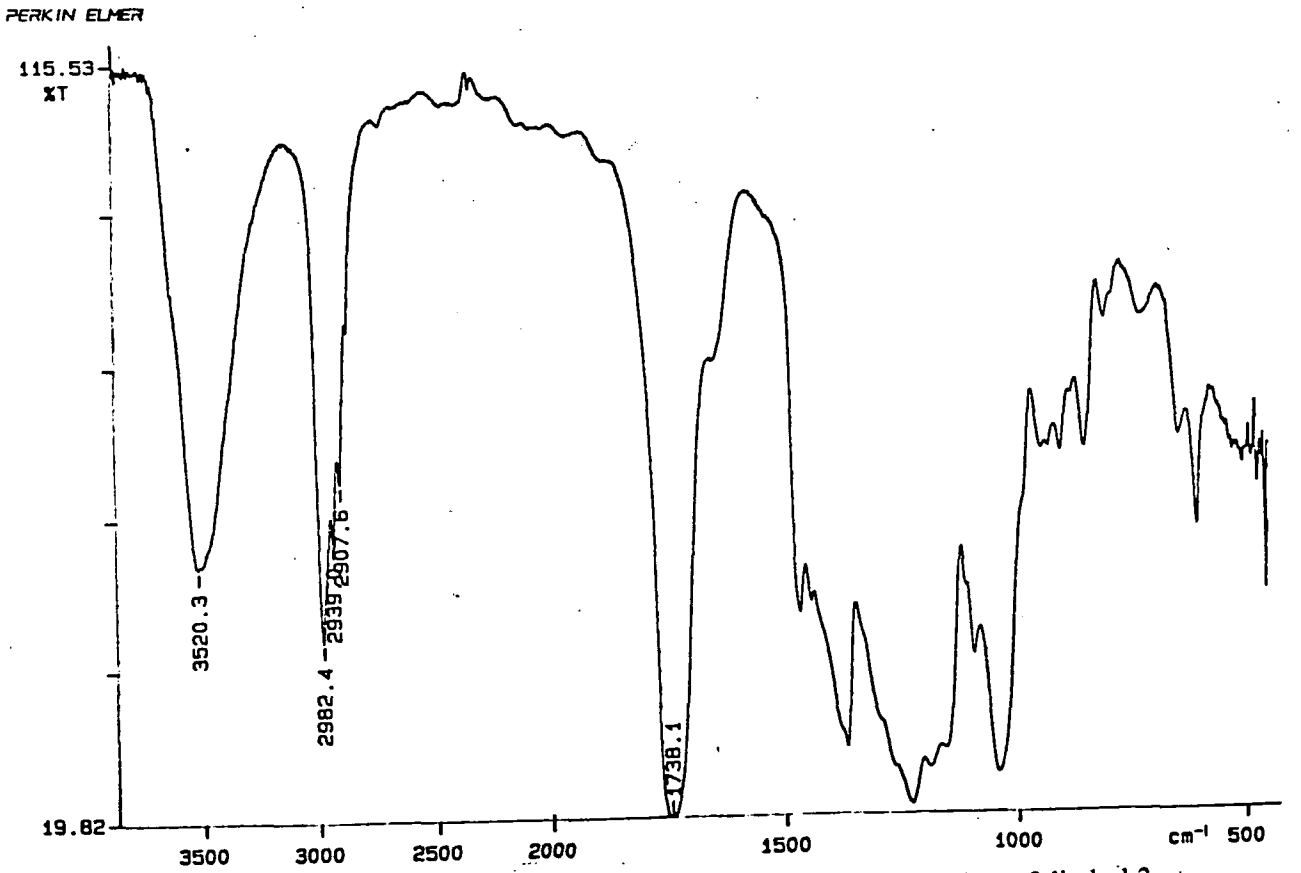

Appendix 4.1 FTIR spectrum of the product of the co-polymerisation of diethyl 3-hydroxyglutarate and PTA (Time of addition = 0 hours)

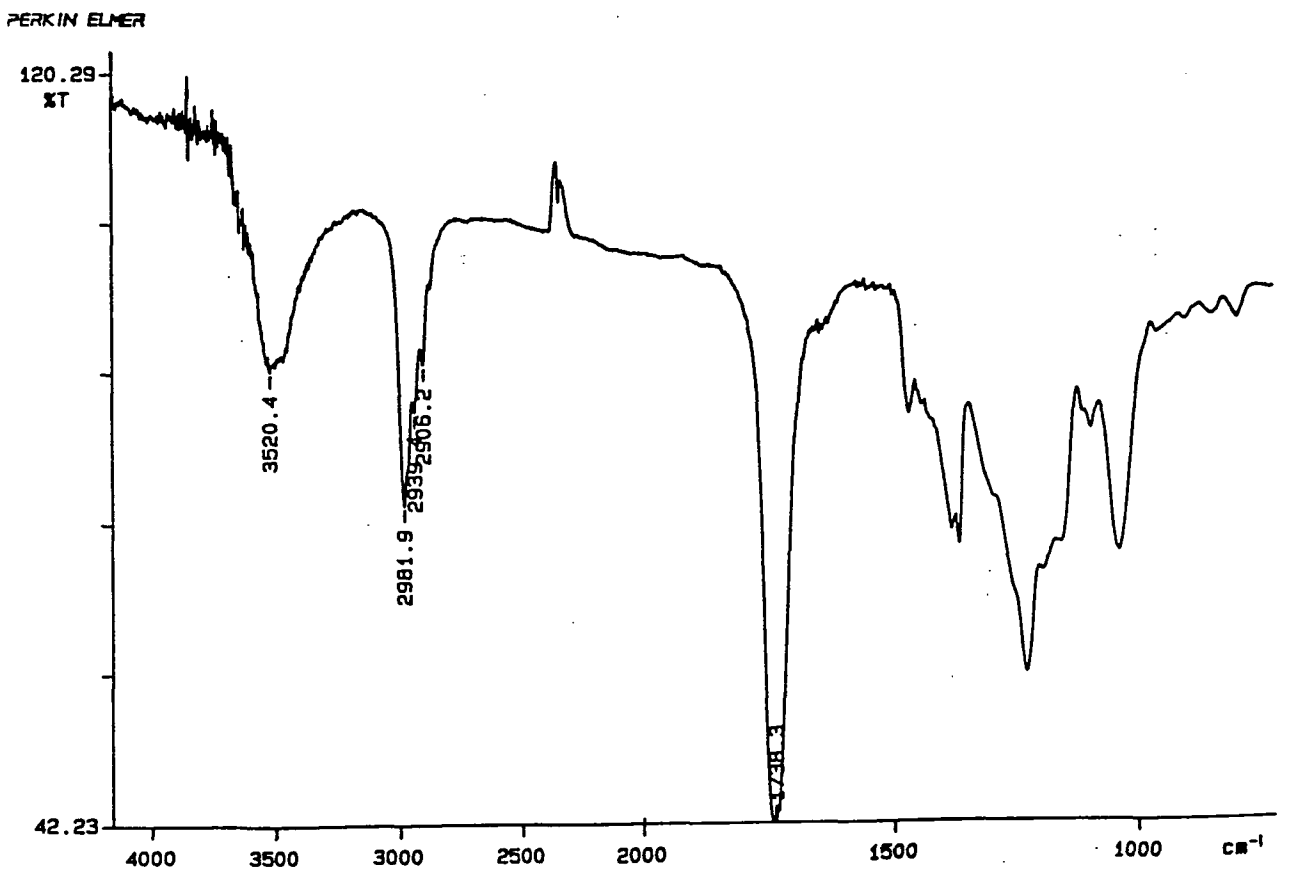

Appendix 4.2 FTIR spectrum of the product of the co-polymerisation of diethyl 3-hydroxyglutarate and PTA (Time of addition = 2 hours)

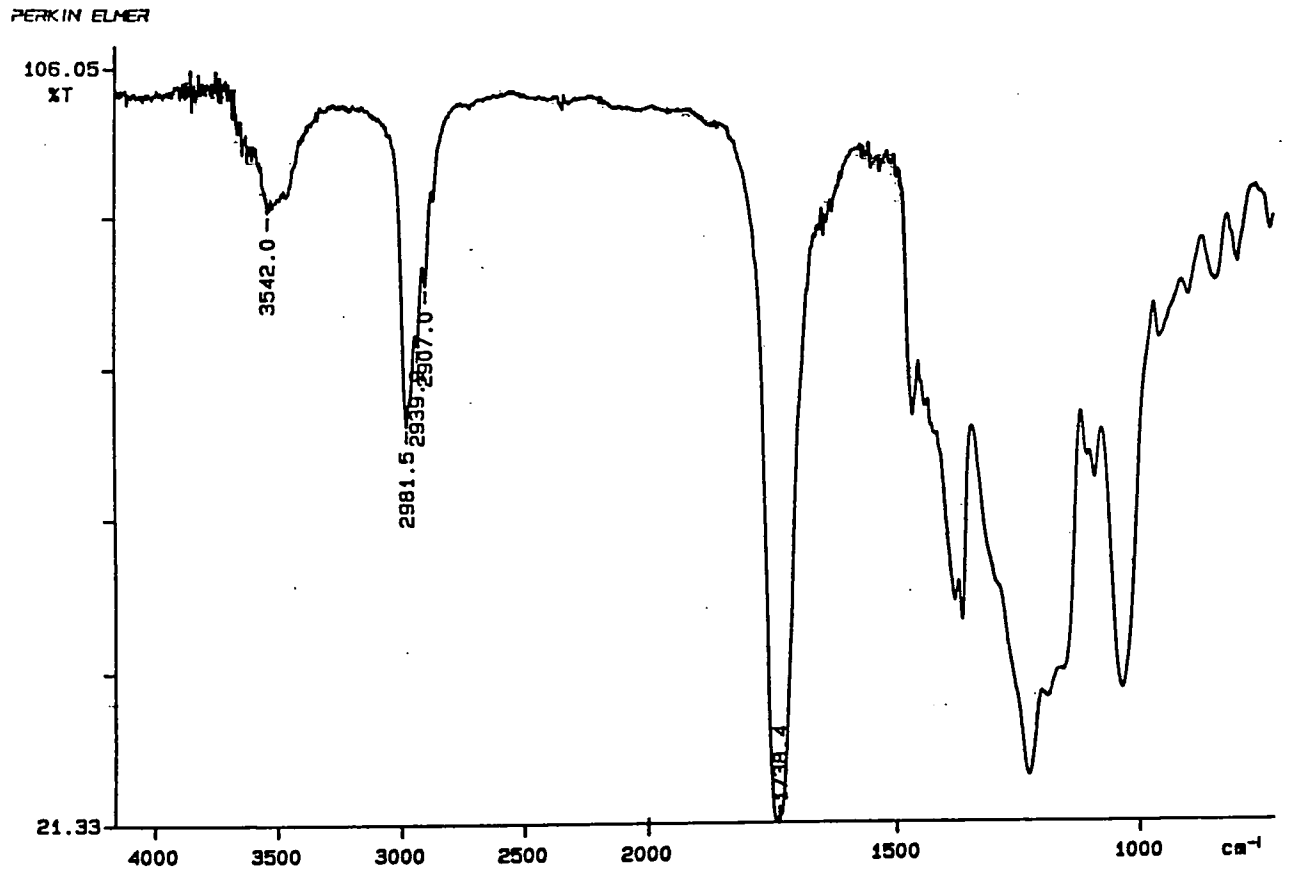

Appendix 4.3 FTIR spectrum of the product of the co-polymerisation of diethyl 3-hydroxyglutarate and PTA (Time of addition = 3 hours)

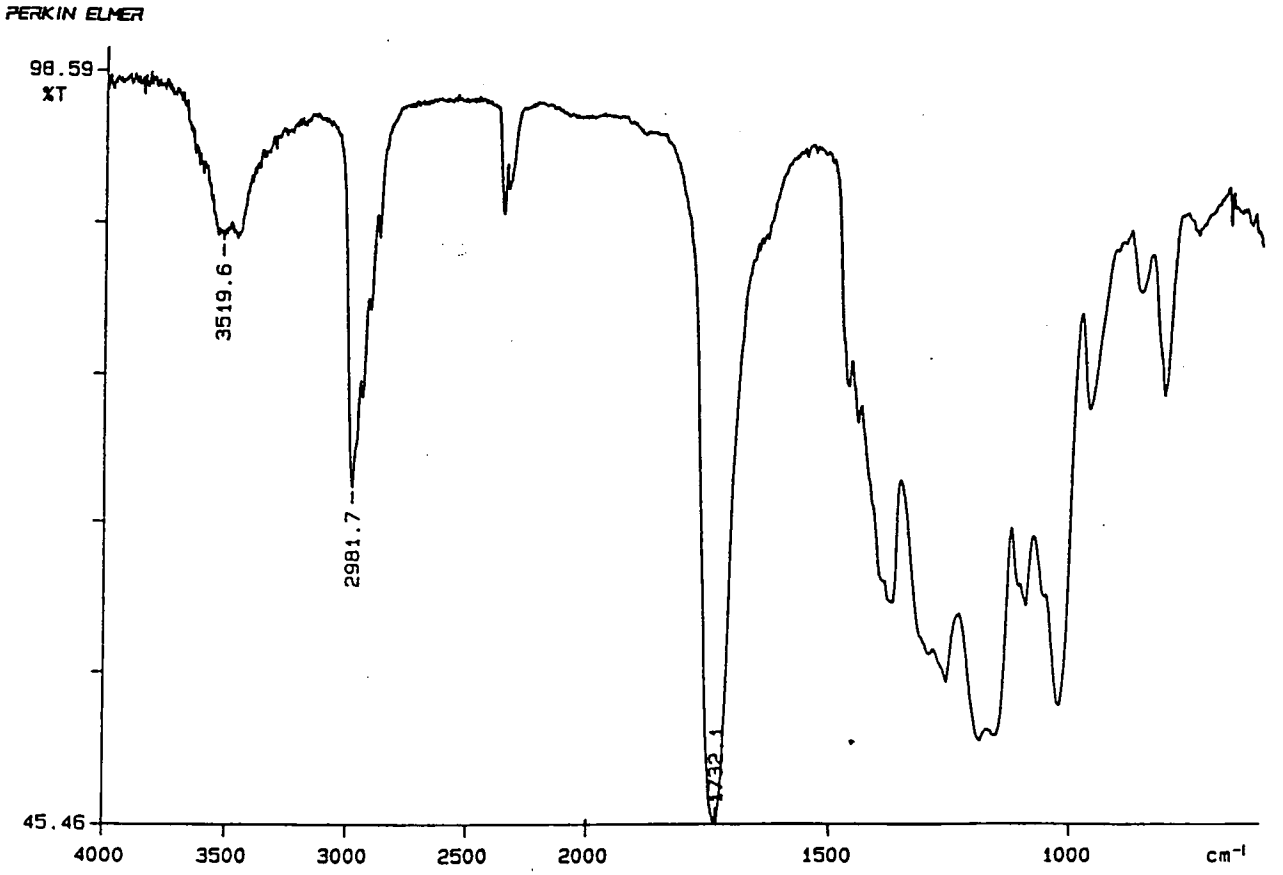

Appendix 4.4 FTIR spectrum of the product of the co-polymerisation of diethyl 3-hydroxyglutarate and 1,5-pentanediol (Time of addition = 2 hours)

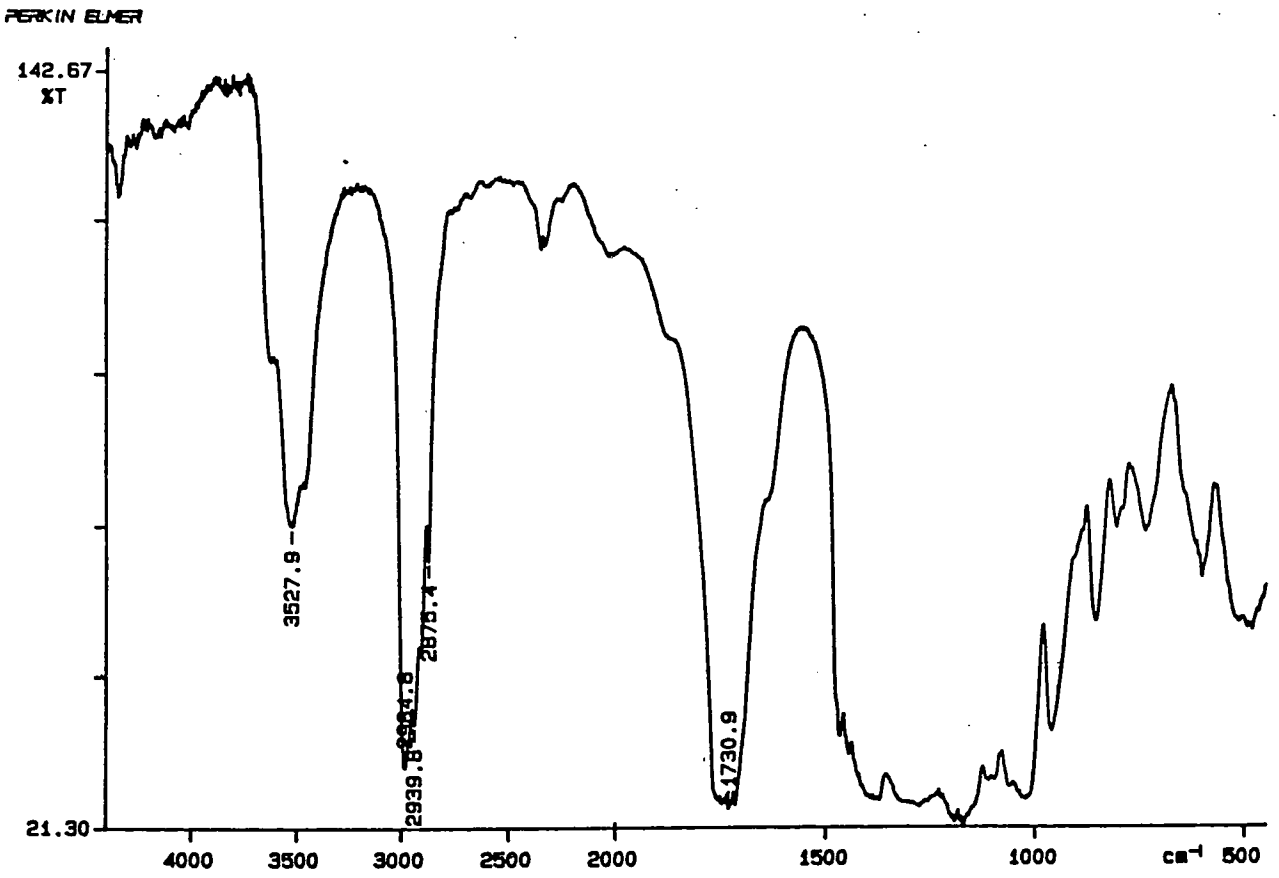

Appendix 4.5 FTIR spectrum of the product of the co-polymerisation of diethyl 3-hydroxyglutarate and 1,5-pentanediol (Time of addition = 3 hours)

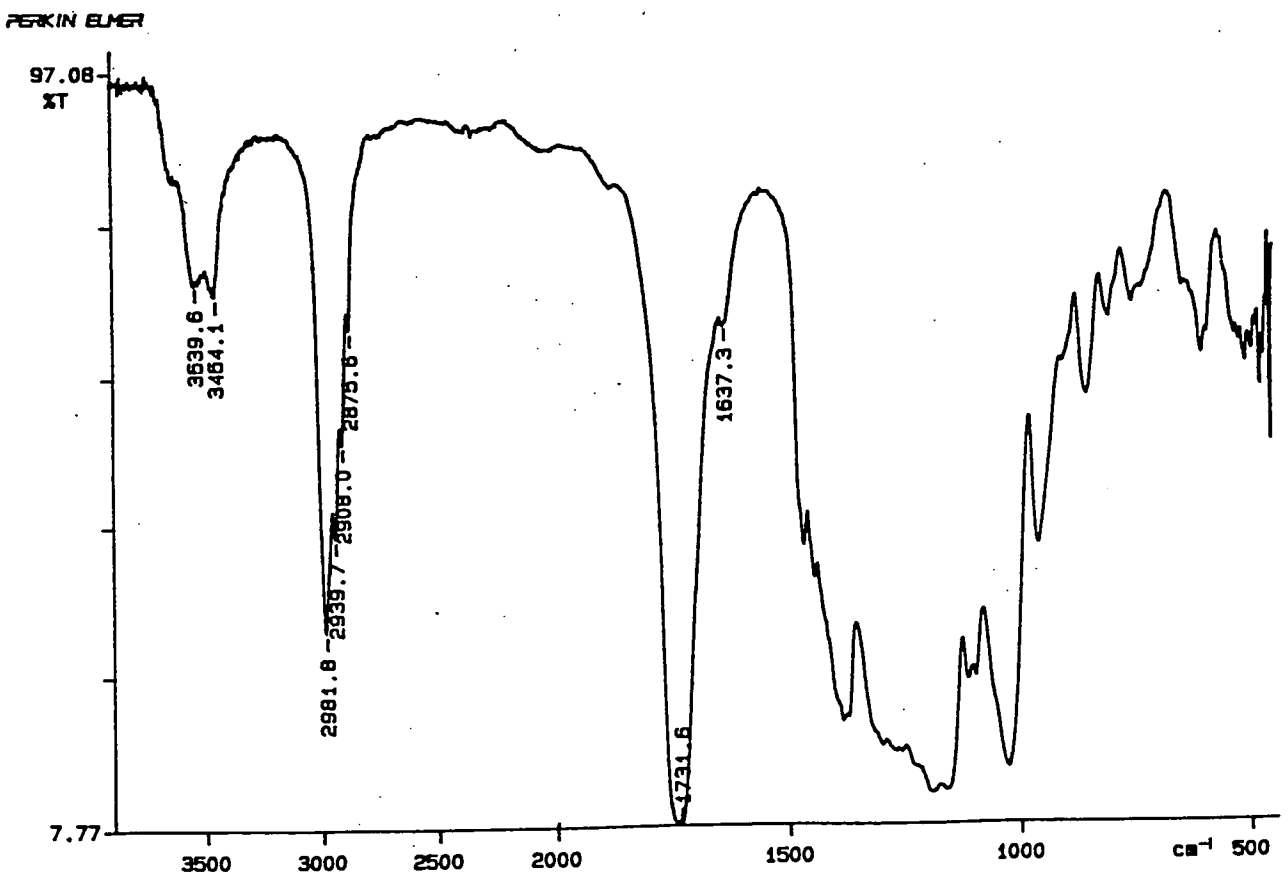

Appendix 4.6 FTIR spectrum of the product of the reaction between poly(diethyl 3-hydroxyglutarate) and PTA at 90°C for 2.5 hours

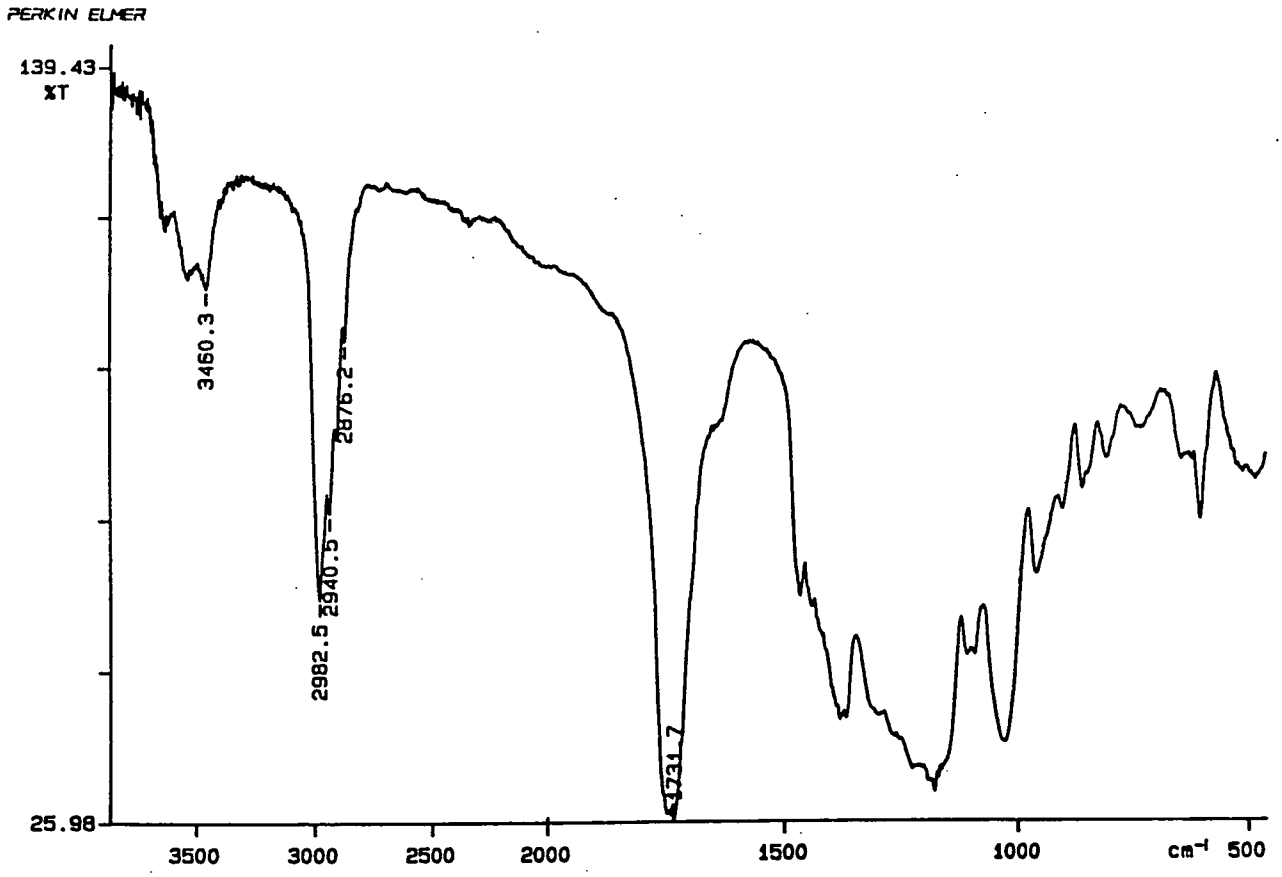

Appendix 4.7 FTIR spectrum of the product of the reaction between poly(diethyl 3-hydroxyglutarate) and PTA at 90°C for 5 hours

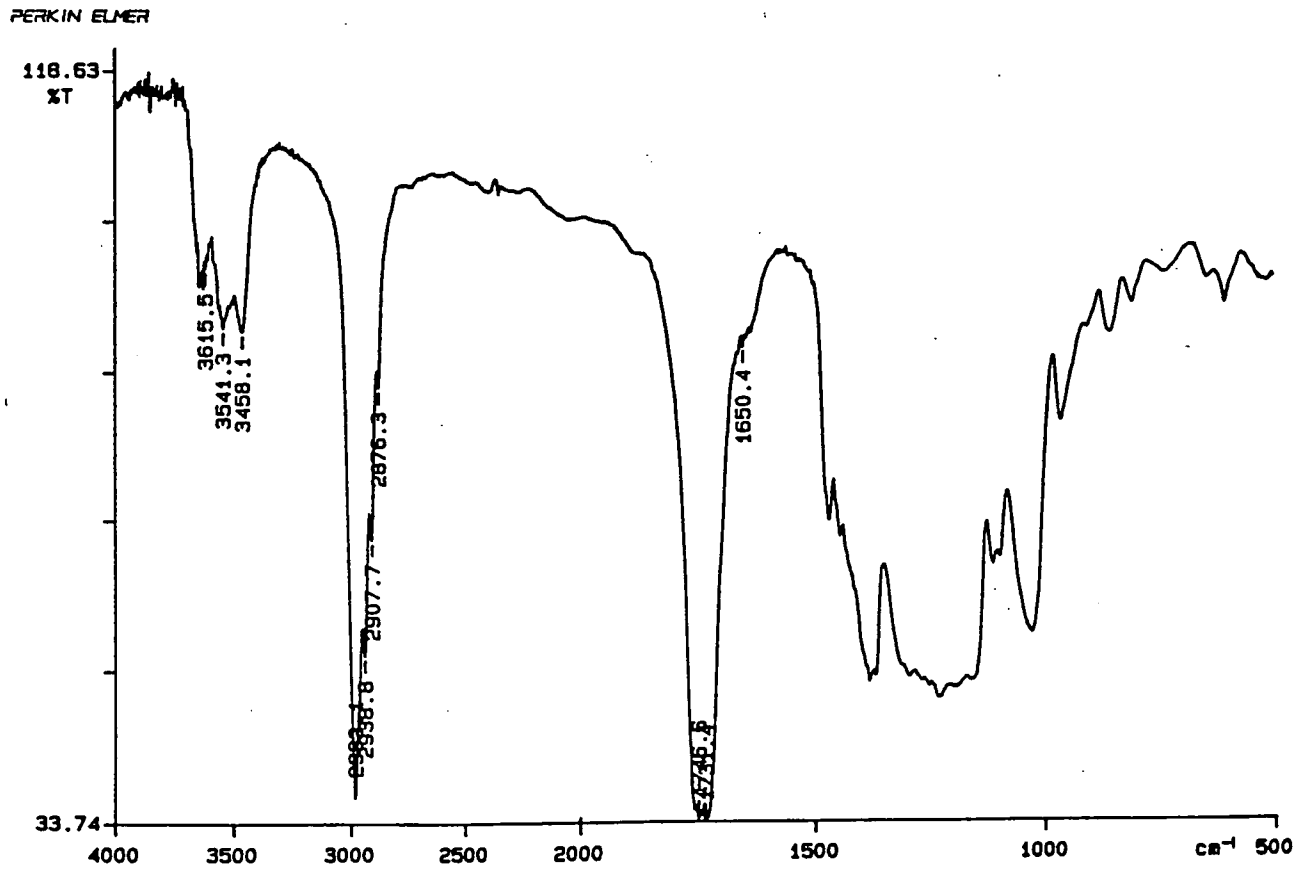

Appendix 4.8 FTIR spectrum of the product of the reaction between poly(diethyl 3-hydroxyglutarate) and PTA at 90°C for 17 hours

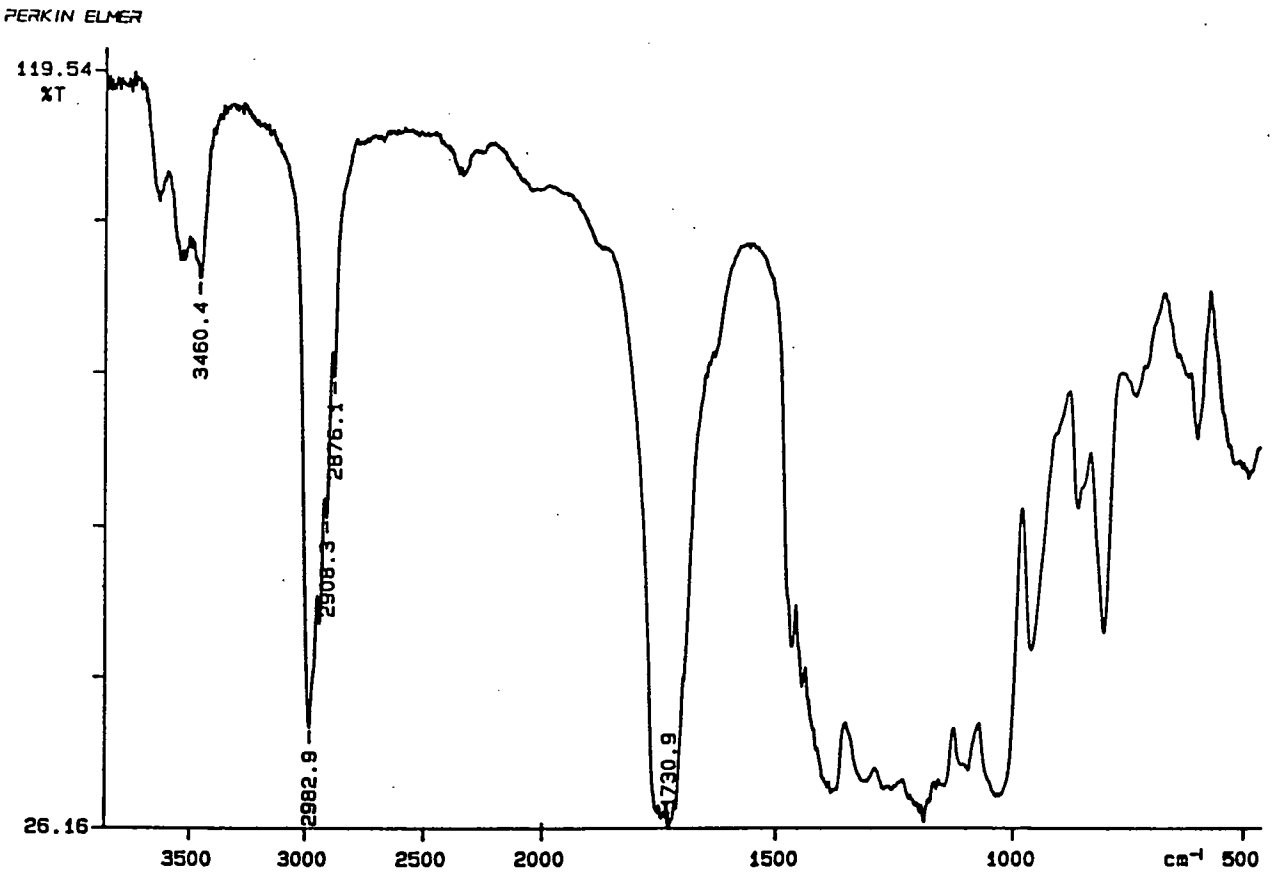

Appendix 4.9 FTIR spectrum of the product of the reaction between poly(diethyl 3-hydroxyglutarate) and PTA at 110°C for 2.5 hours

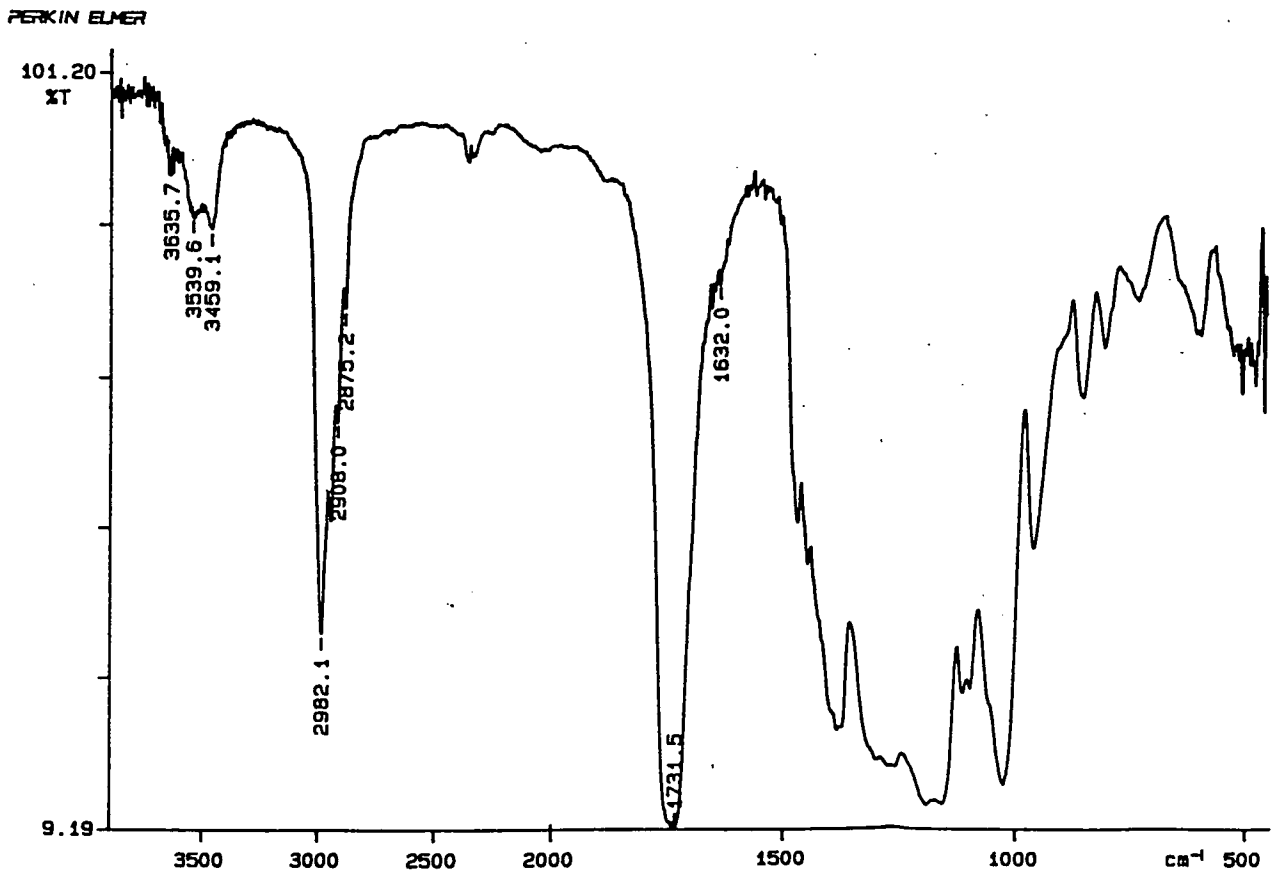

Appendix 4.10 FTIR spectrum of the product of the reaction between poly(diethyl 3-hydroxyglutarate) and PTA at 110°C for 5 hours

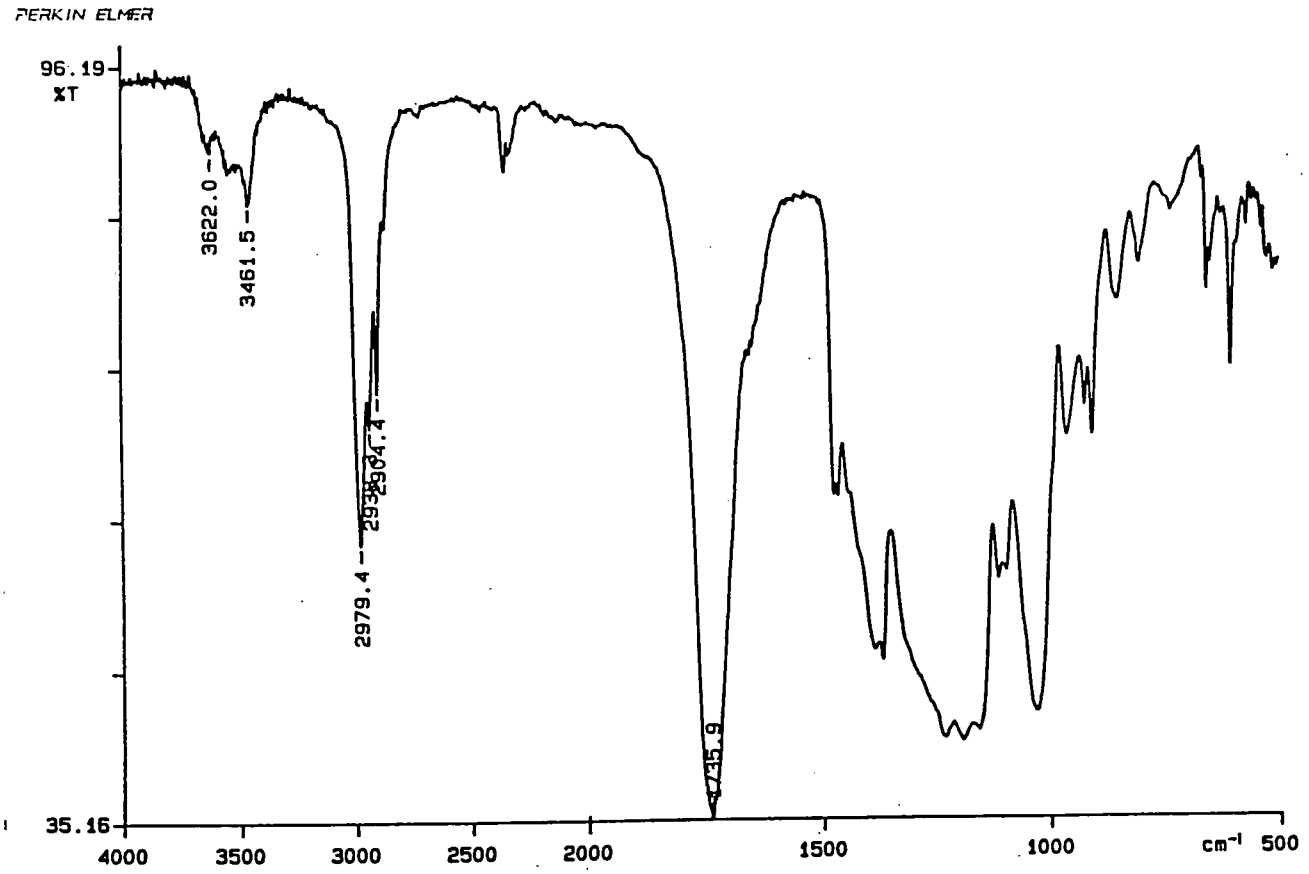

Appendix 4.11 FTIR spectrum of the product of the reaction between poly(diethyl 3-hydroxyglutarate) and PTA at 110°C for 17 hours

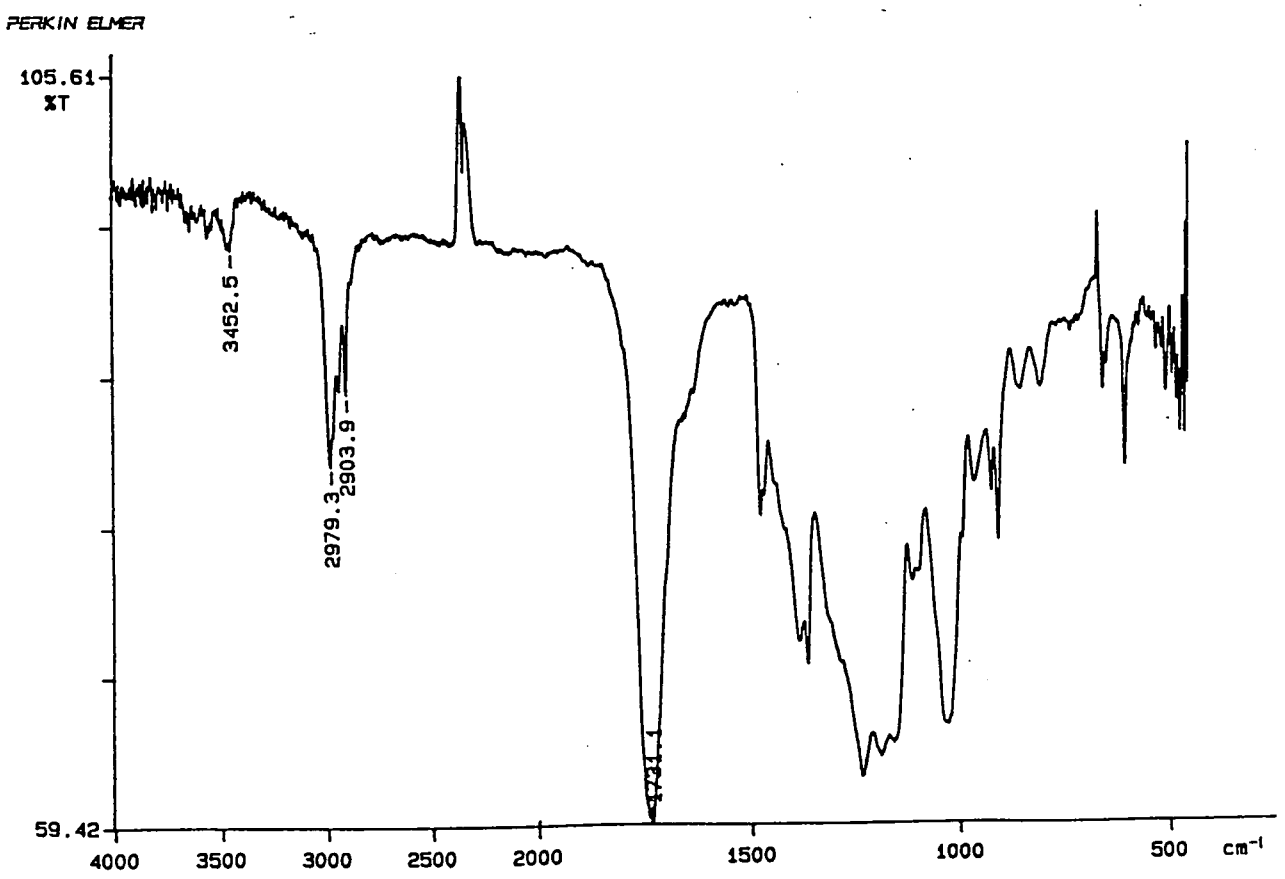

Appendix 4.12 FTIR spectrum of the product of the reaction between poly(diethyl 3-hydroxyglutarate) and PTA at 185°C for 0.25 hours

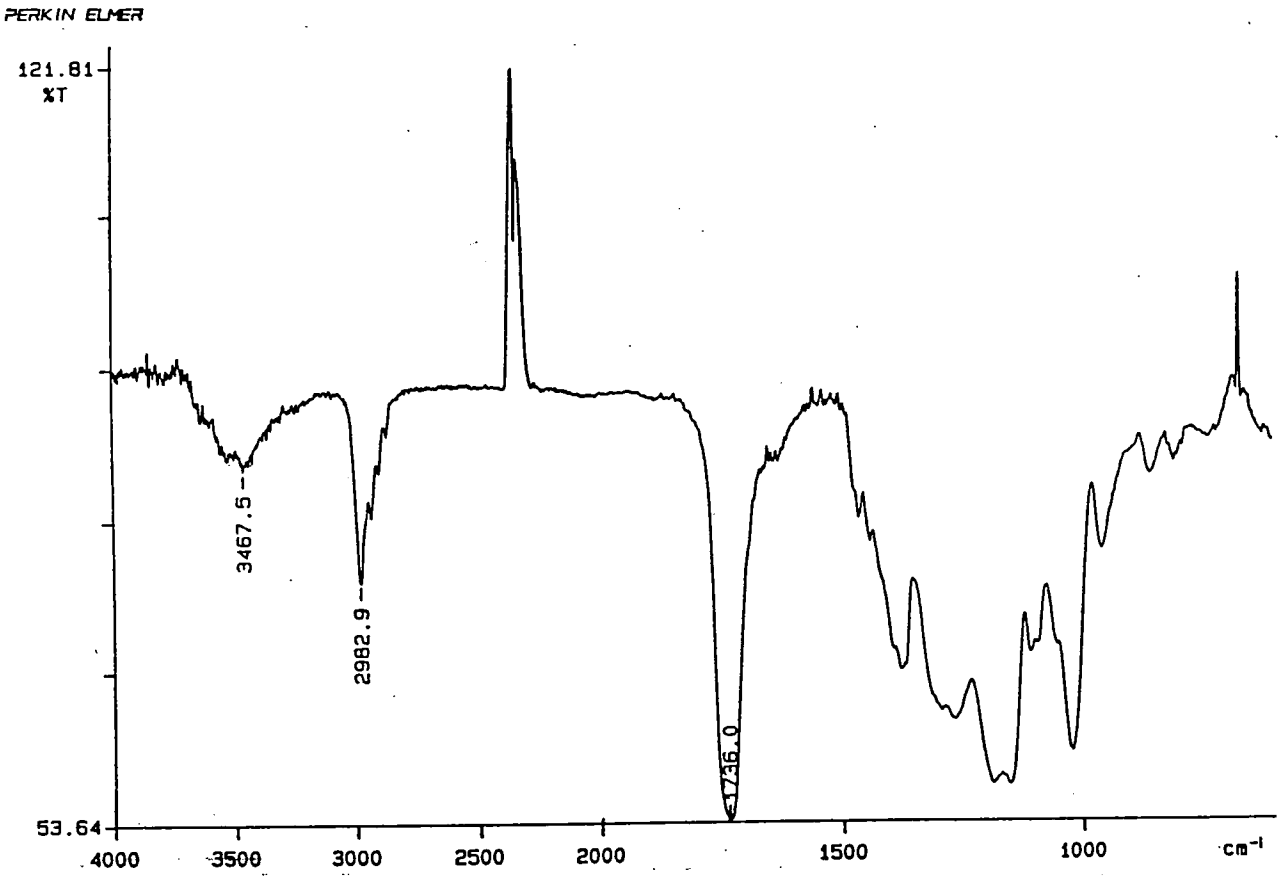

Appendix 4.13 FTIR spectrum of the product of the reaction between poly(diethyl 3-hydroxyglutarate) and 1,5-pentanediol at 90°C for 5 hours

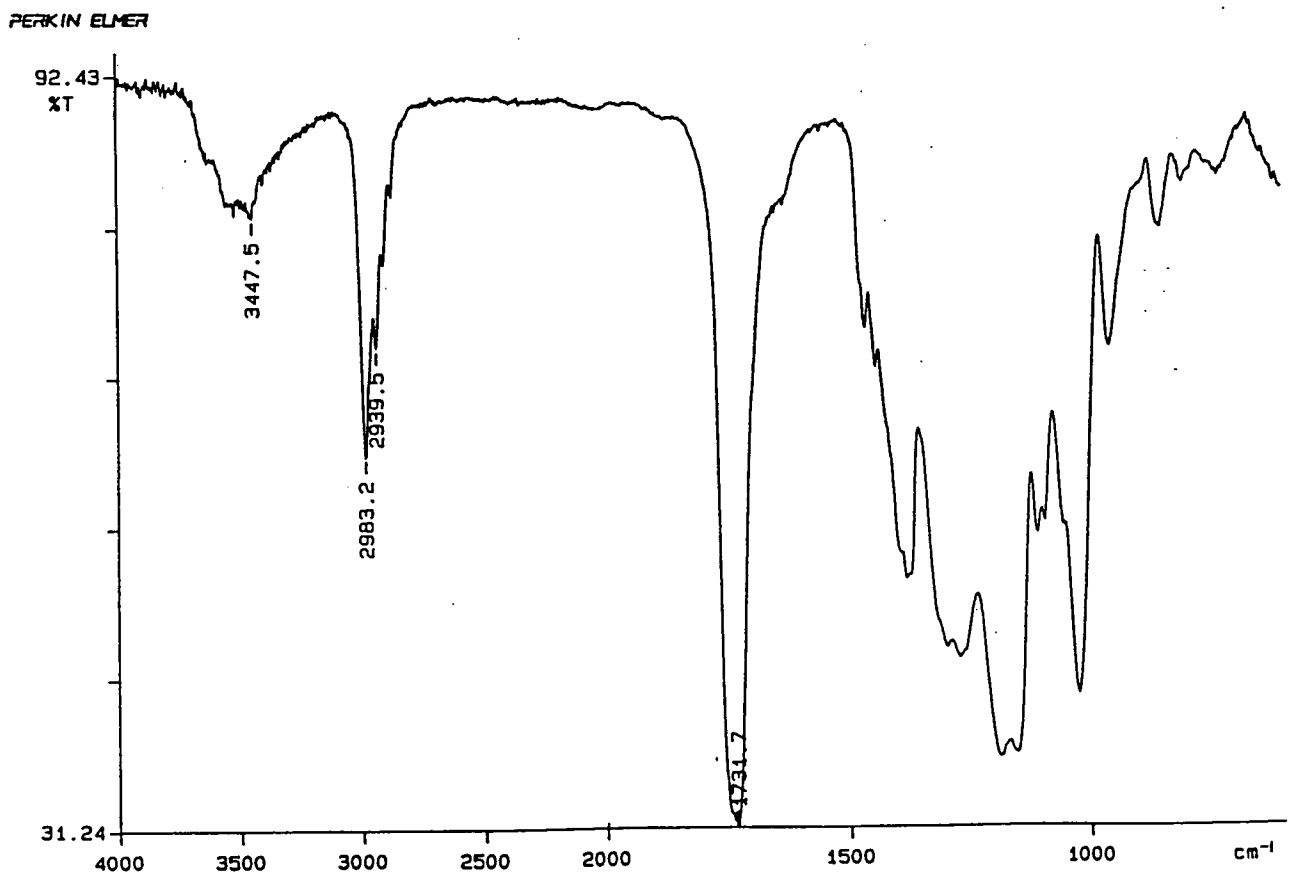

Appendix 4.14 FTIR spectrum of the product of the reaction between poly(diethyl 3-hydroxyglutarate) and 1,5-pentanediol at 90°C for 17 hours

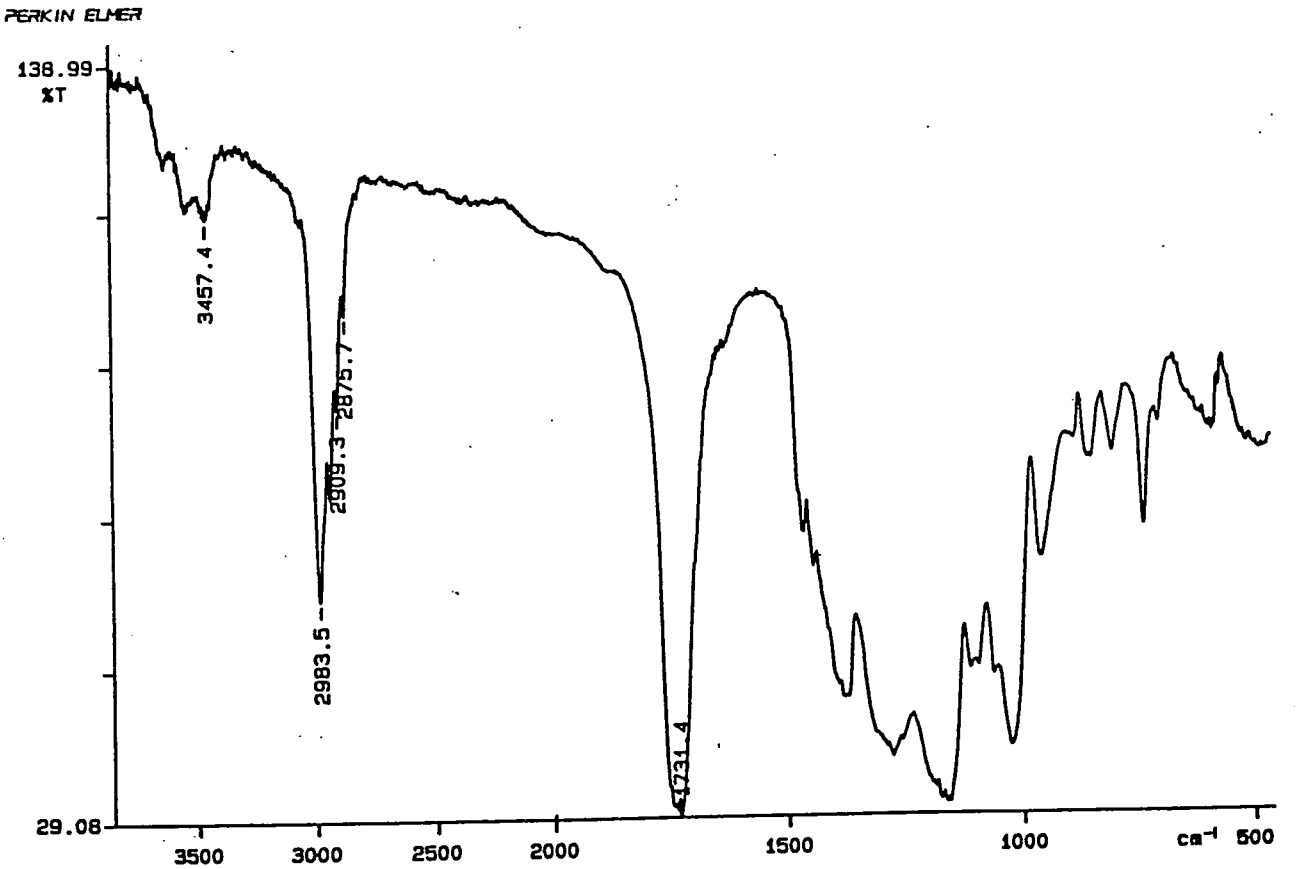

Appendix 4.15 FTIR spectrum of the product of the reaction between poly(diethyl 3-hydroxyglutarate) and 1,5-pentanediol at 110°C for 17 hours

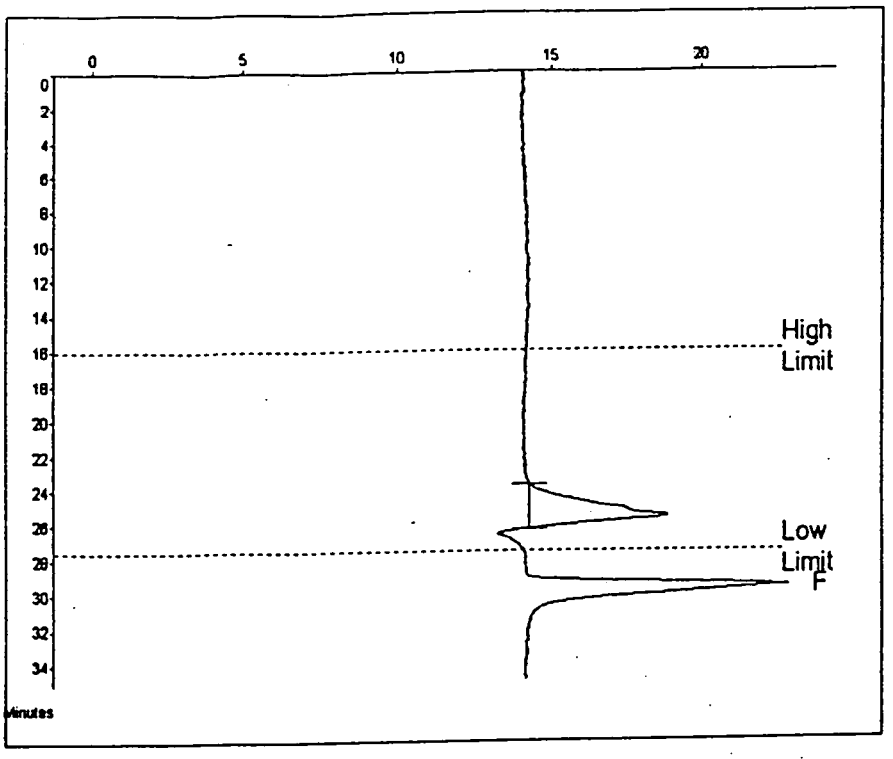

Molecular Weight Averages

Mp =	536	Mz =	721
Mn =	610	Mz+1 =	791
Mw =	660	Mv =	651
Polydispersity =	1.082	Peak Area =	60031

Appendix 4.16 GPC trace of the product of the co-polymerisation of diethyl 3-hydroxyglutarate and PTA (Time of addition = 0 hours)

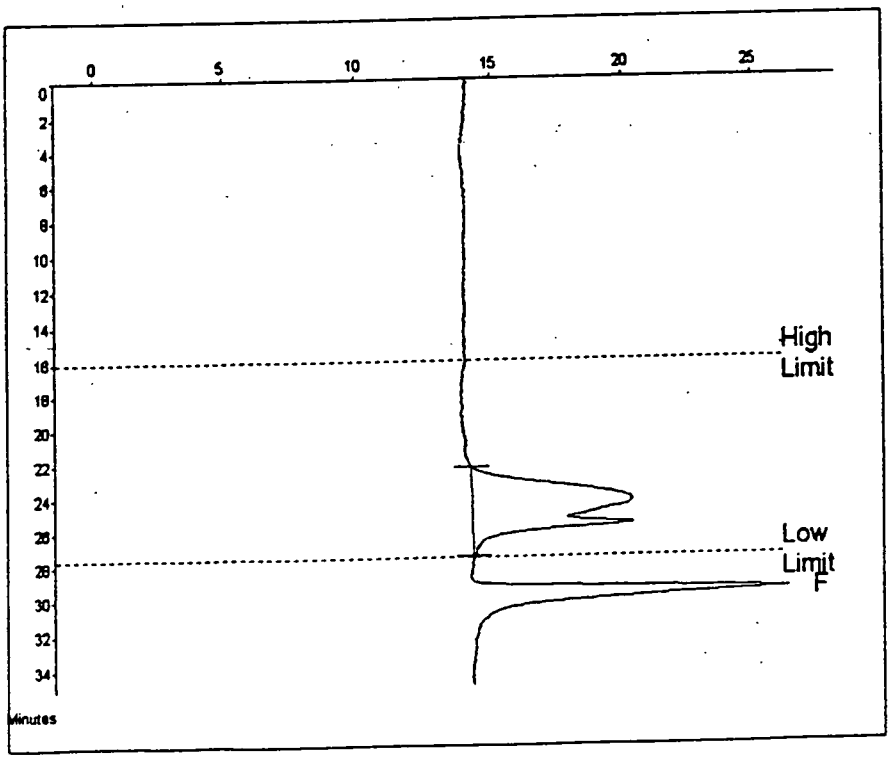

Molecular Weight Averages

Mp =	518	Mz =	1348
Mn =	816	Mz+1 =	1619
Mw =	1069	Mv =	1029
Polydispersity =	1.308	Peak Area =	183805

Appendix 4.17 GPC trace of the product of the co-polymerisation of diethyl 3-hydroxyglutarate and PTA (Time of addition = 2 hours)

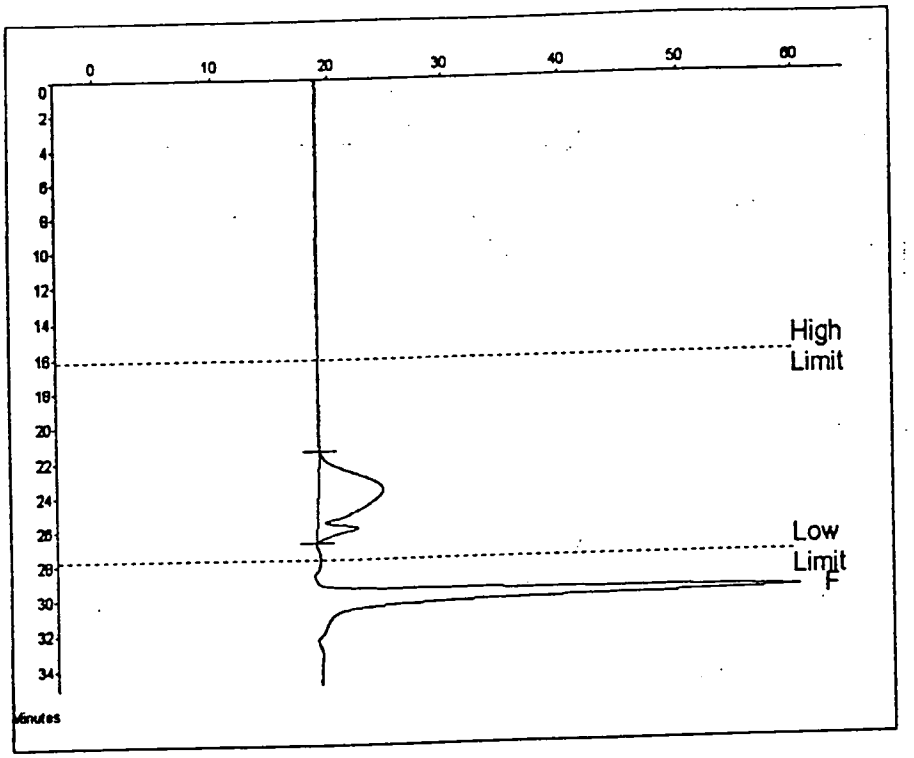

Molecular Weight Averages

Mp =	1747	Mz =	2198
Mn =	1142	Mz+1 =	2725
Mw =	1647	Mv =	1569
Polydispersity =	1.442	Peak Area =	166013

Appendix 4.18 GPC trace of the product of the co-polymerisation of diethyl 3-hydroxyglutarate and PTA (Time of addition = 3 hours)

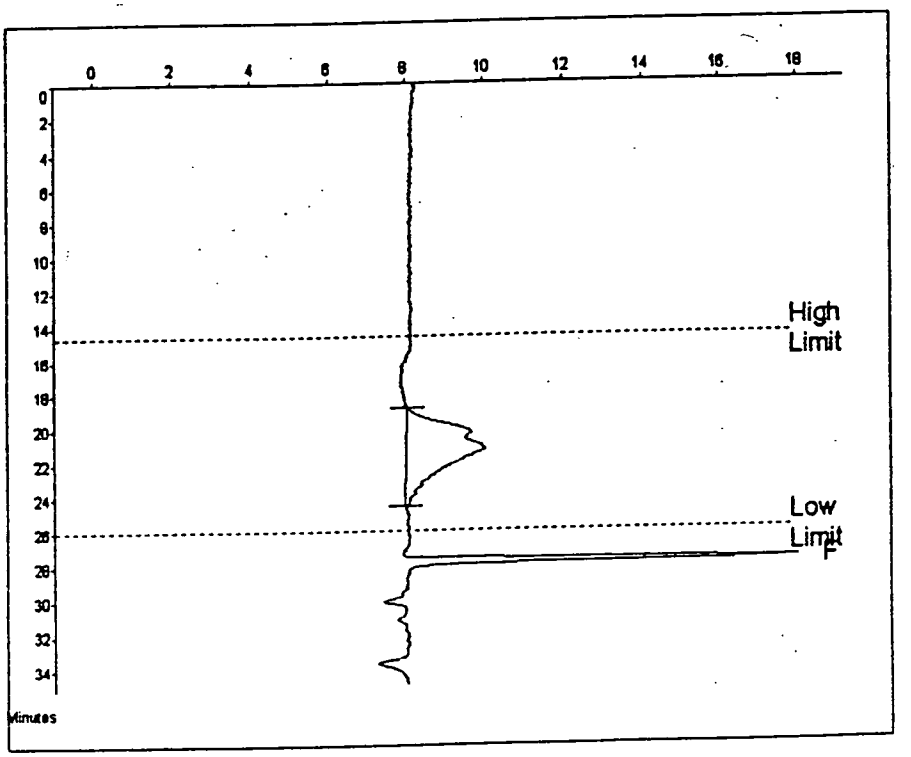

Molecular Weight Averages

Mp =	3214	Mz =	6513
Mn =	2252	Mz+1 =	8941
Mw =	4165	Mv =	3940
Polydispersity =	1.849	Peak Area =	84469

Appendix 4.19 GPC trace of the product of the co-polymerisation of diethyl 3-hydroxyglutarate and 1,5-pentanediol (Time of addition = 2 hours)

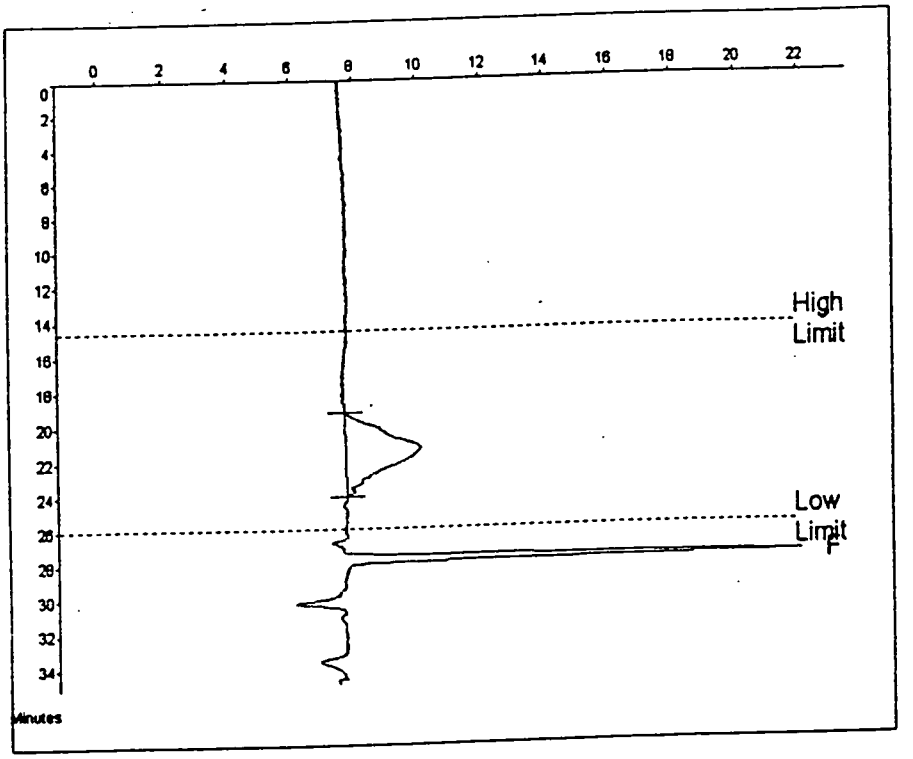

Molecular Weight Averages

Mp =	2997	Mz =	4792
Mn =	2104	Mz+1 =	6438
Mw =	3245	Mv =	3046
Polydispersity =	1.542	Peak Area =	66525

Appendix 4.20 GPC trace of the product of the co-polymerisation of diethyl 3-hydroxyglutarate and 1,5-pentanediol (Time of addition = 3 hours)

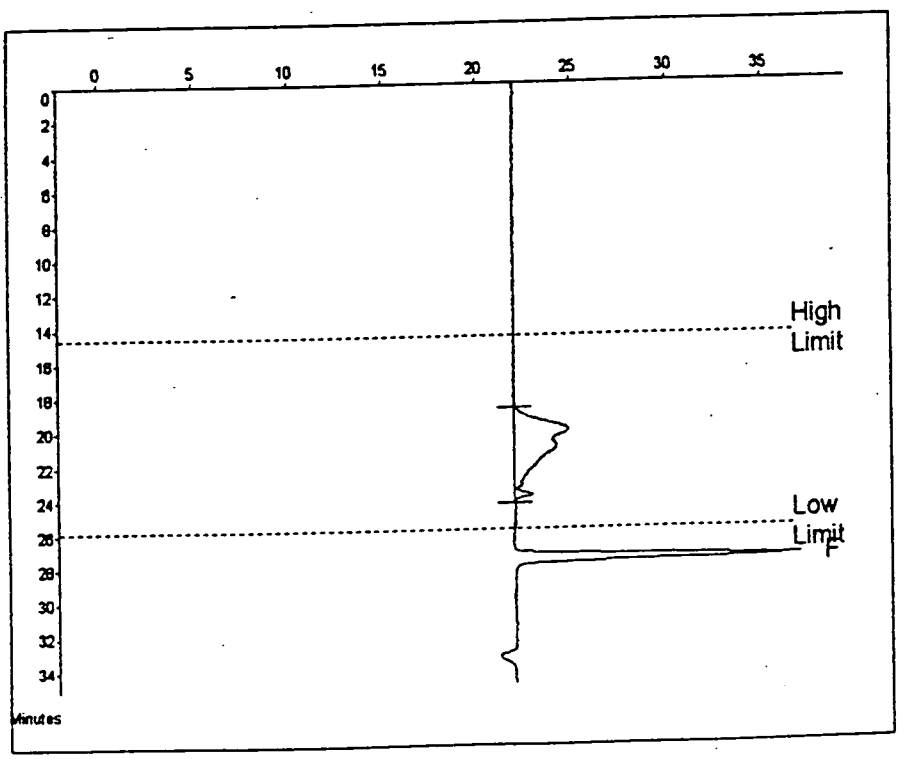

Molecular Weight Averages

Mp =	6608	Mz =	5765
Mn =	2205	Mz+1 =	6838
Mw =	4436	Mv =	4094
Polydispersity =	2.012	Peak Area =	63371

Appendix 4.21 GPC trace of the product of the reaction between poly(diethyl 3-hydroxyglutarate) and PTA at 90°C for 2.5 hours

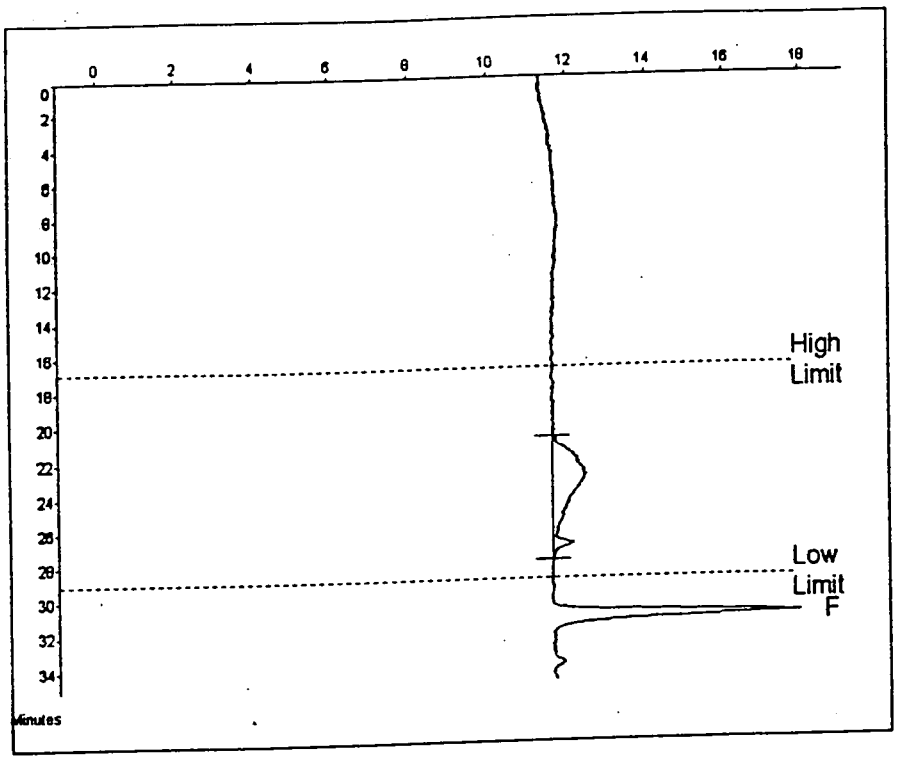

Molecular Weight Averages

Mp =	4652	Mz =	6581
Mn =	1989	Mz+1 =	8527
Mw =	4223	Mv =	3879
Polydispersity =	2.145	Peak Area =	33168

Appendix 4.22 GPC trace of the product of the reaction between poly(diethyl 3-hydroxyglutarate) and PTA at 90°C for 5 hours

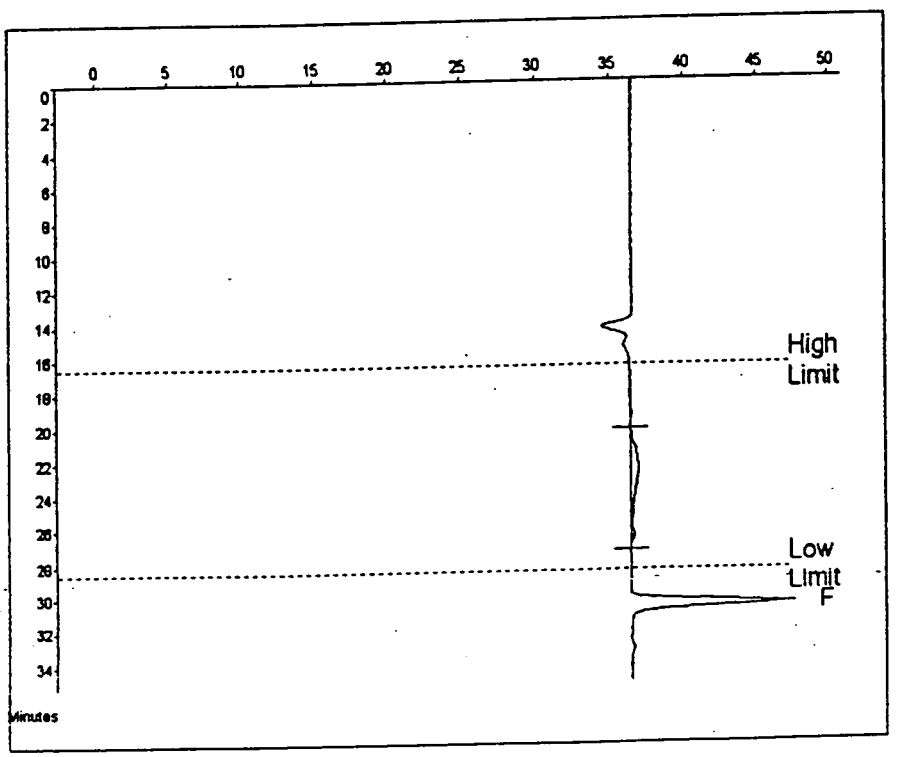

Molecular Weight Averages

Mp =	4518	Mz =	7191
Mn =	2049	Mz+1 =	9691
Mw =	4410	Mv =	4029
Polydispersity =	2.152	Peak Area =	24128

Appendix 4.23 GPC trace of the product of the reaction between poly(diethyl 3-hydroxyglutarate) and PTA at 90°C for 17 hours

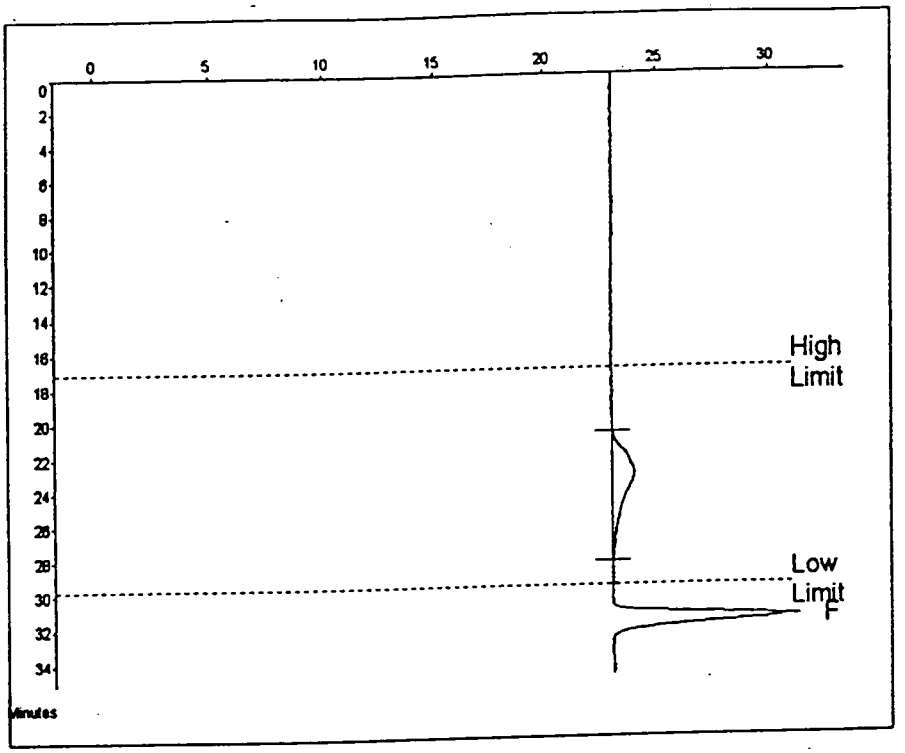

Molecular Weight Averages

Mp =	5182	Mz =	7531
Mn =	2650	Mz+1 =	10052
Mw =	4901	Mv =	4542
Polydispersity =	1.850	Peak Area =	38020

Appendix 4.24 GPC trace of the product of the reaction between poly(diethyl 3-hydroxyglutarate) and PTA at 110°C for 2.5 hours

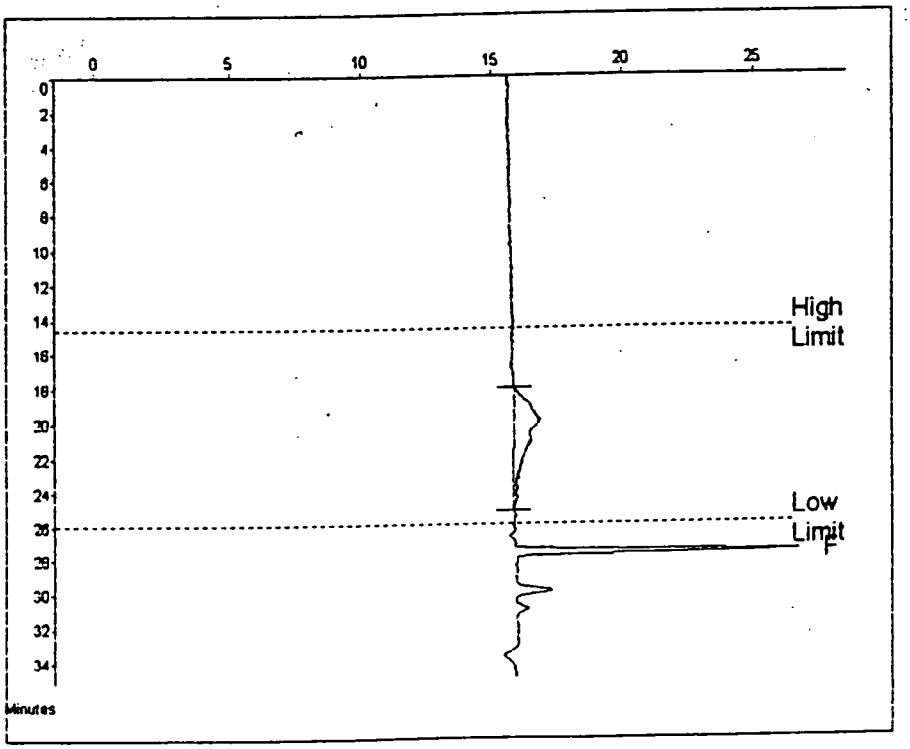

Molecular Weight Averages

Mp =	7783	Mz =	12373
Mn =	2061	Mz+1 =	17002
Mw =	6605	Mv =	5822
Polydispersity =	3.203	Peak Area =	35915

Appendix 4.25 GPC trace of the product of the reaction between poly(diethyl 3-hydroxyglutarate) and PTA at 110°C for 5 hours

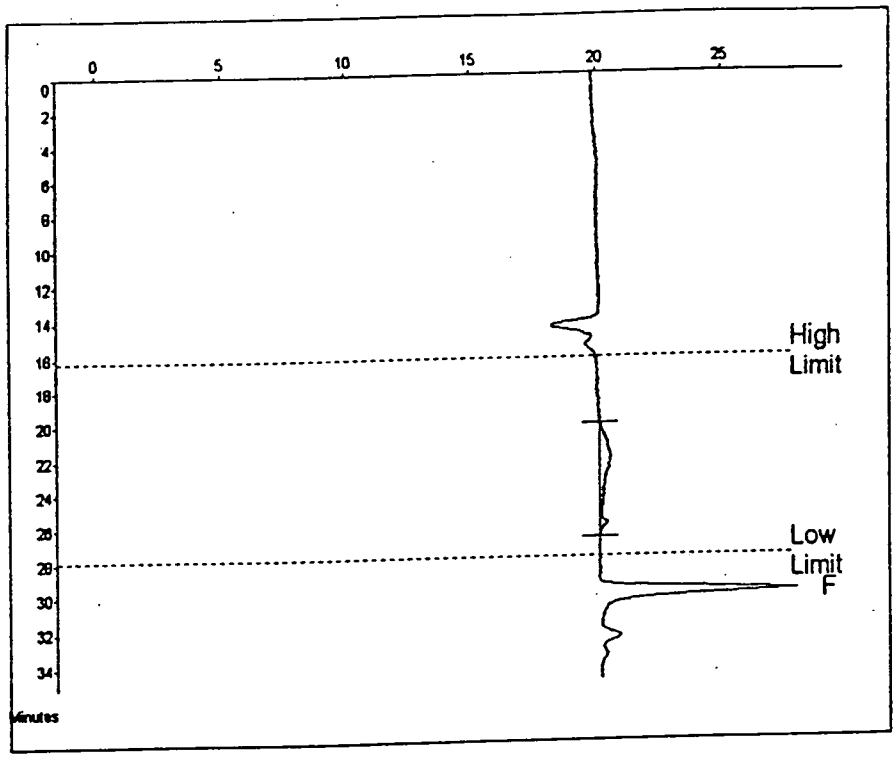

Molecular Weight Averages

Mp =	4992	Mz =	6488
Mn =	1884	Mz+1 =	8500
Mw =	3942	Mv =	3576
Polydispersity =	2.328	Peak Area =	18006

Appendix 4.26 GPC trace of the product of the reaction between poly(diethyl 3-hydroxyglutarate) and PTA at 110°C for 17 hours

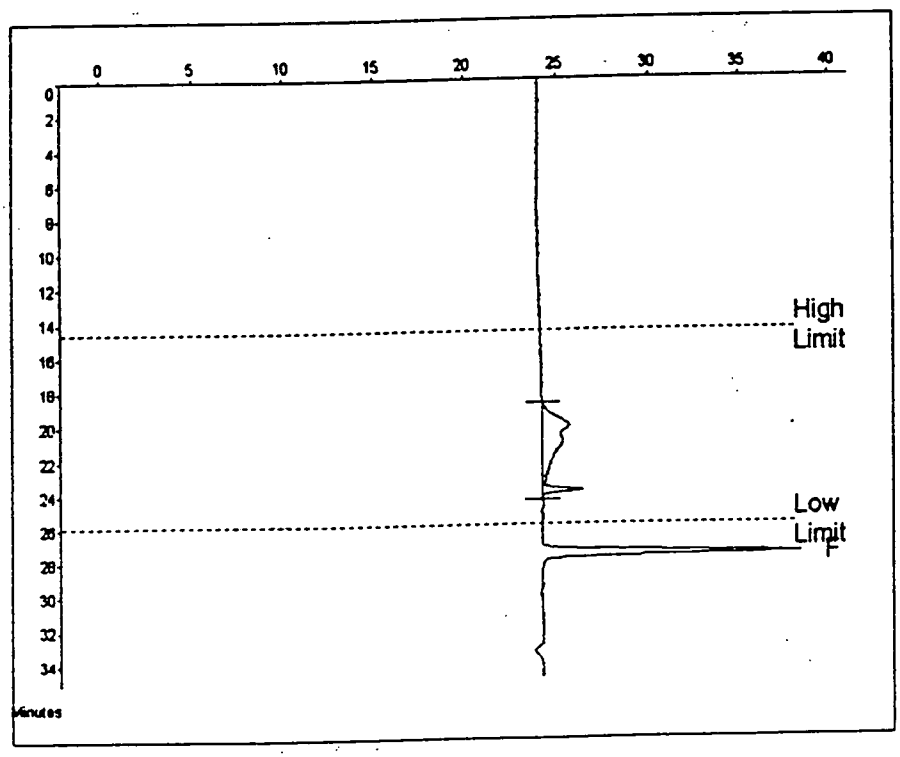

Molecular Weight Averages

Mp =	503	Mz =	6723
Mn =	1545	Mz+1 =	9640
Mw =	3991	Mv =	3584
Polydispersity =	2.582	Peak Area =	46080

Appendix 4.27 GPC trace of the product of the reaction between poly(diethyl 3-hydroxyglutarate) and PTA at 185°C for 0.25 hours

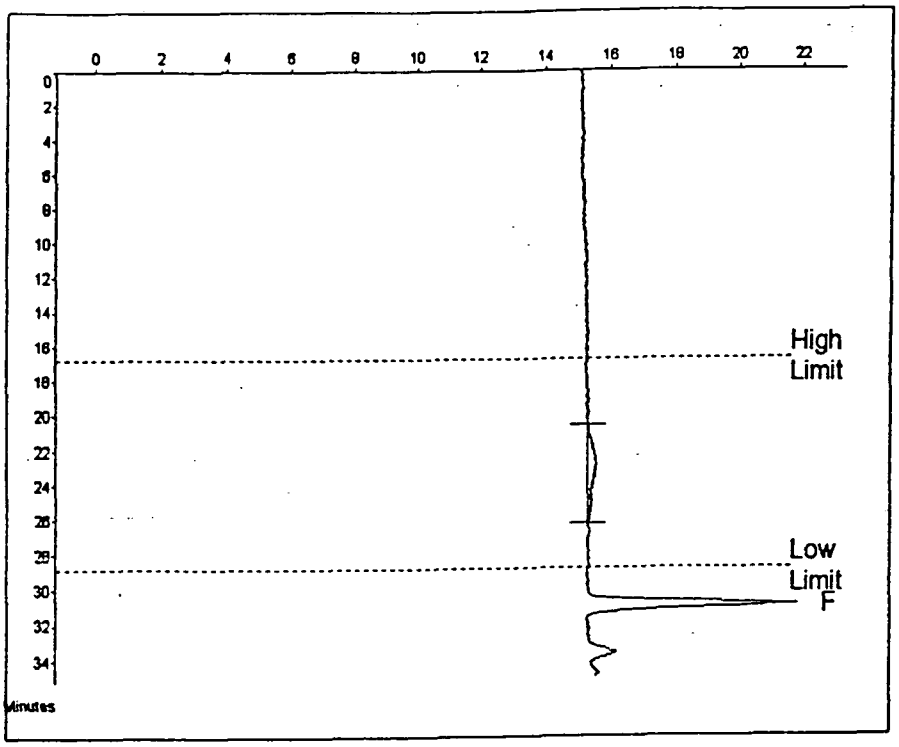

Molecular Weight Averages

Mp =	4693	Mz =	6677
Mn =	2770	Mz+1 =	6764
Mw =	4535	Mv =	4244
Polydispersity =	1.637	Peak Area =	9142

Appendix 4.28 GPC trace of the product of the reaction between poly(diethyl 3-hydroxyglutarate) and 1,5-pentanediol at 90°C for 5 hours

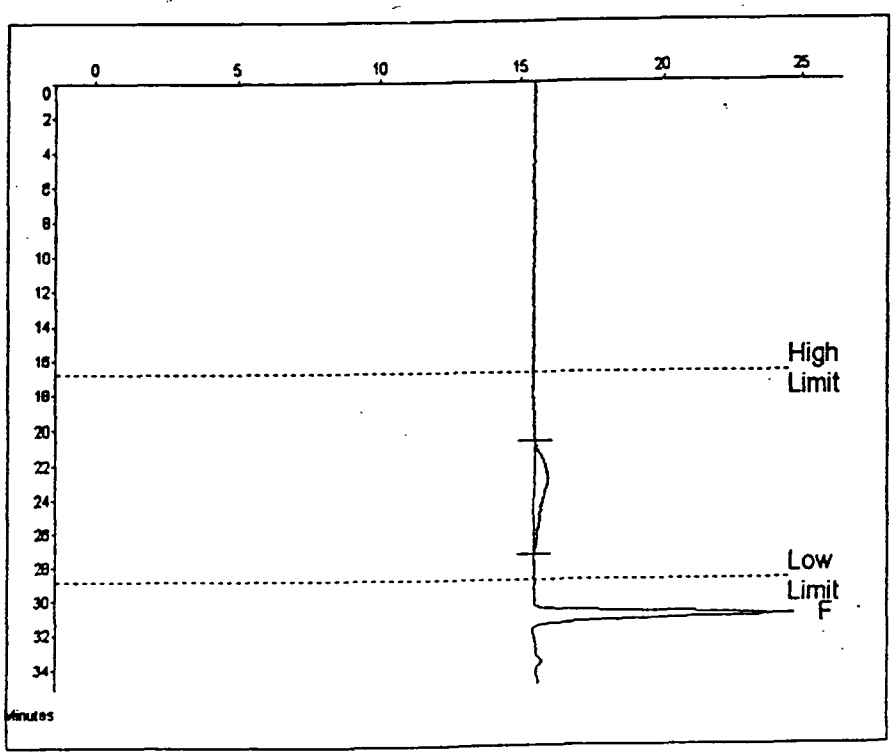

Molecular Weight Averages

Mp =	4681	Mz =	6514
Mn =	2361	Mz+1 =	6514
Mw =	4282	Mv =	3971
Polydispersity =	1.814	Peak Area =	19777

Appendix 4.29 GPC trace of the product of the reaction between poly(diethyl 3-hydroxyglutarate) and 1,5-pentanediol at 90°C for 17 hours

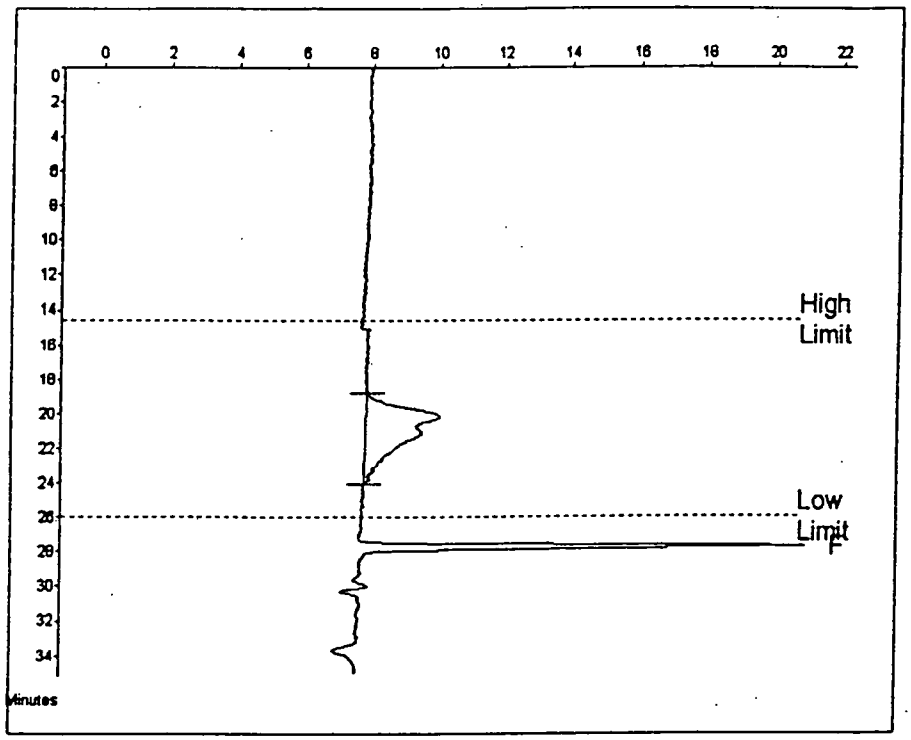

Molecular Weight Averages

Mp =	7104	Mz =	7340
Mn =	2924	Mz+1 =	9223
Mw =	5069	Mv =	4737
Polydispersity =	1.734	Peak Area =	58600

Appendix 4.30 GPC trace of the product of the reaction between poly(diethyl 3-hydroxyglutarate) and 1,5-pentanediol at 110°C for 17 hours

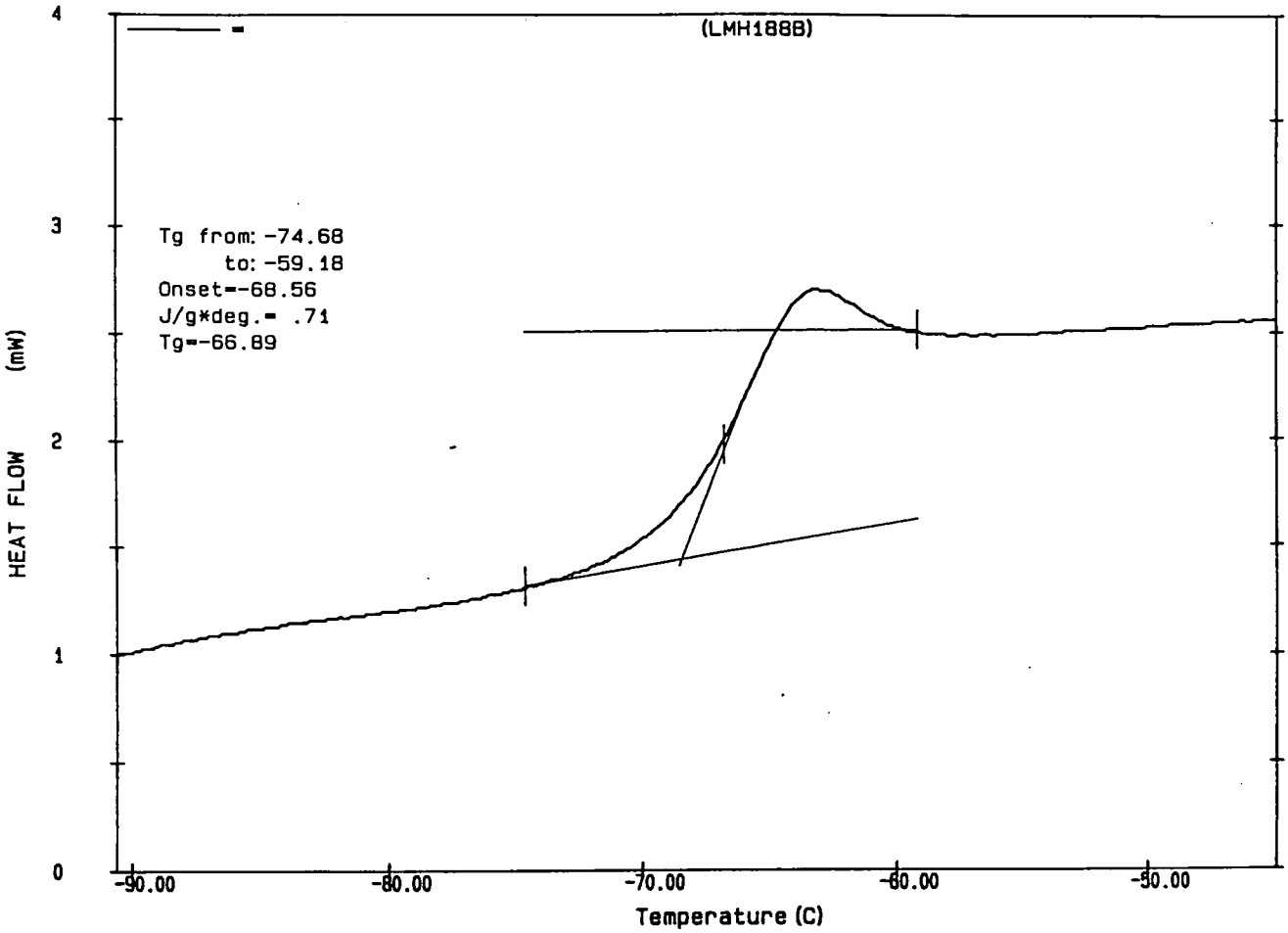

Appendix 4.31 DSC trace of the product of the co-polymerisation of diethyl 3-hydroxyglutarate and PTA (Time of addition = 0 hours)

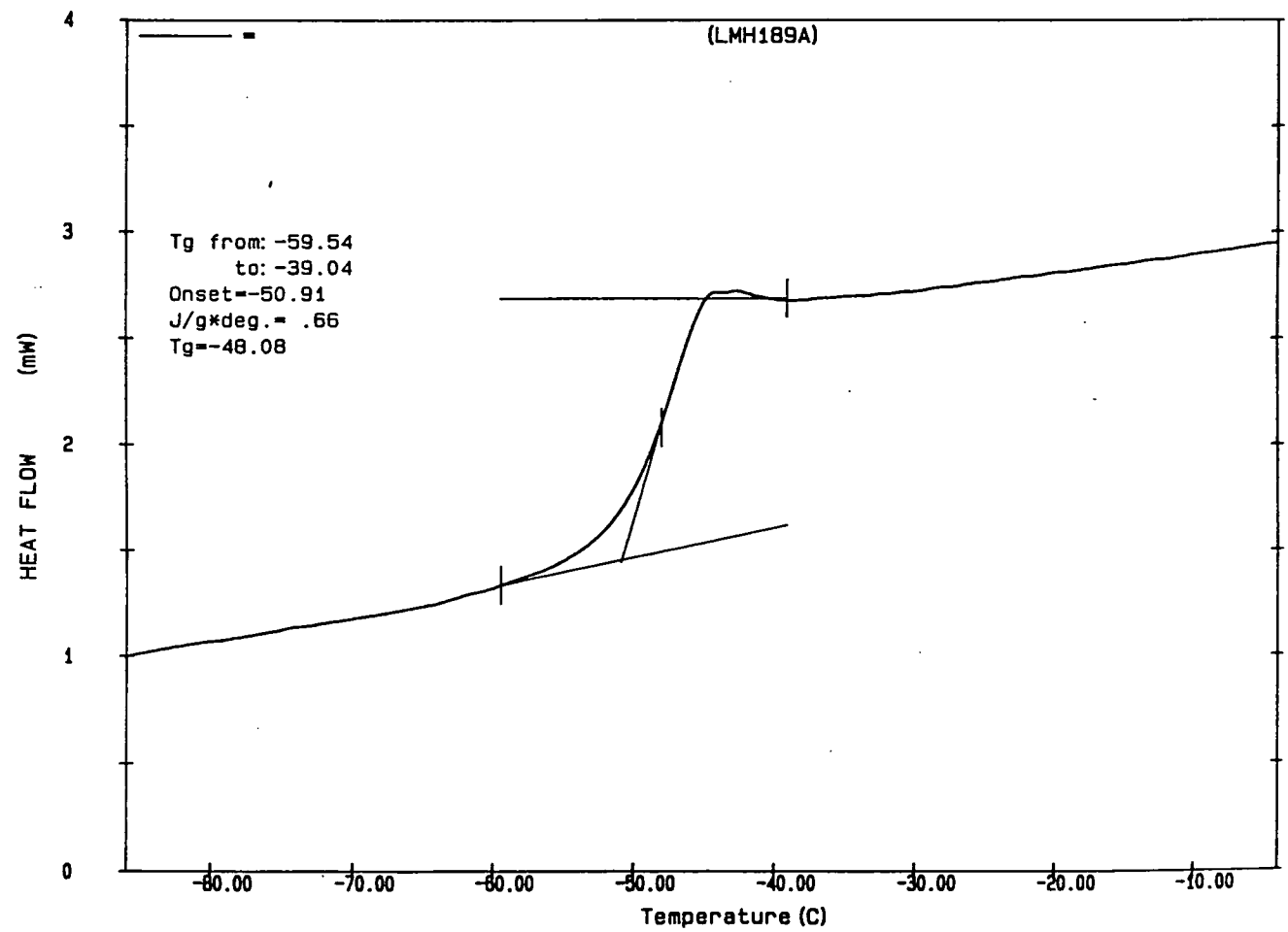

Appendix 4.32 DSC trace of the product of the co-polymerisation of diethyl 3-hydroxyglutarate and PTA (Time of addition = 2 hours)

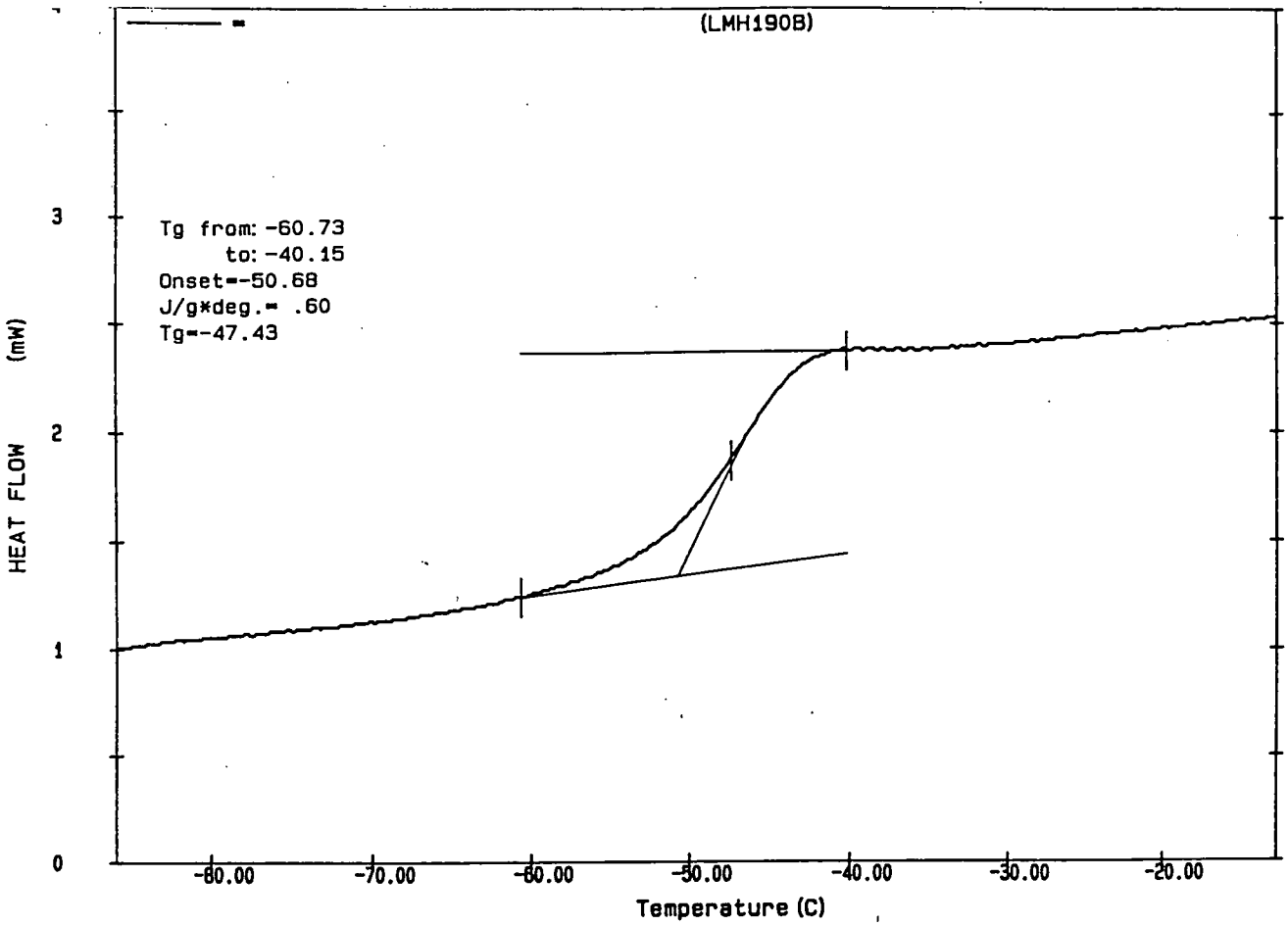

Appendix 4.33 DSC trace of the product of the co-polymerisation of diethyl 3-hydroxyglutarate and PTA (Time of addition = 3 hours)

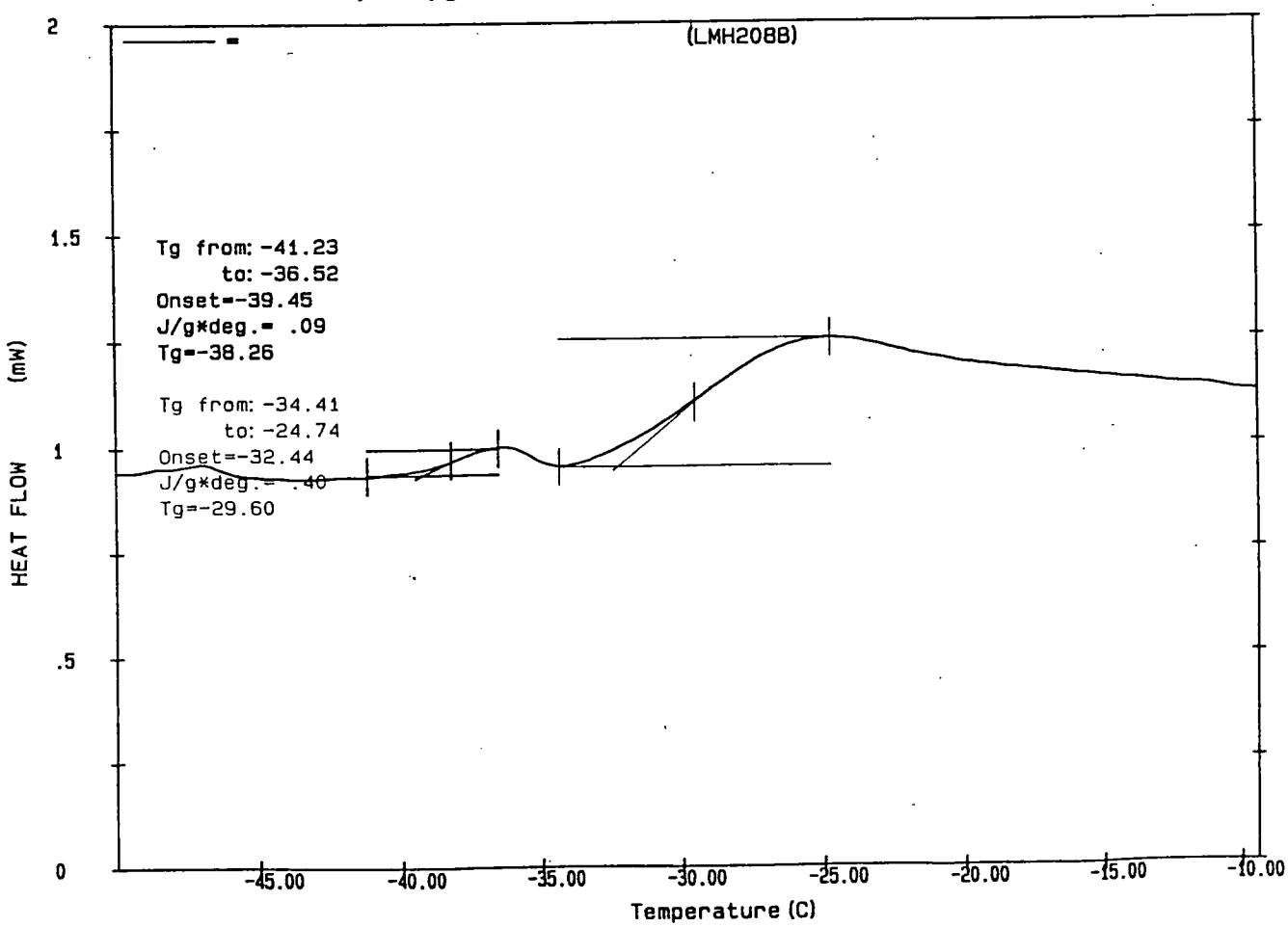

Appendix 4.34 DSC trace of the product of the co-polymerisation of diethyl 3-hydroxyglutarate and 1,5-pentanediol (Time of addition = 2 hours)

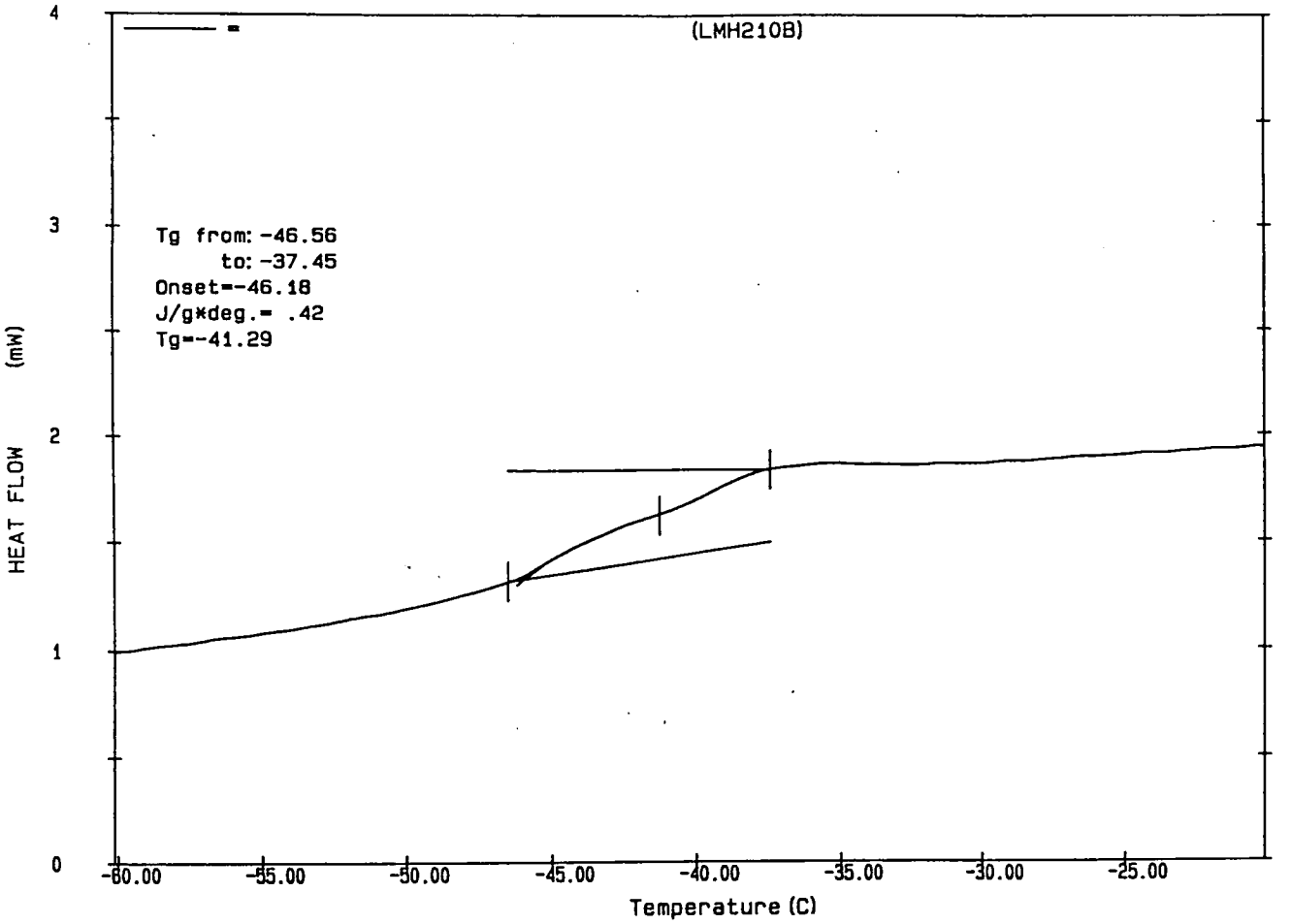

Appendix 4.35 DSC trace of the product of the co-polymerisation of diethyl 3-hydroxyglutarate and 1,5-pentanediol (Time of addition = 3 hours)

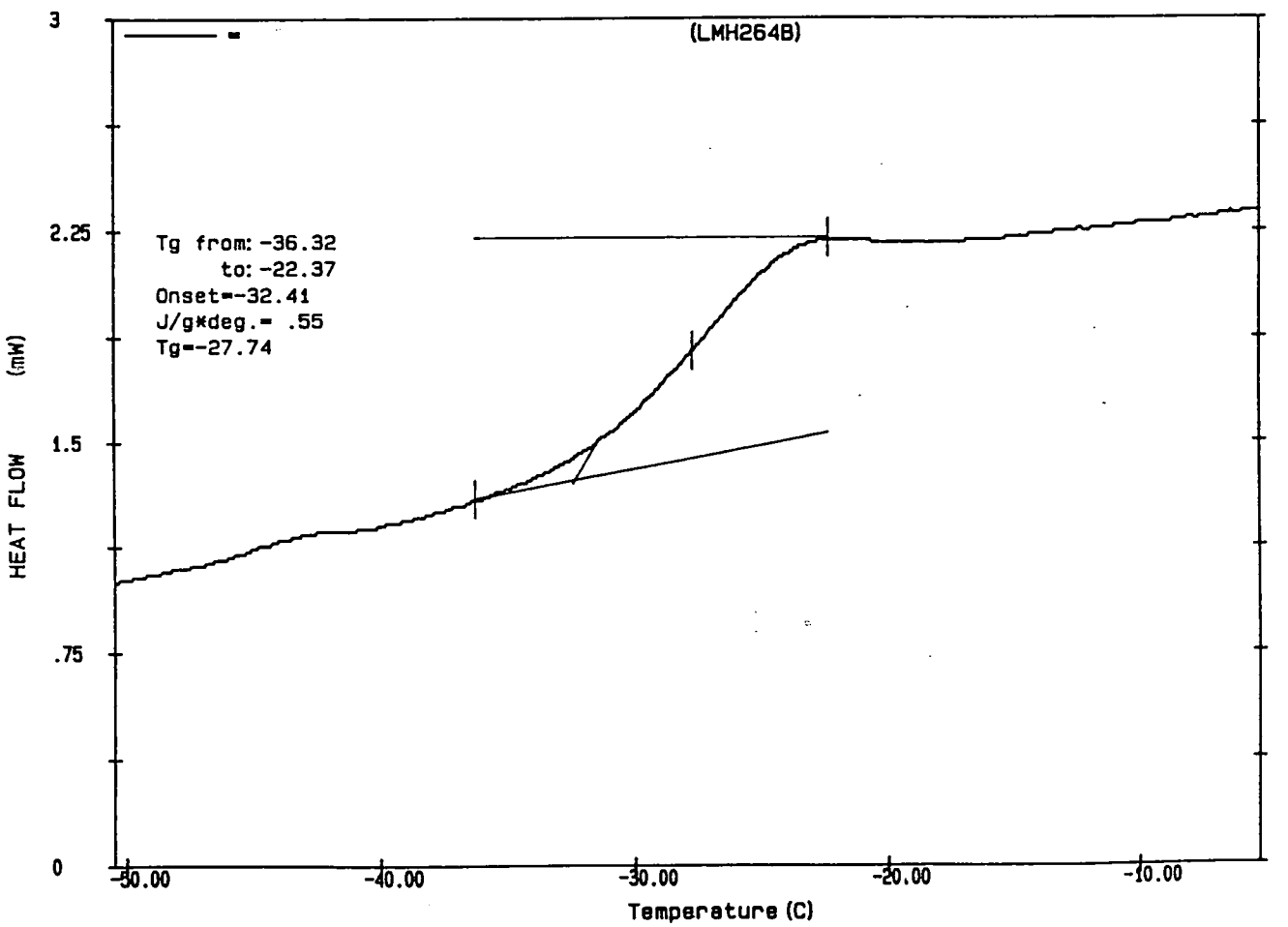

Appendix 4.36 DSC trace of the product of the reaction between poly(diethyl 3-hydroxyglutarate) and PTA at 90°C for 2.5 hours

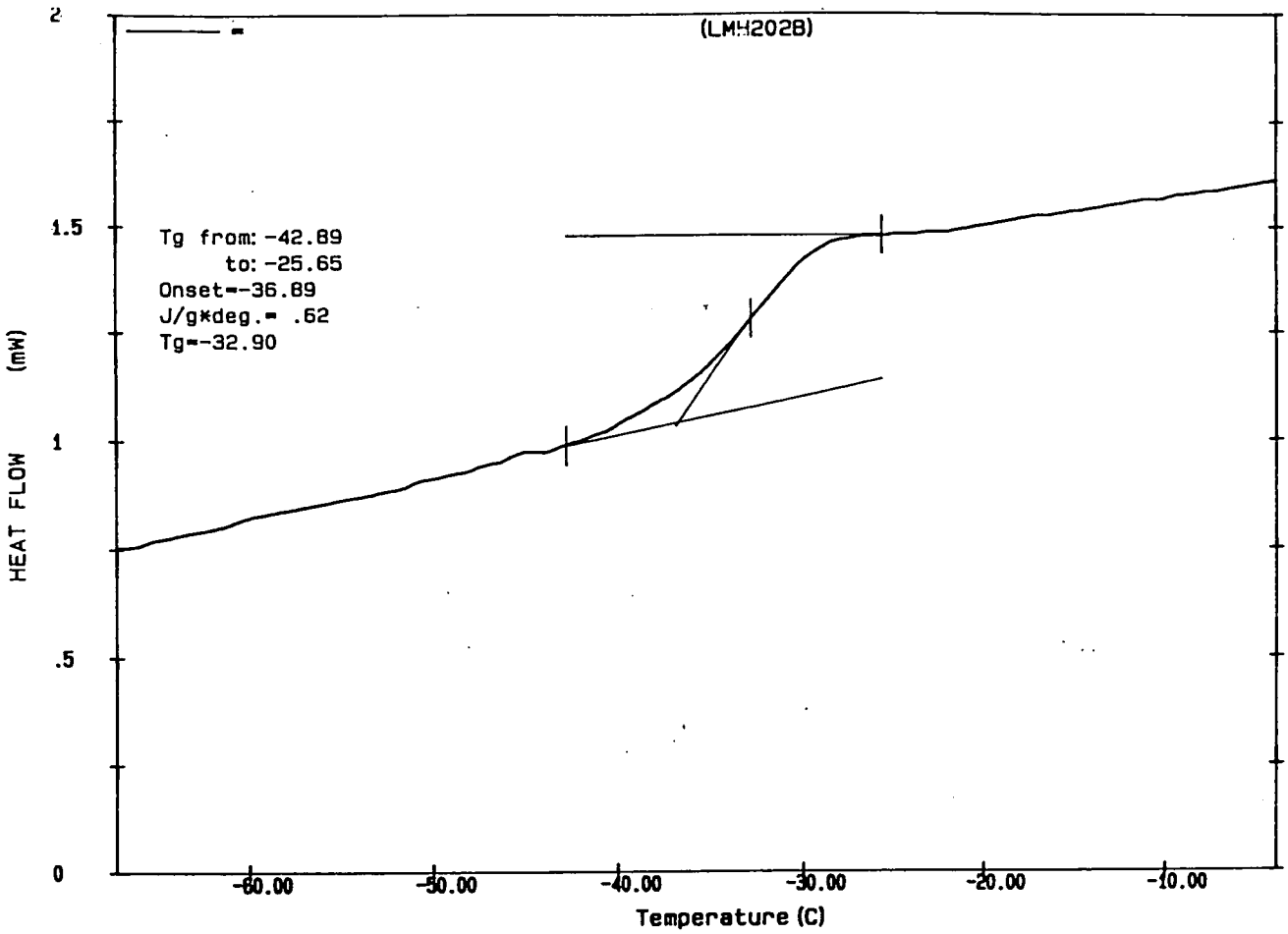

Appendix 4.37 DSC trace of the product of the reaction between poly(diethyl 3-hydroxyglutarate) and PTA at 90°C for 5 hours

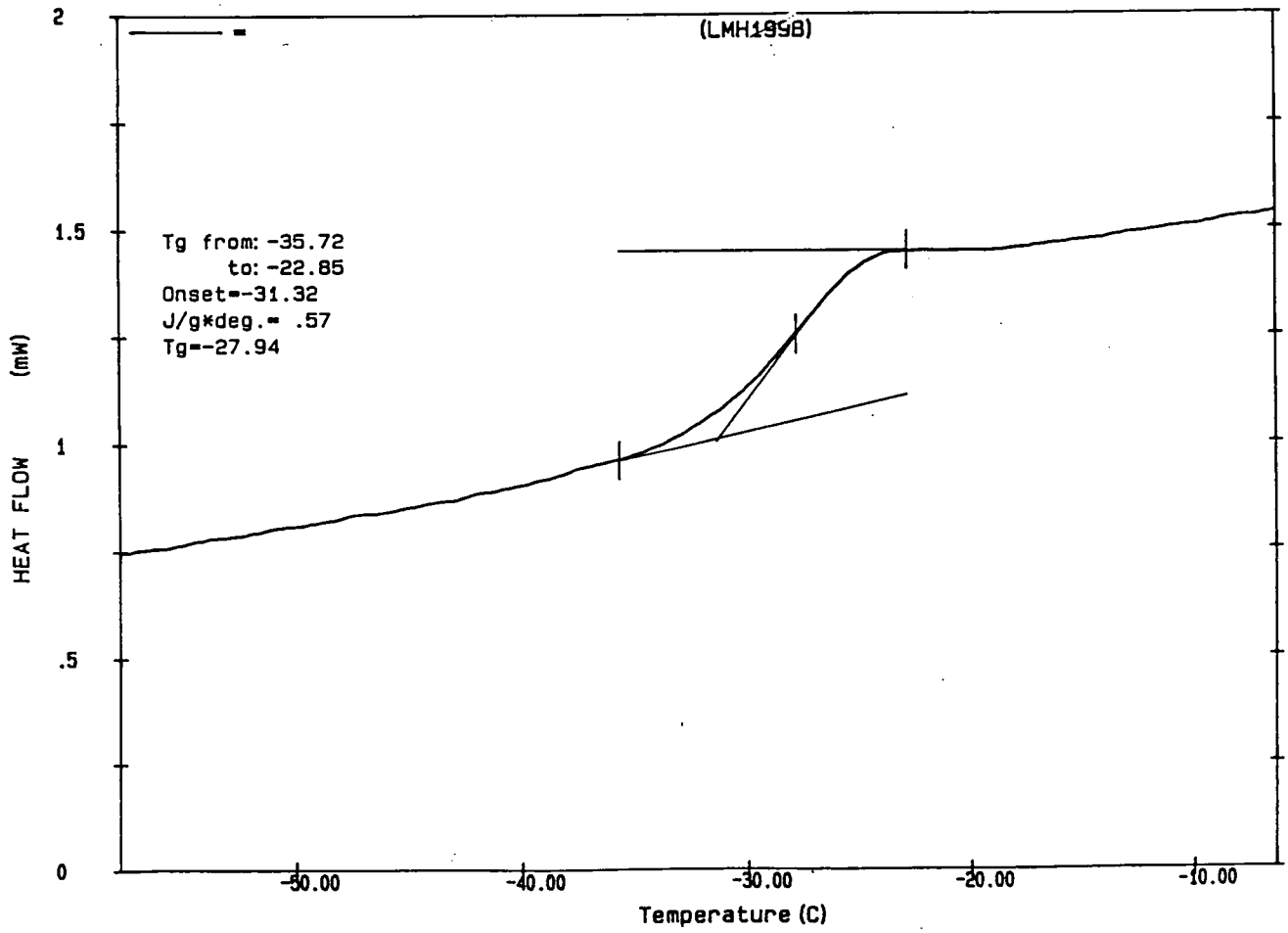

Appendix 4.38 DSC trace of the product of the reaction between poly(diethyl 3-hydroxyglutarate) and PTA at 90°C for 17 hours

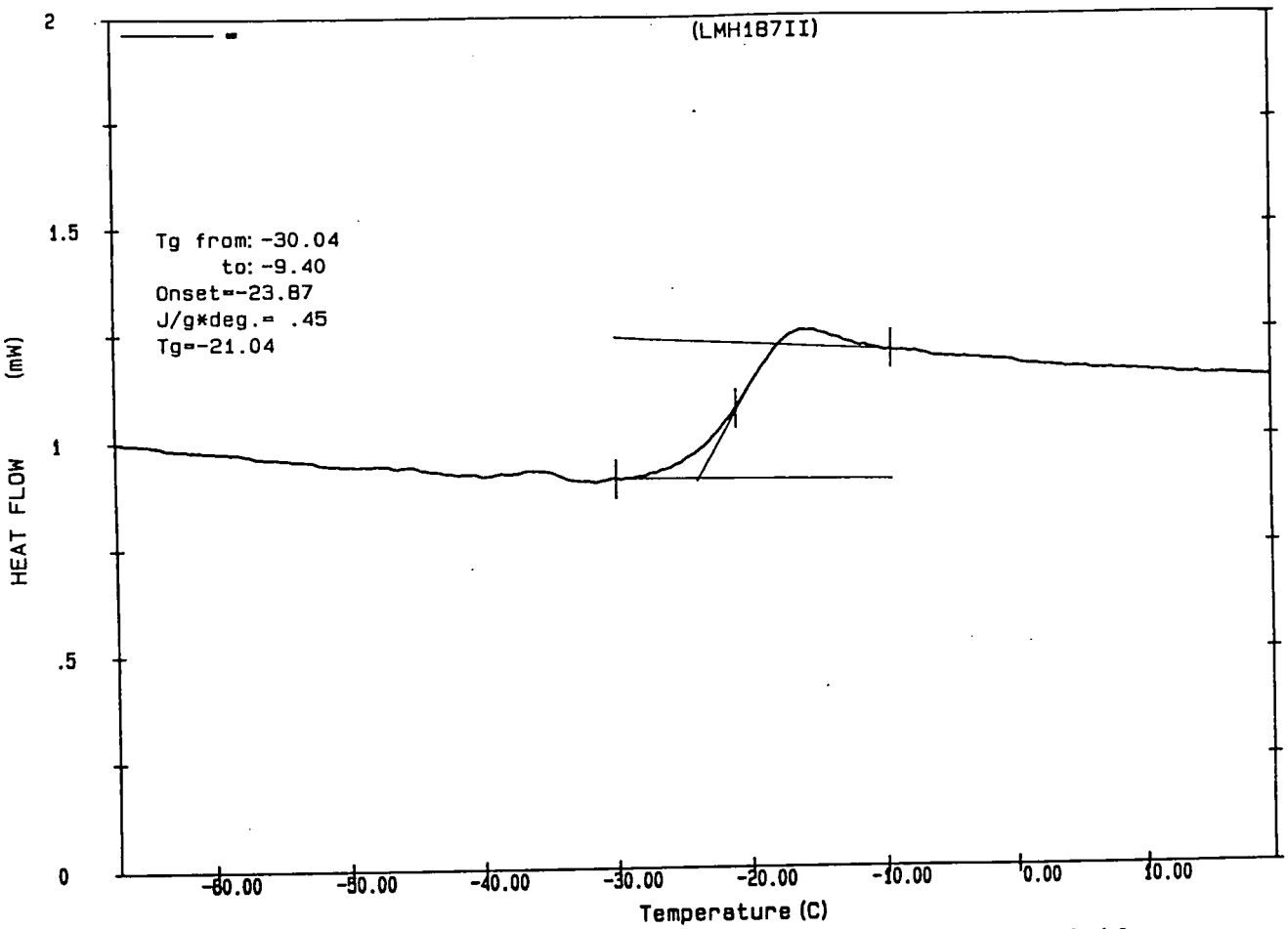

Appendix 4.39 DSC trace of the product of the reaction between poly(diethyl 3-hydroxyglutarate) and PTA at 110°C for 2.5 hours

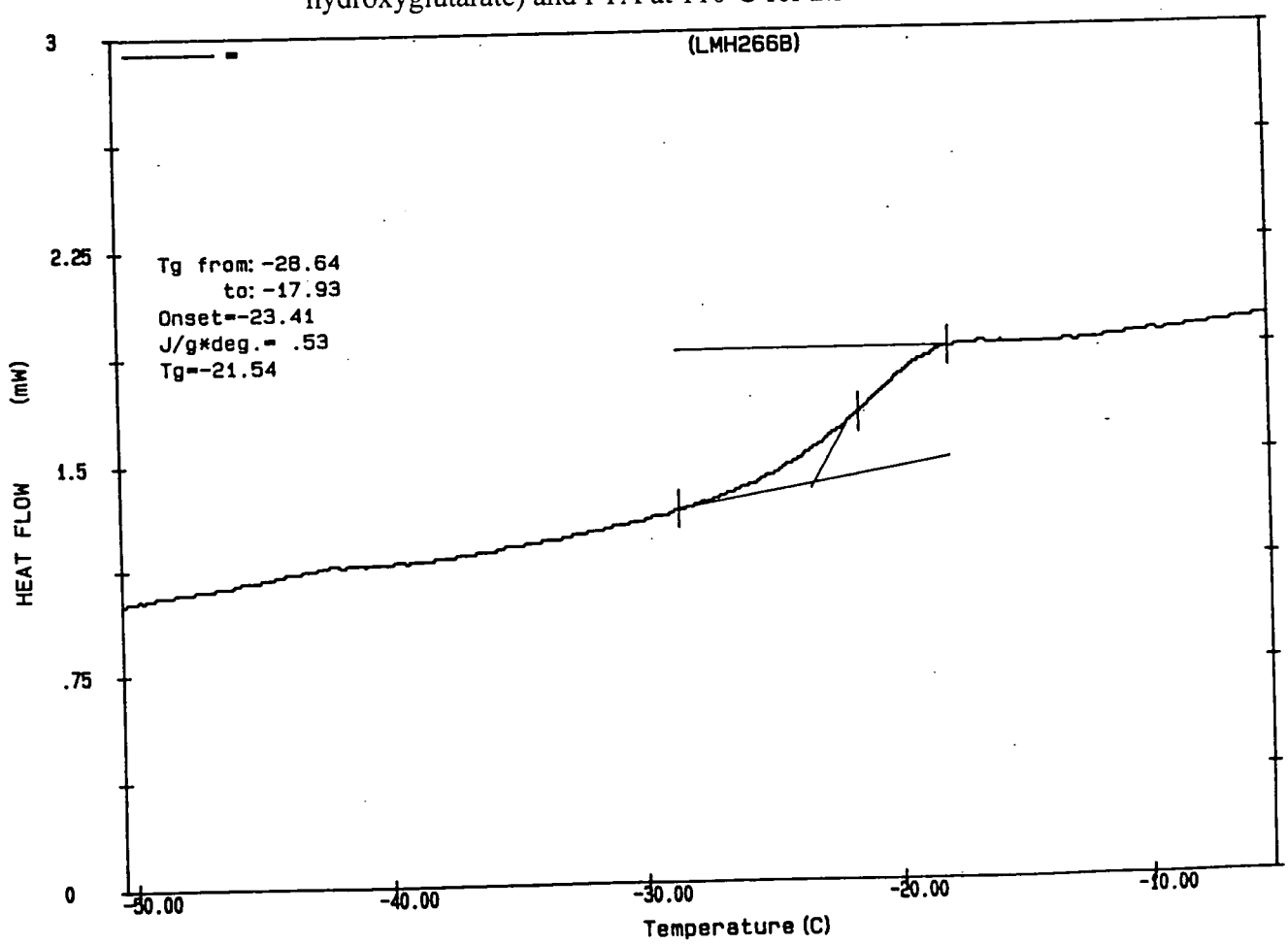

Appendix 4.40 DSC trace of the product of the reaction between poly(diethyl 3-hydroxyglutarate) and PTA at 110°C for 5 hours

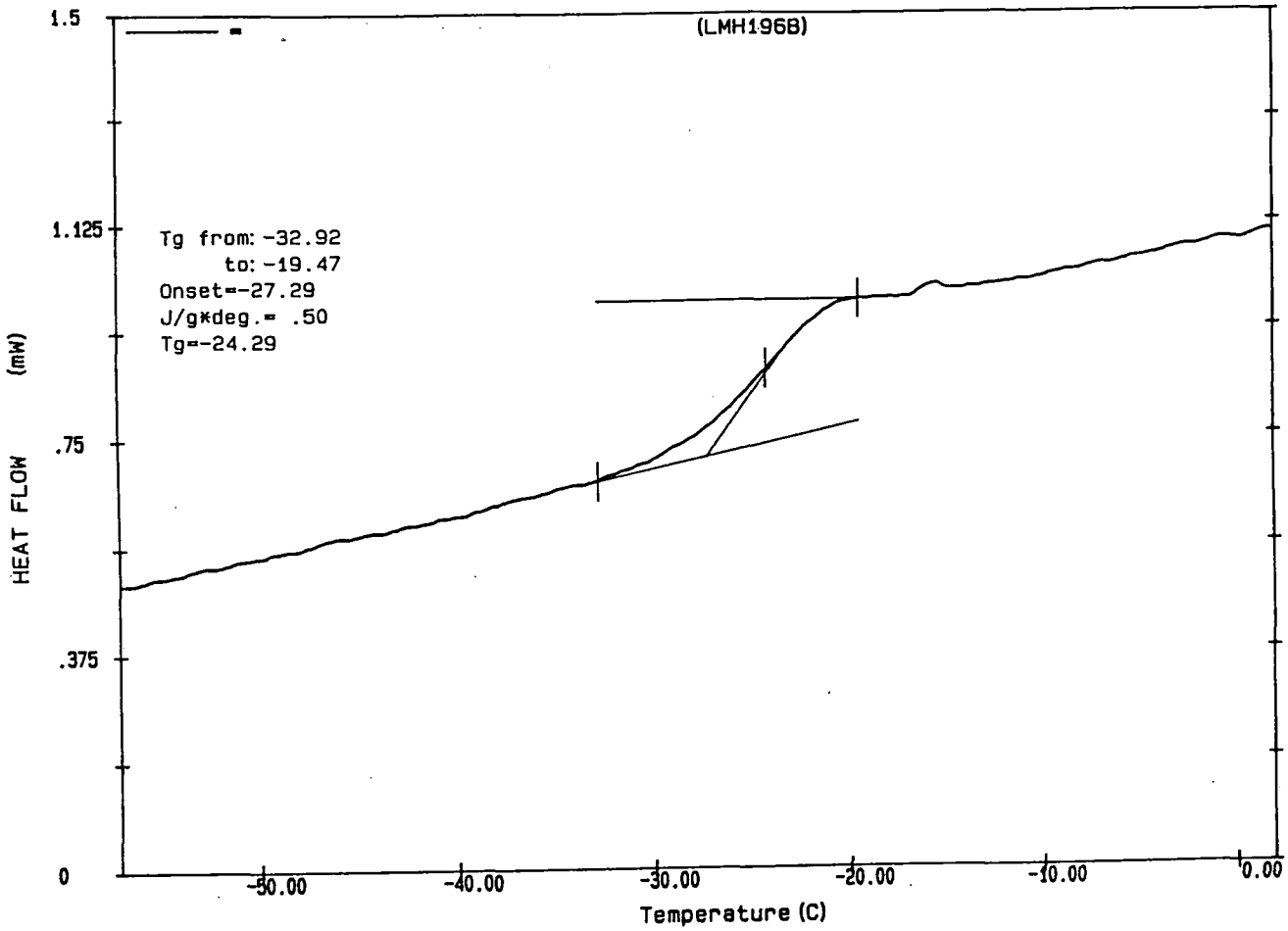

Appendix 4.41 DSC trace of the product of the reaction between poly(diethyl 3-hydroxyglutarate) and PTA at 110°C for 17 hours

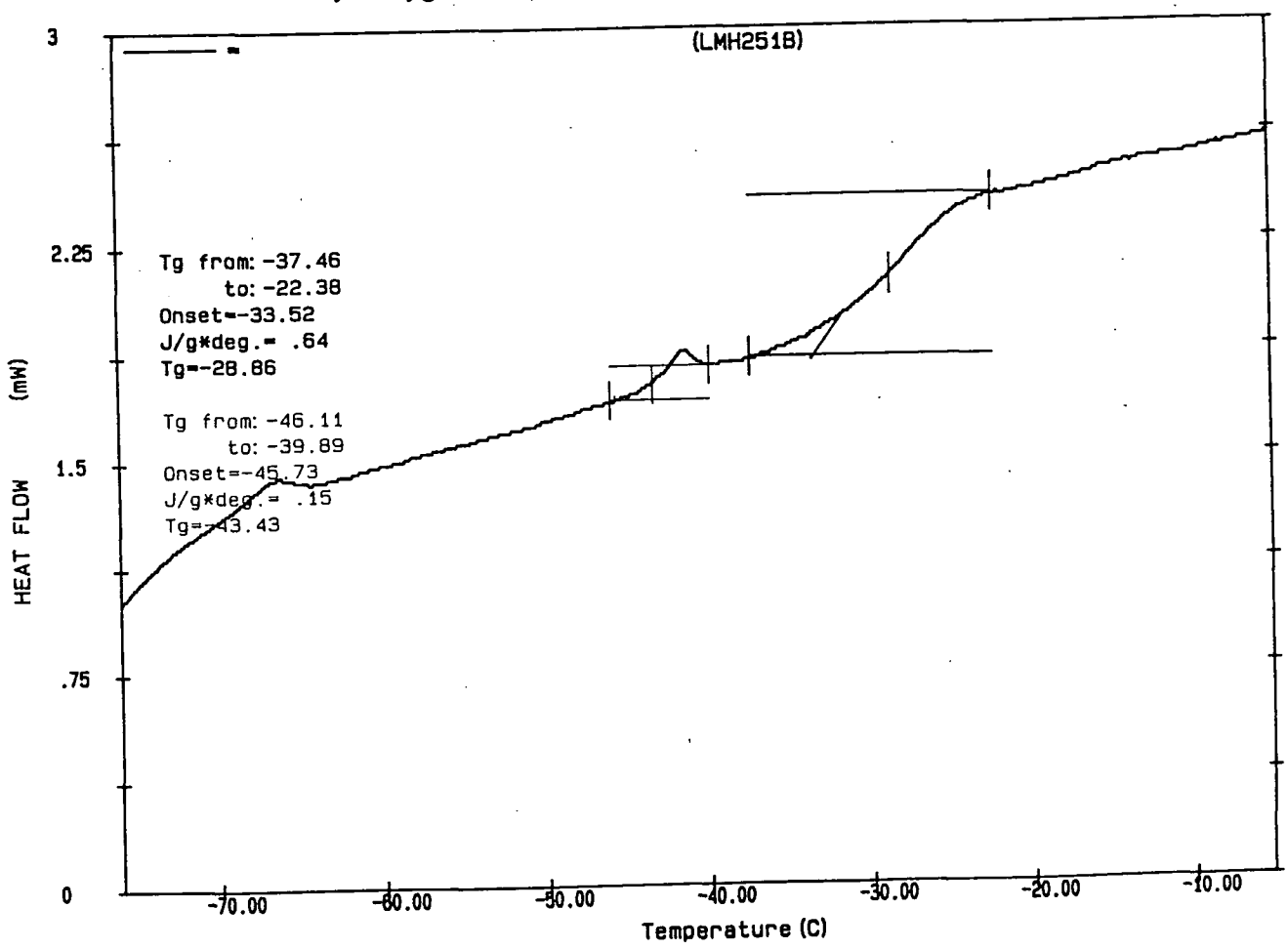

Appendix 4.42 DSC trace of the product of the reaction between poly(diethyl 3-hydroxyglutarate) and PTA at 185°C for 0.25 hours

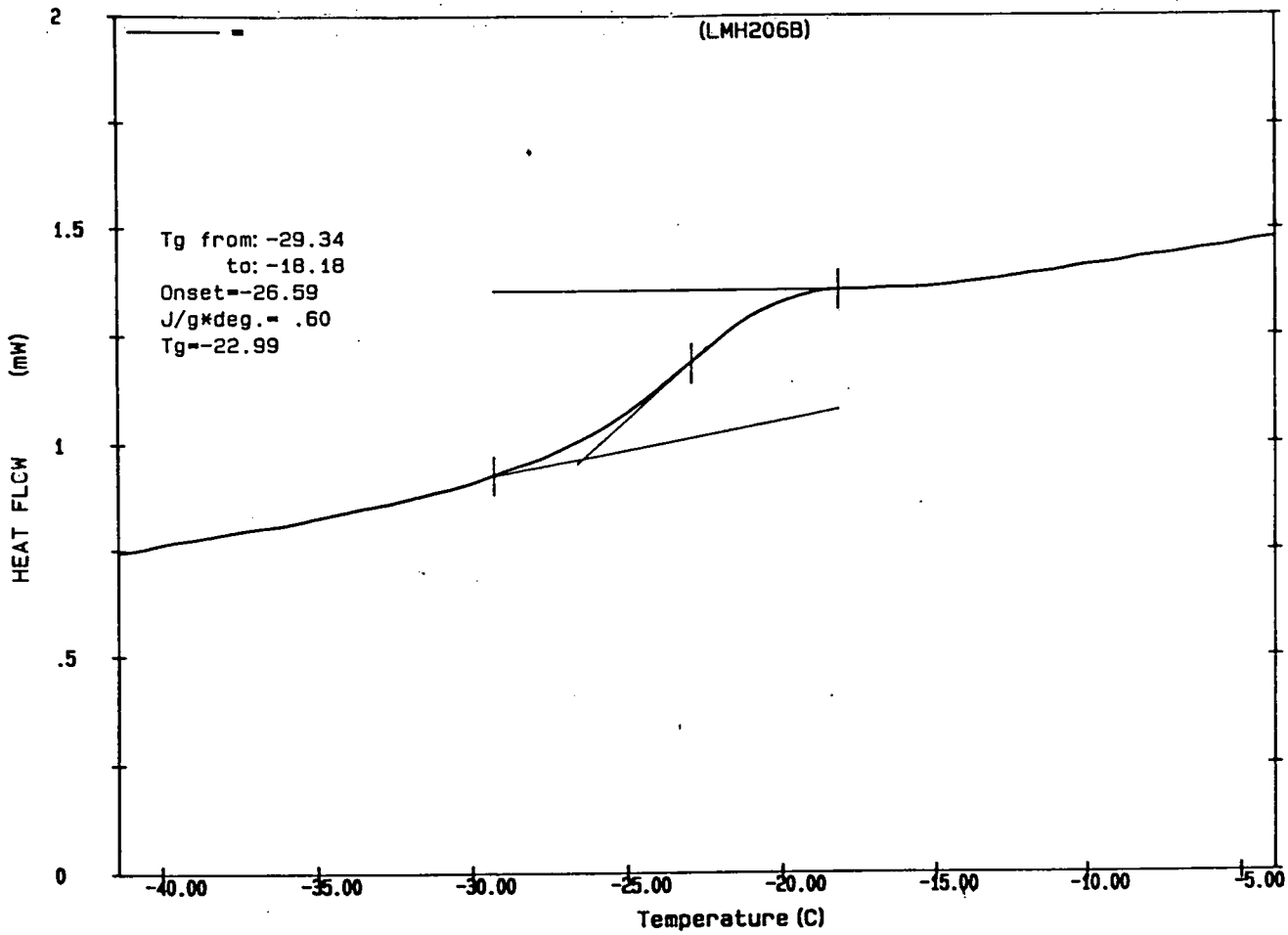

Appendix 4.43 DSC trace of the product of the reaction between poly(diethyl 3-hydroxyglutarate) and 1,5-pentanediol at 90°C for 5 hours

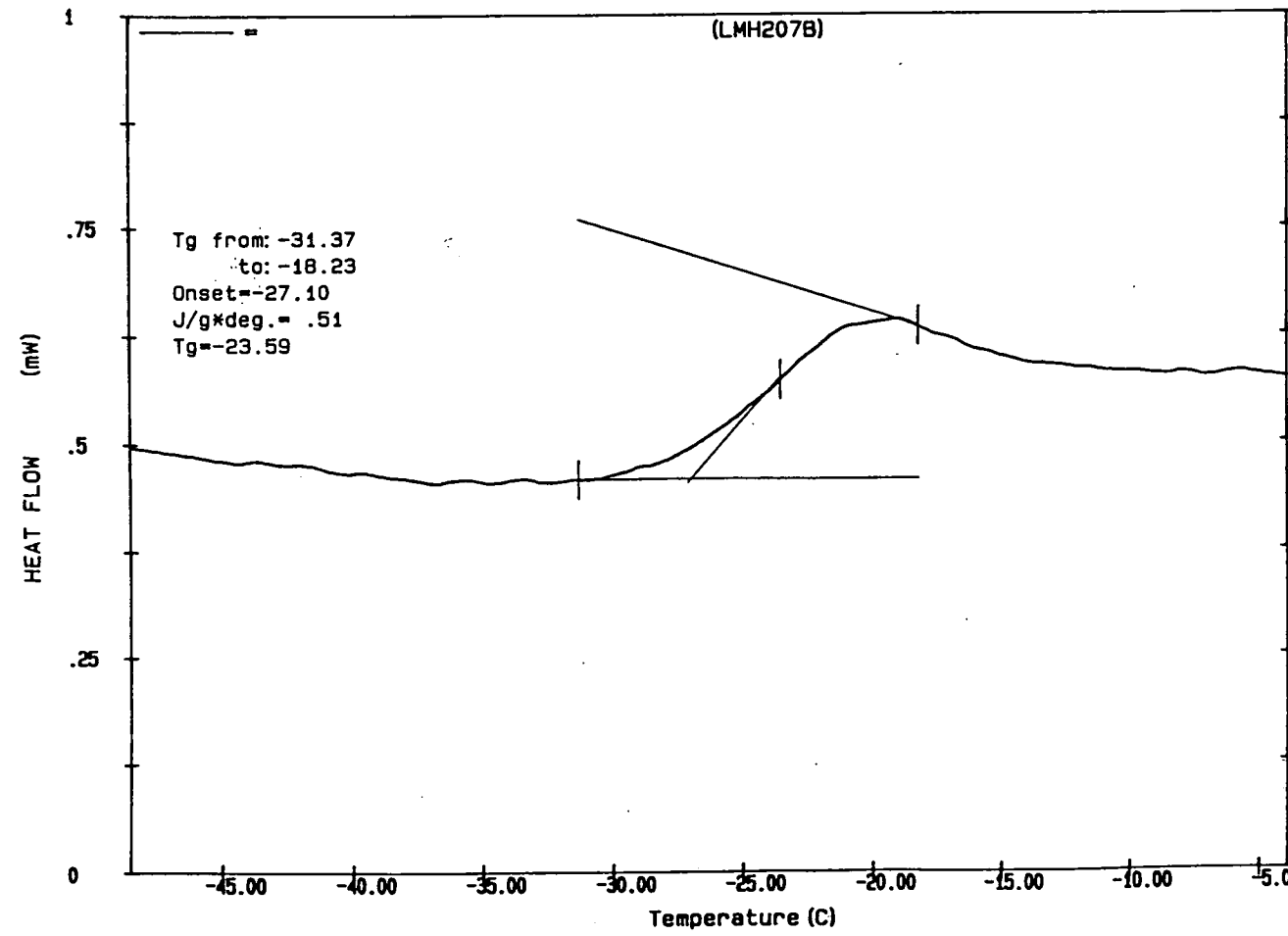

Appendix 4.44 DSC trace of the product of the reaction between poly(diethyl 3-hydroxyglutarate) and 1,5-pentanediol at 90°C for 17 hours

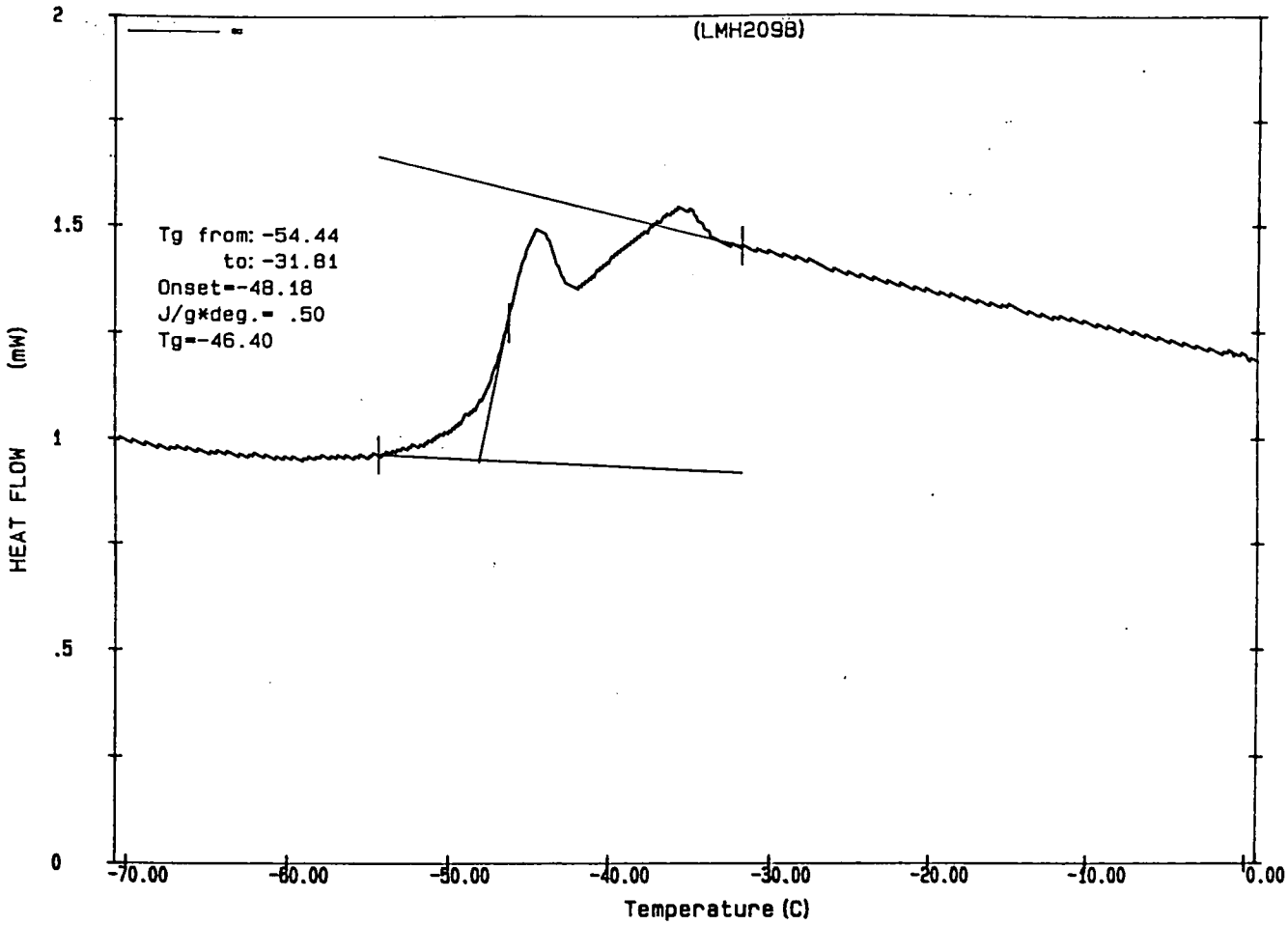

Appendix 4.45 DSC trace of the product of the reaction between poly(diethyl 3-hydroxyglutarate) and 1,5-pentanediol at 110°C for 17 hours

APPENDIX 4

^{1}H and ^{13}C nmr data for the products of the attempted cross-linking reactions described in Chapter 6.

Peak/ppm	Multiplicity	Assignment	Integral
0.93	t	Butyl CH_3	1
1.26	t	Ethyl CH_3	23
2.08	s	PTA CH_3	17.75
2.54	m	Focal CH_2	15.75
2.69	m	Polymeric CH_2	6
3.43	dd	Monomer OH	2.25
4.12	s	PTA CH_2O	16
4.14	m	Ethyl OCH_2	18.25
4.44	m	Focal CH	4
5.56	m	Polymeric CH	1.5

Table 1. ^{1}H nmr results for the product of the copolymerisation of PTA and diethyl 3-hydroxyglutarate (Time of addition = 0 hours)

			2 hours	3 hours
Peak/ppm	Multiplicity	Assignment	Integral	Integral
0.93	t	Butyl CH_3	1	1
1.26	t	Ethyl CH_3	14.89	11.8
2.08	s	PTA CH_3	13.56	11.5
2.54	m	Focal CH_2	4.67	2.4
2.69	m	Polymeric CH_2	12.56	12.6
4.14	m	*Ethyl OCH_2	22.22	18.2
4.44	m	Focal CH	1	0.5
5.56	m	Polymeric CH	3.11	3

Table 2. ^1H nmr results for the product of the copolymerisation of PTA and diethyl 3-hydroxyglutarate (Time of addition = 2 and 3 hours)

*Indicates overlapping signals due to the ethyl OCH_2 and the OCH_2 of PTA

			2 hours	3 hours
Peak/ppm	Multiplicity	Assignment	Integral	Integral
0.93	t	Butyl CH_3	3	1.8
1.26	t	Ethyl CH_3	44	28
1.61	broad s	Diol CH_2	12.67	4.6
2.54	m	Focal CH_2	7.67	5.7
2.69	m	Polymeric CH_2	57.67	34.6
4.14	m	Ethyl OCH_2	38	24.2
4.44	m	Focal CH	1	1
5.56	m	Polymeric CH	15.33	9.6

Table 3. ^{1}H nmr results for the product of the copolymerisation of 1,5-pentanediol and diethyl 3-hydroxyglutarate (Time of addition = 2 and 3 hours)

			2.5 hours	5 hours
Peak/ppm	Multiplicity	Assignment	Integral	Integral
0.93	t	Butyl CH_3	1	1
1.26	t	Ethyl CH_3	28.4	23.2
2.08	s	PTA CH_3	4.4	17.2
2.54	m	Focal CH_2	1.8	2
2.69	m	Polymeric CH_2	34	29.6
4.14	m	*Ethyl OCH_2	22.4	31.6
4.44	m	Focal CH	0.6	0.5
5.56	m	Polymeric CH	8.6	8

Table 4. ^{1}H nmr results for the cross-linking reaction between poly(diethyl 3-hydroxyglutarate) and PTA at 90°C for 2.5 and 5 hours

			17 hours	2.5 hours
Peak/ppm	Multiplicity	Assignment	Integral	Integral
0.93	t	Butyl CH_3	1	1
1.26	t	Ethyl CH_3	22	26.5
2.08	s	PTA CH_3	8.83	1.25
2.54	m	Focal CH_2	1.83	2
2.69	m	Polymeric CH_2	30.5	36.5
4.14	m	*Ethyl OCH_2	25	22.5
4.44	m	Focal CH	0.4	0.38
5.56	m	Polymeric CH	8.83	10

Table 5. ^{1}H nmr results for the cross-linking reaction between poly(diethyl 3-hydroxyglutarate) and PTA at 90°C for 17 hours and 110°C for 2.5 hours

			5 hours	17 hours
Peak/ppm	Multiplicity	Assignment	Integral	Integral
0.93	t	Butyl CH_3	1	1
1.26	t	Ethyl CH_3	29.4	30.5
2.08	s	PTA CH_3	2	20.25
2.54	m	Focal CH_2	2.4	2
2.69	m	Polymeric CH_2	36.8	43.75
4.14	m	*Ethyl OCH_2	22	40.5
4.44	m	Focal CH	0.45	0.28
5.56	m	Polymeric CH	9.4	11.5

Table 6. ^{1}H nmr results for the cross-linking reaction between poly(diethyl 3-hydroxyglutarate) and PTA at 110°C for 5 and 17 hours

Peak/ppm	Multiplicity	Assignment	Integral
0.93	t	Butyl CH_3	1
1.26	t	Ethyl CH_3	30
2.08	s	PTA CH_3	24.8
2.54	m	Focal CH_2	2.6
2.69	m	Polymeric CH_2	36.8
4.14	m	*Ethyl OCH_2	39.2
4.44	m	Focal CH	0.46
5.56	m	Polymeric CH	9

Table 7. ^{1}H nmr results for the cross-linking reaction between poly(diethyl 3-hydroxyglutarate) and PTA at 185°C for 0.25 hours

			5 hours	17 hours
Peak/ppm	Multiplicity	Assignment	Integral	Integral
0.93	t	Butyl CH_3	1	1
1.26	t	Ethyl CH_3	31.5	35.3
1.61	broad s	Diol CH_2	8.75	11
2.54	m	Focal CH_2	2.25	2.67
2.69	m	Polymeric CH_2	43	48
4.14	m	Ethyl OCH_2	25.25	29
4.44	m	Focal CH	0.5	0.46
5.56	m	Polymeric CH	12.25	13

Table 8. ^{1}H nmr results for the cross-linking reaction between poly(diethyl 3-hydroxyglutarate) and 1,5-pentanediol at 90°C for 5 and 17 hours

Peak/ppm	Multiplicity	Assignment	Integral
0.93	t	Butyl CH_3	1
1.26	t	Ethyl CH_3	25.6
1.61	broad s	Diol CH_2	6.6
2.54	m	Focal CH_2	3
2.69	m	Polymeric CH_2	31.6
4.14	m	Ethyl OCH_2	17.8
4.44	m	Focal CH	0.4
5.56	m	Polymeric CH	7.8

Table 9. ^{1}H nmr results for the cross-linking reaction between poly(diethyl 3-hydroxyglutarate) and 1,5-pentanediol at 110°C for 17 hours

0 hours		2 hours	
Peak/ppm	Assignment	Peak/ppm	Assignment
13.89	Butyl CH_3	13.69	Butyl CH_3
14.17	Ethyl CH_3	14.15	Ethyl CH_3
19.06	Butyl CH_2	19.08	Butyl CH_2
20.74	PTA CH_3	20.73	PTA CH_3
30.51	Butyl CH_2	30.53	Butyl CH_2
38.24	Polymeric CH_2	38.38	Polymeric CH_2
40.64	Focal CH_2	40.68	Focal CH_2
40.89	Monomer CH_2	41.16	Butyl CH_2
41.82	PTA C	41.65	PTA C
60.82	Ethyl OCH_2	60.86	Ethyl OCH_2
62.28	PTA OCH_2	62.18	PTA OCH_2
64.76	Focal CH	64.77	Focal CH
66.87	Polymeric CH	67.23	Polymeric CH
67.15	Polymeric CH	168.67	C=O
67.43	Polymeric CH	169.71	C=O
169.78	C=O	169.79	C=O
169.98	C=O	170.53	C=O
170.53	C=O	-	-
171.08	C=O	-	-
171.81	C=O	-	-

Table 10. ^{13}C nmr results for the product of the copolymerisation of PTA and diethyl 3-hydroxyglutarate (Time of addition = 0 and 2 hours)

3 hours	
Peak/ppm	Assignment
13.69	Butyl CH_3
14.15	Ethyl CH_3
19.08	Butyl CH_2
20.74	PTA CH_3
30.54	Butyl CH_2
38.27	Polymeric CH_2
40.68	Focal CH_2
41.65	PTA C
60.85	Ethyl OCH_2
62.28	PTA OCH_2
64.77	Focal CH
67.23	Polymeric CH
168.63	C=O
169.70	C=O
170.53	C=O

Table 11. ^{13}C nmr results for the product of the copolymerisation of PTA and diethyl 3-hydroxyglutarate (Time of addition = 3 hours)

2 hours		3 hours	
Peak/ppm	Assignment	Peak/ppm	Assignment
13.68	Butyl CH_3	13.67	Butyl CH_3
14.14	Ethyl CH_3	14.13	Ethyl CH_3
19.06	Butyl CH_2	19.06	Butyl CH_2
30.52	Butyl CH_2	30.51	Butyl CH_2
38.24	Polymeric CH_2	38.24	Polymeric CH_2
60.83	Ethyl OCH_2	40.62	Focal CH_2
64.74	Focal CH	60.82	Ethyl OCH_2
67.24	Polymeric CH	64.74	Focal CH
168.71	C=O	67.20	Polymeric CH
169.68	C=O	168.59	C=O
-	-	169.67	C=O

Table 12. ^{13}C nmr results for the product of the copolymerisation of 1,5-pentanediol and diethyl 3-hydroxyglutarate (Time of addition = 2 and 3 hours)

2.5 hours		5 hours	
Peak/ppm	Assignment	Peak/ppm	Assignment
13.89	Butyl CH_3	14.15	Ethyl CH_3
14.14	Ethyl CH_3	20.74	PTA CH_3
20.73	PTA CH_3	38.28	Polymeric CH_2
30.52	Butyl CH_2	60.86	Ethyl OCH_2
38.24	Polymeric CH_2	62.28	PTA OCH_2
60.82	Ethyl OCH_2	67.23	Polymeric CH
62.26	PTA OCH_2	169.70	C=O
67.20	Polymeric CH	-	-
168.59	C=O	-	-
169.67	C=O	-	-
170.52	C=O	-	-

Table 13. ^{13}C nmr results for the cross-linking reaction between poly(diethyl 3-hydroxyglutarate) and PTA at 90°C for 2.5 and 5 hours

17 hours		2.5 hours	
Peak/ppm	Assignment	Peak/ppm	Assignment
14.14	Ethyl CH_3	14.15	Ethyl CH_3
20.73	PTA CH_3	19.07	Butyl CH_2
30.94	Butyl CH_2	20.74	PTA CH_3
38.25	Polymeric CH_2	30.52	Butyl CH_2
60.83	Ethyl OCH_2	38.25	Polymeric CH_2
62.27	PTA OCH_2	60.84	Ethyl OCH_2
67.27	Polymeric CH	62.27	PTA OCH_2
169.68	C=O	64.73	Focal CH
170.52	C=O	67.21	Polymeric CH
-	-	168.61	C=O
-	-	169.69	C=O

Table 14. ^{13}C nmr results for the cross-linking reaction between poly(diethyl 3-hydroxyglutarate) and PTA at 90°C for 17 hours and at 110°C for 2.5 hours

5 hours		17 hours	
Peak/ppm	Assignment	Peak/ppm	Assignment
13.94	Butyl CH_3	14.14	Ethyl CH_3
14.13	Ethyl CH_3	20.73	PTA CH_3
19.07	Butyl CH_2	30.26	Butyl CH_2
20.73	PTA CH_3	38.25	Polymeric CH_2
38.25	Polymeric CH_2	60.83	Ethyl OCH_2
60.83	Ethyl OCH_2	62.27	PTA OCH_2
62.27	PTA OCH_2	67.21	Polymeric CH
67.21	Polymeric CH	168.59	C=O
168.69	C=O	169.67	C=O
169.67	C=O	170.52	C=O
-	-	-	-

Table 15. ^{13}C nmr results for the cross-linking reaction between poly(diethyl 3-hydroxyglutarate) and PTA at 110°C for 5 and 17 hours

0.25 hours	
Peak/ppm	Assignment
13.69	Butyl CH_3
14.17	Ethyl CH_3
20.71	PTA CH_3
38.22	Polymeric CH_2
41.60	PTA C
60.78	Ethyl OCH_2
62.24	PTA OCH_2
64.77	Focal CH
67.19	Polymeric CH
168.58	C=O
169.65	C=O
170.49	C=O

Table 16. ^{13}C nmr results for the cross-linking reaction between poly(diethyl 3-hydroxyglutarate) and PTA at 185°C for 0.25 hours

5 hours		17 hours	
Peak/ppm	Assignment	Peak/ppm	Assignment
14.14	Ethyl CH_3	14.14	Ethyl CH_3
38.24	Polymeric CH_2	38.24	Polymeric CH_2
60.82	Ethyl OCH_2	60.82	Ethyl OCH_2
67.20	Polymeric CH	67.20	Polymeric CH
168.59	C=O	168.60	C=O
169.67	C=O	169.67	C=O

Table 17. ^{13}C nmr results for the cross-linking reaction between poly(diethyl 3-hydroxyglutarate) and 1,5-pentanediol at 90°C for 5 and 17 hours

17 hours	
Peak/ppm	Assignment
14.14	Ethyl CH_3
38.24	Polymeric CH_2
60.82	Ethyl OCH_2
67.20	Polymeric CH
168.59	C=O
169,67	C=O

Table 18. ^{13}C nmr results for the cross-linking reaction between poly(diethyl 3-hydroxyglutarate) and 1,5-pentanediol at 110°C for 17 hours

Colloquia, Lectures and Seminars Attended

1993

October 4 Prof. F.J. Feher, University of California, Irvine, USA
Bridging the Gap between Surfaces and Solution with Sessilquioxanes

October 20 Dr. P. Quayle, University of Manchester
Aspects of Aqueous ROMP Chemistry

October 27 Dr. R.A.L. Jones, Cavendish Laboratory, Cambridge
Perambulating Polymers

November 24 Dr. P.G. Bruce, University of St. Andrews
Structure and Properties of Inorganic Solids and Polymers

November 25 Dr. R.P. Wayne, University of Oxford
The Origin and Evolution of the Atmosphere

December 1 Prof. M.A. McKervey, Queen's University, Belfast
Synthesis and Applications of Chemically Modified Calixarenes

1994

January 26 Prof. J. Evans, University of Southampton
Shining Light on Catalysts

February 23 Prof. P.M. Maitlis, University of Sheffield
Across the Border : From Homogeneous to Heterogeneous Catalysis

March 2 Dr. C. Hunter, University of Sheffield
Noncovalent Interactions between Aromatic Molecules

March 9 Prof. F. Wilkinson, Loughborough University of Technology
Nanosecond and Picosecond Laser Flash Photolysis

November 16 Prof. M. Page, University of Huddersfield
Four-membered Rings and b-Lactamase

November 23 Dr J. M. J. Williams, University of Loughborough
New Approaches to Asymmetric Catalysis

December 7 Prof. D. Briggs, ICI and University of Durham
Surface Mass Spectrometry

1995

January 11 Prof. P. Parsons, University of Reading
Applications of Tandem Reactions in Organic Synthesis

January 25 Dr D. A. Roberts, Zeneca Pharmaceuticals
The Design and Synthesis of Inhibitors of the Renin-angiotensin System

February 1 Dr T. Cosgrove, Bristol University
Polymers do it at Interfaces

February 22 Prof. E. Schaumann, University of Clausthal
Silicon- and Sulphur-mediated Ring-opening Reactions of Epoxide

April 26 Dr M. Schroder, University of Edinburgh
Redox-active Macrocyclic Complexes : Rings, Stacks and Liquid Crystals

May 4 Prof. A. J. Kresge, University of Toronto
The Ingold Lecture Reactive Intermediates : Carboxylic-acid Enols and Other Unstable Species

October 11 Prof. P. Lugar, Frei Univ Berlin, FRG
Low Temperature Crystallography

October 25 Dr.D.Martin Davies, University of Northumbria
Chemical reactions in organised systems.

November 1 Prof. W. Motherwell, UCL London
New Reactions for Organic Synthesis

November 17 Prof. David Bergbreiter, Texas A&M, USA
Design of Smart Catalysts, Substrates and Surfaces from Simple Polymers

November 22 Prof. I Soutar, Lancaster University
A Water of Glass? Luminescence Studies of Water-Soluble Polymers.

1996

January 10 Dr Bill Henderson, Waikato University, NZ
Electrospray Mass Spectrometry - a new sporting technique

January 24 Dr Alan Armstrong, Nottingham Univesity
Alkene Oxidation and Natural Product Synthesis

January 31 Dr J. Penfold, Rutherford Appleton Laboratory,
Soft Soap and Surfaces

March 6 Dr Richard Whitby, Univ of Southampton
New approaches to chiral catalysts: Induction of planar and metal centred asymmetry

March 12 RSC Endowed Lecture - Prof. V. Balzani, Univ of Bologna
Supramolecular Photochemistry

March 13 Prof. Dave Garner, Manchester University
Mushrooming in Chemistry

Conferences and Courses Attended

April 1994 Macro Group (UK) Family Meeting
Birmingham University

January 1995 IRC Polymer Physics and Engineering Courses
Leeds and Bradford Universities

July 1995 ISOM 11
Durham University

July 1996 Recent Advances in Polymer Synthesis
York University